frontiers | Research Topics

Advanced bioactive nanomaterials for diagnosis and treatment of major chronic diseases

Edited by
Fan Huang, Chang Li, Yu Zhao and Zhanzhan Zhang

Published in
Frontiers in Bioengineering and Biotechnology
Frontiers in Molecular Biosciences

ISSN 1664-8714
ISBN 978-2-8325-3746-6
DOI 10.3389/978-2-8325-3746-6

About Frontiers

Frontiers is more than just an open access publisher of scholarly articles: it is a pioneering approach to the world of academia, radically improving the way scholarly research is managed. The grand vision of Frontiers is a world where all people have an equal opportunity to seek, share and generate knowledge. Frontiers provides immediate and permanent online open access to all its publications, but this alone is not enough to realize our grand goals.

Frontiers journal series

The Frontiers journal series is a multi-tier and interdisciplinary set of open-access, online journals, promising a paradigm shift from the current review, selection and dissemination processes in academic publishing. All Frontiers journals are driven by researchers for researchers; therefore, they constitute a service to the scholarly community. At the same time, the *Frontiers journal series* operates on a revolutionary invention, the tiered publishing system, initially addressing specific communities of scholars, and gradually climbing up to broader public understanding, thus serving the interests of the lay society, too.

Dedication to quality

Each Frontiers article is a landmark of the highest quality, thanks to genuinely collaborative interactions between authors and review editors, who include some of the world's best academicians. Research must be certified by peers before entering a stream of knowledge that may eventually reach the public - and shape society; therefore, Frontiers only applies the most rigorous and unbiased reviews. Frontiers revolutionizes research publishing by freely delivering the most outstanding research, evaluated with no bias from both the academic and social point of view. By applying the most advanced information technologies, Frontiers is catapulting scholarly publishing into a new generation.

What are Frontiers Research Topics?

Frontiers Research Topics are very popular trademarks of the *Frontiers journals series*: they are collections of at least ten articles, all centered on a particular subject. With their unique mix of varied contributions from Original Research to Review Articles, Frontiers Research Topics unify the most influential researchers, the latest key findings and historical advances in a hot research area.

Find out more on how to host your own Frontiers Research Topic or contribute to one as an author by contacting the Frontiers editorial office: frontiersin.org/about/contact

Advanced bioactive nanomaterials for diagnosis and treatment of major chronic diseases

Topic editors

Fan Huang — China Academy of Chinese Medical Sciences, China
Chang Li — Tongji University, China
Yu Zhao — Tufts University, United States
Zhanzhan Zhang — Tianjin Medical University, China

Citation

Huang, F., Li, C., Zhao, Y., Zhang, Z., eds. (2023). *Advanced bioactive nanomaterials for diagnosis and treatment of major chronic diseases*. Lausanne: Frontiers Media SA. doi: 10.3389/978-2-8325-3746-6

Table of contents

frontiers | Frontiers in Bioengineering and Biotechnology

REVIEW
published: 19 July 2022
doi: 10.3389/fbioe.2022.954470

Nanogels as Novel Nanocarrier Systems for Efficient Delivery of CNS Therapeutics

*Yunhan Zhang, Zhulin Zou, Shuang Liu, Shengjie Miao and Haiyan Liu**

Department of Anatomy, College of Basic Medicine Sciences, Jilin University, Changchun, China

Nanogels have come out as a great potential drug delivery platform due to its prominently high colloidal stability, high drug loading, core-shell structure, good permeation property and can be responsive to environmental stimuli. Such nanoscopic drug carriers have more excellent abilities over conventional nanomaterials for permeating to brain parenchyma *in vitro* and *in vivo*. Nanogel-based system can be nanoengineered to bypass physiological barriers via non-invasive treatment, rendering it a most suitable platform for the management of neurological conditions such as neurodegenerative disorders, brain tumors, epilepsy and ischemic stroke, etc. Therapeutics of central nervous system (CNS) diseases have shown marked limited site-specific delivery of CNS by the poor access of various drugs into the brain, due to the presences of the blood-brain barrier (BBB) and blood-cerebrospinal fluid barrier (BCSFB). Hence, the availability of therapeutics delivery strategies is considered as one of the most major challenges facing the treatment of CNS diseases. The primary objective of this review is to elaborate the newer advances of nanogel for CNS drugs delivery, discuss the early preclinical success in the field of nanogel technology and highlight different insights on its potential neurotoxicity.

Keywords: nanotechnology, nanogel, CNS diseases, blood-brain barrier, smart drug release

OPEN ACCESS

Edited by:
Zhanzhan Zhang,
Tianjin Medical University, China

Reviewed by:
Meng Zheng,
Henan University, China
Chaoyong Liu,
Beijing University of Chemical Technology, China
Xiuli Zhuang,
Changchun Institute of Applied Chemistry (CAS), China

****Correspondence:***
Haiyan Liu
haiyan@jlu.edu.cn

Specialty section:
This article was submitted to Nanobiotechnology, a section of the journal Frontiers in Bioengineering and Biotechnology

Received: *27 May 2022*
Accepted: *20 June 2022*
Published: *19 July 2022*

Citation:
Zhang Y, Zou Z, Liu S, Miao S and Liu H (2022) Nanogels as Novel Nanocarrier Systems for Efficient Delivery of CNS Therapeutics. Front. Bioeng. Biotechnol. 10:954470. doi: 10.3389/fbioe.2022.954470

INTRODUCTION

Neurological diseases and disorders are considered significant challenges to the human health. According to global statistics, more than 1.5 billion people, arguably a quarter of the world's population suffer from CNS diseases (Palmer, 2010; Srikanth and Kessler, 2012; Soni et al., 2016a). A wide spectrum of therapeutic agents, e.g., nucleic acids, polypeptides, proteins and antisense drugs, have been promoted to alleviate CNS diseases, but the majority of these agents are unable to enter the brain parenchyma noninvasively due to a series of challenges. Site-specific delivery of the drugs is one of the most significant challenges due to restrictions imposed by two biochemical barriers, primarily by BBB. To treat CNS diseases, the most lethal and disabling diseases in the world, researchers have attempted to explore the novel treatment strategies using multiple perspectives ranging from more established efforts, such as the disruption of the BBB, the alteration of BBB permeability, and lipidization of water-soluble drugs, to the newer methods such as the development of nanoenabled drug delivery systems.

Nanotechnology is one of the strategies that provide a greater possibility to meet the requirements associated with high doses of the CNS drugs. Nanocarriers for the management of CNS diseases mainly include polymeric nanoparticles, solid lipid nanoparticles (SLNs), lipid nanocapsules, albumin nanoparticles, liposomes, dendrimers, nanoemulsions, hydrogels and nanogels, etc. (Date et al., 2007; Sun et al., 2012; Cojocaru et al., 2020; Bhia et al., 2021) However, these

TABLE 1 | A brief list of properties for nanocarriers used in the field of CNS therapeutics.

Nanocarriers	Type of materials	Advantages/limitations	Drug/agent delivered	References
Polymer NPs	PACA	BBB penetration increased, less immunogenic reaction/	Methotrexate	Tian et al. (2011)
	PLA	High potential toxicity risk	Temozolomide	Javed et al. (2021)
	PLGA		Piperine	Guo et al. (2017)
Dendrimers	PAMAM	Easy functionalization/Ligand-targeted conjugation, suitable for drug entrapment/ limited synthetic route,	*o*-phenylene	(Medina and El-Sayed, 2009; Zain-ul-Abdin et al., 2017)
	PPI	hematological toxicity	Diamine	
	poly(lysine)		Lamivudine	(Dutta and Jain, 2007; Pargoo et al., 2021)
			Doxorubicin	Zhang et al. (2014)
Solid lipid NPs (SLNs)	Sphingomyelin	High BBB permeability, increased drug release, drug levels rise in the brain/Rapid clearance, neurotoxicity from	siRNA	(Jin et al., 2011; Bae et al., 2013; Buyukkoroglu et al., 2016)
	Stearic acid	surfactant	Doxorubicin	(Tangpong et al., 2007; Battaglia et al., 2014)
	Cholesterol		Insulin	Kuo and Shih-Huang, (2013)
	PC		Azidothymidine	Pottoo et al. (2020)
Micelles	Block copolymeric	Drug permeability increased, enhanced oral bioavailability/Low encapsulation efficiency of drugs	Pilocarpine	Meng et al. (2020)
	Micelles		Paclitaxel	Zhang et al. (2012)
	Core-shell micelles		Vinblastine	Wong et al. (2012)
Emulsion	Edible oil	High biocompatibility, drugs uptake increased/Heat	Saquinavir	Mahajan et al. (2014)
	PUFA	decomposition, uncontrollable release, storage instability	Coenzyme Q10	Pastor-Maldonado et al. (2020)
	Flaxseed Oil		Cyclosporin A	Francischi et al. (1997)
Liposome	PC/cholesterol	Large drug loading capacity, extended half-life of the	Daunorubicin	Fassas and Anagnostopoulos, (2005)
	PC/PG	drug/Low distribution in tumor tissue, poor stability	Cisplatin	Huo et al. (2012)
	Phospholipid/ cholesterol		Amikacin	Khan and Chaudary, (2020)
Nanogel	PEG-PLA	Facile synthesis, extended systemic exposure, enhanced bioavailability, respond to external stimuli, high	Methotrexate	(Pourtalebi Jahromi et al., 2018; Pourtalebi Jahromi et al., 2019)
	CHP	distributed in lesion tissue	Nano-NRTI	(Vinogradov et al., 2010; Gerson et al., 2014; Warren et al., 2015)
	PEG-PEI		5-fluorouracil	Zhou et al. (2013)
	PEG-PLA		Antisenseoligonucleotides	(Vinogradov et al., 2004; Wang and Wu, 2017)

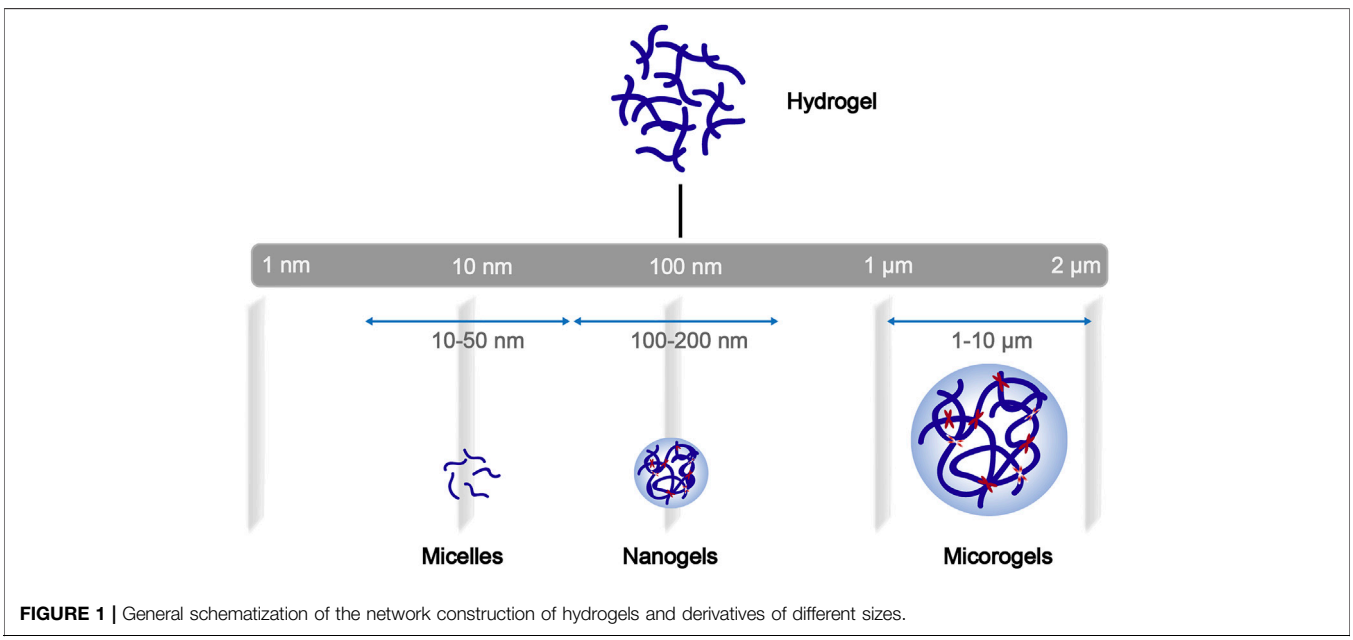

FIGURE 1 | General schematization of the network construction of hydrogels and derivatives of different sizes.

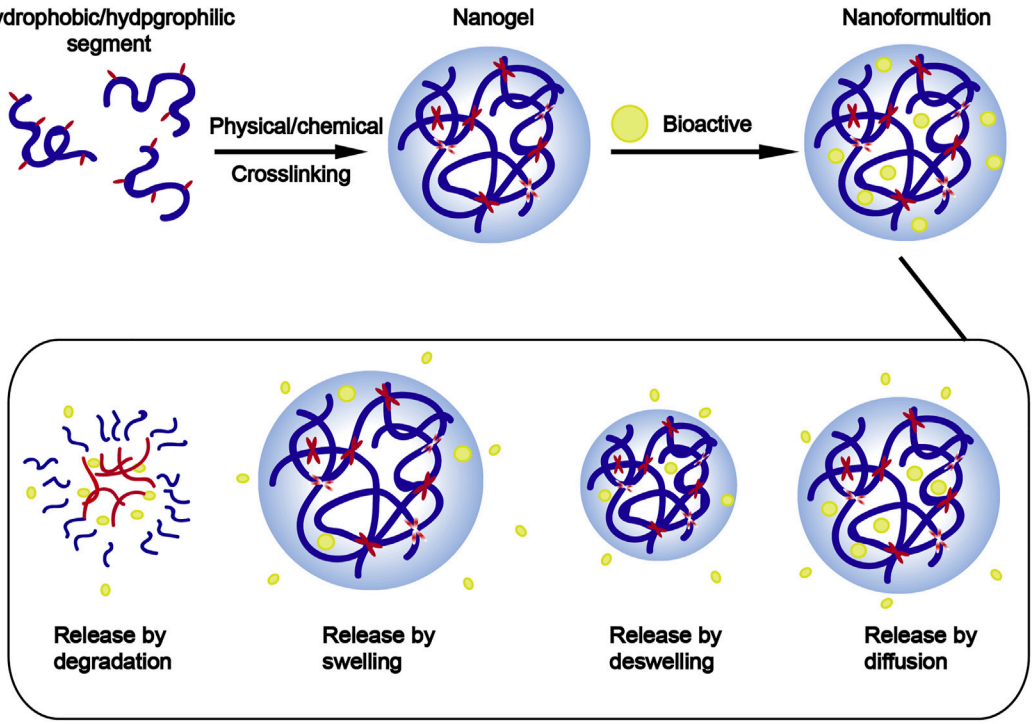

FIGURE 2 | Schematic representation of the synthesis and the release behavior of nanogels.

agents have the following inherent limitations in preclinical applications: 1) liposomes have poor stability and dispersibility; 2) polylactic acid-glycolic acid copolymer NPs but suffer from burst release problems; 3) chitosan nanoparticles have poor dispersibility when used in humans and potential biotoxicity; 5) inorganic-based carriers still cannot achieve biocompatibility; and 6) superparamagnetic iron oxide that contain choline has been mainly been fabricated for *in vivo* imaging studies. These limitations may render drugs unable to treat CNS diseases with ideal effects. **Table 1** summarizes several classes of the drug nanocarriers and their limitations for CNS therapy.

Among these nanotechnologies, the transition from hydrogels to nanogels offers new opportunities to achieve a systemic controlled-release drug delivery platform at the cellular level. Traditional hydrogels exhibit limited BBB penetration ability due to their microstructure, but this obstacle can be overcome by designing nanogels as nanosized colloidal particles (**Figure 1**). (Chen et al., 2021) Nanogels are the nanoscale hydrogel materials consisting of crosslinked polymer networks, which can be easily synthesized by chemical or physical routes (**Figure 2**). (Yin et al., 2008; Merino et al., 2015; Neamtu et al., 2017) Such nanocarrier systems are characterized by excellent ability to cross the BBB and accomplish site-specific delivery of drugs due to high water retention capacity of the hydrogels, their tunable shape, amphiphilic behavior, surface modifiability, and especially to their biodegradability and safety. Currently, nanogel technologies are mainly manifested in the fields of disease diagnosis (medical imaging) and drug delivery. The latter application faces more challenges, especially for therapeutic drug delivery for brain diseases, due to complex physiological responses *in vivo* (Debele et al., 2016; Ma et al., 2017; Neamtu et al., 2017; Ali et al., 2021).

The present review provides insights into nanogels as an effective carrier system for CNS delivery in preclinical applications, the strategies to improve the BBB penetration, and the approaches that are close to clinical applications. The present article considers the major challenges for the nanogels, which remain despite certain advances in the design of CNS nanocarrier, to provide ideal plans for the clinical therapies of CNS diseases.

BIOLOGICAL BARRIERS FOR CNS DRUG DELIVERY

The Blood-Brain Barrier

CNS homeostasis is strictly protected by two peripheral barriers, termed blood-brain barrier (BBB) and blood-cerebrospinal fluid barrier (BCSFB), which strictly regulate a series of the transport and metabolic processes to protect the brain from the periphery (Erickson and Banks, 2018; Ghersi-Egea et al., 2018; Kadry et al., 2020). These biological barriers, particularly the BBB pose the largest obstacle to nanocarriers for the delivery of various drugs into the CNS. In the absence of effective drug carriers, most macromolecules, such as proteins, oligonucleotides, nucleoside analogs, macromolecular drugs and more than 90% of small-molecule drugs cannot enter the brain through the BBB, which is

the key bottleneck in CNS disease treatment (Pardridge, 2005; Wohlfart et al., 2012). These issues are the key bottleneck in the treatment of CNS diseases. Additionally, rapid drug clearance and the failure to achieve a steady release of the drugs in the brain tissue remain among the challenges for the treatment of this group of diseases (Misra et al., 2003; Furtado et al., 2018; Jain, 2020).

The BBB was defined for the first time by Paul Ehrlich in 1885 and is composed of unique CNS microvasculature, including tight junctions (TJs) and adherent junctions, which strictly regulate the metabolism of immune surveillance cells and the entry process of xenobiotics/endogenous materials (Hawkins and Davis, 2005; Engelhardt and Sorokin, 2009; Tietz and Engelhardt, 2015). The functional unit of the BBB is not only constituted by brain capillary endothelial cells (ECs), but also has close interactions with pericytes, perivascular astrocytes and nerve cells. In particular, the tight junction proteins claudins and occludin, which are expressed in brain microvascular cells, account for extremely high transendothelial electrical resistance (TEER, approximately 1,500–2,000 Ω cm^2) of the BBB thus limiting the entry of the neurotherapeutic agents (Baeten and Akassoglou, 2011; Sá-Pereira et al., 2012; Molino et al., 2014; Girolamo et al., 2021).

In addition to impermeable cell barrier, there is a selective membrane-bound barrier regulated by ion channels, receptors, and transporters specifically expressed at the BBB. These molecules include ATP-binding cassette (ABC) transporters expressed in brain ECs, such as multiple drug resistance protein 1 (MDR1), permeability glycoprotein (P-gp), multiple resistance-associated protein 4 (MRP4), and breast cancer resistance protein (BCRP); these protein largely limit the permeability of the neurotherapeutic agents (e.g., anticancer drugs or kinins) through the BBB (Ueno et al., 2010; Alyautdin et al., 2014; Aday et al., 2016; Begicevic and Falasca, 2017; Gil-Martins et al., 2020). The transport of the polypeptides and proteins across the BBB requires the assistance of a series of receptor-binding molecules, such as insulin, insulin-like growth factors (IGF-I and IGF-II), angiotensin, and transferrin (Tf), which undergo receptor-mediated endocytosis (Wang et al., 2009; Soni et al., 2010). Another metabolic barrier is driven jointly by the complex and widely expressed influx/efflux transporters in the BBB. It is well known that P-glycoprotein (P-gp) and selective multidrug resistance protein-1 (MRP-1) are expressed at the high levels in the BBB and act as the efflux channels to confine the therapeutic drugs in combination with metabolic enzymes expressed by ECs (Lee et al., 2001; T. Ronaldson and P. Davis, 2012). Thus, the efficiency of the transport of most cargos from the blood circulation into the brain through the BBB is regulated by various transport systems.

Mounting evidence indicates that the permeability of the BBB is pathologically altered in several CNS diseases, such as neurodegenerative diseases, resulting in the aberrant expression of pivotal carrier/receptor-mediated transporters (e.g., P-gp and neuropeptides) and BBB efflux proteins (Zatta et al., 2009; Meairs, 2015; Logan et al., 2019; Bonsack et al., 2020). Therefore, insight into the pathophysiological characteristics of CNS barriers is essential for the development of a safe and efficient carrier system. The regulation of these transporter proteins and CNS barriers may provide new strategies for targeting of the brain by for neuroprotection and therapy.

Blood-Cerebrospinal Fluid Barrier (BCSFB)

The BCSFB is formed by a rich vascular network surrounding choroid plexus epithelial cells, located in the choroid plexus and meninges, which secrete cerebrospinal fluid into the ventricular system. where it is secreted into the ventricular system by choroid plexus epithelial cells. Similar to many other secretory epithelial cells, but unlike the endothelial cells of the brain capillaries that form the BBB, the endothelial cells of the choroid plexus capillaries are fenestrated. The barrier is composed of choroid plexus epithelial cells and their TJs and restricts the movement of small polar molecules. Thus, the BCSFB also regulates the permeability to nutrients or xenobiotics.

Notably, similar to the BBB, the BCSFB not only acts as both a physical barriers and an enzymatic barrier via endothelial or epithelial cells. These cells express not only a series of cytoplasmic and membrane-related enzymes that can effectively metabolize biologically active drugs, but also express many transport proteins and ion channels. These characteristic enzymatic reactions and polarized expression of proteins are clearly of considerable concern for the design of drug carriers targeting the brain.

Strategies Across the Brain Barriers

A variety of strategies have been developed to overcome the challenge of transporting the drugs across the BBB; however, the discoveries of most of strategies have not resulted in significant advances. **Table 2** describes the strategies to improve the BBB penetration of active drugs/agents. New advances in nanotechnology have produced various opportunities in the field of CNS disorders because nanocarrier systems have been shown to load poorly distributed drugs in the brain, traverse the cellular/metabolic barrier regions of the BBB, and efficiently deliver the drugs into the brain parenchyma (Poovaiah et al., 2018; Prasanna and Upadhyay, 2021; Wang et al., 2021). For example, Harbi et al. designed sertraline (Ser-HCl)-loaded pegylated and glycosylated liposomes. The results of analysis of the transport in endothelial polyoma cells of the mouse brain showed that glycosylated liposomes have a greater ability to target the cerebellum than PEGylated liposomes (Harbi et al., 2016).

The transport of drug nanocarrier systems across the BBB mainly involves the following mechanisms: 1) receptor-mediated endocytosis; 2) adsorptive-mediated endocytosis; 3) carrier-mediated transport; 4) passive diffusion; 5) efflux pump inhibition; and 6) the transient opening of the TJs of BBB. Surface functionalization of nanocarriers is a potential strategy to facilitate crossing of the BBB, enabling their entry into the brain via a transcellular pathway due to their specific targeting. Thus, the development of optimal drug delivery systems for CNS diseases should consider not only the ability to cross the BBB but also the ability to target and accumulate the drugs. Nanoscale particles can traverse the smallest

TABLE 2 | Strategies for drug delivery to access the brain.

Type	Advantages	Limitation	References
Bypass BBB			
ICV	High drug concentration, no metabolic intervention	Invasive injury, infection, elevated intracranial pressure	(Pappu et al., 2016; Heldt et al., 2019; Kazkayasi et al., 2022)
Intrathecal	Less invasive	Infection, dose-dependent drug resistance	(Falagas et al., 2007; Jain et al., 2019; Nau et al., 2021; Sari et al., 2021)
Intranasal	Rapid absorption, no first pass effect on, non-invasive	Poor bioavailability, low drug concentration	(Dowling et al., 2008; Grassin-Delyle et al., 2012)
Intraparenchymal	More clinical prospects	Invasive infection, tissue injury, obvious side effects	(McAteer and Evan, 2008; Tedford et al., 2015)
Across the BBB			
Drug lipidation	Increased BBB permeability	Increased drug efflux, nonspecific systemic administration	(Pardridge, 2003; He et al., 2018)
Prodrug	Drug solubility improvement/absorption	Poor stability, significant toxicity	Jafari et al. (2019)
Analog-based drug design	Suitable for free drug Good stability, good bioavailability, no invasive injury, small side effects	Drug molecule/ capacity size is limited, CNS complications, endogenous nutrient transport interference	Baroud et al. (2021)
Nanocarriers system		Potential toxicity depends on the material used	(Bajracharya et al., 2019; de Souza et al., 2020; Wang et al., 2020)

capillaries, previous studies have demonstrated that after intravenous administration, the particles in the range of 5–10 nm are rapidly removed by the kidney, whereas the particles ranging from 10 to 50 nm are small enough to traverse the capillaries. Additionally, the particles ranging from 50 to 100 nm in size have the longest cycle lifetime, and the particles with a diameter larger than 100 nm are usually blocked by the spleen and removed by phagocytosis, resulting in a short blood circulation time (Vinogradov et al., 2002; De Jong et al., 2008; Kreyling et al., 2014).

Modifying the carrier system with targeting ligands showed better trans-BBB efficiency. The surface of polyamidoamine (PAMAM) dendrimers was conjugated to transferrin (Tf) for improved drug delivery to the brain. The results demonstrated that surface-modified dendrimers show better BBB transport ability in physiological environments.

EMERGENCE OF THE NANOGEL AS A NANOCARRIER SYSTEM

Recently developed available drug nanocarriers for the management of CNS diseases, range from more conventional formulations (e.g., liposomes, solid lipid nanoparticles, polymeric nanoparticles) to advanced formulations (e.g., nanocapsules, albumin, dendrimers (Vigani et al., 2020), and nanogels). Among them, nanogels have been shown to achieve a suitable drug pharmacokinetic profile and higher efficacy and safety compared with other drug nanocarriers.

Properties of the Nanogel

Vinogradov et al. initially introduced the term "NanoGel" in 1999 to describe the particles of a hydrophilic polymer network (PEG-PEI) obtained by crosslinking polyethylene glycol (PEG)

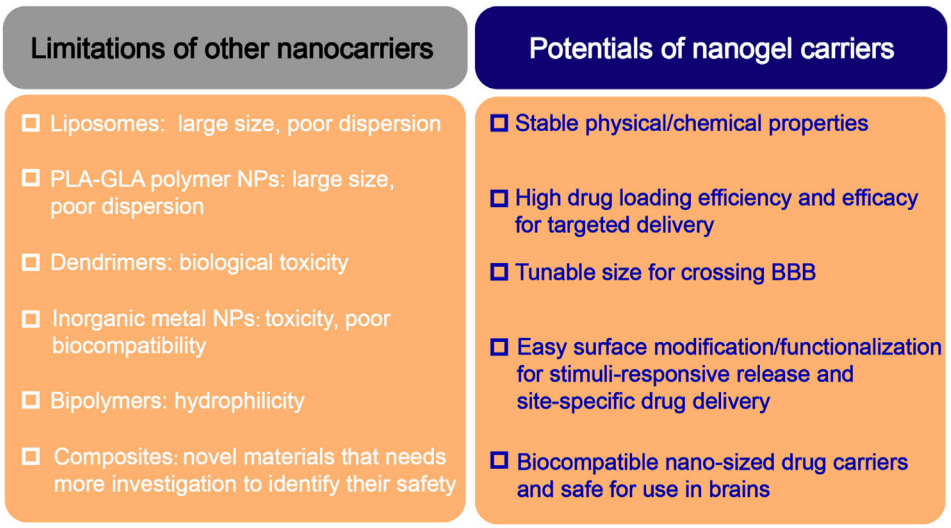

FIGURE 3 | Potentials of nanogels for CNS drug delivery compared with other available nanocarriers.

and polyethyleneimine (PEI) that were able to deliver antisense oligonucleotides (Zhao et al., 2015). These hydrogel nanoparticles are generally defined as three-dimensional colloidal hydrogel nanoparticles obtained by physical or chemical crosslinking of the polymers with a diameter < 200 nm, thus possessing both the advantages of a hydrogel and characteristics of a nanocarrier system (Goldberg et al., 2007; Zhang et al., 2021a). Traditionally, nanogels have been classified as physically or chemically covalently cross-linked according to the synthesis method. Nanogels can also be classified based on the network structure including hollow, core-shell, hairy, multilayered, and core-shell core cross-linking. In addition, according to their responses to environmental stimuli, they can also be divided into response and nonresponse types.

Similar to the hydrogels, the hydrophilic groups in the polymeric structure of nanogels provide for a high water retention capacity (Amoli-Diva et al., 2017; Mauri et al., 2021; Stawicki et al., 2021). Nanogels have unique advantages in CNS drug delivery, especially in increasing the penetration of the drugs through the BBB, enhancing the stability of the bioactive molecules against enzymatic degradation, and reducing the cytotoxic side effects. Compared with other nanocarriers, nanogels have the following unique characteristics (**Figure 3**):1) Tunable nanosize: nanogels have a large specific surface area and, more importantly, can be engineered with an adapted nanosize based on the target tissue/organ, enabling them to efficiently cross cellular and biological barriers. 2) Colloidal stability: nanogels possess higher stability in physiological environments. 3) Swelling behavior: swelling/deswelling is one of the most important properties of nanogels and can be controlled by their design with suitable parameters (such as polymers, cross-linking forms, and functional structures). Furthermore, these behavior properties can be altered by responding to external stimuli. 4) Drug loading and easy surface modification: the diversity of polymeric materials and simple modification of their physical or chemical characteristics enables the creation of nanogels with versatile formulations. Depending on the crosslinked polymer network, such as the hydrophilic/lipophilic groups of the monomers, surfactants, surface charge, and crosslinking agents, various types of nanogels can deliver almost all types of therapeutic agents, including active biomacromolecules (DNA and SiRNA), hydrophobic/hydrophilic drugs, proteins, vaccines and even immunetherapeutics (Coviello et al., 2007; Lombardo et al., 2020; Chander et al., 2021; Tang et al., 2022). 5) Active targeting and controlled release: nanogels can be synthesized by crosslinking natural (e.g., alginate, dextran, and hyaluronic acid) or artificial polymers (e.g., methylcellulose, chitosan, and cyclodextrin). These polymers are nontoxic and stable and ensure high cell viability in the studies, demonstrating that nanogels are inherently biocompatible and biodegradable, which can avoid excessive accumulation in the tissues (Soni et al., 2016b; Mathew et al., 2018). 6) Non immune response: due to their high water-holding capacity a which enables them to absorb large amounts of nonimmunoreactive liquids, usually nanogel formulations do not produce any immune response; 7) Biodegradability: nanogels are synthesized from natural materials or polymers, which can be degraded in a nontoxic manner in living organisms and thus avoid organ accumulation.

Progress of Nanogel Drug Carrier Systems

Nanogels can be accurately modified with respect to their shape, charge, and surface function in response to various internal stimuli (changes in pH, redox conditions, or enzymes), which are usually associated with the majority of physiological conditions *in vivo* because most pathological processes generally induce certain changes in pH, redox levels, or

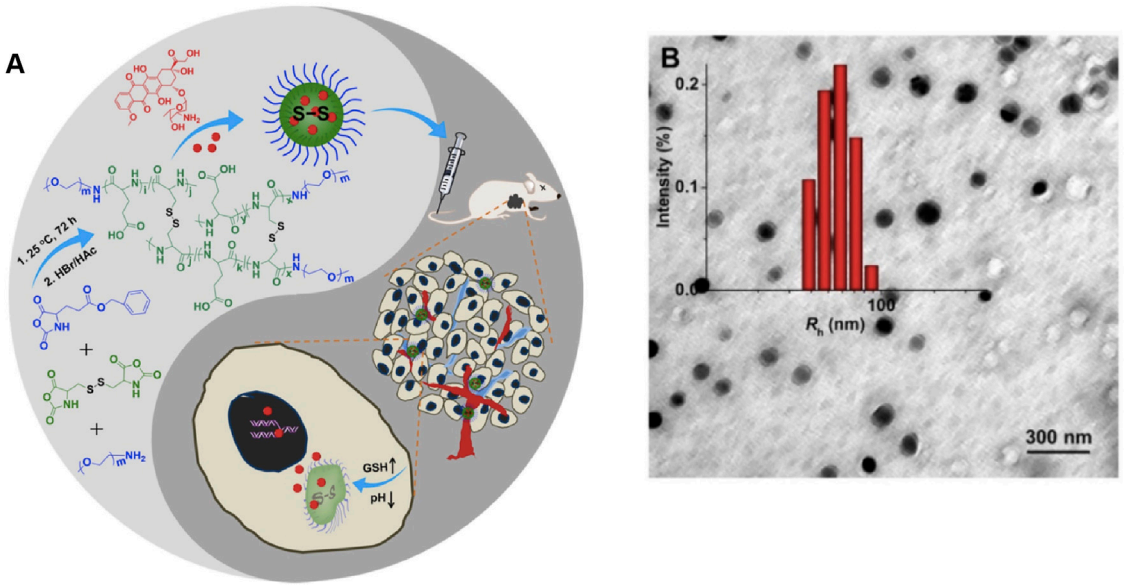

FIGURE 4 | (A) Synthetic pathway for mPEG–P (LG-co-LC) nanogel, illustration of DOX encapsulation by nanogel, and its circulation, intratumoral accumulation, endocytosis, and targeted intracellular DOX release after intravenous injection (Huang et al., 2015). **(B)** Typical TEM micrographs and Rh NG/DOX. Copyright 2017 Ivyspring International Publisher.

specific complementary ligand expression levels. A continuous increase in the availability of the functional and macromolecular monomers can expand the response range of these nanogels (Stuart et al., 2010; Sun et al., 2014). Furthermore, comparison with traditional nanomaterial-based controlled release systems indicates that stimulus-responsive nanogels can react to external stimuli, such as light, electricity, and magnetism, which can control drug release by reversible expansion or contraction of the gels (Zhang et al., 2020). Zhang et al. formed ultra-pH-sensitive nanogels through the self-assembly of an ultra-pH-sensitive hydrogel from the chiral peptide derivative ferrocene-diphenylalanine (FC-FF). The material precisely responds to the changes in pH over a very narrow range (pH 5.7–5.9) (Liu et al., 2020a). Polypeptide, a promising biomedical polymer with biodegradability and biocompatibility, was approved in 1906 α- Ring opening polymerization (ROP) of amino acid n-carboxylic anhydride (NCA) was synthesized for the first time. At present, peptide based nano gel has been applied to the targeted delivery of therapeutic drugs for various diseases (Shi et al., 2017). Previously, our team synthesized the dual-response nanogels, NG/DOX, which respond simultaneously to a low pH level and a high GSH level. After intravenous injection of NG/DOX into tumor-bearing mice, the drug release from nanogel is triggered at a low pH level and a high GSH level. The antitumor effect of NG/DOX is far superior to that of free DOX hydrochloride, and nanogel has extremely low cytotoxicity (**Figure 4**).. (Huang et al., 2015; Suhail et al., 2019)

Ion-induced gelation has attracted considerable attention due to environmentally friendly and time-controlled properties (Lee et al., 2021). Recently, researchers have developed stimuli-responsive DNA noncationic nanogels that can be used for targeted delivery of combination cancer therapeutics with high biocompatibility (Oh et al., 2007). Degradable nanogels loaded with rhodamine B isothiocyanate dextran (RITC DX) were shown to be degraded into a polymeric sol in a reducing environment, thus releasing the encapsulated carbohydrate drugs (Vinogradov, 2010). Based on nanogel technology, many therapeutic strategies for the delivery/release of therapeutic drugs to the brain have been explored to achieve active targeting: 1) by attaching functionalized ligands that recognize homologous receptors on the target organs or tissues, 2) due to noninvasive responsiveness to magnetic field or ultrasound to disrupt the BBB, and 3) due to shutter peptide-mediated BBB crossing (**Figure 5**). (Ganguly et al., 2014; Chaurasiya et al., 2016; Wei et al., 2021) Furthermore, nanogels with encapsulated drugs can be delivered by a variety of methods, such as intravenous or intraperitoneal injection, oral administration, and nasal and intraocular drug delivery (Verma et al., 2011; Zhao et al., 2021). Reports have suggested that PEGylation renders nanogel surface more hydrophilic, shields the drugs, and provides steric hindrance to avoid the interactions with serum proteins, endowing nanogels with a “stealth” feature (Kamaly et al., 2012; Sun et al., 2014).

The modulation of nanogels (e.g., ligands complementary to receptors) can direct them to the affected tissues with lesions, which differentially express the corresponding receptors, thereby facilitating the uptake and retention of the drugs at a target site (Saha et al., 2021). Vinogradov et al. synthesized a new system based on a nanogel network of crosslinked PEG and PEI, which is capable of efficiently delivery of ODNs to the brain across the BBB. The transport efficiency was further improved when the surface of nanogels was modified with Tf or insulin. The results of distribution studies in a mouse model showed that the accumulation of ODN in the brain was increased by more

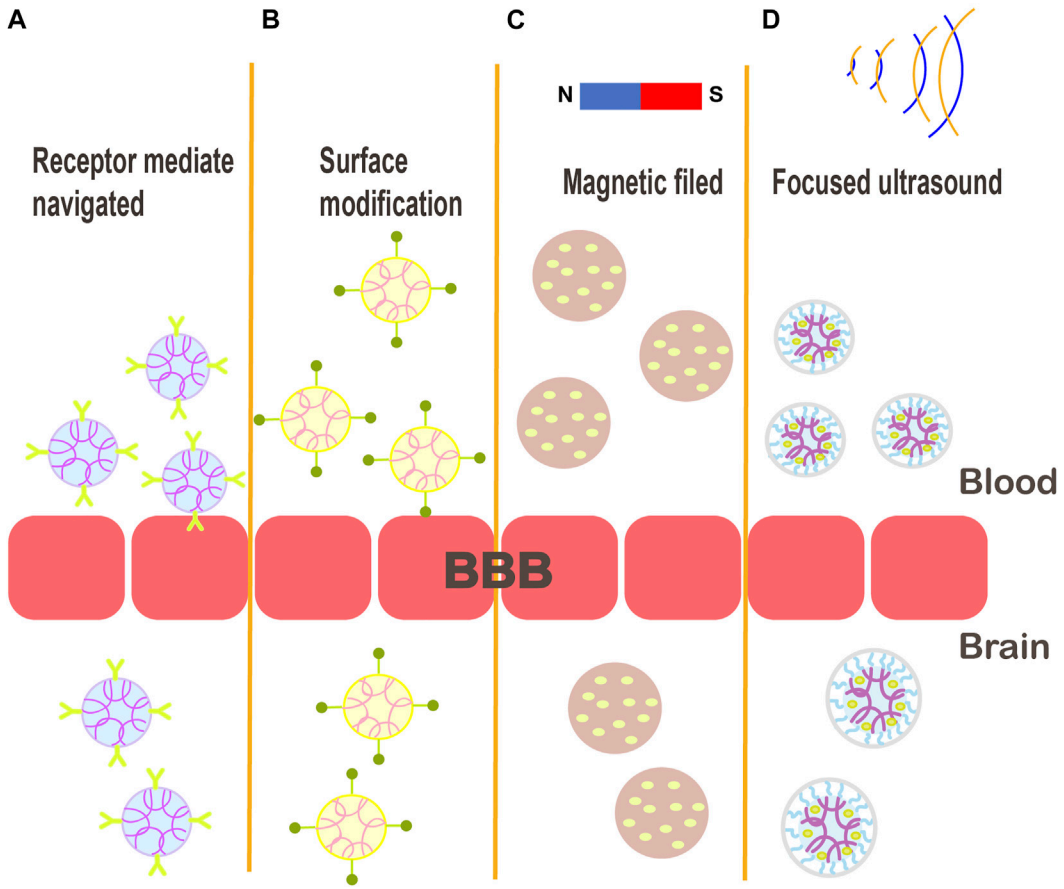

FIGURE 5 | Schematic illustration of the various potential mechanisms for crossing the BBB: **(A)** receptor-mediated endocytosis; **(B)** functionalized ligands that recognize cognate receptors on target organs or tissues; **(C–D)** magnetic field or ultrasound mediated delivery.

than 15-fold after 1 h of intravenous injection compared with the accumulation of unincorporated ODN, and the accumulation of free ODN in the liver and spleen was reduced by 2-fold, implying that clearance of ODN from the blood was not accelerated (Vinogradov et al., 2004). Zwitterionic-based nanogels have greatly broadened the applications of nanogels in drug delivery by virtue of their characteristics such as superhydrophilicity (Peng et al., 2020). In this context, zwitterionic polysulfamide nanogels (PMEDAPA) modified with transferrin (Tf) were synthesized as drug carriers that effectively respond to hyperthermia. These nanogels have their tumor-targeting features shielded at normal temperature; at high temperature, tumor targeting is achieved to enhance the accumulation of chemotherapeutic drugs in the tumor. These finding provides an exciting rationale to achieve tumor targeting of nanogels and to enable on-demand drug release in microwave heating-assisted cancer therapy in a clinical setting (Muresanu et al., 2019).

Overall, nanogels are more novel and advanced nanocarrier that are characterized by superior efficacy, bioavailability, and favorable drug pharmacokinetics, render their the potential side effects are greatly reduced.

APPLICATIONS OF THE NANOGELS FOR CNS DRUG DELIVERY

The advantages of simple and stable synthetic routes, controllable drug release, and high targeting efficiency make nanogel drug carriers one of the preferred options for the treatment of various CNS diseases, such as stroke, neurodegenerative disorders, epilepsy, traumatic brain injury, and brain tumors. **Table 3** summarizes several major studies related to the design of nanogels used for CNS drug delivery.

Ischemic Stroke

Ischemic stroke occurs when a blood clot or embolus locally blocks the middle brain artery, which accounts for 85% of all types of stroke (Houng et al., 2014). Currently, the thrombus-dissolving agents, such as tissue plasminogen activator (tPA), are

TABLE 3 | Summary of representative studies on nanogels for CNS drug delivery.

Formulations	Function	Drugs/Agents	Outcomes	Mechanism Across BBB	References
Nanogel/ODN	Transferrin/insulin-targeting	ODN	Nano-ODN accumulation increased 15 fold in the brain, whereas free ODN accumulated in a large amount in liver and spleen	Ligand- mediated	Vinogradov et al. (2004)
PEG-PEI	Controlled release	Antisense oligonucleotide	Increased *in vitro* uptake, controlled and sustained oligonucleotide release, higher uptake in the brain tissue	Charge adsorption-mediated	Wong et al. (2012)
HCFU	Sustained release	5-fluorouracil	Nanogel coating with polysorbate increased the accumulation from 0.18 to 0.52%, largely enhanced uptake in the brain tissue	Carrier-mediated	Xu et al. (2019)
Dex-FFFKE-ss-EE	Redox-responsive	Taxol/HCPT	Co-delivery nanogel system cantained two complementary anti-cancer drugs, extended drug realse and improved the stability of drugs.	Endocytosis	Teng et al. (2018)
Hollow nanogels (nUK)	Ultrasound-responsive	uPA	nUK has controlled released of uPA taget the clot site under ultrasound, not only enhanced the circulation of the drug, but also increased the safety.	Ultrasound stimulation	Xu et al. (2019)
PCgels	Immunotherapy	T lymphocyte	PCgels had suitable pore size to possess the cellular compatible with T lymphocytes, which retained their localized anti-glioblastoma activity in the PCgels	T lymphocyte-mediated	Mao et al. (2012)
Nano-NRTIs	Anti-viral	NRTIs	Nano-NRTIs exhibited high efficacy against HIV-1 in macrophages at a drug level as low as 1 μmol/L and decreased cytotoxicity compared to NRTIs	Macrophage phagocytosis	Vinogradov et al. (2010)
PEG-PVA/micelle	pH/redox-responsive	TMD/CF	Dual drugs of PEG-PVA/micelle were released significantly increased in alkaline environment	PH stimulation	Mao et al. (2012)

available for the treatment of ischemic stroke; however, a narrow time window for the use of these agents and cerebral ischemia/reperfusion injury often cause serious pathological reactions, which produce unsatisfactory results of these conventional treatment approached for ischemic stroke (Mihalko et al., 2022). Nanogels are expected to expand the arsenal of ischemic stroke treatment strategies by achieving brain targeting of the drugs and local controlled release.

Mihalko et al. designed a fibrin-specific nanogel (FSN) that can be used for the targeted delivery of tPA. *In vivo* experiments confirmed that tPA-FSNs can modulate fibrin/fibrinogen and platelets in thrombi. The distribution of both FSN and tPA-FSNs showed potential clearance and very low toxicity after 24 h. (Cui et al., 2016) A recent study suggested that a new form of urokinase (United Kingdom)-containing PEG-conjugated nanogel with pH-sensitive properties (PEG-UK) was designed to release the payload at a certain pH value. PEG-UKs were detected at the regions of microcirculation with low pH in a rat model of ischemic stroke. Wei Cui at el. demonstrated that the administration of PEG-UKs reduces the infarct volume of ischemic stroke, and this effect protects the BBB, inhibits apoptosis, and decreases neurotoxicity (Kleindorfer et al., 2005). However, high incidence of hemorrhagic events and failure to hospitalize in time usually limit the application of thrombolytic drugs. Statistical data show that very few patients receive thrombolytic therapy within 3 h after ischemic stroke (He et al., 2021). Multiple findings have shown that the generation of reactive oxygen species (ROS) or reactive nitrogen species (RONS) associated with cerebral ischemia and reperfusion worsen the conditions in patients. To reduce ischemic injury caused by oxidative stress, Zhang et al. developed artificial nanogel-zymes with multiple enzyme activities, which were able to provide neuroprotection against ischemic stroke by scavenging RONS. In a rat model of ischemic stroke, RONS levels were significantly reduced, and side effects were minimal (Liu et al., 2021).

The latest studies have shown that administration of microRNAs (miRNAs) can promote blood vessel growth and help restore the function of damaged tissues. Liu et al. encapsulated miRNAs in a nanocapsule platform, which systematically and effectively delivered miRNAs (Davis, 2016). However, the delivery of miRNA by nanogel delivery platform against cerebral ischemia has yet to be investigated. Moreover, future work should assess in detail the ability of these nanoformulations to be translated to the clinic.

Brain Tumors

Specific targeted drug delivery is the future of brain tumor therapy. Gliomas are the most prevalent and malignant CNS tumors, with a median patient survival of less than 15 months despite aggressive use of surgery combined with radiotherapy and chemotherapy (Kim et al., 2018). The blood-brain tumor barrier (BBTB) forms with tumor progression, which blocks almost all small-molecule chemotherapeutics and biomacromolecules. In addition to the limitations of the barriers, most therapeutic agents for glioma are the substrates of biological barrier efflux transporters, and a combination of these obstacles contribute to a high rate of treatment failure (Agarwal et al., 2011; Feng et al., 2019). Gliomas, similar to other solid tumors, have a special tumor microenvironment (TME) characterized by hypoxia, low pH, and chronic inflammation. Intriguingly, the extracellular glutathione concentrations of gliomas are up to 1,000-fold higher than the extracellular glutathione concentrations in the normal tissues, and the pH values in the vicinity of tumor cells are significantly lower (Marí et al., 2009; Wen et al., 2019).

Based on specific characteristics of the tumor tissue, various stimulus-responsive nanogel drug delivery networks have been developed for antitumor drug delivery. Methotrexate, doxorubicin, rituximab, and temozolomide are routine chemotherapeutic agents toxic for glioma cells, which have been formulated as nanomedicines to significantly improve the efficiency of the BBB crossing. The membrane protein connexin 43 (Cx43) and brain-specific anion transporter (BSAT1) are characteristically expressed in gliomas and the adjacent tissues. Recently, cisplatin was loaded into nanogels conjugated to Cx43 and BSAT1 monoclonal antibodies. MRI analysis of tumor-bearing rats showed that the nanoformulation achieved targeted antitumor effects (Gadhave et al., 2021). A recent study demonstrated successful loading of teriflunomide into a nanolipid-based (NLC) carbopol-gellan gum nanogel (TNLCGHG) for the treatment of brain glioma via intranasal administration. These gels were demonstrated to prolong blood circulation and showed significant tumor-suppressive effects (Zhang et al., 2021b). Nanogel formulations have been developed as promising contrast agents. Jiang et al. developed Cy5.5-Lf-MPNA nanogels by labeling lactoferrin (Lf) with Cy5.5. This preparation can target tumor tissue and achieve MR/fluorescence imaging with high sensitivity and specificity in the acidic environment of glioma tissue (Cui et al., 2016). Similarly, Lf/phenylboronic acid (PBA)-reduction-sensitive dual-target nanogels (Lf-DOX/PBNG) were developed for the delivery to deliver doxorubicin (DOX) for glioma therapy. The effective accumulation of Lf-DOX/PBNG was 12.37 times greater than that of free DOX solution (Rizzi et al., 2014).

Alzheimer's Disease

Alzheimer's disease (AD) is the most common cause of dementia, with more than 50 million people worldwide currently living with dementia (DeTure and Dickson, 2019). Clinical therapeutic approaches for AD focus on lowering the levels of the toxic forms of the amyloid beta (Aβ) peptide and τ protein to effectively delay the progression of the disease (Giacobini and Gold, 2013; Yang et al., 2021). A range of limitations account for poor efficacy of most therapeutic drugs, such as hydrophobicity, poor BBB permeability, rapid metabolism, and strong tissue toxicity. Various nanogel technologies have enabled the treatment of neurodegenerative diseases (Jiang et al., 2018).

The development of the dual inhibitor nanosystems is expected to effectively target the inhibition of Aβ aggregation and cytotoxicity induced by drug delivery systems. The biocompatible nanogels of cholesterol-bearing pullulan (CHP) were shown to be able to significantly inhibit the formation of Aβ fibrils. Epigallocatechin-3-gallate (EGCG) and curcumin are able to effectively inhibit Aβ aggregation. These two inhibitors were linked via a modification of hyaluronic acid (HA). The results showed that the EGCG and curcumin dual-modified nanogels (CEHA), which were synthesized by self-assembly, induced 69 and 55% higher inhibition than EGCG- or EHA-loaded single-modified nanogels, respectively. The results of an *in vitro* toxicity assay showed that CEHA significantly improved the viability of SH-SY5Y cells (Zhang et al., 2021c). Another approach to AD therapy involves scavenging of excess ROS induced by mitochondrial dysfunction and inflammatory factor that are overactivated in the brain (McNaught et al., 2002). Oxytocin-loaded angiopep-2-modified AOC NGs were developed to cross the BBB via the transcytosis of a surface-loaded ligand (ANG) for enrichment in the AD lesions. AOC NGs can block the ERK/p38 MAPK and COX-2/iNOS NF-κB signaling pathways, showing the ability to effectively inhibit microglial activation and reduce inflammatory cytokine levels.

Advances in nanotechnology have enabled new prospects for clinical therapeutic strategies for AD; however, the field of AD nanotherapeutics faces several challenges. AD may lead to a variety of clinical complications; hence, the design of the nanogel drugs with multiple drug candidates to achieve a synergistic effect may enhance the benefits of AD treatment.

Parkinson's Disease

Parkinson's disease (PD) is the second most common neurodegenerative disorder characterized by the death of dopaminergic neurons in the substantia nigra and the formation of Lewy bodies (Hawthorne et al., 2016). Dopamine therapy is the primary treatment option for PD; however, the disease is currently considered incurable. The demands for nanomedical studies of PD are mainly focused on achieving a stable concentration of dopamine in the brain (Jiang et al., 2018; Khan et al., 2018).

PEGylated nanogels were engineered to load dopamine and modified ligands of the transferrin receptor. The results of *in vivo* experiments demonstrated that the concentration of dopamine in the brain obtained using this nanogel was nine times higher than that obtained in a rat model treated with free dopamine. The removal of Lewy bodies is another effective strategy for the treatment of PD (Liu et al., 2020b). A study developed the Lewy body antagonist NanoCA using a self-assembly reaction. NanoCA targets the brain, releases its cargo in a controlled manner, and protects the neurons from the neurotoxicity of PD inducers in the animal models. In PD animal models, the nanomaterials are administered by local injection or transdermal absorption. Ropinirole nanogels were proved to enhance the efficacy of transdermal absorption, thus increasing the bioavailability up to two-fold compared with transdermal methods of delivery of the unincorporated free drug (Jafarieh et al., 2015). Jafarieh et al. prepared ropinirole hydrochloride (RH)-loaded chitosan nanoparticles (RH-CSNPs) by the ionic gel method. RH-CSNPs with nasal mucosal absorbability continuously released their cargo for 18 h, and the RH concentration in the brain was significantly increased after intranasal administration (Leoni and Caccia, 2014). The first-line treatment for patients with Parkinson's disease is natural oral levodopa, which has shown higher efficiency than synthetic levodopa. C Chittasupho et al. encapsulated native levodopa from *M. pruriens* seed extract into nanogels for incorporated into a jelly as a functional food for patients with Parkinson's disease.

Finally, although the prospects of using nanogel technology to treat neurodegenerative diseases are very attractive, the actual studies performed to date remain only experimental.

Huntington's Disease

Huntington's disease (HD) is an autosomal dominant neurodegenerative disorder (Arrasate and Finkbeiner, 2012). The known molecular mechanism of HD involves a single mutation of the huntingtin (HTT) gene exon 1, which leads to polyQ expansion, resulting in the misfolding and aggregation of the huntingtin protein in the brain (Li et al., 2020). However, the molecular mechanism by which HTT mutation causes neuronal death remains unclear. At present, many studies have demonstrated that short interfering RNAs (siRNAs) can silence the expression of the mutant proteins, and this application is one of the most recent and promising therapeutic strategies (Godinho et al., 2013).

Godinho et al. developed modified amphiphilic β-cyclodextrin (CD) oligosaccharide molecules as novel neuronal siRNA vectors. The results showed that CD nanoparticles are stable in artificial cerebrospinal fluid. The nanocarrier complex reduces HTT gene expression in ST14A-Htt120q rat striatum cells and primary human HD fibroblasts. A single injection of the CD-siRNA nanoparticles significantly reduces HTT expression in the striatum in a mouse HD model, and multiple injections can alleviate the motor dysfunction in HD mice. In addition, low toxicity of CD-siRNA nanoparticles has been observed in vitro toxicity experiments (Löscher et al., 2020). Numerous efforts have demonstrated the potential efficacy of the nanogel drug delivery systems; however, limited data on *in vivo* toxicity suggest a need to determine potential long-term systemic toxicity.

Epilepsy

Epilepsy is the second most frequent chronic disease of the CNS. Approximately 30% of patients with epilepsy are characterized by poorly controlled drug release and drug resistance during clinical treatment (Hanada, 2014; Shringarpure et al., 2021). Nanogel technology promises to revolutionize the treatment strategies for epilepsy using unique advantages due to the ability to cross the BBB without toxic effects to the brain and other tissues.

Lamotrigine is a broad-spectrum antiepileptic. Only a small amount of potent lamotrigine can exert its antiepileptic effects through the BBB after oral absorption (Xu et al., 2022). The group of Xu designed a polymer hydrogel that specifically responded to electromagnetic radiation. The results of intravital imaging of rats showed that fluorescently labeled lamotrigine nanogels are enriched in the rat brain 3 h after intravenous injection, indicating that lamotrigine nanogels are characterized by enhanced BBB penetration. Comparison with free lamotrigine indicated that the seizures of rats in the lamotrigine nanogel group were continuously and significantly decreased (Wang et al., 2016).

Recently, Wang et al. designed electroresponsive hydrogel nanoparticles (eRHNPs) modified with brain-targeting angiopep-2 (ANG) to facilitate the delivery of the antiepileptic drug phenytoin (PHT) and subsequently developed PHT-loaded ANG-eRHNPs. These formulations achieved a high distribution in the brain and an electrical response in a rat epilepsy model, resulting in a strong release of PHT from nanogels during seizures and achieving better antiepileptic effects (Ying et al., 2014). Brain-targeted ANG peptide-modified electro-responsive nanogels have been confirmed to achieve high-efficiency BBB penetration and enhance the efficacy of alleviating epilepsy (Wilson et al., 2017).

These studies will enable the generation of safe and effective seizure therapeutics. Future attention should also be paid to human clinical trials to evaluate and select precise nanodosage forms and concentrations for subsequent clinical applications.

Traumatic Brain Injury

Traumatic brain injury (TBI) is the main cause of death and disability in young individuals under 45 years of age and a known risk factor for chronic neurodegenerative diseases, such as AD and PD. To date, effective clinical treatments for TBI are lacking (McKee and Robinson, 2014; Gong et al., 2022).

The application of the bioactive scaffold materials is a promising method for tissue regeneration and repair (Marçal et al., 2012). Bladder stroma extracted from the porcine bladder tissue (UBM) showed good performance in promoting and supporting neural cell growth in vitro experiments (Zhang et al., 2013). To improve the biocompatibility of UBM in the brain and the effect of UBM on the function after TBI, a hydrogel-based form of UBM was developed. The results showed that the UBM-hydrogel had weak toxic effects on the healthy brain. After TBI, the application of the nanoscale UBM-hydrogel reduced the volume of the lesions and alleviated myelin sheath breakage induced by traumatic injury (Xu et al., 2019). Unexpectedly, the treatment of TBI using the UBM-hydrogel significantly improved neurobehavioral and vestibulomotor functions. The application of nanogels not only greatly improved the biocompatibility of UBM but also revealed a protective effect on the injured brain tissue. These observations provide valuable insight into the potential efficacy of nanogels in structurally damaged brain tissue.

Recently, Xu et al. successfully demonstrated that nanocapsules loaded with nerve growth factor (NGF) enabled nerve recovery and tissue remodeling in mice with spinal cord injury (Teng et al., 2018). It is suggested that nanogel technology may provide a better approach for TBI and CNS tissue regeneration engineering, which needs to be more explored in the future.

POTENTIAL NEUROTOXICITY

The CNS strongly protects itself from any xenobiotics (pathogens, toxins, and foreign bodies) through strict barrier structures (Nance et al., 2014). Nanocarriers can effectively circumvent the BBB and deliver unevenly distributed drugs to the brain parenchyma (Xiao et al., 2015); however, this delivery also leads to overexposure to the nanomaterials, making the application of the nanomaterials for CNS therapy regarded as a dual-edged sword. Therefore, it is crucial to systematically investigate the potential toxicity of the nanomaterials, which is one of the biggest challenges for the clinical translation of the nanodrug delivery systems.

Existing neurotoxicity studies have shown that the nanocarriers have neurotoxic effects both *in vitro* and *in vivo*

induced by the nanoparticles composed mostly of inorganic materials, whereas complete assessment of potential toxicity of nanogels in humans has not been reported (Wong et al., 2012). The present review analyzed the main reasons associated with neurotoxicity of nanogels. Chemically crosslinked nanogels may release toxic monomers from the matrix during their expected chemical degradation (Lee et al., 2021). Inflammation is one of the main mechanisms of neurotoxicity caused by the nanomaterials. Inflammation is known to eliminate foreign substances from the body and is a protective response; however, overactivation of the inflammatory response will induce substantial damage. Exposure of the brain to nanogels may stimulate glial cells, causing a strong inflammatory response of neuronal mitochondria or other organelles (Trompetero et al., 2018; Wu and Tang, 2018). The mechanism of brain inflammation induced by nanogels needs additional research, and only a few relevant studies of this subject have been performed.

In addition, neuronal exposure to the nanomaterials may induce neurodegenerative diseases. The accumulation of some fibrin aggregates or misfolded proteins is the pathological mechanism of some neurodegenerative diseases (AD, PD, and HD). Plausible interactions between the CNS and nanomaterials may exacerbate the accumulation or misfolding of these protein aggregates (Pichla et al., 2020). The results reported by Alvarez et al. suggest that the induction of a neurodegenerative disease may depend on the size and concentration of the nanoparticles and on their biocompatibility (Oberdörster, 2010). Current data of the assessments of the toxicity of the nanomaterials suggest that rigorous *in vitro*, *in vivo*, and clinical toxicity studies are needed before the clinical transformation of the nanomaterials can be achieved (Wang et al., 2022). Emphasis on detailed toxicity studies of nanogels is needed to provide evolutionary insight into the risks associated with efficient applications of these promising targeting approaches.

DISCUSSION

Overall, nanogel technology can provide the possibilities for advanced treatment in the field of CNS diseases (Sarkar et al., 2017). The BBB is the major anatomical and physiological dynamic barrier, representing one of the narrowest bottlenecks for successful treatment of CNS diseases; hence, the development of safer and more effective targeted nanomedicines has become a major research direction for numerous nanoformulation studies. Continuous development of new nanogel technologies, such as surface modification of the receptors/ligands and magnetic structures, enables various nanogel-based approaches to overcome the BBB to achieve targeted drug delivery. Nanogel-based technologies have been implicated in the development of the nanocarriers of various neuroprotective drugs, including nucleic acids, small-molecule peptides, nerve growth factors, and free radical scavengers (e.g., edaravone). However, the nanogel drug delivery platforms are still in their infancy (Jogani et al., 2008; Kumar et al., 2017; Patel et al., 2021). Therefore, additional in-depth studies on nanogels are required to address several issues before these agents can be widely used in the clinic.

Specific targeted delivery is a future research direction for nanogel studies. Recent discoveries of several specific peptides or receptor-targeting drugs, such as Tf, ANG and human insulin receptor, can facilitate the development of effective nanogels for brain-targeted drug delivery. However, these receptors are not specific; thus, organ/tissue specificity should also be considered in the future studies to provide more specific and rational therapeutic strategies. Due to the outstanding properties associated with the suppression of reactive oxygen species and protein misaggregation, the application of nanogels have been eagerly explored for the treatment of neurological diseases, such as ischemic stroke, AD, PD, brain tumors, and epilepsy (Liu et al., 2018). However, the efficacy of these carrier systems is hindered by the involvement of various pharmacological factors, such as drug loading, controlled release, safety, and biocompatibility *in vivo*. Furthermore, considering the complex structure and unique microenvironment of the brain, additional polymeric materials should be developed to enhance biodegradability and biocompatibility by preparing nanogels with completely eliminated possibilities of potential toxicity.

Most CNS diseases require long-term drug therapy; thus, toxicological studies of the organs, including the kidney, liver, and spleen, should be performed using nanogel formulations (Picone et al., 2018). In the future, advanced diagnostic techniques, such as magnetic resonance imaging, positron emission tomography, and computed tomography, aphy, will be needed to assess nanocarrier-related CNS toxicity.

AUTHOR CONTRIBUTIONS

HL and YZ contributed to conception and design of the study. YZ wrote the first draft of the manuscript. All authors contributed to manuscript revision, read, and approved the submitted version.

FUNDING

This study was funded by National Natural Science Foundation of China (No. 81971174).

REFERENCES

Aday, S., Cecchelli, R., Hallier-Vanuxeem, D., Dehouck, M. P., and Ferreira, L. (2016). Stem Cell-Based Human Blood-Brain Barrier Models for Drug Discovery and Delivery. *Trends Biotechnol.* 34 (5), 382–393. doi:10.1016/j.tibtech.2016.01.001

Agarwal, S., Sane, R., Oberoi, R., Ohlfest, J. R., and Elmquist, W. F. (2011). Delivery of Molecularly Targeted Therapy to Malignant Glioma, a Disease of the Whole Brain. *Expert Rev. Mol. Med.* 13, e17. doi:10.1017/s1462399411001888

Ali, E. S., Sharker, S. M., Islam, M. T., Khan, I. N., Shaw, S., Rahman, M. A., et al. (2021). Targeting Cancer Cells with Nanotherapeutics and Nanodiagnostics: Current Status and Future Perspectives. *Seminars Cancer Biol.* 69, 52–68. doi:10.1016/j.semcancer.2020.01.011

Alyautdin, R., Khalin, I., Nafeeza, M. I., Haron, M. H., and Kuznetsov, D. (2014). Nanoscale Drug Delivery Systems and the Blood-Brain Barrier. *Int. J. Nanomedicine* 9, 795–811. doi:10.2147/IJN.S52236

Amoli-Diva, M., Sadighi-Bonabi, R., and Pourghazi, K. (2017). Switchable On/off Drug Release from Gold Nanoparticles-Grafted Dual Light- and Temperature-Responsive Hydrogel for Controlled Drug Delivery. *Mater. Sci. Eng. C* 76, 242–248. doi:10.1016/j.msec.2017.03.038

Arrasate, M., and Finkbeiner, S. (2012). Protein Aggregates in Huntington's Disease. *Exp. Neurol.* 238 (1), 1–11. doi:10.1016/j.expneurol.2011.12.013

Bae, K. H., Lee, J. Y., Lee, S. H., Park, T. G., and Nam, Y. S. (2013). Optically Traceable Solid Lipid Nanoparticles Loaded with siRNA and Paclitaxel for Synergistic Chemotherapy with *In Situ* Imaging. *Adv. Healthc. Mater.* 2 (4), 576–584. doi:10.1002/adhm.201200338

Baeten, K. M., and Akassoglou, K. (2011). Extracellular Matrix and Matrix Receptors in Blood-Brain Barrier Formation and Stroke. *Devel Neurobio* 71 (11), 1018–1039. doi:10.1002/dneu.20954

Bajracharya, R., Song, J. G., Back, S. Y., and Han, H.-K. (2019). Recent Advancements in Non-invasive Formulations for Protein Drug Delivery. *Comput. Struct. Biotechnol. J.* 17, 1290–1308. doi:10.1016/j.csbj.2019.09.004

Baroud, M., Lepeltier, E., Thepot, S., El-Makhour, Y., and Duval, O. (2021). The Evolution of Nucleosidic Analogues: Self-Assembly of Prodrugs into Nanoparticles for Cancer Drug Delivery. *Nanoscale Adv.* 3 (8), 2157–2179. doi:10.1039/d0na01084g

Battaglia, L., Gallarate, M., Peira, E., Chirio, D., Muntoni, E., Biasibetti, E., et al. (2014). Solid Lipid Nanoparticles for Potential Doxorubicin Delivery in Glioblastoma Treatment: Preliminary *In Vitro* Studies. *J. Pharm. Sci.* 103 (7), 2157–2165. doi:10.1002/jps.24002

Begicevic, R. R., and Falasca, M. (2017). ABC Transporters in Cancer Stem Cells: Beyond Chemoresistance. *Int. J. Mol. Sci.* 18 (11), 2362. doi:10.3390/ijms18112362

Bhia, M., Motallebi, M., Abadi, B., Zarepour, A., Pereira-Silva, M., Saremnejad, F., et al. (2021). Naringenin Nano-Delivery Systems and Their Therapeutic Applications. *Pharmaceutics* 13 (2), 291. doi:10.3390/pharmaceutics13020291

Bonsack, B., Corey, S., Shear, A., Heyck, M., Cozene, B., Sadanandan, N., et al. (2020). Mesenchymal Stem Cell Therapy Alleviates the Neuroinflammation Associated with Acquired Brain Injury. *CNS Neurosci. Ther.* 26 (6), 603–615. doi:10.1111/cns.13378

Buyukkoroglu, G., Senel, B., Basaran, E., Yenilmez, E., and Yazan, Y. (2016). Preparation and *In Vitro* Evaluation of Vaginal Formulations Including siRNA and Paclitaxel-Loaded SLNs for Cervical Cancer. *Eur. J. Pharm. Biopharm.* 109, 174–183.

Chander, S., Kulkarni, G. T., Dhiman, N., and Kharkwal, H. (2021). Protein-Based Nanohydrogels for Bioactive Delivery. *Front. Chem.* 9, 573748. doi:10.3389/fchem.2021.573748

Chaurasiya, B., Mahanty, A., Roy, D., Shen, Y., Tu, J., and Sun, C. (2016). Influence of Tumor Microenvironment on the Distribution and Elimination of Nano-Formulations. *Cdm* 17 (8), 783–798. doi:10.2174/1389200217666160607093347

Chen, Z., Lv, Z., Zhang, Z., Weitz, D. A., Zhang, H., Zhang, Y., et al. (2021). Advanced Microfluidic Devices for Fabricating Multi-structural Hydrogel Microsphere. *Exploration* 1 (3), 1. doi:10.1002/exp.20210036

Cojocaru, F. D., Botezat, D., Gardikiotis, I., Uritu, C. M., Dodi, G., Trandafir, L., et al. (2020). Nanomaterials Designed for Antiviral Drug Delivery Transport across Biological Barriers. *Pharmaceutics* 12 (2), 171. doi:10.3390/pharmaceutics12020171

Coviello, T., Matricardi, P., Marianecci, C., and Alhaique, F. (2007). Polysaccharide Hydrogels for Modified Release Formulations. *J. Control. Release* 119 (1), 5–24. doi:10.1016/j.jconrel.2007.01.004

Cui, W., Liu, R., Jin, H., Lv, P., Sun, Y., Men, X., et al. (2016). pH Gradient Difference Around Ischemic Brain Tissue Can Serve as a Trigger for Delivering Polyethylene Glycol-Conjugated Urokinase Nanogels. *J. Control. Release* 225, 53–63. doi:10.1016/j.jconrel.2016.01.028

Date, A., Joshi, M., and Patravale, V. (2007). Parasitic Diseases: Liposomes and Polymeric Nanoparticles versus Lipid Nanoparticles☆. *Adv. Drug Deliv. Rev.* 59 (6), 505–521. doi:10.1016/j.addr.2007.04.009

Davis, M. E. (2016). Glioblastoma: Overview of Disease and Treatment. *Clin. J. Oncol. Nurs.* 20 (5 Suppl. l), S2–S8. doi:10.1188/16.CJON.S1.2-8

De Jong, W. H., Hagens, W. I., Krystek, P., Burger, M. C., Sips, A. J. A. M., and Geertsma, R. E. (2008). Particle Size-dependent Organ Distribution of Gold Nanoparticles after Intravenous Administration. *Biomaterials* 29 (12), 1912–1919. doi:10.1016/j.biomaterials.2007.12.037

de Souza, M. L., Dos Santos, W. M., de Sousa, A. L. M. D., de Albuquerque Wanderley Sales, V., Nóbrega, F. P., de Oliveira, M. V. G., et al. (2020). Lipid Nanoparticles as a Skin Wound Healing Drug Delivery System: Discoveries and Advances. *Cpd* 26 (36), 4536–4550. doi:10.2174/1381612826666200417144530

Debele, T. A., Mekuria, S. L., and Tsai, H.-C. (2016). Polysaccharide Based Nanogels in the Drug Delivery System: Application as the Carrier of Pharmaceutical Agents. *Mater. Sci. Eng. C* 68, 964–981. doi:10.1016/j.msec.2016.05.121

DeTure, M. A., and Dickson, D. W. (2019). The Neuropathological Diagnosis of Alzheimer's Disease. *Mol. Neurodegener.* 14 (1), 32. doi:10.1186/s13024-019-0333-5

Dowling, J., Isbister, G. K., Kirkpatrick, C. M. J., Naidoo, D., and Graudins, A. (2008). Population Pharmacokinetics of Intravenous, Intramuscular, and Intranasal Naloxone in Human Volunteers. *Ther. Drug Monit.* 30 (4), 490–496. doi:10.1097/ftd.0b013e3181816214

Dutta, T., and Jain, N. K. (2007). Targeting Potential and Anti-HIV Activity of Lamivudine Loaded Mannosylated Poly (Propyleneimine) Dendrimer. *Biochimica Biophysica Acta (BBA) - General Subj.* 1770 (4), 681–686. doi:10.1016/j.bbagen.2006.12.007

Engelhardt, B., and Sorokin, L. (2009). The Blood-Brain and the Blood-Cerebrospinal Fluid Barriers: Function and Dysfunction. *Semin. Immunopathol.* 31 (4), 497–511. doi:10.1007/s00281-009-0177-0

Erickson, M. A., and Banks, W. A. (2018). Neuroimmune Axes of the Blood-Brain Barriers and Blood-Brain Interfaces: Bases for Physiological Regulation, Disease States, and Pharmacological Interventions. *Pharmacol. Rev.* 70 (2), 278–314. doi:10.1124/pr.117.014647

Falagas, M. E., Bliziotis, I. A., and Tam, V. H. (2007). Intraventricular or Intrathecal Use of Polymyxins in Patients with Gram-Negative Meningitis: a Systematic Review of the Available Evidence. *Int. J. Antimicrob. Agents* 29 (1), 9–25. doi:10.1016/j.ijantimicag.2006.08.024

Fassas, A., and Anagnostopoulos, A. (2005). The Use of Liposomal Daunorubicin (DaunoXome) in Acute Myeloid Leukemia. *Leukemia Lymphoma* 46 (6), 795–802. doi:10.1080/10428190500052438

Feng, X., Xu, W., Li, Z., Song, W., Ding, J., and Chen, X. (2019). Immunomodulatory Nanosystems. *Adv. Sci.* 6 (17), 1900101. doi:10.1002/advs.201900101

Francischi, J. N., Pereira, L. S. M., and Castro, M. S. (1997). Cyclosporin Inhibits Hyperalgesia and Edema in Arthritic Rats: Role of the Central Nervous System. *Braz J. Med. Biol. Res.* 30 (1), 101–111. doi:10.1590/s0100-879x1997000100016

Furtado, D., Björnmalm, M., Ayton, S., Bush, A. I., Kempe, K., and Caruso, F. (2018). Overcoming the Blood-Brain Barrier: The Role of Nanomaterials in Treating Neurological Diseases. *Adv. Mater* 30 (46), e1801362. doi:10.1002/adma.201801362

Gadhave, D., Rasal, N., Sonawane, R., Sekar, M., and Kokare, C. (2021). Nose-to-brain Delivery of Teriflunomide-Loaded Lipid-Based Carbopol-Gellan Gum Nanogel for Glioma: Pharmacological and *In Vitro* Cytotoxicity Studies. *Int. J. Biol. Macromol.* 167, 906–920. doi:10.1016/j.ijbiomac.2020.11.047

Ganguly, K., Chaturvedi, K., More, U. A., Nadagouda, M. N., and Aminabhavi, T. M. (2014). Polysaccharide-based Micro/nanohydrogels for Delivering Macromolecular Therapeutics. *J. Control. Release* 193, 162–173. doi:10.1016/j.jconrel.2014.05.014

Gerson, T., Makarov, E., Senanayake, T. H., Gorantla, S., Poluektova, L. Y., and Vinogradov, S. V. (2014). Nano-NRTIs Demonstrate Low Neurotoxicity and High Antiviral Activity against HIV Infection in the Brain. *Nanomedicine Nanotechnol. Biol. Med.* 10 (1), 177–185. doi:10.1016/j.nano.2013.06.012

Ghersi-Egea, J.-F., Strazielle, N., Catala, M., Silva-Vargas, V., Doetsch, F., and Engelhardt, B. (2018). Molecular Anatomy and Functions of the Choroidal Blood-Cerebrospinal Fluid Barrier in Health and Disease. *Acta Neuropathol.* 135 (3), 337–361. doi:10.1007/s00401-018-1807-1

Giacobini, E., and Gold, G. (2013). Alzheimer Disease Therapy-Moving from Amyloid-β to Tau. *Nat. Rev. Neurol.* 9 (12), 677–686. doi:10.1038/nrneurol.2013.223

Gil-Martins, E., Barbosa, D. J., Silva, V., Remião, F., and Silva, R. (2020). Dysfunction of ABC Transporters at the Blood-Brain Barrier: Role in Neurological Disorders. *Pharmacol. Ther.* 213, 107554. doi:10.1016/j.pharmthera.2020.107554

Girolamo, F., de Trizio, I., Errede, M., Longo, G., d'Amati, A., and Virgintino, D. (2021). Neural Crest Cell-Derived Pericytes Act as Pro-angiogenic Cells in Human Neocortex Development and Gliomas. *Fluids Barriers CNS* 18 (1), 14. doi:10.1186/s12987-021-00242-7

Godinho, B. M. D. C., Ogier, J. R., Darcy, R., O'Driscoll, C. M., and Cryan, J. F. (2013). Self-assembling Modified β-Cyclodextrin Nanoparticles as Neuronal siRNA Delivery Vectors: Focus on Huntington's Disease. *Mol. Pharm.* 10 (2), 640–649. doi:10.1021/mp3003946

Goldberg, M., Langer, R., and Jia, X. (2007). Nanostructured Materials for Applications in Drug Delivery and Tissue Engineering. *J. Biomaterials Sci. Polym. Ed.* 18 (3), 241–268. doi:10.1163/156856207779996931

Gong, B., Zhang, X., Zahrani, A. A., Gao, W., Ma, G., Zhang, L., et al. (2022). Neural Tissue Engineering: From Bioactive Scaffolds and *In Situ* Monitoring to Regeneration. *Exploration* 1, 1. doi:10.1002/EXP.20210035

Grassin-Delyle, S., Buenestado, A., Naline, E., Faisy, C., Blouquit-Laye, S., Couderc, L.-J., et al. (2012). Intranasal Drug Delivery: An Efficient and Non-invasive Route for Systemic Administration. *Pharmacol. Ther.* 134 (3), 366–379. doi:10.1016/j.pharmthera.2012.03.003

Guo, D., Lou, C., Wang, N., Chen, M., Zhang, P., Wu, S., et al. (2017). Poly (Styrene-divinyl Benzene-Glycidylmethacrylate) Stationary Phase Grafted with Poly Amidoamine (PAMAM) Dendrimers for Rapid Determination of Phenylene Diamine Isomers in HPLC. *Talanta* 168, 188–195. doi:10.1016/j.talanta.2017.03.053

Hanada, T. (2014). The Discovery and Development of Perampanel for the Treatment of Epilepsy. *Expert Opin. Drug Discov.* 9 (4), 449–458. doi:10.1517/17460441.2014.891580

Harbi, I., Aljaeid, B., El-Say, K. M., and Zidan, A. S. (2016). Glycosylated Sertraline-Loaded Liposomes for Brain Targeting: QbD Study of Formulation Variabilities and Brain Transport. *AAPS PharmSciTech* 17 (6), 1404–1420. doi:10.1208/s12249-016-0481-7

Hawkins, B. T., and Davis, T. P. (2005). The Blood-Brain Barrier/neurovascular Unit in Health and Disease. *Pharmacol. Rev.* 57 (2), 173–185. doi:10.1124/pr.57.2.4

Hawthorne, G. H., Bernuci, M. P., Bortolanza, M., Tumas, V., Issy, A. C., and Del-Bel, E. (2016). Nanomedicine to Overcome Current Parkinson's Treatment Liabilities: A Systematic Review. *Neurotox. Res.* 30 (4), 715–729. doi:10.1007/s12640-016-9663-z

He, Q., Liu, J., Liang, J., Liu, X., Li, W., Liu, Z., et al. (2018). Towards Improvements for Penetrating the Blood-Brain Barrier-Recent Progress from a Material and Pharmaceutical Perspective. *Cells* 7 (4), 24. doi:10.3390/cells7040024

He, W., Zhang, Z., and Sha, X. (2021). Nanoparticles-mediated Emerging Approaches for Effective Treatment of Ischemic Stroke. *Biomaterials* 277, 121111. doi:10.1016/j.biomaterials.2021.121111

Heldt, T., Zoerle, T., Teichmann, D., and Stocchetti, N. (2019). Intracranial Pressure and Intracranial Elastance Monitoring in Neurocritical Care. *Annu. Rev. Biomed. Eng.* 21, 523–549. doi:10.1146/annurev-bioeng-060418-052257

Houng, A. K., Wang, D., and Reed, G. L. (2014). Reversing the Deleterious Effects of α2-antiplasmin on Tissue Plasminogen Activator Therapy Improves Outcomes in Experimental Ischemic Stroke. *Exp. Neurol.* 255, 56–62. doi:10.1016/j.expneurol.2014.02.009

Huang, K., Shi, B., Xu, W., Ding, J., Yang, Y., Liu, H., et al. (2015). Reduction-responsive Polypeptide Nanogel Delivers Antitumor Drug for Improved Efficacy and Safety. *Acta Biomater.* 27, 179–193. doi:10.1016/j.actbio.2015.08.049

Huo, T., Barth, R. F., Yang, W., Nakkula, R. J., Koynova, R., Tenchov, B., et al. (2012). Preparation, Biodistribution and Neurotoxicity of Liposomal Cisplatin Following Convection Enhanced Delivery in Normal and F98 Glioma Bearing Rats. *PLoS One* 7 (11), e48752. doi:10.1371/journal.pone.0048752

Jafari, S., Derakhshankhah, H., Alaei, L., Fattahi, A., Varnamkhasti, B. S., and Saboury, A. A. (2019). Mesoporous Silica Nanoparticles for Therapeutic/diagnostic Applications. *Biomed. Pharmacother.* 109, 1100–1111. doi:10.1016/j.biopha.2018.10.167

Jafarieh, O., Md, S., Ali, M., Baboota, S., Sahni, J. K., Kumari, B., et al. (2015). Design, Characterization, and Evaluation of Intranasal Delivery of Ropinirole-Loaded Mucoadhesive Nanoparticles for Brain Targeting. *Drug Dev. Industrial Pharm.* 41 (10), 1674–1681. doi:10.3109/03639045.2014.991400

Jain, K. K. (2020). An Overview of Drug Delivery Systems. *Methods Mol. Biol.* 2059, 1–54. doi:10.1007/978-1-4939-9798-5_1

Jain, S., Malinowski, M., Chopra, P., Varshney, V., and Deer, T. R. (2019). Intrathecal Drug Delivery for Pain Management: Recent Advances and Future Developments. *Expert Opin. Drug Deliv.* 16 (8), 815–822. doi:10.1080/17425247.2019.1642870

Javed, B., Zhao, X., Cui, D., Curtin, J., and Tian, F. (2021). Enhanced Anticancer Response of Curcumin- and Piperine-Loaded Lignin-G-P (NIPAM-Co-DMAEMA) Gold Nanogels against U-251 MG Glioblastoma Multiforme. *Biomedicines* 9 (11), 1516. doi:10.3390/biomedicines9111516

Jiang, Z., Dong, X., Yan, X., Liu, Y., Zhang, L., and Sun, Y. (2018). Nanogels of Dual Inhibitor-Modified Hyaluronic Acid Function as a Potent Inhibitor of Amyloid β-protein Aggregation and Cytotoxicity. *Sci. Rep.* 8 (1), 3505. doi:10.1038/s41598-018-21933-6

Jin, J., Bae, K. H., Yang, H., Lee, S. J., Kim, H., Kim, Y., et al. (2011). *In Vivo* specific Delivery of C-Met siRNA to Glioblastoma Using Cationic Solid Lipid Nanoparticles. *Bioconjugate Chem.* 22 (12), 2568–2572. doi:10.1021/bc200406n

Jogani, V., Jinturkar, K., Vyas, T., and Misra, A. (2008). Recent Patents Review on Intranasal Administration for CNS Drug Delivery. *Recent Pat. Drug Deliv. Formul.* 2 (1), 25–40. doi:10.2174/187221108783331429

Johanson, C., Stopa, E., McMillan, P., Roth, D., Funk, J., and Krinke, G. (2011). The Distributional Nexus of Choroid Plexus to Cerebrospinal Fluid, Ependyma and Brain. *Toxicol. Pathol.* 39 (1), 186–212. doi:10.1177/0192623310394214

Kadry, H., Noorani, B., and Cucullo, L. (2020). A Blood-Brain Barrier Overview on Structure, Function, Impairment, and Biomarkers of Integrity. *Fluids Barriers CNS* 17 (1), 69. doi:10.1186/s12987-020-00230-3

Kamaly, N., Xiao, Z., Valencia, P. M., Radovic-Moreno, A. F., and Farokhzad, O. C. (2012). Targeted Polymeric Therapeutic Nanoparticles: Design, Development and Clinical Translation. *Chem. Soc. Rev.* 41 (7), 2971–3010. doi:10.1039/c2cs15344k

Kazkayasi, I., Telli, G., Nemutlu, E., and Uma, S. (2022). Intranasal Metformin Treatment Ameliorates Cognitive Functions via Insulin Signaling Pathway in ICV-STZ-Induced Mice Model of Alzheimer's Disease. *Life Sci.* 299, 120538. doi:10.1016/j.lfs.2022.120538

Khan, A. R., Yang, X., Fu, M., and Zhai, G. (2018). Recent Progress of Drug Nanoformulations Targeting to Brain. *J. Control. Release* 291, 37–64. doi:10.1016/j.jconrel.2018.10.004

Khan, O., and Chaudary, N. (2020). The Use of Amikacin Liposome Inhalation Suspension (Arikayce) in the Treatment of Refractory Nontuberculous Mycobacterial Lung Disease in Adults. *Dddt* 14, 2287–2294. doi:10.2147/dddt.s146111

Kim, M., Kizilbash, S. H., Laramy, J. K., Gampa, G., Parrish, K. E., Sarkaria, J. N., et al. (2018). Barriers to Effective Drug Treatment for Brain Metastases: A Multifactorial Problem in the Delivery of Precision Medicine. *Pharm. Res.* 35 (9), 177. doi:10.1007/s11095-018-2455-9

Kleindorfer, D. O., Khatri, P., and Katzan, I. (2005). Reasons for Exclusion from Thrombolytic Therapy Following Acute Ischemic Stroke. *Neurology* 65 (11), 1844. doi:10.1212/01.wnl.0000200031.41939.ac

Kreyling, W. G., Hirn, S., Möller, W., Schleh, C., Wenk, A., Celik, G., et al. (2014). Air-blood Barrier Translocation of Tracheally Instilled Gold Nanoparticles Inversely Depends on Particle Size. *ACS Nano* 8 (1), 222–233. doi:10.1021/nn403256v

Kumar, A., Tan, A., Wong, J., Spagnoli, J. C., Lam, J., Blevins, B. D., et al. (2017). Nanotechnology for Neuroscience: Promising Approaches for Diagnostics, Therapeutics and Brain Activity Mapping. *Adv. Funct. Mater* 27 (39), 1700489. doi:10.1002/adfm.201700489

Kuo, Y.-C., and Shih-Huang, C.-Y. (2013). Solid Lipid Nanoparticles Carrying Chemotherapeutic Drug across the Blood-Brain Barrier through Insulin Receptor-Mediated Pathway. *J. Drug Target.* 21 (8), 730–738. doi:10.3109/1061186x.2013.812094

Lee, G., Dallas, S., Hong, M., and Bendayan, R. (2001). Drug Transporters in the Central Nervous System: Brain Barriers and Brain Parenchyma Considerations. *Pharmacol. Rev.* 53 (4), 569–596.

Lee, K., Kim, T., Kim, Y. M., Yang, K., Choi, I., and Roh, Y. H. (2021). Multifunctional DNA Nanogels for Aptamer-Based Targeted Delivery and Stimuli-Triggered Release of Cancer Therapeutics. *Macromol. Rapid Commun.* 42 (2), e2000457. doi:10.1002/marc.202000457

Leoni, V., and Caccia, C. (2014). Study of Cholesterol Metabolism in Huntington′s Disease. *Biochem. Biophysical Res. Commun.* 446 (3), 697–701. doi:10.1016/j.bbrc.2014.01.188

Li, D., Mastaglia, F. L., Fletcher, S., and Wilton, S. D. (2020). Progress in the Molecular Pathogenesis and Nucleic Acid Therapeutics for Parkinson's Disease in the Precision Medicine Era. *Med. Res. Rev.* 40 (6), 2650–2681. doi:10.1002/med.21718

Liu, C., Wen, J., Li, D., Qi, H., Nih, L., Zhu, J., et al. (2021). Systemic Delivery of microRNA for Treatment of Brain Ischemia. *Nano Res.* 14 (9), 3319–3328. doi:10.1007/s12274-021-3413-8

Liu, J., Liu, C., Zhang, J., Zhang, Y., Liu, K., Song, J.-X., et al. (2020). A Self-Assembled α-Synuclein Nanoscavenger for Parkinson's Disease. *ACS Nano* 14 (2), 1533–1549. doi:10.1021/acsnano.9b06453

Liu, Y., Li, D., Ding, J., and Chen, X. (2020). Controlled Synthesis of Polypeptides. *Chin. Chem. Lett.* 31 (12), 3001–3014. doi:10.1016/j.cclet.2020.04.029

Liu, Z., Qiao, J., Nagy, T., and Xiong, M. P. (2018). ROS-Triggered Degradable Iron-Chelating Nanogels: Safely Improving Iron Elimination *In Vivo*. *J. Control. Release* 283, 84–93. doi:10.1016/j.jconrel.2018.05.025

Logan, S., Arzua, T., Canfield, S. G., Seminary, E. R., Sison, S. L., Ebert, A. D., et al. (2019). Studying Human Neurological Disorders Using Induced Pluripotent Stem Cells: From 2D Monolayer to 3D Organoid and Blood Brain Barrier Models. *Compr. Physiol.* 9 (2), 565–611. doi:10.1002/cphy.c180025

Lombardo, D., Calandra, P., Pasqua, L., and Magazù, S. (2020). Self-assembly of Organic Nanomaterials and Biomaterials: The Bottom-Up Approach for Functional Nanostructures Formation and Advanced Applications. *Mater. (Basel)* 13 (5), 1048. doi:10.3390/ma13051048

Löscher, W., Potschka, H., Sisodiya, S. M., and Vezzani, A. (2020). Drug Resistance in Epilepsy: Clinical Impact, Potential Mechanisms, and New Innovative Treatment Options. *Pharmacol. Rev.* 72 (3), 606–638. doi:10.1124/pr.120.019539

Ma, Y., Ge, Y., and Li, L. (2017). Advancement of Multifunctional Hybrid Nanogel Systems: Construction and Application in Drug Co-delivery and Imaging Technique. *Mater. Sci. Eng. C* 71, 1281–1292. doi:10.1016/j.msec.2016.11.031

Mahajan, H. S., Mahajan, M. S., Nerkar, P. P., and Agrawal, A. (2014). Nanoemulsion-based Intranasal Drug Delivery System of Saquinavir Mesylate for Brain Targeting. *Drug Deliv.* 21 (2), 148–154. doi:10.3109/10717544.2013.838014

Mao, L., Wang, H., Tan, M., Ou, L., Kong, D., and Yang, Z. (2012). Conjugation of Two Complementary Anti-cancer Drugs Confers Molecular Hydrogels as a Co-delivery System. *Chem. Commun.* 48 (3), 395–397. doi:10.1039/c1cc16250k

Marçal, H., Ahmed, T., Badylak, S. F., Tottey, S., and Foster, L. J. R. (2012). A Comprehensive Protein Expression Profile of Extracellular Matrix Biomaterial Derived from Porcine Urinary Bladder. *Regen. Med.* 7 (2), 159–166. doi:10.2217/rme.12.6

Marí, M., Morales, A., Colell, A., García-Ruiz, C., and Fernández-Checa, J. C. (2009). Mitochondrial Glutathione, a Key Survival Antioxidant. *Antioxidants Redox Signal.* 11 (11), 2685–2700. doi:10.1089/ars.2009.2695

Mathew, A. P., Uthaman, S., Cho, K.-H., Cho, C.-S., and Park, I.-K. (2018). Injectable Hydrogels for Delivering Biotherapeutic Molecules. *Int. J. Biol. Macromol.* 110, 17–29. doi:10.1016/j.ijbiomac.2017.11.113

Mauri, E., Giannitelli, S. M., Trombetta, M., and Rainer, A. (2021). Synthesis of Nanogels: Current Trends and Future Outlook. *Gels* 7 (2), 36. doi:10.3390/gels7020036

McAteer, J. A., and Evan, A. P. (2008). The Acute and Long-Term Adverse Effects of Shock Wave Lithotripsy. *Seminars Nephrol.* 28 (2), 200–213. doi:10.1016/j.semnephrol.2008.01.003

McKee, A. C., and Robinson, M. E. (2014). Military-related Traumatic Brain Injury and Neurodegeneration. *Alzheimers Dement.* 10 (3 Suppl. l), S242–S253. doi:10.1016/j.jalz.2014.04.003

McNaught, K. S. P., Belizaire, R., Jenner, P., Olanow, C. W., and Isacson, O. (2002). Selective Loss of 20S Proteasome α-subunits in the Substantia Nigra Pars Compacta in Parkinson's Disease. *Neurosci. Lett.* 326 (3), 155–158. doi:10.1016/s0304-3940(02)00296-3

Meairs, S. (2015). Facilitation of Drug Transport across the Blood-Brain Barrier with Ultrasound and Microbubbles. *Pharmaceutics* 7 (3), 275–293. doi:10.3390/pharmaceutics7030275

Medina, S. H., and El-Sayed, M. E. H. (2009). Dendrimers as Carriers for Delivery of Chemotherapeutic Agents. *Chem. Rev.* 109 (7), 3141–3157. doi:10.1021/cr900174j

Meng, X.-y., Li, J.-j., Ni, T.-j., Xiao-tong, L., He, T., Men, Z.-n., et al. (2020). Electro-responsive Brain-Targeting Mixed Micelles Based on Pluronic F127 and D-α-Tocopherol Polyethylene Glycol Succinate–Ferrocene. *Colloids Surfaces A Physicochem. Eng. Aspects* 601, 124986. doi:10.1016/j.colsurfa.2020.124986

Merino, S., Martín, C., Kostarelos, K., Prato, M., and Vázquez, E. (2015). Nanocomposite Hydrogels: 3D Polymer-Nanoparticle Synergies for On-Demand Drug Delivery. *ACS Nano* 9 (5), 4686–4697. doi:10.1021/acsnano.5b01433

Mihalko, E. P., Nellenbach, K., Krishnakumar, M., Moiseiwitsch, N., Sollinger, J., Cooley, B. C., et al. (2022). Fibrin-specific poly(N-Isopropylacrylamide) Nanogels for Targeted Delivery of Tissue-type Plasminogen Activator to Treat Thrombotic Complications Are Well Tolerated *In Vivo*. *Bioeng. Transl. Med.* 7 (2), e10277. doi:10.1002/btm2.10277

Misra, A., Ganesh, S., Shahiwala, A., and Shah, S. P. (2003). Drug Delivery to the Central Nervous System: a Review. *J. Pharm. Pharm. Sci.* 6 (2), 252–273.

Molino, Y., Jabès, F., Lacassagne, E., Gaudin, N., and Khrestchatisky, M. (2014). Setting-up an *In Vitro* Model of Rat Blood-Brain Barrier (BBB): a Focus on BBB Impermeability and Receptor-Mediated Transport. *J. Vis. Exp.* 88, e51278. doi:10.3791/51278

Muresanu, D. F., Strilciuc, S., and Stan, A. (2019). Current Drug Treatment of Acute Ischemic Stroke: Challenges and Opportunities. *CNS Drugs* 33 (9), 841–847. doi:10.1007/s40263-019-00663-x

Nance, E., Zhang, C., Shih, T.-Y., Xu, Q., Schuster, B. S., and Hanes, J. (2014). Brain-penetrating Nanoparticles Improve Paclitaxel Efficacy in Malignant Glioma Following Local Administration. *ACS Nano* 8 (10), 10655–10664. doi:10.1021/nn504210g

Nau, R., Sörgel, F., and Eiffert, H. (2021). Central Nervous System Infections and Antimicrobial Resistance: an Evolving Challenge. *Curr. Opin. Neurol.* 34 (3), 456–467. doi:10.1097/wco.0000000000000931

Neamtu, I., Rusu, A. G., Diaconu, A., Nita, L. E., and Chiriac, A. P. (2017). Basic Concepts and Recent Advances in Nanogels as Carriers for Medical Applications. *Drug Deliv.* 24 (1), 539–557. doi:10.1080/10717544.2016.1276232

Oberdörster, G. (2010). Safety Assessment for Nanotechnology and Nanomedicine: Concepts of Nanotoxicology. *J. Intern Med.* 267 (1), 89–105. doi:10.1111/j.1365-2796.2009.02187.x

Oh, J. K., Siegwart, D. J., and Matyjaszewski, K. (2007). Synthesis and Biodegradation of Nanogels as Delivery Carriers for Carbohydrate Drugs. *Biomacromolecules* 8 (11), 3326–3331. doi:10.1021/bm070381+

Palmer, A. M. (2010). The Role of the Blood-CNS Barrier in CNS Disorders and Their Treatment. *Neurobiol. Dis.* 37 (1), 3–12. doi:10.1016/j.nbd.2009.07.029

Pappu, S., Lerma, J., and Khraishi, T. (2016). Brain CT to Assess Intracranial Pressure in Patients with Traumatic Brain Injury. *J. Neuroimaging* 26 (1), 37–40. doi:10.1111/jon.12289

Pardridge, W. M. (2003). Blood-brain Barrier Drug Targeting: the Future of Brain Drug Development. *Mol. Interv.* 3 (2), 9051–9105. doi:10.1124/mi.3.2.90

Pardridge, W. M. (2005). The Blood-Brain Barrier: Bottleneck in Brain Drug Development. *Neurotherapeutics* 2 (1), 3–14. doi:10.1602/neurorx.2.1.3

Pargoo, E. M., Aghasadeghi, M. R., Parivar, K., Nikbin, M., Rahimi, P., and Ardestani, M. S. (2021). Lamivudine-conjugated and Efavirenz-loaded G2 Dendrimers: Novel Anti-retroviral Nano Drug Delivery Systems. *IET Nanobiotechnol.* 15 (7), 627–637. doi:10.1049/nbt2.12060

Pastor-Maldonado, C. J., Suárez-Rivero, J. M., Povea-Cabello, S., Álvarez-Córdoba, M., Villalón-García, I., Munuera-Cabeza, M., et al. (2020). Coenzyme Q10: Novel Formulations and Medical Trends. *Int. J. Mol. Sci.* 21 (22), 8432. doi:10.3390/ijms21228432

Patel, V., Chavda, V., and Shah, J. (2021). Nanotherapeutics in Neuropathologies: Obstacles, Challenges and Recent Advancements in CNS Targeted Drug Delivery Systems. *Curr. Neuropharmacol.* 19 (5), 693–710. doi:10.2174/1570159x18666200807143526

Peng, S., Wang, H., Zhao, W., Xin, Y., Liu, Y., Yu, X., et al. (2020). Zwitterionic Polysulfamide Drug Nanogels with Microwave Augmented Tumor Accumulation and On-Demand Drug Release for Enhanced Cancer Therapy. *Adv. Funct. Mater.* 30 (23), 1. doi:10.1002/adfm.202001832

Pichla, M., Bartosz, G., and Sadowska-Bartosz, I. (2020). The Antiaggregative and Antiamyloidogenic Properties of Nanoparticles: A Promising Tool for the

Treatment and Diagnostics of Neurodegenerative Diseases. *Oxid. Med. Cell Longev.* 2020, 3534570. doi:10.1155/2020/3534570

Picone, P., Sabatino, M. A., Ditta, L. A., Amato, A., San Biagio, P. L., Mulè, F., et al. (2018). Nose-to-brain Delivery of Insulin Enhanced by a Nanogel Carrier. *J. Control. Release* 270, 23–36. doi:10.1016/j.jconrel.2017.11.040

Poovaiah, N., Davoudi, Z., Peng, H., Schlichtmann, B., Mallapragada, S., Narasimhan, B., et al. (2018). Treatment of Neurodegenerative Disorders through the Blood-Brain Barrier Using Nanocarriers. *Nanoscale* 10 (36), 16962–16983. doi:10.1039/c8nr04073g

Pottoo, F. H., Sharma, S., Javed, M. N., Barkat, M. A., HarshitaAlam, M. S., et al. (2020). Lipid-based Nanoformulations in the Treatment of Neurological Disorders. *Drug Metab. Rev.* 52 (1), 185–204. doi:10.1080/03602532.2020.1726942

Pourtalebi Jahromi, L., Moghaddam Panah, F., Azadi, A., and Ashrafi, H. (2019). A Mechanistic Investigation on Methotrexate-Loaded Chitosan-Based Hydrogel Nanoparticles Intended for CNS Drug Delivery: Trojan Horse Effect or Not? *Int. J. Biol. Macromol.* 125, 785–790. doi:10.1016/j.ijbiomac.2018.12.093

Pourtalebi Jahromi, L., Mohammadi-Samani, S., Heidari, R., and Azadi, A. (2018). In Vitro- and *In Vivo* Evaluation of Methotrexate-Loaded Hydrogel Nanoparticles Intended to Treat Primary CNS Lymphoma via Intranasal Administration. *J. Pharm. Pharm. Sci.* 21 (1), 305–317. doi:10.18433/jpps29496

Prasanna, P., and Upadhyay, A. (2021). Flavonoid-Based Nanomedicines in Alzheimer's Disease Therapeutics: Promises Made, a Long Way to Go. *ACS Pharmacol. Transl. Sci.* 4 (1), 74–95. doi:10.1021/acsptsci.0c00224

Rizzi, L., Rosset, I., and Roriz-Cruz, M. (2014). Global Epidemiology of Dementia: Alzheimer's and Vascular Types. *Biomed. Res. Int.* 2014, 908915. doi:10.1155/2014/908915

Sá-Pereira, I., Brites, D., and Brito, M. A. (2012). Neurovascular Unit: a Focus on Pericytes. *Mol. Neurobiol.* 45 (2), 327–347. doi:10.1007/s12035-012-8244-2

Saha, P., Ganguly, R., Li, X., Das, R., Singha, N. K., and Pich, A. (2021). Zwitterionic Nanogels and Microgels: An Overview on Their Synthesis and Applications. *Macromol. Rapid Commun.* 42 (13), e2100112. doi:10.1002/marc.202100112

Sari, N. D., Baltali, S., Serin, I., and Antar, V. (2021). Evaluation of Intraventricular/Intrathecal Antimicrobial Therapy in the Treatment of Nosocomial Meningitis Caused by Multidrug-Resistant Gram-Negative Bacteria after Central Nervous System Surgery. *Can. J. Infect. Dis. Med. Microbiol.* 2021, 9923015. doi:10.1155/2021/9923015

Sarkar, A., Fatima, I., Mohammad Sajid Jamal, Q., Sayeed, U., Kalim A. Khan, M., Akhtar, S., et al. (2017). Nanoparticles as a Carrier System for Drug Delivery across Blood Brain Barrier. *Cdm* 18 (2), 129–137. doi:10.2174/1389200218666170113125132

Shi, B., Huang, K., Ding, J., Xu, W., Yang, Y., Liu, H., et al. (2017). Intracellularly Swollen Polypeptide Nanogel Assists Hepatoma Chemotherapy. *Theranostics* 7 (3), 703–716. doi:10.7150/thno.16794

Shringarpure, M., Gharat, S., Momin, M., and Omri, A. (2021). Management of Epileptic Disorders Using Nanotechnology-Based Strategies for Nose-To-Brain Drug Delivery. *Expert Opin. Drug Deliv.* 18 (2), 169–185. doi:10.1080/17425247.2021.1823965

Soni, K. S., Desale, S. S., and Bronich, T. K. (2016). Nanogels: An Overview of Properties, Biomedical Applications and Obstacles to Clinical Translation. *J. Control. Release* 240, 109–126. doi:10.1016/j.jconrel.2015.11.009

Soni, S., Ruhela, R. K., and Medhi, B. (2016). Nanomedicine in Central Nervous System (CNS) Disorders: A Present and Future Prospective. *Adv. Pharm. Bull.* 6 (3), 319–335. doi:10.15171/apb.2016.044

Soni, V., Jain, A., Khare, P., Gulbake, A., and Jain, S. (2010). Potential Approaches for Drug Delivery to the Brain: Past, Present, and Future. *Crit. Rev. Ther. Drug Carr. Syst.* 27 (3), 187–236. doi:10.1615/critrevtherdrugcarriersyst.v27.i3.10

Srikanth, M., and Kessler, J. A. (2012). Nanotechnology-novel Therapeutics for CNS Disorders. *Nat. Rev. Neurol.* 8 (6), 307–318. doi:10.1038/nrneurol.2012.76

Stawicki, B., Schacher, T., and Cho, H. (2021). Nanogels as a Versatile Drug Delivery System for Brain Cancer. *Gels* 7 (2), 63. doi:10.3390/gels7020063

Stuart, M. A. C., Huck, W. T. S., Genzer, J., Müller, M., Ober, C., Stamm, M., et al. (2010). Emerging Applications of Stimuli-Responsive Polymer Materials. *Nat. Mater* 9 (2), 101–113. doi:10.1038/nmat2614

Suhail, M., Rosenholm, J. M., Minhas, M. U., Badshah, S. F., Naeem, A., Khan, K. U., et al. (2019). Nanogels as Drug-Delivery Systems: a Comprehensive Overview. *Ther. Deliv.* 10 (11), 697–717. doi:10.4155/tde-2019-0010

Sun, M., Su, X., Ding, B., He, X., Liu, X., Yu, A., et al. (2012). Advances in Nanotechnology-Based Delivery Systems for Curcumin. *Nanomedicine* 7 (7), 1085–1100. doi:10.2217/nnm.12.80

Sun, T., Zhang, Y. S., Pang, B., Hyun, D. C., Yang, M., and Xia, Y. (2014). Engineered Nanoparticles for Drug Delivery in Cancer Therapy. *Angew. Chem. Int. Ed. Engl.* 53 (46), 12320–12364. doi:10.1002/anie.201403036

Tang, L., Zhang, M., and Liu, C. (2022). Advances in Nanotechnology-Based Immunotherapy for Glioblastoma. *Front. Immunol.* 13, 882257. doi:10.3389/fimmu.2022.882257

Tangpong, J., Cole, M. P., Sultana, R., Estus, S., Vore, M., St. Clair, W., et al. (2007). Adriamycin-mediated Nitration of Manganese Superoxide Dismutase in the Central Nervous System: Insight into the Mechanism of Chemobrain. *J. Neurochem.* 100 (1), 191–201. doi:10.1111/j.1471-4159.2006.04179.x

Tedford, C. E., DeLapp, S., Jacques, S., and Anders, J. (2015). Quantitative Analysis of Transcranial and Intraparenchymal Light Penetration in Human Cadaver Brain Tissue. *Lasers Surg. Med.* 47 (4), 312–322. doi:10.1002/lsm.22343

Teng, Y., Jin, H., Nan, D., Li, M., Fan, C., Liu, Y., et al. (2018). *In Vivo* evaluation of Urokinase-Loaded Hollow Nanogels for Sonothrombolysis on Suture Embolization-Induced Acute Ischemic Stroke Rat Model. *Bioact. Mater.* 3 (1), 102–109. doi:10.1016/j.bioactmat.2017.08.001

Tian, X. H., Lin, X. N., Wei, F., Feng, W., Huang, Z. C., Wang, P., et al. (2011). Enhanced Brain Targeting of Temozolomide in Polysorbate-80 Coated Polybutylcyanoacrylate Nanoparticles. *Int. J. Nanomedicine* 6, 445–452. doi:10.2147/IJN.S16570

Tietz, S., and Engelhardt, B. (2015). Brain Barriers: Crosstalk between Complex Tight Junctions and Adherens Junctions. *J. Cell Biol.* 209 (4), 493–506. doi:10.1083/jcb.201412147

Trompetero, A., Gordillo, A., Del Pilar, M. C., Cristina, V. M., and Bustos Cruz, R. H. (2018). Alzheimer's Disease and Parkinson's Disease: A Review of Current Treatment Adopting a Nanotechnology Approach. *Cpd* 24 (1), 22–45. doi:10.2174/1381612823666170828133059

T. Ronaldson, P., and P. Davis, T. (2012). Blood-brain Barrier Integrity and Glial Support: Mechanisms that Can Be Targeted for Novel Therapeutic Approaches in Stroke. *Curr. Pharm. Des.* 18 (25), 3624–3644. doi:10.2174/138161212802002625

Ueno, M., Nakagawa, T., Wu, B., Onodera, M., Huang, C.-l., Kusaka, T., et al. (2010). Transporters in the Brain Endothelial Barrier. *Cmc* 17 (12), 1125–1138. doi:10.2174/092986710790827816

Verma, S., Domb, A. J., and Kumar, N. (2011). Nanomaterials for Regenerative Medicine. *Nanomedicine* 6 (1), 157–181. doi:10.2217/nnm.10.146

Vigani, B., Rossi, S., Sandri, G., Bonferoni, M. C., Caramella, C. M., and Ferrari, F. (2020). Recent Advances in the Development of *In Situ* Gelling Drug Delivery Systems for Non-parenteral Administration Routes. *Pharmaceutics* 12 (9), 859. doi:10.3390/pharmaceutics12090859

Vinogradov, S. V., Batrakova, E. V., and Kabanov, A. V. (2004). Nanogels for Oligonucleotide Delivery to the Brain. *Bioconjugate Chem.* 15 (1), 50–60. doi:10.1021/bc034164r

Vinogradov, S. V., Bronich, T. K., and Kabanov, A. V. (2002). Nanosized Cationic Hydrogels for Drug Delivery: Preparation, Properties and Interactions with Cells. *Adv. Drug Deliv. Rev.* 54 (1), 135–147. doi:10.1016/s0169-409x(01)00245-9

Vinogradov, S. V. (2010). Nanogels in the Race for Drug Delivery. *Nanomedicine* 5 (2), 165–168. doi:10.2217/nnm.09.103

Vinogradov, S. V., Poluektova, L. Y., Makarov, E., Gerson, T., and Senanayake, M. T. (2010). Nano-NRTIs: Efficient Inhibitors of HIV Type-1 in Macrophages with a Reduced Mitochondrial Toxicity. *Antivir. Chem. Chemother.* 21 (1), 1–14. doi:10.3851/imp1680

Wang, D., and Wu, L.-P. (2017). Nanomaterials for Delivery of Nucleic Acid to the Central Nervous System (CNS). *Mater. Sci. Eng. C* 70 (Pt 2), 1039–1046. doi:10.1016/j.msec.2016.04.011

Wang, J., Ni, Q., Wang, Y., Zhang, Y., He, H., Gao, D., et al. (2021). Nanoscale Drug Delivery Systems for Controllable Drug Behaviors by Multi-Stage Barrier Penetration. *J. Control. Release* 331, 282–295. doi:10.1016/j.jconrel.2020.08.045

Wang, L., Lian, W., Liu, B., Lv, H., Zhang, Y., Wu, X., et al. (2022). Transparent, High-Performance and Stable Sb2 S3 Photoanode Enabled by Heterojunction Engineering with Conjugated Polycarbazole Frameworks for Unbiased Photoelectrochemical Overall Water Splitting Devices. *Adv. Mater* 1, e2200723. doi:10.1002/adma.202200723

Wang, X., Parvathaneni, V., Shukla, S. K., Kulkarni, N. S., Muth, A., Kunda, N. K., et al. (2020). Inhalable Resveratrol-Cyclodextrin Complex Loaded Biodegradable Nanoparticles for Enhanced Efficacy against Non-small Cell Lung Cancer. *Int. J. Biol. Macromol.* 164, 638–650. doi:10.1016/j.ijbiomac.2020.07.124

Wang, Y.-Y., Lui, P. C., and Li, J. Y. (2009). Receptor-mediated Therapeutic Transport across the Blood-Brain Barrier. *Immunotherapy* 1 (6), 983–993. doi:10.2217/imt.09.75

Wang, Y., Ying, X., Chen, L., Liu, Y., Wang, Y., Liang, J., et al. (2016). Electroresponsive Nanoparticles Improve Antiseizure Effect of Phenytoin in Generalized Tonic-Clonic Seizures. *Neurotherapeutics* 13 (3), 603–613. doi:10.1007/s13311-016-0431-9

Warren, G., Makarov, E., Lu, Y., Senanayake, T., Rivera, K., Gorantla, S., et al. (2015). Amphiphilic Cationic Nanogels as Brain-Targeted Carriers for Activated Nucleoside Reverse Transcriptase Inhibitors. *J. Neuroimmune Pharmacol.* 10 (1), 88–101. doi:10.1007/s11481-014-9576-7

Wei, P., Cornel, E. J., and Du, J. (2021). Ultrasound-responsive Polymer-Based Drug Delivery Systems. *Drug Deliv. Transl. Res.* 11 (4), 1323–1339. doi:10.1007/s13346-021-00963-0

Wen, J., Wu, D., Qin, M., Liu, C., Wang, L., Xu, D., et al. (2019). Sustained Delivery and Molecular Targeting of a Therapeutic Monoclonal Antibody to Metastases in the Central Nervous System of Mice. *Nat. Biomed. Eng.* 3 (9), 706–716. doi:10.1038/s41551-019-0434-z

Wilson, L., Stewart, W., Dams-O'Connor, K., Diaz-Arrastia, R., Horton, L., Menon, D. K., et al. (2017). The Chronic and Evolving Neurological Consequences of Traumatic Brain Injury. *Lancet Neurology* 16 (10), 813–825. doi:10.1016/s1474-4422(17)30279-x

Wohlfart, S., Gelperina, S., and Kreuter, J. (2012). Transport of Drugs across the Blood-Brain Barrier by Nanoparticles. *J. Control. Release* 161 (2), 264–273. doi:10.1016/j.jconrel.2011.08.017

Wong, H. L., Wu, X. Y., and Bendayan, R. (2012). Nanotechnological Advances for the Delivery of CNS Therapeutics. *Adv. Drug Deliv. Rev.* 64 (7), 686–700. doi:10.1016/j.addr.2011.10.007

Wu, T., and Tang, M. (2018). The Inflammatory Response to Silver and Titanium Dioxide Nanoparticles in the Central Nervous System. *Nanomedicine* 13 (2), 233–249. doi:10.2217/nnm-2017-0270

Xiao, Y., Liu, F., Yang, J., Zhong, M., Zhang, E., Li, Y., et al. (2015). Over-activation of TLR5 Signaling by High-Dose Flagellin Induces Liver Injury in Mice. *Cell Mol. Immunol.* 12 (6), 729–742. doi:10.1038/cmi.2014.110

Xu, C., Gong, Y., Wang, Y., and Chen, Z. (2022). New Advances in Pharmacoresistant Epilepsy towards Precise Management-From Prognosis to Treatments. *Pharmacol. Ther.* 233, 108026. doi:10.1016/j.pharmthera.2021.108026

Xu, D., Wu, D., Qin, M., Nih, L. R., Liu, C., Cao, Z., et al. (2019). Efficient Delivery of Nerve Growth Factors to the Central Nervous System for Neural Regeneration. *Adv. Mater* 31 (33), e1900727. doi:10.1002/adma.201900727

Yang, J., Wang, L., Huang, L., Che, X., Zhang, Z., Wang, C., et al. (2021). Receptor-targeting Nanomaterials Alleviate Binge Drinking-induced Neurodegeneration as Artificial Neurotrophins. *Exploration* 1 (1), 61–74. doi:10.1002/exp.20210004

Yin, L., Ding, J., Fei, L., He, M., Cui, F., Tang, C., et al. (2008). Beneficial Properties for Insulin Absorption Using Superporous Hydrogel Containing Interpenetrating Polymer Network as Oral Delivery Vehicles. *Int. J. Pharm.* 350 (1-2), 220–229. doi:10.1016/j.ijpharm.2007.08.051

Ying, X., Wang, Y., Liang, J., Yue, J., Xu, C., Lu, L., et al. (2014). Angiopep-conjugated Electro-Responsive Hydrogel Nanoparticles: Therapeutic Potential for Epilepsy. *Angew. Chem. Int. Ed. Engl.* 53 (46), 12436–12440. doi:10.1002/anie.201403846

Zain-ul-Abdin, A., Wang, L., Yu, H., Saleem, M., Akram, M., Khalid, H., et al. (2017). Synthesis of Ethylene Diamine-Based Ferrocene Terminated Dendrimers and Their Application as Burning Rate Catalysts. *J. Colloid Interface Sci.* 487, 38–51. doi:10.1016/j.jcis.2016.10.001

Zatta, P., Drago, D., Bolognin, S., and Sensi, S. L. (2009). Alzheimer's Disease, Metal Ions and Metal Homeostatic Therapy. *Trends Pharmacol. Sci.* 30 (7), 346–355. doi:10.1016/j.tips.2009.05.002

Zhang, C., Pan, D., Luo, K., She, W., Guo, C., Yang, Y., et al. (2014). Peptide Dendrimer-Doxorubicin Conjugate-Based Nanoparticles as an Enzyme-Responsive Drug Delivery System for Cancer Therapy. *Adv. Healthc. Mat.* 3 (8), 1299–1308. doi:10.1002/adhm.201300601

Zhang, G., Zhang, L., Rao, H., Wang, Y., Li, Q., Qi, W., et al. (2020). Role of Molecular Chirality and Solvents in Directing the Self-Assembly of Peptide into an Ultra-pH-sensitive Hydrogel. *J. Colloid Interface Sci.* 577, 388–396. doi:10.1016/j.jcis.2020.05.087

Zhang, L., Zhang, F., Weng, Z., Brown, B. N., Yan, H., Ma, X. M., et al. (2013). Effect of an Inductive Hydrogel Composed of Urinary Bladder Matrix upon Functional Recovery Following Traumatic Brain Injury. *Tissue Eng. Part A* 19 (17-18), 1909–1918. doi:10.1089/ten.TEA.2012.0622

Zhang, M., Asghar, S., Tian, C., Hu, Z., Ping, Q., Chen, Z., et al. (2021). Lactoferrin/phenylboronic Acid-Functionalized Hyaluronic Acid Nanogels Loading Doxorubicin Hydrochloride for Targeting Glioma. *Carbohydr. Polym.* 253, 117194. doi:10.1016/j.carbpol.2020.117194

Zhang, P., Hu, L., Yin, Q., Zhang, Z., Feng, L., and Li, Y. (2012). Transferrin-conjugated Polyphosphoester Hybrid Micelle Loading Paclitaxel for Brain-Targeting Delivery: Synthesis, Preparation and *In Vivo* Evaluation. *J. Control. Release* 159 (3), 429–434. doi:10.1016/j.jconrel.2012.01.031

Zhang, Y., Yang, H., Wei, D., Zhang, X., Wang, J., Wu, X., et al. (2021). Mitochondria-targeted Nanoparticles in Treatment of Neurodegenerative Diseases. *Exploration* 1 (3), 1. doi:10.1002/exp.20210115

Zhang, Z., Ji, Y., Lin, C., and Tao, L. (2021). Thermosensitive Hydrogel-Functionalized Gold Nanorod/mesoporous MnO2 Nanoparticles for Tumor Cell-Triggered Drug Delivery. *Mater. Sci. Eng. C* 131, 112504. doi:10.1016/j.msec.2021.112504

Zhao, F., Yao, D., Guo, R., Deng, L., Dong, A., and Zhang, J. (2015). Composites of Polymer Hydrogels and Nanoparticulate Systems for Biomedical and Pharmaceutical Applications. *Nanomaterials* 5 (4), 2054–2130. doi:10.3390/nano5042054

Zhao, Q., Zhang, S., Wu, F., Li, D., Zhang, X., Chen, W., et al. (2021). Rational Design of Nanogels for Overcoming the Biological Barriers in Various Administration Routes. *Angew. Chem. Int. Ed.* 60 (27), 14760–14778. doi:10.1002/anie.201911048

Zhou, T., Xiao, C., Fan, J., Chen, S., Shen, J., Wu, W., et al. (2013). A Nanogel of On-Site Tunable pH-Response for Efficient Anticancer Drug Delivery. *Acta Biomater.* 9 (1), 4546–4557. doi:10.1016/j.actbio.2012.08.017

Conflict of Interest: TH is employed by Evergreen Therapeutics, Inc.

The author declares that the research was conducted in the absence of any commercial or financial relationships that could be construed as a potential conflict of interest.

Publisher's Note: All claims expressed in this article are solely those of the authors and do not necessarily represent those of their affiliated organizations, or those of the publisher, the editors and the reviewers. Any product that may be evaluated in this article, or claim that may be made by its manufacturer, is not guaranteed or endorsed by the publisher.

frontiers | Frontiers in Bioengineering and Biotechnology

TYPE Original Research
PUBLISHED 15 August 2022
DOI 10.3389/fbioe.2022.962380

OPEN ACCESS

EDITED BY
Chang Li,
Tongji University, China

REVIEWED BY
Hanlin Ou,
Qingdao University, China
Zhaoting Li,
University of Wisconsin-Madison,
United States

*CORRESPONDENCE
Kaikai Wang,
kirk2008@126.com
Hanlin Fu,
fuhanlinzzdx@163.com

†These authors have contributed equally to this work

SPECIALTY SECTION
This article was submitted to Nanobiotechnology, a section of the journal Frontiers in Bioengineering and Biotechnology

RECEIVED 06 June 2022
ACCEPTED 04 July 2022
PUBLISHED 15 August 2022

CITATION
Fu Z, Wang X, Lu X, Yang Y, Zhao L, Zhou L, Wang K and Fu H (2022), Mannose-decorated ginsenoside Rb1 albumin nanoparticles for targeted anti-inflammatory therapy. *Front. Bioeng. Biotechnol.* 10:962380. doi: 10.3389/fbioe.2022.962380

Mannose-decorated ginsenoside Rb1 albumin nanoparticles for targeted anti-inflammatory therapy

Zhihui Fu[1†], Xiaohui Wang[1†], Xuan Lu[2], Ying Yang[2], Lingling Zhao[1], Lin Zhou[1], Kaikai Wang[2*] and Hanlin Fu[1*]

[1]The First Affiliated Hospital of Zhengzhou University, Zhengzhou, China, [2]School of Pharmacy and Affiliated Hospital of Nantong University, Nantong University, Nantong, China

Ginsenoside Rb1 is a potential anti-inflammatory natural molecule, but its therapeutic efficacy was tremendously hampered by the low solubility and non-targeted delivery. In this study, we innovatively developed a mannose (Man)-modified albumin bovine serum albumin carrier (Man-BSA) to overcome the previously mentioned dilemmas of Rb1. The constructed Man-BSA@Rb1 NPs could improve the solubility and increase the cellular uptake of Rb1, finally leading to the enhanced anti-inflammatory effects. The robust therapeutics of Man-BSA@Rb1 NPs were measured in terms of nitrite, tumor necrosis factor-α (TNF-α), and interleukin-6 (IL-6) levels, which might be achieved by potently inhibiting nuclear factor-κB (NF-κB) and mitogen-activated protein kinase (MAPK) signaling pathways in lipopolysaccharide (LPS)-induced Raw264.7 cells. Moreover, the therapeutic efficacy of Man-BSA@Rb1 NPs was further confirmed in the d-Gal/LPS-induced liver injury model. The results indicated that Man-BSA may offer a promising system to improve the anti-inflammatory therapy of Rb1.

KEYWORDS

ginsenoside, mannose, albumin nanoparticles, targeted delivery, inflammation

1 Introduction

Inflammation presents a potential threat to human health, and the unbalanced release of some inflammatory mediators will lead to the occurrence of related diseases such as sepsis shock, arthritis, and inflammatory bowel disease (IBD) (Zhou et al., 2019; Wang Q. et al., 2020; Wang Z. et al., 2020). To date, a variety of herbal-based therapeutic approaches have been attempted to attenuate inflammatory responses. Among them, ginsenoside Rb1 extracted from ginseng has been extensively explored due to its biological functions, including anti-inflammatory, anti-oxidative stress, anti-apoptosis, and acceptable biosafety (Zhou and Xie, 2019; Zhang X. et al., 2021; Jiang et al., 2021). However, the low water solubility and poor bioavailability limit its further application.

A strategy that potentially overcomes the dilemma described above is to utilize nanoparticle (NP)-based materials as delivery carriers (Su et al., 2018; Mitchell et al., 2021;

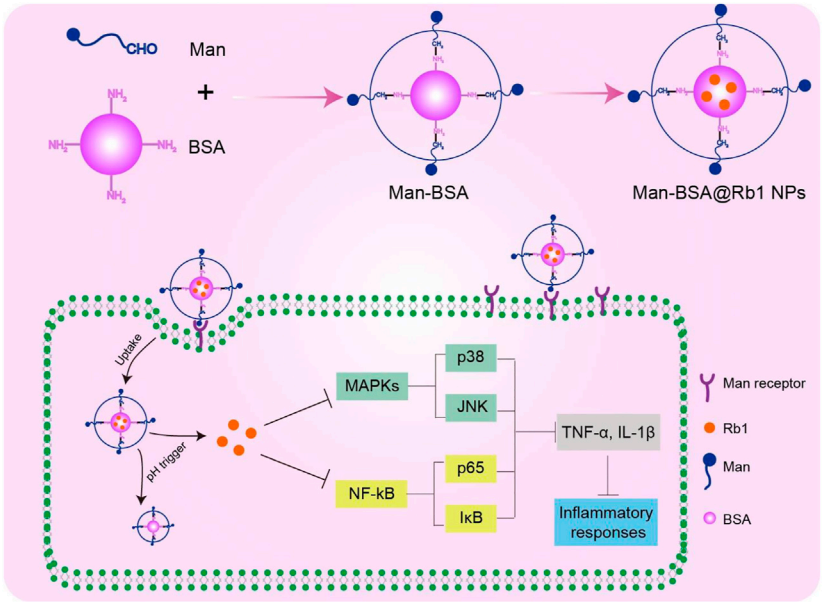

SCHEME 1
Schematic illustration of the preparation and mechanism of Man-BSA@Rb1 NPs.

Zhao et al., 2021). For example, polyethylene glycol (PEG) and poly lactic-co-glycolic acid (PLGA) applied Rb1 NPs were generated to enhance the bioavailability of Rb1 (Zhou et al., 2021). Trimethyl chitosan derivatives developed Rb1 NPs that were generated to improve the oral absorption of Rb1 (Chen et al., 2021). Platelets constructed biomimetic Rb1 NPs that were prepared to improve the bioavailability and stability of Rb1 (Yin et al., 2022). Despite all the progress made by far, the off-target effect remains a bottleneck that limits the therapeutic index of Rb1 NPs. Therefore, it is necessary to develop new Rb1 NPs which contain satisfying properties of biocompatibility, safety, and targeting ability.

The fate of fabricated NPs usually depends on their constituent materials, including various organic or inorganic materials, followed by forming organic NPs (e.g., liposomes, micelles, and polymeric nanoparticles) or inorganic NPs (e.g., magnetic and carbon NPs). With the help of developed nanotechnology, versatile NPs have been extensively explored to offer improved properties of loaded cargos, such as drug loading and therapeutic efficiency (Li and Wang, 2020; Wu et al., 2020; Li Z. et al., 2021). However, NP-associated toxicity and immunogenicity remain as a challenge. Compared with the reported carriers, bovine serum albumin (BSA) is attractive to deliver low solubility and poor bioavailability drugs because it is biodegradable, biologically compatible, and possesses multiple drug-binding abilities (Sleep, 2015; Mazzaferro and Edwards, 2020). Encouragingly, BSA-bound paclitaxel (Abraxane) NPs have been used in clinical treatment of breast cancer (Hama and Ishima, 2021). To endow BSA with targeting ability, mannose (Man) ligand is introduced to target mannose receptors that are overexpressed in pro-inflammatory cells, such as macrophages (Chen and Huang, 2020; Jaynes and Sable, 2020). Man, a simple sugar, has been used in the field of dietary supplements. The advantages of the Man-based ligand are reflected in nontoxicity, biodegradation, and no immunogenicity. Importantly, mannose treatment suppresses macrophage activation through impairing IL-1β production (Torretta et al., 2020; Wang et al., 2021). Thus, the carrier of Man-BSA can deliver the drug into specific cells by the receptor-mediated endocytosis pathway, resulting in enhanced cellular uptake and inflammation alleviation. Moreover, compared with launched NPs (e.g., liposomes), Man-BSA-based NPs can not only protect the degradation of drug in the blood but also promote drug release under acidic conditions (Zhang et al., 2015; Zhu et al., 2015; Lei et al., 2021).

In the present study, we report on the synthesis of Man-BSA and then prepared Man-BSA@Rb1 NPs with BSA@Rb1 NPs as controls. As shown in Scheme 1, Man-BSA@Rb1 NPs could improve Rb1 accumulation into the cells through mannose receptor targeted delivery. After endocytosis, Rb1 could be released in a pH trigger mode to play an anti-inflammatory response by inhibiting nuclear factor-κB (NF-κB) and mitogen-activated protein kinase (MAPK) signaling pathways. The physicochemical characterization of NPs was examined, including structure verification, morphology, particle size, zeta

potential, stability, and drug loading and release. Furthermore, the anti-inflammatory effect of Man-BSA@Rb1 NPs was verified in lipopolysaccharide (LPS)-stimulated Raw264.7 cells *in vitro* and d-Gal/LPS-induced liver inflammation model *in vivo*.

2 Materials and methods

2.1 Chemicals and reagents

The Reactive Oxygen Species (ROS) Assay Kit (cat.no. S0033S), Fluo-4 AM (cat.no S1060), and Nitrite Assay Kit (cat.no S0023) were purchased from Beyotime Biotechnology (Shanghai, China). D-Mannose, BSA, and sodium cyanoborohydride were purchased from Aladdin Bio-Chem Technology Co., Ltd. (Shanghai, China). LPS and D-galactosamine (d-Gal) were purchased from Sigma-Aldrich (United States). The antibodies of p-p65 (3033s), p65 (8242s), p-IκB-α (4812), IκB-α (2859), p-p38 (4511s), p38 (8690s), and β-actin (3700) were purchased from Cell Signaling Technology (United States). The antibodies of p-JNK (76572) and JNK (179461) were purchased from Abcam Co., Ltd. (USK). All other reagents were obtained from Nanjing Jiancheng Bioengineering Institute (Shanghai, China) unless otherwise stated.

2.2 Synthesis of Man-BSA

Man-BSA was synthesized and purified according to a reductive amination method. In brief, D-mannose (100 mg), BSA (68 mg), and sodium cyanoborohydride (100 mg) were co-dissolved in 5.0 ml borate buffer (pH 8.0), and the reacted solution was incubated at 37°C for 24 h. The reaction was terminated by adjusting the pH of the system to 4.0 with acetic acid. The final product of Man-BSA was purified by dialyzing against deionized water three times (molecular weight cut off 1.0 kDa). BSA, Man, and Man-BSA were characterized by ^{1}H-NMR with D_2O as the solvent (Bruker 600 MHz).

2.3 Preparation of BSA@Rb1 NPs and Man-BSA@Rb1 NPs

The Man-BSA@Rb1 NPs were obtained by a typical de-solvation method. In brief, Man-BSA (34 mg BSA) was first dissolved in 4.0 ml borate buffer (pH 8.0) and sonicated for 30 min. Rb1 (10 mg) was weighed and dissolved in 1 ml ethanol, and slowly added to the Man-BSA solution to react for 24 h. Man-BSA@Rb1 NPs were obtained by evaporation and centrifugation to remove ethanol and un-encapsulated Rb1. BSA@Rb1 NPs were also prepared in a similar method to Man-BSA@Rb1 NPs. Rb1, BSA@Rb1, and Man-BSA@Rb1 were also characterized by ^{1}H-NMR with D_2O as the solvent (Bruker 600 MHz).

2.4 Drug encapsulation efficiency

The drug encapsulation efficiency of Rb1 in BSA@Rb1 NPs and Man-BSA@Rb1 NPs was determined by a typical high-pressure liquid chromatography (HPLC) method. In brief, NPs were dissolved in acetonitrile and sonicated to completely release the drug. The concentration of Rb1 in the supernatant was determined by HPLC. The related conditions included C18 column (4.60 mm × 250 mm, 5 μm), a mobile phase of water/acetonitrile (50%/50%, v/v), the flow rate of 1.0 ml/min, the detection wavelength of 203 nm, and the column temperature of 35°C. The formula for drug encapsulation efficiency was as follows:

$$\textit{The drug encapsulation efficiency} = (\textit{weight of Rb1 in the NPs})/(\textit{weight of total Rb1}) \times 100\%$$

2.5 Physicochemical characterization of Man-BSA@Rb1 NPs

The particle size and zeta potential of BSA@Rb1 NPs and Man-BSA@Rb1 NPs were determined by dynamic light scattering (DLS) (Malvern Instruments Ltd., U.K.). The microscopic morphology of Man-BSA@Rb1 NPs was detected using transmission electron microscopy (TEM) (JEM-2100F, JEOL, Japan). The colloidal stability of BSA@Rb1 NPs and Man-BSA@Rb1 NPs was performed by monitoring their particle size in PBS (pH 7.4) for 24 h. The cumulative release of BSA@Rb1 NPs and Man-BSA@Rb1 NPs was tested by incubating them in a dialysis bag (MWCO 3500 Da) with pH 5.0 PBS and pH 7.4 PBS, respectively, and the Rb1 concentration in the medium was determined by HPLC.

2.6 Cell toxicity and cellular uptake

The toxicity study of Man-BSA, Rb1, BSA@Rb1 NPs, and Man-BSA@Rb1 NPs was evaluated by a standard CCK8 method in Raw264.7 cells. In brief, the cells were seeded in 96-well plates until ~80% density and then incubated with different treatments of 10, 25, 50, and 100 μM for 24 h (equal to Rb1 concentration). A standard CCK8 assay was performed to determine the related cytotoxicity.

For the cellular uptake study, Raw264.7 cells were cultured and seeded in confocal dishes for confocal imaging or 12-well plates for flow cytometry measuring. The cells were incubated with BSA@Rb1 NPs and Man-BSA@Rb1 NPs (25 μM, equal to Rb1 concentration) for

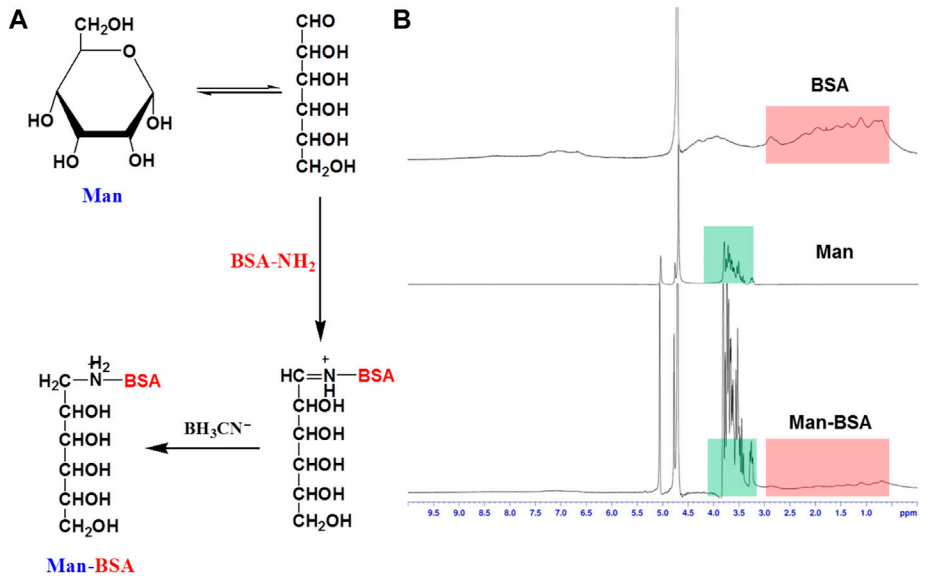

FIGURE 1
Synthesis and characterization of Man-BSA. **(A)** The synthetic route of Man-BSA. **(B)** The ^{1}H-NMR spectra of BSA, Man, and Man-BSA in D_2O.

4 h, and then stained with DAPI before confocal microscopy or collected before flow cytometry.

2.7 Inflammatory cytokines release and protein expression determination

The anti-inflammatory ability of Man-BSA, Rb1, BSA@Rb1 NPs, and Man-BSA@Rb1 NPs was evaluated by kits and the Western blot assay. In brief, Raw264.7 cells were seeded in 6-well plates and pretreated with different treatments (25 μM, equal to Rb1 concentration) for 1 h. After that, the cells were incubated with LPS (1 μg/ml) for another 24 h. The amounts of released cytokines including nitrite, TNF-α, and IL-6 in the medium were assessed by the nitrite assay kit and TNF-α/IL-6 ELISA kits. The cells were washed and isolated according to a standard procedure. The concentrations and levels of p-p65/p65, p-IκB-α/IκB-α, p-JNK/JNK, and p-p38/p38 were determined by a BCA Protein Assay Kit and Western blot, respectively. The intracellular levels of the ROS and calcium Ca^{2+} were determined by ROS assay kit and Fluo-4 AM assay kit, respectively.

2.8 Liver accumulation and therapeutic studies

The animals used in this study were approved by the Animal Care and Use Committee of the First Affiliated Hospital of Zhengzhou University. For the liver accumulation study, female C57BL/6 mice (6 weeks old) were randomly divided into two groups of FITC-labeled BSA@Rb1 NPs and Man-BSA@Rb1 NPs ($n = 3$). All mice were set to perform the procedure of intraperitoneal injection of 400 mg/kg d-Gal and 60 μg/kg LPS. After 0.5 h, the above formulations (20 mg/kg Rb1 equivalent) were administrated by intraperitoneal injection. After another 4 h, the mice were sacrificed, the liver was excised, and immunofluorescence staining was performed. For the therapeutic study, female C57BL/6 mice (6 weeks old) were randomly divided into five groups (n = 5) of saline, untreated, Rb1, BSA@Rb1 NPs, and Man-BSA@Rb1 NPs (20 mg/kg Rb1 equivalent). The treatment was performed at 0.5 h before intraperitoneal injection of 400 mg/kg d-Gal and 60 μg/kg LPS. 12 h after intraperitoneal injection, the mice were sacrificed, and the liver and serum were collected for hematoxylin and eosin (HE) staining, and alanine transaminase (ALT), aspartate transaminase (AST), and TNF-α and IL-1β determination, respectively.

2.9 Biosafety studies

For a potential toxicity study *in vivo*, female C57BL/6 mice (6 weeks old) were randomly divided into two groups. The treatments were administrated with saline and Man-BSA@Rb1 NPs (20 mg/kg Rb1 equivalent). 12 h after the injection, the mice were sacrificed and the major organs were collected for H&E staining. The blood was collected for alanine aminotransferase (ALT), aspartate aminotransferase (AST) determination, and blood analysis of WBCs, lymphocytes, and neutrophils. For the hemolysis assay, red blood cells (RBCs) were collected and

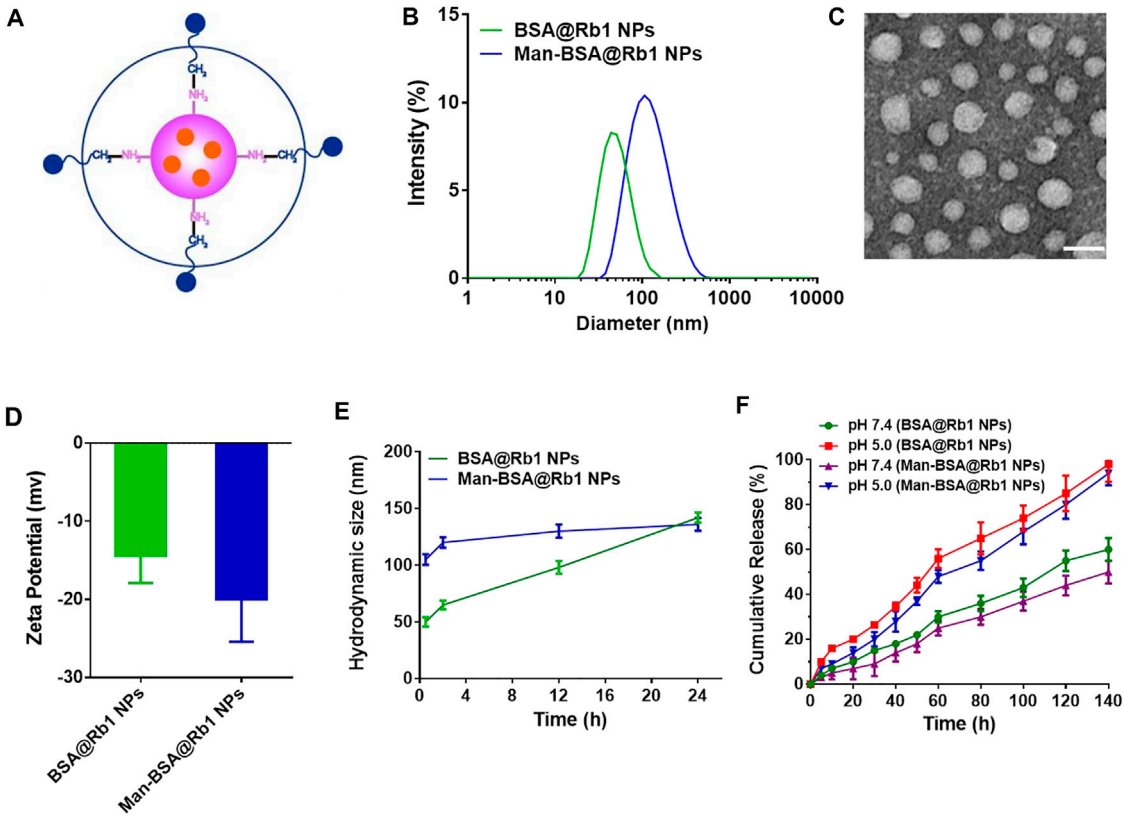

FIGURE 2
Characterization of Man-BSA@Rb1 NPs. **(A)** Structural diagram of Man-BSA@Rb1 NPs. **(B)** Hydrodynamic size distribution of BSA@Rb1 NPs and Man-BSA@Rb1 NPs. **(C)** Representative TEM images of Man-BSA@Rb1 NPs (scale bar = 100 nm). **(D)** Zeta potential of BSA@Rb1 NPs and Man-BSA@Rb1 NPs. **(E)** Stability of BSA@Rb1 NPs and Man-BSA@Rb1 NPs. **(F)** Cumulative release of BSA@Rb1 NPs and Man-BSA@Rb1 NPs at pH 5.0 and pH 7.4 media.

incubated with PBS (pH 7.4), Man-BSA@Rb1 NPs, and 1% Triton. After 2 h, samples were collected and imaged. Then, absorbance of the supernatant was determined with a multimode reader at 540 nm.

2.10 Statistical analysis

Statistical analysis was performed by two-sided Student's t-test for two groups and one-way ANOVA analysis of variance for multiple groups (when $p < 0.05$, the data were considered statistically significant).

3 Results and discussion

3.1 Preparation and characterization of Man-BSA@Rb1 NPs

Man-BSA was first synthesized through the Schiff base reaction between CHO-Man and NH2-BSA (Figure 1A; Mizuta et al., 2021). The structure of Man-BSA was demonstrated by ^{1}H-NMR, which was reflected in the characteristic absorption peak of 0.5–3.0 ppm (Man) and 3.2–3.9 ppm (BSA) (Figure 1B). BSA@Rb1 NPs and Man-BSA@Rb1 NPs were then prepared using the de-solvation method (Dong et al., 2019). Their formation was demonstrated by ^{1}H-NMR and the size distribution study. The characteristic absorption peak of 3.1–3.4 ppm (Rb1) appeared in BSA@Rb1 NPs, which indicated the feasibility of the preparation method in Man-BSA@Rb1 NPs (Supplementary Figure S1). The average particle size of BSA@Rb1 NPs and Man-BSA@Rb1 NPs was 43 and 106 nm, respectively. The modification of Man on the BSA surface would induce an increase in the particle size of BSA@Rb1 NPs (Figures 2A,B). TEM image confirmed the spherical shape of Man-BSA@Rb1 NPs (Figure 2C). The zeta potential of BSA@Rb1 NPs and Man-BSA@Rb1 NPs was -14.4 mV and −20.0 mV, respectively (Figure 2D). These results indicated the successful preparation of BSA@Rb1 NPs and Man-BSA@Rb1 NPs.

The stability and drug release are essential parameters for the efficacy of encapsulated drugs in NPs (Jana et al., 2020; Zhang H.

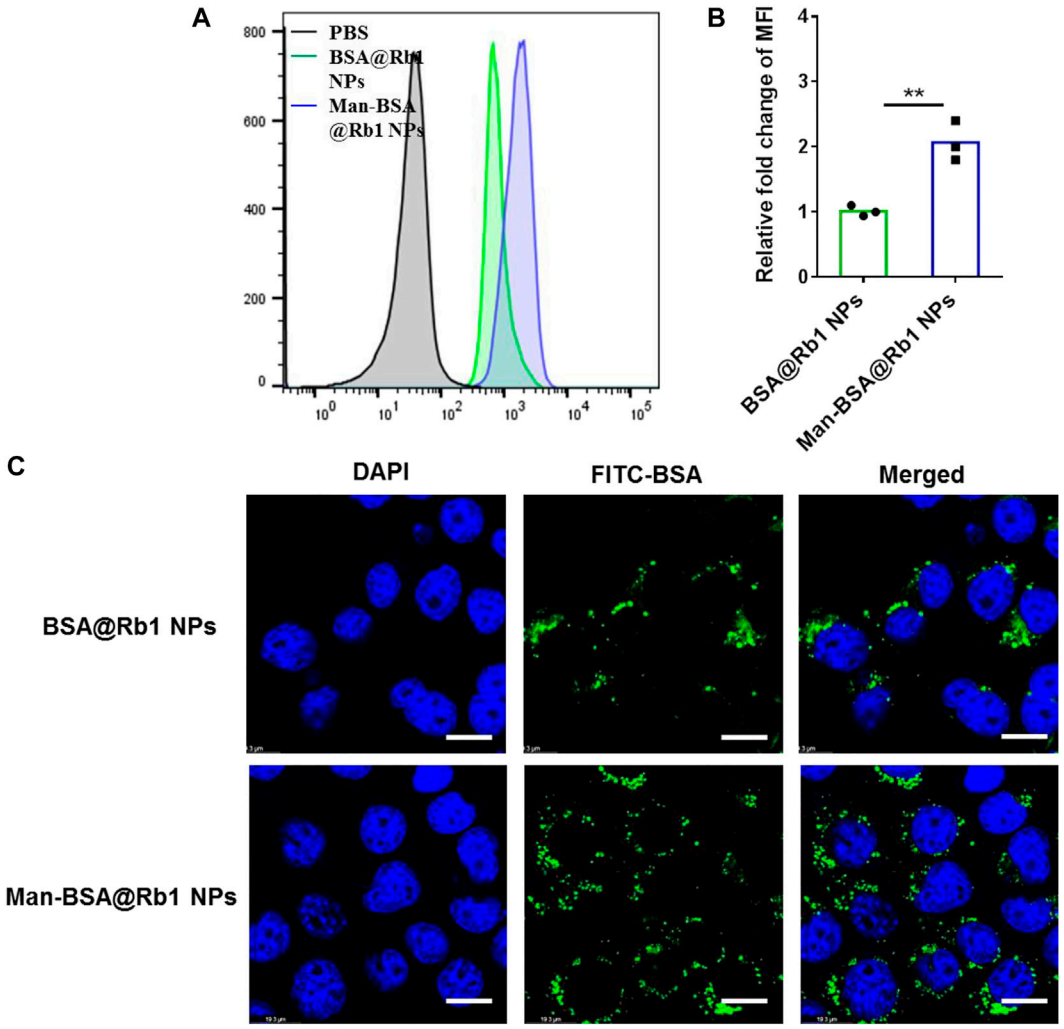

FIGURE 3
Cellular uptake of FITC-labeled Man-BSA@Rb1 NPs. **(A–B)** Flow histogram and MFI detected by flow cytometry. **(C)** Representative images detected by CLSM. Scale bar = 10 μm.

et al., 2021). Therefore, the stability of BSA@Rb1 NPs and Man-BSA@Rb1 NPs was first evaluated in PBS (pH 7.4) media. As shown in Figure 2E, Man-BSA@Rb1 NPs displayed satisfied stability compared with BSA@Rb1 NPs since no significant size change was observed within 24 h. Then, the stability of Man-BSA@Rb1 NPs was further evaluated by incubating Man-BSA@Rb1 NPs in 10% FBS or a combination of PBS (pH 7.4) and 10% FBS. Results indicated that Man-BSA@Rb1 NPs displayed satisfied stability against different media (Supplementary Figure S2). Next, the release profile of Rb1 in NPs exhibited a pH-dependent manner with an increased release rate at pH 5.0 compared to that at pH 7.4. In addition, the cumulative release percentage of Rb1 in BSA@Rb1 NPs was higher than that in Man-BSA@Rb1 NPs at the same time (Figure 2F). Furthermore, the aqueous solution of Man-BSA@Rb1 NPs was clearer than that of BSA@Rb1 NPs and that of Rb1, indicating the enhanced solubility of Rb1 after encapsulating in NPs and the improved hydrophilicity after Man attachment in BSA. As a result, the encapsulation efficiency of Rb1 in BSA@Rb1 NPs and Man-BSA@Rb1 NPs was 65.3 ± 4.5% and 96.7 ± 6.5%, respectively (Supplementary Figure S3A). These results demonstrated the superior properties of Man-BSA@Rb1 NPs in improved solubility of Rb1.

3.2 Cytotoxicity and cellular uptake of Man-BSA@Rb1 NPs

Before the application of Man-BSA@Rb1 NPs in biological functions, we first checked their cytotoxicity in Raw264.7 cells

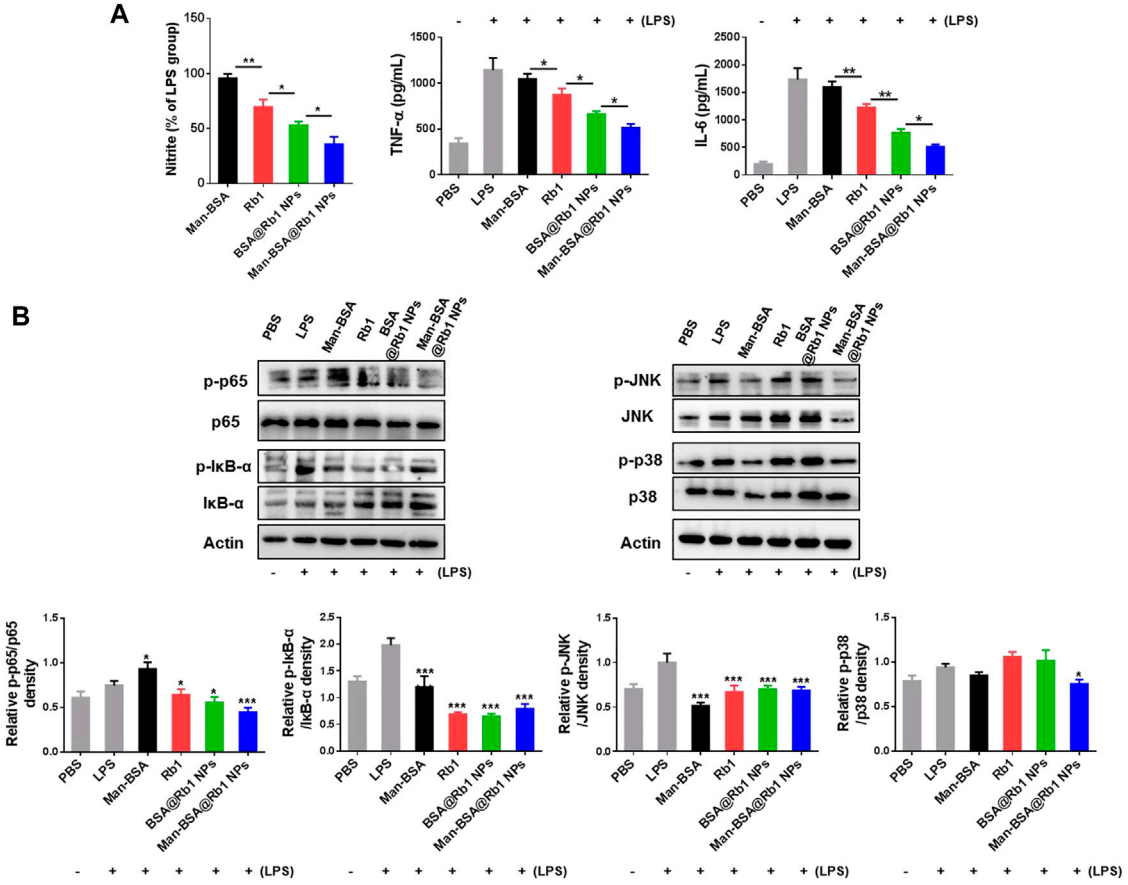

FIGURE 4
Effects of Man-BSA@Rb1 NPs treatment on LPS-induced inflammatory responses in Raw264.7 cells. **(A)** The levels of nitrite, TNF-α, and IL-6 in the medium of Raw264.7 cells. **(B)** The expression of p-p65/p65, p-IκB-α/IκB-α, p-JNK/JNK, and p-p38/p38 in Raw264.7 cells, and their quantitative analysis by ImageJ.

through a CCK8 measurement. As shown in Supplementary Figure S2B, with the increase in concentrations, the carrier of Man-BSA and the drug of Rb1 had no significant effect on the cell viability. However, the cell viability was markedly decreased for Rb1 NPs treatment, especially for Man-BSA@Rb1 NPs (67% viability) when compared with free Rb1 treatment (97% viability) at high concentrations. This result indicated that Rb1 NP formation might increase the cellular uptake of Rb1, leading to enhanced cytotoxicity.

To evaluate the targeting ability of Man-BSA@Rb1 NPs, the cellular uptake of BSA@Rb1 NPs and Man-BSA@Rb1 NPs was evaluated in Raw264.7 cells by flow cytometry and CLSM. FITC-labeled BSA was used as a tool to quantify the accumulation of NPs in cells. As shown in Figures 3A,B, the mean fluorescence intensity (MFI) of FITC in the Man-BSA@Rb1 NP group was ~2 folds as high as that of the BSA@Rb1 NPs group. Furthermore, we confirmed these findings by confocal scanning light microscopy (CLSM), as shown in Figure 3C; the green fluorescence intensity showed an increased manner in the Man-BSA@Rb1 NP group compared with the BSA@Rb1 NP group. These results demonstrated that Man modification could facilitate the uptake and endow the targeting ability of Rb1 NPs, which might be due to the overexpressed Man receptor on macrophages.

3.3 Anti-inflammatory activity of Man-BSA@Rb1 NPs *in vitro*

Some pro-inflammatory cytokines such as nitrite, TNF-α, and IL-6 will be released in the progression of the inflammation occurrence (Yang et al., 2020). To demonstrate the anti-inflammatory activity of Man-BSA@Rb1 NPs, the above mediators were analyzed in LPS-stimulated Raw264.7 cells. As shown in Figure 4A, Man-BSA treatment had no effects on nitrite levels when compared with LPS treatment. Significantly, the main treatments, especially for Man-BSA@Rb1 NP treatment, decreased nitrite levels when compared with Man-BSA treatment. The levels of TNF-α and IL-6 were increased after LPS stimulation, and the main

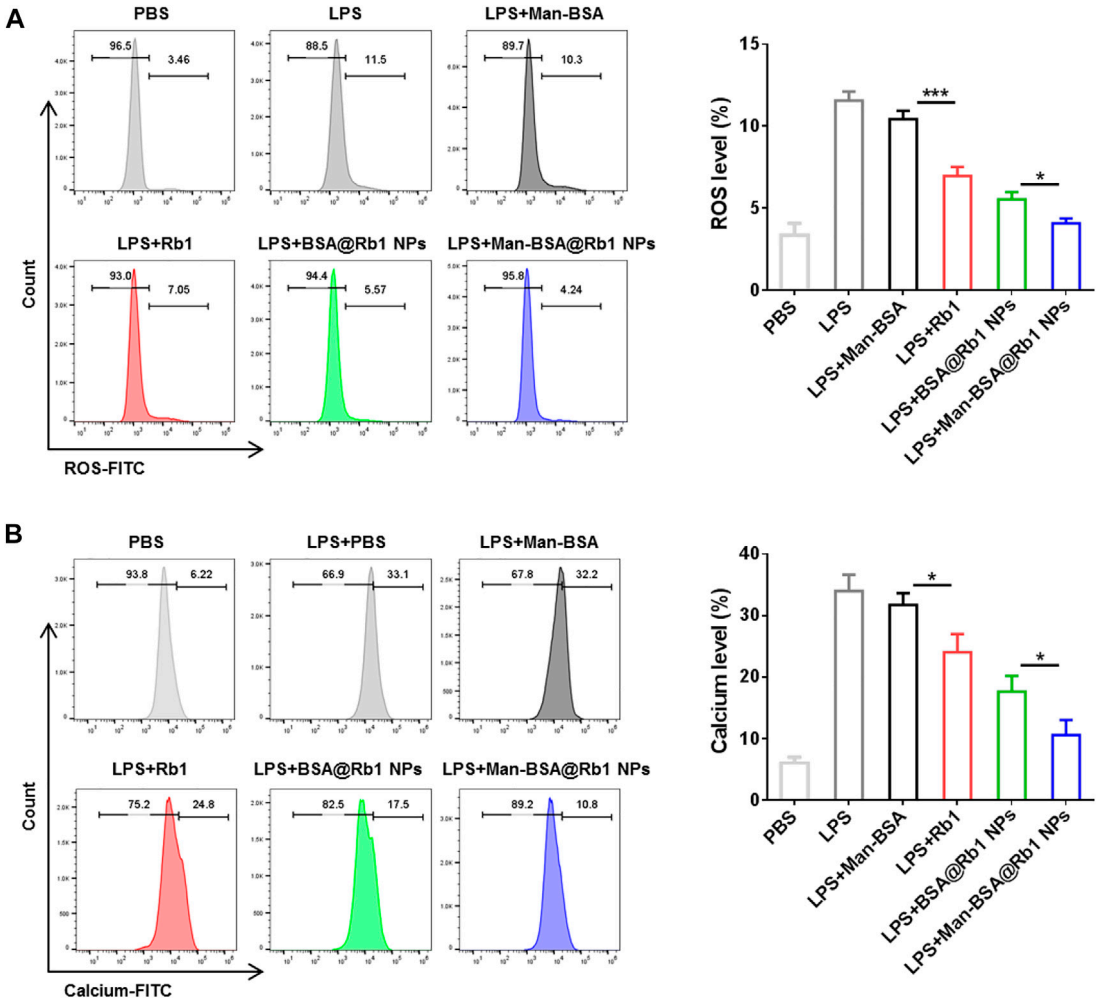

FIGURE 5
Effects of Man-BSA@Rb1 NP treatment on ROS production and Ca^{2+} levels in Raw264.7 cells. **(A)** The ROS levels in Raw264.7 cells determined by flow cytometry. **(B)** The Ca^{2+} levels in Raw264.7 cells determined by flow cytometry.

treatments of Rb1, BSA@Rb1 NPs, and Man-BSA@Rb1 NPs significantly decreased their levels when compared with LPS treatment. Similarly, Man-BSA treatment had no effects on levels of TNF-α and IL-6 when compared with LPS treatment.

The signal pathways involved in macrophage activation and inflammatory responses mainly included the NF-κB and MAPK signaling pathways (Li et al., 2021; Smith and Burger, 2021). Therefore, we evaluated the effects of the above treatments on the expression of p65 and IκB-α (key regulators of NF-κB pathway) and JNK and p38 (key regulators of MAPK pathway) proteins. As shown in Figure 4B, LPS stimulation induced a marked increase in the expression of p-p65 and p-IκB-α, suggesting that LPS led to the activation of the NF-κB pathway in Raw264.7 cells. As anticipated, the main treatments could inhibit its activation by decreasing the expression of p-p65 and p-IκB-α. Notably, the treatment of Man-BSA induced an apparent rise in the expression of p-p65. However, the produced Man-BSA@Rb1 NPs achieved the best silence effect. In addition, LPS stimulation activated JNK and p38 phosphorylation. Compared with other treatment groups, Man-BSA@Rb1 NP treatment exhibited the satisfied silence effect in the expression of p-JNK and p-p38. Interestingly, the carrier of Man-BSA had a positive effect in the expression of p-JNK and p-p38. These results demonstrated that Man-BSA@Rb1 NPs could improve the effects of Rb1 on LPS-induced activation of NF-κB and MAPK pathways.

3.4 Determination of ROS generation and intracellular calcium (Ca^{2+}) levels

ROS generation and Ca^{2+} levels increase are important mediators to reflect the cell damage and inflammation response (Madreiter-

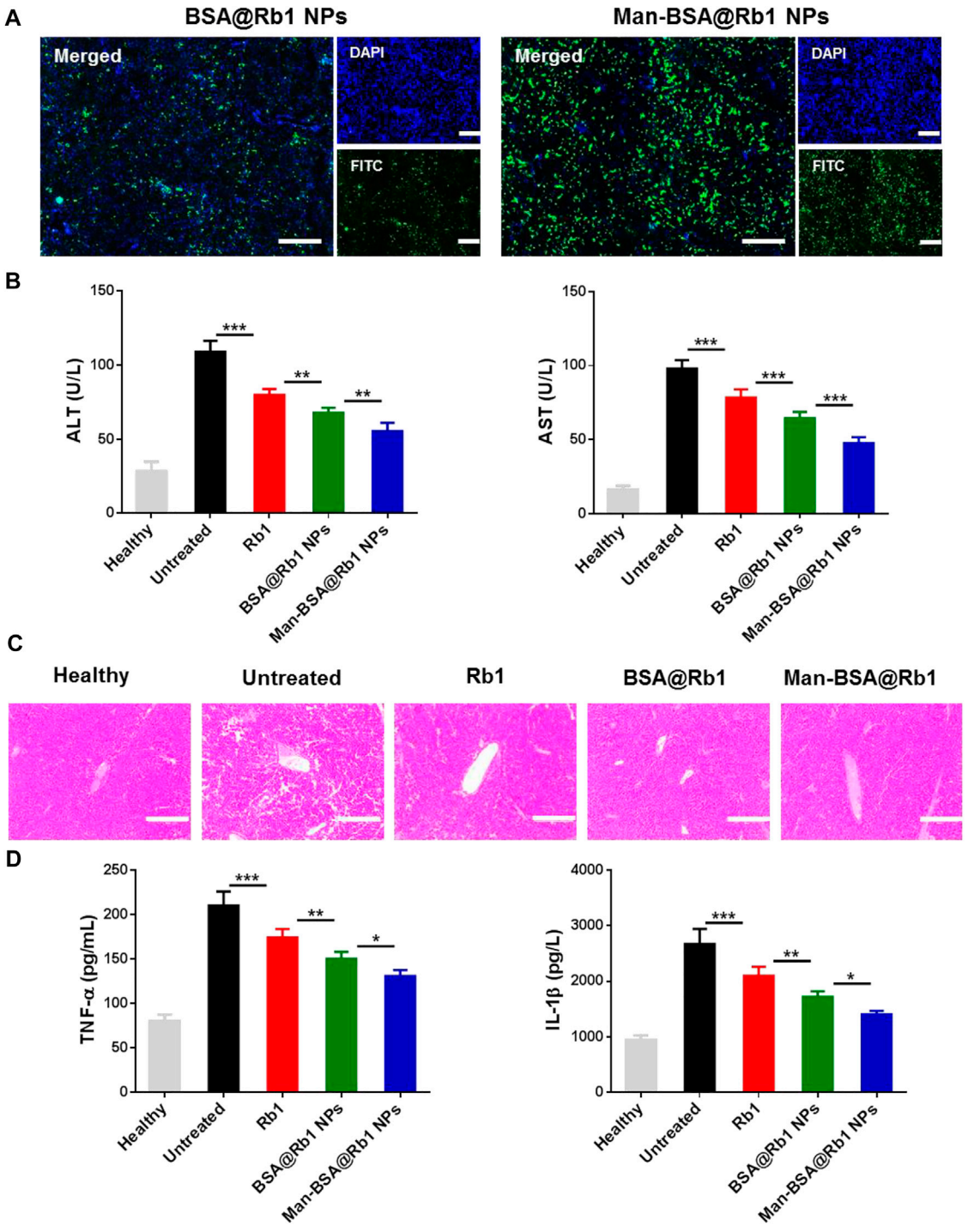

FIGURE 6
Biodistribution and therapeutic efficacy of Man-BSA@Rb1 NPs in d-Gal/LPS-induced liver injury model. **(A)** Analysis of liver accumulation of NPs in liver (scale bar = 200 μm). **(B)** Levels of ALT and AST in serum. **(C)** Representative images of H&E staining of liver tissue sections (scale bar = 200 μm). **(D)** Levels of TNF-α and IL-1β in serum.

Sokolowski et al., 2020). In this study, the effects of Man-BSA@Rb1 NPs on the levels of ROS and Ca^{2+} were evaluated in LPS-induced Raw264.7 cells. As shown in Figure 5, after LPS stimulation, the levels of ROS and Ca^{2+} were significantly increased when compared with the PBS group. The treatments of Rb1 and BSA@Rb1 NPs could effectively decrease the levels of ROS and Ca^{2+}, while

Man-BSA@Rb1 NPs exhibited the best outcome. Interestingly, the delivery carrier of Man-BSA had no effects on the levels of ROS and Ca^{2+}. Therefore, Man-BSA might be a potential carrier to improve the anti-inflammatory activity of Rb1, which was also demonstrated in the aforementioned results.

3.5 Liver accumulation and therapeutic efficacy of Man-BSA@Rb1 NPs *in vivo*

After demonstrating the targeting ability of Man-BSA@Rb1 NPs *in vitro*, their targeting ability was next evaluated by detecting the liver accumulation in injured liver using BSA@Rb1 NPs as controls. As shown in Figure 6A, a strong fluorescent signal was observed in the Man-BSA@Rb1 NP group, while the BSA@Rb1 NP group exhibited the weakest fluorescent signal. Therefore, Man-BSA@Rb1 NP treatment was expected to achieve the best therapeutic efficacy due to the increased Rb1 delivery to the liver.

Next, the anti-inflammatory activity of Man-BSA@Rb1 NPs was evaluated in Gal/LPS-induced liver injury model. The related therapeutic efficacy was assessed by detecting serum levels of ALT and AST (key biomarkers of liver function), analyzing H&E staining of liver sections (histological analysis of liver morphology), and testing the change in TNF-α and IL-1β levels (key mediators of pro-inflammatory factor). As shown in Figure 6B, ALT and AST levels were significantly increased in the untreated group compared with the healthy group. After different treatments, especially for Man-BSA@Rb1 NPs, ALT and AST levels were decreased compared with the untreated group. In Figures 6C, D, H&E results also revealed that the liver structure tended to be normal when compared with the untreated group. Alterations in the pattern of TNF-α and IL-1β levels resembled the trend of ALT and AST levels.

3.6 The safety evaluation of Man-BSA@Rb1 NPs *in vivo*

The potential toxicities of the adopted carrier are ignored factors for the application of the loaded drug. Therefore, the *in vivo* safety of Man-BSA@Rb1 NPs was evaluated by monitoring the liver function, histological section of major organs, and levels of inflammatory cells (Supplementary Figure S3). The results showed that there was no significant change in the levels of ALT and AST between the saline group and Man-BSA@Rb1 NPs. In addition, no pathological change was found in the Man-BSA@Rb1 NP group compared with the saline group, indicating the good biocompatibility of Man-BSA@Rb1 NPs in major organs. The blood analysis of white blood cells (WBCs), lymphocytes, and neutrophils were also performed, and results showed that there was no notable change in the number of blood cells between the Man-BSA@Rb1 NP group and the saline group. Moreover, the hemolytic activity of Man-BSA@Rb1 NPs was evaluated, and results showed that Man-BSA@Rb1 NP treatment exhibited the negligible level of hemolysis.

4 Conclusion

In summary, we have engineered a novel delivery carrier of Man-BSA, which can simultaneously increase Rb1 solubility and endow Rb1 NPs with targeting ability. The fabricated Man-BSA@Rb1 NPs showed attractive properties with a uniform size distribution, spherical shape, high encapsulation efficacy, satisfying stability, and pH-dependent release. The cellular uptake and liver distribution studies demonstrated that Man modification could increase the accumulation of BSA@Rb1 NPs in cells and liver. The improved anti-inflammatory efficacy of Man-BSA@Rb1 NPs was demonstrated in LPS-induced Raw264.7 cells *in vitro* and d-Gal/LPS-induced liver injury model *in vivo*. The related molecular mechanisms were potently involved by inhibiting NF-κB and MAPK signaling pathways, including p-p65/p65, p-IκB-α/IκB-α, p-JNK/JNK, and p-p38/p38 proteins. In addition, Man-BSA@Rb1 NPs exhibited acceptable biosafety *in vivo*. The results presented in this study demonstrate that Man-BSA can play the ideal carrier for Rb1 delivery, which has the potential as an effective delivery platform for enhanced anti-inflammatory therapy.

Data availability statement

The raw data supporting the conclusion of this article will be made available by the authors, without undue reservation.

Ethics statement

The animal study was reviewed and approved by the Animal Care and Use Committee of the First Affiliated Hospital of Zhengzhou University.

Author contributions

ZF, KW, and HF developed the concept of the study, and designed the study. ZF, XW, and XL performed experiments. ZF, YY, and LLZ performed data and statistical analyses. ZF, LZ, and XW wrote the manuscript. KW and HF supervised the whole study. All authors reviewed the manuscript.

Funding

This research was supported by the Science and Technology Development Project of Henan Province (212102310346), the Key Scientific Research Project of Institutions of Higher Learning in Henan Province (21A360026), and Youth Fund of the First Affiliated Hospital of Zhengzhou University (YNQN2017198).

Conflict of interest

The authors declare that the research was conducted in the absence of any commercial or financial relationships that could be construed as a potential conflict of interest.

Publisher's note

All claims expressed in this article are solely those of the authors and do not necessarily represent those of their affiliated organizations, or those of the publisher, the editors, and the reviewers. Any product that may be evaluated in this article, or claim that may be made by its manufacturer, is not guaranteed or endorsed by the publisher.

Supplementary material

The Supplementary Material for this article can be found online at: https://www.frontiersin.org/articles/10.3389/fbioe.2022.962380/full#supplementary-material

References

Chen, F., Huang, G., and Huang, H. (2020). Sugar ligand-mediated drug delivery. *Future Med. Chem.* 12, 161–171. doi:10.4155/fmc-2019-0114

Chen, H., Zhao, Y., Li, R., Chen, B., Luo, Z., Shi, Y., et al. (2021). Preparation and *in vitro* and *in vivo* evaluation of panax notoginseng saponins-loaded nanoparticles coated with trimethyl chitosan derivatives. *J. Pharm. Sci.* 111, 1659–1666. doi:10.1016/j.xphs.2021.11.002

Dong, Y., Fu, R., Yang, J., Ma, P., Liang, L., Mi, Y., et al. (2019). Folic acid-modified Ginsenoside rg5-loaded bovine serum albumin nanoparticles for targeted cancer therapy *in vitro* and *in vivo*. *Int. J. Nanomedicine* 14, 6971–6988. doi:10.2147/ijn.s210882

Hama, M., Ishima, Y., Chuang, V. T. G., Ando, H., Shimizu, T., and Ishida, T. (2021). Evidence for delivery of abraxane via A denatured-albumin transport system. *ACS Appl. Mat. Interfaces* 13, 19736–19744. doi:10.1021/acsami.1c03065

Jana, B. A., Shinde, U., and Wadhwani, A. (2020). Synthetic enzyme-based nanoparticles act as smart catalyst for glucose responsive release of insulin. *J. Biotechnol.* 324, 1–6. doi:10.1016/j.jbiotec.2020.09.023

Jaynes, J. M., and Sable, R. (2020). Mannose receptor (Cd206) activation in tumor-associated macrophages enhances adaptive and innate antitumor immune responses. *Sci. Transl. Med.* 12 (530), eaax6337. doi:10.1126/scitranslmed.aax6337

Jiang, L., Yin, X., Chen, Y. H., Chen, Y., Jiang, W., Zheng, H., et al. (2021). Proteomic analysis reveals Ginsenoside Rb1 attenuates myocardial ischemia/reperfusion injury through inhibiting ros production from mitochondrial complex I. *Theranostics* 11, 1703–1720. doi:10.7150/thno.43895

Lei, C., Liu, X. R., Chen, Q. B., Li, Y., Zhou, J. L., Zhou, L. Y., et al. (2021). Hyaluronic acid and albumin based nanoparticles for drug delivery. *J. Control. Release* 331, 416–433. doi:10.1016/j.jconrel.2021.01.033

Li, S., Wang, H., Ma, R., and Wang, L. (2021). Schisandrin B inhibits epithelial-mesenchymal transition and stemness of large-cell lung cancer cells and tumorigenesis in xenografts via inhibiting the nf-?b and P38 mapk signaling pathways. *Oncol. Rep.* 45, 115. doi:10.3892/or.2021.8066

Li, Z., Wang, Y., Liu, J., Rawding, P., Bu, J., Hong, S., et al. (2021b). Chemically and biologically engineered bacteria-based delivery systems for emerging diagnosis and advanced therapy. *Adv. Mater.* 33, E2102580. doi:10.1002/adma.202102580

Li, Z., and Wang, Y. (2020). Targeting pulmonary tumor microenvironment with cxcr4-inhibiting nanocomplex to enhance anti-Pd-L1 immunotherapy. *Sci. Adv.* 6, Eaaz9240. doi:10.1126/sciadv.aaz9240

Madreiter-Sokolowski, C. T., Thomas, C., and Ristow, M. (2020). Interrelation between ros and Ca(2+) in aging and age-related diseases. *Redox Biol.* 36, 101678. doi:10.1016/j.redox.2020.101678

Mazzaferro, E. M., and Edwards, T. (2020). Update on albumin therapy in critical illness. *Veterinary Clin. N. Am. Small Animal Pract.* 50, 1289–1305. doi:10.1016/j.cvsm.2020.07.005

Mitchell, M. J., Billingsley, M. M., Haley, R. M., Wechsler, M. E., Peppas, N. A., and Langer, R. (2021). Engineering precision nanoparticles for drug delivery. *Nat. Rev. Drug Discov.* 20, 101–124. doi:10.1038/s41573-020-0090-8

Mizuta, Y., Maeda, H., Ishima, Y., Minayoshi, Y., Ichimizu, S., Kinoshita, R., et al. (2021). A mannosylated, pegylated albumin as A drug delivery system for the treatment of cancer stroma cells. *Adv. Funct. Mat.* 31, 2104136. doi:10.1002/adfm.202104136

Sleep, D. (2015). Albumin and its application in drug delivery. *Expert Opin. Drug Deliv.* 12, 793–812. doi:10.1517/17425247.2015.993313

Smith, C. I. E., and Burger, J. A. (2021). Resistance mutations to btk inhibitors originate from the nf-?b but not from the pi3k-ras-mapk arm of the B cell receptor signaling pathway. *Front. Immunol.* 12, 689472. doi:10.3389/fimmu.2021.689472

Su, G., Jiang, H., Xu, B., Yu, Y., and Chen, X. (2018). Effects of protein corona on active and passive targeting of cyclic rgd peptide-functionalized pegylation nanoparticles. *Mol. Pharm.* 15, 5019–5030. doi:10.1021/acs.molpharmaceut.8b00612

Torretta, S., Scagliola, A., Ricci, L., Mainini, F., Di Marco, S., Cuccovillo, I., et al. (2020). D-mannose suppresses macrophage IL-1β production. *Nat. Commun.* 11, 6343. doi:10.1038/s41467-020-20164-6

Wang, J., Jalali Motlagh, N., and Wang, C. (2021). D-mannose suppresses oxidative response and blocks phagocytosis in experimental neuroinflammation. *Biol. Sci.* 118 (44), e2107663118. doi:10.1073/pnas.21076631

Wang, Q., Zhou, X., Yang, L., Zhao, Y., Chew, Z., Xiao, J., et al. (2020a). The natural compound notopterol binds and targets jak2/3 to ameliorate inflammation and arthritis. *Cell Rep.* 32, 108158. doi:10.1016/j.celrep.2020.108158

Wang, Z., Kong, L., Tan, S., Zhang, Y., Song, X., Wang, T., et al. (2020b). Zhx2 accelerates sepsis by promoting macrophage glycolysis via Pfkfb3. *J. I.* 204, 2232–2241. doi:10.4049/jimmunol.1901246

Wu, P., Luo, X., Wu, H., Zhang, Q., Dai, Y., Sun, M., et al. (2020). Efficient and targeted chemo-gene delivery with self-assembled fluoro-nanoparticles for liver fibrosis therapy and recurrence. *Biomaterials* 261, 120311. doi:10.1016/j.biomaterials.2020.120311

Yang, Y., Li, S., Qu, Y., Wang, X., An, W., Li, Z., et al. (2020). Nitrate partially inhibits lipopolysaccharide-induced inflammation by maintaining mitochondrial function. *J. Int. Med. Res.* 48, 030006052090260. doi:10.1177/0300060520902605

Yin, M., Lin, J., Yang, M., Li, C., Wu, P., Zou, J., et al. (2022). Platelet membrane-cloaked selenium/ginsenoside Rb1 nanosystem As biomimetic reactor for atherosclerosis therapy. *Colloids Surfaces B Biointerfaces* 214, 112464. doi:10.1016/j.colsurfb.2022.112464

Zhang, H., Feng, H., Ling, J., Ouyang, X. K., and Song, X. (2021a). Enhancing the stability of zein/fucoidan composite nanoparticles with calcium ions for quercetin delivery. *Int. J. Biol. Macromol.* 193, 2070–2078. doi:10.1016/j.ijbiomac.2021.11.039

Zhang, L., Liu, F., Li, G., Zhou, Y., and Yang, Y. (2015). Twin-arginine translocation peptide conjugated epirubicin-loaded nanoparticles for enhanced tumor penetrating and targeting. *J. Pharm. Sci.* 104, 4185–4196. doi:10.1002/jps.24649

Zhang, X., Wang, L., Guo, R., Xiao, J., Liu, X., Dong, M., et al. (2021b). Ginsenoside Rb1 ameliorates diabetic arterial stiffening via

ampk pathway. *Front. Pharmacol.* 12, 753881. doi:10.3389/fphar.2021.753881

Zhao, Y., Zheng, Y., Zhu, Y., Zhang, Y., Zhu, H., and Liu, T., (2021). M1 macrophage-derived exosomes loaded with gemcitabine and deferasirox against chemoresistant pancreatic cancer. *Pharmaceutics* 13, 1493. doi:10.3390/pharmaceutics13091493

Zhou, S., Lu, S., Guo, S., Zhao, L., Han, Z., and Li, Z., (2021). Protective effect of Ginsenoside Rb1 nanoparticles against contrast-induced nephropathy by inhibiting high mobility group box 1 gene/toll-like receptor 4/nf-?b signaling pathway. *J. Biomed. Nanotechnol.* 17, 2085–2098. doi:10.1166/jbn.2021.3163

Zhou, X., Li, W., Wang, S., Zhang, P., Wang, Q., Xiao, J., et al. (2019). Yap aggravates inflammatory bowel disease by regulating M1/M2 macrophage polarization and gut microbial homeostasis. *Cell Rep.* 27, 1176–1189.e5. E5. doi:10.1016/j.celrep.2019.03.028

Zhu, H., Zhang, S., Ling, Y., Meng, G., Yang, Y., Zhang, W., et al. (2015). Ph-responsive hybrid quantum dots for targeting hypoxic tumor sirna delivery. *J. Control. Release* 220, 529–544. doi:10.1016/j.jconrel.2015.11.017

Zhou, P., and Xie, W. 2019. Ginsenoside rb1 as an anti-diabetic agent and Its underlying mechanism analysis. *Cells* 8(3), 204. doi:10.3390/cells8030204

frontiers | Frontiers in Bioengineering and Biotechnology

TYPE Original Research
PUBLISHED 16 August 2022
DOI 10.3389/fbioe.2022.978846

OPEN ACCESS

EDITED BY
Yu Zhao,
Tufts University, United States

REVIEWED BY
Amir Mirzaie,
Islamic Azad University of Parand, Iran
Donghui Song,
Tufts University, United States

*CORRESPONDENCE
Josthna Penchalaneni,
penchalanenijyo@gmail.com

†These authors have contributed equally to this work

SPECIALTY SECTION
This article was submitted to Nanobiotechnology, a section of the journal Frontiers in Bioengineering and Biotechnology

RECEIVED 26 June 2022
ACCEPTED 20 July 2022
PUBLISHED 16 August 2022

CITATION
Lavudi K, Harika VS, Kokkanti RR, Patchigolla S, Sinha A, Patnaik S and Penchalaneni J (2022), 2-Dimensional *in vitro* culture assessment of ovarian cancer cell line using cost effective silver nanoparticles from *Macrotyloma uniflorum* seed extracts. *Front. Bioeng. Biotechnol.* 10:978846. doi: 10.3389/fbioe.2022.978846

2-Dimensional *in vitro* culture assessment of ovarian cancer cell line using cost effective silver nanoparticles from *Macrotyloma uniflorum* seed extracts

Kousalya Lavudi[1†], Venkata Satya Harika[2], Rekha Rani Kokkanti[2†], Swaroopa Patchigolla[2], Anupriya Sinha[1], Srinivas Patnaik[1] and Josthna Penchalaneni[2*]

[1]KIIT School of Biotechnology, KIIT University, Bhubaneswar, Odisha, India, [2]Department of Biotechnology, Sri Padmavati Mahila Visva Vidyalayam, Tirupati, Andhra Pradesh, India

Our research focused on generating AgNPs using *Macrotyloma uniflorum* (MU) seed extracts and studied their efficacy in combating tumor growth using the 2-Dimensional method for ovarian cancer cell line-PA-1. Characterization studies including a UV-visible spectrophotometer confirmed the surface plasmon resonance peak of 436 nm. Particle size determination data validated the nanoparticle diameter of 91.8 nm. Synthesized AgNPs possess a negative charge of -28.0 mV, which was confirmed through the zeta potential study. Structural characterization studies including XRD determined the crystal phase of AgNPs at four distant peaks at 2θ (38.17, 44.36, 64.52, and 77.46) and were assigned to 111, 200, 220, and 311 planes of the FCC. FTIR studies have confirmed the presence of O-H, N-H, C=O, ethers, C-Br, and C-I groups in AgNPs respectively. DPPH study has confirmed the presence of free radicles and we observed that at 500 µg/ml concentration, 76.08% of free radicles were formed which shows their efficiency. MTT assay shows the efficacy of MU-AgNPs in reducing the cell viability. At lower concentrations of MU-AgNP, 66% viability was observed and 9% of viability was observed at higher dose. ROS production (21%) was observed using MU-AgNPs with respect to 0.45% in controls, which affirms the capacity to induce DNA damage via apoptosis. Standard drug camptothecin generated 26% of ROS production which confirms higher potential of AgNPs in inducing DNA damage in tumor cells without causing lethality to the healthy cells. Further, the Fluorescence-activated cell sorting (FACS) study using a standard Caspase-3 marker confirms the generation of apoptotic bodies using two different concentrations of MU-AgNPs. At 40 µg, 64% of apoptotic cell death was observed, whereas, using 20 µg, 23% of apoptosis was recorded via fluorescent intensity. Propidium iodide-based Cell cycle study has shown a significant decrease in G0/G1 phase compared to control (88.8%), which further confirmed the apoptotic induction. Matrix metalloproteinases (MMP) studies using JC-1 dye, showed a significant increase in green fluorescence owing to lowered membrane potential, thus ensuring the breakdown of mitochondrial potential compared to untreated and standard drugs. With the obtained results, we are

concluding that MU-AgNPs has a tremendous capacity to suppress the ovarian cancer cell proliferation *in vitro* by inducing DNA damage and apoptosis.

KEYWORDS

***in vitro* studies, Mitochondria membrane potential, ovarian cancer, *Macrotyloma uniflorum*, AgNPs**

1 Introduction

Nanoparticles are widely used in industry, cosmetics, biotechnology, and nanomedicine due to their unique features and numerous applications. In recent years, research on metallic nanoparticle applications has become one of the most fascinating fields all around the world (Sagadevan et al., 2020). Among them, biomedical application usage has a vast contribution (Yesilot and Aydin, 2019; Karmous et al., 2020). One of the most widely used and commercialized nanomaterials are silver nanoparticles (AgNPs) gaining popularity due to their broad range of applications in biomedicine. Because of their distinctive qualities, such as photonic and catalytic features, antibacterial, anticancer, and antiangiogenic drugs are all made with AgNPs. They could potentially be utilized in the development of novel and better functional materials (Ghosh, 2019; Sanjay, 2019; Silva et al., 2019). AgNPs are nanoparticles with unique physico-chemical properties ranging from 10 to 100 nm in size. Biological approaches, among the multiple synthetic methods for AgNPs, appear to be simple, rapid, non-toxic, reliable, and green procedures that may produce size and shape that are well defined under ideal conditions for traditional study. Plant-mediated AgNPs are non-toxic, environmentally beneficial, cost-effective, and quickly produced while also acting as reducing, stabilizing, and capping agents. Thus, compared to chemical and physical procedures, the green method of synthesizing AgNPs has several advantages. Green nanoparticles have a high production, solubility, and stability. Metallic nanoparticles that contain medicinal herbs have powerful anti-tumor properties. These metal nanoparticles containing herbs have been utilized to treat ovarian, prostate, oesophageal, stomach and lung cancers, and numerous leukemias in recent years (Shaneza et al., 2018; Mahdavi et al., 2019; Li et al., 2020; Liu et al., 2020).

Ovarian cancer is the world's second most prevalent gynaecological malignancy, and the fifth most common cancer overall (Momenimovahed et al., 2019). Obesity and overweight, gynaecological surgery, hormone therapy, breast cancer, age, family history, reproductive history, human, talcum powder, and HPV are all variables that increase the risk of ovarian cancer (Ebell et al., 2016). Ovarian cancer started as a single aberrant cell that spread throughout the uterus and the rest of the body (Grossmann et al., 2018). Lethargy, weight loss, nausea, bloating, backpain, early satiety, abdominal pain, constipation, sudden vaginal bleeding, urine frequency, bloating, and dyspnoea are all the signs and symptoms of ovarian cancer. Blood tests, biopsy, laparoscopy, pelvic ultrasound and imaging tests like MRI (magnetic resonance imaging), CT scan (computed tomography), PET scan (positron emission tomography), Chest X-ray are all used to diagnose ovarian cancer (Grossmann et al., 2018). Most cases are discovered after they have progressed to an advanced stage (Vargas, 2014). In women with ovarian cancer, preliminary treatment included surgery followed by platinum-based chemotherapy (Brastasz et al., 2006). Even though majority of women respond to first treatment, chemoresistance develops with time. Cancer recurrence is aided by the great degree of heterogeneity found within ovarian tumors, which is a major feature of the disease, as well as between different ovarian cancer subtypes. Chemotherapy, immunotherapy, and radiation therapy are all used by many clinicians to treat various types of malignancies. Patients with ovarian cancer benefit from a combination of chemotherapy at first, but resistance develops over time (Pokhriyal et al., 2019). Chemotherapeutic medications have a negative impact on the body, so developing an effective chemotherapy treatment using metallic nanoparticles is critical nowadays. Natural product exploitation is one of the most effective strategies for discovering new hits and leads among the numerous tactics (Newman and Cragg, 2012).

Reactive oxygen species (ROS) are the main source of cellular oxidative stress. The regulation of ROS equilibrium is crucial for cellular development, metabolism, and survival (Kim et al., 2016). For tumor formation, ROS can be a two-edged sword (Srinivas et al., 2019). ROS-induced oxidative DNA damage, on the other hand, may cause cell death (Wang et al., 2020). One strategy for tumor cells to achieve this goal is to increase the expression of redox protection proteins, which helps to control intracellular ROS levels (Azzouz et al., 2021). This adaptation would allow the tumor-promoting effects of ROS to be separated from their tumor-suppressive effects (Preya et al., 2017). The increased levels of superoxide radicals fluctuate the mitochondrial transmembrane potential and disrupt the signalling pathway, causing apoptosis and cell death (Fani et al., 2016; Kim et al., 2017). Increased ROS generation damages biological components, including DNA fragmentation, lipid membrane peroxidation, and protein carbonylation. Caspases 3 and 9 are activated by altered mitochondrial membrane potential, resulting in cellular death. It then stimulates a number of downstream signalling pathways, resulting in the creation of apoptotic bodies and cell cycle arrest (Ratan et al., 2020). Cell death in tumor cells is triggered by an increase in ROS, cell cycle arrest, and caspase-3 activation (Kumari et al., 2020). Furthermore, ovarian cancer has been

linked to the damaging effects of ROS by reducing the production of antioxidant enzymes (Jiang et al., 2011).

Because of its simplicity and eco-friendliness, plant-mediated biological nanoparticle production has gained popularity in recent years. Plants are a better platform for production of nanoparticles since they are free of hazardous chemicals and contain natural capping agents. Many medicinal plants are used to treat ovarian cancer in traditional medicine, including *Allium sativum*, *Zingiber officinale*, *Dioscorea bulbifera*, *Camellia sinensis*, *Quercus tinctoria*, *Camptotheca acuminate*, *Piper capense*, *Podophyllum peltatum*, *Albizia schimperiana*, *Taxus brevifolia*, *Azadirachta indica*, *Asparagus racemosus*, *Ginkgo biloba*, *Symplocus racemosa*, *Saraca indica*, and *Solanum aculeastrum* (Palanisamy et al., 2021; Aman et al., 2018). Metal nanoparticles produced and manufactured using these plants are expected to have substantially better anti-cancer effects against ovarian cancer cells. Plant-mediated AgNPs have been shown to exhibit anticancer properties in PA-1 (Ovarian cancer cells) (Palle et al., 2020). The G1 phase cell division was delayed by these green synthesized AgNPs, demonstrating that AgNPs can control the cell cycle and limit cell proliferation (Javed and Mashwani, 2020).

Macrotyloma uniflorum Linn. (Horsegram), is one of the less well-known grain legume species belonging to family Fabaceae (Singh et al., 2013). In many parts of India, *Macrotyloma uniflorum* grains are commonly consumed as a green vegetable and are believed to be high in protein and have medicinal benefits (Prasad and Singh, 2015). Horse Gram seeds contain bioactive compounds such as phenolic acids and isoflavonones, which play a key role in enhancing antioxidant enzymes in cancer cells thus imparting anticancer properties (Ingle, et al., 2020). Horsegram, is used for asthma, bronchitis, leukoderma, urine discharges, kidney stones, and heart disease, according to traditional medical sources (Marimuthu and Krishnamoorthi, 2013). Green synthesized AgNPs made from a bioactive fraction of *M. uniflorum* was found to have anti-cancer properties (Anjum et al., 2021). Despite the fact that horse Gram is thought to play a key role in modern diets, little research has been done on its cytotoxic effects. *M. uniflorum* seed methanolic extract is used to make silver nanoparticles in this study. The synthesized nanoparticles using *Macrotyloma Uniflorum*, hereafter mentioned as (MU-AgNPs) were examined using a variety of analytical methods. The biological activity was tested against a common ovarian cancer cell line, PA-1, for antioxidant, cytotoxicity, and anticancer properties.

2 Materials and methods

2.1 Seed collection

Macrotyloma uniflorum seeds were obtained from local markets in Tamilnadu, India. Identification and confirmation of these seeds was done by Dr. B. Nagaraj, Dept. of Botany, Sri Venkateswara University, Tirupati, India. The seeds were washed by removing stones and dried in a shady place. They were then pulverised into a fine powder, sieved, labelled, and kept in a zip lock cover for future investigations.

2.2 Plant extract preparation

Coarsely powdered seeds of *M. uniflorum* was used for extraction using methanol solvent. 5 g of powder was mixed with 100 ml of methanol in a thimble of soxhlet apparatus and extracted for 6 h at 64°C. The extract was weighed after being evaporated in a rotary flash evaporator at 64°C at 100 rpm and air dried at 25–35°C. The sample was collected and stored in a scintillation tube for later use.

2.3 Synthesis of *M. uniflorum* silver nanoparticles

To make up the volume to 5 ml, 2 ml of extracted material was mixed with 3 ml of distilled water. The extract was treated with 10 ml of a 1 mM $AgNO_3$ solution, and the tubes were kept in a water bath at 70–80°C for 20 min to allow the reduction reaction to take place. The presence of silver nanoparticles was confirmed by a shift in color from pale yellow to brown in the solution (AgNPs).

2.4 Characterization of biosynthesized MU-AgNPs

The UV-Visible spectrophotometer (NanoDrop 8,000 Spectrophotometer) in the 200–600 nm range was used to characterize the biosynthesized AgNPs. The crystalline structure of AgNPs was investigated using X-ray diffraction (XRD) was recorded using the XRD6000 (Shimadzu) in the 2θ range (30–80) (Shimadzu IR). The presence of functional groups in MU-AgNPs was detected using the potassium bromide (KBr) pellet approach on a Shimadzu IR 8400 FTIR (Fourier transform-infrared spectrum) Spectrophotometer (Shimadzu IR) in the 4,000–400 cm^{-1} range. Philips EM208S was used to record transmission electron microscopy (TEM) images to assess the size and shape of AgNPs. The average particle size distribution, hydrodynamic diameter, stability, and polydispersity index (PdI) of MU-AgNPs were determined and measured using a dynamic light scattering (DLS) particle size and a zeta potential analyzer (Horiba Nanopartica SZ-100 Nanoparticle analyzer). The clear nanoparticles solution was used for this analysis after the samples were filtered using 0.2 mm syringe filters, with measurements conducted at the appropriate range.

2.5 Antibacterial activity of MU-AgNPs

Anti-bacterial activity was tested against *Escherichia coli*, *Bacillus subtilis*, *Klebsiella pneumonia*, and *Staphylococcus aureus* on nutrient agar plates. Using an L-shaped glass rod, bacterial cultures were evenly dispersed on the surface of the solidified agar media in Petri dishes overnight. 5 mm diameter discs were made using sterile Whatman filter No. 1 paper, and discs were placed equidistantly on each of the inoculated Petri plates with the help of sterile forceps. By using a micropipette and sterile micropipette tips, biosynthesized silver nanoparticles at various concentrations ranging from10–40 μg/ml were added to the discs. The centre of the plate was filled with 30 μl of crude sample disc. Antibiotic disc plates were made by placing levofloxacin antibiotic discs in the centre of the agar plates as a positive control and incubating them overnight or for 12–16 h at 37°C. The clear zone appeared after incubation was measured as an inhibitory zone (Cos et al., 2006).

2.6 DPPH activity of MU-AgNPs

The free radical scavenging assay was determined with the 2,2-Diphenyl-1-picrylhydrazyl radical (DPPH) (Tahvilian et al., 2019). Different concentrations of green synthesized nano and crude samples were taken, 100–500 μg/ml, and made the final volume of 2 ml by adding methanol. To each tube, 1 ml of DPPH was added. The absorbance of the mixtures was measured at 570 nm after 30 min of incubation in dark. 3 ml of DPPH was used as a control. MU-AgNPs and the plant crude extracts were measured and expressed as percentage of inhibition (%).

$$\text{Inhibition (\%)} = \frac{[\text{Abs}]\ \text{control} - [\text{Abs}]\ \text{sample}}{[\text{Abs}]\ \text{control}} X100 \quad (1)$$

2.7 Anti-cancer activity of MU-AgNPs

The antitumor activity of MU-AgNPs was assessed *in vitro* using the MTT (3-(4,5-dimethylthiazol-2-yl)-2,5-diphenyltetrazolium bromide) method against PA-1 cells (You et al., 2012). In a nutshell, cells were grown and maintained in DMEM (Dulbecco's modified Eagle's medium) pH 7.4 with 10% foetal bovine serum (FBS), glutamine (2 mM), penicillin—streptomycin (100 mg/ml). Cells were seeded at a density of 0.1 million in a 96 well plates. After 24 h, the cells were treated with different concentrations of MU-AgNPs ranging from 50–300 μg/ml. After 24 h treatment, each well was filled with 15 μl of MTT (5 mg/ml) in phosphate buffered saline (PBS) and incubated for 4 h at 37°C. The MTT medium was then flicked off, and the formazan crystals that had formed were dissolved in 100 μl of dissolving solution before being measured at 570 nm with a microplate reader. Data was plotted by calculating the viability percentage.

$$\frac{[\text{Abs}]\ \text{Test}}{[\text{Abs}]\text{control}} \text{ x } 100 = \text{Percentage of cell viability} \quad (2)$$

$$\frac{100 - \text{Abs (sample)}}{\text{Abs (control)}} \text{ x } 100 = \text{Percentage of cell inhibition} \quad (3)$$

2.8 Flow cytometric analysis using propidium iodide

PA-1 cells were planted at a density of $1*10^5$ cells per well in a 6-well plate and cultured for 24 h at 37°C in a CO_2 incubator. The cells were treated the next day with the drug, MU-AgNPs, based on the IC_{50} value. The cell control received no treatment. The treatment was administered for two different periods of time, namely 24 and 48 h. Cells were trypsinized and centrifuged at 8,000 rpm for 5 min and the pellet was collected. The cells were rinsed in cold PBS and 1 ml of 70% chilled ethanol was added by vortexing. Ethanol was removed by centrifuging at 2000 rpm for 15 min at 4°C followed by a PBS wash. 50 μl of RNase A was added to the pellet and incubated for 30 min at 37°C. The cells were given 450 μl of PI solution. The cell cycle profile for 10,000 events was obtained using the Fluorescence-activated cell sorting (FACS) calibrator.

2.9 Annexin V/PI apoptotic assay

PA-1 control, untreated and treated (AgNPs) cells were seeded at a density of $3*10^5$ cells/well in 6-well plates, incubated overnight, and then treated with 5 μM of camptothecin or the control (DMSO). Cells were trypsinized, washed once with PBS, and suspended in 1 × binding buffer after 48 h of treatment. After that, each sample was incubated for 15 min at room temperature in the dark with annexin V-FITC (5 μl) and PI (5 μl). Flow cytometry was used to examine the cells (BD Biosciences, San Jose, CA, United States). After 48 h of treatment, cells were trypsinized, washed once with PBS, and then suspended in 1× binding buffer. Annexin V-FITC (5 μl) and PI (5 μl) were then added to each sample, followed by incubation for 15 min at room temperature in the dark. Cells were analyzed using flow cytometry (BD Biosciences, San Jose, CA, United States).

2.10 Cell cycle analysis

PA-1 cells were seeded in six well plate and incubated overnight. After 24 h, cells were treated for 24 h with 40 μg of MU-AgNP extract and camptothecin (5 μM). After trypsinization, the pellet was collected, reconstituted in cold ethanol (70%), and frozen for an hour to improve the staining capacity. The cells were washed twice with cold PBS and centrifuged for 5 min at 3,000 rpm. In 0.5 ml of PI/RNase staining buffer, the pellet was resuspended and incubated at room temperature in the dark for 30 min. A FACS Calibur flow

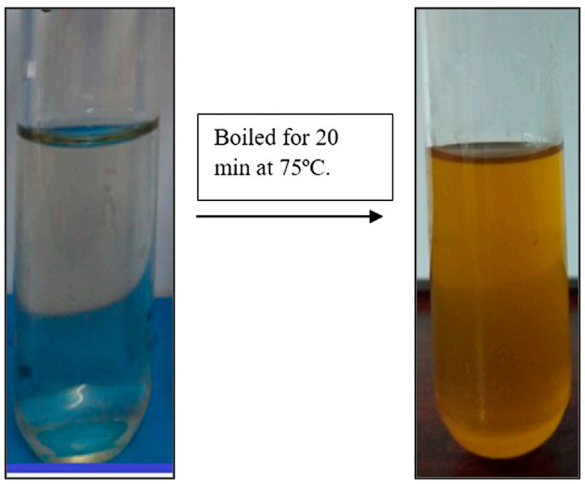

FIGURE 1
Represents the reduction of *Macrotyloma uniflorum* silver nanopracticles. Change colour to light brown confirms the synthesis.

cytometer was used to determine the cell cycle distribution (Becton Dickinson, United States). A total of 10,000 gating occurrences were recorded.

2.11 Mitochondrial membrane potential (ΔΨm)

Changes in mitochondrial membrane potential were determined by flow cytometry using the fluorescent dye 3,3′-dihexyloxacarbocyanine iodide (DiOC6) to understand the role mitochondria play in PA-1 cell death after treatment with MU-AgNPs (Sigma). In 6-well plates, PK-1 cells (3,104 cells/well) were planted. The cells were washed with PBS and resuspended in 10 nM DiOC6 after being incubated with camptothecin (5 μM) or DMSO for 24 and 48 h. The cells were flow cytometrically examined immediately after 30 min of incubation at 37°C.

2.12 Caspase-3 and Caspase-7 activity

The activity of caspase-3 and 7 was evaluated *via* flow cytometry according to the method described by Moraes et al. (2013), with minor modifications. Cells were seeded in 24-well plates (105 cells/ml) and grown in media containing 10% FBS for 24 h after being treated with the AECL or AECR IC_{50}. The cells were centrifuged, washed, and fixed in 4% paraformaldehyde in PBS for 30 min after treatment. The cells were then washed in PBS containing 0.1 M glycine, permeabilized with 0.01% saponin for 30 min, then blocked for 30 min at room temperature in PBS containing 1% bovine serum albumin (BSA). The cells were then incubated in the dark at room temperature for 40 min with an anti-active caspase-3 monoclonal antibody labelled with FITC (BD Pharmingen, San Diego, CA, United States). Fluorescence was analysed using Cell Quest software in a FACS Calibur flow cytometer (Becton Dickinson, United States) after incubation (10,000 events were collected per sample).

2.13 Reactive oxygen species study

In a growth medium, 0.1 million cells were sown in a 6-well plate and incubated for 24 h. Cells were treated for 24 h with MU-AgNPs (20 and 40 μg/ml) and 5 μM Camptothecin. Cells were trypsinized and washed three times with PBS (pH 7) after 24 h of treatment. The supernatant was discarded after centrifuging the cells. The H2DCFDA reagent (2 M, 1 ml) was then applied to the collected pellets, and the cells were incubated at room temperature in the dark for 1 h. The pellet was washed with Dulbecco's phosphate-buffered saline (DPBS), pH 7.4. The fluorescence intensity (FL1-H) of each cell pellet was then measured using FACS equipment (write the model type). A total of 10,000 gate events were measured for each analysis.

2.14 Statistical analysis

Data were expressed as mean ± SEM in triplicate. Statistical analysis was performed using one-way ANOVA (SPSS version 17).

3 Results

3.1 Characterization studies

3.1.1 Green synthesis of silver nanoparticles

The generation of AgNPs was confirmed by the change of color from transparent to dark brown by reduction process. Enhancement of the color is a confirmation for AgNP production. This color change was occurred due to the presence of several bioactive compounds such as tannins, flavonoids, terpenoids, phenols, amines etc. Figure 1 represents the change of colour which confirms the AgNP synthesis.

3.1.2 UV-vis spectrophotometer

Spectrophotometry studies confirmed the distant surface plasmon resonance bands at a peak of 436 nm (Figure 2) in *Macrotyloma uniflorum* seed extracts. Similar results were obtained in Vidhu et al. (2011).

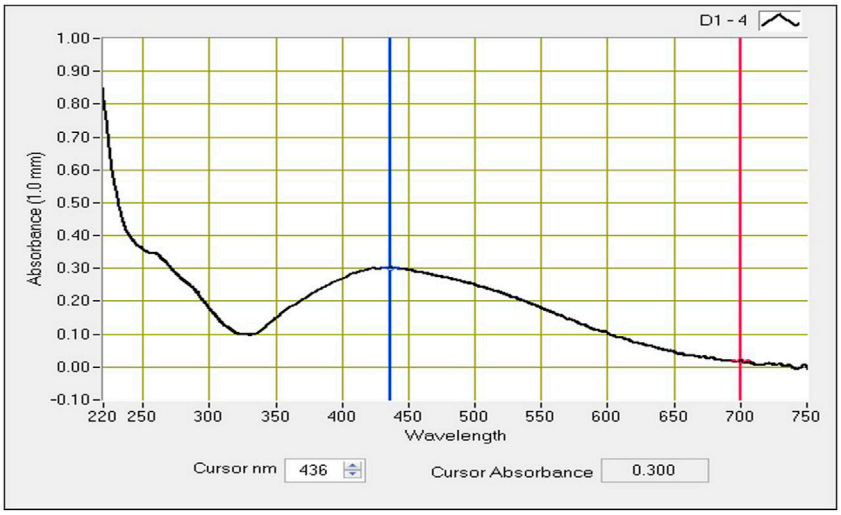

FIGURE 2
UV-visible absorbtion spectra of AgNPs synthesized from *Macrotyloma uniflorum* seed extract with 1 mM silver nitrate.

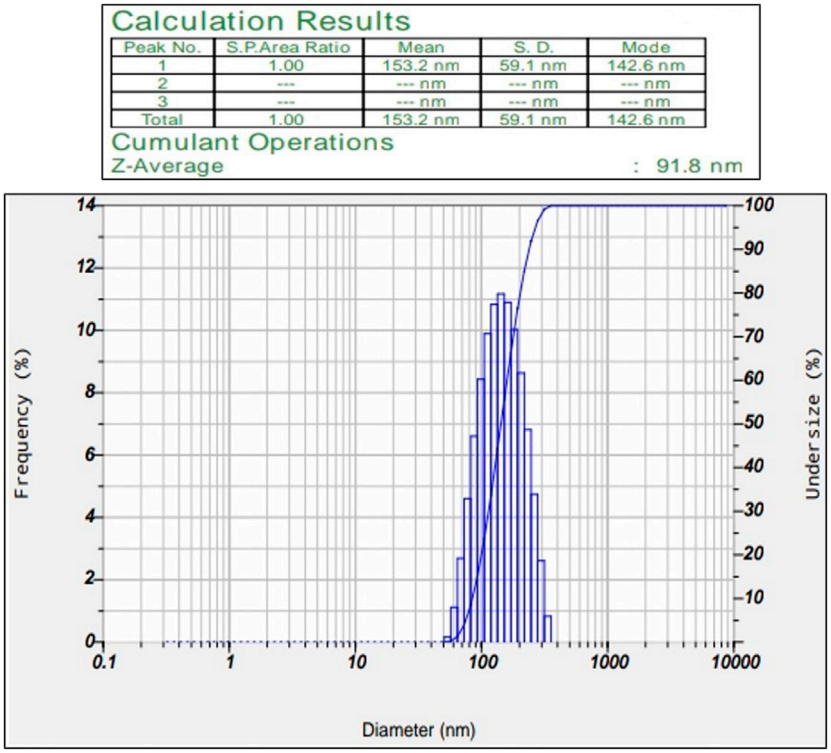

FIGURE 3
Show the average Z-value particle size of synthesized silver nanoparticle.

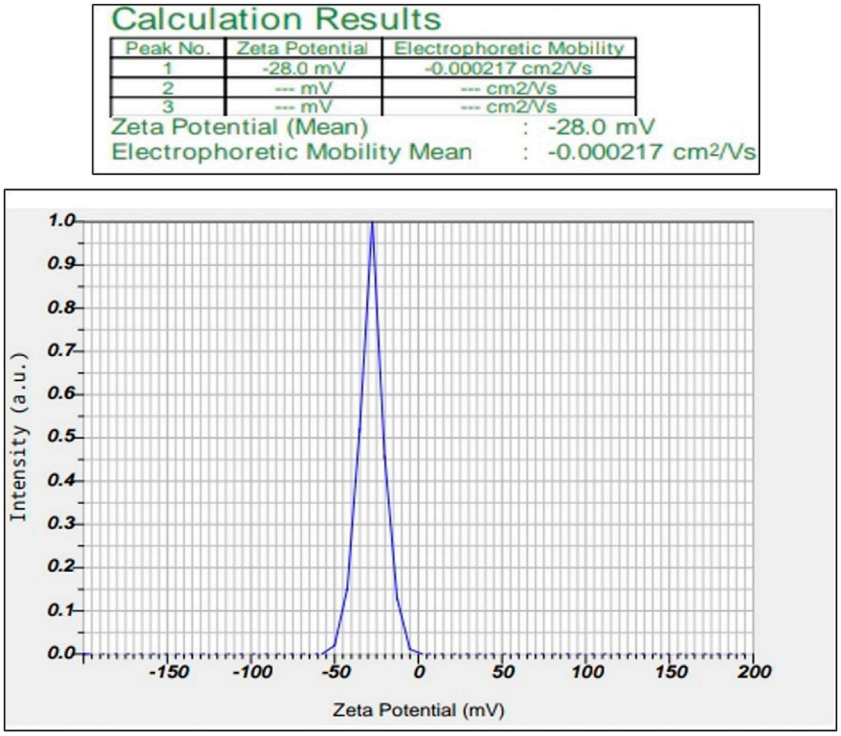

FIGURE 4
Shows Zeta potential of silver nanoparticles *Macrotyloma uniflorum* seed extracts.

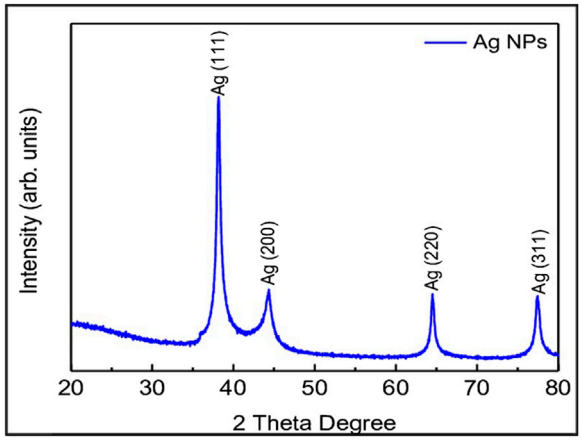

FIGURE 5
The peaks showing X-RAY Diffraction of AgNPs.

3.1.3 Particle size determination

Synthesized silver nanoparticles range from a size of 50–100 nm. Obtained particles in our study have an average diameter of 91.8 nm confirms their identity as AgNPs (Figure 3). Nindawat and Agrawal (2019) studies confirmed the silver nanoparticle size can be either lower (20–60 nm) or medium (200–500 nm). This helps us in confirming the size of the synthesized nanoparticles.

3.1.4 Zeta potential

This study helps us to reveal the possessed charge of the synthesized MU-AgNPs. Electrostatic charge Zeta potential obtained by these particles is −28.0 mV (Figure 4). The negative charge helps the AgNPs from aggregate formation due to the repulsion among themselves. Many studies have confirmed the negative charge in various AgNP synthesized plant extracts.

3.1.5 XRD studies

X-ray diffraction technique (XRD, D/Max 2005; Rigaku) was used to investigate the crystal phase structure of the AgNPs, synthesized using leaf extracts. Crystal phase of AgNPs is determined using XRD. AgNPs, which was synthesized using HG extract (Figure 1) has shown four distinct peaks at 2θ = 38.17, 44.36, 64.52, and 77.46 were assigned to (111, 200, 220, and 311) planes of face centered cubic (FCC) structure of metallic silver (JCPDS 04–0,783) with Fm3m planetary group symmetry (Figure 5). Scherrer's equation is used to calculate the mean crystallite diameter (MCD) of as synthesized nanoparticles, and the size is found to be ≈20–30 nm of AgNPs.

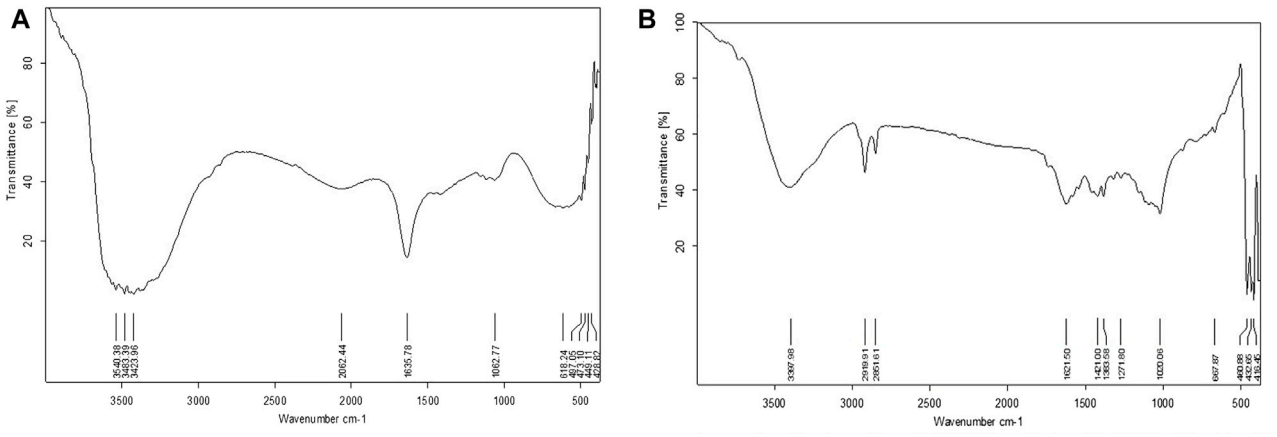

FIGURE 6
FTIR analysis of crude **(A)** and AgNP **(B)** samples of *Macrotyloma uniflorum* seed extracts.

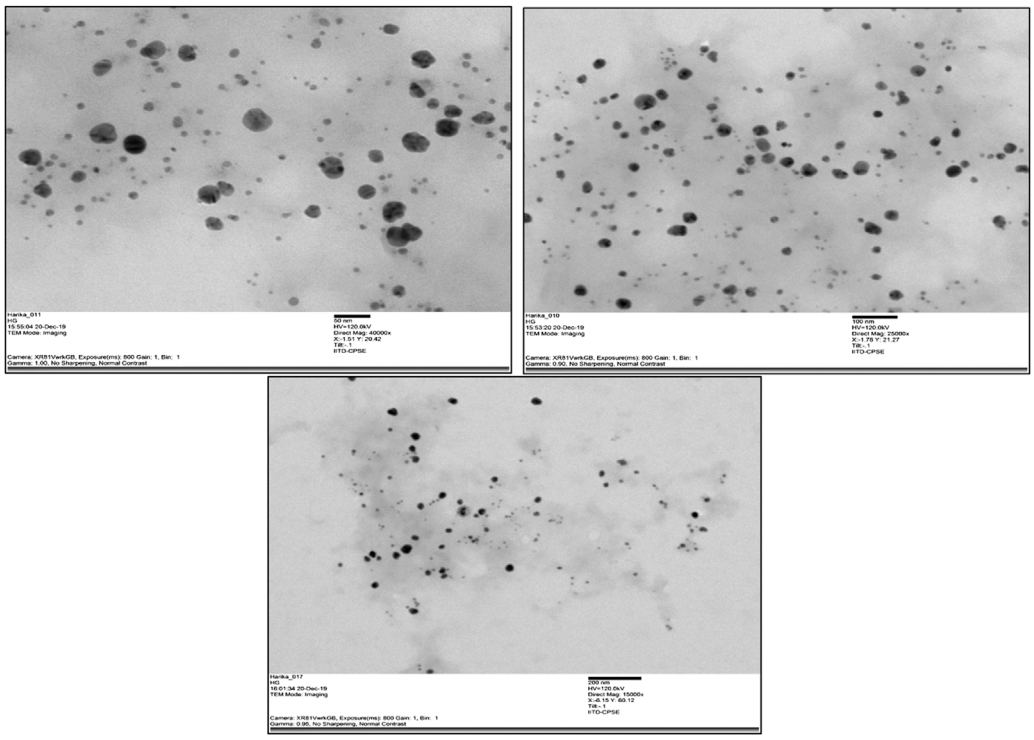

FIGURE 7
TEM images of synthesized nanoparticles from *Macrotyloma uniflorum* at 50, 100, and 200 nm respectively.

3.1.6 FTIR studies

FTIR spectrum of methanolic seed extract showed significant peaks at 3,540.38, 3,483.39, 3,423.96, 1,635.78, 2062.44, 1,062.77, 618.24, 497.05, 473.10, 449.11, and 428.82 cm^{-1} which corresponds to the presence of R-COOH, N-H, C=O, C≡C, Ethers, C-Br, C-I stretch, respectively. The nano extract of seed showed significant peaks at 3,397.98, 1,621.50, 2,919.91, 2,851.61, 1,421.00,

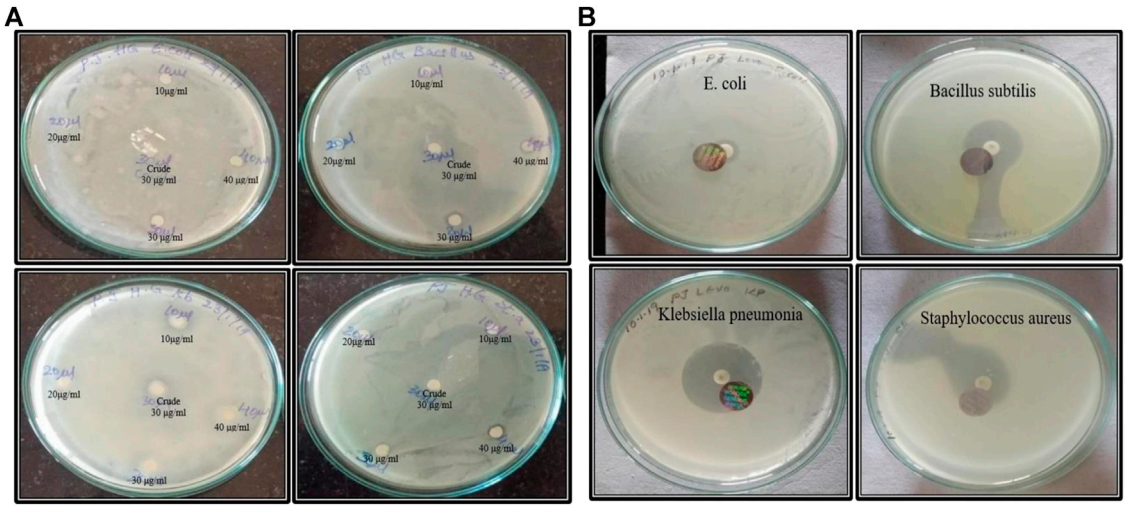

FIGURE 8
(A) Anti-microbial activity of both crude and nano synthesized samples. **(B)**Anti-microbial activity of board-spectrum Levofloxacin antibiotic with *E. coli*, *Bacillus subtilis*, *klebsiella pnemoniae*, and *staphylococcus aureus* respectively.

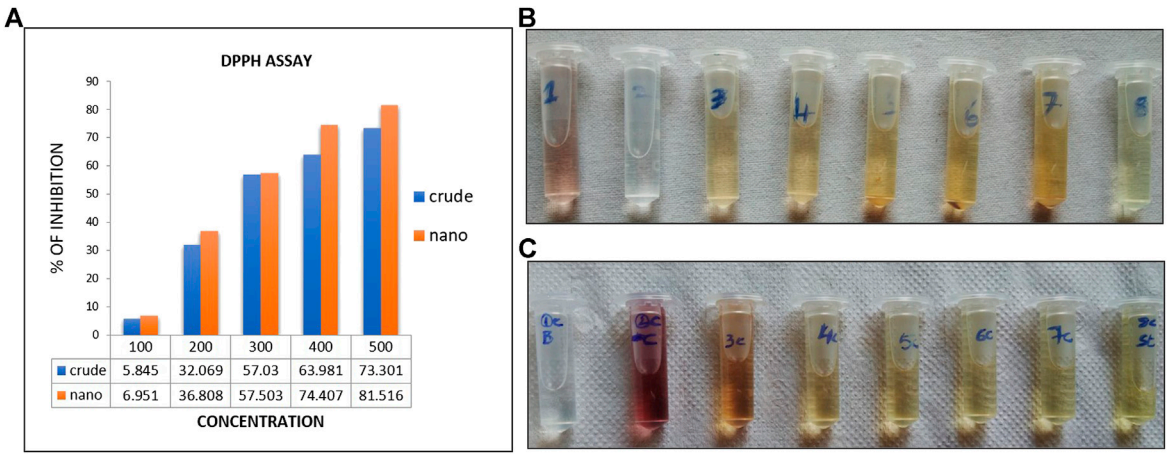

FIGURE 9
(A)-indicates the % of free radicle inhibtion through DPPH activity. **(B,C)** indicates the colur change in crude extracts **(B)**and AgNP **(C)** synthesized extracts.

1,383.58, 1,271.80, 1,020.06, 667.87, 480.88, 432.85, and 416.45 cm^{-1} which corresponds to the presence of O-H, N-H, C=O, C-H, Ethers, C-Br, C-I respectively. (Figure 6).

3.1.7 TEM analysis

The TEM images of the silver nanoparticles biosynthesized from *Macrotyloma uniflorum* shows spherical and oval shapes at 50, 100, and 200 nm. (Figure 7).

3.2 Anti-bacterial activity

By using the disc diffusion technique on nutrient agar plates, the obtained results *S. aureus* has shown a range of inhibition zone compared to other microbes. Hence, we have seen a minute anti-bacterial activity using MU-AgNPs. Figures 8A,B shows the zone of inhibitions between plant extracts and levofloxacin. (Supplementary Table S1).

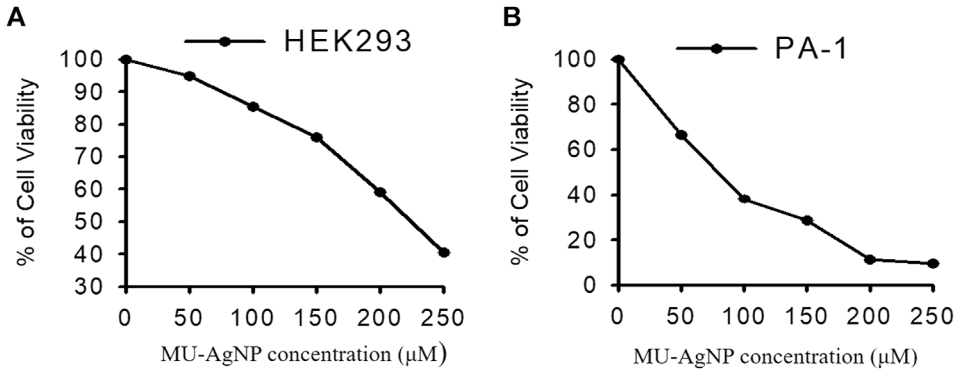

FIGURE 10
Represents the anti cancer activity of Horse Gram AgNP extracts in both **(A)**-HEK293 and **(B)**-PA-1 cells by MTT assay method.

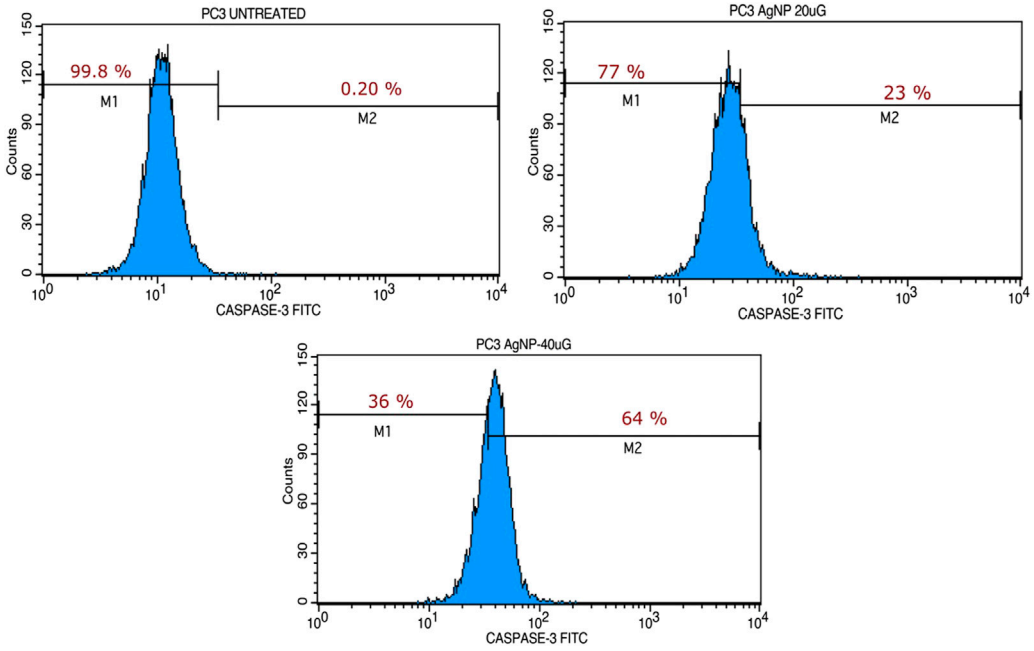

FIGURE 11
Shows the capase the activity at 20 and 40 μg concentration treated with MU-AgNPs.

3.3 Free radicle scavenging assay

Antioxidant activity of crude and AgNPs synthesized from *Macrotyloma uniflorum* plant was checked by DPPH free radical scavenging assay. This method is dependent on the reduction of DPPH radical to the non-radical form DPPH-H in the presence of hydrogen donating antioxidant. The % of inhibition of crude and AgNPs were represented in the Figure 9A. The % of inhibition of AgNPs was increased with increasing concentration and the highest percentage was observed at highest concentration of 500 μg/ml used in this assay and was found to be 76.08%. DPPH assay is an easy, rapid, and sensitive way to survey the antioxidant activity of a specific compound of AgNPs. (Figures 9A–C).

3.4 Cytotoxicity studies

Cytotoxicity studies were performed in Ovarian cancer cell line PA-1 by using MU-AgNP samples at different concentrations (0–250 μg) (Figure 10A). At 50 μg

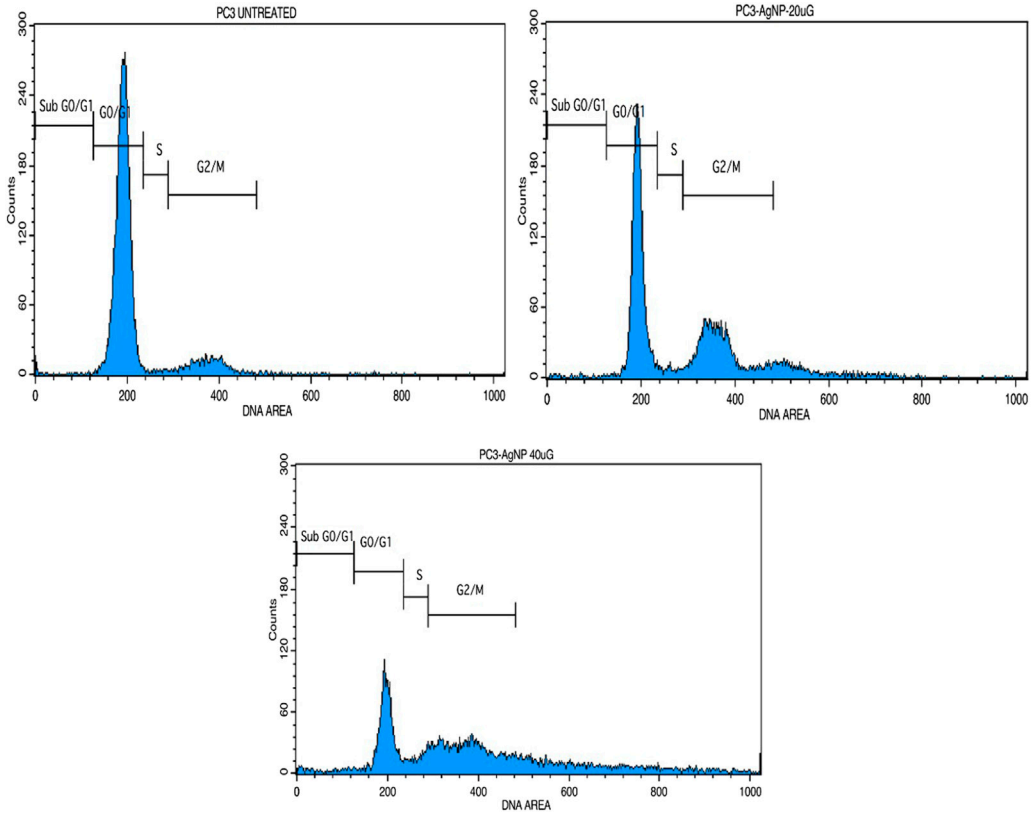

FIGURE 12
Shows the cell cycle analysis of MU-AgNPs treated with control and 20 and 40 μg concentration.

concentration, 66.6% of viability was observed and at 250 μg, 9% viability was observed which shows that these MU-AgNPs have a higher efficiency to inhibit the cancer cell growth compared with the control cell line HEK293 (Figure 10B) which has a viability around 40% at the highest concentration.

3.5 MU-AgNP promotes apoptosis

Our studies indicated the ability of MU-AgNP to influence cell viability. Caspase-3 marker assay is a standard analysis carried out using FACS to understand the potential of a compound as an apoptotic agent. Hence, the Caspase-3 was designed using two different concentrations of Mu-AgNP obtained from Annexin V assay, to evaluate its apoptotic potential in PA-1 cells. FACS analysis of the Caspase-3-FITC stained cells revealed efficient concentration dependent initiation of apoptosis by MU-AgNP. The results showed a significant, MU-AgNP concentration dependent increase in PA-1 cells apoptotic population compared to the control untreated group (Figure 11). At 20 μg & 40 μg MU-AgNP exerts 23 and 64% of apoptotic cell death as per the caspase-3 fluorescent intensity increases in treated cells. Notably the potential of MU-AgNP to selectively to induce apoptosis in a concentration dependent manner is an ideal property for cancer therapy related drugs. The results obtained from FACS were further confirmed by cell cycle analysis and CLSM imaging of the PA-1 cells using other related studies.

3.6 Cell cycle analysis MU-AgNP causes DNA damage and cell cycle arrest

Based on the earlier results it would be of interest to study the influence of MU-AgNP on different phases of PA-1 cell cycle. One of the properties of an effective anticancer drug is to selectively target a specific phase in the life cycle of the cancer cell. PI based cell cycle analysis was carried out using FACS to identify the influence of MU-AgNP on different phases of the PA-1 cell cycle (Figures 12A–C). Results from

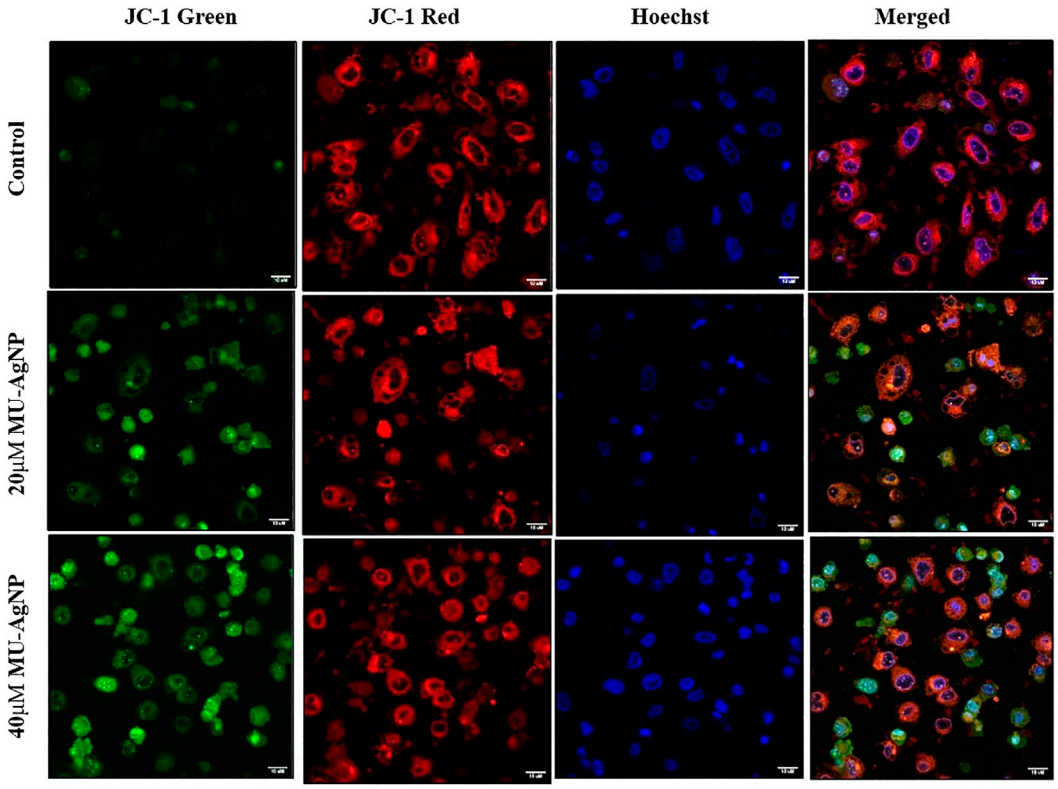

FIGURE 13
Shows the mitochondrial membrane potential activity of MU -AgNPs treated with control and 20 and 40 μM Concentrations. Increase in JC-1 green staining in the treated samples confirms the break down of mitochondria resulted due to apoptosis.

the cell cycle analysis showed increase in G_2/M phase population with a concomitant decrease of cells in the SubG_0/G_1 phase (Figures 12B,C). In contrast there is a considerable increase in SubG_0/G_1 which is characterized by DNA damage and a feature of apoptotic cells. Cells treated with MU-AgNP showed a significant decrease in G_0/G_1 phase (~28.8 & 54%) compared to the control group (88.8%). Whereas the S phase cell population showed significant increasing trend compared to the control group. The cell cycle analysis results further confirmed the potential of MU-AgNP as an anticancer agent with ability to induce apoptosis in PA-1 cell line.

3.7 PC3 AgNP induces mitochondrial membrane damage

Apoptosis is often associated with the induction of cellular oxidative stress and altered membrane function in organelles such as mitochondria. The level of altered membrane function or membrane damages has been shown to have strong correlation with the induction of apoptotic pathway in cells. This mode of apoptotic induction is one of the key features for an anticancer agent. Earlier assay results along with FACS based Caspase-3 assays showed strong ability of MU-AgNP to reduce cell viability of PA-1 cells and induce apoptosis. Hence, the influence of these MU-AgNP on Mitochondrial membrane damages of the PA-cells would be of interest to understand whether the apoptotic pathway of the PA-1 cell is influenced *via* membrane damage. The potential-dependent alteration of membrane potential, treated with MU-AgNP was analyzed using CLSM with the aid of JC-1 dye, the results showed that in comparison with untreated, treated cells showed Significant increase in green fluorescence owing to lowered membrane potential. Thus, the increase in green fluorescence intensity in MU-AgNPs treated cells indicates break-down of the mitochondrial membrane potential in comparison with untreated, which indicates drug induced apoptosis activity. The images concurred with the results observed in FACS indicating that MU-AgNP might be playing a role by altering the mitochondrial membrane potential further leading to apoptosis. (Figure 13).

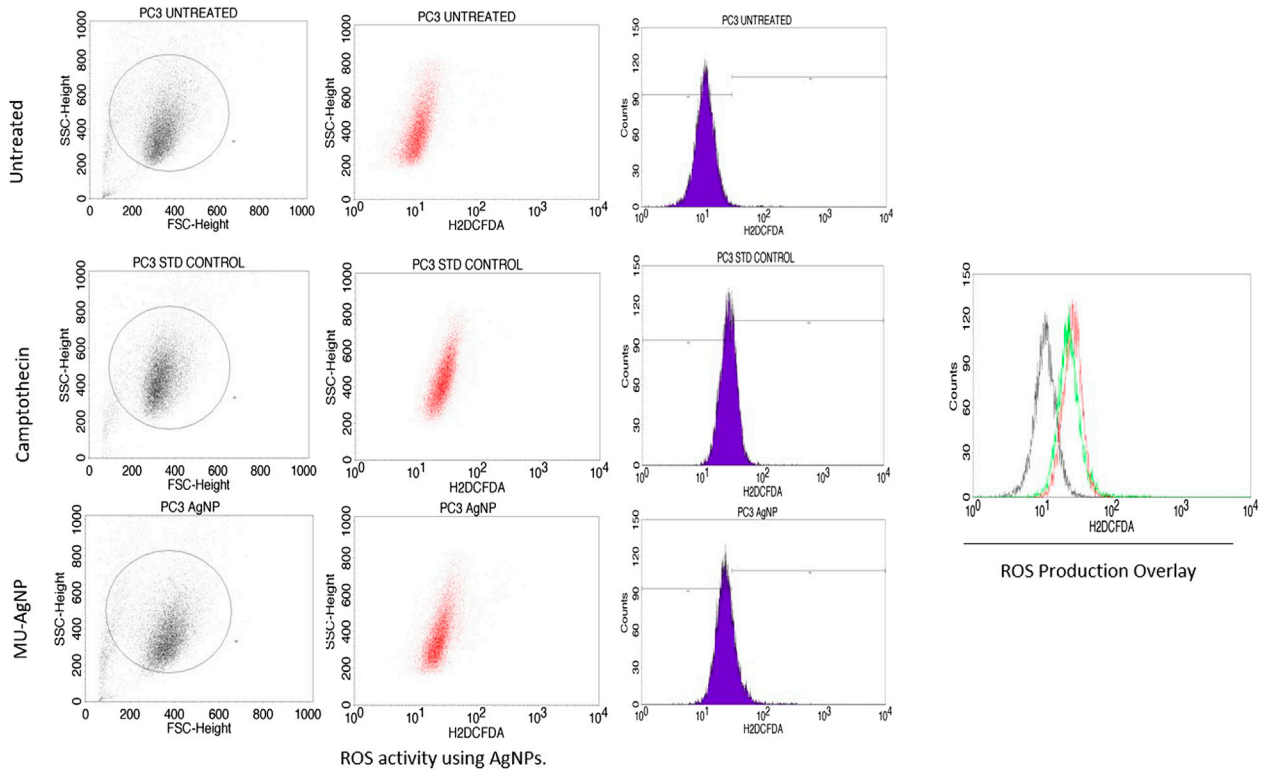

FIGURE 14
Shows the ROS generation in control, standard and AgNP treated samples.

3.8 Reactive oxygen species generation

Several reports have shown that Reactive oxygen species (ROS) is an indication of DNA damage/apoptosis mechanism (Mitra et al., 2019; Ebrahimzadeh et al., 2018). NavaneethaKrishnan et al. (2019) has reported that polyphenols which are a part in phytochemical extracts of a plant are the key compounds for ROS induced DNA damage. MU-AgNP particles has ROS production of 21.3% at 40 µg concentration whereas untreated ones have a percentage of 0.45%. Standard drug camptothecin generated 26% of ROS. Zeta potential studies has shown the negative surface charge of the MU-AgNP which is not the prime factor for both the cytotoxicity and ROS generation. (Cameron et al., 2018). Several studies on cancer using phytochemical extracts from plants and their parts has shown ROS activity as a sign of DNA damage in cancer cells compared to the controls. Ahn and Park (2020) studies have shown that AgNPs has a capacity to generate ROS and thus can cause damage to the DNA in A549 lung cancer cells. Considering this, we reported that ROS production using AgNPs derived from *Macrotyloma uniflorum* seeds have a capacity to generate ROS by damaging the DNA in Ovarian cancer cells along with the standard drug camptothecin. (Figure 14).

4 Discussion

Nano based medicine has gained a huge popularity in past decades because of fewer toxicity. Organic synthesis method enhanced its therapeutic activity and hence could be effective to treat against various ailments. In a recent review by Hembram et al. (2018), choosing AgNPs over AuNPs has been highlighted at *in vivo* level and can be supported by the reason of choosing Eco-friendly synthesis of AgNPs which has gained a vast recognition over globe not only because of their effectivity but also due to the efficacy (Srivastava et al., 2018). Utilising the organic plant extracts in treating diseases specifically cancer is highly required considering no damage to the healthy cells which are surrounding in the tumor microenvironment (Srivastava et al., 2018; Singh et al., 2021).

Considering the above, our research mainly focussed on poor man's legume *Macrotyloma uniflorum* because of its wider availability in the Asian countries. AgNP production was confirmed by analysing the wavelength spectrum from 300–700 nm and observed the wider SPR bands. Macrotyloma seed extracts has showcased a characteristic peak at 436 nm using $AgNO_3$ mixture, which likely confirms green synthesis of AgNPs. These results are quiet similar from the work done

by Vidhu et al. (2011). Particle size of the silver nano particles plays an important role in the therapeutic strategies. The size of the nanoparticle determines whether the AgNP tagged compound has a capacity to penetrate through the cell membrane and bind to the intra cellular compartments. *M. uniflorum* seed extracts has shown an average size of 91.8 nm which falls into AgNP category. Zeta potential studies revealed the negative charge of the synthesized nano particles which shows the repulsion character among themselves by avoiding the aggregate formation. Crystal studies were determined by XRD, which is an advanced technique to study the crystal nature of MU-AgNPs. TEM analysis has confirmed the spherical structure of nanoparticles. However, our data has not shown significant anti-bacterial activity.

In vitro assays have showed significant results which shows similarity with the early reports. MTT assay has showed a significant result in the viability of PA-1 cells compared to the control cell line which confirms that MU-AgNPS have a capacity to inhibit the tumor cell growth (Palle et al., 2020). Further FACS analysis have shown the tremendous in G2/M phase and a concomitant decrease in subG0/G1 phase confirms the presence of apoptotic cells. Further, caspase 3 study by FACS has confirmed the generation of apoptotic cells using different concentration of MU-AgNPs at 23 and 64%. This confirms that MU-AgNPs can cause the tumor cells to death through apoptotic pathway. Our data matches with the other reports who has used different plant AgNP extracts (Bordoni et al., 2021). Finally, mitochondrial membrane potential studies confirmed the reduction of cell viability through apoptosis process, thus staining with JC-1 dye confirmed that MU-AgNPs treated group has shown high intensity thus confers the breakdown of mitochondrial membrane and results in lower membrane potential.

5 Conclusion

We are concluding our finding by saying that MU-AgNPs can be a promising treatment regimen to control the proliferation of Cancer cells, particularly Ovarian cancer. Further studies are highly recommended to see whether they have the similar capability to control the growth of resistant tumors and combinational drug treating of MU-AgNPs alongside primary treatment regimens can be highly appreciated. Studies related to cancer cell signaling pathways are much needed to target specific genes.

Data availability statement

The original contributions presented in the study are included in the article/Supplementary Material, further inquiries can be directed to the corresponding authors.

Author contributions

KL, VH, SP, and AS conducted the experiments. RK and KL drafted the manuscript. JP and SP designed the work. KL, AS, VH, and SP analyzed the data.

Conflict of interest

The authors declare that the research was conducted in the absence of any commercial or financial relationships that could be construed as a potential conflict of interest.

Publisher's note

Supplementary material

The Supplementary Material for this article can be found online at: https://www.frontiersin.org/articles/10.3389/fbioe.2022.978846/full#supplementary-material

References

Ahn, E. Y., and Park, Y. (2020). Anticancer prospects of silver nanoparticles green-synthesized by plant extracts. *Mater. Sci. Eng. C* 116, 111253. doi:10.1016/j.msec.2020.111253

Anjum, A., Farooqi, H., Abdin, M. Z., and Tiwari, A. K. (2021). Combinatorial effect of *Macrotyloma uniflorum* (Lam.) Verdc. seed extract and vorinostat (suberoylanilide hydroxamic acid) in human leukemia cells. *Pharmacogn. Mag.* 17 (6), 213–219. doi:10.4103/pm.pm_70_21

Azzouz, D., Khan, M. A., and Palaniyar, N. (2021). ROS induces NETosis by oxidizing DNA and initiating DNA repair. *Cell. Death Discov.* 7 (1), 113. doi:10.1038/s41420-021-00491-3

Bordoni, V., Sanna, L., Lyu, W., Avitabile, E., Zoroddu, S., Medici, S., et al. (2021). Silver nanoparticles derived by *Artemisia arborescens* reveal anticancer and apoptosis-inducing effects. *Int. J. Mol. Sci.* 22 (16), 8621. doi:10.3390/ijms22168621

Bratasz, A., Weir, N. M., Parinandi, N. L., Zweier, J. L., Sridhar, R., Ignarro, L. J., et al. (2006). Reversal to cisplatin sensitivity in recurrent human ovarian cancer cells by NCX-4016, a nitro derivative of aspirin. *Proc. Natl. Acad. Sci. U. S. A.* 103, 3914–3919. doi:10.1073/pnas.0511250103

Cameron, S. J., Hosseinian, F., and Willmore, W. G. (2018). A current overview of the biological and cellular effects of nanosilver. *Int. J. Mol. Sci.* 19 (7), 2030. doi:10.3390/ijms19072030

Cos, P., Vlietinck, A. J., Berghe, D. V., and Maes, L. (2006). Anti-infective potential of natural products: How to develop a stronger *in vitro* 'proof-of-concept. *J. Ethnopharmacol.* 106 (3), 290–302. doi:10.1016/j.jep.2006.04.003

Ebell, M. H., Culp, M. B., and Radke, T. J. (2016). A systematic review of symptoms for the diagnosis of ovarian cancer. *Am. J. Prev. Med.* 50, 384–394. doi:10.1016/j.amepre.2015.09.023

Ebrahimzadeh, M. A., Tafazoli, A., Akhtari, J., Biparva, P., and Eslami, S. (2018). Engineered silver nanoparticles, a new nanoweapon against cancer. *Anticancer. Agents Med. Chem.* 18 (14), 1962–1969. doi:10.2174/1871520618666180808093040

Fani, S., Kamalidehghan, B., Lo, K., Nigjeh, S. E., Keong, Y. S., Dehghan, F., et al. (2016). Anticancer activity of a monobenzyltin complex C1 against MDA-MB-231 cells through induction of apoptosis and inhibition of breast cancer stem cells. *Sci. Rep.* 6, 38992. doi:10.1038/srep38992

Ghosh, S. (2019). Green synthesis of nanoparticles and fungal infection. *Green Synth. Charact. Appl. nanoparticles.* 7, 75–86. doi:10.1016/B978-0-08-102579-6.00004-6

Grossman, D. C., Curry, S. J., Owens, D. K., Barry, M. J., Davidson, K. W., Doubeni, C. A., et al. (2018). Screening for ovarian cancer: US preventive services task force recommendation statement. *JAMA* 319, 588–594. doi:10.1001/jama.2017.21926

Hembram, K. C., Rahul, K., Laxman, K., Pankaj, K. P., Chanakya, N. K., and Birendra, K. B. (2018). Therapeutic prospective of plant-induced silver nanoparticles: Application as antimicrobial and anticancer agent. *Artif. Cells Nanomed. Biotechnol.* 46, S38–S51. doi:10.1080/21691401.2018.1489262

Ingle, K. P., Al-Khayri, J. M., Chakraborty, P., Narkhede, G. W., and Suprasanna, P. (2020). "Bioactive compounds of horse gram (macrotyloma uniflorum lam. [Verdc.])," in *Bioactive compounds in underutilized vegetables and Legumes.Reference series in phytochemistry*. Editors H. N. Murthy. and K. Y. Paek (Cham: Springer). doi:10.1007/978-3-030-44578-2_36-1

Javed, B., and Mashwani, Z. R. (2020). Synergistic effects of physicochemical parameters on bio-fabrication of mint silver nanoparticles: Structural evaluation and action against HCT116 colon cancer cells. *Int. J. Nanomedicine* 15, 3621–3637. doi:10.2147/IJN.S254402

Jiang, Z., Fletcher, N. M., Ali-Fehmi, R., Diamond, M. P., Abu-Soud, H. M., Munkarah, A. R., et al. (2011). Modulation of redox signaling promotes apoptosis in epithelial ovarian cancer cells. *Gynecol. Oncol.* 122, 418–423. doi:10.1016/j.ygyno.2011.04.051

Karmous, I., Pandey, A., Ben, K., Haj, K. B., and Chaoui, A. (2020). Efficiency of the green synthesized nanoparticles as new tools in cancer therapy: Insights on plant-based bioengineered nanoparticles, biophysical properties, and anticancer roles. *Biol. Trace Elem. Res.* 196, 330–342. doi:10.1007/s12011-019-01895-0

Kim, J., Kim, J., and Bae, J. S. (2016). ROS homeostasis and metabolism: A critical liaison for cancer therapy. *Exp. Mol. Med.* 48, e269. doi:10.1038/emm.2016.119

Kim, S. M., Lee, H. M., Hwang, K. A., and Choi, K. C. (2017). Benzo(a)pyrene induced cell cycle arrest and apoptosis in human choriocarcinoma cancer cells through reactive oxygen species-induced endoplasmic reticulum-stress pathway. *Food Chem. Toxicol.* 107, 339–348. doi:10.1016/j.fct.2017.06.048

Kumari, R., Saini, A. K., Kumar, A., and Saini, R. V. (2020). Apoptosis induction in lung *and prostate cancer cells through silver nanoparticles synthesized from Pinus* roxburghii bioactive fraction. *J. Biol. Inorg. Chem.* 25, 23–37. doi:10.1007/s00775-019-01729-3

Li, Y., Li, N., Jiang, W., Ma, G., and Zangeneh, M. M. (2020). *In situ* decorated Au NPs on pectin-modified Fe3O4 NPs as a novel magnetic nanocomposite (Fe3O4/Pectin/Au) for catalytic reduction of nitroarenes and investigation of its anti-human lung cancer activities. *Int. J. Biol. Macromol.* 163, 2162–2171. doi:10.1016/j.ijbiomac.2020.09.102

Liu, J., Zangeneh, A., Zangeneh, M. M., and Guo, B. (2020). Antioxidant, cytotoxicity, anti-human esophageal squamous cell carcinoma, anti-human caucasian esophageal carcinoma, anti-adenocarcinoma of the gastroesophageal junction, and anti-distal esophageal adenocarcinoma properties of gold nanoparticles green synthesized by Rhus coriaria L. fruit aqueous extract. *J. Exp. Nanosci.* 15 (1), 202–216. doi:10.1080/17458080.2020.1766675

Mahdavi, B., Paydarfard, S., Zangeneh, M. M., Goorani, S., Seydi, N., and Zangeneh, A. (2019). Assessment of antioxidant, cytotoxicity, antibacterial, antifungal, and cutaneous wound healing activities of green synthesized manganese nanoparticles using *Ziziphora clinopodioides* Lam leaves under *in vitro* and *in vivo* condition. *Appl. Organometal. Chem.* 33, e5248. doi:10.1002/aoc.5248

Marimuthu, M., and Krishnamoorthi, K. (2013). Nutrients and functional properties of horse gram (Macrotyloma Uniflorum), an underutilized south Indian food legume. *J. Chem. Pharma. Res.* 5 (5), 390–394.

Mitra, S., Nguyen, L. N., Akter, M., Park, G., Choi, E. H., and Kaushik, N. K. (2019). Impact of ROS generated by chemical, physical, and plasma techniques on cancer attenuation. *Cancers* 11 (7), 1030–1061. doi:10.3390/cancers11071030

Momenimovahed, Z., Tiznobaik, A., Taheri, S., and Salehiniya, H. (2019). Ovarian cancer in the world: Epidemiology and risk factors. *Int. J. Womens Health.* 11, 287–299. doi:10.2147/IJWH.S197604

NavaneethaKrishnan, S., Rosales, J. L., and Lee, K. Y. (2019). ROS-mediated cancer cell killing through dietary phytochemicals. *Oxid. Med. Cell. Longev.* 9051542, 1–16. doi:10.1155/2019/9051542

Newman, J., and Cragg, G. M. (2012). Natural products as sources of new drugs over the 30 years from 1981 to 2010. *J. Nat. Prod.* 75 (3), 311–335. doi:10.1021/np200906s

Nindawat, S., and Agrawal, V. (2019). Fabrication of silver nanoparticles using *Arnebia hispidissima* (Lehm.) A. DC. root extract and unravelling their potential biomedical applications. *Artif. Cells Nanomed. Biotechnol.* 47, 166–180. doi:10.1080/21691401.2018.1548469

Palanisamy, C. P., Cui, B., Zhang, H., Panagal, M., Paramasivam, S., Chinnaiyan, U., et al. (2021). Anti-ovarian cancer potential of phytocompound and extract from South African medicinal plants and their role in the development of chemotherapeutic agents. *Am. J. Cancer Res.* 11 (5), 1828–1844.

Palle, S. R., Penchalaneni, J., Lavudi, K., Gaddam, S. A., Kotakadi, V. S., and Challagundala, V. N. (2020). Green synthesis of silver nanoparticles by leaf extracts of *Boerhavia erecta* and spectral characterization and their antimicrobial, antioxidant ad cytotoxic studies on ovarian cancer cell lines. *Lett. Appl. NanoBioScie.* 9 (3), 1165–1176. doi:10.33263/LIANBS93.11651176

Pokhriyal, R., Hariprasad, R., Kumar, L., and Hariprasad, G. (2019). Chemotherapy resistance in advanced ovarian cancer patients. *Biomark. Cancer* 11, 1179299X1986081. doi:10.1177/1179299X19860815

Prasad, S. K., and Singh, M. K. (2015). Horse gram- an underutilized nutraceutical pulse crop: A review. *J. Food Sci. Technol.* 52 (5), 2489–2499. doi:10.1007/s13197-014-1312-z

Preya, U. H., Lee, K. T., Kim, N. J., Lee, J. Y., Jang, D. S., and Choi, J. H. (2017). The natural terthiophene alpha-terthienylmethanol induces s phase cell cycle arrest of human ovarian cancer cells via the generation of ros stress. *Chem. Biol. Interact.* 272, 72–79. doi:10.1016/j.cbi.2017.05.011

Ratan, Z. A., Haidere, M. F., Nurunnabi, M., Shahriar, S. M., Ahammad, A. J., Shim, Y. Y., et al. (2020). Green chemistry synthesis of silver nanoparticles and their potential anticancer effects. *Cancers* 12 (4), 855. doi:10.3390/cancers12040855

Sagadevan, S., Vennila, S., Muthukrishnan, L., Gurunathan, K., Oh, W. C., Paiman, S., et al. (2020). Exploring the therapeutic potentials of phyto-mediated silver nanoparticles formed via *Calotropis procera* (ait. *J. Exp. Nanosci.* 15 (1), 217–231. doi:10.1080/17458080.2020.1769842

Sanjay, S. S. (2019). Safe nano is green nano. *Green Synth. Charact. Appl. nanoparticles.* 22, 27–36. doi:10.1016/b978-0-08-102579-6.00002-2

Shaneza, A., Gupta, U. K., Singh, D., Khan, T., et al. (2018). Herbal treatment for the ovarian cancer. *SGVU. J. Pharmac. Res. Educ.* 3 (2), 325–329.

Silva, L. P., Pereira, T. M., and Bonatto, C. C. (2019). Frontiers and perspectives in the green synthesis of silver nanoparticles. *Green Synth. Charact. Appl. Nanoparticles*, 137–164. doi:10.1016/b978-0-08-102579-6.00007-1

Singh, M., Agarwal, S., Tiwarim, R. K., Chandam, S., Singhm, K., Agarwalm, P., et al. (2021). Neuroprotective ability of apocynin loaded nanoparticles (apo-nps) as nadph oxidase (nox)-mediated ros modulator for hydrogen peroxide-induced oxidative neuronal injuries. *Molecules* 26 (16), 5011. doi:10.3390/molecules26165011

Singh, M., Hari, D. U., and Ishwari, S. B. (2013). Genetic and genomic resources of grain legume improvement. Pages 1–10. doi:10.1016/B978-0-12-397935-3.00001-3

Srinivas, U. S., Tan, B., Vellayappan, B. A., and Jeyasekharan, A. D. (2019). ROS and the DNA damage response in cancer. *Redox Biol.* 25, 101084. doi:10.1016/j.redox.2018.101084

Srivastava, S., Mohammad, S., Gupta, S., Mahdi, A. A., Dixit, R. K., Singh, V., et al. (2018). Chemoprotective effect of nanocurcumin on 5-fluorouracil-induced-toxicity toward oral cancer treatment. *Natl. J. Maxillofac. Surg.* 9 (2), 160–166. doi:10.4103/njms.NJMS_27_18

Vargas, A. N. (2014). Natural history of ovarian cancer. *Ecancermedicalscience* 8, 465. doi:10.3332/ecancer.2014.465

Vidhu, V. K., Aromalm, S. A., and Philip, D. (2011). Green synthesis of silver nanoparticles using *Macrotyloma uniflorum*. *Spectrochimica Acta Part A Mol. Biomol. Spectrosc.* 83 (1), 392–397. doi:10.1016/j.saa.2011.08.051

Wang, W., Im, J., Kim, S., Jang, S., Han, Y., Yang, K. M., et al. (2020). Ros-induced SIRT2 upregulation contributes to cisplatin sensitivity in ovarian cancer. *Antioxidants (Basel)* 9 (11), 1137. doi:10.3390/antiox9111137

Yesilot, S., and Aydinm, C. (2019). Silver nanoparticles; a new hope in cancer therapy? *East. J. Med.* 24 (1), 111–116. doi:10.5505/ejm.2019.66487

You, C., Han, C., Wang, X., Zheng, Y., Li, Q., Hu, X., et al. (2012). The progress of silver nanoparticles in the antibacterial mechanism, clinical application and cytotoxicity. *Mol. Biol. Rep.* 39, 9193–9201. doi:10.1007/s11033-012-1792-8

frontiers | Frontiers in Bioengineering and Biotechnology

TYPE Original Research
PUBLISHED 31 October 2022
DOI 10.3389/fbioe.2022.1052801

OPEN ACCESS

EDITED BY
Chang Li,
Tongji University, China

REVIEWED BY
Xun Li,
University of Maryland, United States
Yating Xiao,
University of Chinese Academy of Sciences, China
Jiahong Shen,
Northwestern University, United States

*CORRESPONDENCE
Yifang Huang,
0501hyf@163.com
Nannan Cao,
caobeibeicnn@163.com

†These authors have contributed equally to this work

SPECIALTY SECTION
This article was submitted to Nanobiotechnology, a section of the journal Frontiers in Bioengineering and Biotechnology

RECEIVED 24 September 2022
ACCEPTED 17 October 2022
PUBLISHED 31 October 2022

CITATION
Huang Y, Feng W, Zhang G-Q, Qiu Y, Li L, Pan L and Cao N (2022), An enzyme-activatable dual-readout probe for sensitive β-galactosidase sensing and Escherichia coli analysis. *Front. Bioeng. Biotechnol.* 10:1052801. doi: 10.3389/fbioe.2022.1052801

An enzyme-activatable dual-readout probe for sensitive β-galactosidase sensing and *Escherichia coli* analysis

Yifang Huang[1,2*†], Weiwei Feng[3,4†], Guo-Qiang Zhang[5†], Yuling Qiu[6], Linlin Li[1,2], Liqiu Pan[1,2] and Nannan Cao[7*]

[1]Department of Clinical Laboratory, The First Affiliated Hospital of Guangxi Medical University, Nanning, China, [2]Key Laboratory of Clinical Laboratory Medicine of Guangxi Department of Education, Guangxi Medical University, Nanning, China, [3]Department of Gastroenterology, Meizhou People's Hospital, Meizhou, China, [4]Department of Laboratory Medicine and Guangdong Engineering and Technology Research Center for Rapid Diagnostic Biosensors, Nanfang Hospital, Southern Medical University, Guangzhou, China, [5]Key Laboratory of Bioactive Materials, State Key Laboratory of Medicinal Chemical Biology, Key Laboratory of Functional Polymer Ministry of Education, and College of Life Sciences, Nankai University, Tianjin, China, [6]Guangxi Key Laboratory of Thalassemia Research, Guangxi Medical University, Nanning, China, [7]Department of Laboratory Medicine, The Second Affiliated Hospital of Guangzhou University of Chinese Medicine, Guangzhou, China

Rapid and accurate sensing of β-galactosidase (β-gal) activity is particularly critical for the early detection of many diseases and has become a topic of interest in recent years. However, most traditional probes for β-gal sensing often suffer from the disadvantages of narrow dynamic range, low reaction efficiency and are only employed with either colorimetric or fluorescence sensing. Furthermore, β-galactosidase sensing based assay for efficient detection and antibiotic resistance analysis of *Escherichia coli* (*E.coli*) is not available. Here, an enzyme-induced probe assay was reported for dual sensitive fluorescence and colorimetric measurement of β-gal activity, and was further employed for detection of *Escherichia coli* and their antibiotic resistance analysis. The DCM-βgal probe was virtually non-emissive in aqueous solution, while it could be activated by β-gal to produce bright emission. Under optimized conditions, DCM-βgal displayed high sensitivity, selectivity and rapid response to β-gal with a low detection limit of 1.5×10^{-3} U ml^{-1}. Importantly, this assay was successfully applied to sensitive detection of *E. coli* cells with a fast detection process within 5 h and a low detection concentration of 1×10^{3} CFU ml^{-1}. Furthermore, the enzyme-activatable assay was also successfully applied for high throughput *E. coli* antibiotic resistance analysis. The DCM-βgal strategy is applied for the first time on the detection of *E. coli* cells and their antibiotic resistance analysis. It is provided with the advantages of high selectively, a simple operation, low cost and rapid detection. The detection platform can also be extended to analyze the level of β-gal in other types of cells or biological samples. Overall, the simple, effective and dual-readout assay holds promise for efficient sensing of β-gal activity and provides a potential tool for *E. coli* detection and their antibiotic resistance analysis.

KEYWORDS

dual-readout probe, β-galactosidase sensing, *Escherichia coli* detection, antibiotic resistance analysis, enzyme reaction

Introduction

Enzymes play important roles in a variety of biological processes and have served as crucial biomarkers for disease diagnosis and monitoring. Rapid sensing of the specific enzymes activity is emerging as a critical strategy for accurate disease diagnostics and developing simple, effective sensing system has gained considerable attention in past decades. Among these specific enzymes, β-galactosidase (β-gal) is widely known as a common kind of hydrolase in cells and the main biological function of β-gal is to remove galactose residues from substrates (Komatsu and Urano, 2015). In recent years, β-gal has attracted extensive attention as a vital enzyme biomarker because it has been shown to be overexpressed in senescent cells, tumor cells as well as in *Escherichia coli* (*E.coli*) (Munoz-Espin and Serrano, 2014; Chen et al., 2016; Gu et al., 2016; Adkins et al., 2017; Nishihara et al., 2018). Therefore, developing efficient methods to detect β-gal with high efficiency and specificity is thus of great importance for the early diagnosis of the specific diseases and the identification of *E.coli* infection.

Although a number of approaches have been proposed for detecting the activity of β-gal, but most of them suffer from various disadvantages. For example, colorimetric methods have been suggested as convenient assays for visual detection of the β-gal concentration (Chen et al., 2015; Chen et al., 2016; Adkins et al., 2017; Jia et al., 2018). However, most of these enzyme-induced colorimetric strategies often do not have broad color changes enough for quantitative measurement of the enzyme activity. Electrochemical methods are sensitive enough to measure β-gal activity (Adkins et al., 2017; Wang et al., 2017). Unfortunately, they mostly rely upon advanced instrumentation and require cumbersome processes. Furthermore, the above methods are not suitable for the assessment of endogenous β-gal activity *in vivo*. In contrast to colorimetric and electrochemical methods, fluorescent sensors have attracted extensive attention because of their simplicity, high sensitivity, high signal-to-noise ratio, and their ability for imaging β-gal *in vivo* (Jiang et al., 2017; Fu et al., 2019; Gu et al., 2019; Zhang et al., 2019). However, most traditional fluorescent probes suffer from the disadvantages of background fluorescence interference, narrow dynamic range and long response time, which can greatly hamper their application in biological analysis. Thus, it is highly desirable to develop a fluorescent probe capable of detecting β-gal with an improved dynamic range and enhanced reaction efficiency.

E.coli contamination remain major public health challenge and substantial health burden worldwide, accounting for most urinary tract infections and over 90% of food and waterborne diseases (Oliver et al., 2005; Jones et al., 2008; Scharff, 2012). On the other hand, the increasing trend of antibiotics resistance poses another significant threat to public health. Therefore, the rapid and sensitive detection of *E.coli* concentration and *E.coli* antibiotic resistance has been a crucial research topic and is critical to the early diagnosis and prevention of *E.coli* infection. The current gold-standard method, culturing and plate counting, is accurate and reliable for *E.coli* detection. However, it is quite time-consuming and laborious, requiring at least 2 days from sampling to results and even longer for antibiotic resistance analysis (Rompre et al., 2002). Another widely used and promising method for *E. coli* detection is determination of β-gal activity. β-gal is a well-known intracellular enzyme that is encoded by the lacZ operon in *E. coli* cells and it has been widely used as an indicator for the determination of *E. coli* concentration in drinking water and food samples (Colquhoun et al., 1995; Derda et al., 2013; Burnham et al., 2014; Chen et al., 2015; Chen et al., 2016). A number of strategies and probes have been developed to detect β-gal in *E. coli*. Unfortunately, those strategies often take several hours for reaction and are only employed with either colorimetric or fluorescence sensing. Moreover, the requirement of multiple steps of T7 bacteriophage infection and complex chemical reaction in some assays further restrict their clinical application (Chen et al., 2015; Chen et al., 2016; Wang et al., 2017).

Here, we utilized a simple and effective probe, DCM-βgal, for dual sensitive fluorescence and colorimetric measurement of β-gal activity. For this sensing probe, dicyanomethylene-4H-pyran (DCM) chromophore is utilized as reporter, and a β-gal-responsive group (β-galactopyranoside) as the enzyme-active trigger (Figure 1) (Gu et al., 2016). DCM-βgal emits weak background fluorescence in aqueous buffer. In the presence of β-gal, the β-galactopyranoside unit is cleaved, releasing the DCM group, resulting in a remarkable fluorescent emission in the near-infrared region (NIR) and an obvious color shift from yellow to red. The probe enables sensitive and accurate detecting of β-gal activity with high-selectivity and simplicity. Unlike rhodamine derivates, there is only a single cleavage site in DCM-βgal, which makes the kinetic analysis much easier. The sensing strategy was employed to detect *E. coli* in aqueous solutions using β-gal activity as indicator. The bacterial cells were lysed by lysis solution to release β-gal for enzymatic reaction. Once released, β-gal catalyzed the β-gal cleavable unit in DCM-βgal to generate DCM and induced a colorimetric and fluorescence change (Figure 1). The concentration of *E. coli* cells was directly correlated with the colorimetric shift and the fluorescence intensity of emission spectra peak. DCM-βgal possesses several advantages, including a fast response speed, a high light-up ratio and a good sensitivity towards β-gal, making it a promising strategy for rapid sensing of β-gal.

Experimental section

Materials

β-Galactosidase (β-Gal), horseradish peroxidase, alkaline phosphatase, papain, pepsin, and α-mannosidase were purchased from Beyotime (Shanghai, China). Lysozyme, glucose, bovine serum albumin, γ-globulin, transferrin, mannitol tryptophan and proline were purchased from Solarbio (Beijing, China). Ciprofloxacin, ampicillin, kanamycin, dimethyl sulfoxide (DMSO), Polypropylene

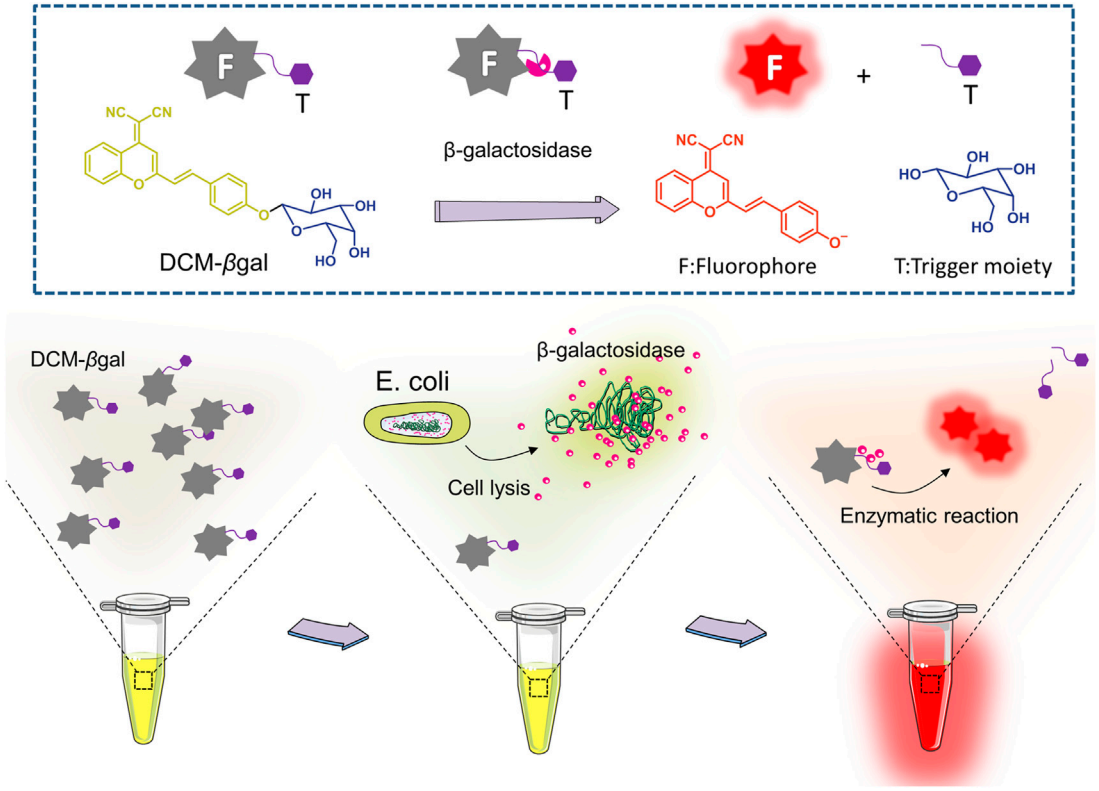

FIGURE 1
Schematic illustration of enzyme-induced probe assay for measuring of β-gal concentration and detection of *Escherichia coli* (*E.coli*). DCM-βgal probe consists of two parts: DCM-OH as the reporter unit and a β-gal-responsive unit. In the presence of β-gal, the responsive unit is cleaved and the DCM group shows enhance fluorescent emission and an obvious color shift from yellow to red. For *E.coli* detection, the bacterial cells are lysed to release β-gal for enzymatic reaction. The concentration of *E. coli* cells is correlated with the colorimetric shift and the fluorescence intensity of emission spectra peak.

pyrrolidone K30 (PVP-K30, MW = 40,000) and all other chemicals and solvents were purchased from Sigma-Aldrich (St. Louis, United States). Luria-Bertani broth (LB) medium was purchased from BD Biosciences (San Jose, CA). All aqueous solutions were prepared with Milli-Q water (≥18 MΩ, Milli-Q, Millipore).

Synthesis of DCM-βgal

DCM-βgal was synthesized according to the processes described in Supplementary Scheme S1 in Supplementary Material. The substrate Ac4β-Gal-Ph-CHO (320 mg, 0.71 mmol, 1 equiv) was dissolved in 15 ml of acetonitrile followed by the addition of piperidine (70 µl, 0.71 mmol, 1 equiv) and dicyanomethyl chromone (DCMC) (221 mg, 1.06 mmol, 1.5 equiv). Reaction mixture was stirred at 70°C for 2 h and monitored by thin layer chromatography (Petroleum ether: Ethyl acetate = 2: 1). Upon completion, the reaction mixture diluted with Ethyl acetate (100 ml) was washed with saturated solution of 0.5 M HCl (100 ml). The organic layer was separated, washed with brine, dried over Na_2SO_4 and evaporated under reduced pressure. The orange residue was purified by column chromatography on silica gel (Petroleum ether: Ethyl acetate = 4: 1) affording Ac4β-Gal-DCM as an orange solid. The residue was dissolved in DCM and MeOH (15 ml, v/v = 1:2), and the MeONa (10 mg, 0.35 mmol, 0.5 equiv) was added into the solution. The mixture was stirred for 50 min, at room temperature and monitored by thin layer chromatography (DCM: MeOH = 10: 1). Upon completion, the reaction mixture was evaporated under reduced pressure. The orange residue was purified by column chromatography on silica gel (DCM: MeOH = 10: 1) affording the target product DCM-βgal as an orange solid (272 mg, 41% yield for two steps). And the NMR data is same as the literature reported (Gu et al., 2016).

UV-vis and fluorescence spectral measurements

DCM-βgal solution was prepared at a concentration of 100 µM in a 2 ml total volume of reaction buffer (pH 7.4, 30% DMSO and

70% PBS). 1 U ml^{-1} β-gal was added into DCM-βgal solution and the mixture was gently agitated and incubated at 37°C for 15 min. UV-vis absorption spectra for DCM-βgal and reaction product were respectively analyzed on a PerkinElmer Lambda 25 UV/vis Spectrometer. Photoluminescence (PL) spectra were analyzed on a PerkinElmer spectrfluorometer LS55 with a wavelength range of 550–800 nm. Fluorescence quantum yields were detected on a Hamamatsu absolute PL quantum yield spectrometer C11347 Quantaurus-QY.

Analytical procedures for detection of β-gal

The stock solution (100 mM) of DCM-βgal was prepared in DMSO and the work solution (100 μM, fDMSO% = 30 vol%) was diluted from the stock solution. Different concentrations of β-gal solution (10 μl) were added into work solution (1 ml) and incubated at 37°C for 15 min. The fluorescence intensity at 675 nm and colorimetric results were recorded for the enzymatic products using PerkinElmer spectrofluorometer LS55.

Photobleaching analysis

1 U ml^{-1} β-gal was added into DCM-βgal solution and the mixture was incubated at 37°C for 15 min. Then enzymatic products were treated with high density bright-light exposure (20 W). The fluorescence intensity of the solution was monitored from 0 to 45 min of exposure.

Bacterial culture

A single colony of *E. coli* was selected from a LB plate and added into LB liquid medium and incubated overnight at 37°C under in the orbital shaker of 200 rpm agitation. The *E. coli* cells was harvested by centrifugation at 6000 g for 3 min and re-suspended in PBS buffer. The centrifugation process was repeated for three times. The re-suspended bacterial solution was then serially diluted into various concentrations for further use. The diluted *E. coli* solution was plated on LB agar plate to confirm the visible counts (CFU ml^{-1}).

Detection of *E. coli* using DCM-βgal based assay

Bacteria suspension with different concentrations was centrifugated by 6000 g for 3 min and discarded the supernatant. Subsequently, 0.7 ml lysis buffer containing 1 mg ml^{-1} lysozyme, 1% (w/v) sodium chloride, 0.2% (w/v) glycerin, 0.01% (w/v) PVP-K30 was added to the bacterial precipitate, mixed gently and incubated at 37°C for 30 min. The dissolved suspension was then added with 100 μM DCM-βgal and 0.3 ml DMSO and incubated at 37°C for 15 min after gently mixed. The fluorescence intensity at 675 nm and colorimetric results were recorded for the enzymatic solution using PerkinElmer spectrofluorometer LS55.

Two-step detection of *E. coli* using DCM-βgal based assay

Different concentrations of bacterial solutions (100 μL, 1×10^5, 5×10^4, 1×10^4, 5×10^3, and 1×10^3 CFU ml^{-1}) were incubated in LB broth (900 μl) at 37°C for 1–3 h with 200 rpm agitation. PBS buffer without bacteria cells was taken as a negative control. After incubation, bacteria suspension was centrifugated and the bacterial precipitate was lysed by 0.7 ml lysis buffer as above. The dissolved suspension was added with 100 μM DCM-βgal and 0.3 ml DMSO and incubated at 37°C for 15 min. The fluorescence intensity and colorimetric results of solutions were recorded.

Bacteria antibiotic resistance analysis

For bacteria antibiotic resistance sensing, LB broth medium was added with different antibiotic drugs (ampicillin, kanamycin, or ciprofloxacin) with varying concentrations (0, 10, 20, 30, 40, and 50 μg ml^{-1}). Then, *E.coli* solutions (10^5 CFU ml^{-1}) were added in LB mixtures at 37°C for 3 h with 200 rpm agitation in a constant temperature shaker. After incubation, bacteria suspension was centrifugated and the bacterial precipitate was lysed by 0.7 ml lysis buffer as above. The dissolved suspension was then added with 100 μM DCM-βgal and 0.3 ml DMSO and incubated at 37°C for 15 min after gently mixed. Then, the supernatant was transferred to 96-well plate and the fluorescence intensity of solutions was analyzed by Cytation 5.

Statistical analysis

All continuous data was presented as means ± standard deviation. Data was statistically analyzed using t-test. $p < 0.05$ was considered statistically significant.

Results and discussion

Spectroscopic properties and optical response to β-gal

The basic chemical structure and the principle of DCM-βgal probe for β-gal activity sensing are shown in Figure 1. The synthetic route of DCM-βgal is display in Supplementary Scheme S1 in Electronic Supplementary Material. DCM derivatives are well-known as laser dyes that produce intense emission in the NIR region and DCM-OH is a commonly used

signal reporter because of its special properties: it is a Donor–π–acceptor (D–π–A) molecule and it has a hydroxyl group that can be easily modified by other groups (Gu et al., 2016; Gu et al., 2019). Thus, DCM-βgal probe consists of two parts: DCM-OH as colorimetric and fluorescent reporter and a β-galactopyranoside unit as β-gal-responsive moiety. Firstly, to test the validity of DCM-βgal, its spectral properties were investigated by UV-vis-NIR spectroscopy and photoluminescence (PL) spectrum. As shown in Figure 2A, the absorption spectrum showed that DCM-βgal exhibited an obvious absorption peak at 440 nm. Upon addition of 1 U ml^{-1} β-gal, the absorption peak significantly decreased at 440 nm and a new absorption peak appeared at 535 nm. This new absorption was in accordance with that of DCM-O-, suggesting that DCM-βgal was cleaved by β-gal and resulting DCM-OH generation (Gu et al., 2016). Then, the emission profile of DCM-βgal was detected. Upon excitation at 535 nm, the fluorescence signal of DCM-βgal was very weak while the probe solution showed a remarkable NIR fluorescence at 675 nm in the presence of β-gal (Figure 2B). In particular, an obvious color shifting from yellow to red could be observed, allowing for the qualitative or semi-quantitative detection of β-gal by direct observation and rapid colorimetric analysis.

Optimization of assay conditions

The reaction solution, temperature and pH are important factors for the sensing system. To obtain the best sensing performance, the optical properties of DCM-βgal were examined in different analytical parameters. Upon addition of 1 U ml^{-1} β-gal, the fluorescence intensity of DCM-βgal at 675 nm was tested in PBS/dimethyl sulfoxide (DMSO) mixtures with different DMSO volume fractions (fDMSO%). As shown in Supplementary Figure S1A,B (Electronic Supplementary Material), the fluorescence intensity of DCM-βgal solution increased quickly with fDMSO% and reached a maximum at fDMSO% = 30 vol%. Specifically, as the DMSO content continued to increase, the fluorescence intensity decreased sharply and DCM-βgal solution showed very weak fluorescence at fDMSO% = 50–100 vol%. Correspondingly, a similar colorimetric change could be observed with the change of fDMSO% (Supplementary Figure S1C in Supplementary Material). Since DCM-βgal is poor solvent in PBS, the addition of DMSO will increase its solubility and induces an increase in fluorescence emission. Thus, PBS solution with 30% DMSO was applied as the optimal reaction solution.

The effect of reaction temperature and pH was then evaluated. The fluorescence response of DCM-βgal to 1 U ml^{-1} β-gal was examined by incubation of the solution from 4°C to 56°C for 15 min. As expected, the fluorescence signal increased with temperature and reached the maximum at 37°C, and then decreased after 37°C (Supplementary Figure S2A in Supplementary Material). Hence, 37°C was selected as optimal reaction temperature. pH is another important factor affecting the rate of enzymatic reaction for the sensing probe. pH was adjusted to the desired value by using 0.1 M NaOH and 0.1 M HCl solutions. The pH was measured with a pH meter. The effect of pH (4.0–11.0) for the emission profiles of DCM-βgal was subsequently evaluated after 15 min of reaction. It can be observed that the fluorescence signal was very weak at pH lower than 6.12 and higher than 8.46, and the maximum fluorescence signal was achieved at pH = 7.59 (Supplementary Figure S2B in Supplementary Material). The result suggested that the enzymatic hydrolysis reaction for DCM-βgal could only be proceeding at the optimal pH range and pH = 7.59 was used as the optimal pH condition. In particular, the color of the solution varied from yellow to red corresponding to temperature and pH of the solution. The distinct color changes of the probe were therefore easily to identify visually (Supplementary Figures S2C,D in Supplementary Material).

Then, the fluorescence signal versus time was analyzed to investigate the enzyme response rate. As shown in Supplementary Figure S3A,B (Supplementary Material), as the incubation with β-gal, the fluorescence intensity of DCM-βgal gradually increased in the early stage and reached the maximum at around 15 min. Moreover, the fluorescence response of β-gal in different concentrations of DCM-βgal was investigated to determine the optimal probe concentration. Increasing concentrations of DCM-βgal (0–140 μM) were incubated with 1 U ml^{-1} β-gal at 37°C for 15 min. As depicted in Supplementary Figure S3C (Supplementary Material), the fluorescent signal increased gradually with increasing the concentration of DCM-βgal and reached a plateau after a concentration of 100 μM. Therefore, a DCM-βgal concentration of 100 μM was selected for further experiments to provide an optimal probe concentration. DCM-βgal displayed similar colorimetric response with the increasing of DCM-βgal concentration and incubation time, suggestive of its feasibility in dual-channel sensing for β-gal (Supplementary Figure S3D,E in Supplementary Material).

Analytical performance of DCM-βgal to β-gal

We next sought to investigate the analytical performance of DCM-βgal for β-gal detection. The fluorescence response of the probe to varying concentrations of β-gal was examined under optimized conditions. As expected, the fluorescence intensity of solution increased with the increasing of β-gal concentration and a 94.84-fold fluorescence enhancement was observed when incubated with 1 U ml^{-1} β-gal (Figures 2C,E). Notably, a good linear relationship between the fluorescence intensity at 675 nm and β-gal concentration in a range from 0 U ml^{-1} to 0.2 U ml^{-1} was observed (Figure 2D). The limit of detection (LOD) was calculated to be as low as 1.5×10^{-3} U ml^{-1} based on the signal of

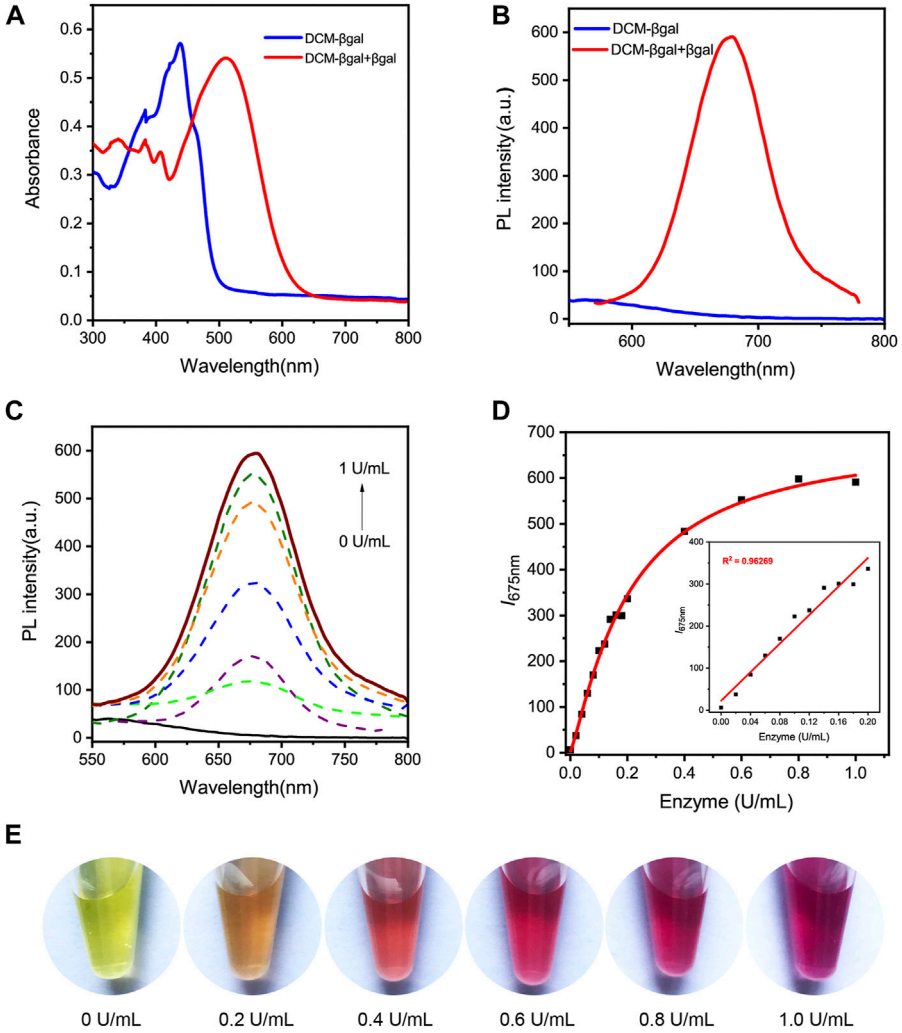

FIGURE 2
Spectral properties of DCM-βgal. **(A)** Normalized UV-vis absorption of DCM-βgal (100 μM) and DCM-βgal (100 μM) incubation with β-gal (1 U ml^{-1}) in aqueous solution (PBS/DMSO = 7:3, v:v, pH = 7.4, 37°C). **(B)** Photoluminescence (PL) spectra of DCM-βgal (100 μM) and DCM-βgal (100 μM) incubation with β-gal (1 U ml^{-1}) in aqueous solution (PBS/DMSO = 7:3, v:v, pH = 7.4, 37°C). **(C)** Emission spectra of DCM-βgal upon addition of different concentrations β-gal (0–1 U ml^{-1}), λex = 535 nm. **(D)** The peak intensity of DCM-βgal at 675 nm toward various concentrations of β-gal (0–1 U ml^{-1}). Inset: the linear relationship between $I_{675\ nm}$ and β-gal concentration in a range from 0 U ml^{-1} to 0.2 U ml^{-1} **(E)** The photographs of DCM-βgal upon addition of various concentrations of β-gal.

blank tests and the standard deviation, indicating the high sensitivity of the probe for the fast and quantitative detection of β-gal. Photo-stability is another important factor to evaluate the performance of the probe in long-term tracking and bioimaging of enzyme activity (Liu et al., 2016). The photo-stability of DCM-βgal was then assessed by time-dependent photobleaching measurements. 1 U ml^{-1} β-gal was added into DCM-βgal solution and the mixture was incubated at 37°C for 15 min. Then enzymatic products were treated with high density bright-light exposure (20 W). The results showed that rounded to 82% of DCM-βgal fluorescence intensity still remained after bright-light exposure for 30 min, indicating the high photo-stability of DCM fluorophore (Supplementary Figure S4 in Supplementary Material). These features make DCM-βgal a promising candidate for long-term tracking and imaging of β-gal in practical applications.

The selectivity of DCM-βgal

Subsequently, the selectivity of probe to β-gal sensing was then evaluated. Control experiments were conducted to investigate the selectivity of DCM-βgal towards of various biological species, including common enzymes (horseradish

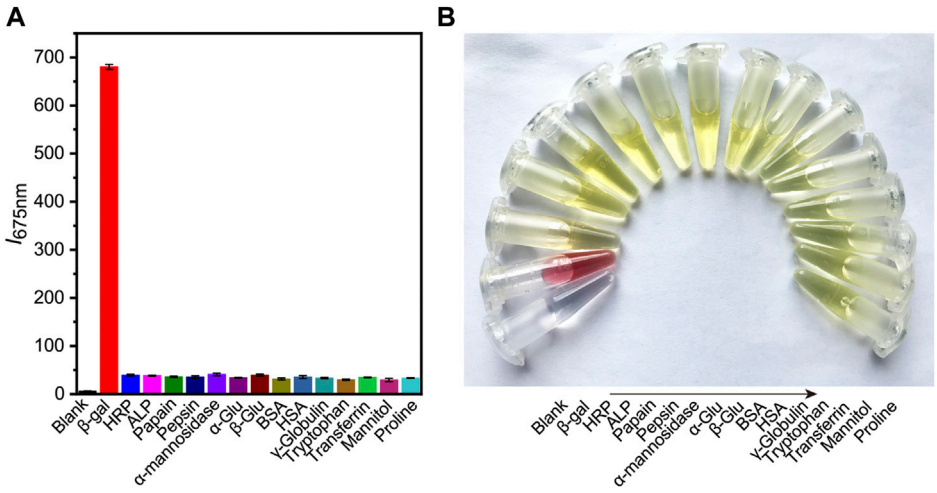

FIGURE 3
The selectivity of DCM-βgal towards of various biological species. Different types of biological samples are added into work solution of DCM-βgal and incubated at 37°C for 15 min. The fluorescence intensity at 675 nm and colorimetric results of solution are then recorded. **(A)** The fluorescence responses ($I_{675\ nm}$) of DCM-βgal to various analytes. Error bars represent the standard deviation of three replicates. **(B)** Corresponding color changes of DCM-βgal treated with different analytes.

peroxidase, alkaline phosphatase, papain, pepsin, and α-mannosidase), bioactive molecules (glucose, bovine serum albumin, γ-globulin, transferrin, and mannitol) and amino acids (tryptophan and proline). As expected, an obvious fluorescence enhancement accompanying with an obvious color change from yellow to red was observed in the presence of β-gal (Figure 3). However, negligible fluorescence and color change was observed for other interferents. These results demonstrated the high selectivity of DCM-βgal for β-gal over other competitive analytes, suggesting its promising use as a bioprobe for detecting β-gal in biological systems.

Application for detection of *Escherichia coli*

Encouraged by the desirable results of DCM-βgal, we next sought to investigate the potential utility of DCM-βgal for detecting β-gal from *E. coli* cells. β-gal is an important bacteria enclosed enzyme encoded by the lacZ gene in *E. coli* cells, and can be used as an indicator for determination of the concentration of *E. coli* (Laczka et al., 2010; Derda et al., 2013; Burnham et al., 2014; Chen et al., 2016). *E. coli* ATCC 25926 was used as a model for investigating the performance of DCM-βgal in *E. coli* detection. Varying concentrations of bacterial cells were firstly lysed, resulting in the release of intracellular β-gal from cells into solution. Then, the solution containing the released β-gal was incubated with DCM-βgal to determine its concentration under optimized conditions. As a result, the *E. coli* concentration could be assessed using the fluorescence intensity of DCM, or directly by the naked eyes. As shown in Figure 4A, the fluorescence intensity and the red color of the enzymatic solution increased with the increasing of bacterial concentration, and distinct signal changes could be reproducibly detected or be distinguished visually for 1×10^5 CFU ml^{-1} of *E. coli* cells (Figure 4B). Compared with previously methods, the DCM-βgal based assay showed a low detection limit and provided a convenient colorimetric readout for visual detection, making it a sensitive and simple strategy for *E. coli* detection.

To test the specificity of the assay to *E. coli*, the responses of the assay to common bacteria strains, including *Staphylococcus aureus* (S.*aureus*), *Klebsiella pneumoniae* (*K. pneumoniae*), *Pseudomonas aeruginosa* (*P. aeruginosa*), *Candida* albicans (*C.albicans*) and *Candida* glabrata (*C.glabrata*), as well as mixtures of different bacteria strains, were investigated. A concentration of 1×10^6 CFU ml^{-1} was used for solutions of each strain or their mixtures. Figures 4C,D shows the fluorescence and colorimetric detection results. No obvious fluorescence signal and color change were observed in S.*aureus*, *P. aeruginosa*, *C.albicans* and *C.glabrata* solutions. In contrast, a significant fluorescence response and distinct color change were detected in *E. coli* solution or in mixtures containing *E. coli*. In particular, the fluorescence intensity of *K. pneumonia* solution was slightly increased and the color of the solution changed from yellow to orange, correspondingly. This result was in accordance with the fact that a certain level of β-gal isoenzymes could be

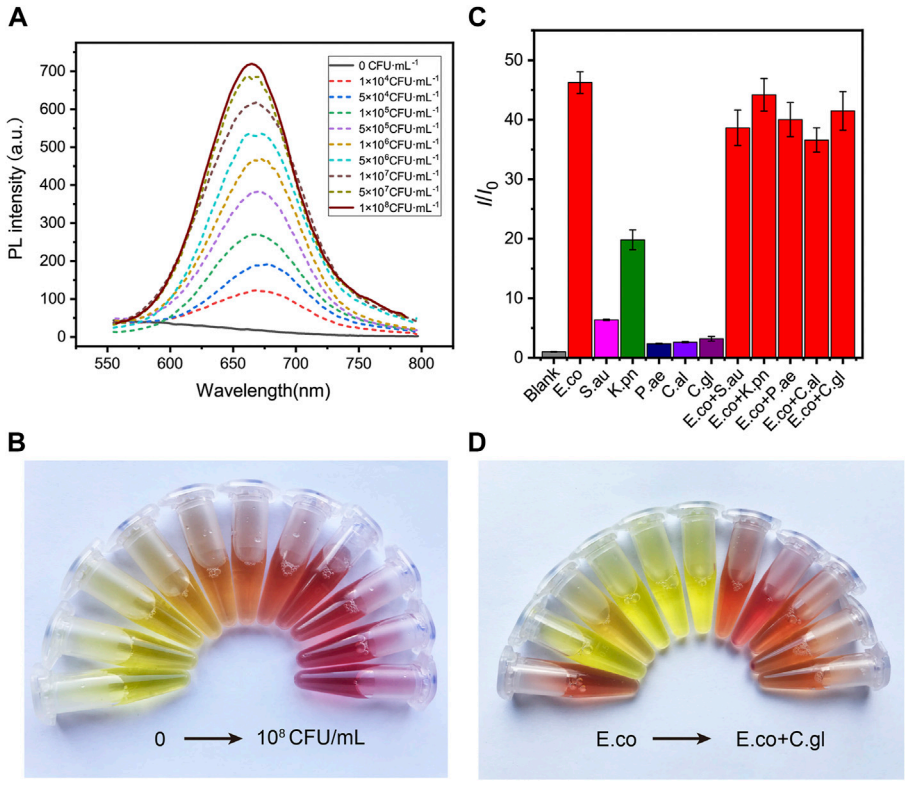

FIGURE 4
The sensitivity and specificity of DCM-βgal based assay to *E. coli*. **(A)** DCM-βgal based assay for the detection of *E.coli* in the concentration range of 0–1.0 × 10^8 CFU ml^{-1} and **(B)** its corresponding color changes. Error bars indicate ± SD of triplicate measurements. **(C)** Fluorescence ratio (I/I_0) of specificity of the DCM-βgal probe against *E.coli*, *S. aureus*, *K. pneumonia*, *P. aeruginosa*, *C.albicans*, *C.glabrata*, *E.coli* + *S. aureus*, *E.coli* + *K. pneumonia*, *E.coli* + *P. aeruginosa*, *E.coli* + *C.albicans* and *E.coli* + *C.glabrata* at concentration of 1.0 × 10^6 CFU ml^{-1}. **(D)** Its corresponding photographs.

encoded by *K. pneumonia* (Wang et al., 2014). These results demonstrated that the dual-channel assay had a good selectively to β-gal for *E. coli* detection.

The concentration of *E. coli* cells is important for the enzymatic response, whereas *E. coli* in clinical urine samples is well below 1 × 10^4 CFU ml^{-1}. To improve the clinical performance of the assay, two-step process was employed to detect *E. coli* cells at low concentrations. Pre-enrichment step was utilized to allow for bacterial growth, and the detection step was then used for determination of *E. coli* cells. Low concentrations of bacteria were incubated in LB liquid medium for 1, 2, and 3 h, respectively. The fluorescence intensity and the color change of solution were investigated after bacteria incubation and enzymatic reaction. As shown in Figures 5A,B, a significant fluorescence and obvious colorimetric response could be detected after 3 h pre-enrichment in all concentrations. *E. coli* cells at the concentration of 1 × 10^5 CFU ml^{-1}, 5 × 10^4 CFU ml^{-1} and 1 × 10^4 CFU ml^{-1} could also be clearly detected after a pre-enrichment step of 2 h incubation. Compared with previous methods, the assay was a more efficient strategy with the whole detection time less than 5 h (Chen et al., 2017; Wang et al., 2017). As shown in Table 1, several similar assays for *E. coli* detection were summarized and compared. Sensitive methods often require advanced instrumentation and cumbersome processes, limiting their use in resource-limited settings. In contrast, the DCM-βgal assay would be a promising method for rapid detection of *E. coli* for their practicality, simplicity and low-cost. These results indicated that the DCM-βgal assay had a good performance for *E. coli* detection at low concentrations incorporating a pre-enrichment step.

Application for *Escherichia coli* antibiotic resistance determination

The prevalence of bacteria's antibiotic resistance is a growing global health concern and it is in urgent need to develop a rapid, efficient strategy for the determination of *E. coli* antibiotic

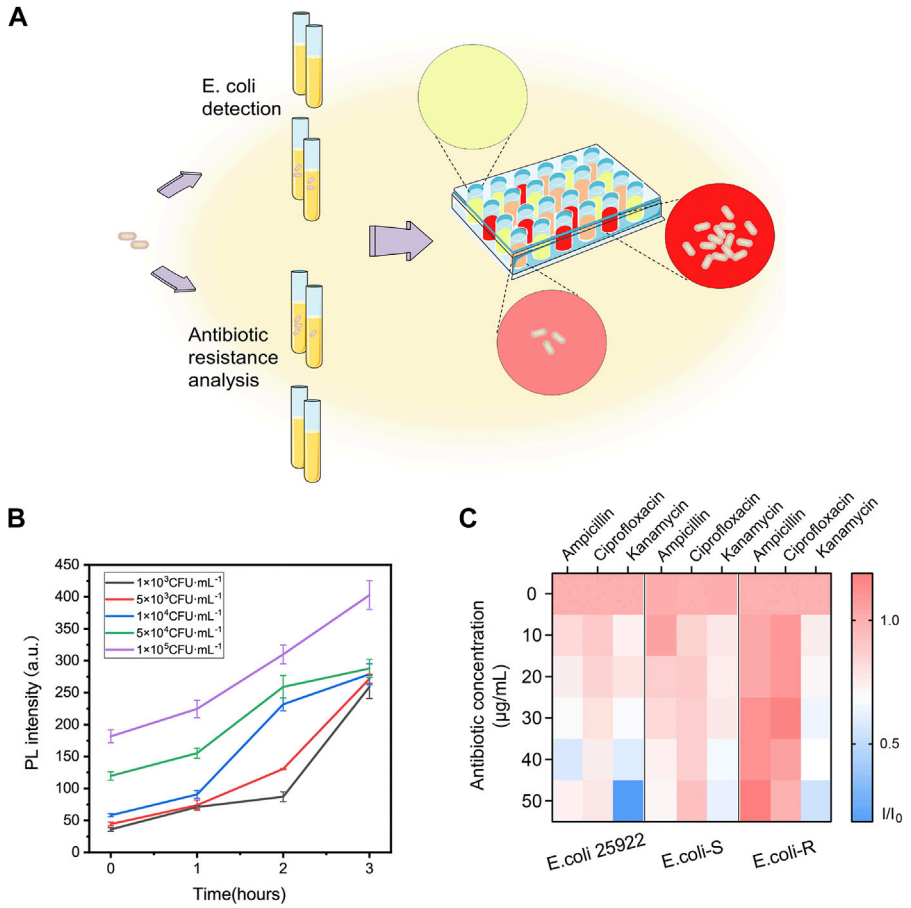

FIGURE 5
Two-step procedure for *E. coli* detection and high-throughput antibiotic screening using DCM-βgal based assay. **(A)** Schematic illustration of two-step procedure and high-throughput antibiotic analysis. *E. coli* cells are lysed to release intracellular β-gal and the signal generation based on enzyme-response is correlated with the concentration of *E. coli* cells. For antibiotic resistance analysis, *E. coli* cells can be treated with various antibiotic concentrations and fluorescence ratio of reaction products in 96-well plate can be high throughput monitored by Cytation. **(B)** Two-step detection of *E. coli* at low concentrations using DCM-βgal based assay. PL intensity (675 nm) with detection time (0–3 h) toward *E. coli* concentration of 1×10^3, 5×10^3, 1×10^4, 5×10^4, and 1×10^5 CFU ml^{-1}. Error bars indicate ± SD of triplicate measurements. **(C)** Heatmap plot of fluorescence ratio (I/I_0) of three types of *E. coli* cells (*E. coli* ATCC 25926, antibiotic-sensitive (*E. coli*-S) and resistant *E. coli* (*E. coli*-R) collected from clinical samples) toward various antibiotic concentrations.

resistance (Walsh, 2000). Conventional test for bacteria antibiotic resistance detection requires cumbersome processes and often takes days to weeks for results. Inspired by the high sensing property of the probe, the ability of DCM-βgal based assay for rapidly detection of *E. coli* antibiotic resistance was then studied (Figure 5A). *E. coli* ATCC 25926, antibiotic-sensitive (E. coli-S) and resistant *E. coli* (E. coli-R) collected from clinical samples were used as bacterial model, and the response of the assay to the bacterial was examined in the presence of three common antibiotics, ampicillin, kanamycin, and ciprofloxacin. *E. coli* cells were incubated in LB liquid medium containing different concentrations of antibiotics at 37°C for 3 h. Bacterial cells were lysed and DCM-βgal probe was then added for enzymatic reaction to determine bacteria concentration. In the presence of effective antibiotic drugs, *E. coli* cells exhibited inhibited growth and a greatly reduced level of β-gal. However, *E. coli* cells showed exponential growth in the presence of antibiotic resistance. Varying levels of β-gal resulted in different levels of enzymatic response, thus providing a simple strategy for antibiotic resistance analysis. With the help of a high throughput fluorescence detection system, Cytation, the fluorescence information of 96-well plate could be easily quantified and monitored. As shown in Figure 5C, for *E. coli* ATCC 25926 and E. coli-S, the fluorescence intensity decreased with the increasing antibiotic concentration when incubated with ampicillin, kanamycin, and ciprofloxacin, indicating that these antibiotics were effective drugs for inhibiting cell growth of these strains. However, for E. coli-R,

TABLE 1 Summary and comparison of techniques for detection of *E. coli* stains.

Method (publication year)	Output	Detection limit	Detection time	Antibiotic resistance analysis	Instruments	Cost	Ref
Our DCM-βgal based assay	Luminescent and Colorimetry	10^3 CFU ml^{-1}	5 h	Yes	Simple	Low	
p-Benzoquinone (2019)	Colorimetry and Electrochemistry	10^4 CFU ml^{-1}	1 h	Yes	Complex	Middle	Sun et al. (2019)
Sequential Immunomagnetic Separation and Paper-Based Isotachophoresis (2019)	Colorimetry	920 CFU ml^{-1}	3 h	No	Middle	Middle	Schaumburg et al. (2019)
Electrochemical methods using engineered bacteriophages (2017)	Electrochemistry	10^2 CFU ml^{-1}	7 h	No	Complex	Middle	Wang et al. (2017)
Printed Paper- and Transparency-Based Analytic Devices (2017)	Colorimetry and Electrochemistry	2.3 × 10^2 CFU ml^{-1}	4 h	No	Complex	Middle	Adkins et al. (2017)
Engineered T7lacZ phage (2017)	Colorimetry	10^2 CFU ml^{-1}	7 h	Yes	Middle	Middle	Chen et al. (2017)
Enzyme-induced silver metallization on the surface of AuNRs (2016)	Colorimetry	10^4 CFU ml^{-1}	2 h	No	Simple	Low	Chen et al. (2016)
T7Bacteriophage-conjugated Magnetic Probe (2015)	Colorimetry	10^4 CFU ml^{-1}	2.5 h	No	Middle	Middle	Chen et al. (2015)
On-site phage-mediated detection (2014)	Luminescent	40 CFU ml^{-1}	8 h	No	Complex	Middle	Burnham et al. (2014)
Filter-Based Assay (2013)	Colorimetry	50 CFU ml^{-1}	Less 4 h	No	Complex	Middle	Derda et al. (2013)
Interdigitated microelectrode arrays (2010)	Electrochemistry	6 × 10^5 CFU ml^{-1}	2 h	No	Complex	Middle	Laczka et al. (2010)
Interdigitated microelectrode arrays (2010)	Electrochemistry	10 CFU ml^{-1}	7 h	No	Complex	Middle	Laczka et al. (2010)
Bacteriophage-amplified bioluminescent sensing (2008)	Luminescent	1 CFU ml^{-1}	12.5 h	No	Complex	Middle	Ripp et al. (2008)
Bead-based immunoassay (2005)	Electrochemistry	2 × 10^6 CFU ml^{-1}	Less 1 h	No	Complex	Middle	Boyaci et al. (2005)
Bead-based immunoassay (2005)	Electrochemistry	20 CFU ml^{-1}	6–7 h	No	Complex	Middle	Boyaci et al. (2005)

no decreasing trend for fluorescence intensity could be observed with the increasing concentration of ampicillin and ciprofloxacin, demonstrating that these antibiotics could not effectively inhibited cell growth of this strain. The resistance results were in consistent with those of Kirby-Bauer tests, a common conventional test. Thus, this enzyme-activatable assay has the potential to provide a simple and accessible tool for *E. coli* antibiotic resistance analysis.

Conclusion

In conclusion, we have proposed an enzyme-responsive NIR probe, DCM-βgal, for sensitive measuring and monitoring β-gal activity. DCM-βgal was almost non-emissive in the absence of β-gal, while it could be induced to produce bright emission upon the addition of β-gal. Particularly, the probe also provided a rapid and convenient colorimetric readout for visual assaying of the β-gal activity. The probe displayed high sensitivity, selectivity and rapid response to β-gal. Simultaneously, the probe also had a good photo-stability, and exhibited a good linear relationship with β-gal concentration from 0 to 0.2 U ml^{-1}, with a low detection limit of 1.5 × 10^{-3} U ml^{-1}. Importantly, this assay was successfully applied to sensitive detection of *E. coli* cells, as well as rapidly determination of the antibiotic resistance profile of *E. coli via* levels of the color response. The strategy provided several advantages for *E. coli* detection, including a fast detection process within 5 h, a low detection concentration of 1 × 10^3 CFU ml^{-1}, a good selectively to *E. coli* sensing and dual fluorescent and colorimetric readout. Further developments include integrating this assay into point of care testing devices, detecting more real and complex samples would provide improved detection outcomes. Overall, the simple, low-cost and friendly-to-user approach provides an accessible tool for efficient quantification of β-gal activity and is promising for *E. coli* detection and antibiotic resistance analysis.

Data availability statement

The original contributions presented in the study are included in the article/Supplementary Material, further inquiries can be directed to the corresponding authors.

Author contributions

YH: Conceptualization, Methodology, Writing—original draft, Supervision. WF: Methodology, Data curation, Investigation. G-QZ: Synthesizing the probe. YQ, LL, and LP: Writing—review and editing. NC: Review and editing, Supervision.

Funding

This study was supported by the Open Project of NHC Key Laboratory of Thalassemia Medicine (GJWJWDP202203).

Acknowledgments

The authors thank Key Laboratory of Bioactive Materials, State Key Laboratory of Medicinal Chemical Biology, Key Laboratory of Functional Polymer Ministry of Education, and College of Life Sciences, Nankai University for their assistance in synthesizing of DCM-βgal probe. We thank Department of Clinical Laboratory, Guangzhou Twelfth People's Hospital, Guangzhou, China for providing the bacterial cells.

Conflict of interest

The authors declare that the research was conducted in the absence of any commercial or financial relationships that could be construed as a potential conflict of interest.

Publisher's note

All claims expressed in this article are solely those of the authors and do not necessarily represent those of their affiliated organizations, or those of the publisher, the editors and the reviewers. Any product that may be evaluated in this article, or claim that may be made by its manufacturer, is not guaranteed or endorsed by the publisher.

Supplementary material

Supplementary Material for this article can be found online at: https://www.frontiersin.org/articles/10.3389/fbioe.2022.1052801/full#supplementary-material

References

Adkins, J. A., Boehle, K., Friend, C., Chamberlain, B., Bisha, B., and Henry, C. S. (2017). Colorimetric and electrochemical bacteria detection using printed paper- and transparency-based analytic devices. *Anal. Chem.* 89 (6), 3613–3621. doi:10.1021/acs.analchem.6b05009

Boyaci, I. H., Aguilar, Z. P., Hossain, M., Halsall, H. B., Seliskar, C. J., and Heineman, W. R. (2005). Amperometric determination of live *Escherichia coli* using antibody-coated paramagnetic beads. *Anal. Bioanal. Chem.* 382 (5), 1234–1241. doi:10.1007/s00216-005-3263-8

Burnham, S., Hu, J., Anany, H., Brovko, L., Deiss, F., Derda, R., et al. (2014). Towards rapid on-site phage-mediated detection of generic *Escherichia coli* in water using luminescent and visual readout. *Anal. Bioanal. Chem.* 406 (23), 5685–5693. doi:10.1007/s00216-014-7985-3

Chen, J., Alcaine, S. D., Jackson, A. A., Rotello, V. M., and Nugen, S. R. (2017). Development of engineered bacteriophages for *Escherichia coli* detection and high-throughput antibiotic resistance determination. *ACS Sens.* 2 (4), 484–489. doi:10.1021/acssensors.7b00021

Chen, J., Alcaine, S. D., Jiang, Z., Rotello, V. M., and Nugen, S. R. (2015). Detection of *Escherichia coli* in drinking water using T7 bacteriophage-conjugated magnetic probe. *Anal. Chem.* 87 (17), 8977–8984. doi:10.1021/acs.analchem.5b02175

Chen, J., Jackson, A. A., Rotello, V. M., and Nugen, S. R. (2016). Colorimetric detection of *Escherichia coli* based on the enzyme-induced metallization of gold nanorods. *Small* 12 (18), 2469–2475. doi:10.1002/smll.201503682

Colquhoun, K. O., Timms, S., and Fricker, C. R. (1995). Detection of *Escherichia coli* in potable water using direct impedance technology. *J. Appl. Bacteriol.* 79 (6), 635–639. doi:10.1111/j.1365-2672.1995.tb00948.x

Derda, R., Lockett, M. R., Tang, S. K., Fuller, R. C., Maxwell, E. J., Breiten, B., et al. (2013). Filter-based assay for *Escherichia coli* in aqueous samples using bacteriophage-based amplification. *Anal. Chem.* 85 (15), 7213–7220. doi:10.1021/ac400961b

Fu, W., Yan, C., Zhang, Y., Ma, Y., Guo, Z., and Zhu, W. H. (2019). Near-infrared aggregation-induced emission-active probe enables *in situ* and long-term tracking of endogenous beta-galactosidase activity. *Front. Chem.* 7, 291. doi:10.3389/fchem.2019.00291

Gu, K., Qiu, W., Guo, Z., Yan, C., Zhu, S., Yao, D., et al. (2019). An enzyme-activatable probe liberating AIEgens: On-site sensing and long-term tracking of beta-galactosidase in ovarian cancer cells. *Chem. Sci.* 10 (2), 398–405. doi:10.1039/c8sc04266g

Gu, K., Xu, Y., Li, H., Guo, Z., Zhu, S., Shi, P., et al. (2016). Real-time tracking and *in vivo* visualization of beta-galactosidase activity in colorectal tumor with a ratiometric near-infrared fluorescent probe. *J. Am. Chem. Soc.* 138 (16), 5334–5340. doi:10.1021/jacs.6b01705

Jia, Z., Sukker, I., Muller, M., and Schonherr, H. (2018). Selective discrimination of Key enzymes of pathogenic and nonpathogenic bacteria on autonomously reporting shape-encoded hydrogel patterns. *ACS Appl. Mat. Interfaces* 10 (6), 5175–5184. doi:10.1021/acsami.7b15147

Jiang, G., Zeng, G., Zhu, W., Li, Y., Dong, X., Zhang, G., et al. (2017). A selective and light-up fluorescent probe for beta-galactosidase activity detection and imaging in living cells based on an AIE tetraphenylethylene derivative. *Chem. Commun.* 53 (32), 4505–4508. doi:10.1039/c7cc00249a

Jones, K. E., Patel, N. G., Levy, M. A., Storeygard, A., Balk, D., Gittleman, J. L., et al. (2008). Global trends in emerging infectious diseases. *Nature* 451, 990–993. doi:10.1038/nature06536

Komatsu, T., and Urano, Y. (2015). Evaluation of enzymatic activities in living systems with small-molecular fluorescent substrate probes. *Anal. Sci.* 31 (4), 257–265. doi:10.2116/analsci.31.257

Laczka, O., Garcia-Aljaro, C., del Campo, F. J., Munoz Pascual, F. X., Mas-Gordi, J., and Baldrich, E. (2010). Amperometric detection of Enterobacteriaceae in river water by measuring beta-galactosidase activity at interdigitated microelectrode arrays. *Anal. Chim. Acta X.* 677 (2), 156–161. doi:10.1016/j.aca.2010.08.001

Liu, X., Qiao, Q., Tian, W., Liu, W., Chen, J., Lang, M. J., et al. (2016). Aziridinyl fluorophores demonstrate bright fluorescence and superior photostability by effectively inhibiting twisted intramolecular charge transfer. *J. Am. Chem. Soc.* 138 (22), 6960–6963. doi:10.1021/jacs.6b03924

Munoz-Espin, D., and Serrano, M. (2014). Cellular senescence: From physiology to pathology. *Nat. Rev. Mol. Cell Biol.* 15 (7), 482–496. doi:10.1038/nrm3823

Nishihara, T., Kuno, S., Nonaka, H., Tabata, S., Saito, N., Fukuda, S., et al. (2018). Beta-galactosidase-responsive synthetic biomarker for targeted tumor detection. *Chem. Commun.* 54 (83), 11745–11748. doi:10.1039/c8cc06068a

Oliver, S. P., Jayarao, B. M., and Almeida, R. A. (2005). Foodborne pathogens in milk and the dairy farm environment: Food safety and public health implications. *Foodborne Pathog. Dis.* 2 (2), 115–129. doi:10.1089/fpd.2005.2.115

Ripp, S., Jegier, P., Johnson, C. M., Brigati, J. R., and Sayler, G. S. (2008). Bacteriophage-amplified bioluminescent sensing of *Escherichia coli* O157:H7. *Anal. Bioanal. Chem.* 391 (2), 507–514. doi:10.1007/s00216-007-1812-z

Rompre, A., Servais, P., Baudart, J., de-Roubin, M. R., and Laurent, P. (2002). Detection and enumeration of coliforms in drinking water: Current methods and emerging approaches. *J. Microbiol. Methods* 49 (1), 31–54. doi:10.1016/s0167-7012(01)00351-7

Scharff, R. L. (2012). Economic burden from health losses due to foodborne illness in the United States. *J. Food Prot.* 75 (1), 123–131. doi:10.4315/0362-028X.JFP-11-058

Schaumburg, F., Carrell, C. S., and Henry, C. S. (2019). Rapid bacteria detection at low concentrations using sequential immunomagnetic separation and paper-based isotachophoresis. *Anal. Chem.* 91 (15), 9623–9630. doi:10.1021/acs.analchem.9b01002

Sun, J., Warden, A. R., Huang, J., Wang, W., and Ding, X. (2019). Colorimetric and electrochemical detection of *Escherichia coli* and antibiotic resistance based on a p-benzoquinone-mediated bioassay. *Anal. Chem.* 91 (12), 7524–7530. doi:10.1021/acs.analchem.8b04997

Walsh, C. (2000). Molecular mechanisms that confer antibacterial drug resistance. *Nature* 406 (6797), 775–781. doi:10.1038/35021219

Wang, D., Chen, J., and Nugen, S. R. (2017). Electrochemical detection of *Escherichia coli* from aqueous samples using engineered phages. *Anal. Chem.* 89 (3), 1650–1657. doi:10.1021/acs.analchem.6b03752

Wang, H., Yang, R., Jiang, X., Hua, X., Zhao, W., Zhang, W., et al. (2014). Expression and characterization of two beta-galactosidases from *Klebsiella pneumoniae* 285 in *Escherichia coli* and their application in the enzymatic synthesis of lactulose and 1-lactulose. *Z Naturforsch C J. Biosci.* 69 (11-12), 479–487. doi:10.5560/znc.2014-0061

Zhang, X., Chen, X., Zhang, Y., Liu, K., Shen, H., Zheng, E., et al. (2019). A near-infrared fluorescent probe for the ratiometric detection and living cell imaging of beta-galactosidase. *Anal. Bioanal. Chem.* 411 (30), 7957–7966. doi:10.1007/s00216-019-02181-7

frontiers | Frontiers in Bioengineering and Biotechnology

TYPE Mini Review
PUBLISHED 01 November 2022
DOI 10.3389/fbioe.2022.1046234

OPEN ACCESS

EDITED BY
Zhanzhan Zhang,
Tianjin Medical University, China

REVIEWED BY
Zhaoting Li,
University of Wisconsin-Madison, United States

*CORRESPONDENCE
Bin Hao,
haobinwl@163.com

SPECIALTY SECTION
This article was submitted to Nanobiotechnology, a section of the journal Frontiers in Bioengineering and Biotechnology

RECEIVED 16 September 2022
ACCEPTED 21 October 2022
PUBLISHED 01 November 2022

CITATION
Hao B, Wei L, Cheng Y, Ma Z and Wang J (2022), Advanced nanomaterial for prostate cancer theranostics. *Front. Bioeng. Biotechnol.* 10:1046234. doi: 10.3389/fbioe.2022.1046234

Advanced nanomaterial for prostate cancer theranostics

Bin Hao[1]*, Li Wei[2], Yusheng Cheng[1], Zhifang Ma[3] and Jingyu Wang[4]

[1]Department of Urology, Central Hospital, China Railway 17th Bureau Group Co., Ltd., Shanxi, China, [2]Internal Medicine, Rongjun Hospital of Shanxi Province, Shanxi, China, [3]Department of Urology, First Hospital of Shanxi Medical University, Shanxi, China, [4]College of Biomedical Engineering and Technology, Tianjin Medical University, Tianjin, China

Prostate cancer (PC) has the second highest incidence in men, according to global statistical data. The symptoms of PC in the early stage are not obvious, causing late diagnosis in most patients, which is the cause for missing the optimal treatment time. Thus, highly sensitive and precise early diagnosis methods are very important. Additionally, precise therapy regimens for good targeting and innocuous to the body are indispensable to treat cancer. This review first introduced two diagnosis methods, containing prostate-specific biomarkers detection and molecular imaging. Then, it recommended advanced therapy approaches, such as chemotherapy, gene therapy, and therapeutic nanomaterial. Afterward, we summarized the development of nanomaterial in PC, highlighting the importance of integration of diagnosis and therapy as the future direction against cancer.

KEYWORDS

nanomaterial, prostate cancer, diagnosis, therapy, theranostics

1 Introduction

Prostate cancer (PC) has become the 4th most commonly diagnosed cancer (7.3% of all sites), according to GLOBOCAN 2020 estimates from the International Agency for Research on Cancer. For men, there is a higher incidence and mortality, which rank 2nd and 5th, respectively, among all cancers according to global statistics. In 2020, there were about 1.4 million new cases and estimated 375,000 deaths worldwide, which attracted increased attention to the theranostics of PC (Sung et al., 2021).

PC patients do not demonstrate evident symptoms in the early stage. Many of the symptoms are easily overlooked because of their similarity with the symptoms of prostatitis and benign prostatic hyperplasia. PC diagnosis, especially in the early phase, is indispensable for curing PC. Digital rectal examination and serum biomarker detection are the simplest non-invasive methods (Carter et al., 2013; Huang et al., 2022). Magnetic resonance imaging (MRI), computed tomography (CT), and ultrasound (US) are very common imaging methods (Carter et al., 2013; Huang et al., 2022). Aspiration biopsy is usually used as a gold standard to improve accuracy. The cure rate of PC is largely dependent on the PC stage at diagnosis. Treatment plans also rely on staging.

Surgery is a ubiquitous therapy that is almost always applied to malignant tumors. Androgen ablation is a unique method of PC treatment since this type of cancer is a hormone-dependent illness (Seidenfeld et al., 2000). In some PC stages, radiotherapy and chemotherapy are effectively employed to delay clinical metastasis and further progression. These diagnosis and treatment strategies induce a decrease in mortality rate, especially in high-income countries (Sung et al., 2021). Although these efforts are beginning to show results, there are still some issues, such as low diagnosis sensitivity, limited options of targeted drugs, and a high recurrence rate.

Nanomaterials, which have an enhanced permeability and retention (EPR) effect, are emerging as carriers or drug molecules to address the problems mentioned before(Li et al., 2020b; Li et al., 2022). This review focused on the frontiers of nanomaterials in PC theranostics. First, we discussed the diagnosis of PC, containing prostate-specific biomarkers detection and molecular imaging. Then, we provided some therapeutic approaches, of which chemotherapy is the most widespread one. Selecting appropriate targets and nanomaterials to reduce side effects and drug resistance is essential in cancer treatment. Gene therapy, containing polymers, membrane vesicles, etc., as the carriers, is used in certain cases. Therapeutic nanomaterials are also introduced, such as selenium nanoparticles, graphene, and targeting peptides. Lastly, we proposed that the integration of diagnosis and therapy should be a significant breakthrough in cancer management.

2 Diagnosis of PC

2.1 Prostate-specific biomarkers detection

Different biomarkers, such as serum, urine, and exosome biomarkers, are effectively used for cancer detection and screening (Carter et al., 2013; Salimi et al., 2013; Patra et al., 2015; Kowalczyk et al., 2022; Yan et al., 2022). Among these biomarkers, prostate-specific antigen (PSA) is the most common one used to diagnose PC. PSA is the biomarker for primary tumor diagnosis approved by the US Food and Drug Administration (FDA), and it has been generally employed to diagnose PC in the clinic (Sanders et al., 2014). Although efficient testing occurred due to the evidence of PC spike during the early 1990s, after its widespread uptake (Siegel et al., 2022), this method frequently provides false-positive and false-negative results and leads to overdiagnosis (Huang et al., 2022; Kshirsagar et al., 2022). More sensitive and accurate detection means are emerging to optimize PSA testing.

The most widely used method for detecting proteins is enzyme-linked immunosorbent assay (ELISA) (Patra et al., 2015; Sharafeldin et al., 2017). Besides, many other optimized methods can screen PSA, such as fluorescence resonance energy transfer (FRET) (Furukawa et al., 2016), electrochemical sensor (Salimi et al., 2013; Wei et al., 2018), electrochemiluminescence (ECL) (Khoshfetrat et al., 2019), localized surface plasmon resonance (LSPR) (Acimovic et al., 2014; Sanders et al., 2014), surface-enhanced Raman scattering (SERS) (Cheng et al., 2017), and some combined methods (Duan et al., 2018). Development of various approaches results in great improvement; for example, PSA can be evaluated not only in male but also in female serum, although the value of PSA in women is very limited, and PSA detection is difficult (Patra et al., 2015). In the review, we mainly concentrated on electrochemistry and SERS to diagnose PSA.

Timely medical interference and sensitive testing methods are necessary. As shown in Figure 1A, a polydimethylsiloxane (PDMS) slice is decorated with 8 × 8 nano-Au electrodes. The slice is then modified with the primary antibody by the magnetic force between the magnetic beads (MBs) and nano-Au electrodes. In the presence of PSA, which is to be detected, the three-in-one compounds, the second antibody-horse radish peroxidase (HRP)-Au nanorods, are added to bind with PSA. The reduction reaction of H_2O_2, the added substrate, triggers the generation of electrochemical signals, which can quantitatively evaluate PSA with good selectivity and appropriate detection limit. This assay provides a new direction to detect PSA more precisely and accurately (Liu et al., 2014).

Elevated serum PSA, specifically 4–10 ng ml^{-1}, is not only associated with PC but also with benign prostate hyperplasia and prostatitis (Liu et al., 2014). Therefore, using only PSA to diagnose PC is insufficient. Prostate-specific membrane antigen (PSMA) is a protein of prostatic epithelial cell membrane with higher specificity (Liu et al., 2014; Sharafeldin et al., 2017). In a study, graphene oxide (GO) nanosheets were deposited with Fe_3O_4 nanoparticles (Fe_3O_4@GO). The first antibody was loaded onto the magnetic Fe_3O_4@GO composite by chemical crosslinking, which could specifically capture the biomarker. The biomarker-laden Fe_3O_4@GO was delivered into a detection chamber, which was coated with the second antibody. The interaction between the second antibody and the biomarker made an amperometric response after adding H_2O_2, as catalyzed by Fe_3O_4@GO, which had peroxidase-like activity. This system could simultaneously detect PSA and PSMA, which might promote the sensitivity and preciseness of using biomarker-based diagnosis in the clinic (Sharafeldin et al., 2017).

Another biomarker to address the nonspecific expression of PSA in PC is free PSA (f-PSA). Most PSA, easily attaching to other proteins, exists in serum as a complex. For example, PSA and protease inhibitors create stable complexed PSA (c-PSA). In contrast, another PSA not binding to any proteins is known as f-PSA. According to a report, f-PSA decreases in men with PC compared with those with benign prostate hyperplasia or prostatitis (Cheng et al., 2017). Therefore, in clinical diagnosis, the decline in free to total PSA (t-PSA) ratio is employed to identify PC as an important index to distinguish PC and other benign diseases. As shown in Figure 1B, magnetic beads (MBs) are loaded with t-PSA antibodies, which can

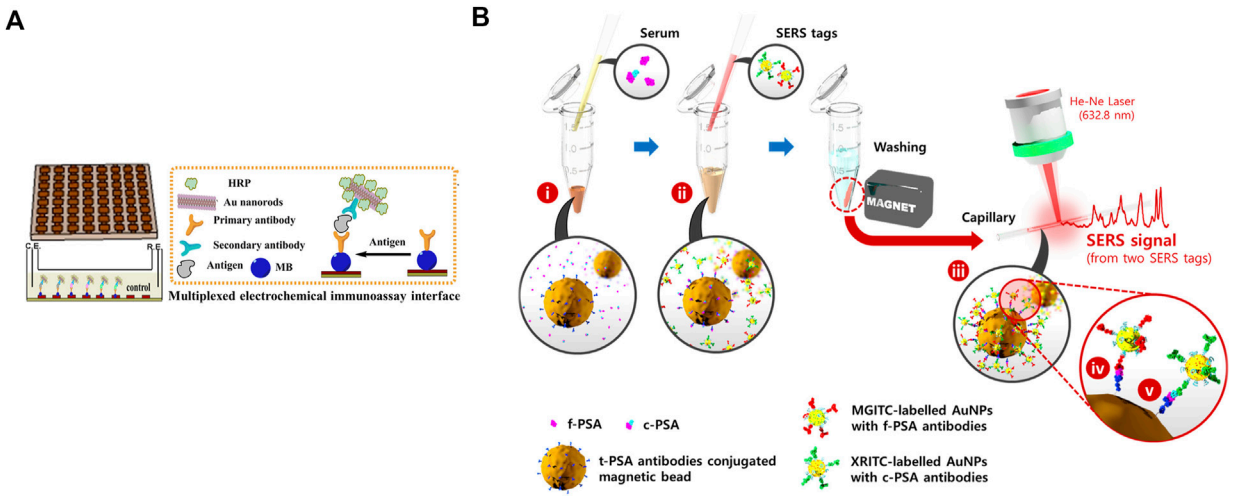

FIGURE 1
(A) Preparation of magnetic slice and multiplexed electrochemical immunoassay interface. Reprinted with permission from (Liu et al., 2014). Copyright 2014, American Chemical Society. **(B)** Preparation of t-PSA antibody-loaded beads, two characteristic SERS tags, and detection of two biomarkers. Reprinted with permission from (Cheng et al., 2017). Copyright 2017, American Chemical Society.

simultaneously bind to f-PSA and c-PSA. Two tags are prepared based on SERS, with conjugation of f-PSA and c-PSA antibodies, respectively. Adding SERS tags to the centrifuge tube forms sandwich complexes. The beads are separated by the magnetic bar, which produces SERS signals to quantify f-PSA and c-PSA according to characteristic Raman peaks of two different tags (Cheng et al., 2017). This easy-to-perform and accurate approach might help develop new methods for the primary diagnosis of PC.

2.2 Molecular imaging

Molecular imaging, such as MRI and CT (Hurley et al., 2016; Schilham et al., 2021), can also diagnose diseases. Additionally, the preparation of aspiration biopsy may depend on CT or transrectal ultrasound (TRUS) (Logan et al., 2014). MRI, which avoids ionizing radiation exposure, is more acceptable. This technology was developed several decades ago. MRI usually uses a contrast agent (CA) as the adjuvant to increase sensitivity and improve imaging quality. Basically, CA is divided into two categories: paramagnetic and superparamagnetic. Paramagnetic agent, such as gadolinium (Gd), which can increase signals, is also named positive CA. In contrast, the superparamagnetic one, commonly called negative CA, has the effect of decreasing signals to enhance contrast. Iron oxide is representative of this type (Liu et al., 2021b; Jiang et al., 2021). There are still some issues with MRI. For example, retention of CA is limited for quick body clearance, affecting imaging quality and accuracy. In recent years, many different categories of nanomaterials have been applied in MRI, qualitatively enhancing its specificity and sensitivity.

Yang et al. (2015) have reported a nanomaterial based on CA. Graphene oxide (GO) nanosheets were grafted with dendrimers (DEN), and then gadolinium diethylene triamine pentaacetate (Gd-DTPA) and prostate stem cell antigen (PSCA) monoclonal antibody (mAb) were sequentially added (GO-DEN [Gd-DTPA]-mAb). GO-DEN (Gd-DTPA)-mAb could target PSCA overexpressing cells (PC3), inducing enhancement of T1-weighted contrast. In *vivo* experiment, after 1 h or 4 h of intravenous injection, compared with GO-DEN (Gd-DTPA), GO-DEN (Gd-DTPA)-mAb triggered a more obvious increase in the image signal to PC3 tumor (Guo et al., 2016). This work was based on the interaction between antigen and antibody, implying the promise of targeting nanomaterials in MRI and other imaging modalities.

3 PC therapy

3.1 Chemotherapy

Chemotherapy originated during a war when scientists accidentally found that nitrogen mustard played a role in inhibiting lymphoma (Rahmani and Abdollahi, 2017). Now, it is frequently employed for advanced/metastatic cancer or after surgery to prevent relapse (Adahoun et al., 2017). According to the source and mechanism, chemotherapeutics categorize into different types, such as alkylating agents (Liang et al., 2018),

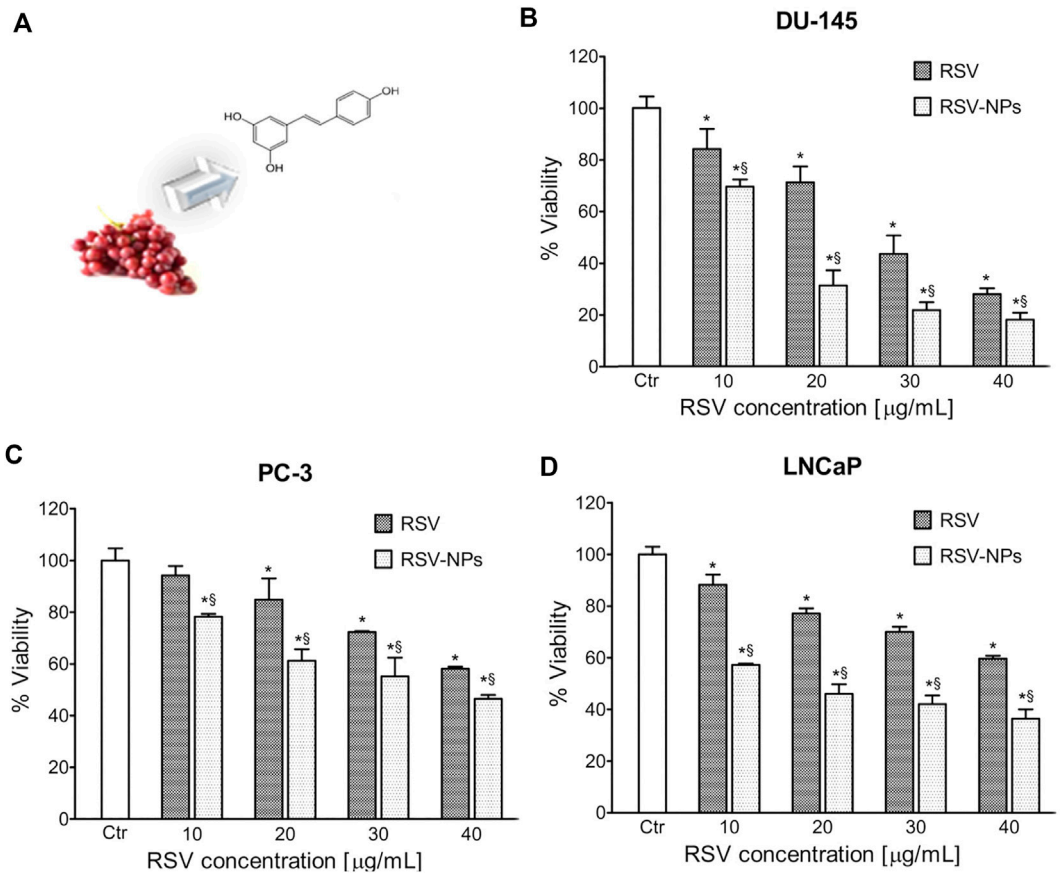

FIGURE 2
(A) Extraction of RSV from grapes and molecular structure of RSV. Toxicity of RSV/RSV-NPs to different cell lines: **(B)** DU-145, **(C)** PC-3, and **(D)** LNCaP. Reprinted with permission from (Sanna et al., 2013). Copyright 2013, American Chemical Society.

antimetabolites (Ren et al., 2014), compounds extracted from plants (Zhang et al., 2018), metals (Cai et al., 2017). One group of these drugs, which is extracted from plants, comprises nature molecules and serves as a very promising and safe choice to treat cancers.

As shown in Figure 2A, trans-resveratrol (RSV), present in multiple plants, such as grapes and peanuts, has good antiaging and antitumor effects. Nevertheless, this molecule has some drawbacks also commonly found in other antitumoral drugs, such as poor solubility and bioavailability, instability, and low intracellular penetration. Polymeric nanoparticles (NPs), composed of a mix of poly (epsilon-caprolactone) (PCL) and poly (D,L-lactic-co-glycolic acid)-poly (ethylene glycol) conjugate (PLGA-PEG-COOH), can overcome this challenge. With NPs as the carrier, this system exhibits high RSV loading ability, controlled RSV release, and enhanced toxicity in all three PC cell lines compared to free RSV (Figures 2B,D) (Sanna et al., 2013). This system, addressing the issues that exist in RSV, might be further applied to other natural drugs.

Although these drugs are effective in cancer cells, other indexes, such as the biocompatibility to body index, also need evaluation. There is the nanomaterial based on genistein. Genistein (5, 7-dihydroxy-3-[-4-hydroxyphenyl]-4H-1-benzopyran-4-one) is also a natural molecule present in Leguminosae family, particularly in soy. Soy genistein (Gen) has proved to reduce the proliferation of PC cells (Vodnik et al., 2021). Due to the limitation of chemotherapy for its poor solubility and retention, which is similar to RSV, two variants of genistein-gold conjugates are provided: Gen@AuNPs1 and Gen@AuNPs2. The two nanoparticles are classified by different concentrations of Gen and Au^{3+}. This system shows toxicity to all three PC cells (LNCaP, DU145, and PC3). More importantly, the nanoparticles maintain low toxicity to noncancerous cells (MRC-5, primary human cells) (Vodnik et al., 2021). This work highlights Au nanoparticles as the carrier to inhibit cancer cells and protect normal ones, broadening the applications of nanomaterial.

Nanomaterial is widely used for its excellent performance, but the addition of extra substances into natural drugs increases its unsafety. There is an intriguing approach to prepare a

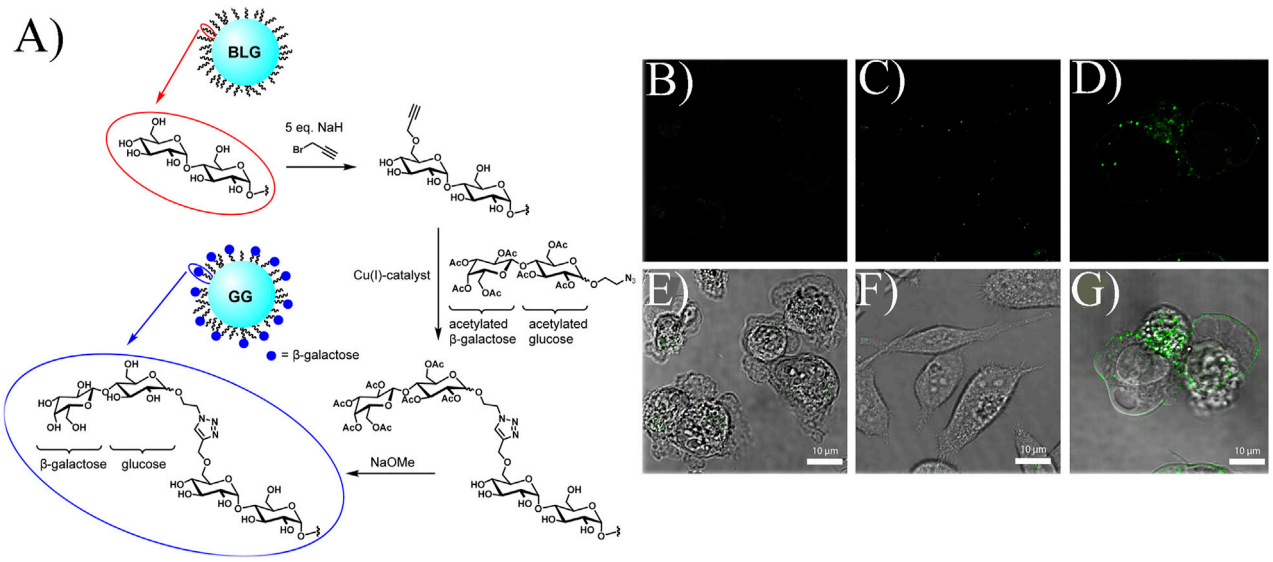

FIGURE 3
(A) Formation of GG. Confocal microscopy and bright field images of different compounds: **(B,E)** control, **(C,F)** FITC-labeled BLG, **(D,G)** FITC-labeled GG incubating PC cells. Reprinted with permission from (Besford et al., 2017). Copyright 2017, American Chemical Society.

nanodrug (Bhawana et al., 2011). Curcumin ([E, E]-1,7-bis [4-hydroxy-3-methoxy-phenyl]-1,6-heptadiene-3,5-ione) (CUR) is another natural drug derived from rhizome of *Curcuma longa*. It is described as an antitumor, anti-inflammatory, and antimicrobial compound. In a study, the authors used a wet-milling technique to form CUR nanoparticles (nanocurcumin), which displayed good solubility and bioavailability. Nanocurcumin showed enhanced antitumor activity compared with parent CUR. Moreover, it had low toxicity to normal cells (HEK, human embryonic kidney cell line) (Adahoun et al., 2017). This work provided an innovative direction to improve the safety of nanomaterial delivery systems, motivating scientists to study other nanodrugs besides CUR.

Although an increasing number of natural drugs have been found, while some, for example, taxol, have been used as the first-line anticancer drugs, there still are some general problems. These include the disadvantage of all anticancer drugs used in the clinic. It is inevitable to induce side effects after chemotherapy; for example, patients suffer from vomiting, loss of appetite, and diarrhea (Zhang et al., 2022), making it a frightening therapy. Additionally, drug and even multidrug resistance (MDR) can be easily developed. Concentrating on these issues, the topical subjects are the selection of a target and using nanomaterial to reduce adverse effects and overcome drug resistance.

3.1.1 Selection of a target to reduce side effects

The key issue in overcoming side effects is how to deliver drugs directly to tumor sites rather than to the whole body. The first question is how to select an effective target (Tong et al., 2010; Al-Mansoori et al., 2021). Galectin-1, a galactoside binding lectin, is upregulated in PC cells during disease development. Hence, galectin-1 is usually employed as the target to specifically inhibit PC cell survival. In one study, glyconanoparticles were used as they are more likely to bind lectin (Besford et al., 2017). As shown in Figure 3A, the bovine liver glycogen (BLG) nanoparticle is a branched polymer of glucose. After a series of chemical reactions, terminal galactoside is linked to BLG, named galactoside-glycogen (GG). This is a kind of nanoparticle that can specifically interact with galectin-1. To prove this point, fluorescein isothiocyanate (FITC, a fluorescent dye)-labeled BLG and GG were used. As shown in Figures 3B,G, compared with BLG, the fluorescence of GG was stronger, indicating that the improved nanoparticles had better performance in specifically binding to the PC cell membrane (Besford et al., 2017). This work selected galectin-1 as the target, proving that the biomarkers are indispensable in tumor management.

Although efficient, targeting agents have some problems. For instance, since the transferrin receptor (TfR) is overexpressed in numerous types of cancer cells, transferrin (Tf), which can specifically target TfR, is usually used as a targeting agent. However, it easily dissociates from TfR after losing an iron molecule in cells. In a study, a Tf variant (oxalate Tf) was adopted. Doxorubicin (DOX)-loaded poly (lactide-co-glycolide) (PLGA) nanoparticles (DPs), encapsulating Tf/oxalate Tf and polyethylene glycol (PEG), were the targeting system named Tf-PEG-DPs (TPDPs). It was then incorporated into a three-dimensional PLGA network, forming the system to

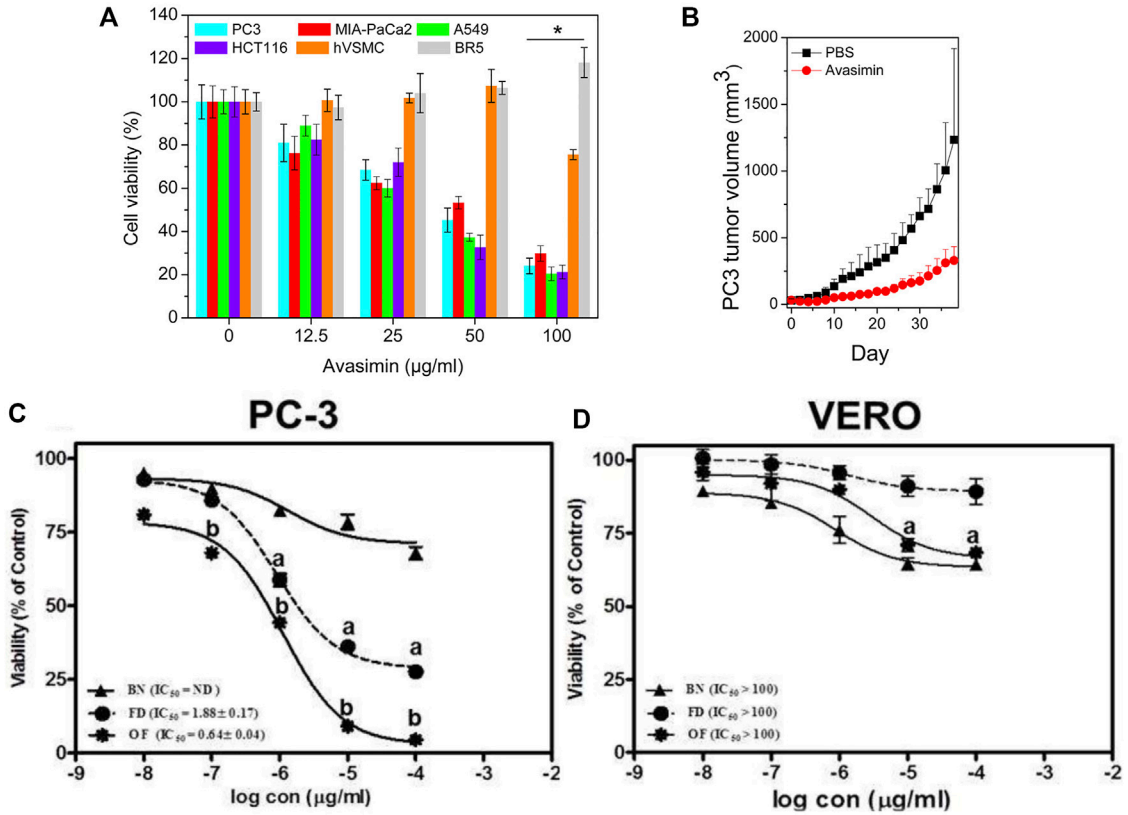

FIGURE 4
(A) Cell viability after treatment of avasimin in various cells. **(B)** PC3 tumor volume after the treatment with avasimin. Reprinted with permission from (Lee et al., 2015). Copyright 2015, American Chemical Society. Viability after the treatment with three substances in different cell lines: **(C)** PC3; **(D)** VERO. BN: blank niosomes, FD: Free drug. Reproduced with permission from (Ali et al., 2021).

release drugs controllably. Compared with the native TPDPs, the one containing oxalate was more effective in reducing the survival of PC cells (Lopes et al., 2017). This was the first example of using oxalate Tf in the PLGA network to enhance the inhibition effect against PC, which might promote the development of other targeting systems.

3.1.2 Selection of nanomaterial to reduce adverse effects

The selection of a target is indispensable to a specific controlled drug release system. However, the choice of nanomaterial is more important (Shin et al., 2014). The nanomaterial requires good biocompatibility, appropriate rate of release and degradation, easy synthesis, etc. Avasimibe is an antitumor agent that works in many kinds of cancers. However, it has low solubility in water, inducing poor bioavailability in blood circulation. In a study, human serum albumin (HSA) was used to conjugate avasimibe, forming water-soluble nanoparticles named avasimin (Lee et al., 2015). As shown in Figure 4A, avasimin played a role in high PC3 inhibition and non-toxicity to normal cells (BR5: dermal fibroblast), showing excellent biocompatibility. The same results happened in *vivo* experiment, as shown in Figure 4B. H&E staining showed that there was no harm to the vital organs (Lee et al., 2015). These results verified the importance of nanomaterials regarding good performance.

Some drugs are very promising and even going into clinical trials. We should focus not only on these drugs but also drugs in suspension. For example, ZSTK474 (ZSTK) is an anticancer drug, especially against advanced cancer. Although it can inhibit phosphatidylinositol 3-kinase (PI3K), which is over-activated in PC, it has been withdrawn in the early clinical investigation because it activates macrophage polarization. Macrophages are very important in the tumor microenvironment. They can be polarized into two types: classical macrophage (M1) and alternative macrophage (M2). M1 inhibits cancers by activating the immune system. However, M2 plays the role in surviving tumor cells. Indomethacin (IND), an anti-inflammatory drug, can combine with ZSTK due to its reduction effect on M1 to M2 polarization, which enhances the immune response. Nevertheless, the issue of toxic ZSTK affecting normal tissues has not been solved. Hence, adding nanoparticles

to this drug is necessary. A cancer cell membrane can be considered as a natural nanoparticle, and it can specifically target cancer cells and escape body clearance, thus, stabilizing the particle in long blood circulation. However, the source of the cell membrane is limited; therefore, it is necessary to search for an alternative. In a study, ZSTK was initially synthesized into nanoparticles named ZNPs. Then, IND was encapsulated in a liposome, which is a commercial agent similar to the cellular membrane but more accessible. Hybridizing the PC3 cracked cell membrane in IND/liposome generated I@CML. Afterward, ZNPs were decorated with I@CML, termed ZNPs/I@CML, to form the drug release system. Concrete experimental data *in vivo* and *in vitro* were shown, confirming the speculation of M1 creation and the higher inhibitory activity of ZNPs/I@CML in PC3 tumor mice compared with free Z + I and ZNPs/I@Lip. Additionally, H&E staining showed no obvious tissue damage and proved the biosafety of ZNPs/I@CML (Zhang et al., 2022). This system utilized the advantage of ZSTK, IND, and cellular membrane to inhibit PC cells, highlighting the importance of appropriate nanomaterial in optimizing therapeutic drugs.

Some cancers, such as PC and breast cancer, are different in their hormone dependence. Hence, antihormone drugs attract more attention. Flutamide (FLT) is currently a clinical drug for PC therapy. However, its poor solubility, low bioavailability, and short half-life (5–6 h) affect the therapy. Increasing the dose from 250 mg to 750 mg per day worsens FLT side effects, such as hepatotoxicity and a decrease in sexual desire. Optimizing nanomaterial containing particle size and surface charge thus is indispensable. In a study, FLT-loaded optimized niosomes (optimized formula, OF) were prepared. This system had reasonable drug release and a good inhibitory effect on PC. As shown in Figures 4C,D, compared to PC3, green monkey epithelial kidney cells (VERO) were almost not sensitive to OF (Ali et al., 2021). This was an example of nanovesicle optimization as the carrier of antiandrogen drugs, and it might be a promising method to optimize other antihormone drugs, such as estrogen.

3.1.3 Overcoming drug resistance

Drug resistance is common in patients receiving chemotherapy for a long time. Glycolysisgenerally occurs in the absence of oxygen. Tumor cells have a rapid metabolic rate and consume large amounts of glucose. Hence, they generate different metabolic characteristics, such as aerobic glycolysis, which was first observed by Otto Warburg and was named the Warburg effect. Therefore, aerobic glycolysis can be employed in cancer therapy. Pyruvate kinase muscle isoform 2 (PKM2) is a very important enzyme converting phosphoenolpyruvate to pyruvate in aerobic glycolysis. Additionally, the dimers type, not the tetramers type, of PKM2 can function in this kind of glucose metabolism. Therefore, PKM2 activators, which transfer PKM2 dimers to its tetramers, have the potency to prevent the Warburg effect and promote tumor inhibition. Serine (Ser) is this kind of activators, but the effect is not sufficient. O-GlcNAcase (OGA), which is overexpressed in many malignant tumors, can improve the proliferation of tumor cells by inhibiting PKM2. In a study, nanomaterial based on OGA was designed: S (GlcNAc)-K (TPA-1) LVFF termed GPNA1. It contained four motifs: 1) ser (β-N-acetylglucosamine) (S [GlcNAc]) motif containing PKM2 activator and OGA targeting agent, 2) Lys (K) motif as the linker, 3) TPA-1 as the fluorescent molecule 4) Leu-Val-Phe-Phe (LVFF) motif for self-assembly. GPNA1 first formed nanoparticles in the water. After it specifically targeted cancer cells, upregulated OGA catalyzed GlcNAc removal, exposing Ser. The nano-activator was transformed from nanoparticles to nanofibers, promoting the formation of PKM2 tetramers and inhibiting tumor metabolism. Compared with GPNA2, GPNA1 showed higher toxicity to highly metastatic PC cell lines (PC-3M IE8 cells). GPNA2 was similar to GPNA1 but had Ala-Ala-Gly-Gly (AAGG) peptide to substitute the self-assembly motif, LVFF. Additionally, compared with GPNA2, GPNA1 could sensitize cells to docetaxel (DTX), overcoming chemotherapy resistance, in *vitro* and *in vivo* experiments (Hou et al., 2022). This project used enzymes as the target to prevent tumor metabolism, highlighting the function of self-assembly peptides against chemotherapy resistance.

Docetaxel (DTX), which can disturb mitosis in the cell cycle to induce cell death, is the standard chemotherapy in advanced PC (Bharali et al., 2017). However, the side effect and drug resistance are inevitable, as shown in clinical trials. Curcumin (CUR), a natural drug, has been shown to affect PC. Furthermore, many molecules that explain the inhibitory effect, such as nuclear factor (NF)-κB and p53, are relevant to DTX resistance. Hence, CUR can prevent DTX resistance and reduce PC cell survival. In a study, the lipid-polymer nanoparticles were synthesized, containing PLGA, lecithin, and PEG-DSPE (LPNs). LPNs were conjugated with DTX and CUR, termed DTX-CUR-LPNs. PLGA nanoparticles without lecithin and PEG-DSPE were used as a control to encapsulate DTX and CUR, named DTX-CUR-NPs. The *in vivo* antitumor efficacy was evaluated. Compared with LPNs, free CUR, free DTX, CUR-LPNs, DTX-LPNs, DTX-CUR-NPs, and DTX-CUR-LPNs exhibited the highest activity against PC, proving the synergistic effect of DTX and CUR (Yan et al., 2016). This was an example of effective combined drugs, paving the way for a double drug release system to prevent tumor progression.

3.2 Gene therapy

Gene therapy is usually used in tumors and monogenic diseases. It has achieved significant progress, such as in the treatment of hemophilia and leukemia (Nathwani et al., 2014; Kuehn, 2017). Many therapeutic regimens have been approved,

such as Zynteglo, authorized by European Union for treating β-thalassemia (Harrison, 2019) and Luxturna (Darrow, 2019) and Kymriah (The, 2017), permitted by the FDA for the cure of genetic eye disease and acute lymphocytic leukemia, respectively. Although it has been developing for many years and many patients have been cured, there are still some failures, such as the death of an American boy, Jesse Gelsinger (Lehrman, 1999), and phase II clinical failure of a drug for heart failure, CUPID2 (Ratner, 2015).

There are some reasons for the mentioned failures, such as inappropriate vectors and limited target-gene expression. As the vector of a target gene, viruses are the most widely used for their high transfection efficacy. Nonetheless, a virus has non-negligible safety problems. For example, in 2000, after the treatment of severe combined immunodeficiency disease (SCID) by a retrovirus, some patients had genetic mutations and symptoms similar to those of leukemia (Check, 2003). Adenovirus can lower this risk because it functions not necessarily to insert its genome into the host genome. However, the immunogenicity of adenovirus is too high (Lehrman, 1999). According to the research, adeno-associated virus (AAV) has become a very promising vector for its low immunogenicity, but its capacity is poor, usually less than 5 kb. Meanwhile, although the virus vector has been remodified to delete a pathogenic gene, uncertain genetic recombination still exists in virus packing, increasing the risk of causing an illness. Some physical methods, which are not dependent on the carrier, usually need very expensive equipment, and they are generally harmful to cells, causing the limitation of wide employment. Therefore, a non-viral vector is emerging to overcome these drawbacks.

Non-viral vector is currently in the basic research phase. This kind of vector does not necessarily insert its genetic material into the host genome, which is relatively safe. Additionally, the length of the loaded gene is not restricted. There are many non-viral vector types, such as mesoporous silicon (Wang et al., 2020), metal nanoparticles (Peng et al., 2018), linear and dendritic polymers (Han et al., 2018), liposome and its derivatives (Fenton et al., 2017), proteins (Ping et al., 2017), and peptides and their derivatives (Guan et al., 2019). The research on non-viral vectors is not limited to *in vitro* experiments, and some *in vivo* experiments have had a very good effect. Therefore, the non-viral vector is developing for practical applications and has a remarkable efficiency in some diseases, such as eye disease (Jiang et al., 2019), degenerative disease, and cancer (Guo et al., 2012; Liu et al., 2019).

The most widely used commercial transfection agent is polyethylenimine (PEI). However, PEI has no targeting motif, limiting its applications. Therefore, there are large amounts of PEI derivatives to enhance transfection efficacy. There are some reports about the usage of two receptors of some viruses for uptake into host cells. Hence, simultaneously targeting two receptors to mimic a virus is a clever design. In a study, B6 peptide (Ac-CGHKAKGPRKNH2) was employed to substitute transferrin (Tf), a protein capable of increasing the interaction with tumor cells. Another peptide motif was RGD, well known for its facilitation of attaching to cells. In this work, PEI derivatives were designed, containing B6/RGD dual-targeted system, B6, or RGD single targeted system. Luciferase expression was used to evaluate the transfection efficiency. The dual-targeted polyplex showed almost equal efficacy compared to PEI in two PC cells and higher efficacy than any of the single systems (Nie et al., 2011). This work provided a dual-targeted system of gene therapy, paving the way to find more effective transfection agents.

Small interfering RNA (siRNA), which knockdowns the complementary mRNA to regulate gene expression, has been developed in the cancer therapy field (Li et al., 2020a). O'Driscoll et al. have reported a polymer nanocarrier to deliver siRNA. The compound of PEGylation of poly-L-lysine-cholic acid (PEG-PLL-CA) was designed. The linker between PEG and PLL was acid-sensitive, which made it cleavable in a tumor site. The release of PEG made it a more appropriate system to load drugs into cells. In this work, the vascular endothelial growth factor (VEGF) siRNA was used to inhibit tumor proliferation in transgenic adenocarcinoma of the mouse prostate cell (TRAMP C1) tumor mice. The efficacy of PEG-PLL-CA was comparable with JetPEI, a commercial *in vivo* PEI (Guo et al., 2012). This work showed siRNA encapsulated in polymer to inhibit tumors, which might stimulate the development of more efficient polymers, even surpassing the commercial transfection agents.

Polymers, such as PEI, have the drawbacks of low transfection efficacy and high toxicity to cells. There are commercial substitutes, such as lipo2000 and lipo3000. In a study, membrane vesicles, which have the targeting capability, were used to deliver drugs for many diseases, such as cancer and HIV/AIDS. This system was termed nanoghosts (NGs). In this work, plasmid cDNA was used to encode the C-terminal motif of matrix metalloprotease-2, named the hemopexin-like domain (PEX). This kind of protein is toxic to cancer cells. As shown in Figure 5A, the tumor size after the treatment with NG-pPEX showed obvious shrink compared with control, proving its effective transfection (Kaneti et al., 2016). This work used innovative NGs as the vector, highlighting the development of membrane systems in gene therapy.

The above-discussed projects showed different carriers. Sometimes, there are other technologies added to enhance the transfection. A schematic illustration is shown in Figure 5B. The dickkopfs (DKKs) protein family is related to PC development. DKK-2 pDNA-loaded chitosan/perfluorohexane nanodroplets (CNDs) are added to the LNCaP cells, and then ultrasound is applied. The expression of DKKs protein prevents the proliferation of PC cells. Figure 5C exhibits the transfection effect of different groups, proving the importance of ultrasound (pDNA also encodes enhanced green fluorescent protein [EGFP] to evaluate transfection efficacy) (Liu et al.,

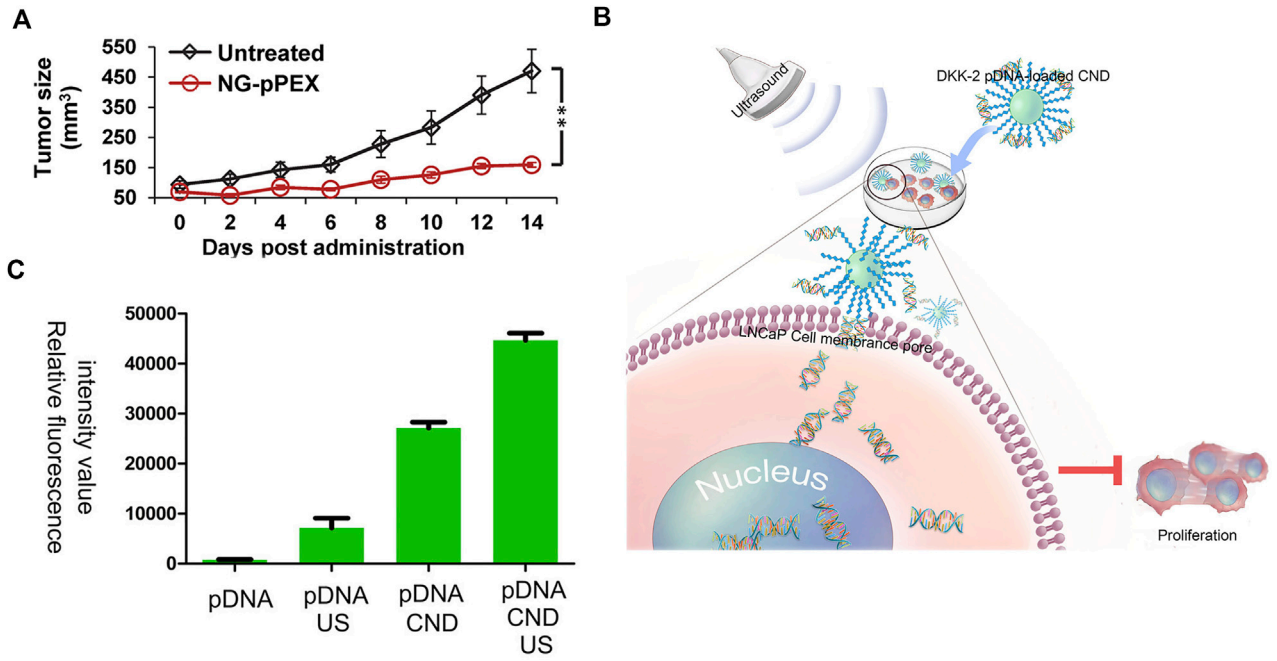

FIGURE 5
(A) Prostate tumor volume after the treatment with NG-pPEX using the untreated group as the control. Reprinted with permission from (Kaneti et al., 2016). Copyright 2016, American Chemical Society. **(B)** Schematic illustration of DKK-2 pDNA delivery into LNCaP cells. **(C)** Relative fluorescence intensity of pDNA/pDNA + US/pDNA + CND/pDNA + CND + US in LNCaP cells. Reproduced with permission from (Liu et al., 2021a).

2021a). This approach, dependent on ultrasound, is innovative and might be used in PC therapy in further clinical research.

3.3 Therapeutic nanomaterial

Nanomaterial functions not only as a carrier but also as a drug. Some nanomaterials are toxic to cancer cells, specifically inhibiting tumor proliferation. The trace element selenium can prevent cancer, and selenium nanoparticles (Nano-Se) are safer than other selenium compounds, such as sodium selenite and selenomethionine. Gao et al. have reported the function of Nano-Se. It showed the inhibitory activity of LNCaP cells, proving the potential of selenium nanomaterial in cancer therapy (Kong et al., 2011).

It is well known that metastasis of tumors is an issue in cancer therapy, dramatically shortening patients' lives. Wei et al. have reported the function of graphene in tumor migration and invasion. In their work, graphene (Gra) and graphene oxide (GO) were used to suppress three kinds of cancer cells (MDA-MB-231: human breast cancer cell line, PC3, and B16F10: mouse melanoma cell line). The inhibitory activity was dose-dependent, and 90% of cells were viable after the treatment with Gra or GO at 20 μg/ml for 24 h. Nonetheless, under this condition, migration and invasion were prevented compared with control (Zhou et al., 2014). This work proved the function of Gra and GO in tumor migration and invasion, providing innovative insight into future cancer therapy.

Targeting agents are very indispensable in designing functional nanomaterial. Self-assembled peptides are very useful for inhibiting pathogenic cells, such as tumor cells and bacteria, and maintaining the physiological functions of normal tissues (Wang et al., 2021). In a study, tandem self-assembled peptide systems based on the targets were designed. As shown in Figure 6A, compound 1 contained four motifs: 1) NBD as the capped fluorescent motif, 2) GFF_RY as the self-assembly and alkaline phosphatase (ALP)-targeting motif, 3) ss as the glutathione (GSH) targeting motif, 4) RGD as the targeting motif to cancer cells. Adding ALP to compound 1 formed compound 2, which was a nanoparticle imaged by a transmission electron microscope (TEM) scan. By further using GSH, compound 3 was formed, generating the hydrogel. TEM image showed the nanofibers in the yellow hydrogel. Some cell experiments were conducted to further prove the tandem self-assembly. In many cancer cells, ALP and GSH are overexpressed. Nanoparticle formation by ALP catalysis and further formation of nanofibers by GSH cleavage in liver cancer cells had been evidenced by confocal laser scanning microscopy. This tandem self-assembly system was toxic to various cancer cells containing PC3 but was almost innocuous

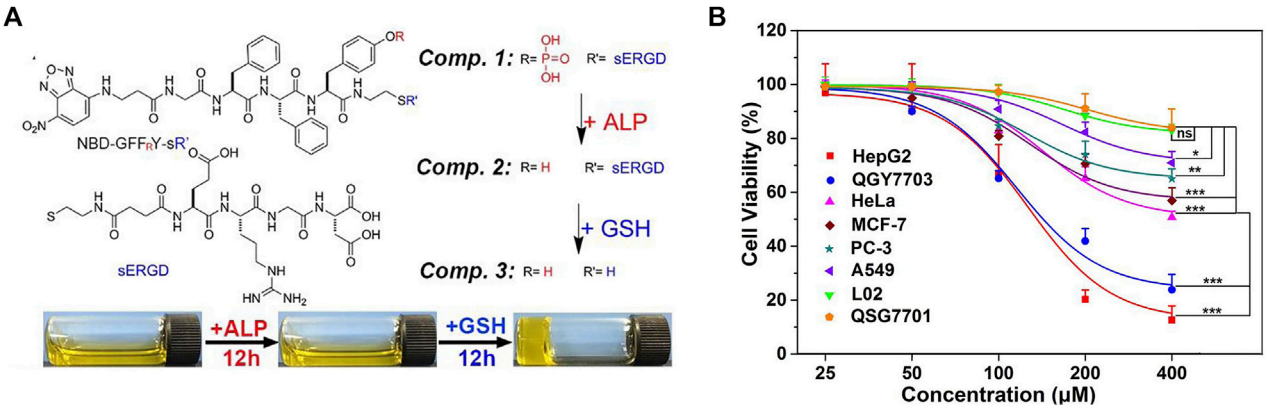

FIGURE 6
(A) Molecular structures of compounds 1, 2, and 3, tandem self-assembly formation, and a photograph after adding ALP and GSH to compound 1. **(B)** Cell viability after the treatment with different concentrations of compound 1 for 48 h of six cancer cells and two normal cells. Reproduced with permission from (Zhan et al., 2018)

to normal liver cells, LO2 and QSG7701, as shown in Figure 6B (Zhan et al., 2018). Although this system had a less inhibitory effect on PC cells than liver cancer ones, it provided the theoretical and experimental basis for tandem self-assembly, which might benefit the development of more efficient nanomaterials in future research on PC.

This review mainly introduced chemotherapy, gene therapy, and therapeutic nanomaterial. Besides these methods, there are some other PC therapies, such as photodynamic therapy (PDT) (Lin et al., 2016), sonodynamic therapy (SDT) (Hadi et al., 2021), and combined therapy (Lee et al., 2011; Min et al., 2017; Mirjolet et al., 2017). Immunotherapy is effective in many diseases, such as allergic rhinitis (Liu et al., 2015), diabetes (Bluestone et al., 2015), HIV infection (Caskey et al., 2015), and especially cancer (Kanapathipillai et al., 2012; Hu et al., 2015; Stephan et al., 2015). Immunotherapy combination with other therapies, such as chemotherapy, is very popular and efficient. Jon et al. have reported a delivery system based on chemoimmunotherapy. CpG is an oligonucleotide that can stimulate the immune system. CpG-dendrimer conjugate was used as the carrier to load doxorubicin (Dox), an antitumor drug in the clinic. This system showed more effective antitumor activity than free Dox with the same dose in the 22RV1 (a kind of PC cell line) tumor model (Lee et al., 2011). Chemotherapy can combine not only with immune treatment but also with radiotherapy. Docetaxel (DTX) can sensitize cells to radiotherapy, but side effects and drug resistance limit its applications. There was a report based on titanate nanotubes (TiONts) to solve this challenge. This nano-carrier-loaded docetaxel (TiONts-DTX) enhanced the radiosensitivity. The effect of radiotherapy correlated with TiONts-DTX was assessed in PC3 tumor mice. The dual therapy system had stronger inhibitory efficacy compared to single therapy (Mirjolet et al., 2017). These data confirmed the effect of chemotherapy with other treatments. Additionally, combined gene therapy has been reported. Gold nanorods (GNR) were decorated with dipicolyl amine (DPA), which could bind Zn^{2+} cations, forming Zn (II)/DPA-GNR nanoparticles. They could deliver siRNA because of the interaction between Zn (II)/DPA and siRNA. More importantly, this system also enabled photothermal therapy, benefiting from GNR, exhibiting significant inhibitory activity in PC3 tumor mice (Min et al., 2017). In summary, a combined therapy system, which is superior to a single therapy, is a direction in future research and more applicable to individualized treatment.

4 Outlook

Most cases of PC are diagnosed at an advanced stage, III or IV, missing the best time to treat cancer. Aspiration biopsy is invasive to patients. Therefore, less invasive diagnosing methods in the early stage are requisite. Nanomaterial provides a strategy to enhance the sensitivity and accuracy of these methods. Traditional therapies for cancer include surgery, chemotherapy, and radiotherapy. However, some issues, such as side effects, MDR, metastasis, and relapse, limit the development of cancer therapy. Some innovative approaches based on nanotechnology are emerging, such as PDT and SDT. However, sometimes, the bioavailability of these drugs is still very low. Real-time detection and treatment become urgent needs. The word “theranostics” has been first introduced by John Funkhouser (Choudhury and Gupta, 2018). It means using one nanomaterial system to simultaneously diagnose and treat disease. For example, Ray et al. have reported a multifunctional gold nanoparticle system based on surface-

enhanced Raman scattering (SERS). It had a triple function: diagnosis and treatment of PC cells and monitoring the photothermal regimen response (Lu et al., 2010). Therefore, integration of diagnosis and treatment may be another direction to overcome the barriers in PC therapy. Although most of these methods are in the basic research stage, they lay the foundation should the nanomaterial apply in the clinic in the future.

Although some anticancer nanomedicines have been applied in the clinic, such as Myocet, approved by European Medicines Agency (EMA) in 2000 to fight against breast cancer and DHP 107, authorized by South Korea in 2016 for gastric cancer therapy (He et al., 2019), there are still some disadvantages of nanomaterials, limiting their development. For example, the degradation and biodistribution of nanomaterial in*in vivo* are uncontrollable. Appropriate degradation rate and biodistribution of nanomaterial in *vivo* are necessary in the PC diagnosis and therapy. Therefore, precise design of nanomaterial is indispensable, containing charge, hydrophilia, size, configuration, and so on (Yang et al., 2015). To simplify the procedure, computer aided design is popularly used (Lai et al., 2017; Shao et al., 2020). Another common uncertain factor of nanomaterial used in *vivo* is the biocompatibility. Many of the nanomaterials are toxic to the vital organs or trigger the inflammatory response of the body, which makes us urgently establish an integrated evaluation system to screen nanomedicines (Heller et al., 2020). Although there are some difficulties in screening cancer nanomedicines, it is more attractive to scientists to study the characteristics of nanomaterial and further overcome the challenges (Sun et al., 2020).

Since the first nano-based cancer drug (Doxil) was approved by FDA in 1995, nanomedicines have been authorized in a few kinds of cancers therapies, such as ovarian and non-small-cell lung cancer, myeloma, osteogenic sarcoma (He et al., 2019; Zhao et al., 2022). There are a few PC nanomedicines employed in clinical phase Ⅱ, such as BIND-014, Tecemotide, and CT-2103 and clinical data shows the positive efficiency of BIND-014 (Autio et al., 2018; He et al., 2019). BIND-014 is a docetaxel nanoparticle which targets the prostate-specific membrane antigen (PSMA). Although PC, especially in the advanced period, can shorten the lives and cause the pain of patients, it is still hopeful by the effective clinical data. More importantly, the basic researches have been developing fast, and they might provide theoretical and experimental foundation for the clinical progress in the future.

Author contributions

BH wrote and revised the paper; LW, YC, ZM, and JW revised the format of the pictures and text in the paper.

Conflict of interest

BH and YC were employed by Department of Urology, Central Hospital, China Railway 17th Bureau Group Co., Ltd.

The remaining authors declare that the research was conducted in the absence of any commercial or financial relationships that could be construed as a potential conflict of interest.

The handling editor ZZ declared a shared affiliation with the author JW at the time of the review.

Publisher's note

References

Acimovic, S. S., Ortega, M. A., Sanz, V., Berthelot, J., Garcia-Cordero, J. L., Renger, J., et al. (2014). LSPR chip for parallel, rapid, and sensitive detection of cancer markers in serum. *Nano Lett.* 14, 2636–2641. doi:10.1021/nl500574n

Adahoun, M. A., AL-Akhras, M. H., Jaafar, M. S., and Bououdina, M. (2017). Enhanced anti-cancer and antimicrobial activities of curcumin nanoparticles. *Artif. Cells Nanomed. Biotechnol.* 45, 98–107. doi:10.3109/21691401.2015.1129628

AL-Mansoori, L., Elsinga, P., and Goda, S. K. (2021). Bio-vehicles of cytotoxic drugs for delivery to tumor specific targets for cancer precision therapy. *Biomed. Pharmacother.* 144, 112260. doi:10.1016/j.biopha.2021.112260

Ali, M. A., Mohamed, M. I., Megahed, M. A., Abdelghany, T. M., and EL-Say, K. M. (2021). Cholesterol-based nanovesicles enhance the *in vitro* cytotoxicity, *ex vivo* intestinal absorption, and *in vivo* bioavailability of flutamide. *Pharmaceutics* 13, 1741. doi:10.3390/pharmaceutics13111741

Autio, K. A., Dreicer, R., Anderson, J., Garcia, J. A., Alva, A., Hart, L. L., et al. (2018). Safety and efficacy of BIND-014, a docetaxel nanoparticle targeting prostate-specific membrane antigen for patients with metastatic castration-resistant prostate cancer: A phase 2 clinical trial. *JAMA Oncol.* 4, 1344–1351. doi:10.1001/jamaoncol.2018.2168

Besford, Q. A., Wojnilowicz, M., Suma, T., Bertleff-Zieschang, N., Caruso, F., and Cavalieri, F. (2017). Lactosylated glycogen nanoparticles for targeting prostate cancer cells. *ACS Appl. Mat. Interfaces* 9, 16869–16879. doi:10.1021/acsami.7b02676

Bharali, D. J., Sudha, T., Cui, H., Mian, B. M., and Mousa, S. A. (2017). Anti-CD24 nano-targeted delivery of docetaxel for the treatment of prostate cancer. *Nanomedicine Nanotechnol. Biol. Med.* 13, 263–273. doi:10.1016/j.nano.2016.08.017

BhawanaBasniwal, R. K., Buttar, H. S., Jain, V. K., and Jain, N. (2011). Curcumin nanoparticles: preparation, characterization, and antimicrobial study. *J. Agric. Food Chem.* 59, 2056–2061. doi:10.1021/jf104402t

Bluestone, J. A., Buckner, J. H., Fitch, M., Gitelman, S. E., Gupta, S., Hellerstein, M. K., et al. (2015). Type 1 diabetes immunotherapy using polyclonal regulatory T cells. *Sci. Transl. Med.* 7, 315ra189. doi:10.1126/scitranslmed.aad4134

Cai, Y., Shen, H., Zhan, J., Lin, M., Dai, L., Ren, C., et al. (2017). Supramolecular "trojan horse" for nuclear delivery of dual anticancer drugs. *J. Am. Chem. Soc.* 139, 2876–2879. doi:10.1021/jacs.6b12322

Carter, H. B., Albertsen, P. C., Barry, M. J., Etzioni, R., Freedland, S. J., Greene, K. L., et al. (2013). Early detection of prostate cancer: AUA guideline. *J. Urology* 190, 419–426. doi:10.1016/j.juro.2013.04.119

Caskey, M., Klein, F., Lorenzi, J. C., Seaman, M. S., West, A. P., JR., Buckley, N., et al. (2015). Viraemia suppressed in HIV-1-infected humans by broadly neutralizing antibody 3BNC117. *Nature* 522, 487–491. doi:10.1038/nature14411

Check, E. (2003). Second cancer case halts gene-therapy trials. *Nature* 421, 305. doi:10.1038/421305a

Cheng, Z., Choi, N., Wang, R., Lee, S., Moon, K. C., Yoon, S. Y., et al. (2017). Simultaneous detection of dual prostate specific antigens using surface-enhanced Raman scattering-based immunoassay for accurate diagnosis of prostate cancer. *ACS Nano* 11, 4926–4933. doi:10.1021/acsnano.7b01536

Choudhury, P. S., and Gupta, M. (2018). Differentiated thyroid cancer theranostics: radioiodine and beyond. *Br. J. Radiol.* 91, 20180136. doi:10.1259/bjr.20180136

Darrow, J. J. (2019). Luxturna: FDA documents reveal the value of a costly gene therapy. *Drug Discov. Today* 24, 949–954. doi:10.1016/j.drudis.2019.01.019

Duan, F., Zhang, S., Yang, L., Zhang, Z., He, L., and Wang, M. (2018). Bifunctional aptasensor based on novel two-dimensional nanocomposite of MoS2 quantum dots and g-C3N4 nanosheets decorated with chitosan-stabilized Au nanoparticles for selectively detecting prostate specific antigen. *Anal. Chim. Acta X.* 1036, 121–132. doi:10.1016/j.aca.2018.06.070

Fenton, O. S., Kauffman, K. J., Kaczmarek, J. C., Mcclellan, R. L., Jhunjhunwala, S., Tibbitt, M. W., et al. (2017). Synthesis and biological evaluation of ionizable lipid materials for the *in vivo* delivery of messenger RNA to B lymphocytes. *Adv. Mat.* 29, 1606944. doi:10.1002/adma.201606944

Furukawa, K., Ueno, Y., Takamura, M., and Hibino, H. (2016). Graphene FRET aptasensor. *ACS Sens.* 1, 710–716. doi:10.1021/acssensors.6b00191

Guan, S., Munder, A., Hedtfeld, S., Braubach, P., Glage, S., Zhang, L., et al. (2019). Self-assembled peptide-poloxamine nanoparticles enable *in vitro* and *in vivo* genome restoration for cystic fibrosis. *Nat. Nanotechnol.* 14, 287–297. doi:10.1038/s41565-018-0358-x

Guo, J., Cheng, W. P., Gu, J., Ding, C., Qu, X., Yang, Z., et al. (2012). Systemic delivery of therapeutic small interfering RNA using a pH-triggered amphiphilic poly-L-lysine nanocarrier to suppress prostate cancer growth in mice. *Eur. J. Pharm. Sci.* 45, 521–532. doi:10.1016/j.ejps.2011.11.024

Guo, L., Shi, H., Wu, H., Zhang, Y., Wang, X., Wu, D., et al. (2016). Prostate cancer targeted multifunctionalized graphene oxide for magnetic resonance imaging and drug delivery. *Carbon* 107, 87–99. doi:10.1016/j.carbon.2016.05.054

Hadi, M. M., Nesbitt, H., Masood, H., Sciscione, F., Patel, S., Ramesh, B. S., et al. (2021). Investigating the performance of a novel pH and cathepsin B sensitive, stimulus-responsive nanoparticle for optimised sonodynamic therapy in prostate cancer. *J. Control. Release* 329, 76–86. doi:10.1016/j.jconrel.2020.11.040

Han, J., Hwang, H. S., and Na, K. (2018). TRAIL-secreting human mesenchymal stem cells engineered by a non-viral vector and photochemical internalization for pancreatic cancer gene therapy. *Biomaterials* 182, 259–268. doi:10.1016/j.biomaterials.2018.08.024

Harrison, C. (2019). First gene therapy for beta-thalassemia approved. *Nat. Biotechnol.* 37, 1102–1103. doi:10.1038/d41587-019-00026-3

He, H., Liu, L., Morin, E. E., Liu, M., and Schwendeman, A. (2019). Survey of clinical translation of cancer nanomedicines-lessons learned from successes and failures. *Acc. Chem. Res.* 52, 2445–2461. doi:10.1021/acs.accounts.9b00228

Heller, D. A., Jena, P. V., Pasquali, M., Kostarelos, K., Delogu, L. G., Meidl, R. E., et al. (2020). Grouping all carbon nanotubes into a single substance category is scientifically unjustified. *Nat. Nanotechnol.* 15, 164–166. doi:10.1038/s41565-020-0654-0

Hou, D. Y., Xiao, W. Y., Wang, J. Q., Yaseen, M., Wang, Z. J., Fei, Y., et al. (2022). OGA activated glycopeptide-based nano-activator to activate PKM2 tetramerization for switching catabolic pathways and sensitizing chemotherapy resistance. *Biomaterials* 284, 121523. doi:10.1016/j.biomaterials.2022.121523

Hu, Q. L., Wu, M., Fang, C., Cheng, C. Y., Zhao, M. M., Fang, W. H., et al. (2015). Engineering nanoparticle-coated bacteria as oral DNA vaccines for cancer immunotherapy. *Nano Lett.* 15, 2732–2739. doi:10.1021/acs.nanolett.5b00570

Huang, Y. T., Tseng, N. C., Chen, Y. K., Huang, K. H., Lin, H. Y., Huang, Y. Y., et al. (2022). The detection performance of 18 F-Prostate-Specific membrane antigen-1007 PET/CT in primary prostate cancer : A systemic review and meta-analysis. *Clin. Nucl. Med.* 47, 755–762. doi:10.1097/rlu.0000000000004228

Hurley, K. R., Ring, H. L., Etheridge, M., Zhang, J., Gao, Z., Shao, Q., et al. (2016). Predictable heating and positive MRI contrast from a mesoporous silica-coated iron oxide nanoparticle. *Mol. Pharm.* 13, 2172–2183. doi:10.1021/acs.molpharmaceut.5b00866

Jiang, K., Hu, Y., Gao, X., Zhan, C., Zhang, Y., Yao, S., et al. (2019). Octopus-like flexible vector for noninvasive intraocular delivery of short interfering nucleic acids. *Nano Lett.* 19, 6410–6417. doi:10.1021/acs.nanolett.9b02596

Jiang, Q., Liu, X., Liang, G., and Sun, X. (2021). Self-assembly of peptide nanofibers for imaging applications. *Nanoscale* 13, 15142–15150. doi:10.1039/d1nr04992e

Kanapathipillai, M., Mammoto, A., Mammoto, T., Kang, J. H., Jiang, E., Ghosh, K., et al. (2012). Inhibition of mammary tumor growth using lysyl oxidase-targeting nanoparticles to modify extracellular matrix. *Nano Lett.* 12, 3213–3217. doi:10.1021/nl301206p

Kaneti, L., Bronshtein, T., Malkah Dayan, N., Kovregina, I., Letko Khait, N., Lupu-Haber, Y., et al. (2016). Nanoghosts as a novel natural nonviral gene delivery platform safely targeting multiple cancers. *Nano Lett.* 16, 1574–1582. doi:10.1021/acs.nanolett.5b04237

Khoshfetrat, S. M., Khoshsafar, H., Afkhami, A., Mehrgardi, M. A., and Bagheri, H. (2019). Enhanced visual wireless electrochemiluminescence immunosensing of prostate-specific antigen based on the luminol loaded into MIL-53(Fe)-NH2 accelerator and hydrogen evolution reaction mediation. *Anal. Chem.* 91, 6383–6390. doi:10.1021/acs.analchem.9b01506

Kong, L., Yuan, Q., Zhu, H., Li, Y., Guo, Q., Wang, Q., et al. (2011). The suppression of prostate LNCaP cancer cells growth by Selenium nanoparticles through Akt/Mdm2/AR controlled apoptosis. *Biomaterials* 32, 6515–6522. doi:10.1016/j.biomaterials.2011.05.032

Kowalczyk, A., Wrzecinska, M., Czerniawska-Piatkowska, E., and Kupczynski, R. (2022). Exosomes - spectacular role in reproduction. *Biomed. Pharmacother.* 148, 112752. doi:10.1016/j.biopha.2022.112752

Kshirsagar, P., Seshacharyulu, P., Muniyan, S., Rachagani, S., Smith, L. M., Thompson, C., et al. (2022). DNA-gold nanoprobe-based integrated biosensing technology for non-invasive liquid biopsy of serum miRNA: A new frontier in prostate cancer diagnosis. *Nanomedicine Nanotechnol. Biol. Med.* 43, 102566. doi:10.1016/j.nano.2022.102566

Kuehn, B. M. (2017). The promise and challenges of CAR-T gene therapy. *JAMA* 318, 2167–2169. doi:10.1001/jama.2017.15605

Lai, C. T., Rosi, N. L., and Schatz, G. C. (2017). All-atom molecular dynamics simulations of peptide amphiphile assemblies that spontaneously form twisted and helical ribbon structures. *J. Phys. Chem. Lett.* 8, 2170–2174. doi:10.1021/acs.jpclett.7b00745

Lee, I. H., An, S., Yu, M. K., Kwon, H. K., Im, S. H., and Jon, S. (2011). Targeted chemoimmunotherapy using drug-loaded aptamer-dendrimer bioconjugates. *J. Control. Release* 155, 435–441. doi:10.1016/j.jconrel.2011.05.025

Lee, S. S., Li, J., Tai, J. N., Ratliff, T. L., Park, K., and Cheng, J. X. (2015). Avasimibe encapsulated in human serum albumin blocks cholesterol esterification for selective cancer treatment. *ACS Nano* 9, 2420–2432. doi:10.1021/nn504025a

Lehrman, S. (1999). Virus treatment questioned after gene therapy death. *Nature* 401, 517–518. doi:10.1038/43977

Li, Z., Ding, Y., Liu, J., Wang, J., Mo, F., Wang, Y., et al. (2022). Depletion of tumor associated macrophages enhances local and systemic platelet-mediated anti-PD-1 delivery for post-surgery tumor recurrence treatment. *Nat. Commun.* 13, 1845. doi:10.1038/s41467-022-29388-0

Li, Z., Wang, Y., Shen, Y., Qian, C., Oupicky, D., and Sun, M. (2020a). Targeting pulmonary tumor microenvironment with CXCR4-inhibiting nanocomplex to enhance anti-PD-L1 immunotherapy. *Sci. Adv.* 6, eaaz9240. doi:10.1126/sciadv.aaz9240

Li, Z., Zhu, L., Sun, H., Shen, Y., Hu, D., Wu, W., et al. (2020b). Fluorine assembly nanocluster breaks the shackles of immunosuppression to turn the cold tumor hot. *Proc. Natl. Acad. Sci. U. S. A.* 117, 32962–32969. doi:10.1073/pnas.2011297117

Liang, C., Zhang, L., Zhao, W., Xu, L., Chen, Y., Long, J., et al. (2018). Supramolecular nanofibers of drug-peptide amphiphile and affibody suppress HER2+ tumor growth. *Adv. Healthc. Mat.* 7, e1800899. doi:10.1002/adhm.201800899

Lin, T. Y., Guo, W., Long, Q., Ma, A., Liu, Q., Zhang, H., et al. (2016). HSP90 inhibitor encapsulated photo-theranostic nanoparticles for synergistic combination cancer therapy. *Theranostics* 6, 1324–1335. doi:10.7150/thno.14882

Liu, H. J., Zhang, A. F., Zhao, N., and Li, X. Z. (2015). Role of miR-146a in enforcing effect of specific immunotherapy on allergic rhinitis. *Immunol. Invest.* 45, 1–10. doi:10.3109/08820139.2015.1085390

Liu, J., Lu, C. Y., Zhou, H., Xu, J. J., and Chen, H. Y. (2014). Flexible gold electrode array for multiplexed immunoelectrochemical measurement of three protein

biomarkers for prostate cancer. *ACS Appl. Mat. Interfaces* 6, 20137–20143. doi:10.1021/am505726b

Liu, S., Gao, Y., Zhou, D., Zeng, M., Alshehri, F., Newland, B., et al. (2019). Highly branched poly(β-amino ester) delivery of minicircle DNA for transfection of neurodegenerative disease related cells. *Nat. Commun.* 10, 3307. doi:10.1038/s41467-019-11190-0

Liu, X., Shi, D., Guo, L., Zhou, X., Shang, M., Sun, X., et al. (2021a). Echogenic, ultrasound-sensitive chitosan nanodroplets for spatiotemporally controlled DKK-2 gene delivery to prostate cancer cells. *Int. J. Nanomedicine* 16, 421–432. doi:10.2147/ijn.s286474

Liu, Z., Liang, G., and Zhan, W. (2021b). *In situ* activatable peptide-based nanoprobes for tumor imaging. *Chem. Res. Chin. Univ.* 37, 889–899. doi:10.1007/s40242-021-1181-8

Logan, J. K., Rais-Bahrami, S., Turkbey, B., Gomella, A., Amalou, H., Choyke, P. L., et al. (2014). Current status of magnetic resonance imaging (MRI) and ultrasonography fusion software platforms for guidance of prostate biopsies. *BJU Int.* 114, 641–652. doi:10.1111/bju.12593

Lopes, A. M., Chen, K. Y., and Kamei, D. T. (2017). A transferrin variant as the targeting ligand for polymeric nanoparticles incorporated in 3-D PLGA porous scaffolds. *Mater. Sci. Eng. C* 73, 373–380. doi:10.1016/j.msec.2016.12.091

Lu, W., Singh, A. K., Khan, S. A., Senapati, D., Yu, H., and Ray, P. C. (2010). Gold nano-popcorn-based targeted diagnosis, nanotherapy treatment, and *in situ* monitoring of photothermal therapy response of prostate cancer cells using surface-enhanced Raman spectroscopy. *J. Am. Chem. Soc.* 132, 18103–18114. doi:10.1021/ja104924b

Min, K. H., Kim, Y. H., Wang, Z., Kim, J., Kim, J. S., Kim, S. H., et al. (2017). Engineered Zn(II)-Dipicolylamine-Gold nanorod provides effective prostate cancer treatment by combining siRNA delivery and photothermal therapy. *Theranostics* 7, 4240–4254. doi:10.7150/thno.22435

Mirjolet, C., Boudon, J., Loiseau, A., Chevrier, S., Boidot, R., Oudot, A., et al. (2017). Docetaxel-titanate nanotubes enhance radiosensitivity in an androgen-independent prostate cancer model. *Int. J. Nanomedicine* 12, 6357–6364. doi:10.2147/ijn.s139167

Nathwani, A. C., Reiss, U. M., Tuddenham, E. G., Rosales, C., Chowdary, P., Mcintosh, J., et al. (2014). Long-term safety and efficacy of factor IX gene therapy in hemophilia B. *N. Engl. J. Med. Overseas. Ed.* 371, 1994–2004. doi:10.1056/nejmoa1407309

Nie, Y., Schaffert, D., Rodl, W., Ogris, M., Wagner, E., and Gunther, M. (2011). Dual-targeted polyplexes: one step towards a synthetic virus for cancer gene therapy. *J. Control. Release* 152, 127–134. doi:10.1016/j.jconrel.2011.02.028

Patra, S., Roy, E., Madhuri, R., and Sharma, P. K. (2015). Nano-iniferter based imprinted sensor for ultra trace level detection of prostate-specific antigen in both men and women. *Biosens. Bioelectron. X.* 66, 1–10. doi:10.1016/j.bios.2014.10.076

Peng, S., Bie, B., Sun, Y., Liu, M., Cong, H., Zhou, W., et al. (2018). Metal-organic frameworks for precise inclusion of single-stranded DNA and transfection in immune cells. *Nat. Commun.* 9, 1293. doi:10.1038/s41467-018-03650-w

Ping, Y., Ding, D., Ramos, R., Mohanram, H., Deepankumar, K., Gao, J., et al. (2017). Supramolecular beta-sheets stabilized protein nanocarriers for drug delivery and gene transfection. *ACS Nano* 11, 4528–4541. doi:10.1021/acsnano.6b08393

Rahmani, S., and Abdollahi, M. (2017). Novel treatment opportunities for sulfur mustard-related cancers: genetic and epigenetic perspectives. *Arch. Toxicol.* 91, 3717–3735. doi:10.1007/s00204-017-2086-7

Ratner, M. (2015). Heart failure gene therapy disappoints but experts keep the faith. *Nat. Biotechnol.* 33, 573–574. doi:10.1038/nbt0615-573a

Ren, C., Xu, C., Li, D., Ren, H., Hao, J., and Yang, Z. (2014). Gemcitabine induced supramolecular hydrogelations of aldehyde-containing short peptides. *RSC Adv.* 4, 34729–34732. doi:10.1039/c4ra05808a

Salimi, A., Kavosi, B., Fathi, F., and Hallaj, R. (2013). Highly sensitive immunosensing of prostate-specific antigen based on ionic liquid-carbon nanotubes modified electrode: application as cancer biomarker for prostate biopsies. *Biosens. Bioelectron. X.* 42, 439–446. doi:10.1016/j.bios.2012.10.053

Sanders, M., Lin, Y., Wei, J., Bono, T., and Lindquist, R. G. (2014). An enhanced LSPR fiber-optic nanoprobe for ultrasensitive detection of protein biomarkers. *Biosens. Bioelectron. X.* 61, 95–101. doi:10.1016/j.bios.2014.05.009

Sanna, V., Siddiqui, I. A., Sechi, M., and Mukhtar, H. (2013). Resveratrol-loaded nanoparticles based on poly(epsilon-caprolactone) and poly(D, L-lactic-co-glycolic acid)-poly(ethylene glycol) blend for prostate cancer treatment. *Mol. Pharm.* 10, 3871–3881. doi:10.1021/mp400342f

Schilham, M. G. M., Zamecnik, P., Prive, B. M., Israel, B., Rijpkema, M., Scheenen, T., et al. (2021). Head-to-Head comparison of (68)Ga-Prostate-Specific membrane antigen PET/CT and ferumoxtran-10-enhanced MRI for the diagnosis of lymph node metastases in prostate cancer patients. *J. Nucl. Med.* 62, 1258–1263. doi:10.2967/jnumed.120.258541

Seidenfeld, J., Samson, D. J., Hasselblad, V., Aronson, N., Albertsen, P. C., Bennett, C. L., et al. (2000). Single-therapy androgen suppression in men with advanced prostate cancer: a systematic review and meta-analysis. *Ann. Intern. Med.* 132, 566–577. doi:10.7326/0003-4819-132-7-200004040-00009

Shao, Q., Wong, K. M., Seroski, D. T., Wang, Y., Liu, R., Paravastu, A. K., et al. (2020). Anatomy of a selectively coassembled beta-sheet peptide nanofiber. *Proc. Natl. Acad. Sci. U. S. A.* 117, 4710–4717. doi:10.1073/pnas.1912810117

Sharafeldin, M., Bishop, G. W., Bhakta, S., EL-Sawy, A., Suib, S. L., and Rusling, J. F. (2017). Fe3O4 nanoparticles on graphene oxide sheets for isolation and ultrasensitive amperometric detection of cancer biomarker proteins. *Biosens. Bioelectron. X.* 91, 359–366. doi:10.1016/j.bios.2016.12.052

Shin, S. W., Song, W. C., Kim, A. R., Cho, S. W., Kim, D. I., and Um, S. H. (2014). Novel stem-loop RNA and drug-bearing DNA hybrid nanostructures specific to LNCaP prostate carcinoma. *Biomater. Sci.* 2, 76–83. doi:10.1039/c3bm60136f

Siegel, R. L., Miller, K. D., Fuchs, H. E., and Jemal, A. (2022). Cancer statistics, 2022. *Ca. A Cancer J. Clin.* 72, 7–33. doi:10.3322/caac.21708

Stephan, S. B., Taber, A. M., Jileaeva, I., Pegues, E. P., Sentman, C. L., and Stephan, M. T. (2015). Biopolymer implants enhance the efficacy of adoptive T-cell therapy. *Nat. Biotechnol.* 33, 97–101. doi:10.1038/nbt.3104

Sun, B., Chang, R., Cao, S., Yuan, C., Zhao, L., Yang, H., et al. (2020). Acid-activatable transmorphic peptide-based nanomaterials for photodynamic therapy. *Angew. Chem. Int. Ed. Engl.* 59, 20763–20769. doi:10.1002/ange.202008708

Sung, H., Ferlay, J., Siegel, R. L., Laversanne, M., Soerjomataram, I., Jemal, A., et al. (2021). Global cancer statistics 2020: GLOBOCAN estimates of incidence and mortality worldwide for 36 cancers in 185 countries. *Ca. A Cancer J. Clin.* 71, 209–249. doi:10.3322/caac.21660

The, L. (2017). CAR T-cells: an exciting frontier in cancer therapy. *Lancet* 390, 1006. doi:10.1016/s0140-6736(17)32395-4

Tong, R., Yala, L., Fan, T. M., and Cheng, J. (2010). The formulation of aptamer-coated paclitaxel–polylactide nanoconjugates and their targeting to cancer cells. *Biomaterials* 31, 3043–3053. doi:10.1016/j.biomaterials.2010.01.009

Vodnik, V. V., Mojic, M., Stamenovic, U., Otonicar, M., Ajdzanovic, V., Maksimovic-Ivanic, D., et al. (2021). Development of genistein-loaded gold nanoparticles and their antitumor potential against prostate cancer cell lines. *Mater. Sci. Eng. C* 124, 112078. doi:10.1016/j.msec.2021.112078

Wang, J., Li, H., and Xu, B. (2021). Biological functions of supramolecular assemblies of small molecules in the cellular environment. *RSC Chem. Biol.* 2, 289–305. doi:10.1039/d0cb00219d

Wang, Y., Tang, J., Yang, Y., Song, H., Fu, J., Gu, Z., et al. (2020). Functional nanoparticles with a reducible tetrasulfide motif to upregulate mRNA translation and enhance transfection in hard-to-transfect cells. *Angew. Chem. Int. Ed. Engl.* 59, 2717–2721. doi:10.1002/ange.201914264

Wei, B., Mao, K., Liu, N., Zhang, M., and Yang, Z. (2018). Graphene nanocomposites modified electrochemical aptamer sensor for rapid and highly sensitive detection of prostate specific antigen. *Biosens. Bioelectron. X.* 121, 41–46. doi:10.1016/j.bios.2018.08.067

Yan, J., Wang, Y., Zhang, X., Liu, S., Tian, C., and Wang, H. (2016). Targeted nanomedicine for prostate cancer therapy: docetaxel and curcumin co-encapsulated lipid-polymer hybrid nanoparticles for the enhanced anti-tumor activity *in vitro* and *in vivo*. *Drug Deliv. (Lond).* 23, 1757–1762. doi:10.3109/10717544.2015.1069423

Yan, R., Lu, N., Han, S., Lu, Z., Xiao, Y., Zhao, Z., et al. (2022). Simultaneous detection of dual biomarkers using hierarchical MoS2 nanostructuring and nano-signal amplification-based electrochemical aptasensor toward accurate diagnosis of prostate cancer. *Biosens. Bioelectron. X.* 197, 113797. doi:10.1016/j.bios.2021.113797

Yang, C., Chu, L., Zhang, Y., Shi, Y., Liu, J., Liu, Q., et al. (2015). Dynamic biostability, biodistribution, and toxicity of L/D-peptide-based supramolecular nanofibers. *ACS Appl. Mat. Interfaces* 7, 2735–2744. doi:10.1021/am507800e

Zhan, J., Cai, Y., He, S., Wang, L., and Yang, Z. (2018). Tandem molecular self-assembly in liver cancer cells. *Angew. Chem. Int. Ed. Engl.* 57, 1831–1834. doi:10.1002/ange.201710237

Zhang, X., Wang, Y., Hua, Y., Duan, J., Chen, M., Wang, L., et al. (2018). Kinetic control over supramolecular hydrogelation and anticancer properties of taxol. *Chem. Commun.* 54, 755–758. doi:10.1039/c7cc08041g

Zhang, Z., Hou, L., Yu, Z., Xu, Z., Li, S., Wang, Y., et al. (2022). Biomimetic Small-Molecule Self-Assembly of PI3K inhibitor integrated with immunomodulator to amplify anticancer efficacy. *Chem. Eng. J.* 433, 133747. doi:10.1016/j.cej.2021.133747

Zhao, J., Zhang, C., Wang, W., Li, C., Mu, X., and Hu, K. (2022). Current progress of nanomedicine for prostate cancer diagnosis and treatment. *Biomed. Pharmacother.* 155, 113714. doi:10.1016/j.biopha.2022.113714

Zhou, H., Zhang, B., Zheng, J., Yu, M., Zhou, T., Zhao, K., et al. (2014). The inhibition of migration and invasion of cancer cells by graphene via the impairment of mitochondrial respiration. *Biomaterials* 35, 1597–1607. doi:10.1016/j.biomaterials.2013.11.020

frontiers | Frontiers in Bioengineering and Biotechnology

TYPE Review
PUBLISHED 17 November 2022
DOI 10.3389/fbioe.2022.1042986

OPEN ACCESS

EDITED BY
Zhanzhan Zhang,
Tianjin Medical University, China

REVIEWED BY
Zhongmin Geng,
Qingdao University, China
Hanlin Ou,
Qingdao University, China

*CORRESPONDENCE
Yanyan Cao,
caoyanyan1991@sina.com

SPECIALTY SECTION
This article was submitted to Nanobiotechnology, a section of the journal Frontiers in Bioengineering and Biotechnology

RECEIVED 13 September 2022
ACCEPTED 02 November 2022
PUBLISHED 17 November 2022

CITATION
Cao Y and Zhang R (2022), The application of nanotechnology in treatment of Alzheimer's disease. *Front. Bioeng. Biotechnol.* 10:1042986. doi: 10.3389/fbioe.2022.1042986

The application of nanotechnology in treatment of Alzheimer's disease

Yanyan Cao* and Run Zhang

Department of Neurology, First Affiliated Hospital of Wannan Medical College, Wuhu, China

The buildup of beta-amyloid plaques in the brain results in Alzheimer's disease (AD), a neurodegenerative condition. A permanent treatment for AD is not yet available. Only a slowing down of its advancement is possible with the current pharmaceutical options. Nevertheless, nanotechnology has proven to be advantageous in medical applications. It has a lot of potential for AD therapy, particularly in diagnosing the condition and providing an alternative course of treatment. In this review, we outline the developments and benefits of nanomedicines in treating AD. Prospective nanomedicines for diagnosing and surveillance therapeutic interventions for AD and other diseases of the central nervous system (CNS) may be clinically accessible, persuading the development of investigation in this field.

KEYWORDS

nanotechnology, nanomedicine, brain disorder, Alzheimer, chronic disease

Introduction

The most prevalent type of dementia, Alzheimer's disease (AD), affects close to 50 million people worldwide. Because of the rise in the average life expectancy, it is anticipated that this population will reach 150 million in the year 2050 (Gaudreault and Mousseau, 2019). Then, AD is expected to remain a clinical, social, and economic concern. Several approaches are being investigated to find novel treatments for AD (Loureiro et al., 2014). Dealing with the pathology of AD has some restrictions. The intranasal administration of drugs targeting neurotransmitters or enzyme modulation is exploited to treat the cognitive deficits caused by AD (Sood et al., 2014). Only four treatments for AD have been approved by the Food and Drug Administration (FDA), and these all target different aspects of the disease's two main molecular pathways: the buildup of Aβ peptide and neurofibrillary tangles (NFT) of p-tau protein (Sabbagh, 2020). However, using these medications causes a significant increase in therapy failures because of their poor absorption in the neuronal cell membranes, instability, neurotoxicity, and a number of other pharmacokinetic and pharmacodynamic characteristics (Suri et al., 2015; Guo et al., 2020). This emphasizes the necessity for developing alternative therapeutic interventions. Recognition of different molecular targets that could result in new treatments is anticipated to result from the finding of new biomarkers, which are also expected to strengthen previous AD diagnoses. The development of novel therapies needs to describe the pathophysiological mechanisms underlying AD and the best biomarkers to discover them. Furthermore, it is essential to deliver diagnostic and therapeutic compounds to the target sites

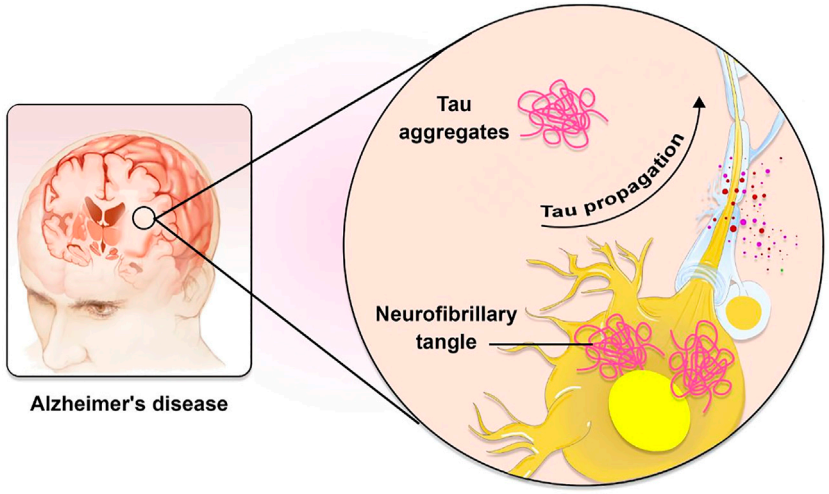

FIGURE 1
The role of Tau in AD pathogenesis. Tau is known to spread in a predictable way along neuronal networks in neurofibrillary tangles (NFTs). It is possible that the characteristic development of AD neuropathology is caused by interneuron transfer of the pathogenic form of tau.

in these mechanisms effectively and precisely. Because of their diverse chemical properties and their predisposition for chemical change to modulate and refine desired characteristics, nanoparticles (NPs) have enabled significant advancements in drug delivery, treatment, and disease diagnosis (Duskey et al., 2017; Mulvihill et al., 2020). Due to the enhancement of the medicine's pharmacological effects, the necessary doses to generate therapeutic effects are reduced when drugs are delivered using nanocarriers. This results in a reduction in the number of adverse effects experienced by patients (Wais et al., 2016). The main components of NPs involve a wide range of substances encapsulating compounds with various chemical properties, including lipids, polymers, and metals. The ability of NPs to deliver compounds to difficult-to-reach organs, like the CNS, where the blood-brain barrier (BBB) must be crossed and controlled kinetic drug releases are necessary for long-term therapies, is indispensable for chronic CNS diseases (Wilczewska et al., 2012). The purpose of this study is to provide a high-level summary of how AD treatment has evolved as a direct result of the application of nanotechnology. A strong focus is also put on the significant challenges that currently exist as well as the prospects for the future of this industry.

Alzheimer's disease pathogenesis and molecular basis

AD is a massively complicated and progressive neurodegenerative disorder (Association, 2015). Extracellular accumulations of Aβ plaques and intracellular accumulations of NFTs constituted of hyperphosphorylated microtubule-associated τ have been reported as AD's histopathological features. Plaques composed of Aβ first appear in the brain's basal, temporal, and orbitofrontal neocortices. As the disease progresses, however, it spreads throughout the neocortex, hippocampus, amygdala, diencephalon, and basal ganglia. In severe cases, the mesencephalon, cerebellar cortex, and lower brain stem contain Aβ. The development of tau-tangles, which can be observed in the locus coeruleus and the transentorhinal and entorhinal regions of the brain, is triggered when a concentration of Aβ is present. It propagates to the hippocampus and neocortex during the critical phase (Figure 1) (Goedert, 2015). Also, AD development is influenced by several physiological variables summarized in Table 1.

Despite the progress made in understanding the biology of the AD and developing treatments for it, we do not yet have a molecule that may postpone and/or prevent the progression of the disease in aged people and patients with AD. There are two distinct etiologies of AD: early-onset familial AD and late-onset sporadic AD. Investigations of Alzheimer's disease brains obtained *via* autopsies found that there are no discernible differences between the early-onset familial form of the disease and the late-onset sporadic form (Ayodele et al., 2021). Early-onset familial AD is caused by mutations in three different loci: the amyloid precursor protein (APP), presenilin 1 (PS1), and presenilin 2 (PS2). It is hypothesized that these genetic changes make a person more susceptible to increased mitochondrial dysfunction (Hyman et al., 2012; Reddy et al., 2018). If a person has these genetic antecedents, it is more probable that they will get AD in their 50s rather than in their 70s or later in life. In addition, having the

TABLE 1 The involvement of physiological factors in AD pathogenesis.

Variable	Distinction	Reference
Hypertension	It is thought that hypertension can influence AD through its relationship with cerebrovascular pathology. Hypertension, commonly known as high blood pressure, is another factor that may have a role in the pathophysiology of AD. According to the research, hypertension is the cause of increased plaque development in the brain	Nehls (2016)
Homocysteine	It contributes to the progression of beta amyloid (Aβ) plaque development. In addition, there is speculation that homocysteine plays a role in the elevation of oxidative stress in the brain, which is a factor in the advancement of AD diseases	Pacheco-Quinto et al. (2006)
Inflammation	A significant correlation with the overall risk of dementia	Mrak and Griffin (2005)
Physical activity	Exercising produces anti-inflammatory effects and offers a myriad of additional advantages through a variety of routes, all of which have the potential to slow or stop the advancement of AD.	Schlegel et al. (2019); Valenzuela et al. (2020)
Diabetes mellitus	There is a theoretical support has been depicted on the relationship between diabetes and Alzheimer's disease, along with novel strategies to prevent diabetic people from developing AD. It has also been found that AD can be alleviated by taking preventative measures against diabetes such as maintaining a healthy weight and diet, participating in sports, and engaging in other physically active pursuits	Sun et al. (2020)

apolipoprotein E allele 4 (APOE4) increases a person's risk of developing late-onset sporadic AD since this allele plays a role in the accumulation of amyloid protein (Hyman et al., 2012). In addition, the development of both types of AD is caused by age-related variables such as reactive oxygen species (ROS), malfunction in mitochondria, and phosphorylation of tau (Kritsilis et al., 2018; Reddy et al., 2018). Additionally, synaptic loss and mitochondrial dysfunction are early events or triggers in the progression of the disease. Mitochondria, sometimes known as the "powerhouses of the cell," are accountable for the vast majority of the metabolic activities that are necessary for human survival. Unfortunately, when these super organelles are not functioning properly, it leaves us open to the development of serious, debilitating illnesses (Oliver and Reddy, 2019).

Blood-brain barrier in Alzheimer's disease

The BBB plays a pivotal role in the movement of biomolecules into and out of the brain's neuronal system. Hence, to enhance the delivery of drugs to the brain, it is necessary to gain a comprehension of the structural and functional features of the BBB (Sharifzad et al., 2019; Alahmari, 2021). Two specialized barriers, the cerebrospinal fluid barrier (CSFB) and BBB distinguish the complex human CNS (Pathan et al., 2009; Dabbagh et al., 2022). Both cognitive impairment and dementia are caused by cerebrovascular dysfunction, which may result in cerebral amyloid angiopathy in AD. In addition, it acts as a mediator for the buildup of Aβ peptides within the brain. The advanced glycation end product (RAGE) receptor and the low-density lipoprotein receptor related protein 1 (LRP1) are the two main receptors that enable the BBB to control the regulation of Aβ transport to the brain (Sagare et al., 2012).

The perseverance required for the selective transport of small molecules over the BBB is provided by cohesive domains bound to the endothelial cells (Abbott et al., 2010). A regulated intracellular transport *via* transcytosis takes place to fulfill the needs of proteins and peptides for brain homeostasis. Endothelial cells, with the assistance of a wide variety of specialized transporting proteins, can enable the transport of molecules. However, this ability is contingent on the nature of the compounds (hydrophilic or hydrophobic). In preclinical investigations, several various nanocarriers have been reported as having the potential to cure brain illnesses like AD. To cross the BBB, these carriers encapsulate the AD medications as cargo (Mulvihill et al., 2020).

Nanotechnology in Alzheimer's disease

Nanotechnology aims to design, produce, and use nanomaterials-materials with at least one dimension falling between 1 and 100 nm. At this scale, materials frequently exhibit bulk-independent properties that are considered interesting to the medical community, including superparamagnetism or surface plasmon resonance (Khan et al., 2019). Additionally, because proteins and nucleic acids are in the same size range as nanomaterials, particularly nanoparticles, they are well-suited for interacting with those biomolecules and, as a result, with cells. Likewise, a large surface-volume ratio associated with nanometric size offers benefits in applications of biological recognition, particularly in sensing. Therapeutic uses of these compounds have undergone extensive testing (Auría-Soro et al., 2019; Li et al.,

2019; He et al., 2021). Applications of nanomaterials have also been studied in the field of precision medicine for the past few years (Mura and Couvreur, 2012). Because of the drug's inability to circumvent the BBB, the only treatment for AD currently on the market focuses on symptomatic relief. Due to its many benefits, nanotechnology-based therapy may overcome this restriction (Ling et al., 2021). The FDA has given its blessing for the use of commercially available medications to a wide variety of nanocarriers that range in size from very tiny to very large. These nanocarriers are used in the treatment of neurological conditions such as AD and brain cancer (Association, 2013; Patra et al., 2018). Nanomedicines are comprised of various nanocarriers containing different drugs. The potential for nanomaterials to manage the pathologies of AD is receiving extensive investigation. The treatment of AD currently uses nanostructure-based delivery systems, which will be discussed in the following sections. Most of them are classified as either metallic NPs, organic nanostructures, or lipid-based nanoparticles.

Liposomes

The phospholipid bilayer of liposomes is the most probable solution to the problem of transporting medications across the BBB. However, it is forbidden to cross the BBB. Numerous surface modifications have been implemented to boost liposomal carrier transport across the BBB (Spuch and Navarro, 2011). Numerous proteins, peptides, antibodies, and other ligand receptors may be present on the surface of the BBB. Transcytosis can be facilitated by applying surface-active ligands, including those found in these compounds. Transcytosis and cationic liposome absorption into the BBB take place simultaneously. Liposomes are typically coated with nutrients like glucose to make it easier for them to move through the body. Once the liposomes have entered the brain, the passive diffusion mechanism can proceed. This process is triggered by the brain's passive efflux (Noble et al., 2014). Through associated receptors on BBB cells, curcumin-loaded liposomes can substantially improve drug delivery to the CNS (Lajoie and Shusta, 2015). The liposome carrier system that has been modified with a surface with mannose ligand and cell-penetrating peptides (CPPs) has been employed to deliver apolipoprotein E (ApoE2) in the brain injured by AD. The findings show that functionalized liposomes can deliver a significant concentration of genes to the target tissues safely and effectively for the treatment of AD (Arora et al., 2020). Osthole (Ost) is an anti-AD compound because of its prophylactic impacts on hippocampus neurons and anti-Aβ characteristics. Bioavailability and exposure to target sites in the AD mice brain have been addressed by developing an Ost-liposomes carrier system (Kong et al., 2020).

Polymeric-based nanoparticles

Designing and testing polymeric biodegradable NPs functionalized with antibody and polyethylene glycol (PEG) in transgenic AD mice was productive. According to recent research, exposure to PEGylated NPs can rectify memory deficits and significantly lower levels of Aβ-soluble peptides. The AD disease can therefore be treated with the designed formulation (Carradori et al., 2018). Research has been carried out in which biodegradable polymeric NPs are synthesized using the double emulsion method. The purpose of this study is to determine whether or not loading memantine into these NPs will increase its effectiveness in treating AD. Memantine-loaded NPs can significantly reduce Aβ plaques and AD-related inflammatory processes when used to treat AD brain tissue (Sánchez-López et al., 2018). When applied to mice with AD, targeting the brain with zinc-loaded polymeric NPs can reduce the size of amyloid plaques and help alleviate other neuronal deficiencies (Vilella et al., 2018). To transport the acetylcholinesterase inhibitor known as huperzine A, mucoadhesive and target poly lactic-co-glycolic acid nanoparticles (PLGA-NPs) that have had their surfaces changed with lactoferrin-conjugated N-trimethylated chitosan have been used. The formulation has shown promising results in both its sustained-release action and its ability to target AD pathology (Meng et al., 2018).

Thymoquinone (TQ), a bioactive component found in *Nigella sativa* seed essential oil, has been demonstrated to have a variety of medicinal applications (Javidi et al., 2016). Numerous preliminary pharmacological investigations have been carried out to study the therapeutic utilization of TQ; however, further research is required to decide whether or not it is beneficial in treating neurological diseases. Recent studies have demonstrated that TQ is a potential treatment for AD (Abulfadl et al., 2018).

TQ-containing NPs coated with polysorbate-80 (P-80) may be a viable and dependable method of delivering nanoscale to the brain through the BBB (Yusuf et al., 2021). PLGA is a biodegradable polymer because it can be hydrolyzed into its non-toxic endogenous metabolites, including glycolic acid and lactic acid. Hydrophobic PLGA tends to opsonize and be eliminated by the reticuloendothelial system (RES), despite its widespread use for CNS-targeted drug administration. Since the PLGA-NPs are coated with surfactant P-80, non-toxic, non-ionic, biodegradable, and hydrophilic, they are protected from being opsonized and cleared (Sempf et al., 2013).

The significant contribution of drug release from the matrix through diffusion caused by pore formation comes from the autocatalytic hydrolytic breakdown of PLGA to lactic and glycolic acid. Through the autocatalytic breakdown of the matrix, it may be possible to accomplish both high porosity and strong drug diffusion. Because of the hydrophilicity of the P-80 coating, TQ from P-80-TQN could be easily derived (Tığlı

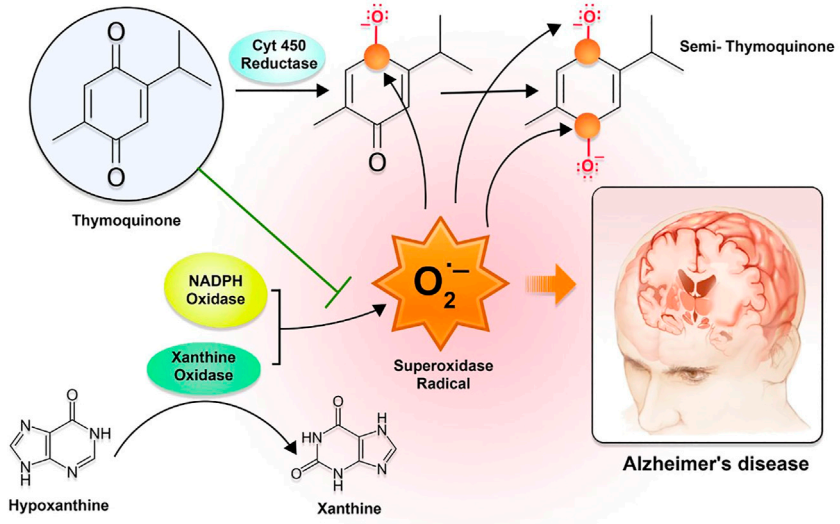

FIGURE 2
The mechanism of action of thymoquinone with regard to oxidative stress-mediated AD symptoms. The interaction between TQ and PLGA may have led to a further sluggish release, which may have restricted the amount of TQ that was released. The TQ primarily exerts its effect by inhibiting the enzyme xanthine-oxidase and lowering the production of superoxide radicals. In contrast, the semi-TQ that is produced by cytochrome 450 reductase offers electron-deficient platforms at the first and fourth positions, which in turn offers electron-deficient centers for superoxide radicals.

Aydın et al., 2016; Zeng et al., 2020). The interaction between TQ and PLGA may have led to an additional delayed discharge, which may have restricted the amount of TQ delivery. The primary mechanism by which TQ exerts its effect is by inhibiting the enzyme xanthine-oxidase, thereby lowering the production of superoxide radicals. In contrast, the semi-TQ produced by cytochrome 450 reductase offers electron-deficient platforms at the first and fourth positions, thereby supplying electron-deficient centers for superoxide radicals. Because of the reduction in OS and AD, these processes can bring the number of superoxide radicals in the environment down to a safer level (Figure 2).

The cationic mucoadhesive polymer chitosan (CH) was also used in the study because it can form gels by absorbing water, extending the period at the site of action. When medications are taken orally, CH is said to enhance medication penetration through the nasal mucosa and assist in opening tight junctions, as stated in several studies (Ariful Islam et al., 2015; Wang et al., 2018; Duan et al., 2022). Utilizing this material as a shell makes it possible to employ CH to increase the residence period and improve medication permeation.

Accumulation of inhibitors of Aβ could help treat AD. Various drugs can destabilize the A fibrils *in vitro*, preventing Aβ accumulation and neurotoxic effects. Much research has been done on the inhibitory action of NPs. The functional NPs have the potential to avoid the aggregation of proteins efficiently. Light-activated gold nanoparticles (AuNPs) containing peptides have the potential to cause the disintegration of preformed fibrils. Detrimental ions are precluded from being released from the nanocarrier whenever the surface is appropriately functionalized (Meenambal and Bharath, 2020).

NPs may disrupt small fibers and avoid their accumulation. Experiments may successfully avoid Aβ accumulation and fibrillation when applying the small AuNPs because they decelerate the nucleation mechanism. Theoretical perspectives for therapeutic candidates to treat AD may thus be gained through synthesizing AuNPs.

Curcumin is an antioxidant with low toxicity and a free radical scavenger, a naturally occurring phytochemical (Azizi et al., 2018; Sharifi-Rad et al., 2020). The most appealing method for treating AD is administering curcumin to the brain, inhibiting tau protein accumulation and exhibiting anti-amyloid characteristics at concentrations in the micromolar range (Yang et al., 2022a). Poor stability and bioavailability of curcumin during brain delivery contribute to its reduced brain absorption (Gao et al., 2020). The use of nanocarriers is favored as a means of addressing these concerns because of the safety benefits associated with this method and the increased and sustained brain exposure it provides. It is also possible to establish a stable and sustained distribution of curcumin across the BBB by utilizing a nanoemulsion of red blood cell membrane-coated PLGA particles loaded with T807 molecules implanted on the surface of the red blood cell membrane (T807/RPCNP). The mutual actions of these proteins show strong inhibitory effects of T807, 807/RPCNP on tau-associated pathogenesis (Gao et al., 2020). Additionally, to expedite the

phagocytosis of the Aβ peptide and enhance drug permeation, curcumin loaded with chitosan and bovine serum albumin NPs is used to mitigate AD manifestations (Yang et al., 2018). Through various kinase pathways, curcuminoids control the proliferation of neuronal stem cells in the Aβ-induced rat model (Ling et al., 2021). In order to alleviate the symptoms of AD, curcumin that has been loaded with chitosan and bovine serum albumin NPs has been shown to boost the drug penetration and speed the phagocytosis of the Aβ peptide. Other biological benefits of curcumin-based nanomedicines for treating brain disorders include their ability to protect neurons against dopaminergic toxicity by activating the transcription factor Nrf2, which is renowned as a master regulator of the antioxidant response (Szwed and Miłowska, 2012; Yang et al., 2018; Chen et al., 2021).

Nanogels

It has been shown that the use of nanogels for the delivery of pharmaceuticals is more effective than the administration of free drugs. This was established in comparison to the effectiveness of the administration of free drugs. This happens as a result of a number of reasons, some of which include enhanced cellular absorption of the medication, decreased drug toxicity, higher drug loading, and controlled release of the loaded drug at the targeted site (Neamtu et al., 2017). The potential of nanogels to bind active compounds, macromolecules, and drugs make them attractive drug delivery systems that have been used to address many problems related to various pathologies, such as AD (Aderibigbe and Naki, 2018). According to a recent study, one of the most effective treatments for AD involves delivering deferoxamine as nanogels employing the chitosan and tripolyphosphate approach (Ashrafi et al., 2020). Polysaccharide pullulan backbones modified with cholesterol moieties serve as artificial chaperones that have been proven to alleviate AD pathology by preventing the development of Aβ amyloids (Ikeda et al., 2006). The nose-to-brain delivery of insulin, a candidate drug for AD, has been assessed and found to be increased by employing nanogels as a carrier during a preclinical experiment conducted on mice (Picone et al., 2018). When combined with polysaccharides, the NPs had a number of benefits, including the fact that they were non-toxic, very stable, hydrophilic, and biodegradable (Meng et al., 2018).

Dendrimers

For the treatment of AD, dendrimers are viewed as a potentially useful compound (Aliev et al., 2019). Combining low-generation dendrimers and lactoferrin to deliver memantine to specific brain regions in AD-induced mice has resulted in a discovery. An important effect on target mice's memory aspects was noted in recent research (Gothwal et al., 2019).

Dendrimers with an ethylenediamine core, generation 4.0 and 4.5, are commonly used to improve the drug solubility and bioavailability for greater permeation across the BBB to target the damaged parts in the brain to increase the efficacy of drug-related CNS disorders such as AD and polyamidoamine (PAMAM). This is done to increase the efficacy of drug-related CNS disorders such as AD and PAMAM (Igartúa et al., 2018; Yang et al., 2022b). Dendrimers composed of a poly (propylene imine) core and a maltose-histidine shell (G4HisMal) have been effectively developed, and they may show significant alleviation of AD manifestations like memory dysfunction. To improve biocompatibility and lessen the toxic effects of medications employed to treat AD, tacrine has also been administered in combination with generation 4.0 and PAMAM dendrimers as nanocomposites (Jin and Wang, 2016; Igartúa et al., 2020). Moreover, the disposable immune platforms for the concurrent identification of the biomarkers for AD have been designed using the nanocomposites of PAMAM dendrimers and gold NPs (Figure 3) (Serafín et al., 2021).

Micelle

In the form of drinking water, double transgenic AD mice are given a micelle water-soluble formulation of coenzyme Q10 (UbisolQ10). The findings indicate that it is effective in enhancing long-term memories and lowering the concentrations of circulated Aβ plaques (Muthukumaran et al., 2018). The availability and effectiveness of curcumin in treating AD symptoms have been found to increase when Tween-80 is mixed with micelles to develop curcumin micelles (Hagl et al., 2015). In recent research, neuronal N2 cells have examined how PEG ceramide nanomicelles influence the cells. Nanomicelles have been demonstrated to be an efficient tool for mediating tau protein disintegration and inducing autophagy in target cells (Gao and Jiang, 2006). Another study demonstrates the use of curcumin-loaded polymeric nanomicelles as a targeted therapeutic delivery system in conjunction with the glycation method of bovine serum albumin in the presence of phosphate-buffered saline results in significant inhibition of the amyloidogenesis process in mice with AD (Mirzaie et al., 2019). In addition to this, it was demonstrated that an artificial chaperone comprised of mixed-shell polymeric micelles (MSPMs) has been developed with variable surface characteristics that serves as a suppressor of AD. This artificial chaperone was inspired by a natural molecular chaperone. MSPM-based chaperones have the ability to maintain A homeostasis through a variety of mechanisms, including the inhibition of A fibrillation, the facilitation of A

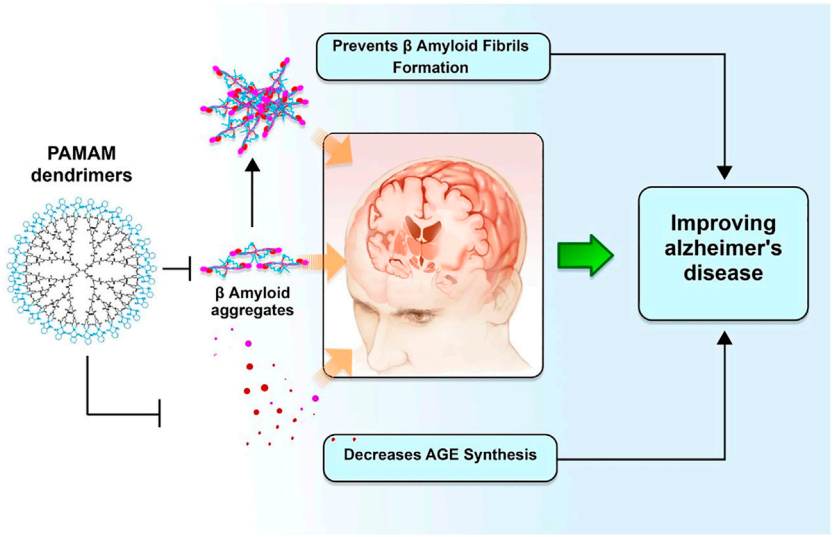

FIGURE 3
Dendrimers and their potential role in improving AD pathogenesis. Polyamidoamine dimers, also known as PAMAM, serve as modulators for amyloid fibrillar production. This, in turn, enhances biocompatibility and degradation of synapses against A oligomers, hence preventing a deterioration in memory associated with Alzheimer's disease.

aggregate clearance, and the reduction of A-mediated neurotoxicity at the same time (Huang et al., 2014). MSPMs were able to lessen the load of A, dampen the inflammation caused by A, and ultimately repair the cognitive abnormalities shown in APP/PS1 transgenic AD mice (Yang et al., 2019). An additional nanochaperone was developed by designing a VQIINK hexapeptide that was obtained from the tau protein onto the surface of a self-assembly micelle that was outfitted with chaperone-like hydrophobic microdomains and restricted spaces. This nanochaperone is able to collect pathogenic tau without affecting normal tau, and it inhibits their ability to aggregate by a significant amount because to the synergistic action of tau-recognizing peptides and limited hydrophobic microdomains on the surface (Xu et al., 2022).

Selenium nanoparticles

As was mentioned earlier, one of the most important steps in treating AD is lowering the level of ROS in the brain. Active ROS inhibitors can be found in many different trace elements, including selenium (II), sodium selenite (VI), and sodium selenite (IV). Because selenium and selenite are essential micronutrients for the human body and have the potential for use in biomedical applications of selenium nanoformulation, nanoparticles containing selenium and selenite have been shown to reduce oxidative stress and prevent the cytotoxicity of cells. As a result, they can potentially be used in the treatment of neurodegenerative disorders such as AD (Rajeshkumar et al., 2019). The BBB has been discovered to be permeable to modified selenium NPs containing sialic acid, and their exposure has been shown to inhibit the Aβ accumulation reactions (Yin et al., 2015). Aβ aggregation might also be blocked by using sialic acid-modified selenium NPs coated with high BBB permeability peptide-B6 and epigallocatechin-3-gallate (EGCG) (Zhang et al., 2020). One promising delivery system for AD treatment is a new modified nanoformulation of selenium NPs entrapped in PLGA nanospheres with curcumin, demonstrating potent inhibitory impacts against Aβ accumulation in a transgenic AD mouse model (Huo et al., 2019).

Antibody-based nanoparticles

When immunotherapy doses are given to treat AD, complications such as meningoencephalitis could emerge (Hoskin et al., 2019). Applying NPs coated with antibodies directed against specific target proteins is the most effective alternative to immunotherapy for locating and dissolving protein aggregates in brain cells. Secondary ion mass spectrometry is employed to image proteins associated with AD in the brain using antibodies coated with metal oxide NPs (Moon et al., 2020). Nanovehicles coated with chitosan and Aβ fragments have been used to target amyloid-containing cells in AD. NP-Aβ absorption across the BBB is boosted by contrast agents like fluorescein isothiocyanate (FITC) and Alexa Fluor (Agyare et al., 2008). The therapy of AD with the class A receptor activator XD4 (W20/XD4-SPIONs) and the A oligomer-specific

scFv-AbW20 coupled to superparamagnetic iron oxide NPs (SPIONs) has shown some encouraging results (Liu et al., 2020a). Outstanding early diagnostic potential for AD was found in superparamagnetic iron oxide NPs when they were associated with an A-oligomer-specific antibody and a category A scavenger receptor activator (Liu et al., 2020b).

Receptor-based targeted treatment of Alzheimer's disease

Through a process known as receptor-mediated transcytosis, macromolecular ligands such as proteins (plasma proteins), hormones, enzymes, and growth factors are transported to the brain. This process begins with the ligand binding to a specific trans-membrane receptor; next, the membrane invaginates, and the receptor-ligand complex forms a vesicle that is transported across the endothelial barrier; finally, the vesicle dissociates In the case of drug carriers, targeting ligands are first linked to the surface of the carrier so that they may bind to the receptors, and only after this step can the medication be released into the intended target region. For the treatment of AD, researchers have investigated a number of receptors, including transferrin lactoferrin, insulin, low density lipoproteins, and toll-like receptors, in the hopes of delivering the drug moiety to the target region in the brain while avoiding the BBB (Wong et al., 2019).

The brain's capillary endothelial cells contain low-density lipoprotein (LDL) receptors and LDL receptor related protein receptor 1 (LRP1), which may accept or bind a variety of ligands for signaling and scavenging. They are therefore appropriate for the targeted delivery of drugs to the brain. LRP1 is likewise an APOE and APP receptor (Holtzman et al., 2012).

Lactoferrin is an iron-binding glycoprotein and a member of the transferrin family. Both neurons and brain endothelial cells have been found to have high levels of lactoferrin receptor expression. Therefore, lactoferrin receptors may be targeted by employing lactoferrin ligands to deliver medications to the brain in order to treat AD. Transferrin receptors are found in high concentrations in the endothelium of brain capillaries. It is possible to circumvent the BBB when it comes to the delivery of medications for AD by conjugating the drug delivery system with ligands that target the transferrin receptor. In a similar manner, substantial amounts of insulin receptors have been discovered on the cell surface of brain vascular endothelial cells. When compared to transferrin receptors, insulin receptors are substantially more successful in crossing the BBB, which means that targeting insulin receptors could more effectively carry therapeutic molecules into the brain (Wong et al., 2019).

Combinatorial nanomedicines in the management of Alzheimer's disease

In view of the failure of treatments aimed at a single target, it would seem that multi-target combination therapies, which include the simultaneous administration of a number of drugs, offer the most potential for treating AD. It has been shown that nanomaterials are capable of delivering many drugs (such as chemical compounds, genes, peptides, and antibodies) all at once, suggesting that they may have a future use in the treatment of AD. There have been some really ground-breaking advances made in the treatment of AD as well as in its diagnosis because to nanomaterials (Chopra et al., 2022).

For instance, in the Chinese patent CN110559454B (2022), CRT (cathode ray tube) targeting peptides and QSH (quadrupole superparamagnetic ferrite) are used to modify a medicine-carrying nano micelle. This nano micelle is used to transport a medication that contains an anti-amyloid protein and superparamagnetic ferrite, and it is intended to treat AD. The nano composite medicine incorporates both the diagnosis and treatment of AD as well as image tracing using MRI technology. The invention combines a QSH targeting peptide and a CRT targeting peptide in order to enable drug-loaded nano-micelles to pass across the BBB by targeting both AD protein and transferrin. This is accomplished by combining the QSH targeting peptide and the CRT targeting peptide. By concurrently focusing on AD protein and transferrin, it is possible to boost the concentration of a medicine at a specified spot while also extending the amount of time it takes for the drug to have its effect (Patents, 2022a).

The invention protected by patent CN110507830A centers on a particular kind of nano-probe and the process of producing it for the purpose of detecting AD pathogenic protein (CN110507830A, 2022). In order to create the multi-modal nano-probe that is the subject of the present invention, a polyethyleneglycol derivative and a phenothiazine derivative are used as key building blocks. An extra-small ferrite nanometer particle is located in the center of the nano-probe, and the nano-outside probe's layer is composed of a polyethylene glycol segment that is coupled with the phenothiazine derivative. In addition to its one-of-a-kind impact of improving the contrast of near-infrared fluorescent labels and its effect of improving the contrast of T1–T2 nuclear magnetic resonance images, the multi-modal nano-probe may be particularly useful when used in conjunction with beta-amyloid protein patches. The probe has a high application potential in the early detection of AD, in addition to its small size, great biocompatibility, radiation-free features, and a range of without any neurotoxicity (Patents, 2022b).

Gene therapy

Recently, gene therapy for AD has received a lot of interest. A gene that expresses an enzyme or growth factor was included into the medication as a generic option. The fundamental objective of this strategy is to maintain the therapeutic expression levels of chosen genes over the long term. Altering or activating certain proteins that are involved in the pathological process of neurodegenerative illness is one way to achieve neuroprotection and neurorestoration. These two goals can be accomplished simultaneously. When it comes to the treatment of neurodegenerative diseases, gene therapy is an exceedingly complex process that involves a number of variables, including the specificity of time and place, the regulation of genes, the transport of genes, and more (Sudhakar and Richardson, 2019). The target illness dictates whether an integrating or non-integrating form of gene transfer is used, and whether *in vivo* or *ex vivo* therapy is administered for treatment (genetic disease vs. complex acquired ailment). To a large extent, this is achieved by the enhancement of the gene, the inhibition of the gene, and editing of the genome (Soofiyani et al., 2013). Additionally, there are small, single-stranded antisense oligonucleotides that connect with RNA messengers to prevent a particular gene from being translated (also known as AS-Ons). The antisense oligonucleotides known as IONIS MAPTRx, which are intended to restrict the synthesis of tau, have been in clinical studies with the intention of serving as a novel technique to reduce tau production in the brain, as has been known for some time (Jadhav et al., 2019).

Conclusion and future prospective

Improving the delivery of drugs, therapeutic proteins, and antiamyloids across the BBB is one of the applications of nanotechnology that can be found in treating AD. Bioimaging and proteomics advancements are potential uses of nanotechnology in treating AD. The potential for chronic toxicity needs to be further investigated for potential clinical applications, notwithstanding the recent developments in using nanotechnology for AD treatment. The future of nanomedicines utilized in AD seems bright. We recommend that the existing procedures be revised in order to take into account the aspects that have been ignored at the nano–bio interface. This will help to reduce the likelihood that the results will be misinterpreted in the future. It is also advised that multifunctional NPs with many therapeutic capabilities be used (for example, providing a range of therapeutic moieties to regulate inflammation, oxidative stress tau phosphorylation, and mitochondrial dysfunctionality). Furthermore, the difficulties of producing reproducible NPs on a big scale must be addressed. Given the present medications' major targets of tau proteins, neuroinflammation, and Aβ proteins, there is an urgent need to create treatments with novel targets that may not only cure symptoms but also prevent disease development at an early stage, eventually leading to a higher quality of life.

Author contributions

YC and RZ had full access to all the data in the study and administrative support and the design. YC and RZ: Study concept and detailed design, and draft preparation; YC and RZ: Data collecting, interpretation, and critical revision of the manuscript for important intellectual content. All authors have read and approved the final version of the manuscript.

Conflict of interest

The authors declare that the research was conducted in the absence of any commercial or financial relationships that could be construed as a potential conflict of interest.

Publisher's note

All claims expressed in this article are solely those of the authors and do not necessarily represent those of their affiliated organizations, or those of the publisher, the editors and the reviewers. Any product that may be evaluated in this article, or claim that may be made by its manufacturer, is not guaranteed or endorsed by the publisher.

References

Abbott, N. J., Patabendige, A. A., Dolman, D. E., Yusof, S. R., and Begley, D. J. (2010). Structure and function of the blood–brain barrier. *Neurobiol. Dis.* 37 (1), 13–25. doi:10.1016/j.nbd.2009.07.030

Abulfadl, Y., El-Maraghy, N., Ahmed, A. E., Nofal, S., Abdel-Mottaleb, Y., and Badary, O. A. (2018). Thymoquinone alleviates the experimentally induced Alzheimer's disease inflammation by modulation of TLRs signaling. *Hum. Exp. Toxicol.* 37 (10), 1092–1104. doi:10.1177/0960327118755256

Aderibigbe, B. A., and Naki, T. (2018). Design and efficacy of nanogels formulations for intranasal administration. *Molecules* 23 (6), 1241. doi:10.3390/molecules23061241

Agyare, E. K., Curran, G. L., Ramakrishnan, M., Yu, C. C., Poduslo, J. F., and Kandimalla, K. K. (2008). Development of a smart nano-vehicle to target cerebrovascular amyloid deposits and brain parenchymal plaques observed in Alzheimer's disease and cerebral amyloid angiopathy. *Pharm. Res.* 25 (11), 2674–2684. doi:10.1007/s11095-008-9688-y

Alahmari, A. (2021). Blood-brain barrier overview: Structural and functional correlation. *Neural Plast.* 2021, 1–10. doi:10.1155/2021/6564585

Aliev, G., Ashraf, G. M., Tarasov, V. V., Chubarev, V. N., Leszek, J., Gasiorowski, K., et al. (2019). Alzheimer's disease–future therapy based on dendrimers. *Curr. Neuropharmacol.* 17 (3), 288–294. doi:10.2174/1570159x16666180918164623

Ariful Islam, M., Park, T-E., Reesor, E., Cherukula, K., Hasan, A., Firdous, J., et al. (2015). Mucoadhesive chitosan derivatives as novel drug carriers. *Curr. Pharm. Des.* 21 (29), 4285–4309. doi:10.2174/1381612821666150901103819

Arora, S., Layek, B., and Singh, J. (2020). Design and validation of liposomal ApoE2 gene delivery system to evade blood–brain barrier for effective treatment of Alzheimer's disease. *Mol. Pharm.* 18 (2), 714–725. doi:10.1021/acs.molpharmaceut.0c00461

Ashrafi, H., Azadi, A., Mohammadi-Samani, S., and Hamidi, M. (2020). New candidate delivery system for Alzheimer's disease: Deferoxamine nanogels. *Biointerface Res. Appl. Chem.* 10 (6), 7106–7119.

Association, As. (2015). 2015 Alzheimer's disease facts and figures. *Alzheimer's. &amp. Dement.* 11 (3), 332–384. doi:10.1016/j.jalz.2015.02.003

Association, As. FDA-approved treatments for Alzheimer's. 2013.

Auría-Soro, C., Nesma, T., Juanes-Velasco, P., Landeira-Viñuela, A., Fidalgo-Gomez, H., Acebes-Fernandez, V., et al. (2019). Interactions of nanoparticles and biosystems: Microenvironment of nanoparticles and biomolecules in nanomedicine. *Nanomater. (Basel)* 9 (10), 1365. doi:10.3390/nano9101365

Ayodele, T., Rogaeva, E., Kurup, J. T., Beecham, G., and Reitz, C. (2021). Early-onset alzheimer's disease: What is missing in research? *Curr. Neurol. Neurosci. Rep.* 21 (2), 4. doi:10.1007/s11910-020-01090-y

Azizi, M., Pasbakhsh, P., Nadji, S. A., Pourabdollah, M., Mokhtari, T., Sadr, M., et al. (2018). Therapeutic effect of perinatal exogenous melatonin on behavioral and histopathological changes and antioxidative enzymes in neonate mouse model of cortical malformation. *Int. J. Dev. Neurosci.* 68, 1–9. doi:10.1016/j.ijdevneu.2018.03.008

Carradori, D., Balducci, C., Re, F., Brambilla, D., Le Droumaguet, B., Flores, O., et al. (2018). Antibody-functionalized polymer nanoparticle leading to memory recovery in Alzheimer's disease-like transgenic mouse model. *Nanomedicine Nanotechnol. Biol. Med.* 14 (2), 609–618. doi:10.1016/j.nano.2017.12.006

Chen, L., Huang, Y., Yu, X., Lu, J., Jia, W., Song, J., et al. (2021). Corynoxine protects dopaminergic neurons through inducing autophagy and diminishing neuroinflammation in rotenone-induced animal models of Parkinson's disease. *Front. Pharmacol.* 12, 642900. doi:10.3389/fphar.2021.642900

Chopra, H., Bibi, S., Singh, I., Kamal, M. A., Islam, F., Alhumaydhi, F. A., et al. (2022). Nanomedicines in the management of alzheimer's disease: Current view and future prospects. *Front. Aging Neurosci.* 14, 879114. doi:10.3389/fnagi.2022.879114

Dabbagh, F., Schroten, H., and Schwerk, C. (2022). *In vitro* models of the blood–cerebrospinal fluid barrier and their applications in the development and research of (Neuro)Pharmaceuticals. *Pharmaceutics* 14 (8), 1729. doi:10.3390/pharmaceutics14081729

Duan, C., Deng, H., Xiao, S., Xie, J., Li, H., Zhao, X., et al. (2022). Accelerate gas diffusion-weighted MRI for lung morphometry with deep learning. *Eur. Radiol.* 32 (1), 702–713. doi:10.1007/s00330-021-08126-y

Duskey, J. T., Belletti, D., Pederzoli, F., Vandelli, M. A., Forni, F., Ruozi, B., et al. (2017). Current strategies for the delivery of therapeutic proteins and enzymes to treat brain disorders. *Int. Rev. Neurobiol.* 137, 1–28. doi:10.1016/bs.irn.2017.08.006

Gao, J., Chen, X., Ma, T., He, B., Li, P., Zhao, Y., et al. (2020). <p>PEG-Ceramide nanomicelles induce autophagy and degrade tau proteins in N2a cells</p>. *Int. J. Nanomedicine* 15, 6779–6789. doi:10.2147/ijn.s258311

Gao, K., and Jiang, X. (2006). Influence of particle size on transport of methotrexate across blood brain barrier by polysorbate 80-coated polybutylcyanoacrylate nanoparticles. *Int. J. Pharm.* 310 (1-2), 213–219. doi:10.1016/j.ijpharm.2005.11.040

Gaudreault, R., and Mousseau, N. (2019). Mitigating alzheimer's disease with natural polyphenols: A review. *Curr. Alzheimer Res.* 16 (6), 529–543. doi:10.2174/1567205016666190315093520

Goedert, M. (2015). NEURODEGENERATION. Alzheimer's and Parkinson's diseases: The prion concept in relation to assembled Aβ, tau, and α-synuclein. *Science* 349 (6248), 1255555. doi:10.1126/science.1255555

Gothwal, A., Kumar, H., Nakhate, K. T., Ajazuddin, Dutta, A., Borah, A., et al. (2019). Lactoferrin coupled lower generation PAMAM dendrimers for brain targeted delivery of memantine in aluminum-chloride-induced Alzheimer's disease in mice. *Bioconjug. Chem.* 30 (10), 2573–2583. doi:10.1021/acs.bioconjchem.9b00505

Y. Guo, S. Liu, Y. Zhang, and X. Guo (Editors) (2020). "Indian journal of pharmaceutical sciences," *Low noise engineering cost budget model considering the health status of patients with neuroweakness* (SANTA CRUZ EAST, MUMBAI, 00000, INDIA: INDIAN PHARMACEUTICAL ASSOC KALINA).

Hagl, S., Kocher, A., Schiborr, C., Kolesova, N., Frank, J., and Eckert, G. P. (2015). Curcumin micelles improve mitochondrial function in neuronal PC12 cells and brains of NMRI mice–Impact on bioavailability. *Neurochem. Int.* 89, 234–242. doi:10.1016/j.neuint.2015.07.026

He, X., Zhu, Y., Yang, L., Wang, Z., Wang, Z., Feng, J., et al. (2021). Embryonic stem cell pluripotency: MgFe-LDH nanoparticles: A promising leukemia inhibitory factor replacement for self-renewal and pluripotency maintenance in cultured mouse embryonic stem cells (adv. Sci. 9/2021). *Adv. Sci. (Weinh).* 8 (9), 2170049. doi:10.1002/advs.202170049

Holtzman, D. M., Herz, J., and Bu, G. (2012). Apolipoprotein E and apolipoprotein E receptors: Normal biology and roles in alzheimer disease. *Cold Spring Harb. Perspect. Med.* 2 (3), a006312. doi:10.1101/cshperspect.a006312

Hoskin, J. L., Sabbagh, M. N., Al-Hasan, Y., and Decourt, B. (2019). Tau immunotherapies for Alzheimer's disease. *Expert Opin. investigational drugs* 28 (6), 545–554. doi:10.1080/13543784.2019.1619694

Huang, F., Wang, J., Qu, A., Shen, L., Liu, J., Liu, J., et al. (2014). Maintenance of amyloid β peptide homeostasis by artificial chaperones based on mixed-shell polymeric micelles. *Angew. Chem. Int. Ed.* 53 (34), 8985–8990. doi:10.1002/anie.201400735

Huo, X., Zhang, Y., Jin, X., Li, Y., and Zhang, L. (2019). A novel synthesis of selenium nanoparticles encapsulated PLGA nanospheres with curcumin molecules for the inhibition of amyloid β aggregation in Alzheimer's disease. *J. Photochem. Photobiol. B Biol.* 190, 98–102. doi:10.1016/j.jphotobiol.2018.11.008

Hyman, B. T., Phelps, C. H., Beach, T. G., Bigio, E. H., Cairns, N. J., Carrillo, M. C., et al. (2012). National Institute on Aging-Alzheimer's Association guidelines for the neuropathologic assessment of Alzheimer's disease. *Alzheimer's. &amp. Dement.* 8 (1), 1–13. doi:10.1016/j.jalz.2011.10.007

Igartúa, D. E., Martinez, C. S., del, V., Alonso, S., and Prieto, M. J. (2020). Combined therapy for alzheimer's disease: Tacrine and PAMAM dendrimers co-administration reduces the side effects of the drug without modifying its activity. *AAPS PharmSciTech* 21 (3), 110–114. doi:10.1208/s12249-020-01652-w

Igartúa, D. E., Martinez, C. S., Temprana, C. F., Alonso, SdV., and Prieto, M. J. (2018). PAMAM dendrimers as a carbamazepine delivery system for neurodegenerative diseases: A biophysical and nanotoxicological characterization. *Int. J. Pharm.* 544 (1), 191–202. doi:10.1016/j.ijpharm.2018.04.032

Ikeda, K., Okada, T., Sawada, S., Akiyoshi, K., and Matsuzaki, K. (2006). Inhibition of the formation of amyloid beta-protein fibrils using biocompatible nanogels as artificial chaperones. *FEBS Lett.* 580 (28-29), 6587–6595. doi:10.1016/j.febslet.2006.11.009

Jadhav, S., Avila, J., Schöll, M., Kovacs, G. G., Kövari, E., Skrabana, R., et al. (2019). A walk through tau therapeutic strategies. *acta neuropathol. Commun.* 7 (1), 22–31. doi:10.1186/s40478-019-0664-z

Javidi, S., Razavi, B. M., and Hosseinzadeh, H. (2016). A review of neuropharmacology effects of Nigella sativa and its main component, thymoquinone. *Phytother. Res.* 30 (8), 1219–1229. doi:10.1002/ptr.5634

Jin, H-Y., and Wang, Z-A. (2016). Boundedness, blowup and critical mass phenomenon in competing chemotaxis. *J. Differ. Equations* 260 (1), 162–196. doi:10.1016/j.jde.2015.08.040

Khan, I., Saeed, K., and Khan, I. (2019). Nanoparticles: Properties, applications and toxicities. *Arabian J. Chem.* 12 (7), 908–931. doi:10.1016/j.arabjc.2017.05.011

Kong, L., Li, X., Ni, Y., Xiao, H., Yao, Y., Wang, Y., et al. (2020). <p>Transferrin-Modified osthole PEGylated liposomes travel the blood-brain barrier and mitigate alzheimer's disease-related pathology in APP/PS-1 mice</p>. *Int. J. Nanomedicine* 15, 2841–2858. doi:10.2147/ijn.s239608

Kritsilis, M. S., Koutsoudaki, P. N., Evangelou, K., Gorgoulis, V. G., and Papadopoulos, D. (2018). Ageing, cellular senescence and neurodegenerative disease. *Int. J. Mol. Sci.* 19 (10), 2937. doi:10.3390/ijms19102937

Lajoie, J. M., and Shusta, E. V. (2015). Targeting receptor-mediated transport for delivery of biologics across the blood-brain barrier. *Annu. Rev. Pharmacol. Toxicol.* 55, 613–631. doi:10.1146/annurev-pharmtox-010814-124852

Li, Y., Yao, C-F., Xu, F-J., Qu, Y-Y., Li, J-T., Lin, Y., et al. (2019). APC/CCDH1 synchronizes ribose-5-phosphate levels and DNA synthesis to cell cycle progression. *Nat. Commun.* 10 (1), 2502–2516. doi:10.1038/s41467-019-10375-x

Ling, T. S., Chandrasegaran, S., Xuan, L. Z., Suan, T. L., Elaine, E., Nathan, D. V., et al. (2021). The potential benefits of nanotechnology in treating Alzheimer's disease. *Biomed. Res. Int.* 2021, 1–9. doi:10.1155/2021/5550938

Liu, X., Zhang, L., Lu, S., Liu, D., Huang, Y., Zhu, J., et al. (2020). Superparamagnetic iron oxide nanoparticles conjugated with Aβ oligomer-specific scFv antibody and class A scavenger receptor activator show therapeutic potentials for Alzheimer's Disease. *J. Nanobiotechnology* 18 (1), 160–213. doi:10.1186/s12951-020-00723-1

Liu, X-G., Zhang, L., Lu, S., Liu, D-Q., Zhang, L-X., Yu, X-L., et al. (2020). <p>Multifunctional superparamagnetic iron oxide nanoparticles conjugated with Aβ oligomer-specific scFv antibody and class A scavenger receptor activator show early diagnostic potentials for alzheimer's disease</p>. *Int. J. Nanomedicine* 15, 4919–4932. doi:10.2147/ijn.s240953

Loureiro, J. A., Crespo, R., Börner, H., Martins, P. M., Rocha, F. A., Coelho, M., et al. (2014). Fluorinated beta-sheet breaker peptides. *J. Mat. Chem. B* 2 (16), 2259–2264. doi:10.1039/c3tb21483d

Meenambal, R., and Bharath, M. S. (2020). Nanocarriers for effective nutraceutical delivery to the brain. *Neurochem. Int.* 140, 104851. doi:10.1016/j.neuint.2020.104851

Meng, Q., Wang, A., Hua, H., Jiang, Y., Wang, Y., Mu, H., et al. (2018). Intranasal delivery of Huperzine A to the brain using lactoferrin-conjugated N-trimethylated chitosan surface-modified PLGA nanoparticles for treatment of Alzheimer’s disease. *Int. J. Nanomedicine* 13, 705–718. doi:10.2147/ijn.s151474

Mirzaie, Z., Ansari, M., Kordestani, S. S., Rezaei, M. H., and Mozafari, M. (2019). Preparation and characterization of curcumin-loaded polymeric nanomicelles to interference with amyloidogenesis through glycation method. *Biotechnol. Appl. Biochem.* 66 (4), 537–544. doi:10.1002/bab.1751

Moon, D. W., Park, Y. H., Lee, S. Y., Lim, H., Kwak, S., Kim, M. S., et al. (2020). Multiplex protein imaging with secondary ion mass spectrometry using metal oxide nanoparticle-conjugated antibodies. *ACS Appl. Mat. Interfaces* 12 (15), 18056–18064. doi:10.1021/acsami.9b21800

Mrak, R. E., and Griffin, W. S. T. (2005). Potential inflammatory biomarkers in Alzheimer's disease. *J. Alzheimer's Dis.* 8 (4), 369–375. doi:10.3233/jad-2005-8406

Mulvihill, J. J., Cunnane, E. M., Ross, A. M., Duskey, J. T., Tosi, G., and Grabrucker, A. M. (2020). Drug delivery across the blood–brain barrier: Recent advances in the use of nanocarriers. *Nanomedicine* 15 (2), 205–214. doi:10.2217/nnm-2019-0367

Mura, S., and Couvreur, P. (2012). Nanotheranostics for personalized medicine. *Adv. drug Deliv. Rev.* 64 (13), 1394–1416. doi:10.1016/j.addr.2012.06.006

Muthukumaran, K., Kanwar, A., Vegh, C., Marginean, A., Elliott, A., Guilbeault, N., et al. (2018). Ubisol-Q 10 (a nanomicellar water-soluble formulation of CoQ 10) treatment inhibits Alzheimer-type behavioral and pathological symptoms in a double transgenic mouse (TgAPEswe, PSEN1dE9) model of Alzheimer's disease. *J. Alzheimer's Dis.* 61 (1), 221–236. doi:10.3233/jad-170275

Neamtu, I., Rusu, A. G., Diaconu, A., Nita, L. E., and Chiriac, A. P. (2017). Basic concepts and recent advances in nanogels as carriers for medical applications. *Drug Deliv.* 24 (1), 539–557. doi:10.1080/10717544.2016.1276232

Nehls, M. (2016). Unified theory of alzheimer's disease (UTAD): Implications for prevention and curative therapy. *J. Mol. Psychiatry* 4 (1), 3–52. doi:10.1186/s40303-016-0018-8

Noble, G. T., Stefanick, J. F., Ashley, J. D., Kiziltepe, T., and Bilgicer, B. (2014). Ligand-targeted liposome design: Challenges and fundamental considerations. *Trends Biotechnol.* 32 (1), 32–45. doi:10.1016/j.tibtech.2013.09.007

Oliver, D., and Reddy, P. H. (2019). Molecular basis of alzheimer's disease: Focus on mitochondria. *J. Alzheimer's Dis.* 72, S95–S116. doi:10.3233/jad-190048

Pacheco-Quinto, J., de Turco, E. B. R., DeRosa, S., Howard, A., Cruz-Sanchez, F., Sambamurti, K., et al. (2006). Hyperhomocysteinemic Alzheimer's mouse model of amyloidosis shows increased brain amyloid β peptide levels. *Neurobiol. Dis.* 22 (3), 651–656. doi:10.1016/j.nbd.2006.01.005

Patents (2022). *A kind of nano-probe and its preparation for alzheimer disease pathogenic protein – google patents*. [Internet]. Available from: https://patents.google.com/patent/CN110507830A/en?q=alzheimer+disease+nano&oq=alzheimer+disease+nano.

Patents (2022). *Nano composite medicine for diagnosing and treating alzheimer's disease – google patents*. [Internet]. Available from: https://patents.google.com/patent/CN110559454B/en?q=alzheimer+disease+nano&oq=alzheimer+disease+nano.

Pathan, S. A., Iqbal, Z., Zaidi, S., Talegaonkar, S., Vohra, D., Jain, G. K., et al. (2009). CNS drug delivery systems: Novel approaches. *Recent Pat. Drug Deliv. Formul.* 3 (1), 71–89. doi:10.2174/187221109787158355

Patra, J. K., Das, G., Fraceto, L. F., Campos, E. V. R., Rodriguez-Torres, MdP., Acosta-Torres, L. S., et al. (2018). Nano based drug delivery systems: Recent developments and future prospects. *J. Nanobiotechnology* 16 (1), 71. doi:10.1186/s12951-018-0392-8

Picone, P., Sabatino, M. A., Ditta, L. A., Amato, A., San Biagio, P. L., Mulè, F., et al. (2018). Nose-to-brain delivery of insulin enhanced by a nanogel carrier. *J. Control. release* 270, 23–36. doi:10.1016/j.jconrel.2017.11.040

Rajeshkumar, S., Ganesh, L., and Santhoshkumar, J. (2019). Selenium nanoparticles as therapeutic agents in neurodegenerative diseases. *Nanobiotechnology Neurodegener. Dis.* 8, 209–224. doi:10.1007/978-3-030-30930-5

Reddy, P. H., Manczak, M., Yin, X., Grady, M. C., Mitchell, A., Tonk, S., et al. (2018). Protective effects of Indian spice curcumin against amyloid-β in Alzheimer's disease. *J. Alzheimers Dis.* 61 (3), 843–866. doi:10.3233/jad-170512

Sabbagh, M. N. (2020). *Alzheimer's disease drug development pipeline 2020*. Germany: Springer, 66–67.

Sagare, A. P., Bell, R. D., and Zlokovic, B. V. (2012). Neurovascular dysfunction and faulty amyloid β-peptide clearance in Alzheimer disease. *Cold Spring Harb. Perspect. Med.* 2 (10), a011452. doi:10.1101/cshperspect.a011452

Sánchez-López, E., Ettcheto, M., Egea, M. A., Espina, M., Cano, A., Calpena, A. C., et al. (2018). Memantine loaded PLGA PEGylated nanoparticles for alzheimer's disease: *In vitro* and *in vivo* characterization. *J. Nanobiotechnology* 16 (1), 32–16. doi:10.1186/s12951-018-0356-z

Schlegel, P., Novotny, M., Klimova, B., and Valis, M. (2019). Muscle-gut-brain axis": Can physical activity help patients with alzheimer's disease due to microbiome modulation? *J. Alzheimer's Dis.* 71 (3), 861–878. doi:10.3233/jad-190460

Sempf, K., Arrey, T., Gelperina, S., Schorge, T., Meyer, B., Karas, M., et al. (2013). Adsorption of plasma proteins on uncoated PLGA nanoparticles. *Eur. J. Pharm. Biopharm.* 85 (1), 53–60. doi:10.1016/j.ejpb.2012.11.030

Serafín, V., Razzino, C. A., Gamella, M., Pedrero, M., Povedano, E., Montero-Calle, A., et al. (2021). Disposable immunoplatforms for the simultaneous determination of biomarkers for neurodegenerative disorders using poly (amidoamine) dendrimer/gold nanoparticle nanocomposite. *Anal. Bioanal. Chem.* 413 (3), 799–811. doi:10.1007/s00216-020-02724-3

Sharifi-Rad, J., Rayess, Y. E., Rizk, A. A., Sadaka, C., Zgheib, R., Zam, W., et al. (2020). Turmeric and its major compound curcumin on health: Bioactive effects and safety profiles for Food, pharmaceutical, biotechnological and medicinal applications. *Front. Pharmacol.* 11, 01021. doi:10.3389/fphar.2020.01021

Sharifzad, F., Yasavoli-Sharahi, H., Mardpour, S., Fakharian, E., Nikuinejad, H., Heydari, Y., et al. (2019). Neuropathological and genomic characterization of glioblastoma-induced rat model: How similar is it to humans for targeted therapy? *J. Cell. Physiol.* 234 (12), 22493–22504. doi:10.1002/jcp.28813

Sood, S., Jain, K., and Gowthamarajan, K. (2014). Intranasal therapeutic strategies for management of Alzheimer's disease. *J. drug Target.* 22 (4), 279–294. doi:10.3109/1061186x.2013.876644

Soofiyani, S. R., Baradaran, B., Lotfipour, F., Kazemi, T., and Mohammadnejad, L. (2013). Gene therapy, early promises, subsequent problems, and recent breakthroughs. *Adv. Pharm. Bull.* 3 (2), 249–255. doi:10.5681/apb.2013.041

Spuch, C., and Navarro, C. (2011). Liposomes for targeted delivery of active agents against neurodegenerative diseases (Alzheimer's disease and Parkinson's disease). *J. drug Deliv.* 2011, 1–12. doi:10.1155/2011/469679

Sudhakar, V., and Richardson, R. M. (2019). Gene therapy for neurodegenerative diseases. *Neurotherapeutics* 16 (1), 166–175. doi:10.1007/s13311-018-00694-0

Sun, Y., Ma, C., Sun, H., Wang, H., Peng, W., Zhou, Z., et al. (2020). Metabolism: A novel shared link between diabetes mellitus and alzheimer's disease. *J. diabetes Res.* 2020, 1–12. doi:10.1155/2020/4981814

Suri, K., Wolfram, J., Shen, H., and Ferrari, M. (2015). "Novel approaches and strategies for biologics, vaccines and cancer therapies: Elsevier," in *Advances in nanotechnology-based drug delivery platforms and novel drug delivery systems* (Netherlands: Elsevier), 41–58.

Szwed, A., and Miłowska, K. (2012). The role of proteins in neurodegenerative disease. *Postepy Hig. Med. Dosw.* 66, 187–195. doi:10.5604/17322693.991446

Tığlı Aydın, R. S., Kaynak, G., and Gümüşderelioğlu, M. (2016). Salinomycin encapsulated nanoparticles as a targeting vehicle for glioblastoma cells. *J. Biomed. Mat. Res. A* 104 (2), 455–464. doi:10.1002/jbm.a.35591

Valenzuela, P. L., Castillo-Garcia, A., Morales, J. S., de la Villa, P., Hampel, H., Emanuele, E., et al. (2020). Exercise benefits on Alzheimer's disease: State-of-the-science. *Ageing Res. Rev.* 62, 101108. doi:10.1016/j.arr.2020.101108

Vilella, A., Belletti, D., Sauer, A. K., Hagmeyer, S., Sarowar, T., Masoni, M., et al. (2018). Reduced plaque size and inflammation in the APP23 mouse model for Alzheimer's disease after chronic application of polymeric nanoparticles for CNS targeted zinc delivery. *J. Trace Elem. Med. Biol.* 49, 210–221. doi:10.1016/j.jtemb.2017.12.006

Wais, U., Jackson, A. W., He, T., and Zhang, H. (2016). Nanoformulation and encapsulation approaches for poorly water-soluble drug nanoparticles. *Nanoscale* 8 (4), 1746–1769. doi:10.1039/c5nr07161e

Wang, D., Zhao, R., Qu, Y-Y., Mei, X-Y., Zhang, X., Zhou, Q., et al. (2018). Colonic lysine homocysteinylation induced by high-fat diet suppresses DNA damage repair. *Cell Rep.* 25 (2), 398–412.e6. e6. doi:10.1016/j.celrep.2018.09.022

Wilczewska, A. Z., Niemirowicz, K., Markiewicz, K. H., and Car, H. (2012). Nanoparticles as drug delivery systems. *Pharmacol. Rep.* 64 (5), 1020–1037. doi:10.1016/s1734-1140(12)70901-5

Wong, K. H., Riaz, M. K., Xie, Y., Zhang, X., Liu, Q., Chen, H., et al. (2019). Review of current strategies for delivering Alzheimer's disease drugs across the blood-brain barrier. *Int. J. Mol. Sci.* 20 (2), 381. doi:10.3390/ijms20020381

Xu, L., Ding, Y., Ma, F., Chen, Y., Chen, G., Zhu, L., et al. (2022). Engineering a pathological tau-targeted nanochaperone for selective and synergetic inhibition of

tau pathology in Alzheimer's Disease. *Nano Today* 43, 101388. doi:10.1016/j.nantod.2022.101388

Yang, H., Li, X., Zhu, L., Wu, X., Zhang, S., Huang, F., et al. (2019). Heat shock protein inspired nanochaperones restore amyloid-β homeostasis for preventative therapy of Alzheimer's disease. *Adv. Sci. (Weinh).* 6 (22), 1901844. doi:10.1002/advs.201901844

Yang, H., Zeng, F., Luo, Y., Zheng, C., Ran, C., and Yang, J. (2022). Curcumin scaffold as a multifunctional tool for Alzheimer's disease research. *Molecules* 27 (12), 3879. doi:10.3390/molecules27123879

Yang, R., Zheng, Y., Wang, Q., and Zhao, L. (2018). Curcumin-loaded chitosan–bovine serum albumin nanoparticles potentially enhanced Aβ 42 phagocytosis and modulated macrophage polarization in Alzheimer's disease. *Nanoscale Res. Lett.* 13 (1), 330–339. doi:10.1186/s11671-018-2759-z

Yang, W., Liu, W., Li, X., Yan, J., and He, W. (2022). Turning chiral peptides into a racemic supraparticle to induce the self-degradation of MDM2. *J. Adv. Res*. doi:10.1016/j.jare.2022.05.009

Yin, T., Yang, L., Liu, Y., Zhou, X., Sun, J., and Liu, J. (2015). Sialic acid (SA)-modified selenium nanoparticles coated with a high blood–brain barrier permeability peptide-B6 peptide for potential use in Alzheimer's disease. *Acta biomater.* 25, 172–183. doi:10.1016/j.actbio.2015.06.035

Yusuf, M., Khan, M., Alrobaian, M. M., Alghamdi, S. A., Warsi, M. H., Sultana, S., et al. (2021). Brain targeted Polysorbate-80 coated PLGA thymoquinone nanoparticles for the treatment of Alzheimer's disease, with biomechanistic insights. *J. Drug Deliv. Sci. Technol.* 61, 102214. doi:10.1016/j.jddst.2020.102214

Zeng, Q., Bie, B., Guo, Q., Yuan, Y., Han, Q., Han, X., et al. (2020). Hyperpolarized Xe NMR signal advancement by metal-organic framework entrapment in aqueous solution. *Proc. Natl. Acad. Sci. U. S. A.* 117 (30), 17558–17563. doi:10.1073/pnas.2004121117

Zhang, L., Yang, S., Wong, L. R., Xie, H., and Ho, P. C-L. (2020). *In vitro* and *in vivo* comparison of curcumin-encapsulated chitosan-coated poly (lactic-co-glycolic acid) nanoparticles and curcumin/hydroxypropyl-β-Cyclodextrin inclusion complexes administered intranasally as therapeutic strategies for Alzheimer's Disease. *Mol. Pharm.* 17 (11), 4256–4269. doi:10.1021/acs.molpharmaceut.0c00675

frontiers | Frontiers in Molecular Biosciences

TYPE Review
PUBLISHED 04 January 2023
DOI 10.3389/fmolb.2022.1105540

OPEN ACCESS

EDITED BY
Yu Zhao,
Tufts University, United States

REVIEWED BY
Zhongfeng Ye,
Tufts University, United States
Jundong Shao,
Guangzhou Medical University, China
Xiuguo Han,
Xinhua Hospital, School of Medicine, Shanghai Jiao Tong University, China

*CORRESPONDENCE
Shijie Chen,
shijiechencsu@csu.edu.cn

†These authors have contributed equally to this work and share first authorship

SPECIALTY SECTION
This article was submitted to Nanobiotechnology, a section of the journal Frontiers in Molecular Biosciences

RECEIVED 22 November 2022
ACCEPTED 14 December 2022
PUBLISHED 04 January 2023

CITATION
Wang D, Peng Y, Li Y, Kpegah JKSK and Chen S (2023), Multifunctional inorganic biomaterials: New weapons targeting osteosarcoma.
Front. Mol. Biosci. 9:1105540.
doi: 10.3389/fmolb.2022.1105540

Multifunctional inorganic biomaterials: New weapons targeting osteosarcoma

Dong Wang[1†], Yi Peng[1†], Yuezhan Li[1,2†], Julius K. S. K. Kpegah[3] and Shijie Chen[1,4*]

[1]Department of Spine Surgery, The Third Xiangya Hospital of Central South University, Changsha, Hunan, China, [2]College of Medicine, Nursing and Health Science, School of Medicine, Regenerative Medicine Institute (REMEDI), University of Galway, Galway, Ireland, [3]Xiangya School of Medicine, Central South University, Changsha, Hunan, China, [4]Shanghai Key Laboratory of Regulatory Biology, Institute of Biomedical Sciences and School of Life Sciences, East China Normal University, Shanghai, China

Osteosarcoma is the malignant tumor with the highest incidence rate among primary bone tumors and with a high mortality rate. The anti-osteosarcoma materials are the cross field between material science and medicine, having a wide range of application prospects. Among them, biological materials, such as compounds from black phosphorous, magnesium, zinc, copper, silver, etc., becoming highly valued in the biological materials field as well as in orthopedics due to their good biocompatibility, similar mechanical properties with biological bones, good biodegradation effect, and active antibacterial and anti-tumor effects. This article gives a comprehensive review of the research progress of anti-osteosarcoma biomaterials.

KEYWORDS

osteosarcoma, material, black phosphorus, magnesium, zinc, copper, silver

1 Introduction

Osteosarcoma is the malignant tumor with the highest incidence among primary bone tumors (Mirabello et al., 2009; Rojas et al., 2021). It usually occurs in children and adolescents and often occurs in the distal femur, proximal tibia, and proximal humerus (Ritter and Bielack, 2010). For primary osteosarcoma without metastasis, the current clinical methods are surgery such as amputation, combined with radiotherapy and chemotherapy and others, with a high 5-year survival rate reaching 70% (Souhami, 1989; Heng et al., 2020). However, there are still 20% of patients who will have metastasis during treatment, especially prone to lung metastases (Ward et al., 1994; Meazza and Scanagatta, 2016). Once metastasis occurs, such as lung metastasis, the 5-year survival rate may be less than 30% (Tsuchiya et al., 2002). Until recently, extensive radical resection was used as the main treatment for osteosarcoma. More importantly, the continuous emergence of chemotherapy resistance in osteosarcoma further reduces the survival rate of patients, leading to low clinical benefits and poor postoperative quality of life for patients (Li et al., 2015). But, with the development of imaging, the application of angiography and interventional techniques, advances in neoadjuvant chemoradiotherapy

TABLE 1 The Comparison of features of different biomaterials.

Type of material	Anti-tumor effect	Toxicity	Inflammatory response	Bone regeneration capacity	Flaw
Magnesium	Phototherapy and nanoparticle targeting effects	Electrolyte disturbances	Less, depending on the concentration	Excellent	Rapid degradation rate and local hydrogen production
Zinc	nanoparticle targeting effects	Anemia and impaired immune function	Less, depending on the concentration	Good	Poor corrosion resistance
Copper	Photothermal therapy and nano drug delivery system	Liver function lesions and tubular necrosis and nephritis	Less, depending on the concentration	Good	Potential toxicity
Silver	nanoparticle targeting effects	Potential cytotoxicity	Less	General	Complex preparation process
Black phosphorus	Phototherapy and nanoparticle targeting effects	No obvious cytotoxicity	Less	Excellent	Unstable properties and low preparation efficiency
Poly (lactic acid-co-glycolic acid) (PLGA)	nanoparticle targeting effects	No obvious cytotoxicity	More	General	Poor mechanical properties

and surgical techniques as well as rapid progress in immunotherapy, the treatment of osteosarcoma has undergone major changes and limb preservation surgery has an increasing ratio (Ferrari et al., 1997; Muscolo et al., 2005; Wong and Kumta, 2013; Takeuchi et al., 2019; Gill and Gorlick, 2021). Regrettably, to completely remove the tumor, a large number of tissues need to be removed during a limb-preserving surgery, which results in some challenges to the preservation and functional reconstruction of limbs. Therefore, the treatment of primary lesions is very important, especially those osteosarcomas that grow in the pelvis or the spine, which cannot be completely removed due to surgical limitations. Inevitably, there will be residual tumor tissue after surgery. However, the currently used autologous bone, allogeneic bone, and prosthesis only play the role of reconstruction, and cannot eliminate the local residual tumor tissue. Meanwhile, the various physical and chemical inactivation methods commonly used at present, such as neoadjuvant radiotherapy and chemotherapy, may damage the normal tissues while destroying the tumor tissue simultaneously, and these methods have no reconstruction effect. Therefore, finding an ideal material that can not only fill in but also kill the residual tumor cells, reducing the probability of recurrence, and metastasis and thereby promoting bone repair to treat osteosarcoma, has become a hot topic (Marques et al., 2014; Ma et al., 2020; Liao et al., 2021).

For this reason, many kinds of anti-osteosarcoma materials have emerged, and previous studies have mainly focused on the polymer compounds, such as poly (lactic acid-co-glycolic acid) (PLGA) and chitosan, etc., (Ma et al., 2014; He et al., 2022). These polymer compounds often require multiple modifications before they can function as anti-osteosarcoma, and they have no obvious advantages in promoting osteogenesis and mechanical properties (Table 1). For that matter, there's a limitation to the clinical application of these polymers.

But, in recent years, biological materials, such as black phosphorous (BP), magnesium (Mg), zinc (Zn), copper (Cu), silver (Ag), etc., have become more and more valuable in tissue engineering and orthopedics fields due to their good biocompatibility, mechanical properties similar to those of biological bones, biodegradation, antibacterial and anti-tumor effects (Figure 1) (Choi et al., 2018; Ambrosio et al., 2021). For instance, copper, magnesium and other metal ions can inhibit inflammation by promoting the polarization of macrophages from M1 to M2, which is conducive to bone regeneration and repair (Yang et al., 2021c; Diez-Tercero et al., 2021). Of these, the anti-tumor effect of biomaterials is mainly reflected in phototherapy. Phototherapy, as a minimally invasive and high-efficiency anticancer approach, has sparked extensive research interest (Hou et al., 2018). Phototherapy includes photodynamic therapy (PDT) and photothermal therapy (PTT) which have very different therapy mechanisms under the same stimulus. For PTT, a light at a specific wavelength irradiates photothermal agents, which heats up and kills tumor cells; however, in PDT, photosensitizers can produce large amounts of singlet oxygen ($^1O_2$) that can kill tumor cells under specific light exposure. Besides, several studies have found that local hyperthermia can activate heat shock proteins and promote the expression of osteogenesis-related genes, such as RUNX2, and BMP2, through the PI3K/AKT signaling pathway and ERK1/2 signaling pathway (Chen et al., 2015; Sayed et al., 2019; Wang et al., 2022). It can also increase the expression of alkaline phosphatase and promote bone differentiation (Shui and Scutt, 2001; Norgaard et al., 2006).

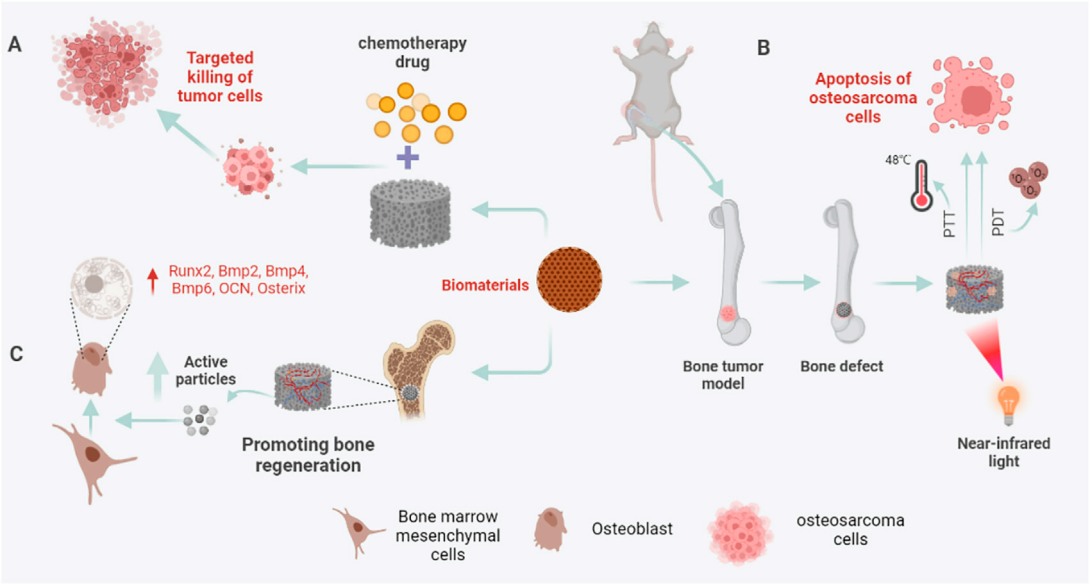

FIGURE 1
Biomaterials in bone reconstruction after osteosarcoma surgery. **(A)** Under near-infrared (NIR) light, biomaterials eliminate residual osteosarcoma cells through PTT and PDT to prevent a recurrence. **(B)** Biomaterials can be used as drug-loaded systems to target residual osteosarcoma cells, release chemotherapeutic drugs, and kill osteosarcoma cells. **(C)** After osteosarcoma resection, the 3D printed biomaterial scaffold can not only play the role of bone support and bone connection but also release some active particles, such as Ag^{+}, Cu^{+}, PO_4^{3-}, etc., to up-regulate the expression of osteogenesis-specific genes and promote bone regeneration.

These make phototherapy, especially PTT, attract the interest of many researchers in the process of bone repair after osteosarcoma surgery. At the same time, nanomaterials, such as nano-silver, BP nanosheets, etc., have shown great advantages in drug loading, tumor imaging, promoting osteogenesis, and anti-tumor properties (Gui et al., 2018; Qing et al., 2020; Ge et al., 2022; Zhu et al., 2022). Nanoparticles (NPs) usually refer to particles with a diameter between 1 nm and 100 nm, which can be used as biocatalysts, infrared absorbing materials, etc. Studies have shown that particles with a diameter of 5.5 nm–100 nm are not easily filtered by the kidney, but when passing through the tumor blood vessels, they can pass through the leaking blood vessels at the tumor, and then accumulate in large quantities in the tumor (Maeda, 2001; Poon et al., 2019). This is known as the enhanced permeability and retention (EPR) effect, which makes nanomaterials excellent for tumor therapy (Wu, 2021). Overall, this review describes recent advances and challenges in biomaterials for osteosarcoma treatment, inspiring future osteosarcoma research.

2 Magnesium, zinc, and their alloy

Mg, Zn, and their alloys exert excellent anti-tumor effects by influencing the metabolism and phenotype of tumor cells, inducing tumor cell proliferation inhibition, cell cycle arrest, and cell apoptosis (Krol et al., 2017; Zhou et al., 2021). Studies by Wu et al. have shown that magnesium-zinc alloy can inhibit the proliferation of osteosarcoma cell line U20S cells by arresting the G2/M phase of the cell cycle, and promote the apoptosis of U20S tumor cells through a mitochondrial-dependent pathway; at the same time, the alloy solution can inhibit the metastasis of U20S tumor cells through the MAPK pathway (Wu et al., 2016).

Moreover, Mg, as an essential trace element in the human body, indirectly affects mineral metabolism through its role in ATP metabolism and as a cofactor for more than 300 enzymes (Palacios, 2006). Therefore, Mg plays a more prominent role in bone tissue engineering by its excellent biocompatibility and biodegradability. Besides, the PTT of mg and the hydrogen generated from its degradation have also received increased attention in tumor therapy. On the ground, Long et al. have designed innovative multifunctional PLGA/Mg porous scaffolds with excellent biodegradability and biocompatibility by low-temperature three-dimensional (3D) printing technology (Long et al., 2021). *In vivo* experiments, Mg particles exhibit excellent photothermal effects for tumor eradication and Mg ions released from PLGA/Mg porous scaffolds could promote bone regeneration, which gives the PLGA/Mg scaffolds dual functions of inhibiting OS recurrence and continuously repairing bone defects. On the other hand, after intra-tumoral injection, Zhou et al. found that micro-scale Mg/PLGA exhibited stronger cytotoxicity, PTT, and anti-tumor effect than nano-scale Mg/

PLGA (Zhou et al., 2021). This inspires the design of Mg scaffolds in the reconstruction of bone defects after osteosarcoma surgery. Besides, Zan et al. designed a magnesium-based biomaterial that can release hydrogen in a controlled manner, giving full play to the anti-tumor effect of Mg (Zan et al., 2022). Then, the generated hydrogen can promote the expression of tumor suppressor gene P53 and activate the mitochondria-related apoptosis pathway. At last, several studies also revealed that Mg can induce the apoptosis of osteosarcoma cells (MG63 and U2-OS cells) by shortening the half-life of Snail1 (Zan et al., 2020). However, although the human toxicity of Mg has been controversial, recent studies have reported that high concentrations of magnesium particles can inhibit osteoblast activity (Wang J. L. et al., 2020). This contradicts the potential osteogenic ability of Mg, which may be related to the concentration of Mg^{2+} in the bone microenvironment. The underlying mechanism is still unclear, and more research is needed to explore the metabolic mechanism of Mg^{2} in the bone microenvironment. In general, the toxicity study of magnesium-containing bone repair materials requires further studies (Table 1).

Nano-zinc biomaterials have also received increased attention in anti-tumor. For instance, He et al. (2018) revealed that zinc ions from ZnO NPs could suppress osteosarcoma cell proliferation by causing S phase arrest. Intercellular Zn ions also can target and damage the mitochondria, which could contribute to excessive reactive oxygen species (ROS) generation to promote apoptosis, which contributes to osteosarcoma cell death. They also found that there is an enhancing autophagosome formation and impaired lysosomal function with an upregulation of the LC3-II/LC3-I ratio after ZnO NPs treatment. Furthermore, there is crosstalk, in which apoptosis inhibition would contribute to autophagy, between apoptosis and autophagy in ZnO NPs-induced human osteosarcoma cell death. In addition, He et al. also revealed firstly an interplay between HIF-1α and the autophagy–Zn^{2+}–reactive oxygen species (ROS)–autophagy cycle axis and confirmed that ZnO NPs could up-regulate HIF-1α in osteosarcoma cells mainly due to the combined effect of Zn^{2+} and ROS (He et al., 2020). Then, the studies *in vivo* experiments have shown that ZnO NPs could inhibit subcutaneous osteosarcoma proliferation with good biosafety by activating HIF-1α, apoptosis, and autophagy. Besides, Zn, like Mg, is mostly stored in the bones and may play a significant role in bone disease and osteogenesis (Palacios, 2006; Huang et al., 2020; Song et al., 2020). Based on this, a zinc-containing hydroxyapatite nanorod that promotes osteogenic differentiation of bone marrow mesenchymal cells in the absence of osteo-inductive factors is engineered (Fernandes et al., 2020). However, scaffolds of Mg, Zn, and their alloys often require a high-temperature fabrication process and are prone to corrosion after being placed in the body, which limits their clinical application (Table 1) (Koons et al., 2020). Therefore, while ensuring the degradability of metals, future research also needs to focus on the corrosion resistance of metallic materials. Additionally, to further exert the role of Zn and Mg biomaterials in bone repair after osteosarcoma surgery, the underlying molecular mechanisms need to be further explored.

3 Copper

As a constituent microelement of the human body and a cofactor for metalloenzymes, Cu plays an important role in human tissue regeneration, hemostasis, antibacterial, and anti-tumor (Harris, 1992; Palacios, 2006; Mendel et al., 2007; Yang J. et al., 2021). Thus, the imbalance of Cu in the internal environment will affect the normal function of tissues and organs, leading to adverse reactions such as anemia, malnutrition, neurodegenerative disease, and osteoporosis (Palacios, 2006; Brewer, 2010). Recently, some studies reported the design of scaffolds with antitumor and bone repair promotion by adding Cu elements (Kargozar et al., 2021; Solak et al., 2021). A new type of metal framework copper tetrakis (4-carboxyphenyl) porphyrin (Cu-TCPP) nanosheet interface structure is combined with β tricalcium phosphate (TCP) to make a Cu-TCPP-TCP scaffold (Dang et al., 2020). On one hand, the Cu-TCPP-TCP scaffold material uses near-infrared (NIR) irradiated light to exhibit photothermal performance, then killing the osteosarcoma cells by releasing heat energy. On the other hand, *in vitro* studies have found that the Cu-TCPP-TCP scaffold stimulates human bone marrow stromal stem cells (hBMSCs) and human umbilical vein endothelial cells (HUVEC), and significantly enhances the expression of osteogenic differentiation-related genes in hBMSCs and differentiation-related genes in vascular endothelial cells. In animal experiments, implanting a Cu-TCPP-TCP scaffold into a rabbit's bone defect site can promote bone regeneration.

In addition, it is worth noting that a nano-Cu-based drug-targeted delivery system will also bring new benefits to osteosarcoma patients (Figure 2). For example, Wang et al. (2016) reported that a smart therapeutic nanoplatform based on CuS@Zeolitic imidazolate framework-8 (ZIF-8) NPs have been developed (Gao et al., 2019). On this basis, they observe for the first time that after the loading of DOX the CuS@ZIF-8 NPs have synergistic chemo- and PTT effects on tumor cells *in vitro*/vivo studies. The low pH-sensitive property of the ZIF-8 framework makes a progress in integrating light/low pH triggered the release and chemo-photothermal therapy into one system which shows superior anticancer effects over the chem- or phototherapy alone. However, the toxicity of Cu limits further applications (Brewer, 2010; Ameh and Sayes, 2019). Several works of literature point out that Cu^{2+} can combine with a variety of organic substances and disrupt the normal homeostasis and physiological processes of the human body. In the body, Cu^{2+} is often accumulated in the liver, affecting

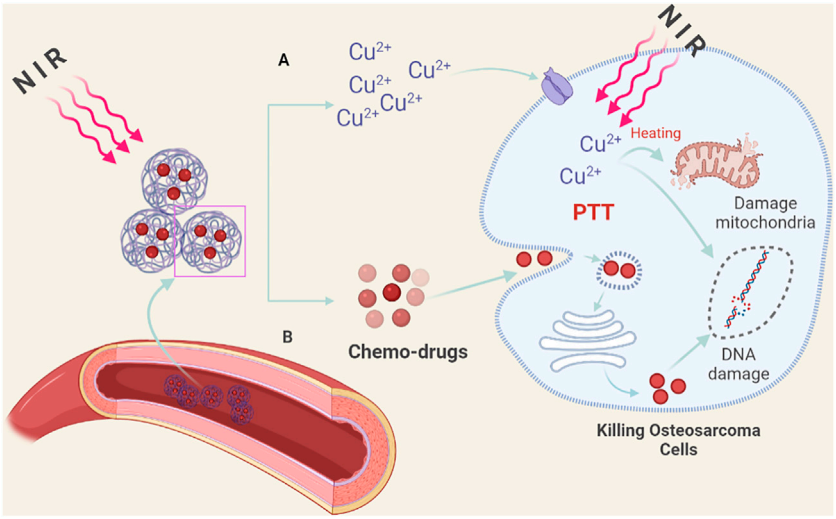

FIGURE 2
Nano-copper-based drug targeted delivery system. **(A)** Under the irradiation of NIR light, the nano-Cu-chemotherapy drug targeted delivery system decomposes and releases Cu^{2+} locally in the tumor, which can destroy the tumor cell membrane structure through PPT, kill tumor cells, and improve the sensitivity of chemotherapeutic drugs. **(B)** Under NIR light, the released chemotherapy drugs target tumor cells, causing DNA damage. At the same time, the damage to normal tissue cells is reduced.

liver metabolism and causing liver function lesions; in the kidney, it can cause tubular necrosis and nephritis (Table 1) (Chen et al., 2006). Based on this, more research is needed to explore the biodegradability or controlled release of Cu^{2+} in bone repair scaffolds.

4 Silver

Ag has been employed for biomedical purposes since ancient times owing to its anti-microbial properties (Xu et al., 2020). And, in the early 19th century, Ag preparations were developed for wound disinfection and burn care, and Ag nitrate was used for wound care and instrument disinfection. Regrettably, in the 1940s, the medical use of Ag gave way to the clinical use of antibiotics. But, with the development of nanotechnology, nano-silver particles (AgNPs) have received special interest due to their excellent antibacterial and antitumor effects. They are also used to promote wound repair and bone healing, as well as vaccine adjuvants, anti-diabetics and biosensors, etc., (Qing et al., 2018). Besides, several studies have also reported the role of Ag nanorods in photoacoustic (PA) imaging of inflammatory tissue, which is worthy of further exploration in the role of osteosarcoma imaging (Mei et al., 2020).

Then, AgNPs have been observed to exhibit good anticancer activities in breast cancer, cervical cancer, colon cancer, ovarian cancer, pancreatic ductal adenocarcinoma, lung cancer, hepatocellular carcinoma, melanoma, osteosarcoma, etc., (Chugh et al., 2018; Xu et al., 2020). And several studies have confirmed that the anticancer activity of AgNPs varies in various sizes, shapes, and doses/concentrations in different cancer cells (Jo et al., 2015; Dziedzic et al., 2016). In general, AgNPs show broad-spectrum anticancer effects through size, dose/concentration, and time-dependent ways. Smaller AgNPs can induce enhanced endocytosis and more significant cytotoxicity and genotoxicity. Compared with other shapes, spherical AgNPs exhibit greater cytotoxicity due to a higher surface-volume ratio. And higher doses of AgNPs generally lead to more apoptosis than lower doses. On the basis, taking advantage of the lack of function of the P53 gene in a variety of tumors, Kovacs et al. proposed a clever idea based on a therapeutic strategy that stimulates the function of P53, prepared Ag nanoparticles, and tested their cytotoxic effect on the osteosarcoma cells (U20S, Saos-2) which lack the function of P53 tumor suppressor gene (Kovacs et al., 2016). The results showed that the mitochondrial structure and function of osteosarcoma cells treated with citric acid-coated AgNPs were disordered, and the apoptosis rate was increased, indicating that the NPs did not depend on the functional state of P53 in killing the osteosarcoma cells. This feature makes AgNPs become another choice for chemotherapy strategies.

Furthermore, Recent research further explores the use of smaller-scale angstrom silver (one-tenth of a nanometer, AgAP) in cancer therapy. On the one hand, Xie et al. announced for the first time the broad-spectrum anti-cancer properties of AgAP and the body's good tolerance (no obvious side effects) to AgAP (Wang Z. X. et al., 2019). It is precise because smaller particles have greater cellular toxicity, Xie et al. speculated that AgAP particles have stronger anti-tumor effects (Jo et al., 2015). And

they independently developed automatic "metal vapor-condensation" equipment based on physical high temperature and pressure gasification methods for the preparation of angstrom material. At the same time, by using fructose to modify AgAP, AgAP stably existing in the solution was obtained. The results of cell and animal experiments show that AgAP injection exhibits killing effects on lung cancer, pancreatic cancer, and other tumors, but has no obvious toxic or side effects on normal tissues. Furthermore, Xie et al. found that fructose-coated angstrom silver (F-AgÅPs; 9.38 nm ± 4.11 nm) can effectively kill a variety of osteosarcoma cell lines and primary osteosarcoma cells (Hu et al., 2020). Compared with cisplatin, one of the first-line drugs for osteosarcoma treatment, F-AgÅPs can more effectively inhibit the growth of osteosarcoma transplanted subcutaneously in nude mice and *situ* osteosarcoma, reduce the damage of *in situ* osteosarcoma to bone and inhibit its metastasis to lung, and has no obvious effect on normal cells and tissues at therapeutic doses. Tissue distribution and metabolism results show that after intravenous injection of F-AgÅPs, Ag presents a high level of accumulation in tumor tissues and is mainly excreted through feces (the excretion rate through feces after one week is about 68% of the injected dose). On the other hand, tumor cells still mainly use glycolysis rather than mitochondrial oxidative phosphorylation to break down glucose and produce ATP (Warburg effect) even under the condition of adequate oxygen supply (Bonnet et al., 2007). Aerobic glycolysis can prevent tumor cells with active oxidative metabolism from producing excessive ROS and protect them from apoptosis caused by ROS (Stacpoole, 2017; Woolbright et al., 2019). Pyruvate dehydrogenase kinase (PDK) is a mitochondrial enzyme that can selectively phosphorylate pyruvate dehydrogenase (PDH) E1α subunit to inactivate it, thereby prompting the cell glucose metabolism to switch from aerobic oxidation to glycolysis. Mechanism studies have shown that F-AgÅPs can activate PDH by inhibiting PDK so that the glucose metabolism state of osteosarcoma cells changes from glycolysis to mitochondrial aerobic oxidation, thereby selectively inducing osteosarcoma cells (rather than normal cells) to generate ROS-mediated apoptosis (Hu et al., 2020).

Moreover, several studies have reported on the creation of nanocomposites that promote bone regeneration (Xu et al., 2020). AgNPs are one of them, exhibiting an excellent ability to promote bone repair. For example, Zhang et al. have uncovered that AgNPs induce proliferation and osteogenic differentiation of MSCs *in vitro*, stimulate callus formation and accelerate the healing of fractured bone in an osteogenic mouse model (C57BL/6 mice) (Zhang R. et al., 2015). Mahmood et al. have confirmed that AgNPs significantly enhanced osteocyte mineralization and differentiation in MC3T3-E1 cells (an *in vitro* model) compared with several other NPs and many genes related to the osteogenesis pathway were expressed in both control cell cultures and those exposed to AgNPs (Qing et al., 2018). However, in response to AgNPs exposure, there was a significant increase in key factors including Bmp4, Bmp6, and Fosl1, associated with osteoclast pathways. At last, they revealed that AgNPs accelerated the differentiation and proliferation of McT3-e1 cells by the differential expression genes (DEGs) and functional analysis. Besides, Han et al. fabricated AgNPs-loaded Gel hydrogels (AgNPs/Gel) by a simple method under sunlight using gelatin as a stabilizing agent which shows an excellent effect on bone regeneration and fracture treatment (Han et al., 2021). These innovative explorations reveal the advantages of AgNP as a multifunctional biomaterial, which may help to solve the problem of large bone defects and recurrence after osteosarcoma surgery.

In addition, Xie et al. also first reported that Carbomer gel loaded with AgAPs (simplified as AgAPs gel) can promote the repair and regeneration of damaged skin by potent sterilization and reducing inflammation (Chen et al., 2020). It has been proved that AgAPs gel can effectively kill a variety of bacteria *in vitro* (including *Pseudomonas aeruginosa*, methicillin-resistant, and methicillin-sensitive *Staphylococcus aureus*), inhibit the bacteria colonization in skin defect sites of diabetic mice, and the large scalded area of the common mice, reduce the inflammation of the wound, and thus accelerate the healing of the wound. The AgAPs r gel of therapeutic dose has no significant effect on the *in vitro* activity of normal skin repair-related cells and the multiple physiological functions and organ tissue structures in mice and the topical application of AgAPs gel for several days did not cause Ag accumulation in other organs in mice. This significant discovery will inspire us to further explore the potential and more meaningful applications, such as bone repair, of AgAPs s in nanomedicine.

However, despite the remarkable effects of AgAPs and AgNPs in anti-inflammatory, anti-tumor, and promoting bone repair, the process requirements and high energy consumption of its fabrication also hinder wide clinical applications (Zhang X. F. et al., 2016). Moreover, due to the natural high affinity of Ag to sulfur, AgAPs and AgNPs can bind proteins or sulfur-containing macromolecules *in vivo*, thereby promoting membrane damage, ROS generation, protein oxidation, and denaturation, mitochondrial dysfunction, DNA damage and inhibition of cell proliferation (Table 1) (Tortella et al., 2020). But, there is no doubt that AgNPs biomaterials still hold great promise in bone tissue engineering, and further exploration to obtain slow-release or locally degraded silver biomaterials may help to address these challenges.

5 Black phosphorus

BP nanomaterials, also known as phosphenes, a new member in the two-dimensional (2D) material family, have sparked considerable research interest (Kou et al., 2015). In the monolayer BP, each phosphorus atom is covalently linked

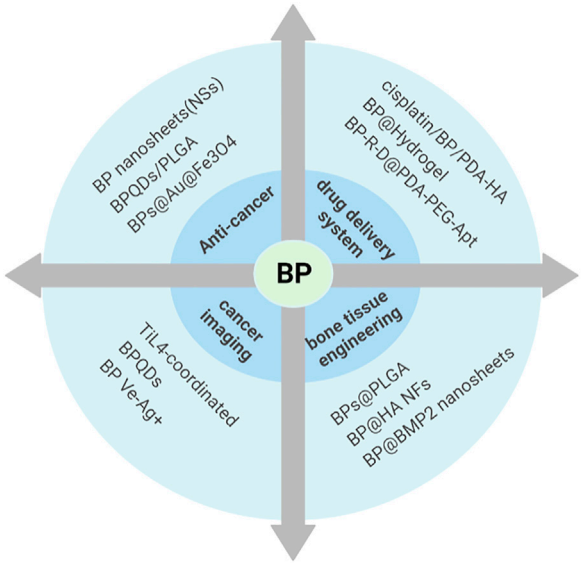

FIGURE 3
Biomedical applications of BP. With its unique structure, BP has been more and more favored in anti-tumor, drug-targeted delivery, photoacoustic imaging, and bone tissue engineering after various modifications.

with three adjacent phosphorus atoms to form a puckered phosphorus layer structure, and the phosphorus layer and surface are closely bonded by the van der Waals force (Choi et al., 2018). Compared with other 2D nanomaterials, the BP at the nanometer level has a fold structure and a bilayer structure along the Zigzag direction, which makes the BP have a higher specific surface area. This structural anisotropy contributes to its excellent properties, including its optical properties, mechanical properties, electrical conductivity, thermoelectric properties, and properties that distinguish its topology from other 2D materials. In addition, another zero-dimensional structure nanomaterial of BP, black phosphorus quantum dots (BPQDs), was successfully synthesized by chemical methods and attracted wide attention (Sun et al., 2015). In 2015, Zhang et al. achieved the first breakthrough in the preparation of BPQDs (Zhang X. et al., 2015). Using a facile liquid-phase sonication technique to fabricate BPQDs, Zhang and colleagues successfully prepared BPQDs with uniform size and better dispersion. Then, BPQDs have exhibited significant application in biomedicine (Gui et al., 2018). In general, BP nanomaterials have attracted widespread attention for biomedical applications, such as PTT, PDT, drug delivery, bioimaging, and tissue engineering since it was first discovered in 2014 (Figure 3). For example, Yang et al. (2018) based on the PTT and osteogenesis of BP, made a breakthrough in integrating 2D BP nanosheets into 3D printed bioglass (BG) scaffolds (Figure 4A). From the micro-scale to the macro-level, Yang successfully prepared multifunctional biomaterials with osteogenic and anti-osteosarcoma properties *in vitro* and *in vivo*. And, in this section, we will discuss the biomedical applications of the properties of black phosphorus.

5.1 Anticancer properties of BP

Owing to its excellent photothermal conversion properties, black phosphorus has been explored and used as a PTT agent or a photosensitizer in PDT *in vivo* cancer therapy (Qi et al., 2021).

Shao et al. (2016) used the emulsification solvent volatilization method to prepare core-shell structured nanospheres with high polymer (PLGA) encapsulating BPQDs. PLGA is a degradable hydrophobic biomedical polymer, and the formed polymer shell can isolate the internal BPQDs from the physiological environment, ensuring the stable performance of the BPQDs during the treatment process. After the PTT is over, the BPQDs will be slowly released and degraded with the gradual degradation of the PLGA shell, and then safely metabolized out of the body. Cell and animal experiments show that BPQDs/PLGA has good biological safety and passive tumor targeting, and shows high PTT efficiency. Five minutes of near-infrared light can effectively kill tumors. This promotes the actual clinical application of PTT. In addition, several reports have revealed that a large number of tumor antigens and alarmins, acting as an endogenous stimulatory signal that can improve tumor immunogenicity, are produced when BP kills tumors through PDT (Li W. et al., 2019; Alzeibak et al., 2021).

More importantly, recent studies have attempted to combine BP phototherapy with tumor immunotherapy, to achieve innovative breakthroughs in the treatment of osteosarcoma. Generally speaking, in the tumor microenvironment, when interacting with signal regulatory protein-alpha (SIRPα) which is expressed on macrophages, CD47 can realize the function of "do not eat me" (Liu M. et al., 2019). On the ground, Xie et al. (2020) found that BP-based PTT plus in combination with anti-CD47 antibodies (aCD47) can prompt the repolarization of tumor-associated macrophages (TAMs) from M2-like to M1-like macrophages, block the "do not eat me" signal of CD47-SIRPα in tumor cells and promote phagocytosis of macrophages (Figure 4B). Then, activated macrophages may enhance the local cross-presentation of tumor-specific antigens and facilitate the production of tumor antigen-specific T cells against distant metastatic tumor cells. Yang et al. (2017) have fabricated a novel nanocomposite, showing highly biocompatible and excellent tumor suppression due to synergistic PTT and PDT mediated by low-power near-infrared lasers, by assembling iron oxide (Fe_3O_4) NPs and Au nanoparticles on BP sheets (BPs@Au@ Fe_3O_4). Besides, there are also several reports that more precise and efficient PTT and PDT have been obtained by modifying black phosphorus or combining it with other materials. For example, by combining the plasmonic photothermal effect of Au nanoparticles with MRI of Fe_3O_4

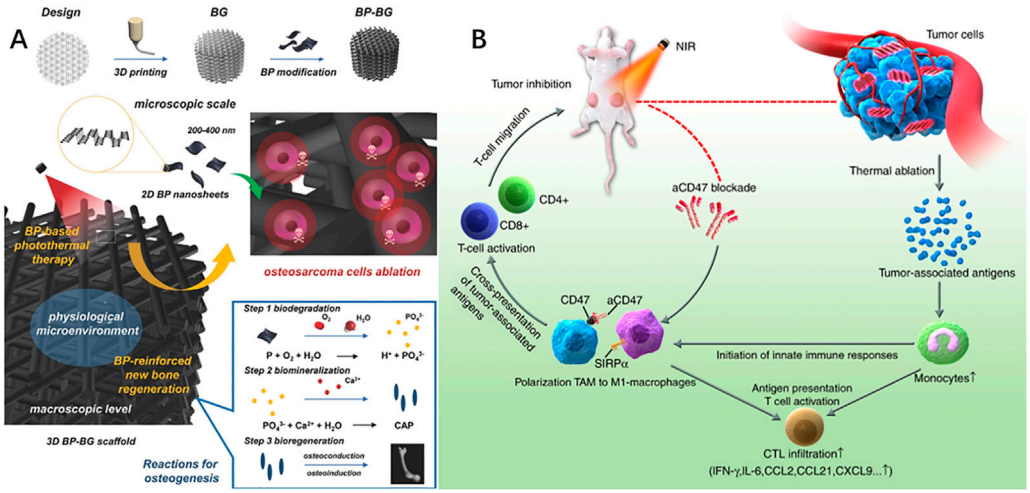

FIGURE 4
(A) 2D-Black-Phosphorus-Reinforced 3D-Printed Scaffolds. Schematic illustration of the fabrication process for BP-BG scaffold and the stepwise therapeutic strategy for the elimination of osteosarcoma followed by osteogenesis by BP-BG. **(B)** Black phosphorus-based photothermal therapy with aCD47-mediated immunotherapy. Black phosphorus in combination with anti-CD47 antibody activates innate and adaptive immunity and promotes local and systemic anticancer immune responses, thereby providing a synergistic enhancement in inhibiting tumor progression and suppressing metastatic cancer. **(A)**: Yang et al. (2018). 2D-Black-Phosphorus-Reinforced 3D-Printed Scaffolds: A Stepwise Countermeasure for Osteosarcoma. *Adv Mater 30(10)*. doi: 10.1002/adma.201705611. **(B)**: Xie et al. (2020). Black phosphorus-based photothermal therapy with aCD47-mediated immune checkpoint blockade for enhanced cancer immunotherapy. *Light Sci Appl* 9, 161. doi: 10.1038/s41377-020-00388-3.

NPs for the first time, BPs@Au@ Fe_3O_4 shows a more significant photothermal treatment effect and more selective targeted therapy. However, although BP-based phototherapy has achieved some gains in cancer treatment, its clinical application in osteosarcoma remains a formidable challenge, and more research is needed to achieve this translation. Meanwhile, the damage of PTT of BP to the normal tissue around the tumor has also sparked controversy, and the subsequent mild photothermal therapy may be its potential solution (Jiang et al., 2021).

5.2 BP-based drug delivery system

For cancer, traditional drug therapy often has more or fewer defects, such as easy degradation, adverse reactions, and lack of targeting ability. But, Over the past decade, as 2D nanomaterials, such as graphene oxide (GO), BP, and molybdenum disulfide with various unique physical and chemical properties have been widely studied, more and more research is turning interest in these biomaterials to overcoming these challenges (Biju, 2014; Yin et al., 2017; Liu et al., 2018). Among them, BP has also been widely discussed as a drug delivery system with a large surface area, fold-like structure, good biodegradability, and active nano-interactions (Tao et al., 2017; Wang S. et al., 2019; Liu W. et al., 2021).

On the one hand, the current exploration is mainly to modify BP through polymer compounds, such as hydrogels, and PLGA, to increase the anti-tumor drug carrying capacity of BP nanosheets, increase the stability of the BP structure, and achieve a controllable and sustained drug release (Tao et al., 2017; Choi et al., 2018). Qiu et al. (2018) used the non-contact probe ultrasonic liquid peeling method to successfully prepare two-dimensional layered phosphorene nanosheets, and integrate them with anticancer drugs into the biodegradable temperature-sensitive hydrogel material to prepare black phosphorus hydrogel material. Under the irradiation of near-infrared light, the black phosphorus in the material can generate local high heat, which can not only kill tumor cells directly through photothermal action but also target tumor tissue to release drugs. The rate of drug release can be more precisely controlled by various parameters such as the intensity of the laser light field, irradiation time, and black phosphorus concentration, and ultimately achieve the effect of treating tumors. Besides, Li Y. et al., 2021 have designed a BP nanosheet-based nano-assembly containing cisplatin and used polydopamine (PDA) and hyaluronic acid (HA) to modify the surface of black phosphorus, achieving higher stability, a stronger photothermal effect, and targeting ability. Then in the tumor microenvironment, cisplatin/BP/PDA-HA (CBPH) would start to degrade and release cisplatin in a controlled manner by responding to internal or external stimuli, such as low pH, hydrogen peroxide, and near-infrared light. Therefore, *in vivo* experiments further revealed that there is a greater accumulation of cisplatin in tumor tissue and smaller primary tumors, and fewer lung metastases under the stimulation of light.

On the other hand, it has been pointed out that after black phosphorus is taken up by tumor cells, the active phosphorus produced can play an anti-tumor effect. Studies by Geng et al. (2020) have found that due to the vigorous endocytosis of cancer cells compared to normal cells, faster metabolic rate, and strong oxidative pressure, BP nanosheets are easily taken up by cancer cells rather than normal cells through endocytosis, and are rapidly degraded, resulting in the production of a lot of phosphate ions in the cell. This process leads to changes in the internal environment of cancer cells, causing G2/M phase blockade, thereby effectively inducing apoptosis and autophagy in cancer cells, which brings a better therapeutic effect than the traditional chemotherapy drug doxorubicin (DOX) *in vitro* and *in vivo* experiments. The research team named this selective killing of cancer cells derived from the natural biological activity of black phosphorus, "Bioactive Phosphorus-based Therapy" ("BPT").

So, the deepening of biomaterial research also provides new therapy options for the treatment of recurrent or metastatic osteosarcoma.

5.3 BP for cancer imaging

Recently, with high image contrast and sensitivity, high spatial resolution with depth up to several centimeters, and depth resolution 3D imaging, photoacoustic (PA) imaging has attracted widespread interest, then reducing unnecessary biopsies and facilitating image-guided therapy (Lemaster and Jokerst, 2017). However, although PA imaging has been researched to be superior to many other traditional optical imaging techniques, there are still many problems to be solved in its clinical application. In the early stage of the tumor, the PA signal from the tumor is very low, so we need a contrast agent to enhance the signal and obtain more accurate *in vivo* imaging of PA. Lately, several studies have reported nanomaterials, such as metals, semiconductors, and reduced graphene oxide (RGO) with NIR absorption as contrast agents for better imaging, but have been limited by their potential toxicity in clinical applications (Fu et al., 2019).

Fortunately, BP is emerging as an alternative material for contrast agents in photoacoustic imaging, considering its excellent electronic and optical properties (Gui et al., 2018). On the other hand, the degradation of black phosphorus to phosphate *in vivo* avoids potential toxicity limitations. In the way that mixes BPQDs prepared by a liquid exfoliation technique and titanium ligand (TiL_4) in N-methyl-2-pyrrolidone (NMP) at room temperature for 15 h, Sun et al. (2017) have fabricated TiL4-coordinated BPQDs, showing better PA performance *in vivo*. Titanium ligand sulfonates made BPQDs more stable in aqueous media through the surface ligands of BPQDs. In addition, a few studies have further reported that BPQDs exhibit higher spatial resolution, deeper penetration, lower optical absorption and scattering from biological tissues, and lower autofluorescence for PA imaging in the second NIR (NIR-II, 950 nm–2,000 nm) window (Fu et al., 2019; Xu et al., 2019). On this basis, an exogenous NIR stimulus responsive BPQDs vesicle (BP Ve) was constructed by Li Z. et al. (2020) and can chelate and release Ag^+ ions. Then Ag^+ ions-coupled BP Ve shows not only more effective NIR-II PA imaging ability but also synergistic photodynamic/Ag^+ therapy owing to enhanced light absorption and PA intensity in the NIR-II window. Therefore, more research is needed to further explore the potential value of BP in oncology, to address these challenges in the early diagnosis and treatment of recurrent or metastatic osteosarcoma.

5.4 BP for bone tissue engineering

According to recent research, BP nanomaterials have many advantages in bone regeneration. First, compared with other 2D materials, they have good biocompatibility and are biodegradable in the physiological environment (Qing et al., 2020). The BP is completely biodegradable, and the final degradation products are harmless H_2O, CO_2, and PO_4^{3-}, which can be used as essential bone components (Tong et al., 2019). Based on this, the preparation of a photo-responsive BP@Hydrogel provides an *in situ* mineralized model controlled by timing and direction of light, exhibiting high potential for mechanical properties and bone induction (Shao et al., 2020). Therefore, this platform provides a good mimicking extracellular matrix (ECM) microenvironment for promoting osteoblast differentiation and bone regeneration (Figure 5A).

Besides, due to the strong light absorption capacity of BP in the NIR, BP based nanomaterials or 3D printed scaffolds have a stable and reliable light-controlled release mode, to achieve the purpose of targeted and sustained release. Simultaneously, its unique photothermal conversion ability can both promote bone regeneration and repair by up-regulating alkaline phosphatase (ALP) and heat shock proteins (HSP) through hyperthermia, and also killing tumor cells by increasing local temperature (Figure 5B) (Qing et al., 2020). In this regard, a chitosan/hydroxypropyl trimethylammonium chloride chitosan/hydroxyapatite/black phosphorus (CS/HC/HA/BP) composite scaffold is designed to take advantage of these characteristics of black phosphorus, aiming to deal with the clinical problems of tumor recurrence, bone defect and chronic bone loss after bone tumor surgery (Zhao et al., 2023).

At last, due to their large surface area and fold-like structure, BP nanomaterials have greater active agent-carrying capacity including various drugs, biomolecules, and nanoparticles. For the first time, Li Z. et al. (2021) designed a Ca^+ ion-supplying BP-based 3D nanocomposite fiber scaffold *via* microfluidic technology, which brings new therapeutic prospects to elderly patients with bone defects or bone damage caused by calcium loss. In addition, by integrating BP nanosheets and

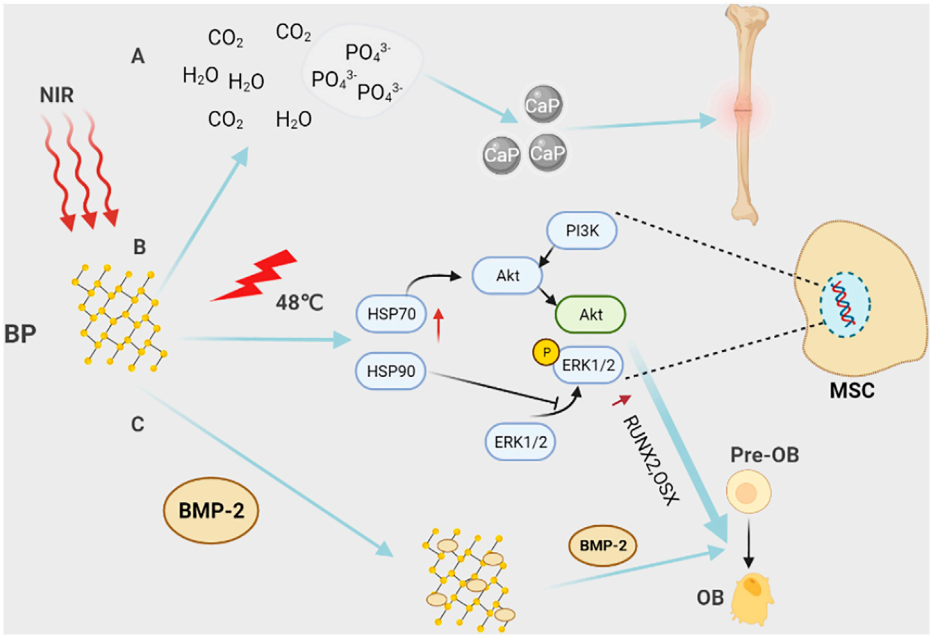

FIGURE 5
Black phosphorus in bone tissue engineering. **(A)** Black phosphorus is completely degraded in the body into harmless H_20, CO_2, and PO_4^{3-}. PO_4^{3-} is one of the basic components of the bone matrix, which is beneficial to promote bone repair. **(B)** Under NIR light, BP locally generates heat through the photothermal effect, activates heat shock proteins, and then promotes the expression of osteogenic-specific genes, such as RUNX2, BMP2, and the differentiation of pre-osteoblasts into osteoblasts through activating ERK1/2 signaling pathway and PI3K/AKT signaling pathway. **(C)** With their unique structure, black phosphorus nanosheets can carry BMP2, etc., and regulate bone formation in the bone microenvironment. For example, BMP2 promotes the differentiation of pre-osteoblasts into osteoblasts.

hydroxyapatite-silica (SiO_2) nanoparticles onto 3D PLGA nanofibers, the scaffold has a better Ca/P ratio, variable pore size distribution, and highly porous interconnected structure, providing a better microenvironment for the bone repair compared to other composites based on BP. Further, based on black phosphorus can provide a negative surface and strong bone morphogenetic protein$_2$ (BMP_2) loading capacity, BMP_2-modified black phosphorus (BP@BMP_2) nanosheets are used to bind on a polylactic acid (PLLA) electrospun fibrous scaffold by microsol-electrospinning technique, realizing successfully a bioinspired staged bone regeneration strategy (Figure 5C) (Cheng et al., 2020). On this basis, BMP-2 can recruit pre-osteoblasts and promote their differentiation. Phosphate generated from BP also chelates Ca^+ ions to deposit on electrospun fibrous scaffolds in a 3D manner. At last, P-BP@BMP2 nanofibrous scaffolds exhibit excellent bone regeneration ability.

A recent study has also found that the binding of extracellular vesicles (EVs) to black phosphorus can regulate intercellular communication to promote bone regeneration. In 2019, wang et al. engineered matrix bioinspired matrix vesicles (MVs), termed Apt-bioinspired MVs, through the intercalation of black phosphorus and functionalization of cell-specific aptamers (Apt) (Wang Y. et al., 2019). MVs, as a kind of EVs, are involved in the regulation of mineralization in the body (Hasegawa, 2018). Apt-bioinspired MVs can be directed to osteoblasts in bone tissue under the guidance of the aptamer and take advantage of the photothermal effect of black phosphorus to achieve the up-regulation of heat shock proteins and alkaline phosphatase. Simultaneously, the degradation product phosphate, as a component of bone, from BP can also promote the biomineralization process as a component of bone.

6 Other bio-materials

With the continuous progress of physical and chemical processing, other innovative smart multi-functional materials provided with both structural and therapeutical properties have been also discovered and prepared (Ambrosio et al., 2021). These biomaterials, such as bio-ceramics, molybdenum disulfide (MoS_2), selenium (Se), natural polymers, etc., have also received more and more attention in the process of bone reconstruction after bone tumor surgery due to excellent osteogenesis-promoting ability, biodegradability, drug-loading ability, and anti-tumor effect of phototherapy, etc. (Table 2) (Turnbull et al., 2018; Koons et al., 2020).

TABLE 2 The main features of other bio-materials.

Type of bio-materials	Strengths	Flaws	Instance
Bio-ceramics	Corrosion resistance; good biocompatibility; bioactive ions, pressure resistance	Excessive brittleness	Calcium silicate $CaCO_3$-PCL scaffold
MoS_2	two-dimensional surface area; high near-infrared strong absorbance	Potential toxicity	MoS2-HA-DTPA-Gd/Gef
Selenium	Thermal and chemical stability	Acute or chronic poisoning; lack of targeting	Se-doped HA scaffolds Se-CaP
Natural polymers	Mimicking extracellular matrix; no toxicity	Potential immunogenicity; lower mechanical properties	Chitosan Curcumin Alginate

Bio-ceramics can release lots of bioactive ions, such as calcium ions, copper ions, silicon ions, magnesium ions, etc., to play the role of promoting osteogenesis and angiogenesis (Hoppe et al., 2011; Jones, 2013). In addition, some new breakthroughs have been made in bio-ceramics as a repair material for bone defects after osteosarcoma surgery recently (Chen et al., 2019; Elfeky et al., 2020; Yang et al., 2020). Firstly, bio-ceramics tend to mimic the extracellular matrix during bone tissue regeneration by providing mechanical support and an appropriate environment for mesenchymal stem cell attachment, proliferation, and differentiation (Shin et al., 2003; Kim et al., 2017). Besides, the bio-ceramic scaffold, functionalized with appropriate materials, also has the effect of photothermal anti-tumor. Meanwhile, bio-ceramic-based composites have important roles in anticancer drug delivery systems, including the treatment of osteosarcoma (Liu Y. et al., 2021; Oliveira et al., 2021). For, example, a 3D-printed calcium silicate material, after high photothermal functionalization, has the functions of anti-osteosarcoma, promoting bone regeneration and drug loading (Truong et al., 2021). On this basis, He et al. designed a 3D printed polymeric polycaprolactone fibers coated with porous calcium carbonate structures (PCL/CaCO3) scaffold and surface-modified it with 2D inorganic Egyptian blue nanosheets (CaPCu) (He et al., 2021). Here, Egyptian blue (EB, $CaCuSi_4O_{10}$), one of the oldest synthetic pigments containing silicon, copper, and calcium, has been revealed in previous studies to promote osteogenesis. To conclude, compared with other bone repair materials, the scaffold has greater advantages in terms of stronger photothermal ability under NIR-II laser irradiation, synergistic osteogenesis and antitumor ability, and orthotopic transplantation. Finally, bio-ceramics, as a biomaterial with both anti-tumor and promotion of bone repair, have also made some progress in the study of its mechanism. For instance, several reports have also found that nanoscale hydroxyapatite can inhibit the proliferation and migration of osteosarcoma by down-regulating the FAK/PI3K/Akt signaling pathways *in vitro* and *in vivo* (Wang R. et al., 2020). However, despite the advantages of bio-ceramics in high compressive modulus and provision of bioactive ions, the excessive brittleness limits further clinical applications. Therefore, the synthesis of potentially tough bio-ceramic polymer hybrids may help to overcome this challenge.

Beyond graphene and BP nanosheets, a new 2D material, MoS_2, is attracting researchers' attention due to its unique visible photoluminescence with high absorption (Shi et al., 2020). MoS_2 disulfide has been reported to exhibit an indirect-to-direct semiconducting transition in the exfoliation from bulk to monolayer, which has led to the widespread use of MoS_2 in electronic devices and catalysts (Voiry et al., 2016). More importantly, the application of MoS_2 in the biomedical field has been continuously explored due to its large two-dimensional surface area and high near-infrared strong absorbance (Chou et al., 2013). For example, by combining MoS_2 with hyaluronic acid, the instability of MoS_2 and the low efficiency of the PTT in tissues are overcome (Shin et al., 2019). Meanwhile, hyaluronic acid promotes the accumulation of MoS_2 in tumor cells through its mediated endocytosis, which enhances the efficiency of PTT and PA imaging of tumors (Lemaster and Jokerst, 2017; Fu et al., 2019). On this basis, Liu J. et al. (2019) designed a nanoplatform based on MoS_2 and functionalized with hyaluronic acid for tumor MRI and synergistic chemo-photothermal therapy. This nanoplatform enables co-targeted delivery of gadolinium (Gd) based contrast agents and gefitinib (Gef). Both *in vitro* and *in vivo* experiments have demonstrated that under near-infrared radiation, MoS2-HA-DTPA-Gd/Gef can induce tumor cell apoptosis through the phosphatidylinositol 3 kinase (PI3K)/protein kinase B (Akt) signaling pathway, which provides new ideas for tumor diagnosis and treatment. Unfortunately, reports on the application of MoS_2 in bone reconstruction after osteosarcoma surgery are rare. Besides, MoS_2, as a transition metal dihalide, has a non-negligible low toxicity (Chen et al., 2018). In general, based on its unique properties, the application of MoS_2 in the treatment and diagnosis of bone tumors deserves further exploration.

Selenium (Se), as one of the essential trace elements in the human body and a cofactor for dozens of enzymes in the body, is an indispensable part of the body's oxidation, stress, immunity,

and other reaction (Prabhu and Lei, 2016). Several previous reports have revealed the toxic effects of Se in various tumors, such as colon cancer, prostate cancer, breast cancer, etc. (Pang and Chin, 2019). Recently, it has also been reported that Se can improve the multidrug resistance (MDR) of osteosarcoma cells by inducing apoptosis in osteosarcoma treatment. For instance, Wang et al. found that selenium-doped nano-hydroxyapatite (Se-HANs) could exert an antitumor effect through the synergistic effect of caspase-dependent apoptosis and ROS-induced apoptosis (Li X. et al., 2020). On this basis, selenium-doped calcium phosphate (Se-CaP) organisms were engineered to carry the chemotherapeutic drug doxorubicin to target doxorubicin-resistant osteosarcoma cell line MG63/DXR in a xenografted BALB/c nude mice (Hu et al., 2021). In addition to caspase-dependent apoptosis and ROS-induced apoptosis, Se-CaP can downregulate the expression of MDR-associated ATP-binding cassette (ABC) transporters (ABCB1 and ABCC1) to reverse MDR (Hu et al., 2021). Besides, an article found that compared with hydroxyapatite, Se-doped hydroxyapatite scaffolds can synergistically promote the differentiation of human adipose-derived mesenchymal stem cells (hAD-MSCs) into bone tissue, thereby enhancing ALP activity and osteogenesis (Zakhireh et al., 2021). Furthermore, Li et al. found that the porous Se@SiO2 nanocomposite avoided the apoptosis of H_2O_2 on BMSCs through the BMP/SMAD pathway and promoted the osteogenic differentiation of BMSCs (Li C. et al., 2019). Overall, Se-doped bio-scaffolds may offer new clinical benefits for bone tissue engineering (Zeng et al., 2013). However, although Se deficiency may be associated with some biological disturbances, Se can also cause acute or chronic poisoning, often manifesting as brittle and falling nails, gastrointestinal disturbances, rashes, fatigue, irritability, and neurological abnormalities (Cao et al., 2012; Cardoso et al., 2021). Therefore, the design of Se-doped scaffolds for sustained release of Se to obtain a safe concentration in the body may be the focus of future research.

Natural polymers, such as chitosan, curcumin, alginate, etc., have received a lot of attention in bone tissue engineering due to their advantages of mimicking ECM, providing cell adhesion sites, and low cost. Recently, unlike previous studies, an article has revealed that extracellular matrix elasticity, rather than matrix adherence, modulates tumor cell growth through integrin-mediated focal adhesion (FA) signaling (Chaudhuri et al., 2014; Jiang et al., 2019). In contrast, normal cells, such as osteoblasts, are primarily affected by ECM adhesion ligands through integrin-mediated regulation of the adherens junction (AJ) signaling pathway (Steinbacher and Ebnet, 2018). This provides new insights into bone tissue engineering. Based on this, Tan et al. designed an injectable curcumin microsphere/IR820 hybrid bifunctional hydrogel, which can not only play the role of photothermal anti-tumor but also promote bone remodeling through the sustained release of curcumin (Tan et al., 2021). Meanwhile, the heat generated by PTT *in vivo* accelerates the release of curcumin and induces apoptosis of osteosarcoma cells. In addition, studies have confirmed that 3D-printed hydroxyapatite scaffolds added with chitosan can further promote the development of new bone tissue *in vitro* and vivo, which is beneficial to osseointegration (Zafeiris et al., 2021). The degradability of the scaffolds will benefit patients in terms of improved quality of life while avoiding some complications. However, although natural polymers are more and more widely used as multifunctional materials in bone defects after osteosarcoma surgery, their existing problems, such as potential immunogenicity and lower mechanical properties, should also be paid attention to several studies have made progress on the lack of rigidity by 3D-printing hybrid scaffolds made by combining natural polymers with bio-ceramics. But this is not enough, more modified natural polymers are needed for better clinical application.

Recently, ferroptosis as a form of regulated cell death has also attracted great interest in tumor research (Dixon et al., 2012; Zhang et al., 2022). The earliest studies found that ferroptosis is mainly caused by an iron-dependent accumulation of lipid peroxidation, inactivation/depletion of anti-lipid peroxidation molecules, and increased mitochondrial membrane density. On this basis, several studies have made some progress in the non-surgical treatment of tumors by inducing ferroptosis of tumor cells through biomaterials (Yang et al., 2021d; Han et al., 2022). For example, Fu et al. (2021) designed a mesoporous silica nanoplatform integrating doxorubicin and ferrate by assembling a solid-liquid phase change material of *n*-heneicosane, thus realizing the co-release of doxorubicin and ferrate under ultrasound (US). Surprisingly, exogenous iron derived from the metabolism of this nanodrug can induce ferroptosis in tumor cells and exert a synergistic anti-tumor effect. Furthermore, an article found that singlet oxygen generated by photodynamic therapy of nanomaterials can promote the ferroptosis of tumor cells (Li J. et al., 2021). In conclusion, combining photothermal therapy, photodynamic therapy, and ferroptosis with nanomaterials provides a new perspective for dealing with the issue of tumor tissue recurrence after osteosarcoma surgery and the chemoresistance of osteosarcoma. However, the current problem is that studies on ferroptosis in osteosarcoma are rare. Therefore, new explorations based on nano-biomaterials are highly required to deal with the challenges of killing residual tumor cells and bone remodeling after osteosarcoma surgery.

7 Prospects and clinical translation

With excellent anti-tumor and bone-promoting effects, the above biomaterials have become a hot spot in the current spotlight, and have also been preliminaries explored in clinical translational research. Then, we briefly describe the prospects and clinical translation of magnesium, silver and black phosphorus.

7.1 Magnesium

Mg has been regarded as a promising bioactive material for bone regeneration due to its sufficient mechanical properties, biodegradability and osteogenic activity. But in fact, the application of pure Mg implants still faces some challenges, such as rapid degradation, excessive hydrogen formation, and the difficulty of fabricating magnesium-based multi-pore scaffolds.

Encouragingly, the use of orthopedic devices or implants, for instance screws based on magnesium or its alloys in fracture repair has been reported in China and Germany in recent years, with promising osteogenic results compared to titanium (Windhagen et al., 2013; Zhao et al., 2016; Zhao et al., 2017). Besides, as mentioned earlier, magnesium particles are integrated into biodegradable polymer substrates such as PLGA to create composite scaffolds (PLGA/Mg) to circumvent these defects (Long et al., 2021). On the other hand, the surface modification of Mg alloy, enhancing the corrosion resistance and mechanical strength of Mg metal and avoiding a large amount of local hydrogen accumulation, can also pave the way for the clinical translation of Mg implants (Gao et al., 2021).

Less noticed but as important, magnetic hyperthermia (MHT) was found to be able to ablate the tumor using an alternating magnetic field (AMF) to heat a magnetothermal agent (magnetic nanoparticles including magnesium particles) applied to the tumor (Yang N. et al., 2021). The potential interaction between human biological magnetic field and this MHT may bring different prospects for clinical application of Mg materials.

Mg-induced osteogenesis is mediated by local neuronal production of calcitonin gene-related peptide 1 (CGRP1) and has been demonstrated in fractured mice suggesting that magnesium may be involved in the neural regulation of bone defects and thus in the regulation of bone homeostasis (Zhang Y. et al., 2016). This means that other roles of magnesium in the process of bone reconstruction after bone tumor surgery, such as pain regulation and angiogenesis, are also worth further investigation.

7.2 Silver

As described above, silver has been used in our clinical practice for hundreds of years, from antibacterial and regenerative to today's anti-tumor. At present, the academic research mainly focuses on nanoscale silver particles, such as AgNP and AgAP, due to their excellent tumor targeting, killing effects and potential osteogenesis.

Consequently, current clinical studies aim to improve cancer treatment by modifying Ag NPs to track and specifically bind tumor cells *in vivo*, thereby improving cancer treatment with minimal risk to normal cells. Beyond that, the exploration of different nanoparticle shapes for optimal drug delivery is the focus of current clinical research (Malik and Mukherjee, 2018). But regrettably, this part of clinical research is lacking in osteosarcoma. Therefore, the potential widespread application of silver nanoparticles in preclinical and clinical stages of osteosarcoma should not stop exploration, although the current research and development is still in its infancy and face many difficulties.

7.3 Black phosphorus

Black phosphorus not only can be completely degraded into non-toxic phosphate, but also can fully kill tumors through phototherapy, making it a favorite in the field of biomaterials, especially in the field of bone tumors.

The broad prospect of clinical translational application of BP has attracted the attention of researchers mainly because of its unique pre-osteogenic ability in the field of bone repair. For example, chitosan thermal response hydrogel therapy can be used to treat bone defects caused by arthritis rheumatoid arthritis (RA) by adding BP nanosheets to platelet-rich plasma (PRP) (Pan et al., 2020). Yet, in the case of osteosarcoma, the clinical translation of black phosphorus-based biomaterials is still in the infant segment, despite ongoing exploration of the immune and metabolic microenvironment during bone defect reconstruction. Fortunately, black phosphorus, with its high electrical conductivity, seems to be a breakthrough point for clinical translational research by participating in nerve fiber repair to promote bone regeneration (Grassel, 2014; Qian et al., 2019). In conclusion, the clinical application prospect of BP can be predicted, based on its three major properties of promoting *in situ* mineralization through degradation product phosphate, inducing nerve regeneration and regulating bone repair, and photothermal treatment killing tumor although the mainstream research of black phosphorus in osteosarcoma is still concentrated in the experimental stage.

8 Summary and discussion

This article introduces biomaterials of recent years, such as black phosphorus, magnesium, zinc, copper, silver, etc., with their good biocompatibility, biodegradation antibacterial, and anti-tumor effects, they have received high attention and consideration from researchers. Many studies have been successful in cell or animal experiments. However, in looking for an ideal material that can not only fill in but also kill the residual tumor cells, reducing the probability of recurrence and metastasis, and hence promoting bone repair, there is still a long way to go in the clinical treatment of osteosarcoma.

Overall, magnesium-zinc alloys and copper are relatively under-studied, while silver and black phosphorus are relatively

studied and are on the rise due to their various functions and safe use. Additionally, MoS_2 and bio-ceramics, etc. have also attracted a lot of interest in bone tissue engineering. Above all, for the study of silver, the advantage is that it has anti-tumor and antibacterial effects, but there are few studies on long-term toxic and side effects, and it is worth continuing to explore. At the same time, currently, the targeted therapy of AgNPs and AgAPs is mainly targeting the acidic environment of tumors through the effect of EPR, so more accurate targeted therapy for tumors is urgently needed. For black phosphorus, the biologically active phosphorus-based drug therapy has just started, and the specific molecular mechanism may be a direction worth exploring. However, although a controlled degradation mode can be obtained by irradiation with near infrared light, how to improve the targeting of black phosphorus nanomaterials is also a clinical problem. But targeted therapy based on specific molecules on the surface of the osteosarcoma may help improve targeting although osteosarcoma is a highly heterogeneous tumor. Secondly, for zinc, magnesium, and copper, the rapid development of nanotechnology has made them another breakthrough after being used as the substrate for 3D printing scaffolds. Among them, potential toxicity and rapid degradation of zinc limit its application in bone reconstruction after osteosarcoma surgery. However, combining zinc coating with 3D-printed scaffolds, such as PLGA, BG may produce unexpected applications. Due to excellent osteogenic activity and surface modification, Mg has made great strides in clinical conversion applications, despite its rapid degradation rate and excessive local hydrogen production. In the meantime, the research on the MHT and neural regulation of magnesium has opened up a new direction for the study of magnesium. Then, MoS_2, a discovery of two-dimensional materials after black phosphorus nanosheets, possesses excellent anti-tumor effects and photoacoustic imaging capabilities. However, research in osteosarcoma is rare, and its application in osteosarcoma deserves further exploration. Finally, the research of modified polymer compounds and selenium in bone tissue engineering has also attained a new turning point.

In general, we consider the latest application of biomaterials in bone reconstruction after osteosarcoma surgery as a remedy for large bone defects after osteosarcoma surgery as well as recurrence and metastasis caused by residual tumor tissue. At the same time, advances in nanomaterials have enabled the better use of phototherapy, tumor imaging, and targeted drug delivery. It is expected that this will inspire future research to bring further developments in the treatment of patients with osteosarcoma.

Author contributions

SC, DW, and YP contributed to the conception and design of the article. DW and YP designed and drew all the figures. YL designed and drew the table. DW and YL wrote the first draft of the manuscript. All authors contributed to the revision of the manuscript, read and approved the submitted version.

Funding

This work was supported by the National Natural Science Foundation of China (Grant Nos 82172594 and 81772866), the Wisdom Accumulation and Talent Cultivation Project of the Third Xiangya Hospital of Central South University (YX202001), Natural Science Foundation of Hunan Province (2022JJ40752), and Natural Science Foundation of Changsha (kq2202426).

Conflict of interest

The authors declare that the research was conducted in the absence of any commercial or financial relationships that could be construed as a potential conflict of interest.

Publisher's note

All claims expressed in this article are solely those of the authors and do not necessarily represent those of their affiliated organizations, or those of the publisher, the editors and the reviewers. Any product that may be evaluated in this article, or claim that may be made by its manufacturer, is not guaranteed or endorsed by the publisher.

Supplementary material

The Supplementary Material for this article can be found online at: https://www.frontiersin.org/articles/10.3389/fmolb.2022.1105540/full#supplementary-material

References

Alzeibak, R., Mishchenko, T. A., Shilyagina, N. Y., Balalaeva, I. V., Vedunova, M. V., and Krysko, D. V. (2021). Targeting immunogenic cancer cell death by photodynamic therapy: Past, present and future. *J. Immunother. Cancer* 9 (1), e001926. doi:10.1136/jitc-2020-001926

Ambrosio, L., Raucci, M. G., Vadala, G., Ambrosio, L., Papalia, R., and Denaro, V. (2021). Innovative biomaterials for the treatment of bone cancer. *Int. J. Mol. Sci.* 22 (15), 8214. doi:10.3390/ijms22158214

Ameh, T., and Sayes, C. M. (2019). The potential exposure and hazards of copper nanoparticles: A review. *Environ. Toxicol. Pharmacol.* 71, 103220. doi:10.1016/j.etap.2019.103220

Biju, V. (2014). Chemical modifications and bioconjugate reactions of nanomaterials for sensing, imaging, drug delivery and therapy. *Chem. Soc. Rev.* 43 (3), 744–764. doi:10.1039/c3cs60273g

Bonnet, S., Archer, S. L., Allalunis-Turner, J., Haromy, A., Beaulieu, C., Thompson, R., et al. (2007). A mitochondria-K+ channel axis is suppressed in cancer and its normalization promotes apoptosis and inhibits cancer growth. *Cancer Cell* 11 (1), 37–51. doi:10.1016/j.ccr.2006.10.020

Brewer, G. J. (2010). Risks of copper and iron toxicity during aging in humans. *Chem. Res. Toxicol.* 23 (2), 319–326. doi:10.1021/tx900338d

Cao, J. J., Gregoire, B. R., and Zeng, H. (2012). Selenium deficiency decreases antioxidative capacity and is detrimental to bone microarchitecture in mice. *J. Nutr.* 142 (8), 1526–1531. doi:10.3945/jn.111.157040

Cardoso, B. R., Cominetti, C., and Seale, L. A. (2021). Editorial: Selenium, human health and chronic disease. *Front. Nutr.* 8, 827759. doi:10.3389/fnut.2021.827759

Chaudhuri, O., Koshy, S. T., Branco da Cunha, C., Shin, J. W., Verbeke, C. S., Allison, K. H., et al. (2014). Extracellular matrix stiffness and composition jointly regulate the induction of malignant phenotypes in mammary epithelium. *Nat. Mater* 13 (10), 970–978. doi:10.1038/nmat4009

Chen, C. Y., Yin, H., Chen, X., Chen, T. H., Liu, H. M., Rao, S. S., et al. (2020). Angstrom-scale silver particle-embedded carbomer gel promotes wound healing by inhibiting bacterial colonization and inflammation. *Sci. Adv.* 6 (43), eaba0942. doi:10.1126/sciadv.aba0942

Chen, E., Xue, D., Zhang, W., Lin, F., and Pan, Z. (2015). Extracellular heat shock protein 70 promotes osteogenesis of human mesenchymal stem cells through activation of the ERK signaling pathway. *FEBS Lett.* 589 (24), 4088–4096. doi:10.1016/j.febslet.2015.11.021

Chen, L., Deng, C., Li, J., Yao, Q., Chang, J., Wang, L., et al. (2019). 3D printing of a lithium-calcium-silicate crystal bioscaffold with dual bioactivities for osteochondral interface reconstruction. *Biomaterials* 196, 138–150. doi:10.1016/j.biomaterials.2018.04.005

Chen, W., Qi, W., Lu, W., Chaudhury, N. R., Yuan, J., Qin, L., et al. (2018). Direct assessment of the toxicity of molybdenum disulfide atomically thin film and microparticles via cytotoxicity and patch testing. *Small* 14 (12), e1702600. doi:10.1002/smll.201702600

Chen, Z., Meng, H., Xing, G., Chen, C., Zhao, Y., Jia, G., et al. (2006). Acute toxicological effects of copper nanoparticles *in vivo*. *Toxicol. Lett.* 163 (2), 109–120. doi:10.1016/j.toxlet.2005.10.003

Cheng, L., Chen, Z., Cai, Z., Zhao, J., Lu, M., Liang, J., et al. (2020). Bioinspired functional black phosphorus electrospun fibers achieving recruitment and biomineralization for staged bone regeneration. *Small* 16 (50), e2005433. doi:10.1002/smll.202005433

Choi, J. R., Yong, K. W., Choi, J. Y., Nilghaz, A., Lin, Y., Xu, J., et al. (2018). Black phosphorus and its biomedical applications. *Theranostics* 8 (4), 1005–1026. doi:10.7150/thno.22573

Chou, S. S., Kaehr, B., Kim, J., Foley, B. M., De, M., Hopkins, P. E., et al. (2013). Chemically exfoliated MoS2 as near-infrared photothermal agents. *Angew. Chem. Int. Ed. Engl.* 52 (15), 4160–4164. doi:10.1002/anie.201209229

Chugh, H., Sood, D., Chandra, I., Tomar, V., Dhawan, G., and Chandra, R. (2018). Role of gold and silver nanoparticles in cancer nano-medicine. *Artif. Cells Nanomed Biotechnol.* 46 (1), 1210–1220. doi:10.1080/21691401.2018.1449118

Dang, W., Ma, B., Li, B., Huan, Z., Ma, N., Zhu, H., et al. (2020). 3D printing of metal-organic framework nanosheets-structured scaffolds with tumor therapy and bone construction. *Biofabrication* 12 (2), 025005. doi:10.1088/1758-5090/ab5ae3

Diez-Tercero, L., Delgado, L. M., Bosch-Rue, E., and Perez, R. A. (2021). Evaluation of the immunomodulatory effects of cobalt, copper and magnesium ions in a pro inflammatory environment. *Sci. Rep.* 11 (1), 11707. doi:10.1038/s41598-021-91070-0

Dixon, S. J., Lemberg, K. M., Lamprecht, M. R., Skouta, R., Zaitsev, E. M., Gleason, C. E., et al. (2012). Ferroptosis: An iron-dependent form of nonapoptotic cell death. *Cell* 149 (5), 1060–1072. doi:10.1016/j.cell.2012.03.042

Dziedzic, A., Kubina, R., Buldak, R. J., Skonieczna, M., and Cholewa, K. (2016). Silver nanoparticles exhibit the dose-dependent anti-proliferative effect against human squamous carcinoma cells attenuated in the presence of berberine. *Molecules* 21 (3), 365. doi:10.3390/molecules21030365

Elfeky, S. A., Elsayed, A., Moawad, M., and Ahmed, W. A. (2020). Hydroxyapatite nanocomposite as a potential agent in osteosarcoma PDT. *Photodiagnosis Photodyn. Ther.* 32, 102056. doi:10.1016/j.pdpdt.2020.102056

Fernandes, M. H., Alves, M. M., Cebotarenco, M., Ribeiro, I. A. C., Grenho, L., Gomes, P. S., et al. (2020). Citrate zinc hydroxyapatite nanorods with enhanced cytocompatibility and osteogenesis for bone regeneration. *Mater Sci. Eng. C Mater Biol. Appl.* 115, 111147. doi:10.1016/j.msec.2020.111147

Ferrari, S., Bacci, G., Picci, P., Mercuri, M., Briccoli, A., Pinto, D., et al. (1997). Long-term follow-up and post-relapse survival in patients with non-metastatic osteosarcoma of the extremity treated with neoadjuvant chemotherapy. *Ann. Oncol.* 8 (8), 765–771. doi:10.1023/a:1008221713505

Fu, J., Li, T., Yang, Y., Jiang, L., Wang, W., Fu, L., et al. (2021). Activatable nanomedicine for overcoming hypoxia-induced resistance to chemotherapy and inhibiting tumor growth by inducing collaborative apoptosis and ferroptosis in solid tumors. *Biomaterials* 268, 120537. doi:10.1016/j.biomaterials.2020.120537

Fu, Q., Zhu, R., Song, J., Yang, H., and Chen, X. (2019). Photoacoustic imaging: Contrast agents and their biomedical applications. *Adv. Mater* 31 (6), e1805875. doi:10.1002/adma.201805875

Gao, J., Su, Y., and Qin, Y. X. (2021). Calcium phosphate coatings enhance biocompatibility and degradation resistance of magnesium alloy: Correlating *in vitro* and *in vivo* studies. *Bioact. Mater* 6 (5), 1223–1229. doi:10.1016/j.bioactmat.2020.10.024

Gao, L. C. Q., Gong, T., Liu, J., and Li, C. (2019). "Ecent advancement of imidazolate framework (ZIF-8) based nanoformulations for synergistic tumor therapy," in *Nanoscale*.

Ge, X., Wong, R., Anisa, A., and Ma, S. (2022). Recent development of metal-organic framework nanocomposites for biomedical applications. *Biomaterials* 281, 121322. doi:10.1016/j.biomaterials.2021.121322

Geng, S., Pan, T., Zhou, W., Cui, H., Wu, L., Li, Z., et al. (2020). Bioactive phospho-therapy with black phosphorus for *in vivo* tumor suppression. *Theranostics* 10 (11), 4720–4736. doi:10.7150/thno.43092

Gill, J., and Gorlick, R. (2021). Advancing therapy for osteosarcoma. *Nat. Rev. Clin. Oncol.* 18 (10), 609–624. doi:10.1038/s41571-021-00519-8

Grassel, S. G. (2014). The role of peripheral nerve fibers and their neurotransmitters in cartilage and bone physiology and pathophysiology. *Arthritis Res. Ther.* 16 (6), 485. doi:10.1186/s13075-014-0485-1

Gui, R., Jin, H., Wang, Z., and Li, J. (2018). Black phosphorus quantum dots: Synthesis, properties, functionalized modification and applications. *Chem. Soc. Rev.* 47 (17), 6795–6823. doi:10.1039/c8cs00387d

Han, W., Duan, X., Ni, K., Li, Y., Chan, C., and Lin, W. (2022). Co-delivery of dihydroartemisinin and pyropheophorbide-iron elicits ferroptosis to potentiate cancer immunotherapy. *Biomaterials* 280, 121315. doi:10.1016/j.biomaterials.2021.121315

Han, X., He, J., Wang, Z., Bai, Z., Qu, P., Song, Z., et al. (2021). Fabrication of silver nanoparticles/gelatin hydrogel system for bone regeneration and fracture treatment. *Drug Deliv.* 28 (1), 319–324. doi:10.1080/10717544.2020.1869865

Harris, E. D. (1992). Copper as a cofactor and regulator of copper, zinc superoxide dismutase. *J. Nutr.* 122 (3), 636–640. doi:10.1093/jn/122.suppl_3.636

Hasegawa, T. (2018). Ultrastructure and biological function of matrix vesicles in bone mineralization. *Histochem Cell Biol.* 149 (4), 289–304. doi:10.1007/s00418-018-1646-0

He, C., Dong, C., Yu, L., Chen, Y., and Hao, Y. (2021). Ultrathin 2D inorganic ancient pigment decorated 3D-printing scaffold enables photonic hyperthermia of osteosarcoma in NIR-II biowindow and concurrently augments bone regeneration. *Adv. Sci. (Weinh)* 8 (19), e2101739. doi:10.1002/advs.202101739

He, G., Ma, Y., Zhu, Y., Yong, L., Liu, X., Wang, P., et al. (2018). Cross talk between autophagy and apoptosis contributes to ZnO nanoparticle-induced human osteosarcoma cell death. *Adv. Healthc. Mater* 7 (17), e1800332. doi:10.1002/adhm.201800332

He, G., Pan, X., Liu, X., Zhu, Y., Ma, Y., Du, C., et al. (2020). HIF-1α-Mediated mitophagy determines ZnO nanoparticle-induced human osteosarcoma cell death both *in vitro* and *in vivo*. *ACS Appl. Mater Interfaces* 12 (43), 48296–48309. doi:10.1021/acsami.0c12139

He, P., Xu, S., Guo, Z., Yuan, P., Liu, Y., Chen, Y., et al. (2022). Pharmacodynamics and pharmacokinetics of PLGA-based doxorubicin-loaded implants for tumor therapy. *Drug Deliv.* 29 (1), 478–488. doi:10.1080/10717544.2022.2032878

Heng, M., Gupta, A., Chung, P. W., Healey, J. H., Vaynrub, M., Rose, P. S., et al. (2020). The role of chemotherapy and radiotherapy in localized extraskeletal osteosarcoma. *Eur. J. Cancer* 125, 130–141. doi:10.1016/j.ejca.2019.07.029

Hoppe, A., Güldal, N. S., and Boccaccini, A. R. (2011). A review of the biological response to ionic dissolution products from bioactive glasses and glass-ceramics. *Biomaterials* 32 (11), 2757–2774. doi:10.1016/j.biomaterials.2011.01.004

Hou, X., Tao, Y., Pang, Y., Li, X., Jiang, G., and Liu, Y. (2018). Nanoparticle-based photothermal and photodynamic immunotherapy for tumor treatment. *Int. J. Cancer* 143 (12), 3050–3060. doi:10.1002/ijc.31717

Hu, J., Jiang, Y., Tan, S., Zhu, K., Cai, T., Zhan, T., et al. (2021). Selenium-doped calcium phosphate biomineral reverses multidrug resistance to enhance bone tumor chemotherapy. *Nanomedicine* 32, 102322. doi:10.1016/j.nano.2020.102322

Hu, X. K., Rao, S. S., Tan, Y. J., Yin, H., Luo, M. J., Wang, Z. X., et al. (2020). Fructose-coated Angstrom silver inhibits osteosarcoma growth and metastasis via promoting ROS-dependent apoptosis through the alteration of glucose metabolism by inhibiting PDK. *Theranostics* 10 (17), 7710–7729. doi:10.7150/thno.45858

Huang, T., Yan, G., and Guan, M. (2020). Zinc homeostasis in bone: Zinc transporters and bone diseases. *Int. J. Mol. Sci.* 21 (4), 1236. doi:10.3390/ijms21041236

Jiang, T., Xu, G., Chen, X., Huang, X., Zhao, J., and Zheng, L. (2019). Impact of hydrogel elasticity and adherence on osteosarcoma cells and osteoblasts. *Adv. Healthc. Mater* 8 (9), e1801587. doi:10.1002/adhm.201801587

Jiang, Z., Li, T., Cheng, H., Zhang, F., Yang, X., Wang, S., et al. (2021). Nanomedicine potentiates mild photothermal therapy for tumor ablation. *Asian J. Pharm. Sci.* 16 (6), 738–761. doi:10.1016/j.ajps.2021.10.001

Jo, D. H., Kim, J. H., Lee, T. G., and Kim, J. H. (2015). Size, surface charge, and shape determine therapeutic effects of nanoparticles on brain and retinal diseases. *Nanomedicine* 11 (7), 1603–1611. doi:10.1016/j.nano.2015.04.015

Jones, J. R. (2013). Review of bioactive glass: From hench to hybrids. *Acta Biomater.* 9 (1), 4457–4486. doi:10.1016/j.actbio.2012.08.023

Kargozar, S., Mozafari, M., Ghodrat, S., Fiume, E., and Baino, F. (2021). Copper-containing bioactive glasses and glass-ceramics: From tissue regeneration to cancer therapeutic strategies. *Mater Sci. Eng. C Mater Biol. Appl.* 121, 111741. doi:10.1016/j.msec.2020.111741

Kim, H. D., Amirthalingam, S., Kim, S. L., Lee, S. S., Rangasamy, J., and Hwang, N. S. (2017). Biomimetic materials and fabrication approaches for bone tissue engineering. *Adv. Healthc. Mater* 6 (23), 1700612. doi:10.1002/adhm.201700612

Koons, G. L., Diba, M., and Mikos, A. G. (2020). Materials design for bone-tissue engineering. *Nat. Rev. Mater.* 5 (8), 584–603. doi:10.1038/s41578-020-0204-2

Kou, L., Chen, C., and Smith, S. C. (2015). Phosphorene: Fabrication, properties, and applications. *J. Phys. Chem. Lett.* 6 (14), 2794–2805. doi:10.1021/acs.jpclett.5b01094

Kovacs, D., Igaz, N., Keskeny, C., Belteky, P., Toth, T., Gaspar, R., et al. (2016). Silver nanoparticles defeat p53-positive and p53-negative osteosarcoma cells by triggering mitochondrial stress and apoptosis. *Sci. Rep.* 6, 27902. doi:10.1038/srep27902

Krol, A., Pomastowski, P., Rafinska, K., Railean-Plugaru, V., and Buszewski, B. (2017). Zinc oxide nanoparticles: Synthesis, antiseptic activity and toxicity mechanism. *Adv. Colloid Interface Sci.* 249, 37–52. doi:10.1016/j.cis.2017.07.033

Lemaster, J. E., and Jokerst, J. V. (2017). What is new in nanoparticle-based photoacoustic imaging? *Wiley Interdiscip. Rev. Nanomed Nanobiotechnol* 9 (1). doi:10.1002/wnan.1404

Li, C., Wang, Q., Gu, X., Kang, Y., Zhang, Y., Hu, Y., et al. (2019). Porous Se@SiO2 nanocomposite promotes migration and osteogenic differentiation of rat bone marrow mesenchymal stem cell to accelerate bone fracture healing in a rat model. *Int. J. Nanomedicine* 14, 3845–3860. doi:10.2147/IJN.S202741

Li, J., Li, J., Pu, Y., Li, S., Gao, W., and He, B. (2021). PDT-enhanced ferroptosis by a polymer nanoparticle with pH-activated singlet oxygen generation and superb biocompatibility for cancer therapy. *Biomacromolecules* 22 (3), 1167–1176. doi:10.1021/acs.biomac.0c01679

Li, S., Sun, W., Wang, H., Zuo, D., Hua, Y., and Cai, Z. (2015). Research progress on the multidrug resistance mechanisms of osteosarcoma chemotherapy and reversal. *Tumour Biol.* 36 (3), 1329–1338. doi:10.1007/s13277-015-3181-0

Li W, W., Yang, J., Luo, L., Jiang, M., Qin, B., Yin, H., et al. (2019). Targeting photodynamic and photothermal therapy to the endoplasmic reticulum enhances immunogenic cancer cell death. *Nat. Commun.* 10 (1), 3349. doi:10.1038/s41467-019-11269-8

Li, X., Wang, Y., Chen, Y., Zhou, P., Wei, K., Wang, H., et al. (2020). Hierarchically constructed selenium-doped bone-mimetic nanoparticles promote ROS-mediated autophagy and apoptosis for bone tumor inhibition. *Biomaterials* 257, 120253. doi:10.1016/j.biomaterials.2020.120253

Li, Y., Xiong, J., Guo, W., Jin, Y., Miao, W., Wang, C., et al. (2021). Decomposable black phosphorus nano-assembly for controlled delivery of cisplatin and inhibition of breast cancer metastasis. *J. Control Release* 335, 59–74. doi:10.1016/j.jconrel.2021.05.013

Li, Z., Fu, Q., Ye, J., Ge, X., Wang, J., Song, J., et al. (2020). Ag(+) -coupled black phosphorus vesicles with emerging NIR-II photoacoustic imaging performance for cancer immune-dynamic therapy and fast wound healing. *Angew. Chem. Int. Ed. Engl.* 59 (49), 22202–22209. doi:10.1002/anie.202009609

Li, Z., Zhang, X., Ouyang, J., Chu, D., Han, F., Shi, L., et al. (2021). Ca(2+)-supplying black phosphorus-based scaffolds fabricated with microfluidic technology for osteogenesis. *Bioact. Mater* 6 (11), 4053–4064. doi:10.1016/j.bioactmat.2021.04.014

Liao, J., Han, R., Wu, Y., and Qian, Z. (2021). Review of a new bone tumor therapy strategy based on bifunctional biomaterials. *Bone Res.* 9 (1), 18. doi:10.1038/s41413-021-00139-z

Liu, J., Dong, J., Zhang, T., and Peng, Q. (2018). Graphene-based nanomaterials and their potentials in advanced drug delivery and cancer therapy. *J. Control Release* 286, 64–73. doi:10.1016/j.jconrel.2018.07.034

Liu, J., Zheng, J., Nie, H., Zhang, D., Cao, D., Xing, Z., et al. (2019). Molybdenum disulfide-based hyaluronic acid-guided multifunctional theranostic nanoplatform for magnetic resonance imaging and synergetic chemo-photothermal therapy. *J. Colloid Interface Sci.* 548, 131–144. doi:10.1016/j.jcis.2019.04.022

Liu M, M., O'Connor, R. S., Trefely, S., Graham, K., Snyder, N. W., and Beatty, G. L. (2019). Metabolic rewiring of macrophages by CpG potentiates clearance of cancer cells and overcomes tumor-expressed CD47-mediated 'don't-eat-me' signal. *Nat. Immunol.* 20 (3), 265–275. doi:10.1038/s41590-018-0292-y

Liu W, W., Dong, A., Wang, B., and Zhang, H. (2021). Current advances in black phosphorus-based drug delivery systems for cancer therapy. *Adv. Sci. (Weinh)* 8 (5), 2003033. doi:10.1002/advs.202003033

Liu, Y., Raina, D. B., Sebastian, S., Nagesh, H., Isaksson, H., Engellau, J., et al. (2021). Sustained and controlled delivery of doxorubicin from an *in-situ* setting biphasic hydroxyapatite carrier for local treatment of a highly proliferative human osteosarcoma. *Acta Biomater.* 131, 555–571. doi:10.1016/j.actbio.2021.07.016

Long, J., Zhang, W., Chen, Y., Teng, B., Liu, B., Li, H., et al. (2021). Multifunctional magnesium incorporated scaffolds by 3D-Printing for comprehensive postsurgical management of osteosarcoma. *Biomaterials* 275, 120950. doi:10.1016/j.biomaterials.2021.120950

Ma, H., He, C., Cheng, Y., Li, D., Gong, Y., Liu, J., et al. (2014). PLK1shRNA and doxorubicin co-loaded thermosensitive PLGA-PEG-PLGA hydrogels for osteosarcoma treatment. *Biomaterials* 35 (30), 8723–8734. doi:10.1016/j.biomaterials.2014.06.045

Ma, L., Feng, X., Liang, H., Wang, K., Song, Y., Tan, L., et al. (2020). A novel photothermally controlled multifunctional scaffold for clinical treatment of osteosarcoma and tissue regeneration. *Mater. Today* 36, 48–62. doi:10.1016/j.mattod.2019.12.005

Maeda, H. (2001). The enhanced permeability and retention (EPR) effect in tumor vasculature: The key role of tumor-selective macromolecular drug targeting. *Adv. Enzyme Regul.* 41 (1), 189–207. doi:10.1016/s0065-2571(00)00013-3

Malik, P., and Mukherjee, T. K. (2018). Recent advances in gold and silver nanoparticle based therapies for lung and breast cancers. *Int. J. Pharm.* 553 (1-2), 483–509. doi:10.1016/j.ijpharm.2018.10.048

Mao, C., Xiang, Y., Liu, X., Cui, Z., Yang, X., Li, Z., et al. (2018). Repeatable photodynamic therapy with triggered signaling pathways of fibroblast cell proliferation and differentiation to promote bacteria-accompanied wound healing. *ACS Nano* 12 (2), 1747–1759. doi:10.1021/acsnano.7b08500

Marques, C., Ferreira, J. M., Andronescu, E., Ficai, D., Sonmez, M., and Ficai, A. (2014). Multifunctional materials for bone cancer treatment. *Int. J. Nanomedicine* 9, 2713–2725. doi:10.2147/IJN.S55943

Meazza, C., and Scanagatta, P. (2016). Metastatic osteosarcoma: A challenging multidisciplinary treatment. *Expert Rev. Anticancer Ther.* 16 (5), 543–556. doi:10.1586/14737140.2016.1168697

Mei, Z., Gao, D., Hu, D., Zhou, H., Ma, T., Huang, L., et al. (2020). Activatable NIR-II photoacoustic imaging and photochemical synergistic therapy of MRSA infections using miniature Au/Ag nanorods. *Biomaterials* 251, 120092. doi:10.1016/j.biomaterials.2020.120092

Mendel, R. R., Smith, A. G., Marquet, A., and Warren, M. J. (2007). Metal and cofactor insertion. *Nat. Prod. Rep.* 24 (5), 963–971. doi:10.1039/b703112m

Miao, Y., Shi, X., Li, Q., Hao, L., Liu, L., Liu, X., et al. (2019). Engineering natural matrices with black phosphorus nanosheets to generate multi-functional therapeutic nanocomposite hydrogels. *Biomater. Sci.* 7 (10), 4046–4059. doi:10.1039/c9bm01072f

Mirabello, L., Troisi, R. J., and Savage, S. A. (2009). Osteosarcoma incidence and survival rates from 1973 to 2004: Data from the surveillance, epidemiology, and end results program. *Cancer* 115 (7), 1531–1543. doi:10.1002/cncr.24121

Muscolo, D. L., Ayerza, M. A., Aponte-Tinao, L. A., and Ranalletta, M. (2005). Partial epiphyseal preservation and intercalary allograft reconstruction in high-grade metaphyseal osteosarcoma of the knee. *J. Bone Jt. Surg. Am.* 87 (2), 226–236. doi:10.2106/JBJS.E.00253

Norgaard, R., Kassem, M., and Rattan, S. I. (2006). Heat shock-induced enhancement of osteoblastic differentiation of hTERT-immortalized mesenchymal stem cells. *Ann. N. Y. Acad. Sci.* 1067, 443–447. doi:10.1196/annals.1354.063

Oliveira, T. M., Berti, F. C. B., Gasoto, S. C., Schneider, B., Jr., Stimamiglio, M. A., and Berti, L. F. (2021). Calcium phosphate-based bioceramics in the treatment of

osteosarcoma: Drug delivery composites and magnetic hyperthermia agents. *Front. Med. Technol.* 3, 700266. doi:10.3389/fmedt.2021.700266

Palacios, C. (2006). The role of nutrients in bone health, from A to Z. *Crit. Rev. Food Sci. Nutr.* 46 (8), 621–628. doi:10.1080/10408390500466174

Pan, W., Dai, C., Li, Y., Yin, Y., Gong, L., Machuki, J. O., et al. (2020). PRP-chitosan thermoresponsive hydrogel combined with black phosphorus nanosheets as injectable biomaterial for biotherapy and phototherapy treatment of rheumatoid arthritis. *Biomaterials* 239, 119851. doi:10.1016/j.biomaterials.2020.119851

Pang, K. L., and Chin, K. Y. (2019). Emerging anticancer potentials of selenium on osteosarcoma. *Int. J. Mol. Sci.* 20 (21), 5318. doi:10.3390/ijms20215318

Poon, W., Zhang, Y. N., Ouyang, B., Kingston, B. R., Wu, J. L. Y., Wilhelm, S., et al. (2019). Elimination pathways of nanoparticles. *ACS Nano* 13 (5), 5785–5798. doi:10.1021/acsnano.9b01383

Prabhu, K. S., and Lei, X. G. (2016). Selenium. *Adv. Nutr.* 7 (2), 415–417. doi:10.3945/an.115.010785

Qi, F., Ji, P., Chen, Z., Wang, L., Yao, H., Huo, M., et al. (2021). Photosynthetic cyanobacteria-hybridized black phosphorus nanosheets for enhanced tumor photodynamic therapy. *Small* 17 (42), e2102113. doi:10.1002/smll.202102113

Qian, Y., Yuan, W. E., Cheng, Y., Yang, Y., Qu, X., and Fan, C. (2019). Concentrically integrative bioassembly of a three-dimensional black phosphorus nanoscaffold for restoring neurogenesis, angiogenesis, and immune homeostasis. *Nano Lett.* 19 (12), 8990–9001. doi:10.1021/acs.nanolett.9b03980

Qing, T., Mahmood, M., Zheng, Y., Biris, A. S., Shi, L., and Casciano, D. A. (2018). A genomic characterization of the influence of silver nanoparticles on bone differentiation in MC3T3-E1 cells. *J. Appl. Toxicol.* 38 (2), 172–179. doi:10.1002/jat.3528

Qing, Y., Li, R., Li, S., Li, Y., Wang, X., and Qin, Y. (2020). Advanced black phosphorus nanomaterials for bone regeneration. *Int. J. Nanomedicine* 15, 2045–2058. doi:10.2147/IJN.S246336

Qiu, M., Wang, D., Liang, W., Liu, L., Zhang, Y., Chen, X., et al. (2018). Novel concept of the smart NIR-light-controlled drug release of black phosphorus nanostructure for cancer therapy. *Proc. Natl. Acad. Sci. U. S. A.* 115 (3), 501–506. doi:10.1073/pnas.1714421115

Ritter, J., and Bielack, S. S. (2010). Osteosarcoma. *Ann. Oncol.* 21 (7), vii320–325. doi:10.1093/annonc/mdq276

Rojas, G. A., Hubbard, A. K., Diessner, B. J., Ribeiro, K. B., and Spector, L. G. (2021). International trends in incidence of osteosarcoma (1988-2012). *Int. J. Cancer* 149 (5), 1044–1053. doi:10.1002/ijc.33673

Sayed, S., Faruq, O., Hossain, M., Im, S. B., Kim, Y. S., and Lee, B. T. (2019). Thermal cycling effect on osteogenic differentiation of MC3T3-E1 cells loaded on 3D-porous Biphasic Calcium Phosphate (BCP) scaffolds for early osteogenesis. *Mater Sci. Eng. C Mater Biol. Appl.* 105, 110027. doi:10.1016/j.msec.2019.110027

Shao, J., Ruan, C., Xie, H., Chu, P. K., and Yu, X. F. (2020). Photochemical activity of black phosphorus for near-infrared light controlled *in situ* biomineralization. *Adv. Sci. (Weinh)* 7 (14), 2000439. doi:10.1002/advs.202000439

Shao, J., Xie, H., Huang, H., Li, Z., Sun, Z., Xu, Y., et al. (2016). Biodegradable black phosphorus-based nanospheres for *in vivo* photothermal cancer therapy. *Nat. Commun.* 7, 12967. doi:10.1038/ncomms12967

Shi, J., Li, J., Wang, Y., Cheng, J., and Zhang, C. Y. (2020). Recent advances in MoS2-based photothermal therapy for cancer and infectious disease treatment. *J. Mater Chem. B* 8 (27), 5793–5807. doi:10.1039/d0tb01018a

Shin, H., Jo, S., and Mikos, A. G. (2003). Biomimetic materials for tissue engineering. *Biomaterials* 24 (24), 4353–4364. doi:10.1016/s0142-9612(03)00339-9

Shin, M. H., Park, E. Y., Han, S., Jung, H. S., Keum, D. H., Lee, G. H., et al. (2019). Multimodal cancer theranosis using hyaluronate-conjugated molybdenum disulfide. *Adv. Healthc. Mater* 8 (1), e1801036. doi:10.1002/adhm.201801036

Shui, C., and Scutt, A. (2001). Mild heat shock induces proliferation, alkaline phosphatase activity, and mineralization in human bone marrow stromal cells and Mg-63 cells *in vitro*. *J. Bone Min. Res.* 16 (4), 731–741. doi:10.1359/jbmr.2001.16.4.731

Solak, K., Mavi, A., and Yilmaz, B. (2021). Disulfiram-loaded functionalized magnetic nanoparticles combined with copper and sodium nitroprusside in breast cancer cells. *Mater Sci. Eng. C Mater Biol. Appl.* 119, 111452. doi:10.1016/j.msec.2020.111452

Song, Y., Wu, H., Gao, Y., Li, J., Lin, K., Liu, B., et al. (2020). Zinc silicate/nano-hydroxyapatite/collagen scaffolds promote angiogenesis and bone regeneration via the p38 MAPK pathway in activated monocytes. *ACS Appl. Mater. Interfaces* 12 (14), 16058–16075. doi:10.1021/acsami.0c00470

Souhami, R. L. (1989). Chemotherapy for osteosarcoma. *Br. J. Cancer* 59 (2), 147–148. doi:10.1038/bjc.1989.30

Stacpoole, P. W. (2017). Therapeutic targeting of the pyruvate dehydrogenase complex/pyruvate dehydrogenase kinase (PDC/PDK) Axis in cancer. *J. Natl. Cancer Inst.* 109 (11). doi:10.1093/jnci/djx071

Steinbacher, T., and Ebnet, K. (2018). The regulation of junctional actin dynamics by cell adhesion receptors. *Histochem Cell Biol.* 150 (4), 341–350. doi:10.1007/s00418-018-1691-8

Sun, Z., Xie, H., Tang, S., Yu, X. F., Guo, Z., Shao, J., et al. (2015). Ultrasmall black phosphorus quantum dots: Synthesis and use as photothermal agents. *Angew. Chem. Int. Ed. Engl.* 54 (39), 11526–11530. doi:10.1002/anie.201506154

Sun, Z., Zhao, Y., Li, Z., Cui, H., Zhou, Y., Li, W., et al. (2017). TiL4 -coordinated black phosphorus quantum dots as an efficient contrast agent for *in vivo* photoacoustic imaging of cancer. *Small* 13 (11), 1602896. doi:10.1002/smll.201602896

Takeuchi, A., Yamamoto, N., Hayashi, K., Matsubara, H., Miwa, S., Igarashi, K., et al. (2019). Joint-preservation surgery for pediatric osteosarcoma of the knee joint. *Cancer Metastasis Rev.* 38 (4), 709–722. doi:10.1007/s10555-019-09835-z

Tan, B., Wu, Y., Wu, Y., Shi, K., Han, R., Li, Y., et al. (2021). Curcumin-Microsphere/IR820 hybrid bifunctional hydrogels for *in situ* osteosarcoma chemo-co-thermal therapy and bone reconstruction. *ACS Appl. Mater Interfaces* 13 (27), 31542–31553. doi:10.1021/acsami.1c08775

Tao, W., Zhu, X., Yu, X., Zeng, X., Xiao, Q., Zhang, X., et al. (2017). Black phosphorus nanosheets as a robust delivery platform for cancer theranostics. *Adv. Mater* 29 (1), 1603276. doi:10.1002/adma.201603276

Tong, L., Liao, Q., Zhao, Y., Huang, H., Gao, A., Zhang, W., et al. (2019). Near-infrared light control of bone regeneration with biodegradable photothermal osteoimplant. *Biomaterials* 193, 1–11. doi:10.1016/j.biomaterials.2018.12.008

Tortella, G. R., Rubilar, O., Duran, N., Diez, M. C., Martinez, M., Parada, J., et al. (2020). Silver nanoparticles: Toxicity in model organisms as an overview of its hazard for human health and the environment. *J. Hazard Mater* 390, 121974. doi:10.1016/j.jhazmat.2019.121974

Truong, L. B., Medina Cruz, D., Mostafavi, E., O'Connell, C. P., and Webster, T. J. (2021). Advances in 3D-printed surface-modified Ca-Si bioceramic structures and their potential for bone tumor therapy. *Mater. (Basel)* 14 (14), 3844. doi:10.3390/ma14143844

Tsuchiya, H., Kanazawa, Y., Abdel-Wanis, M. E., Asada, N., Abe, S., Isu, K., et al. (2002). Effect of timing of pulmonary metastases identification on prognosis of patients with osteosarcoma: The Japanese musculoskeletal oncology group study. *J. Clin. Oncol.* 20 (16), 3470–3477. doi:10.1200/JCO.2002.11.028

Turnbull, G., Clarke, J., Picard, F., Riches, P., Jia, L., Han, F., et al. (2018). 3D bioactive composite scaffolds for bone tissue engineering. *Bioact. Mater* 3 (3), 278–314. doi:10.1016/j.bioactmat.2017.10.001

Voiry, D., Fullon, R., Yang, J., de Carvalho Castro, E. S. C., Kappera, R., Bozkurt, I., et al. (2016). The role of electronic coupling between substrate and 2D MoS2 nanosheets in electrocatalytic production of hydrogen. *Nat. Mater* 15 (9), 1003–1009. doi:10.1038/nmat4660

Wang J L, J. L., Xu, J. K., Hopkins, C., Chow, D. H., and Qin, L. (2020). Biodegradable magnesium-based implants in orthopedics-A general review and perspectives. *Adv. Sci. (Weinh)* 7 (8), 1902443. doi:10.1002/advs.201902443

Wang, L., Hu, P., Jiang, H., Zhao, J., Tang, J., Jiang, D., et al. (2022). Mild hyperthermia-mediated osteogenesis and angiogenesis play a critical role in magnetothermal composite-induced bone regeneration. *Nano Today* 43, 101401. doi:10.1016/j.nantod.2022.101401

Wang, R., Liu, W., Wang, Q., Li, G., Wan, B., Sun, Y., et al. (2020). Anti-osteosarcoma effect of hydroxyapatite nanoparticles both *in vitro* and *in vivo* by downregulating the FAK/PI3K/Akt signaling pathway. *Biomater. Sci.* 8 (16), 4426–4437. doi:10.1039/d0bm00898b

Wang, S., Shao, J., Li, Z., Ren, Q., Yu, X. F., and Liu, S. (2019). Black phosphorus-based multimodal nanoagent: Showing targeted combinatory therapeutics against cancer metastasis. *Nano Lett.* 19 (8), 5587–5594. doi:10.1021/acs.nanolett.9b02127

Wang, Y., Hu, X., Zhang, L., Zhu, C., Wang, J., Li, Y., et al. (2019). Bioinspired extracellular vesicles embedded with black phosphorus for molecular recognition-guided biomineralization. *Nat. Commun.* 10 (1), 2829. doi:10.1038/s41467-019-10761-5

Wang, Z., Tang, X., Wang, X., Yang, D., Yang, C., Lou, Y., et al. (2016). Near-infrared light-induced dissociation of zeolitic imidazole framework-8 (ZIF-8) with encapsulated CuS nanoparticles and their application as a therapeutic nanoplatform. *Chem. Commun. (Camb)* 52 (82), 12210–12213. doi:10.1039/c6cc06616j

Wang, Z. X., Chen, C. Y., Wang, Y., Li, F. X. Z., Huang, J., Luo, Z. W., et al. (2019). Ångstrom-scale silver particles as a promising agent for low-toxicity broad-spectrum potent anticancer therapy. *Adv. Funct. Mater.* 29 (23), 1808556. doi:10.1002/adfm.201808556

Wang, Z., Zhao, J., Tang, W., Hu, L., Chen, X., Su, Y., et al. (2019). Multifunctional nanoengineered hydrogels consisting of black phosphorus

nanosheets upregulate bone formation. *Small* 15 (41), e1901560. doi:10.1002/smll.201901560

Ward, W. G., Mikaelian, K., Dorey, F., Mirra, J. M., Sassoon, A., Holmes, E. C., et al. (1994). Pulmonary metastases of stage IIB extremity osteosarcoma and subsequent pulmonary metastases. *J. Clin. Oncol.* 12 (9), 1849–1858. doi:10.1200/JCO.1994.12.9.1849

Windhagen, H., Radtke, K., Weizbauer, A., Diekmann, J., Noll, Y., Kreimeyer, U., et al. (2013). Biodegradable magnesium-based screw clinically equivalent to titanium screw in hallux valgus surgery: Short term results of the first prospective, randomized, controlled clinical pilot study. *Biomed. Eng. Online* 12, 62. doi:10.1186/1475-925X-12-62

Wong, K. C., and Kumta, S. M. (2013). Joint-preserving tumor resection and reconstruction using image-guided computer navigation. *Clin. Orthop. Relat. Res.* 471 (3), 762–773. doi:10.1007/s11999-012-2536-8

Woolbright, B. L., Rajendran, G., Harris, R. A., and Taylor, J. A., 3rd (2019). Metabolic flexibility in cancer: Targeting the pyruvate dehydrogenase kinase: pyruvate dehydrogenase Axis. *Mol. Cancer Ther.* 18 (10), 1673–1681. doi:10.1158/1535-7163.MCT-19-0079

Wu, J. (2021). The enhanced permeability and retention (EPR) effect: The significance of the concept and methods to enhance its application. *J. Pers. Med.* 11 (8), 771. doi:10.3390/jpm11080771

Wu, Y., He, G., Zhang, Y., Liu, Y., Li, M., Wang, X., et al. (2016). Unique antitumor property of the Mg-Ca-Sr alloys with addition of Zn. *Sci. Rep.* 6, 21736. doi:10.1038/srep21736

Xie, Z., Peng, M., Lu, R., Meng, X., Liang, W., Li, Z., et al. (2020). Black phosphorus-based photothermal therapy with aCD47-mediated immune checkpoint blockade for enhanced cancer immunotherapy. *Light Sci. Appl.* 9, 161. doi:10.1038/s41377-020-00388-3

Xu, L., Wang, Y. Y., Huang, J., Chen, C. Y., Wang, Z. X., and Xie, H. (2020). Silver nanoparticles: Synthesis, medical applications and biosafety. *Theranostics* 10 (20), 8996–9031. doi:10.7150/thno.45413

Xu, Y., Ren, F., Liu, H., Zhang, H., Han, Y., Liu, Z., et al. (2019). Cholesterol-modified black phosphorus nanospheres for the first NIR-II fluorescence bioimaging. *ACS Appl. Mater Interfaces* 11 (24), 21399–21407. doi:10.1021/acsami.9b05825

Yang, B., Yin, J., Chen, Y., Pan, S., Yao, H., Gao, Y., et al. (2018). 2D-Black-Phosphorus-Reinforced 3D-printed scaffolds:A stepwise countermeasure for osteosarcoma. *Adv. Mater* 30 (10), 1705611. doi:10.1002/adma.201705611

Yang, D., Yang, G., Yang, P., Lv, R., Gai, S., Li, C., et al. (2017). Assembly of Au plasmonic photothermal agent and iron oxide nanoparticles on ultrathin black phosphorus for targeted photothermal and photodynamic cancer therapy. *Adv. Funct. Mater.* 27 (18), 1700371. doi:10.1002/adfm.201700371

Yang, J., Qin, H., Chai, Y., Zhang, P., Chen, Y., Yang, K., et al. (2021). Molecular mechanisms of osteogenesis and antibacterial activity of Cu-bearing Ti alloy in a bone defect model with infection *in vivo*. *J. Orthop. Transl.* 27, 77–89. doi:10.1016/j.jot.2020.10.004

Yang, N., Gong, F., Cheng, L., Lei, H., Li, W., Sun, Z., et al. (2021). Biodegradable magnesium alloy with eddy thermal effect for effective and accurate magnetic hyperthermia ablation of tumors. *Natl. Sci. Rev.* 8 (1), nwaa122. doi:10.1093/nsr/nwaa122

Yang, Q., Yin, H., Xu, T., Zhu, D., Yin, J., Chen, Y., et al. (2020). Engineering 2D mesoporous Silica@MXene-integrated 3D-printing scaffolds for combinatory osteosarcoma therapy and NO-augmented bone regeneration. *Small* 16 (14), e1906814. doi:10.1002/smll.201906814

Yang, Y., Guo, L., Wang, Z., Liu, P., Liu, X., Ding, J., et al. (2021c). Targeted silver nanoparticles for rheumatoid arthritis therapy via macrophage apoptosis and Re-polarization. *Biomaterials* 264, 120390. doi:10.1016/j.biomaterials.2020.120390

Yang, Y., Tian, Q., Wu, S., Li, Y., Yang, K., Yan, Y., et al. (2021d). Blue light-triggered Fe(2+)-release from monodispersed ferrihydrite nanoparticles for cancer iron therapy. *Biomaterials* 271, 120739. doi:10.1016/j.biomaterials.2021.120739

Yin, F., Hu, K., Chen, S., Wang, D., Zhang, J., Xie, M., et al. (2017). Black phosphorus quantum dot based novel siRNA delivery systems in human pluripotent teratoma PA-1 cells. *J. Mater Chem. B* 5 (27), 5433–5440. doi:10.1039/c7tb01068k

Zafeiris, K., Brasinika, D., Karatza, A., Koumoulos, E., Karoussis, I. K., Kyriakidou, K., et al. (2021). Additive manufacturing of hydroxyapatite-chitosan-genipin composite scaffolds for bone tissue engineering applications. *Mater Sci. Eng. C Mater Biol. Appl.* 119, 111639. doi:10.1016/j.msec.2020.111639

Zakhireh, S., Adibkia, K., Beygi-Khosrowshahi, Y., and Barzegar-Jalali, M. (2021). Osteogenesis promotion of selenium-doped hydroxyapatite for application as bone scaffold. *Biol. Trace Elem. Res.* 199 (5), 1802–1811. doi:10.1007/s12011-020-02309-2

Zan, R., Ji, W., Qiao, S., Wu, H., Wang, W., Ji, T., et al. (2020). Biodegradable magnesium implants: A potential scaffold for bone tumor patients. *Sci. China Mater.* 64 (4), 1007–1020. doi:10.1007/s40843-020-1509-2

Zan, R., Wang, H., Cai, W., Ni, J., Luthringer-Feyerabend, B. J. C., Wang, W., et al. (2022). Controlled release of hydrogen by implantation of magnesium induces P53-mediated tumor cells apoptosis. *Bioact. Mater* 9, 385–396. doi:10.1016/j.bioactmat.2021.07.026

Zeng, H., Cao, J. J., and Combs, G. F., Jr. (2013). Selenium in bone health: Roles in antioxidant protection and cell proliferation. *Nutrients* 5 (1), 97–110. doi:10.3390/nu5010097

Zeng, X., Luo, M., Liu, G., Wang, X., Tao, W., Lin, Y., et al. (2018). Polydopamine-modified black phosphorous nanocapsule with enhanced stability and photothermal performance for tumor multimodal treatments. *Adv. Sci. (Weinh)* 5 (10), 1800510. doi:10.1002/advs.201800510

Zhang, R., Lee, P., Lui, V. C., Chen, Y., Liu, X., Lok, C. N., et al. (2015). Silver nanoparticles promote osteogenesis of mesenchymal stem cells and improve bone fracture healing in osteogenesis mechanism mouse model. *Nanomedicine* 11 (8), 1949–1959. doi:10.1016/j.nano.2015.07.016

Zhang, W., Yu, L., Jiang, Y., and Guo, C. (2021). Phycocyanin-functionalized black phosphorus quantum dots enhance PDT/PTT therapy by inducing ROS and irreparable DNA damage. *Biomater. Sci.* 9 (15), 5302–5318. doi:10.1039/d1bm00106j

Zhang, X. F., Liu, Z. G., Shen, W., and Gurunathan, S. (2016). Silver nanoparticles: Synthesis, characterization, properties, applications, and therapeutic approaches. *Int. J. Mol. Sci.* 17 (9), 1534. doi:10.3390/ijms17091534

Zhang, X., Li, X., Zheng, C., Yang, C., Zhang, R., Wang, A., et al. (2022). Ferroptosis, a new form of cell death defined after radiation exposure. *Int. J. Radiat. Biol.* 98, 1201–1209. doi:10.1080/09553002.2022.2020358

Zhang, X., Xie, H., Liu, Z., Tan, C., Luo, Z., Li, H., et al. (2015). Black phosphorus quantum dots. *Angew. Chem. Int. Ed. Engl.* 54 (12), 3653–3657. doi:10.1002/anie.201409400

Zhang, Y., Xu, J., Ruan, Y. C., Yu, M. K., O'Laughlin, M., Wise, H., et al. (2016). Implant-derived magnesium induces local neuronal production of CGRP to improve bone-fracture healing in rats. *Nat. Med.* 22 (10), 1160–1169. doi:10.1038/nm.4162

Zhao, D., Huang, S., Lu, F., Wang, B., Yang, L., Qin, L., et al. (2016). Vascularized bone grafting fixed by biodegradable magnesium screw for treating osteonecrosis of the femoral head. *Biomaterials* 81, 84–92. doi:10.1016/j.biomaterials.2015.11.038

Zhao, D., Witte, F., Lu, F., Wang, J., Li, J., and Qin, L. (2017). Current status on clinical applications of magnesium-based orthopaedic implants: A review from clinical translational perspective. *Biomaterials* 112, 287–302. doi:10.1016/j.biomaterials.2016.10.017

Zhao, Y., Peng, X., Xu, X., Wu, M., Sun, F., Xin, Q., et al. (2023). Chitosan based photothermal scaffold fighting against bone tumor-related complications: Recurrence, infection, and defects. *Carbohydr. Polym.* 300, 120264. doi:10.1016/j.carbpol.2022.120264

Zhou, W., Zhang, Y., Meng, S., Xing, C., Ma, M., Liu, Z., et al. (2021). Micro-/Nano-Structures on biodegradable magnesium@PLGA and their cytotoxicity, photothermal, and anti-tumor effects. *Small Methods* 5 (2), e2000920. doi:10.1002/smtd.202000920

Zhu, X., Li, L., Tang, J., Yang, C., Yu, H., Liu, K., et al. (2022). Cascade-responsive nano-assembly for efficient photothermal-chemo synergistic inhibition of tumor metastasis by targeting cancer stem cells. *Biomaterials* 280, 121305. doi:10.1016/j.biomaterials.2021.121305

frontiers | Frontiers in Molecular Biosciences

TYPE Review
PUBLISHED 26 January 2023
DOI 10.3389/fmolb.2023.1121429

OPEN ACCESS

EDITED BY
Zhanzhan Zhang,
Tianjin Medical University, China

REVIEWED BY
Jingyu Wang,
Tianjin Medical University, China
Jiulong Zhao,
Naval Medical University, China

*CORRESPONDENCE
Yi Yi,
shkudo221@gmail.com

SPECIALTY SECTION
This article was submitted to Nanobiotechnology, a section of the journal Frontiers in Molecular Biosciences

RECEIVED 11 December 2022
ACCEPTED 17 January 2023
PUBLISHED 26 January 2023

CITATION
Liu Y, Yi Y, Zhong C, Ma Z, Wang H, Dong X, Yu F, Li J, Chen Q, Lin C and Li X (2023), Advanced bioactive nanomaterials for diagnosis and treatment of major chronic diseases.
Front. Mol. Biosci. 10:1121429.
doi: 10.3389/fmolb.2023.1121429

Advanced bioactive nanomaterials for diagnosis and treatment of major chronic diseases

Yongfei Liu[1], Yi Yi[1]*, Chengqian Zhong[2], Zecong Ma[1], Haifeng Wang[1], Xingmo Dong[1], Feng Yu[1], Jing Li[1], Qinqi Chen[1], Chaolu Lin[1] and Xiaohong Li[2]

[1]Department of Urology, Longyan First Hospital Affiliated to Fujian Medical University, Longyan, China, [2]Longyan First Hospital Affiliated to Fujian Medical University, Longyan, China

With the rapid innovation of nanoscience and technology, nanomaterials have also been deeply applied in the medical and health industry and become one of the innovative methods to treat many diseases. In recent years, bioactive nanomaterials have attracted extensive attention and have made some progress in the treatment of some major chronic diseases, such as nervous system diseases and various malignant tumors. Bioactive nanomaterials depend on their physical and chemical properties (crystal structure, surface charge, surface functional groups, morphology, and size, etc.) and direct produce biological activity and play to the role of the treatment of diseases, compared with the traditional nanometer pharmaceutical preparations, biological active nano materials don't exert effects through drug release, way more directly, also is expected to be more effective for the treatment of diseases. However, further studies are needed in the evaluation of biological effects, fate *in vivo*, structure-activity relationship and clinical transformation of bionanomaterials. Based on the latest research reports, this paper reviews the application of bioactive nanomaterials in the diagnosis and treatment of major chronic diseases and analyzes the technical challenges and key scientific issues faced by bioactive nanomaterials in the diagnosis and treatment of diseases, to provide suggestions for the future development of this field.

KEYWORDS

nanomaterials (A), neurodegenerative disease, cancer, bioactivity, biomimetic nanomaterials, inorganic nanomaterials, organic nanomaterials, nanozyme

1 Introduction

Nanomaterials are short for nanoscale structural materials. In a narrow sense, they refer to solid materials composed of nanoparticles with a size of no more than 100 nm, and in a broad sense, they refer to all kinds of solid ultra-fine materials with at least one dimension of the three-dimensional spatial scale of microstructure in the nanometer scale (1–100 nm) (Cheng et al., 2020). Nanotechnology is a comprehensive subject with strong intersection, and the research content involves a broad field of modern science and technology, from microtechnology including microelectronics to nanotechnology. Human beings are becoming more and more in-depth to the microscopic world, and the level of people's understanding and transformation of the microscopic world has increased to an unprecedented height. At present, nanotechnology has included nano-electronics, nano-mechanics, nanomaterials science, nano-chemistry, nano-biology, and other disciplines. With the continuous research and development of nanoscience and technology, it has been widely used in energy and environment, electronics and information, medicine, and health

(Zheng et al., 2015; Li et al., 2017a; Kumawat et al., 2017), etc., and has a profound impact on the rapid development of related industries. Biological detection, drug delivery, and disease diagnosis and prevention have become the research hotspots of nanoscience in the field of health care. Currently, ph-responsive, and enzyme-responsive nanomaterials, which are widely used in targeted drug delivery and controlled drug release (Zhao et al., 2021), are materials that can change their physical and chemical properties (such as surface charge and chemical structure) in response to external stimuli such as light and heat, reactive oxygen species (ROS) levels, and pH changes. In recent years, bioactive nanomaterials have attracted extensive attention and attention. Bioactive nanomaterials are bioactive nanomaterials that interact with proteins, cells or tissues *in vivo* and cause biological reactions depending on their physical and chemical properties (crystal structure, surface charge, surface functional group, morphology and size, etc.) (Zhou et al., 2019a; Xu et al., 2021). Since Larry Hench in the 60 s of last century Since the concept of bioactive materials was first proposed in the 1960s by discovering that bioactive glass can closely integrate with the surrounding bone tissue at the interface (Henchll, 2002), bioactive nanomaterials have been developed with nanoscale size and precise structure, which enable them to accurately regulate the interaction between materials and biological systems, and thus exhibit unique biological activities (Islam et al., 2020). This is also far beyond the scope defined by Larry Hench in the past. Due to the absence of therapeutic drug loading and drug release process, bioactive nanomaterials are more direct than the target mode of action, which is expected to achieve better therapeutic effects, and have made certain research progress in the treatment of some major chronic diseases such as nervous system diseases and various malignant tumors. However, there are still few systematic summaries of bioactive nanomaterials and their related applications. This article reviews the latest research progress and reports of bioactive nanomaterials in the diagnosis and treatment of major chronic diseases, systematically introduces the typical applications of bioactive nanomaterials in the biomedical field and analyzes the technical challenges and key scientific issues faced by bioactive nanomaterials in the diagnosis and treatment of diseases, to provide suggestions for the future development of this field.

2 Influencing factors of biological activity of nanomaterials

Traditional biological nanomaterials respond to external stimuli such as pH changes, reactive oxygen species levels, light and heat, and then change their physical and chemical properties such as surface charge and chemical structure to play a role. However, the chemical structure and surface properties of bioactive nanomaterials are usually relatively clear (Kerativitayanan et al., 2015), and they directly interact with proteins, cells, or tissues *in vivo* and cause biological reactions through their physical structure, surface properties and nano-topography (Zhou et al., 2019b). Therefore, these characteristics such as structure and properties are important factors affecting the biological activity of materials.

2.1 Nano-morphology

Studies have found that the adhesion of Embryonic stem cells (ESCs) is affected by the roughness of the surface (Chen et al., 2012). Compared with the rough surface, the smooth surface is easier to make undifferentiated cells adhere. In addition, rough surfaces can induce the differentiation of ESCs, while smooth surfaces can maintain the self-renewal ability of ESCs. Kwon et al. also showed that cells on surfaces with different roughness or different nanotopography would exhibit distinct behaviors (Kwon et al., 2012), and these studies revealed that cell behaviors were affected by nanotopography.

2.2 Surface properties

The biological activity of bioactive nanomaterials is affected by surface properties. For example, bioactive ligands such as small molecules, peptides and proteins are modified to the surface of materials by chemical modification (Eivazzadeh-Keihan et al., 2020), and the surface charge, hydrophilic and hydrophobic properties of bioactive nanomaterials are adjusted to become bioactive nanomaterials with specific biological functions. Some studies have found that the use of polymer nanoparticles to modify the surface of cellular-mesenchymal epithelial transition factor (c-MET) peptide bioactive nanoinhibitors and Mesenchymal epithelial transition factor (MET). The affinity of MET is three orders of magnitude higher than that of free c-MET peptide (KD = 3.96 × 10-7 mol/L) (KD = 1.32 × 10-10 mol/L) (Wu et al., 2018). It has also been found that positively charged (+7 mV) Au NPs have no effect on the aggregation of Aβ protein, while negatively charged (−38 mV) Au NPs can effectively inhibit the aggregation of β-amyloid (Aβ) to form toxic oligomers.

2.3 Physical structure

The physical structure of nanomaterials can affect their biological activity. For example, Molecular imprinting polymer (MINP) can bind target biomolecules with high affinity. The specific biological activity depends on the fine structure of the nanoparticle itself. Different fine structures show different biological activities. Some scholars have developed a MINP that can capture vascular epidermal growth factor and thus reduce angiogenesis in the tumor to inhibit tumor growth (Koide et al., 2017), and some studies have reported a borate-based MINP that inhibits tumor growth by blocking the human epidermal growth factor receptor-2 signaling pathway (Dong et al., 2019). These studies have shown that MINP with different fine structures can be developed for the treatment of various diseases such as cancer (Tang et al., 2017; Zhang, 2020). In addition, the particle size of the material also plays an important role in the influence of its biological activity. The specific surface area of nanoparticles is opposite to the particle size, the smaller the particle size, the larger the specific surface area. Jong et al. (Park et al., 2011) found that Ag NPs and Ag+ with large particle size were less toxic by measuring the cytotoxicity of Ag NPs, which are widely used in medicine for antibacterial treatment. Therefore, particle size plays an important role in determining the biological activity of nanomaterials.

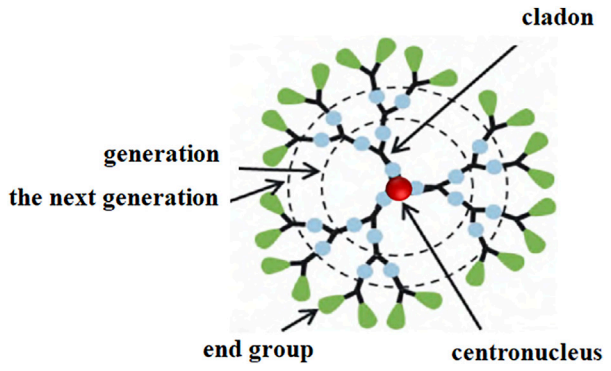

FIGURE 1
Schematic of the basic structure of the tree molecule.

3 Classification of bioactive nanomaterials

With the rapid development of materials science and the development of various bioactive nanomaterials, bioactive nanomaterials have been widely used in biomedicine. Bioactive nanomaterials can be classified into organic nanomaterials, inorganic nanomaterials, bioactive nanoenzymes, and biologically active biomimetic nanomaterials.

3.1 Bioactive organic nanomaterials

Bioactive organic nanomaterials include bioactive nanofibers and bioactive tree molecules. Nanofibers have the characteristics of high specific surface area, high porosity, and good mechanical properties (Shikhi-Abadi and Irani, 2021). One-dimensional nanolinear assemblies with a diameter of 50–500 nm and an aspect ratio of more than 1: 200 are prepared from organic polymer solutions or melts, which have antibacterial and anti-inflammatory properties. For example, poly (ε -caprolactam)—β -poly (ethylenimine) (PCL- β -PEI) nanofibers can prevent CpG oligodeoxynucleotide (ODN) from stimulating dendritic cells and macrophages to secrete cytokines α, tumor necrosis factor (TNF-α) and interferon-γ by electrostatic adsorption of ODN (Kang and Yoo, 2014). While N-trimethyl chitosan nanofibers can generate pressure by electrostatic binding of polycations on the membrane to negatively charged parts of the bacterial cell wall, leading to lysis and death of bacterial cells, and then inhibit inflammatory response (Cheah et al., 2019). However, such nanofibers are prepared based on cationic polymers, and the cell membrane of mammals is also negatively charged, so it is easy to produce cytotoxicity. Tree molecules are usually a kind of spherical nanoscale molecules (Figure 1) composed of three parts: a central core, a branching unit, and a terminal group. The more generations they have, the larger the particle size. Tree molecules can inhibit virus entry into host cells by modifying groups that block the ability of virus to attach to host cells, modifying cationic groups such as zwitterions (Mintzer et al., 2012), organic metals (Abd-El-Aziz et al., 2015), amino acids, and glycopeptides (Michaud et al., 2016), etc. The introduction of hydrophobic chains can damage the cell membrane (Zielińska et al., 2015) or enhance the electrostatic interaction with the bacterial cell membrane to play a role in anti-infection and anti-inflammation. Polyamide amine tree molecules with carboxyl and benzene ends can inhibit the aggregation of β-amyloid peptides through hydrophobic binding and electrostatic repulsion, thus playing a role in nervous system diseases (Wang et al., 2018; Wang et al., 2019a). Polyacylthiourea tree molecules can be modified by polyethylene glycol (PEG) to efficiently chelate copper ions, thereby downregulating the expression of vascular endothelial growth factor (VEGF) in tumor sites and inhibiting the formation of tumor neovascularization (Shao et al., 2017), thus achieving anti-tumor effects. However, few bioactive tree molecules have entered clinical research and application, and only one naphthalene disulfonate-modified polylysine tree molecule has been approved as an antiviral additive for condoms in Australia, which needs to be further evaluated for safety and biocompatibility.

3.2 Bioactive inorganic nanomaterials

Inorganic nanomaterials are a class of nanomaterials with inorganics as the main body (Nethi et al., 2019), including biologically active carbon nanomaterials, biologically active precious metal nanomaterials, biologically active metal oxide nanomaterials, and biologically active non-metallic nanomaterials. They usually have higher mechanical stability.

3.2.1 Bioactive noble metal nanomaterials

Nanomaterials prepared from gold, silver, platinum, etc., are commonly referred to as precious metal nanomaterials. It has been found that gold nanomaterials can exert antibacterial, anti-inflammatory, anti-tumor, and other biological activities according to their specific size, morphology and surface sealing groups. Gold nanoparticles with a size of about 1 nm can induce the production of many reactive oxygen species (ROS) in bacteria, and gold nanopins with high aspect ratio can induce bacterial dissolution through mechanical pressure to achieve the purpose of antibacterial (Zheng et al., 2017; Elbourne et al., 2019). It can also achieve anti-inflammatory effect by regulating related signaling pathways. Some studies have found that gold nanomaterials also have a certain effect on anti-tumor (De Carvalho et al., 2018; Hao et al., 2021), but the structure-activity relationship and biological effect need to be further studied. In particular, the potential toxicity caused by long-term accumulation of inorganic materials in organs and tissues needs to be further clarified.

3.2.2 Biologically active non-metallic nanomaterials

Common bioactive non-metallic nanomaterials mainly include selenium and black phosphorus. As one of the essential non-metallic elements for human body, selenium exerts its biological activity by binding to the structure of selenoproteins in the body. Selenium nanoparticles can exert anti-inflammatory and anti-oxidative effects by activating Nrf2 and its downstream genes, inhibiting ROS production and scavenging superoxide and DPPH free radicals (Cheng et al., 2017; Song et al., 2017). It can also achieve antibacterial effects by inducing ROS production, consuming internal ATP to interfere with bacterial metabolism, destroying membrane structure, disturbing membrane potential, and decomposing mature extracellular polysaccharide matrix produced by bacteria (Cremonini et al., 2016; Huang et al., 2019). Black

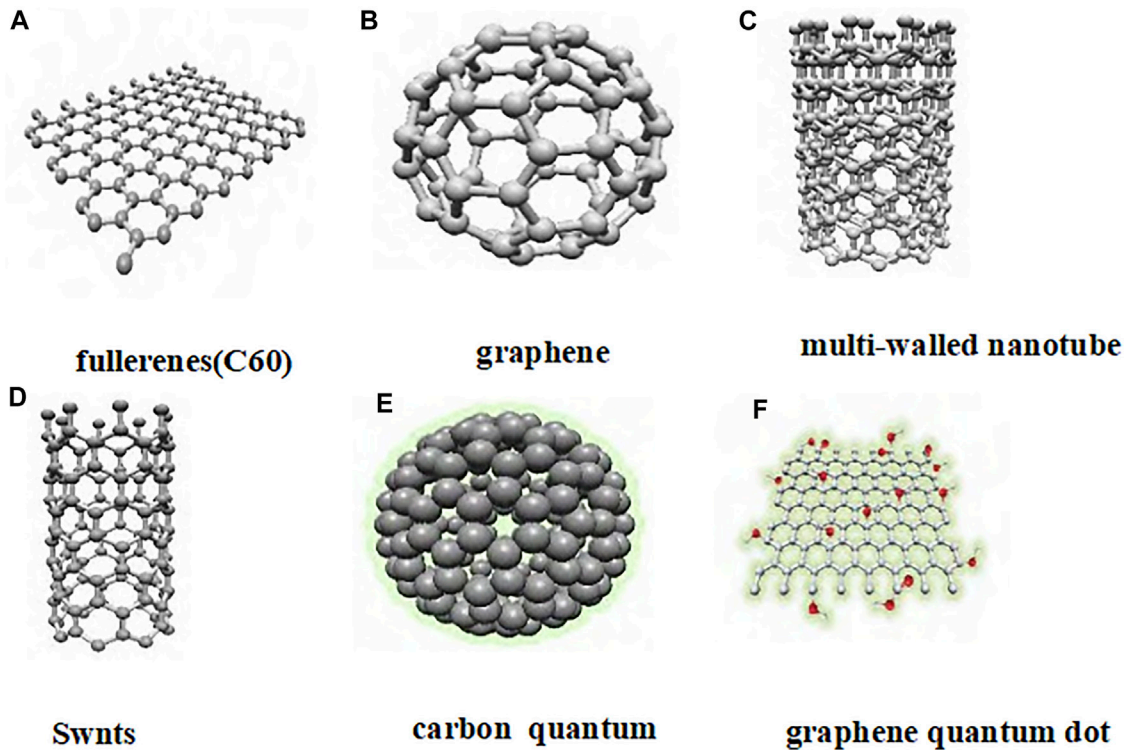

FIGURE 2
Different types of carbon nanomaterials.

phosphorus (BP) nanosheets can induce bacterial apoptosis by producing ROS, and can cause physical damage to the bacterial cell membrane to kill bacteria to achieve antibacterial effect (Xiong et al., 2018). At the same time, it can also interfere with cell multipolar spindle and mitosis, and cause cell apoptosis, thereby exerting great anti-tumor potential (Shao et al., 2021).

3.2.3 Biologically active carbon nanomaterials

Carbon nanomaterials have attracted increasing attention due to their unique electrical, optical, thermal, and mechanical properties (Wang et al., 2014; Lin et al., 2016; Tiwari et al., 2016; Zhang et al., 2017) Carbon nanomaterials include graphene, fullerene (C60), carbon nanotubes, carbon dots, graphene quantum dots, etc., (Figure 2). Carbon nanomaterials are widely used in the biomedical field due to their excellent biological activity and controllable functional design. Studies have found that carbon nanomaterials not only have nanoenzyme activity, but also have antibacterial, anti-infection, anti-tumor, and other biological activities. For example, graphene oxide (GO) nanosheets can affect the formation of dendritic cell -T cell synapses and enhance the activation and proliferation of antigen-specific $CD8^+$ T cells as DC vaccine adjuvants, thus playing an anti-infection role (Zhou et al., 2021). Quaternary ammonium modified carbon quantum dots (QCQD) can play an antibacterial role by interfering with protein translation, post-translational modification, and protein transport in bacteria (Zhao et al., 2020). Graphy-oxide acetylic acid (GDYO) can interact with signal transduction proteins and transcription factor STAT3 in the intracellular, and turn the pro-tumor M2 macrophages into anti-tumor M1 macrophages, thereby reversing the tumor immunosuppressive microenvironment and playing an anti-tumor role (Guo et al., 2021a). However, there are some key problems in the cli nical transformation of carbon nanomaterials, such as the metabolism and clearance process in the body cannot be fully elucidated, and their safety *in vivo* needs to be further studied.

3.2.4 Bioactive metal oxide nanomaterials

Metal oxide refers to the binary compounds composed of oxygen and another metal chemical element, including basic oxide, acid oxide, peroxide, superoxide, amphotericin oxide, etc. In addition to the high specific surface area and high mechanical strength due to its size effect, metal oxide nanoparticles also have the advantages of wide source and stable structure. They play a very important role in many fields such as physics, chemistry, and materials science. It can exhibit insulator, semiconductor or metal characteristics depending on the oxidation state of the metal and the environment. Studies have confirmed that metal oxides of specific sizes have anti-inflammatory, antibacterial, anti-tumor, and other biological activities. For example, tiO2 nanoparticles can inactivate thrombin by promoting the formation of thrombin-antithrombin complex in plasma, thereby blocking the way that thrombin causes inflammatory response through protease activated receptors, and can inhibit oxidative stress response induced by the activation of Toll-like receptors on the surface of platelets (Seisenbaeva et al., 2017). In addition, zno nanoparticles can also improve the antioxidant capacity of the colon and reduce inflammatory damage (Li et al., 2017b). Nanoparticles such as zinc oxide, copper oxide and iron oxide can achieve anti-tumor

effects by causing membrane leakage of tumor cells, inducing oxidative stress and promoting apoptosis (Wahab et al., 2014; Nagajyothi et al., 2017; Yousefvand et al., 2021).

3.3 Bioactive nanozymes

Nanomaterials containing catalytic properties like those of natural enzymes are called nanozymes (Wei and Wang, 2013; Wu et al., 2019), including multiple enzyme-like active nanozymes, peroxidase-like and oxidases, catalase-like active nanozymes, superoxide dismutase-like active nanozymes, etc., due to their low cost, good stability, and easy mass production. They are widely used in many fields such as biomedicine, physical chemistry, materials, agriculture, environmental management, national defense, and security (Wang et al., 2016). A variety of enzyme-active nanozymes can exhibit different types of enzyme-like activities under different conditions. For example, manganese dioxide doped nanoparticles (MnO2 NPs) have a variety of enzyme-like activities that are more stable than natural enzymes, and nitrogen carbon nanomaterials (N-CNMs) can simulate a variety of enzyme-like activities, which can change the intracellular microenvironment of tumor cells and achieve anti-tumor effects (Fan et al., 2018).

3.4 Biologically active biomimetic nanomaterials

By learning the micro and nano multi-scale structure, composition, function and principle in life systems, nanomaterials are designed and prepared to imitate various functions in life systems, which are called biomimetic nanomaterials. These materials include bioactive biomolecular assembly nanomaterials, bioactive cell-like nanomaterials, etc. Biomacromolecules in the body can achieve similar biological activities by rationally designing the physical and chemical properties of materials and mimicking the structure and properties of natural biomacromolecule assemblies. For example, the synthesis of quinazolinone derivatives with arylboric acid connecting groups (BQA-GGFF) can simulate the neutrophil extracellular traps to capture pathogenic microorganisms *in vivo*, thus playing an antibacterial role (Huang et al., 2020). Polymer micelles prepared by polyuamine- β -polycaprolactone (PAE- β -PCL) and polyethylene glycol- β -polycaprolactone (PEG-β-PCL) mimic the role of heat shock protein molecular chaperones to specifically recognize and adsorb hydrophobic fragments in abnormal proteins, so as to play a therapeutic effect in inflammatory response and nervous system diseases (Xu et al., 2019).

4 Application of bioactive nanomaterials in biomedicine

After decades of development, bioactive nanomaterials have been widely used in real life. They have been well used in anti- infection therapy, inflammatory disease treatment, cancer treatment, and neurodegenerative disease treatment.

4.1 Application of bioactive nanomaterials in anti-infection

In recent years, researchers have found that bioactive nanomaterials can play an excellent role in anti-inflammatory and anti-infection (Yang et al., 2019a). In the treatment of infectious diseases, some nanomaterials can strongly interact with cell membranes, thereby destroying the integrity of biofilms. For example, N-trimethyl chitosan nanofibers can electrostatically combine with negatively charged parts of bacterial cell wall through polycations on the membrane to generate pressure, leading to lysis and death of bacterial cells (Cheah et al., 2019). Zinc oxide nanoparticles have a positive charge, which can bind to and damage the negatively charged bacterial cell membrane, leading to the leakage of bacterial cell contents and bacterial death (Król et al., 2017). However, gold nanonail with high aspect ratio can induce bacterial dissolution through mechanical pressure, thus effectively inhibiting bacterial adhesion and bacterial biofilm formation (Elbourne et al., 2019). In addition, copper/carbon nanozymes modified by copper oxide can release Cu2+ and cause membrane damage of Gram-negative bacteria, while selenium nanoparticles can kill bacteria by disturbing membrane potential and destroying membrane structure (Cremonini et al., 2016; Huang et al., 2019). Other researchers (Joseph et al., 2016) have reported a series of quaternary phosphine and quaternary ammonium groups modified columnar aromatic hydrocarbons for antibacterial applications. Wang et al. (Guo et al., 2021b) constructed a new type of Guanidinium-modified pillar (Zhao et al., 2021) arene (GP5), which can rapidly combine with the negative electrical components on the biofilm and the phospholipid components on the bacterial membrane through a salt bridge to dissolve the bacteria, to achieve antibacterial and anti-infection effects. Some nanomaterials can also play a role in inhibiting bacteria by trapping or blocking bacteria. For example, Wang et al. (Zhang et al., 2020) designed a human defensin-6 mimic peptide, which can specifically recognize bacteria and form a nanofiber network *in situ* to trap bacteria (Figure 3). Other nanomaterials can directly kill bacteria by producing reactive oxygen species (ROS). Two types of nanozymes, peroxidase-like and oxidase-like active nanozymes, can catalyze the production of ROS (Gao et al., 2014; Fang et al., 2018a). For example, copper-modified copper/carbon nanozymes can kill bacteria by producing ROS through peroxidase-like catalysis (Figure 4); Metal-based nanomaterials such as Au, ZnO, TiO2 and graphene-based nanomaterials can also show good bactericidal effect by producing ROS (Liu et al., 2019).

4.2 Application of bioactive nanomaterials in inflammatory diseases

Routine physiological activities of the human body produce large amounts of free radicals, including reactive oxygen species (ROS) and reactive nitrogen species (RNS) (Mittal et al., 2014; Kwon et al., 2021), and the production and clearance of free radicals are balanced in the body through a variety of mechanisms (Closa, 2013). As one of the by-products of respiration, ROS play an important role in the occurrence of many inflammatory diseases. Inflammation can activate epithelial cells, neutrophils, and macrophages to produce a variety of inflammatory cytokines and other inflammatory

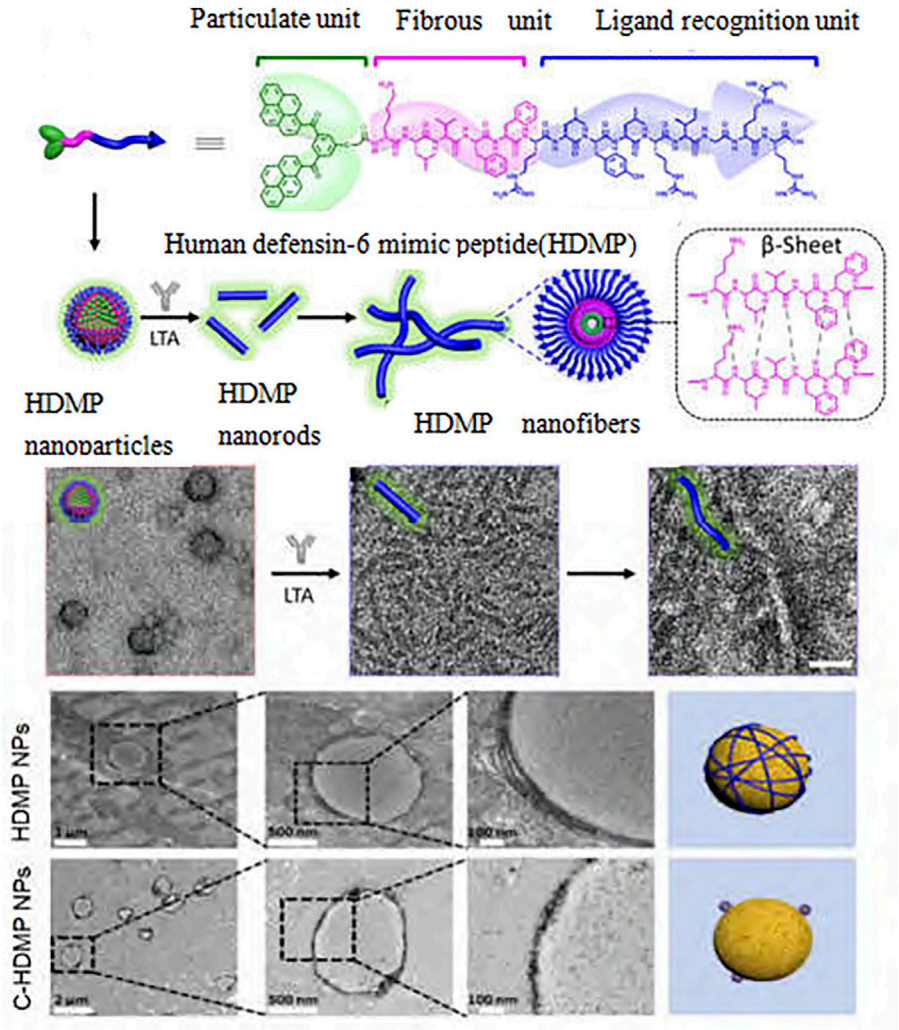

FIGURE 3
HDMP for antibacterial applications.

mediators, which in turn impair the free radical scavenging function or reduce the expression of enzymes in the body (Jena et al., 2012; Piechota-Polanczyk and Fichna, 2014; Zhang et al., 2021a). The production and clearance of free radicals in the body cannot be balanced, leading to oxidative damage to proteins, DNA, and lipids. And further accelerate the progression of inflammation (Kawanishi et al., 2006; Zhu and Li, 2012; Vaghari-Tabari et al., 2018). Therefore, the timely removal of excessive free radicals plays a crucial role in inhibiting inflammation (Zhao et al., 2019; Zhang et al., 2021b; Weng et al., 2021). In recent years, nanomaterials have found many applications in scavenging ROS. Xie et al. (2022) reported a simple and inexpensive method to synthesize Mose2—PVP NPs with high physiological stability and biosafety levels, which mimicked the intrinsic antioxidant properties of superoxide dismutase (SOD), catalase (CAT), peroxidase (POD), and glutathione peroxidase (GPx). It can eliminate a variety of ROS (such as H2O2, OH and O2−) and RNS (such as DPPH) in mitochondria and cells, thereby improving acute pancreatitis (AP). In recent years, the incidence of inflammatory bowel disease (IBD) has gradually increased, and the pathogenesis of IBD is usually related to genetic, environmental, intestinal barrier, and immune factors (Ramos and Papadakis, 2019). With the increasing understanding of the pathogenesis of IBD, more and more new drugs and therapeutic avenues have been investigated, such as nanoparticles (Scarpignato and Pelosini, 2005), natural algae (Zhang et al., 2022), and hydrogels (Liu et al., 2021). Among them, hydrogels have become one of the most competitive materials due to their loose and porous 3D network structure and hydrophilicity. Hydrogels used to treat IBD are made of natural polymers such as chitosan (Xu et al., 2017), alginate (Cheng et al., 2022), hyaluronic acid (Liu et al., 2021), and dextran (Pitarresi et al., 2007) as well as proteins such as chondroitin sulfate (Zhang et al., 2019) and gelatin (Zhang et al., 2021c). A recent review (Ouyang et al., 2022) summarized relevant reports on the types of hydrogels used to load drugs, peptides, and proteins and immunomodulators, as well as probiotics, and found that hydrogel carriers have excellent physical and chemical properties and are well used in IBD treatment. In addition, phosphorus- based dendrimer-based molecules can inhibit the maturation of pro-inflammatory $CD4^+$

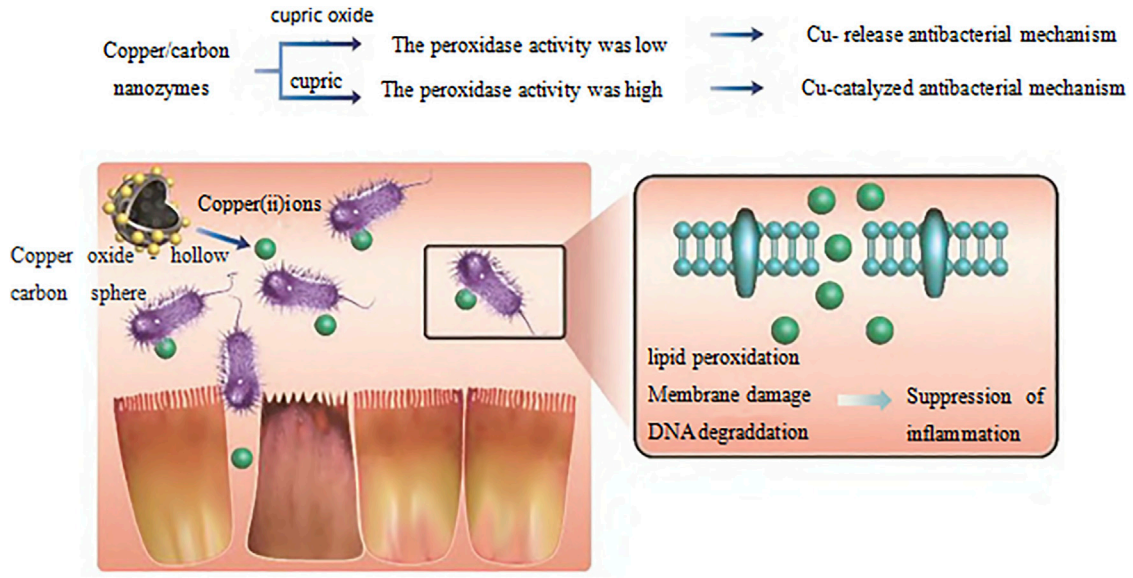

FIGURE 4
Cu/carbon hybrid nanozymes modified with different valence states.

T lymphocytes and dendritic cells (DC), Poly (ε-caprolactone)—β-poly (ethylenimine) (PCL—β- PEI) nanofibers can inhibit the secretion of cytokines α, tumor necrosis factor α (TNF- α) and interferon- γ (Ifn- γ) by dendritic cells and macrophages stimulated by CpG oligodeoxynucleotides (ODNs) through electrostatic adsorption. Thus, the nanofibers can inhibit inflammation (Kang and Yoo, 2014). Gold nanoparticles in precious metal nanomaterials can treat liver injury in rats by regulating AKT/PI3K and MAPK signaling pathways, downregulating the activity of Kupffer cells and hepatic stellate cells in the liver, inhibiting proinflammatory cytokines oxidative stress and fibrosis (De Carvalho et al., 2018). Zinc oxide nanoparticles in metal oxide nanomaterials can inhibit the secretion of pro-inflammatory cytokines IL-1 β and TNF- α and the activity of peroxidase in the colitis model by down-regulating the production of ROS and malondialdehyde in the colon (Li et al., 2017b). Selenium nanoparticles can protect the intestinal barrier from oxidative stress-induced inflammatory damage by activating Nrf2 and its downstream genes. Song et al. (2017) In addition, PLGA bioactive cellmionic nanoparticles coated with neutrophil membranes can effectively a dsorb the pro-inflammatory cytokines TNF- α and IL-1β in the joint cavity of RA. In addition, PLGA bioactive nanoparticles can effectively adsorb the proinflammatory factors Tnf- α and Il-1β in the joint space of RA (Deng et al., 2018).

4.3 Application of bioactive nanomaterials in cancer therapy

In recent years, bioactive nanomaterials have also been more and more widely used in cancer treatment. For example, PLGA bioactive cell-like nanomaterials coated with natural killer cell membranes can induce or enhance the polarization of local M1 macrophages in tumors to play an anti-tumor role (Fang et al., 2018b). Polyethylene glycol (PEG) modified polyacylthiourea tree molecules can down-regulate the expression of vascular endothelial growth factor (VEGF) at the tumor site and inhibit the formation of tumor neovascularization by highly efficient chelation of copper ions, thereby inhibiting tumor cells and tumor metastasis (Shao et al., 2017). In addition, graphite oxide acetylene (GDYO) can interact with signal transduction proteins and transcription factor STAT3 to reverse the tumor immunosuppressive microenvironment, thereby improving the role of tumor immunotherapy (Guo et al., 2021a). Gold nanoparticles can inhibit the growth of prostate cancer cells by inhibiting the expression of related metalloproteinases (Hao et al., 2021). Copper oxide and iron oxide nanomaterials can cause leakage of tumor cell membrane. Copper oxide and iron oxide nanoparticles play an anti-tumor role by activating caspase-9 and caspase-3 mediated pro-apoptotic effects (Nagajyothi et al., 2017; Yousefvand et al., 2021), while zinc oxide nanoparticles can kill tumor cells by inducing oxidative stress and pro-apoptotic pathways (Wahab et al., 2014). Black phosphorus (BP) nanosheets have shown great anticancer potential by causing cell multipolar spindle and mitosis to be delayed, and eventually cell apoptosis (Shao et al., 2021). In addition, catalase like active nanoenzymes catalyze hydrogen peroxide to generate oxygen at the tumor site, thereby enhancing the anti-tumor effect of photodynamic therapy or photothermal therapy. Bioactive nanomaterials can also regulate the interaction between Tumor-associated antigens (TAAs) and APC, thereby enhancing the uptake and presentation of TAAs by APC, thereby enhancing the degree of immune activation and playing an anti-tumor effect. For example, Min et al. (2017) constructed a biodegradable antigen-capturing nanoparticles (AC-NPs) based on Poly (lactic-co-glycolic acid) (PLGA). Yang et al. (2020) proposed a mannose-modified stearic acid-grafted chitosan micellar particle (MChSA), and (Wang et al., 2019b) proposed a Upconverting nanoparticle (UCNP) antigen-capturing nano system (UCNP/ICG/RB-MAL), thereby

promoting antigen presentation and inducing tumor-specific immune response to play an anti-tumor effect. It has also been reported that nanoparticles effectively promote the maturation of APC by directly activating inflammatory cytokine receptors, thereby inducing T cell-mediated anti-tumor immunity (Roy et al., 2014). It has also been found (Kim et al., 2019) that folate-functionalized bioactive glass nanoparticles BGN (F) can effectively alleviate the immunosuppression of TME by depleting or repolarizing immunosuppressive cells. Lee et al. (2021) reported an antibody-like polymer nanoparticle (APN), which can effectively remove the immunosuppressive factor Gal-1 in the tumor, to alleviate the immunosuppression of TME and achieve the effect of anti-tumor immunity. In addition, Zhang et al. (2021d) designed a hydrogel that combines the ability of tumor photodynamic therapy (PDT) and photothermal therapy (PTT) for anti-tumor recurrence. This hydrogel is biocompatible and biodegradable, with good photothermal conversion, drug loading and CT imaging capabilities, laying the foundation for the rational design of biodegradable multifunctional hydrogels. Liu et al. (2022) reported the use of a gelatin methacrylate/oxidized dextran/montmorilite-strontium/polypyrrole (GOMP) hydrogel for synergistic treatment of osteosarcoma and potential bone regeneration. This hydrogel has a dual network structure, formed by photoinitiator-initiated double bond polymerization and Schiff base reaction. The hydrogel has good biocompatibility and excellent biodegradability *in vitro* and *in vivo*. This multifunctional DOX-loaded GOMP hydrogel with bone regeneration, photothermal therapy, and chemotherapy functions has great potential for application in the treatment of osteosarcoma.

4.4 Application of bioactive nanomaterials in the treatment of neurodegenerative diseases

Neurodegenerative diseases (ND), usually referring to Alzheimer's disease, Parkinson's disease, etc., (Marie-Therese, 2016). affect many people worldwide and are often debilitating; unfortunately, there are few treatment options for such diseases. The application of some bioactive nanomaterials with unique properties, which can play a role by inhibiting protein aggregation or eliminating formed protein aggregates, has shown great potential in the treatment of neurodegenerative diseases, providing more options for therapeutic drugs. It has been found that (Huang et al., 2014) Mixed shells polymer micelles (MSPMs) which has a unique surface phase separation structure composed of hydrophilic chain segments and hydrophobic microregions can be used for the treatment of AD. In addition, Yang et al. (2019b) reported A bioactive nanocomposite with a surface-integrated Aβ-capturing peptide (LVFF), and Xu et al. (2019) reported a new method for the treatment of AD by co-assembling Calixarene (CA) and Cyclodextrin (CD) and the preparation of supramolecular nanoparticles (CA-CD), Zhu et al. (2021) reported a TLK [(D)-TLKIVW] integrated polymer micelle particles, etc., which can play a role by inhibiting protein aggregation. In addition, in the treatment of Alzheimer's disease, polyamide amine dendrimer molecules with carboxyl and benzene rings can inhibit the aggregation of β-amyloid peptides through hydrophobic binding and electrostatic repulsion, thus playing an anti-Alzheimer's disease function (Wang et al., 2018; Wang et al., 2019a). It has also been found that bioactive nanomaterials can promote the removal of protein aggregates by regulating the interaction between microglia and proteins (Waisman et al., 2015; Pan et al., 2021) combined Aβ42 with A novel Aβ inhibitor (Gca-CD) to form A positively charged Gca-CD/Aβ copolymer to promote the removal of Aβ aggregates by microglia. Gu et al. (2021) reported A neuroprotective nano-scavenger that could remove Aβ oligomers from the brain and significantly improve the cognitive behavior of AD mice.

5 Discussion

The application of bioactive nanomaterials in biomedicine provides more options for the treatment of diseases. Compared with traditional nanomedicine preparations, bioactive nanomaterials do not exert drug effects through drug release but rely on their physical and chemical properties to interact with proteins, cells, or tissues *in vivo* and cause biological reactions to play a role in the treatment of diseases. Their biological activity is mainly affected by their physical structure, surface properties, and nanomorphology. In recent years, bioactive nanomaterials have been more and more widely studied and applied in the treatment of diseases, such as anti-inflammatory diseases, anti-infectious diseases, anti-tumor, and anti-neurodegenerative diseases. However, the development of bioactive nanomaterials still faces some challenges, such as biological effect evaluation, *in vivo* fate, structure-activity relationship, and clinical translation, etc. Further research is still needed. The main problems are summarized as follows:

(1) There are many uncertainties in the mechanism of action: At present, most of the pharmacological activities of bioactive nanomaterials refer to the ideas of pharmacological activities of small molecule drugs. However, the structure-activity relationship related to their special physical and chemical characteristics, such as size effect, interface effect, and mechanical properties, still need to be further studied to provide guidance for the rational design and development of bioactive nanomaterials.
(2) Lack of *in vivo* safety evaluation: At present, most of the research on bioactive nanomaterials focuses on their biological activity and mechanism of action, such as bioactive tree molecules, which lack safety and biocompatibility evaluation, and mostly stay at the *in vitro* level. The research on *in vivo* metabolism needs to be further improved, and the distribution, metabolism, and clearance process *in vivo* need to be further studied. In addition, the tissue targeting, biodistribution, biodegradation and immunogenicity of biomaterials need to be further solved to accelerate the *in vivo* application and clinical transformation of bioactive nanomaterials.
(3) Lack of safe and effective nanomaterials: The safety of bioactive nanomaterials includes the safety of the starting materials for preparing nanomaterials and the safety of nanomaterials themselves, and their pharmacological activity is closely related to their physical and chemical properties. Therefore, it is still a great challenge to develop nanomaterials with good biological safety. Therefore, the development of nanomaterials with good biological safety is still a great challenge. The processes and technologies that are suitable for the preparation of bioactive nanomaterials on industrial scale while ensuring uniformity and batch-to-batch stability need to be further developed.
(4) Clinical transformation needs to be further studied: The clinical application and research of bioactive nanomaterials have obvious interdisciplinary aspects, including nanoscience, materials science and engineering, and life science. In the future, it is necessary to

strengthen the cooperation and communication among various disciplines, integrate advantages, and focus on the safety evaluation of materials *in vivo*, how to prepare, sterilization and storage in large amounts, to accelerate the clinical translation of bioactive nanomaterials.

Although there are still various problems in the clinical translation and application of bioactive nanomaterials, with the continuous deepening of research and breakthroughs in key scientific issues, it is believed that bioactive nanomaterials will play a greater role in the treatment of diseases in the future.

Author contributions

YL and YY wrote the manuscript. YL, YY, CZ, and ZM planned the study and supervised the entire project. YL, ZM, HW, JL, and XL searched the reference papers. YY, XD, FY, QC, and CL edited the manuscript. All authors read and approved the final manuscript.

Conflict of interest

The authors declare that the research was conducted in the absence of any commercial or financial relationships that could be construed as a potential conflict of interest.

Publisher's note

References

Abd-El-Aziz, A. S., Agatemor, C., Etkin, N., Overy, D. P., Lanteigne, M., McQuillan, K., et al. (2015). Antimicrobial organometallic dendrimers with tunable activity against multidrug-resistant bacteria. *Biomacromolecules* 16 (11), 3694–3703. doi:10.1021/acs.biomac.5b01207

Cheah, W. Y., Show, P. L., Ng, I. S., Lin, G. Y., Chiu, C. Y., and Chang, Y. K. (2019). Antibacterial activity of quaternized chitosan modified nanofiber membrane. *Int. J. Biol. Macromol.* 126, 569–577. doi:10.1016/j.ijbiomac.2018.12.193

Chen, W., Villa-Diaz, L. G., Sun, Y., Weng, S., Kim, J. K., Lam, R. H. W., et al. (2012). Nanotopography influences adhesion, spreading, and self-renewal of human embryonic stem cells. *ACS Nano* 6 (5), 4094–4103. doi:10.1021/nn3004923

Cheng, C., Cheng, Y., Zhao, S., Wang, Q., Li, S., Chen, X., et al. (2022). Multifunctional nanozyme hydrogel with mucosal healing activity for single-dose ulcerative colitis therapy. *Bioconjug Chem.* 33 (1), 248–259. doi:10.1021/acs.bioconjchem.1c00583

Cheng, L., Wang, X., Gong, F., Liu, T., and Liu, Z. (2020). 2D nanomaterials for cancer theranostic applications. *Adv. Mater* 32 (13), e1902333. doi:10.1002/adma.201902333

Cheng, Y., Xiao, X., Li, X., Song, D., Lu, Z., Wang, F., et al. (2017). Characterization, antioxidant property and cytoprotection of exopolysaccharide-capped elemental selenium particles synthesized by Bacillus paralicheniformis SR14. *Carbohydr. Polym.* 178, 18–26. doi:10.1016/j.carbpol.2017.08.124

Closa, D. (2013). Free radicals and acute pancreatitis: Much ado about . . . something something. *Free Radic. Res.* 47, 934–940. doi:10.3109/10715762.2013.829571

Cremonini, E., Zonaro, E., Donini, M., Lampis, S., Boaretti, M., Dusi, S., et al. (2016). Biogenic selenium nanoparticles: Characterization, antimicrobial activity and effects on human dendritic cells and fibroblasts. *Microb. Biotechnol.* 9 (6), 758–771. doi:10.1111/1751-7915.12374

De Carvalho, T. G., Garcia, V. B., De Araújo, A. A., da Silva Gasparotto, L. H., Silva, H., Guerra, G. C. B., et al. (2018). Spherical neutral gold nanoparticles improve anti-inflammatory response, oxidative stress and fibrosis in alcohol-methamphetamine-induced liver injury in rats. *Int. J. Pharm.* 548 (1), 1–14. doi:10.1016/j.ijpharm.2018.06.008

Deng, G., Sun, Z., Li, S., Peng, X., Li, W., Zhou, L., et al. (2018). Cell-membrane immunotherapy based on natural killer cell membrane coated nanoparticles for the effective inhibition of primary and abscopal tumor growth. *ACS Nano* 12 (12), 12096–12108. doi:10.1021/acsnano.8b05292

Dong, Y., Li, W., Gu, Z., Xing, R., Ma, Y., Zhang, Q., et al. (2019). Inhibition of HER2-positive breast cancer growth by blocking the HER2 signaling pathway with HER2-glycan-imprinted nanoparticles. *Angew. Chem. Int. Ed. Engl.* 58 (31), 10621–10625. doi:10.1002/anie.201904860

Eivazzadeh-Keihan, R., Bahojb Noruzi, E., Khanmohammadi Chenab, K., Jafari, A., Radinekiyan, F., Hashemi, S. M., et al. (2020). Metal-based nanoparticles for bone tissue engineering. *J. Tissue Eng. Regen. Med.* 14 (12), 1687–1714. doi:10.1002/term.3131

Elbourne, A., Coyle, V. E., Truong, V. K., Sabri, Y. M., Kandjani, A. E., Bhargava, S. K., et al. (2019). Multi-directional electrodeposited gold nanospikes for antibacterial surface applications. *Nanoscale Adv.* 1 (1), 203–212. doi:10.1039/c8na00124c

Fan, K., Xi, J., Fan, L., Wang, P., Zhu, C., Tang, Y., et al. (2018). *In vivo* guiding nitrogen-doped carbon nanozyme for tumor catalytic therapy. *Nat. Commun.* 9 (1), 1440. doi:10.1038/s41467-018-03903-8

Fang, G., Li, W., Shen, X., Perez-Aguilar, J. M., Chong, Y., Gao, X., et al. (2018). Differential Pd-nanocrystal facets demonstrate distinct antibacterial activity against Gram-positive and Gram-negative bacteria. *Nat. Commun.* 9 (1), 129. doi:10.1038/s41467-017-02502-3

Fang, R. H., Kroll, A. V., Gao, W., and Zhang, L. (2018). Cell membrane coating nanotechnology. *J. Adv. Mater.* 30 (23), 1706759. doi:10.1002/adma.201706759

Gao, L., Giglio, K. M., Nelson, J. L., Sondermann, H., and Travis, A. J. (2014). Ferromagnetic nanoparticles with peroxidase-like activity enhance the cleavage of biological macromolecules for biofilm elimination. *Nanoscale* 6 (5), 2588–2593. doi:10.1039/c3nr05422e

Gu, Y., Zhao, Y., Zhang, Z., Hao, J., Zheng, Y., Liu, Q., et al. (2021). An antibody-like polymeric nanoparticle removes intratumoral galectin-1 to enhance antitumor T-cell responses in cancer immunotherapy. *ACS Appl. Mater Interfaces* 13 (19), 22159–22168. doi:10.1021/acsami.1c02116

Guo, S., Zhao, L., Liu, J., Wang, X., Yao, H., Chang, X., et al. (2021a). The underlying function and structural organization of the intracellular protein corona on graphdiyne oxide nanosheet for local immunomodulation. *Nano Lett.* 21 (14), 6005–6013. doi:10.1021/acs.nanolett.1c01048

Guo, S., Huang, Q., Chen, Y., Wei, J., Zheng, J., Wang, L., et al. (2021b). Synthesis and bioactivity of guanidinium-functionalized pillar [5] arene as a biofilm disruptor. *Angew. Chem. Int. Ed. Engl.* 60 (2), 618–623. doi:10.1002/anie.202013975

Hao, Y., Hu, J., Wang, H., and Wang, C. (2021). Gold nanoparticles regulate the antitumor secretome and have potent cytotoxic effects against prostate cancer cells. *J. Appl. Toxicol.* 41 (8), 1286–1303. doi:10.1002/jat.4117

Henchll, P. J. M. (2002). Third-generation biomedicalmaterials. *Science* 295 (5557), 1014–1017. doi:10.1126/science.1067404

Huang, F., Wang, J., Qu, A., Shen, L., Liu, J., Liu, J., et al. (2014). Maintenance of amyloid β peptide homeostasis by artificial chaperones based on mixed-shell polymeric micelles. *Angew. Chem. Int. Ed. Engl.* 53 (34), 8985–8990. doi:10.1002/anie.201400735

Huang, T., Holden, J. A., Heath, D. E., O'Brien-Simpson, N. M., and O'Connor, A. J. (2019). Engineering highly effective antimicrobial selenium nanoparticles through control of particle size. *Nanoscale* 11 (31), 14937–14951. doi:10.1039/c9nr04424h

Huang, Z., Liu, Y., Wang, L., Ali, A., Yao, Q., Jiang, X., et al. (2020). Supramolecular assemblies mimicking neutrophil extracellular traps for MRSE infection control. *biomaterials* 253, 120124. doi:10.1016/j.biomaterials.2020.120124

Islam, M. M., Shahruzzaman, M., Biswas, S., Nurus Sakib, M., and Rashid, T. U. (2020). Chitosan based bioactive materials in tissue engineering applications-A review. *Bioact. Mater* 5 (1), 164–183. doi:10.1016/j.bioactmat.2020.01.012

Jena, G., Trivedi, P. P., and Sandala, B. (2012). Oxidative stress in ulcerative colitis: An old concept but a new concern. *Free Radic. Res.* 46, 1339–1345. doi:10.3109/10715762.2012.717692

Joseph, R., Kaizerman, D., Herzog, I. M., Hadar, M., Feldman, M., Fridman, M., et al. (2016). Phosphonium pillar [5] arenes as a new class of efficient biofilm inhibitors: Importance of charge cooperativity and the pillar platform. *Chem. Commun. (Camb)* 52 (70), 10656–10659. doi:10.1039/c6cc05170g

Kang, J., and Yoo, H. S. (2014). Nucleic acid-scavenging electrospun nanofibrous meshes for suppressing inflammatory responses. *Biomacromolecules* 15 (7), 2600–2606. doi:10.1021/bm500437e

Kawanishi, S., Hiraku, Y., and Pinlaor, S. (2006). Oxidative and nitrative DNA damage in animals and patients with inflammatory diseases in relation to inflammation-related carcinogenesis. *Biol. Chem.* 387, 365–372. doi:10.1515/BC.2006.049

Kerativitayanan, P., Carrow, J. K., and Gaharwar, A. K. (2015). Nanomaterials for engineering stem cell responses. *Adv. Healthc. Mater* 4 (11), 1600–1627. doi:10.1002/adhm.201500272

Kim, T. H., Kang, M. S., Mandakhbayar, N., El-Fiqi, A., Kim, H. W., et al. (2019). Anti-inflammatory actions of folate-functionalized bioactive ion-releasing nanoparticles imply drug-free nanotherapy of inflamed tissues. *Biomaterials* 207, 23–38. doi:10.1016/j.biomaterials.2019.03.034

Koide, H., Yoshimatsu, K., Hoshino, Y., Lee, S. H., Okajima, A., Ariizumi, S., et al. (2017). A polymer nanoparticle with engineered affinity for a vascular endothelial growth factor (VEGF165). *Nat. Chem.* 9 (7), 715–722. doi:10.1038/nchem.2749

Król, A., Pomastowski, P., Rafińska, K., Railean-Plugaru, V., and Buszewski, B. (2017). Zinc oxide nanoparticles: Synthesis, antiseptic activity and toxicity mechanism. *Adv. Colloid Interface Sci.* 249, 37–52. doi:10.1016/j.cis.2017.07.033

Kumawat, M. K., Thakur, M., Gurung, R. B., and Srivastava, R. (2017). Graphene quantum dots for cell proliferation, nucleus imaging, and photoluminescent sensing applications. *Sci. Rep.* 7 (1), 15858. doi:10.1038/s41598-017-16025-w

Kwon, K. W., Park, H., Song, K. H., Choi, J. C., Ahn, H., Park, M. J., et al. (2012). Nanotopography-guided migration of T cells. *J. Immunol.* 189 (5), 2266–2273. doi:10.4049/jimmunol.1102273

Kwon, N., Kim, D., Swamy, K. M. K., and Yoon, J. (2021). Metal-coordinated fluorescent and luminescent probes for reactive oxygen species (ROS) and reactive nitrogen species (RNS). *Coord. Chem. Rev.* 427, 213581. doi:10.1016/j.ccr.2020.213581

Lee, J. H., Shin, G., Baek, J. Y., and Kang, T. J. (2021). An electricity-generating window made of aTransparent energy harvester of thermocells. *ACS Appl. Mater Interfaces* 13 (18), 21157–21165. doi:10.1021/acsami.1c00164

Li, S., Chen, H., Wang, B., Cai, C., Yang, X., Chai, Z., et al. (2017b). ZnO nanoparticles act as supportive therapy in DSS-induced ulcerative colitis in mice by maintaining gut homeostasis and activating Nrf2 signaling. *Sci. Rep.* 7 (1), 43126. doi:10.1038/srep43126

Li, S., Zhou, S., Li, Y., Li, X., Zhu, J., Fan, L., et al. (2017a). Exceptionally high payload of the IR780 iodide on folic acid-functionalized graphene quantum dots for targeted photothermal therapy. *ACS Appl. Mater Interfaces* 9 (27), 22332–22341. doi:10.1021/acsami.7b07267

Lin, G., Mi, P., Chu, C., Zhang, J., and Liu, G. (2016). Inorganic nanocarriers overcoming multidrug resistance for cancer theranostics. *Adv. Sci. (Weinh).* 3 (11), 1600134. doi:10.1002/advs.201600134

Liu, H., Cai, Z., Wang, F., Hong, L., Deng, L., Zhong, J., et al. (2021). Colon-targeted adhesive hydrogel microsphere for regulation of gut immunity and flora. *Adv. Sci. (Weinh).* 8 (18), e2101619. doi:10.1002/advs.202101619

Liu, X., Zhang, Y., Wu, H., Tang, J., Zhou, J., Zhao, J., et al. (2022). A conductive gelatin methacrylamide hydrogel for synergistic therapy of osteosarcoma and potential bone regeneration. *Int. J. Biol. Macromol.* 228, 111–122. doi:10.1016/j.ijbiomac.2022.12.185

Liu, Y., ShiSu, L. L., van der Mei, H. C., Jutte, P. C., Ren, Y., et al. (2019). Nanotechnology-based antimicrobials and delivery systems for biofilm-infection control. *Chem. Soc. Rev.* 48 (2), 428–446. doi:10.1039/c7cs00807d

Marie-Therese, S. (2016). Neurodegenerative diseases [J]. *Nat. Heemels* 539 (7628), 179–180.

Michaud, G., Visini, R., Bergmann, M., Salerno, G., Bosco, R., Gillon, E., et al. (2016). Overcoming antibiotic resistance in *Pseudomonas aeruginosa* biofilms using glycopeptide dendrimers. *Chem. Sci.* 7 (1), 166–182. doi:10.1039/c5sc03635f

Min, Y., Roche, K. C., Tian, S., Eblan, M. J., McKinnon, K. P., Caster, J. M., et al. (2017). Antigen-capturing nanoparticles improve the abscopal effect and cancer immunotherapy. *Nat. Nanotechnol.* 12 (9), 877–882. doi:10.1038/nnano.2017.113

Mintzer, M. A., Dane, E. L., O'toole, G. A., and Grinstaff, M. W. (2012). Exploiting dendrimer multivalency to combat emerging and re-emerging infectious diseases. *Mol. Pharm.* 9 (3), 342–354. doi:10.1021/mp2005033

Mittal, M., Siddiqui, M. R., Tran, K., Reddy, S. P., and Malik, A. B. (2014). Reactive oxygen species in inflammation and tissue injury. *Antioxid. Redox Signal* 20, 1126–1167. doi:10.1089/ars.2012.5149

Nagajyothi, P. C., Pandurangan, M., Kim, D. H., Sreekanth, T. V. M., and Shim, J. (2017). Green synthesis of iron oxide nanoparticles and their catalytic and *in vitro* anticancer activities. *J. Clust. Sci.* 28 (1), 245–257. doi:10.1007/s10876-016-1082-z

Nethi, S. K., Das, S., Patra, C. R., and Mukherjee, S. (2019). Recent advances in inorganic nanomaterials for wound-healing applications. *Biomater. Sci.* 7 (7), 2652–2674. doi:10.1039/c9bm00423h

Ouyang, Y., Zhao, J., and Wang, S. (2022). Multifunctional hydrogels based on chitosan, hyaluronic acid and other biological macromolecules for the treatment of inflammatory bowel disease: A review. *Int. J. Biol. Macromol.* 227, 505–523. doi:10.1016/j.ijbiomac.2022.12.032

Pan, Y., Wang, H., and Xu, X. (2021). Coassembly of macrocyclic amphiphiles for anti-β-amyloid therapy of Alzheimer's disease [J]. *CCS Chem.* 3 (9), 2485–2497.

Park, M. V., Neigh, A. M., Vermeulen, J. P., de la Fonteyne, L. J. J., Verharen, H. W., Briede, J. J., et al. (2011). The effect of particle size on the cytotoxicity, inflammation, developmental toxicity, and genotoxicity of silver nanoparticles. *Biomaterials* 32 (36), 9810–9817. doi:10.1016/j.biomaterials.2011.08.085

Piechota-Polanczyk, A., and Fichna, J. (2014). Review article: The role of oxidative stress in pathogenesis and treatment of inflammatory bowel diseases. *Schmiedeb. Arch. Pharmacol.* 387, 605–620. doi:10.1007/s00210-014-0985-1

Pitarresi, G., Casadei, M. A., Mandracchia, D., Paolicelli, P., Palumbo, F. S., and Giammona, G. (2007). Photocrosslinking of dextran and polyaspartamide derivatives: A combination suitable for colon-specific drug delivery. *J. Control Release* 119 (3), 328–338. doi:10.1016/j.jconrel.2007.03.005

Ramos, G. P., and Papadakis, K. A. (2019). Mechanisms of disease: Inflammatory bowel diseases. *Mayo Clin. Proc.* 94 (1), 155–165. doi:10.1016/j.mayocp.2018.09.013

Roy, R., Singh, S. K., Das, M., Tripathi, A., and Dwivedi, P. D. (2014). Toll-like receptor 6 mediated inflammatory and functional responses of zinc oxide nanoparticles Primed macrophages. *Immunology* 142 (3), 453–464. doi:10.1111/imm.12276

Scarpignato, C., and Pelosini, I. (2005). Rifaximin, a poorly absorbed antibiotic: Pharmacology and clinical potential. *Chemotherapy* 51 (1), 36–66. doi:10.1159/000081990

Seisenbaeva, G. A., Fromell, K., Vinogradov, V. V., Terekhov, A. N., Pakhomov, A. V., Nilsson, B., et al. (2017). Dispersion of TiO_2 nanoparticles improves burn wound healing and tissue regeneration through specific interaction with blood serum proteins [J]. *Sci. Rep.* 7 (1), 15448. doi:10.1038/s41598-017-15792-w

Shao, S., Zhou, Q., Si, J., Tang, J., Liu, X., Wang, M., et al. (2017). A non-cytotoxic dendrimer with innate and potent anticancer and anti-metastatic activities. *Nat. Biomed. Eng.* 1 (9), 745–757. doi:10.1038/s41551-017-0130-9

Shao, X., Ding, Z., Zhou, W., Li, Y., Cui, H., et al. (2021). Intrinsic bioactivity of black phosphorus nanomaterials on mitotic centrosome destabilization through suppression of PLK1 kinase. *Nat. Nanotechnol.* 16, 1150–1160. doi:10.1038/s41565-021-00952-x

Shikhi-Abadi, P. G., and Irani, M. (2021). A review on the applications of electrospun chitosan nanofibers for the cancer treatment. *Int. J. Biol. Macromol.* 183, 790–810. doi:10.1016/j.ijbiomac.2021.05.009

Song, D., Cheng, Y., Li, X., Wang, F., Lu, Z., Xiao, X., et al. (2017). Biogenic nanoselenium particles effectively attenuate oxidative stress-induced intestinal epithelial barrier injury by activating the Nrf2 antioxidant pathway. *ACS Appl. Mater. interfaces* 9 (17), 14724–14740. doi:10.1021/acsami.7b03377

Tang, X., Li, F., Jia, J., Yang, C., Liu, W., Jin, B., et al. (2017). Synthesis of magnetic molecularly imprinted polymers with excellent biocompatibility for the selective separation and inhibition of testosterone in prostate cancer cells. *Int. J. Nanomedicine* 12, 2979–2993. doi:10.2147/IJN.S133009

Tiwari, J. N., Vij, V., Kemp, K. C., and Kim, K. S. (2016). Engineered carbon-nanomaterial-based electrochemical sensors for biomolecules. *ACS Nano* 10 (1), 46–80. doi:10.1021/acsnano.5b05690

Vaghari-Tabari, M., Moein, S., Qujeq, D., Kashifard, M., and Hajian-Tilaki, K. (2018). Positive correlation of fecal calprotectin with serum antioxidant enzymes in patients with inflammatory bowel disease: Accidental numerical correlation or a new finding? *Am. J. Med. Sci.* 355, 449–455. doi:10.1016/j.amjms.2017.12.009

Wahab, R., Siddiqui, M. A., Saquib, Q., Dwivedi, S., Ahmad, J., Musarrat, J., et al. (2014). ZnO nanoparticles induced oxidative stress and apoptosis in HepG2 and MCF-7 cancer cells and their antibacterial activity. *Colloids Surfaces B Biointerfaces* 117, 267–276. doi:10.1016/j.colsurfb.2014.02.038

Waisman, A., Liblau, R. S., and Becher, B. (2015). Innate and adaptive immune responses in the CNS. *Lancet Neurol.* 14 (9), 945–955. doi:10.1016/S1474-4422(15)00141-6

Wang, L., Wang, X., Bhirde, A., Cao, J., Zeng, Y., Huang, X., et al. (2014). Carbon-dot-based two-photon visible nanocarriers for safe and highly efficient delivery of siRNA and DNA. *Adv. Healthc. Mater* 3 (8), 1203–1209. doi:10.1002/adhm.201300611

Wang, Z., Song, J., Zhou, F., Hoover, A. R., Murray, C., Zhou, B., et al. (2019b). NIR-triggered phototherapy, and immunotherapy via an antigen-capturing nanoplatform for metastatic cancer treatment. *Adv. Sci. (Weinh)* 6 (10), 1802157. doi:10.1002/advs.201802157

Wang, X., Hu, Y., and Wei, H. (2016). Nanozymes in bionanotechnology: From sensing to therapeutics and beyond. *Inorg. Chem. Front.* 3 (1), 41–60. doi:10.1039/c5qi00240k

Wang, Z., Dong, X., and Sun, Y. (2018). Hydrophobic modification of carboxyl-terminated polyamidoamine dendrimer surface creates a potent inhibitor of amyloid-β fibrillation. *Langmuir* 34 (47), 14419–14427. doi:10.1021/acs.langmuir.8b02890

Wang, Z., Dong, X., and Sun, Y. (2019a). Mixed carboxyl and hydrophobic dendrimer surface inhibits amyloid-β fibrillation: New insight from the generation number effect. *Langmuir* 35 (45), 14681–14687. doi:10.1021/acs.langmuir.9b02527

Wei, H., and Wang, E. (2013). Nanomaterials with enzyme-like characteristics (nanozymes): Next-generation artificial enzymes. *Chem. Soc. Rev.* 42 (14), 6060–6093. doi:10.1039/c3cs35486e

Weng, Q. J., Sun, H., Fang, C. Y., Xia, F., Liao, H., Lee, J., et al. (2021). Catalytic activity tunable ceria nanoparticles prevent chemotherapy-induced acute kidney injury without interference with chemotherapeutics. *Nat. Commun.* 12, 1436. doi:10.1038/s41467-021-21714-2

Wu, J., Wang, X., Wang, Q., Lou, Z., Li, S., Zhu, Y., et al. (2019). Nanomaterials with enzyme-like characteristics (nanozymes): Next-generation artificial enzymes (II). *Chem. Soc. Rev.* 48 (4), 1004–1076. doi:10.1039/c8cs00457a

Wu, Y., Fan, Q., Zeng, F., Zhu, J., Chen, J., Fan, D., et al. (2018). Peptide-functionalized nanoinhibitor restrains brain tumor growth by abrogating mesenchymal-epithelial transition factor (MET) signaling. *Nano Lett.* 18 (9), 5488–5498. doi:10.1021/acs.nanolett.8b01879

Xie, P., Zhang, L., Shen, H., Wu, H., Zhao, J., Wang, S., et al. (2022). Biodegradable MoSe2-polyvinylpyrrolidone nanoparticles with multi-enzyme activity for ameliorating acute pancreatitis. *J. Nanobiotechnology* 20 (1), 113. doi:10.1186/s12951-022-01288-x

Xiong, Z., Zhang, X., Zhang, S., Lei, L., Ma, W., Li, D., et al. (2018). Bacterial toxicity of exfoliated black phosphorus nanosheets. *Ecotoxicol. Environ. Saf.* 161, 507–514. doi:10.1016/j.ecoenv.2018.06.008

Xu, J., Tam, M., Samaei, S., Lerouge, S., Barralet, J., Stevenson, M. M., et al. (2017). Mucoadhesive chitosan hydrogels as rectal drug delivery vessels to treat ulcerative colitis. *Acta Biomater.* 48, 247–257. doi:10.1016/j.actbio.2016.10.026

Xu, S., Chang, L., Hu, Y., Zhao, X., Huang, S., Chen, Z., et al. (2021). Tea polyphenol modified, photothermal responsive and ROS generative black phosphorus quantum dots as nanoplatforms for promoting MRSA infected wounds healing in diabetic rats. *J. Nanobiotechnology* 19 (1), 362. doi:10.1186/s12951-021-01106-w

Xu, Z., Jia, S., Wang, W., Yuan, Z., Jan Ravoo, B., and Guo, D. S. (2019). Heteromultivalent peptide recognition by co-assembly of cyclodextrin and calixarene amphiphiles enables inhibition of amyloid fibrillation. *Nat. Chem.* 11 (1), 86–93. doi:10.1038/s41557-018-0164-y

Yang, C., Lou, W., Zhong, G., Lee, A., Leong, J., Chin, W., et al. (2019a). Degradable antimicrobial polycarbonates with unexpected activity and selectivity for treating multidrug-resistant *Klebsiella pneumoniae* lung infection in mice. *Acta Biomater.* 94, 268–280. doi:10.1016/j.actbio.2019.05.057

Yang, C., Li, X., Zhu, L., Wu, X., Zhang, S., Huang, F., et al. (2019b). Heat shock protein inspired nanochaperones restore amyloid-β homeostasis for preventative therapy of Alzheimer's disease. *Adv. Sci.* 6 (22), 1901844. doi:10.1002/advs.201901844

Yang, X., Yu, T., Zeng, Y., Lian, K., Zhou, X., Li, S., et al. (2020). Tumor-draining lymph node targeting chitosan micelles as antigen-capturing adjuvants for personalized immunotherapy. *Carbohydr. Polym.* 240, 116270. doi:10.1016/j.carbpol.2020.116270

Yousefvand, P., Mohammadi, E., Zhuang, Y., Bloukh, S. H., Edis, Z., Gamasaee, N. A., et al. (2021). Biothermodynamic, antiproliferative and antimicrobial properties of synthesized copper oxide nanoparticles. *J. Mol. Liq.* 324, 114693. doi:10.1016/j.molliq.2020.114693

Zhang, D., Zhong, D., Ouyang, J., He, J., Qi, Y., Chen, W., et al. (2022). Microalgae-based oral microcarriers for gut microbiota homeostasis and intestinal protection in cancer radiotherapy. *Nat. Commun.* 13 (1), 1413. doi:10.1038/s41467-022-28744-4

Zhang, D. Y., Liu, H. K., Zhu, K. S., Younis, M. R., Yang, C., et al. (2021b). Prussian blue-based theranostics for ameliorating acute kidney injury. *J. Nanobiotechnol* 19, 266. doi:10.1186/s12951-021-01006-z

Zhang, D. Y., Younis, M. R., Liu, H. K., Lei, S., Wan, Y., Qu, J., et al. (2021a). Multi-enzyme mimetic ultrasmall iridium nanozymes as reactive oxygen/nitrogen species scavengers for acute kidney injury management. *Biomaterials* 271, 120706. doi:10.1016/j.biomaterials.2021.120706

Zhang, D. Y., Zheng, Y., Tan, C. P., Sun, J. H., Zhang, W., Ji, L. N., et al. (2017). Graphene oxide decorated with Ru(II)-Polyethylene glycol complex for lysosome-targeted imaging and photodynamic/photothermal therapy. *ACS Appl. Mater Interfaces* 9 (8), 6761–6771. doi:10.1021/acsami.6b13808

Zhang, H. (2020). Molecularly imprinted nanoparticles for biomedical applications. *Adv. Mater* 32 (3), e1806328. doi:10.1002/adma.201806328

Zhang, L., Jing, D., Jiang, N., Rojalin, T., Baehr, C. M., Zhang, D., et al. (2020). Transformable peptide nanoparticles arrest HER2 signalling and cause cancer cell death *in vivo*. *Nat. Nanotechnol.* 15 (2), 145–153. doi:10.1038/s41565-019-0626-4

Zhang, D. Y., Kang, L., Hu, S., Hu, J., Fu, Y., Hu, Y., et al. (2021c). Carboxymethyl chitosan microspheres loaded hyaluronic acid/gelatin hydrogels for controlled drug delivery and the treatment of inflammatory bowel disease. *Int. J. Biol. Macromol.* 167, 1598–1612. doi:10.1016/j.ijbiomac.2020.11.117

Zhang, X., Ma, Y., Ma, L., Zu, M., Song, H., and Xiao, B. (2019). Oral administration of chondroitin sulfate-functionalized nanoparticles for colonic macrophage-targeted drug delivery. *Carbohydr. Polym.* 223, 115126. doi:10.1016/j.carbpol.2019.115126

Zhang, D. Y., Zhu, C., Zhang, Z., Zhao, J., Yuan, Y., and Wang, S. (2021d). Oxidation triggered formation of polydopamine-modified carboxymethyl cellulose hydrogel for anti-recurrence of tumor. *Colloids Surf. B Biointerfaces* 207, 112025. doi:10.1016/j.colsurfb.2021.112025

Zhao, C., Wu, L., Wang, X., Weng, S., Ruan, Z., Liu, Q., et al. (2020). Quaternary ammonium carbon quantum dots as an antimicrobial agent against gram-positive bacteria for the treatment of MRSA-infected pneumonia in mice. *Carbon* 163, 70–84. doi:10.1016/j.carbon.2020.03.009

Zhao, J. L., Gao, W., Cai, X. J., Xu, J., Zou, D., Li, Z., et al. (2019). Nanozyme-mediated catalytic nanotherapy for inflammatory bowel disease. *Theranostics* 9, 2843–2855. doi:10.7150/thno.33727

Zhao, Y., Li, Q., Chai, J., and Liu, Y. (2021). Cargo-templated crosslinked polymer nanocapsules and their biomedical applications. *Adv. NanoBiomed Res.* 1 (4), 2000078. doi:10.1002/anbr.202000078

Zheng, K., Setyawati, M. I., Leong, D. T., and Xie, J. (2017). Antimicrobial gold nanoclusters. *ACS Nano* 11 (7), 6904–6910. doi:10.1021/acsnano.7b02035

Zheng, X. T., Ananthanarayanan, A., Luo, K. Q., and Chen, P. (2015). Glowing graphene quantum dots and carbon dots: Properties, syntheses, and biological applications. *Small* 11 (14), 1620–1636. doi:10.1002/smll.201402648

Zhou, Q., Gu, H., Sun, S., Zhang, Y., Hou, Y., Li, C., et al. (2021). Large-sized graphene oxide nanosheets increase DC-T-cell synaptic contact and the efficacy of DC vaccines against SARS-CoV-2. *Adv. Mater.* 33 (40), 2102528. doi:10.1002/adma.202102528

Zhou, W., Pan, T., Cui, H., Zhao, Z., Chu, P. K., and Yu, X. F. (2019b). Black phosphorus: Bioactive nanomaterials with inherent and selective chemotherapeutic effects. *Angew. Chem. Int. Ed. Engl.* 58 (3), 769–774. doi:10.1002/anie.201810878

Zhou, W., Pan, T., and Cui, H. (2019a). Black phosphorus: Bioactive nanomaterials with inherent and selective chemotherapeutic effects [J]. *Angew. Chem. Int. Ed.* 131 (3), 779–784.

Zhu, H., and Li, Y. R. (2012). Oxidative stress and redox signaling mechanisms of inflammatory bowel disease: Updated experimental and clinical evidence. *Exp. Biol. Med.* 237, 474–480. doi:10.1258/ebm.2011.011358

Zhu, L., Xu, L., Wu, X., Deng, F., Ma, R., Liu, Y., et al. (2021). Tau-targeted multifunctional nanoinhibitor for Alzheimer's disease. *ACS Appl. Mater Interfaces* 13 (20), 23328–23338. doi:10.1021/acsami.1c00257

Zielińska, P., Staniszewska, M., Bondaryk, M., Koronkiewicz, M., and Urbanczyk-Lipkowska, Z. (2015). Design and studies of multiple mechanism of anti-Candida activity of a new potent Trp-rich peptide dendrimers. *Eur. J. Med. Chem.* 105, 106–119. doi:10.1016/j.ejmech.2015.10.013

frontiers | Frontiers in Bioengineering and Biotechnology

TYPE Original Research
PUBLISHED 28 April 2023
DOI 10.3389/fbioe.2023.1164942

OPEN ACCESS

EDITED BY
Zhanzhan Zhang,
Tianjin Medical University, China

REVIEWED BY
Jiahong Shen,
Northwestern University, United States
Jiulong Zhao,
Naval Medical University, China
Jing Cao,
Hunan Institute of Science and Technology, China

*CORRESPONDENCE
Xueguan Xie,
erpen731@163.com

RECEIVED 13 February 2023
ACCEPTED 04 April 2023
PUBLISHED 28 April 2023

CITATION
Hu H, Huang X, Dai Y, Zhu K, Ye X, Meng S, Zhang Q and Xie X (2023), Organic metal matrix Mil-88a nano-enzyme for joint repair in the osteoarthritis mouse model. *Front. Bioeng. Biotechnol.* 11:1164942. doi: 10.3389/fbioe.2023.1164942

Organic metal matrix Mil-88a nano-enzyme for joint repair in the osteoarthritis mouse model

Hao Hu, Xu Huang, Yankun Dai, Kairun Zhu, Xuwen Ye, Shengdong Meng, Qing Zhang and Xueguan Xie*

Huai'an Second People's Hospital, Huaian, China

Introduction: In this paper we tried to conduct a novel nanomaterial strategy to overcome osteoarthritis (OA) in a mouse model.

Methods: In this regard, after synthesizing the Mil-88a nanozyme, as a certain Fe-MOF, its toxic effects were detected by CCK-8 method and live-dead staining. The OA model of mouse was constructed, and paraffin sections of joints were taken for histological evaluation. In addition, immunofluorescence and immunohistochemistry were used to identify the OA progression and OARSI was used to evaluate the OA grades. We observed that Mil-88a could be easily synthesized and has high biocompatibility.

Results: We observed that Mil-88a could significantly promote the expression of OA anabolism-related genes such as *Col2* and also significantly inhibit the expression of OA catabolism-related genes *MMP13*. Besides, we observed better OARSI score in animals treated with Mil-88a nano-enzyme loading on organic metal matrix.

Discussion: Overall, Mil-88a nano-enzyme could be used as a novel strategy to treat OA.

KEYWORDS

nano-enzyme, osteoarthritis, mouse model, Mil-88a, organic metal

Introduction

Osteoarthritis (OA) is also known as degenerative bone disease, and its clinical symptoms are usually manifested as joint swelling and pain, limited mobility, etc., and even lead to joint deformity and muscle atrophy (Wang et al., 2020). Clinically, the symptomatic treatment for OA is to mainly relieve pain and reduce deformity (Zhang et al., 2019). At present, a large number of basic research studies have carried out a closer understanding of the occurrence and development of OA, but its specific pathogenesis is still unclear. It is mainly believed that the most important reason for the pathogenesis of OA is the imbalance of reactive oxygen species (ROS) (Ding et al., 2020).

Reactive oxygen species (ROS) are known to be essential to cellular processes and are essential byproducts of cell metabolism, including superoxide anions (O_2•), hydrogen peroxide (H_2O_2), and hydroxyl radicals (•OH) (Tsvetkov et al., 2022). ROS typically play a key role in the regulation of cell signaling pathways that normally control cell proliferation, growth, cycle, and death (Yi et al., 2021). ROS break the structure of signaling proteins by oxidizing redox-reactive residues on proteins, leading to the regulation of protein function (Gaurav et al., 2021). However, due to the oxidation of proteins, DNA, and membrane lipids, excess ROS may be a major cause of various inflammatory diseases (Zhai et al., 2021). Strategies to remove ROS by

antioxidant molecules such as vitamins or natural enzymes such as superoxide dismutase (SOD) when the anti-ROS system is disrupted have a wide range of effects (Sun et al., 2018).

Spectroscopic capabilities have been shown to be effective biological therapeutic agents to combat oxidative stress in the treatment of various inflammatory diseases (Li et al., 2022). While there is promise in reducing ROS levels, many conventional antioxidant molecular treatments are less efficient than natural enzymes (He et al., 2020). At the same time, natural enzymes are subjected to many limitations, such as sensitivity to environmental conditions, limited functional stability, and difficulty in large-scale production (Li et al., 2017; Chen et al., 2018; Wan et al., 2020; Zhang et al., 2023). Recently, with the rapid and significant advances in nanotechnology, a series of biocatalytic or antioxidant nanostructures have been designed with unique ROS-scavenging capabilities, demonstrating promising activity to overcome these core challenges in clinical anti-ROS and anti-oxidation (Chen et al., 2020; Shetty et al., 2021). This is compared to conventional anti-inflammatory drugs, where biocatalytic or antioxidant nanostructures can achieve anti-inflammatory effects by eliminating a broad spectrum of reactive oxygen species, rather than targeting only specific inflammatory pathways or molecules, which may provide better therapeutic efficiency and greater biosafety than current clinical drugs (Zhang et al., 2018; Zhu et al., 2020; Cheng et al., 2021).

Thus, the idea of using biocatalytic or antioxidant nanostructures opens up new avenues for ROS clearance of ROS-related biotherapeutics, such as metal–organic framework (MOF) and polyphenol nanoparticles. Overall, biocatalytic or antioxidant nanostructures exhibit significant advantages, such as a remarkable ROS-scavenging capacity compared to natural enzymes, a broad spectrum of ROS elimination activity, robust stability in physiological environments, and satisfactory biocompatibility and biosafety (Li et al., 2020).

Eventually, we can regulate ROS levels to treat inflammatory diseases. It has also been reported that MOF nanoparticles have the ability to remove reactive oxygen species (Bian et al., 2020). ROS cleared by MOFs is a promising candidate for therapeutic applications due to its high biocompatibility, 3D matrix, and modification capabilities. Therefore, a novel, safe, and effective drug targeting ROS imbalance needs to be developed urgently. Nanozyme is a kind of nanomaterial with enzymatic activity similar to proteins. Mil-88a belongs to the family of metal–organic framework (MOF) nanozyme with peroxidase mimetic activity and good biocompatibility (Kasula et al., 2022) and thus is considered to be a promising nano-enzyme repair system for promoting OA repair. This study investigated the role of Mil-88a nanozyme co-loaded with the organic metal matrix in promoting OA repair in a mouse model.

Materials and methods

Material synthesis

The preparation process of Mil-88a was carried out based on the improved techniques of the existing literature (Gaurav et al., 2021; Yi et al., 2021). First of all, 0.9744 g (8.4 mmol) fumaric acid and 2.2722 g (8.4 mmol) $FeCl_3$ were weighed. Then, the mixture was dissolved in 42 mL ultrapure water and stirred for 2 h. The solution was placed in the reaction kettle in a blast drying oven and then in a drying oven. The reaction was carried out at 85°C for 2 h. The reactor was taken out and cooled to room temperature. After the reaction kettle was cooled, the solution was centrifuged at 10,000 rpm for 10 min to obtain a brick-red solid. The precipitate was washed three times with absolute ethanol and dried in a vacuum drying oven at 100°C for 6 h. Ultimately, the solid obtained by drying was the metal–organic framework Mil-88a and was stored for future use.

Characterization of Mil-88a

The aforementioned dried precipitate was used for SEM, XRD, TGA, and FTIR characterization. In addition, a small amount of the powder was ultrasonically dispersed in ultrapure water for particle size analysis by DLS.

Detection of the SOD clearance rate of Mil-88a

Using the principle of the xanthine oxidase system to generate superoxide anion, according to the kit instructions (Beijing Solarbio Science & Technology Co., 100T/48S), the WST working solution and the enzyme working solution were prepared, respectively. A small amount of the sample powder was prepared as the mother solution, and then different proportions of the mother solution were mixed with pure water in a 1.5-mL tube to obtain sample solutions of different concentrations. The solution was incubated at 37°C for 20 min and was fully centrifuged to remove the material. The absorbance at 450 nm of the supernatant was measured, calculated, and compared with the control group, and the process was repeated three times for each group.

Detection of the hydroxyl radical-scavenging rate of Mil-88a

Using the principle that hydroxyl radicals are generated by the Fenton reaction and the interaction between hydroxyl radicals and chromogenic reagents (BOXBIO, AKAO013M), different concentrations of Mil-88a solutions were prepared according to the kit instructions, and the hydroxyl radical-scavenging efficiency of Mil-88a at different concentrations was measured. The process was repeated three times.

Primary culture of chondrocytes

Cartilage tissue was isolated from 5-day-old SD rats and washed with PBS containing 10% double antibody to remove blood clots. After incubation with 0.25% trypsin for 1.5 h at 37°C, 0.02% type II collagenase was replaced with 0.02% collagenase overnight to separate free cells. After the dissociated cells adhered to the wall, the medium was changed every 2 days and passed to the P3–P5 generation for use.

Biocompatibility testing

CCK-8 method: A density of 5×10^4 P3–P5 chondrocytes was inoculated in a 96-well plate overnight. After the cells adhered to the

wall, the medium was changed and 100 μL, 1 μg/mL, and 2 μg/mL chondrocytes were added, respectively. Mil-88a was resuspended in 0.25 mL of fresh media to get different concentrations (0 μg/mL, 1 μg/mL, 2 μg/mL, 5 μg/mL, 10 μg/mL, 20 μg/mL, 50 μg/mL, and 100 μg/mL). After allowing culturing in the cell incubator for 24 h, the medium was completely removed and rinsed with PBS twice to completely remove the material. A measure of 110 μL of CCK-8 containing the medium prepared at a ratio of 1:10 was added and incubated at 37°C for 1 h. After incubation, the supernatant medium was carefully pipetted to a new 96-well plate, and the absorbance at 450 nm was measured using a microplate reader. Then, the process was repeated three times per set. Staining of live and dead cells: A total of 5,000 P3–P5 chondrocytes were seeded in a 96-well plate overnight, and then the original medium was replaced by 0.2 mL of the fresh medium containing different concentrations of Mil-88a (0 μg/mL, 1 μg/mL, 2 μg/mL, 5 μg/mL, 10 μg/mL, 20 μg/mL, 50 μg/mL, and 100 μg/mL) for 24 h. The medium was removed and washed two times with PBS. A measure of 100 μL of calcein-AM/PI staining working solution was added in the dark for 20 min, PBS was used to remove excess dye, and three fields of view were randomly selected for observation under a confocal microscope at ×100 magnification.

PCR detection

A density of 3×10^5 cells per well was inoculated in a six-well plate, and after culturing for 24 h, the old medium was removed and washed thoroughly with PBS, and then 1 mL of H_2O_2 induction solution prepared in a serum-free medium with a concentration of 450 μmol/L was added. After the cells were fully induced, equal volumes of Mil-88a solutions prepared with the serum-free medium of different concentrations were added, and culturing was continued for 24 h. Subsequently, the medium containing nanomaterials was removed by thorough rinsing with PBS. Ultimately, RNA was extracted for PCR experiments.

Immunofluorescence

Each well was seeded with 75,000 chondrocytes of the same generation in a 24-well plate that had been placed on the slides. After adhering overnight, the cells were induced by oxidative stress in 0.25 mL of the serum-free medium mixed with H_2O_2 for 20 min. Then, the serum-free medium was replaced by 0.25 mL of the fresh medium containing different concentrations of Mil-88a (0 μg/mL, 1 μg/mL, 2 μg/mL, 5 μg/mL, 10 μg/mL, 20 μg/mL, 50 μg/mL, and 100 μg/mL). The treated cells were incubated for another 24 h, and it was washed three times with PBS buffer, fixed with 4% paraformaldehyde for 25 min, washed with PBS three times, then incubated with 3% H_2O_2 for 15 min, washed with PBS three times, and then incubated with goat serum for 30 min. After the blocking treatment, the diluted IL-1β primary antibody (1:200) was added dropwise to the slides and incubated overnight in a refrigerator at 4°C. Subsequently, the cells were incubated with biotinylated goat anti-rabbit secondary antibody (1:500) and allowed dilution for 1 h. Finally, the nuclei were labeled with 4′,6-diamidino-2-phenylindole (DAPI), incubated in the dark for 10 min, washed with buffer three times, dried the water on the slide, and sealed with neutral resin. After slicing, the sections were observed and photographed using a fluorescence microscope.

OARSI score

In this study, the Osteoarthritis Research Society International (OARSI) score was used to evaluate the degree of articular cartilage degeneration (Chen et al., 2018). OARSI grade (grade) is divided into six grades, and the higher the score, the more serious the cartilage degeneration. Grade 0: normal, with normal cartilage surface and chondrocytes; grade 1: slight fibrosis on the articular cartilage surface, unevenness, but no cartilage loss, and no involvement but middle and deep cartilage; grade 2: fissures on the articular cartilage surface and cartilage loss, the middle layer of cartilage is involved, fibrosis, chondrocyte proliferation and death, abnormal cartilage matrix staining, etc.; grade 3: the fissure involves the deep cartilage, and chondrocyte death and proliferation are mainly distributed along the fissure; grade 4: the matrix around the fissure is lost and articular cartilage erosion; grade 5: articular cartilage erosion, full-thickness erosion of unmineralized hyaline cartilage, mineralized cartilage, and subchondral bone exposed on the articular surface; grade 6: joint deformation, articular surface fibrocartilage, osteophyte formation, etc. In this study, the OARSI score was independently completed by two sports medicine doctors with clinical work experience under the light microscope (×100) according to the scoring rules, and the average score was taken as the final score, and the sample grouping was not informed.

Statistical analysis

SPSS and GraphPad Prism statistical software were used to analyze data, measurement data were expressed as mean ± standard deviation ($\bar{x} \pm s$), and a *t*-test was used for the comparison between groups. Comparisons among multiple groups were performed using one-way analysis of variance (ANOVA). $p < 0.05$ was regarded as a statistically significant difference.

Results

Evaluating Mil-88a by scanning electron microscopy and characterization by XRD, TGA, and FTIR

Electron microscopy showed that the synthesized Mil-88a was in the shape of hexagonal rods, as shown in Figure 1A. The overall main peak of Mil-88a did not show a large shift in the whole spectrum. There were three characteristic peaks in the range of 6°–15°, which were 2.8°, 10.4°, and 12.9°, respectively, as shown in Figures 1B and C. The mass retention of Mil-88a was basically unchanged in the range of 100°C–300°C. FTIR showed that Mil-88a had all the characteristic peaks of $FeCl_3$ and fumaric acid, as shown in Figures 1D, E. Next, the size of Mil-88a was characterized by dynamic light scattering (DLS) analysis, which demonstrated an ideal and uniform morphology with an average diameter of approximately 100 nm (Supplementary Figure S1).

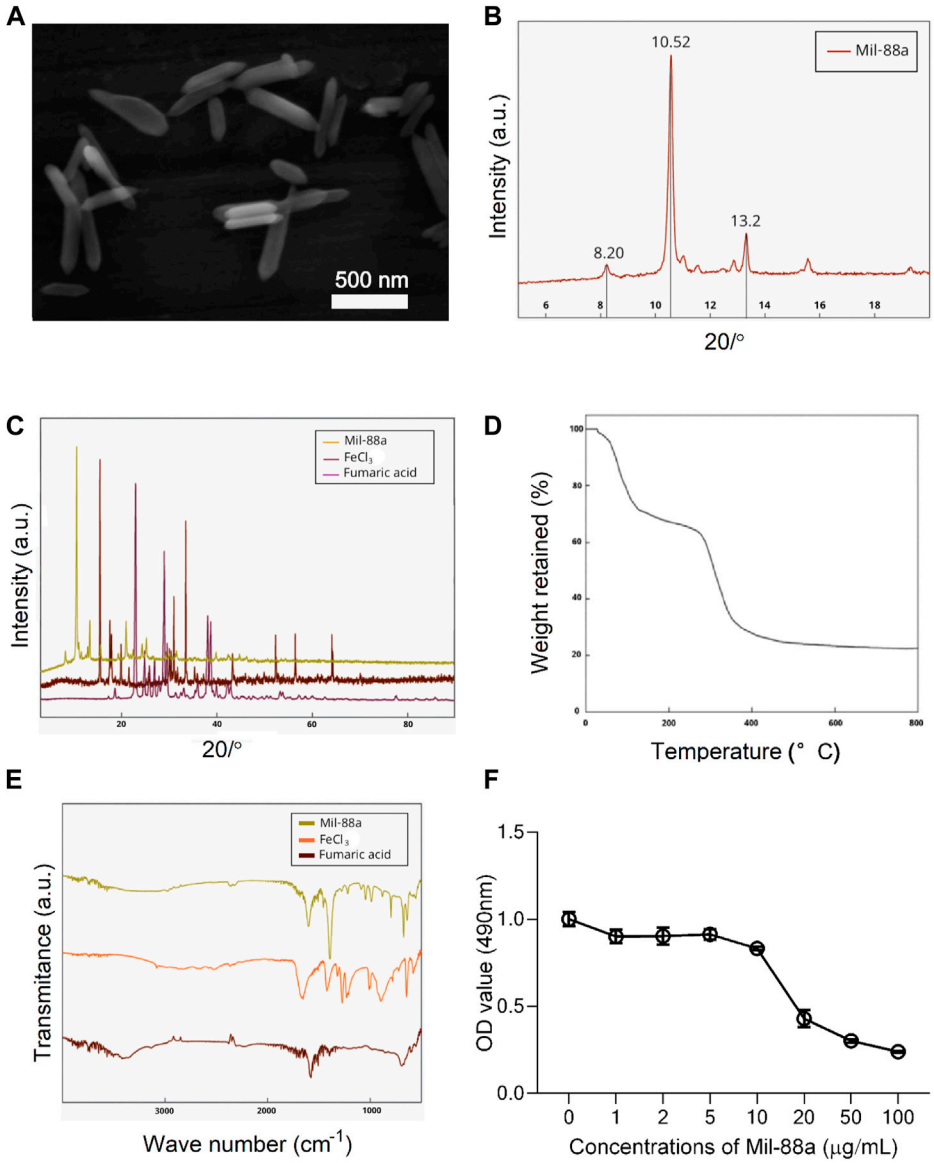

FIGURE 1
Characterization of Mil-88a. **(A)** Electron microscopy image of Mil-88a. **(B)** XRD characterization of Mil-88a. **(C)** XRD characterization of Mil-88a, $FeCl_3$, and fumaric acid. **(D)** TGA characterization of Mil-88a. **(E)** FTIR characterization of Mil-88a. **(F)** Effects of different concentrations of Mil-88a on chondrocyte proliferation for 24 h.

Biocompatibility evaluation of Mil-88a

CCK-8 method: When the concentration of Mil-88a was in the range of 1–10 μg/mL, the chondrocyte survival rate was maintained above 80%, as shown in Figure 1F. Staining of live and dead cells: When the concentration was greater than 10 μg/mL, it showed strong toxicity to chondrocytes ($p < 0.001$), as shown in Figures 2A, B. ROS-scavenging effect of Mil-88a: With the increase in the Mil-88a concentration, the SOD-scavenging rate of Mil-88a gradually increased ($p < 0.001$; Figure 2C), and the hydroxyl radical-scavenging rate was different from that of Fe_3O_4, but the scavenging efficiency did not change with Mil-88a ($p < 0.05$, Figure 2D). This phenomenon takes place because when the nanoreactor reaches the tumor site, a high concentration of glutathione reduces Fe^{3+}, triggering the structural collapse of MOF and the release of Fe^{2+}, while GOx catalyzes the oxidation of glucose to H_2O_2. Then, the Fenton reaction occurs between H_2O_2 and Fe^{2+}, producing the hydroxyl radical (•OH). Therefore, after Mil-88a, as a Fe-MOF, is taken up by cells, SOD is only consumed and •OH is consumed and increased. In addition, we evaluated the expression of IL-1β to figure out the effect of Mil-88a on pro-inflammatory cytokines (Figure 2E; Supplementary Figure S2). We observed that Mil-88a could significantly decrease the expression of IL-1β in a dose-dependent manner.

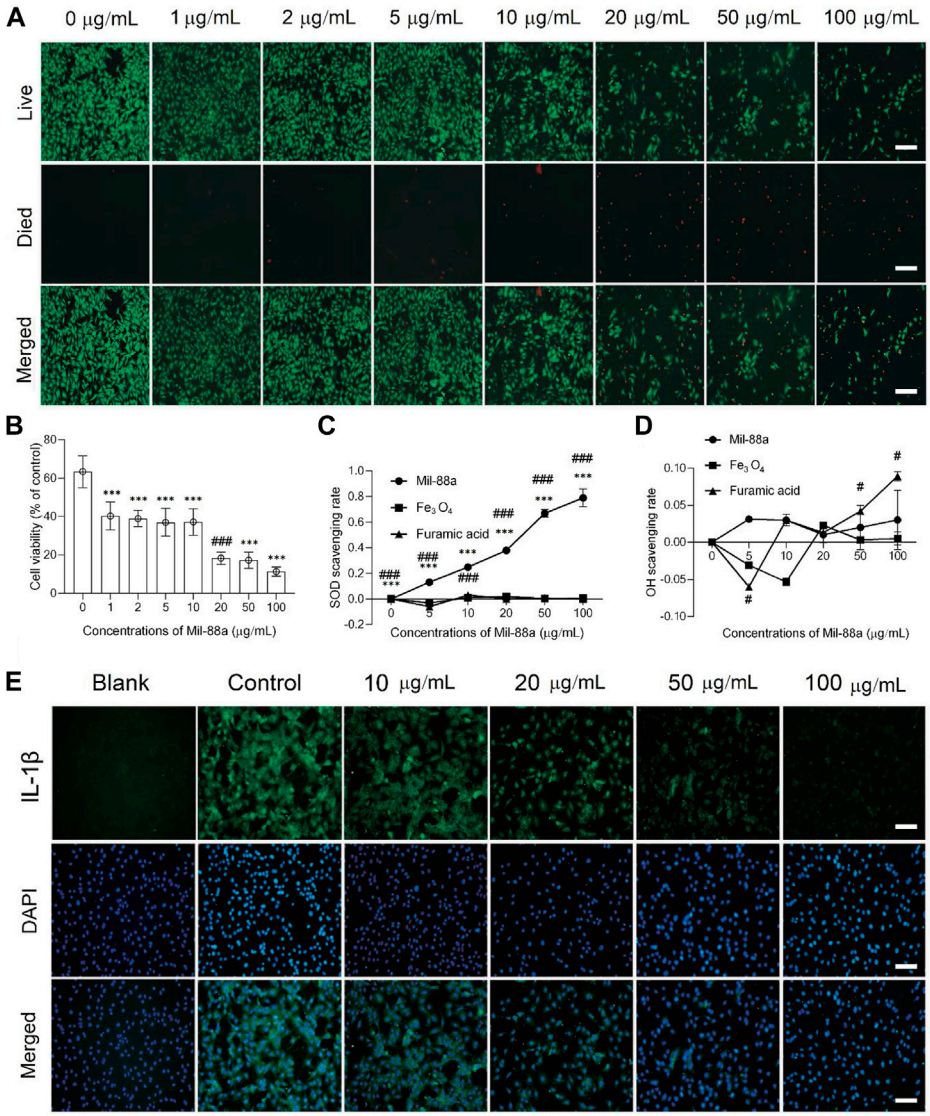

FIGURE 2
Cytotoxicity and biocompatibility testing of Mil-88a *in vitro*. **(A)** Fluorescence microscopy images of calcein-AM/PI staining in cells treated with different concentrations of Mil-88a (1, 2, 5, 10, 20, 50, and 100 μg/mL). Live, live cells (green); died, dead cells (red); merge, overlay. **(B)** Cell viabilities of chondrocyte cells treated with different concentrations of Mil-88a (1, 2, 5, 10, 20, 50, and 100 μg/mL and $n = 4$). The effects of different concentrations of Mil-88a (1, 2, 5, 10, 20, 50, and 100 μg/mL and $n = 4$) on SOD- **(C)** and OH- **(D)** scavenging rates for 24 h, and IL-1β **(E)**. ***$p < 0.001$ compared with 0 μg/mL; ###$p < 0.001$ compared with 10 μg/mL. Scale bar = 100 μm.

Mil-88a alleviated the pathological manifestations of OA *in vivo*

To explore the effect of Mil-88a nano-enzyme on the osteoarthritis mouse model, Mil-88a nano-enzyme was administered by local injection into the joint cavity. Safranin O staining of paraffin sections of rat knee joints showed that rats on a high-cholesterol diet showed a more severe OA phenotype than those on a normal diet (Figure 3A). The joint surface was not smooth, the safranin O staining and immunohistochemical staining intensity of type II collagen (col2) decreased, and the immunohistochemical staining intensity of MMP13 (matrix metalloproteinases 13) increased, indicating that the ECM proteoglycan content of articular cartilage Mil-88a nano-enzyme treatment can significantly increase the content of protein polysaccharide and type II collagen, effectively improve the degenerative lesions of the aforementioned knee cartilage tissue, and alleviate the progression of OA (Figure 3A). The severity of OA in the mouse was scored using the OARSI score. The results showed that the OARSI scores of MTP (Figure 3B) and MFC (Figure 3C) of the animals treated with Mil-88a were significantly lower than those of the animals in the non-treated group. This indicated that the degenerative lesions of the cartilage tissue in the Mil-88a-treated group were milder. Scoring of Col2 (Figure 3D) and MMP13 (Figure 3E) immunohistochemistry also showed this trend. The results suggest that Mil-88a could alleviate the progression of OA.

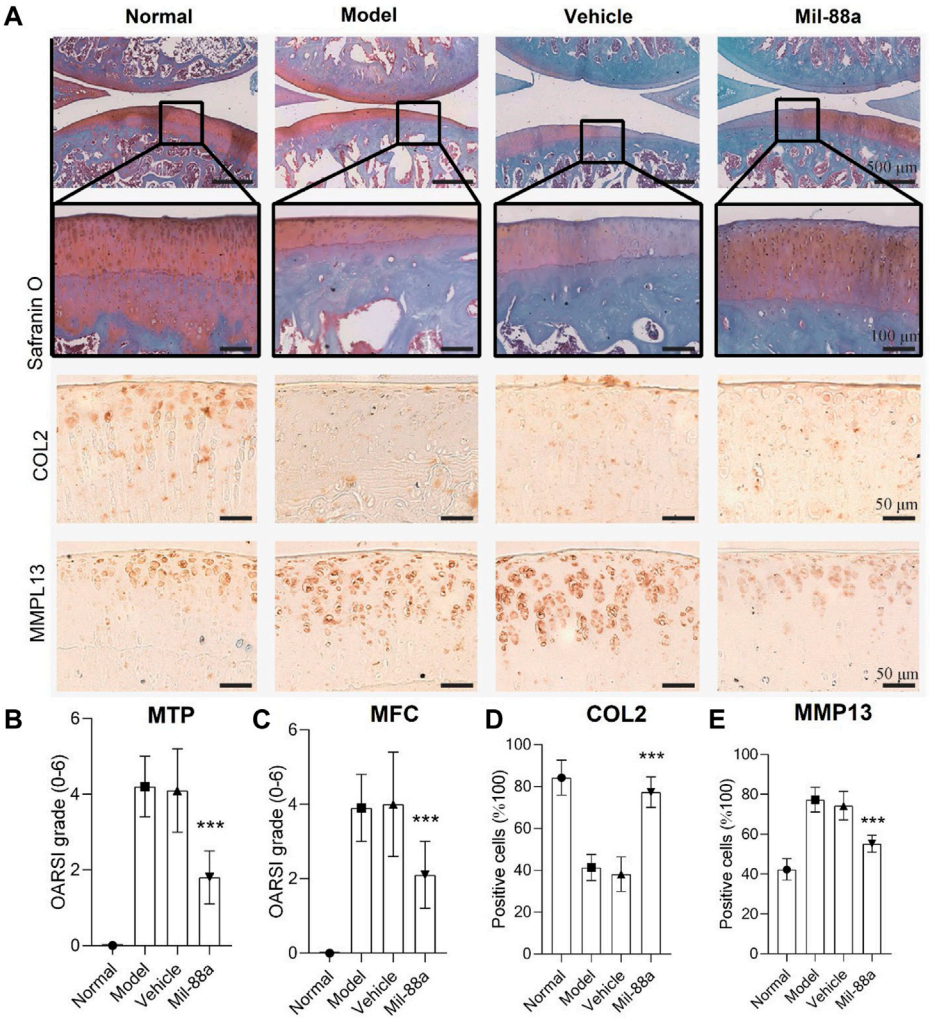

FIGURE 3
Mil-88a alleviates the pathological manifestations of OA. **(A)** Safranin O staining of paraffin sections of rat knee tissue, scale bar = 500 or 100 μm, and immunohistochemical staining of Col2 and MMP13, scale bar = 50 μm. **(B, C)** OARSI score. **(D, E)** Positive cell statistics of Col2 and MMP13. (n = 6). ns, no statistical difference; $*p < 0.05$; $**p < 0.01$; $***p < 0.001$.

Evaluation of the effect

In this section, we first tried to evaluate the conduction of OA in the mouse model using luminescence imaging (Figures 4A, B, 5). We observed high intensity of luminescence in the joints with the conduction of OA in comparison to normal mice (Figure 4B). In addition, we observed a significant drop in luminescence density in joints treated with Mil-88a. These results suggested that Mil-88a could improve OA *in vivo*. In addition, we applied a micro-CT scan to assess the effect of Mil-88a on bone density (Figures 4C, D). Dramatically, we observed that Mil-88a could increase bone density at the site of femoral joints (Figures 4E–H). These results suggested that Mil-88a could significantly increase bone formation to improve OA.

Discussion

Approximately 16.2% of patients in China suffer from OA for a long time. The unbearable pain and extremely high disability rate seriously affect the quality of life of patients and destroy the stability of families and society (Xu et al., 2022). Although a lot of basic research has been carried out, the etiology and pathogenesis of OA are still inconclusive, and it is mainly believed to be related to factors such as age, occupation, strain, and endocrine (Lan et al., 2019; Qiu et al., 2020). Excessive ROS is the cause of arthritis inflammatory lesions. One of the important factors, as a potential target for the treatment of OA, is how to reverse the ROS imbalance, which has become the key to curing OA (Hou et al., 2021). MOFs are nanoparticles with a special 3D network structure formed by the self-assembly of metal nodes and organic ligands through chemical bonds. With a large specific surface area, adjustable pore size, and stable physicochemical properties, it is considered a promising biomimetic nanozyme (Xiong et al., 2022). Wu et al. (Zhou et al., 2022) reported that the special metal node structure of MOFs has oxidase analog activity, which is considered an ideal nanozyme for scavenging ROS. In this study, electron microscopy of Mil-88a showed a hexagonal rod shape, and XRD showed three characteristic peaks

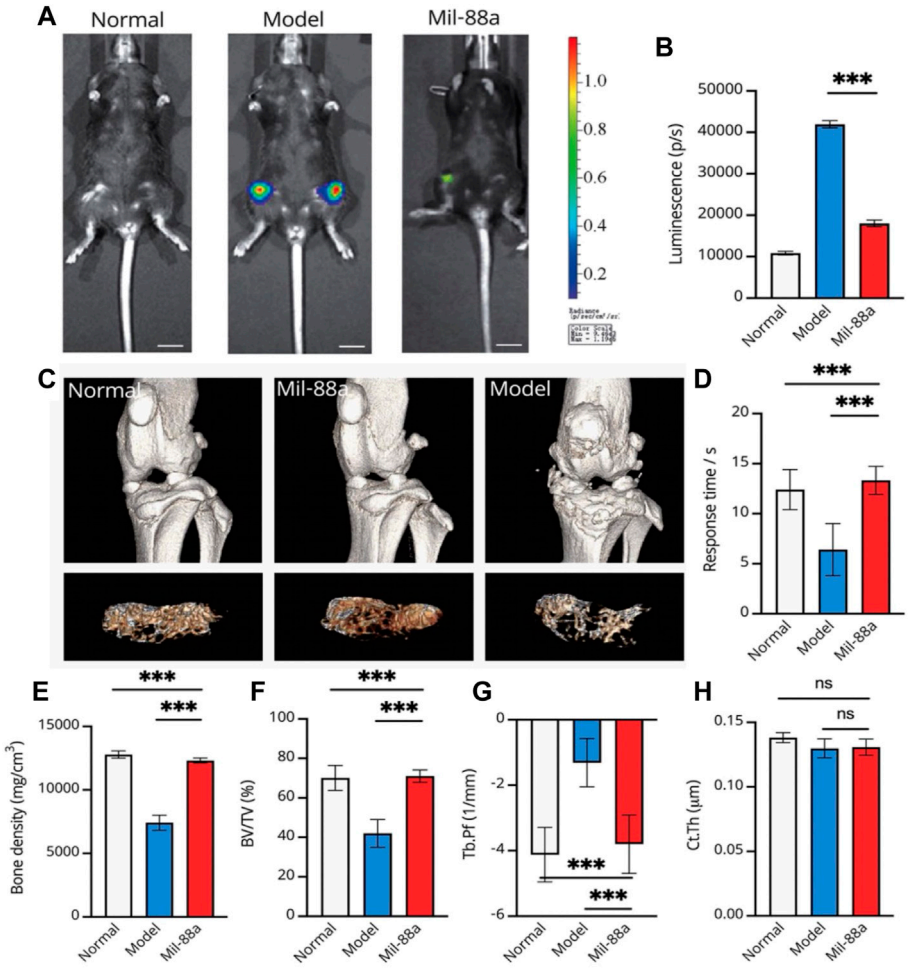

FIGURE 4
Representative luminescence imaging *in vivo* and evaluation of bone density in the mouse joint using micro-CT. Evaluation of osteoarthritis using luminescence imaging **(A, B)**. The 3D reconstruction of CT indicates the bone changes, and the tibial plateau section shows the structure of bone trabeculae **(C)**. For evaluating the response time, mice were placed on the heating platform at 55°C, and the reaction time of licking and jumping was shown; a micro-CT scan of the joints of mice was performed **(C, D)**. Bone density (mg/cm^3) **(E)**, bone volume fraction (BV/TV) **(F)**, trabecular pattern factor (Tb.Pf, 1/mm) **(G)**, and cortical bone thickness **(H)** were used to assess subchondral bone changes in osteoarthritis by quantitative CT. Values were presented as mean ± SD. ***$p < 0.001$ ($n = 5$).

in the range of 6°–15°, which was consistent with the previous report (Chen et al., 2022). FTIR has all the characteristic peaks of raw materials, and TGA confirms that Mil-88a still has good stability in the range of approximately 100°C–300°C. In order to verify the cytotoxicity of Mil-88a, CCK-8 and live–dead staining indicated that when the concentration of Mil-88a was less than 10 μg/mL, there was basically no cytotoxicity ($p < 0.001$). In conclusion, Mil-88a was successfully synthesized with good biocompatibility. OA is mainly manifested as a cartilage defect. Reducing the oxidative stress of chondrocytes and removing excess reactive oxygen species will be beneficial to the regeneration of cartilage (He et al., 2021; Ma et al., 2022). ROS include SOD and OH (Chen et al., 2021). The ROS clearance rate of Mil-88a was further verified. The results showed that the SOD clearance rate of Mil-88 was concentration-dependent, and the OH clearance rate did not change with the concentration but was still higher than that of Fe_3O_4 ($p < 0.05$), suggesting that it is not simply due to its porous physical structure that scavenges ROS and the specific mechanism remains to be further studied. The results suggested that Mil-88a has the potential to act as a ROS-scavenging nanozyme in the joint cavity. ROS is an important signaling molecule that regulates inflammation. The imbalance of ROS leads to the abnormal expression of TNF-α and IL-1β inflammatory factors. Previous works of literature reported that TNF-α and IL-1β are closely related to cartilage destruction and the occurrence of synovitis (Ma et al., 2020; Cao et al., 2023). TNF-α, as a key inhibitor of cartilage collagen production, promotes the apoptosis of chondrocytes, and the activation of TNF-α causes the occurrence of the inflammatory cascade by upregulating the inflammatory trigger of IL-1β (Liu et al., 2021; Peng et al., 2021).

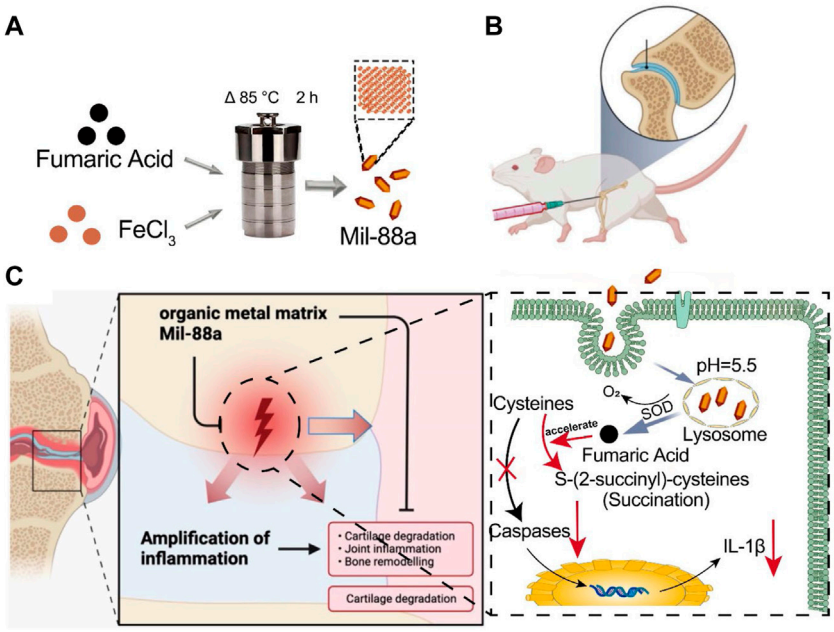

FIGURE 5
Schematic of how Mil-88a could improve OA in a mouse model. **(A)** Flow diagram of the prepared Mil-88a. **(B)** Illustration of the injected method of Mil-88a. **(C)** The treatment process for suppressing the expression of IL-1β and relief of inflammatory response.

Conclusion

In summary, we synthesized a novel platform based on Fe-MOF (Mil-88a) to overcome osteoarthritis (OA), which has good biosafety and can downregulate the expression of oxidative and inflammatory factors in OA-induced chondrocytes. In this regard, after synthesizing the Mil-88a nanozyme, its toxic effects were detected by the CCK-8 method and live–dead staining. The OA mouse model was constructed, and paraffin sections of the joints were obtained for histological evaluation. In addition, immunofluorescence and immunohistochemistry were used to identify the OA progression, and the OARSI score was used to evaluate the OA grades. We observed that Mil-88a could be easily synthesized and has high biocompatibility. We observed that Mil-88a could significantly promote the expression of OA anabolism-related genes such as *Col2* and also significantly inhibit the expression of OA catabolism-related genes such as *MMP13*. In addition, we observed better OARSI scores in animals treated with Mil-88a nano-enzyme loaded on the organic metal matrix. Overall, Mil-88a co-loaded with the organic metal matrix could be used as a novel nano-enzyme strategy in the treatment of OA. We also observed that Mil-88a nanozyme could significantly improve OARSI scores and OA in the mouse model in this study. Thus, our Mil-88a might be particularly meaningful and readily adapted to OA in a broad diversity of the current situation.

Data availability statement

The raw data supporting the conclusion of this article will be made available by the authors, without undue reservation.

Ethics statement

The animal study was reviewed and approved by Huai'an Second People's Hospital.

Author contributions

XX and HH conceived the presented idea and together with XH designed the experiment. YD and KZ carried out most of the experiments. XY and SM contributed to sample preparation and data analysis. QZ wrote the manuscript. All authors discussed the results, provided critical feedback, and contributed to the final manuscript.

Conflict of interest

The authors declare that the research was conducted in the absence of any commercial or financial relationships that could be construed as a potential conflict of interest.

Publisher's note

All claims expressed in this article are solely those of the authors and do not necessarily represent those of their affiliated organizations, or those of the publisher, the editors, and the reviewers. Any product that may be evaluated in this article, or claim that may be made by its manufacturer, is not guaranteed or endorsed by the publisher.

Supplementary material

The Supplementary Material for this article can be found online at: https://www.frontiersin.org/articles/10.3389/fbioe.2023.1164942/full#supplementary-material

References

Bian, Y., Liu, B., Liang, S., Ding, B., Zhao, Y., Jiang, F., et al. (2020). Cu-based MOFs decorated dendritic mesoporous silica as tumor microenvironment responsive nanoreactor for enhanced tumor multimodal therapy. *Chem. Eng. J.* 435, 135046. doi:10.1016/j.cej.2022.135046

Cao, Z., Wang, H., Chen, J., Zhang, Y., Mo, Q., Zhang, P., et al. (2023). Silk-based hydrogel incorporated with metal-organic framework nanozymes for enhanced osteochondral regeneration. *Bioact. Mater.* 20, 221–242. doi:10.1016/j.bioactmat.2022.05.025

Chen, C., Wang, Z., Jia, S., Zhang, Y., Ji, S., Zhao, Z., et al. (2020). Evoking highly immunogenic ferroptosis aided by intramolecular motion-induced photo-hyperthermia for cancer therapy. *Adv. Sci.* 9, e2104885. doi:10.1002/advs.202104885

Chen, J., Wei, X., Tang, H., Munyemana, J. C., Guan, M., Zhang, S., et al. (2021). Deep eutectic solvents-assisted synthesis of ZnCo2O4 nanosheets as peroxidase-like nanozyme and its application in colorimetric logic gate. *Talanta* 222, 121680. doi:10.1016/j.talanta.2020.121680

Chen, S., Jia, Q., Zheng, X., Wen, Y., Liu, W., Zhang, H., et al. (2018). PEGylated carbon dot/MnO_2 nanohybrid: A new pH/H_2O_2-driven, turn-on cancer nanotheranostics. *Sci. China Mater.* 61, 1325–1338. doi:10.1007/s40843-018-9261-x

Chen, Y., Wang, Y., Chen, Z., Cai, J., Li, K., Huang, H., et al. (2022). NIR-driven polydopamine-based nano-enzymes as ROS scavengers to suppress osteoarthritis progression. *Mater. Today Nano* 19, 100240. doi:10.1016/j.mtnano.2022.100240

Cheng, Y., Wen, C., Sun, Y. Q., Yu, H., and Yin, X. B. (2021). Mixed-metal MOF-derived hollow porous nanocomposite for trimodality imaging guided reactive oxygen species-augmented synergistic therapy. *Adv. Funct. Mater.* 31 (37), 2104378. doi:10.1002/adfm.202104378

Ding, S. S., He, L., Bian, X. W., and Tian, G. (2020). Metal-organic frameworks-based nanozymes for combined cancer therapy. *Nano Today* 35, 100920. doi:10.1016/j.nantod.2020.100920

Gaurav, K., Nirmal, P., Venkateswaran, V., and Sang-Jae, K. (2021). Biodegradable metal-organic framework MIL-88A for triboelectric nanogenerator. *iScience* 24, 102064. doi:10.1016/j.isci.2021.102064

He, H., Du, L., Guo, H., An, Y., Lu, L., Chen, Y., et al. (2020). Redox responsive metal organic framework nanoparticles induces ferroptosis for cancer therapy. *Small* 16, 2001251. doi:10.1002/smll.202001251

He, S. B., Yang, L., Lin, M. T., Noreldeen, H. A., Yu, R. X., Peng, H. P., et al. (2021). Acetaminophen sensor based on the oxidase-like activity and interference self-elimination ability of chondroitin sulfate-modified platinum nanozyme. *Sensors Actuators B Chem.* 347, 130627. doi:10.1016/j.snb.2021.130627

Hou, W., Ye, C., Chen, M., Gao, W., Xie, X., Wu, J., et al. (2021). Excavating bioactivities of nanozyme to remodel microenvironment for protecting chondrocytes and delaying osteoarthritis. *Bioact. Mater.* 6 (8), 2439–2451. doi:10.1016/j.bioactmat.2021.01.016

Kasula, M., Le, T., Thomsen, A., and Rabbani Esfahani, M. (2022). Silver metal organic frameworks and copper metal organic frameworks immobilized on graphene oxide for enhanced adsorption in water treatment. *Chem. Eng. J.* 439, 135542. doi:10.1016/j.cej.2022.135542

Lan, G., Ni, K., Veroneau, S. S., Luo, T., You, E., and Lin, W. 2019. Nanoscale metal-organic framework hierarchically combines high-Z components for multifarious radio-enhancement. *J. Am. Chem. Soc.* 141, pp.6859–6863. doi:10.1021/jacs.9b03029

Li, C., Shen, J., Wu, K., and Yang, N. (2022). Metal centers and organic ligands determine electrochemistry of metal-organic frameworks. *Small. Mar.* 18, e2106607. doi:10.1002/smll.202106607

Li, P. X., Xie, Z. X., Jin, A. P., Li, J., and Guo, G. C. (2020). A new photochromic Gd-MOF with photoswitchable bluish-white to greenish-yellow emission based on electron transfer. *Chem. Commun. (Camb).* 56, 14689–14692. doi:10.1039/d0cc06019d

Li, S. Y., Cheng, H., Xie, B. R., Qiu, W. X., Zeng, J. Y., Li, C. X., et al. (2017). Cancer cell membrane camouflaged cascade bioreactor for cancer targeted starvation and photodynamic therapy. *ACS Nano* 11, 7006–7018. doi:10.1021/acsnano.7b02533

Liu, Y., Qing, Y., Jing, L., Zou, W., and Guo, R. (2021). Platinum–copper bimetallic colloid nanoparticle cluster nanozymes with multiple enzyme-like activities for scavenging reactive oxygen species. *Langmuir* 37 (24), 7364–7372. doi:10.1021/acs.langmuir.1c00697

Lopez-Cantu, D. O., González-González, R. B., Sharma, A., Bilal, M., Parra-Saldívar, R., and Iqbal, H. M. (2022). Bioactive material-based nanozymes with multifunctional attributes for biomedicine: Expanding antioxidant therapeutics for neuroprotection, cancer, and anti-inflammatory pathologies. *Coord. Chem. Rev.* 469, 214685. doi:10.1016/j.ccr.2022.214685

Ma, J., Qiu, J., and Wang, S. (2020). Nanozymes for catalytic cancer immunotherapy. *ACS Appl. Nano Mater.* 3 (6), 4925–4943. doi:10.1021/acsanm.0c00396

Ma, X., Hao, J., Wu, J., Li, Y., Cai, X., and Zheng, Y. (2022). Prussian blue nanozyme as a pyroptosis inhibitor alleviates neurodegeneration. *Adv. Mater.* 34 (15), 2106723. doi:10.1002/adma.202106723

Mou, X., Wu, Q., Zhang, Z., Liu, Y., Zhang, J., Zhang, C., et al. (2022). Nanozymes for regenerative medicine. *Small Methods* 6, 2200997. doi:10.1002/smtd.202200997

Peng, Y., He, D., Ge, X., Lu, Y., Chai, Y., Zhang, Y., et al. (2021). Construction of heparin-based hydrogel incorporated with Cu5.4O ultrasmall nanozymes for wound healing and inflammation inhibition. *Bioact. Mater.* 6 (10), 3109–3124. doi:10.1016/j.bioactmat.2021.02.006

Qiu, Q., Wang, T., Jing, L., Huang, K., and Qin, D. (2020). Tetra-carboxylic acid based metal-organic framework as a high-performance bifunctional electrocatalyst for HER and OER. *Int. J. Hydrogen Energy* 45, 11077–11088. doi:10.1016/j.ijhydene.2020.02.033

Rajeshri, D. P., Mihir, K. R., and Navin, R. S. (2020). Formation of Diacerein – fumaric acid eutectic as a multi-component system for the functionality enhancement. *J. Drug Deliv. Sci. Technol.* 58, 101562. doi:10.1016/j.jddst.2020.101562

Shetty, S. C., Yandrapalli, N., Pinkwart, K., Krafft, D., Vidakovic-Koch, T., Ivanov, I., et al. (2021). Directed signaling cascades in monodisperse artificial eukaryotic cells. *ACS Nano* 15, 15656–15666. doi:10.1021/acsnano.1c04219

Sun, L., Li, Y. H., and Shi, H. (2018). A ketone functionalized Gd (III)-MOF with low cytotoxicity for anti-cancer drug delivery and inhibiting human liver cancer cells. *J. Clust. Sci.* 30, 251–258. doi:10.1007/s10876-018-1482-3

Tsvetkov, P., Coy, S., Petrova, B., Dreishpoon, M., Verma, A., Abdusamad, M., et al. (2022). Copper induces cell death by targeting lipoylated TCA cycle proteins. *Sci. Mar* 18 (375), 1254–1261. doi:10.1126/science.abf0529

Wan, X., Song, L., Pan, W., Zhong, H., Li, N., and Tang, B. (2020). Tumor-targeted cascade nanoreactor based on metal–organic frameworks for synergistic ferroptosis–starvation anticancer therapy. *ACS Nano* 14, 11017–11028. doi:10.1021/acsnano.9b07789

Wang, D., Jana, D., and Zhao, Y. (2020). Metal–organic framework derived nanozymes in biomedicine. *Accounts Chem. Res.* 53 (7), 1389–1400. doi:10.1021/acs.accounts.0c00268

Wu, H., Li, F., Shao, W., Gao, J., and Ling, D. (2019). Promoting angiogenesis in oxidative diabetic wound microenvironment using a nanozyme-reinforced self-protecting hydrogel. *ACS central Sci.* 5 (3), 477–485. doi:10.1021/acscentsci.8b00850

Xiong, H., Zhao, Y., Xu, Q., Xie, X., Wu, J., Hu, B., et al. (2022). Biodegradable hollow-structured nanozymes modulate phenotypic polarization of macrophages and relieve hypoxia for treatment of osteoarthritis. *Small* 18 (32), 2203240. doi:10.1002/smll.202203240

Xu, W., Wang, T., Qian, J., Wang, J., Hou, G., Wang, Y., et al. (2022). Fe (II)-hydrazide coordinated all-active metal organic framework for photothermally enhanced tumor penetration and ferroptosis-apoptosis synergistic therapy. *Chem. Eng. J.* 437, 135311. doi:10.1016/j.cej.2022.135311

Yi, X., Ji, H., Wang, C., Li, Y., Li, Y. H., Zhao, C., et al. (2021). Photocatalysis-activated SR-AOP over PDINH/MIL-88A(Fe) composites for boosted chloroquine phosphate degradation: Performance, mechanism, pathway and DFT calculations. *Appl. Catal. B Environ.* 293, 120229. doi:10.1016/j.apcatb.2021.120229

Zhai, Y., Wang, J., Lang, T., Kong, Y., Rong, R., Cai, Y., et al. (2021). T lymphocyte membrane-decorated epigenetic nanoinducer of interferons for cancer immunotherapy. *Nat. Nanotechnol. Nov.* 16, 1271–1280. doi:10.1038/s41565-021-00972-7

Zhang, D., Wu, M., Cai, Z., Liao, N., Ke, K., Liu, H., et al. (2018). Chemotherapeutic drug based metal-organic particles for microvesicle-mediated deep penetration and programmable pH/NIR/hypoxia activated cancer photochemotherapy. *Adv. Sci.* 5, 1700648. doi:10.1002/advs.201700648

Zhang, X., Li, G., Wu, D., Li, X., Hu, N., Chen, J., et al. (2019). Recent progress in the design fabrication of metal-organic frameworks-based nanozymes and their applications to sensing and cancer therapy. *Biosens. Bioelectron.* 137, 178–198. doi:10.1016/j.bios.2019.04.061

Zhang, Z., Zhao, J., Chen, Z., Wub, H., and Wang, S. (2023). A molybdenum-based nanoplatform with multienzyme mimicking capacities for oxidative stress-induced acute liver injury treatment. *Inorg. Chem. Front.* 10, 1305–1314. doi:10.1039/d2qi02318k

Zhou, T., Ran, J., Xu, P., Shen, L., He, Y., Ye, J., et al. (2022). A hyaluronic acid/platelet-rich plasma hydrogel containing MnO2 nanozymes efficiently alleviates osteoarthritis *in vivo*. *Carbohydr. Polym.* 292, 119667. doi:10.1016/j.carbpol.2022.119667

Zhu, Y., Xin, N., Qiao, Z., Chen, S., Zeng, L., Zhang, Y., et al. (2020). Bioactive MOFs based theranostic agent for highly effective combination of multimodal imaging and chemo-phototherapy. *Adv. Healthc. Mater.* 9 (14), 2000205. doi:10.1002/adhm.202000205

frontiers | Frontiers in Bioengineering and Biotechnology

TYPE Review
PUBLISHED 24 July 2023
DOI 10.3389/fbioe.2023.1240529

OPEN ACCESS

EDITED BY
Zhanzhan Zhang,
Tianjin Medical University, China

REVIEWED BY
Guotao Yuan,
Sun Yat-sen University, China
Jingyu Wang,
Tianjin Medical University, China
Chunxiong Zheng,
Sun Yat-sen University, China

*CORRESPONDENCE
Jie Lv,
lvjie@ylu.edu.cn
Xianhai Zeng,
zxhklwx@163.com
Wei Jiang,
13667452911@163.com

†These authors have contributed equally to this work

RECEIVED 15 June 2023
ACCEPTED 14 July 2023
PUBLISHED 24 July 2023

CITATION
Zhang P, Ye G, Xie G, Lv J, Zeng X and Jiang W (2023), Research progress of nanomaterial drug delivery in tumor targeted therapy.
Front. Bioeng. Biotechnol. 11:1240529.
doi: 10.3389/fbioe.2023.1240529

Research progress of nanomaterial drug delivery in tumor targeted therapy

Peng Zhang[1†], Guihua Ye[2†], Guofeng Xie[3], Jie Lv[4*], Xianhai Zeng[1*] and Wei Jiang[3*]

[1]Department of Otorhinolaryngology, Longgang Otorhinolaryngology Hospital & Shenzhen Key Laboratory of Otorhinolaryngology, Shenzhen Institute of Otorhinolaryngology, Shenzhen, China, [2]Shanghai Ninth People's Hospital Hainan Branch, Hainan Western Central Hospital, Danzhou, China, [3]Affiliated Cancer Hospital and Institute of Guangzhou Medical University, Guangzhou, China, [4]School of Computer Science and Engineering, Yulin Normal University, Yulin, China

Cancer is one of the most lethal diseases in human society, and its incidence is gradually increasing. However, the current tumor treatment often meets the problem of poor efficacy and big side effects. The unique physical and chemical properties of nanomaterials can target the delivery of drugs to tumors, which can improve the therapeutic effect while reducing the damage of drugs to normal cells. This makes nanomaterials become a hot topic in the field of biomedicine. This review summarizes the recent progress of nanomaterials in tumor targeted therapy.

KEYWORDS

nanomaterials, tumor, targeted therapy, drug delivery, tumorigenic factors

1 Introduction

Malignant tumor is a new organism, that is seriously disturbed in the regulation of cell growth under the action of various tumorigenic factors, resulting in the abnormal proliferation of cells in the body. It often presents as abnormal tissue clumps in the body. Tumors can escape the surveillance of the immune system, grow without limit, and metastasize through blood, lymphatic, or implantation (Robert, 2013). There are still great challenges in the treatment of malignant tumors. In 2022, 1918030 new cancer cases and 609360 cancer deaths are projected to occur in the United States. Although the incidence of lung cancer is gradually slowing down, the incidence of breast cancer and advanced stage prostate cancer is still increasing (Siegel and Miller, 2022). According to the National Cancer Center of China, the number of new cases of malignant tumor in China in 2016 was 4.0640 million, of which 2.2343 million were men and 1.829,600 were women. The crude and age-standardized incidence rates (ASIR) were 293.91 and 186.46 per 100,000 population, respectively (Zheng et al., 2022). Nowadays, the traditional treatment methods are mainly surgery, chemotherapy and radiotherapy. However, the therapeutic effect is still not satisfactory. The main reasons include side effects, drug resistance and insensitivity of tumor cells to radiation (Zhang et al., 2018). Therefore, the search for a highly targeted, efficient and low toxicity therapy has become an important direction in cancer therapy research.

At present, many targeted drugs have been applied in clinical practice, which have the advantages of good targeting and few side effects. Targeted therapy can inhibit the growth of tumor cells by targeting drugs on key genes of tumor growth and division, such as EGFR, HER-2, KRAS, ALK, etc (Rouviere et al., 2015; Saito et al., 2018; Meric-Bernstam et al., 2019).

However, the mutation rate of target genes in patient population is not high, so many patients are not suitable for using targeted drugs. In addition, in clinical practice, targeted drugs may miss the target. Long-term use is easy to resist drugs, and the price is expensive. Therefore, it has broad application prospect to find a new therapeutic method which is applicable to a wide population and stable targeting performance. At present, the commonly used targeted drugs in clinical practice include Bevacizumab, Trastuzumab, Cetuximab, Pertuzumab, Osimertinib, Lenvatinib, etc. These targeted drugs can mainly be used in the treatment of lung cancer, bowel cancer, breast cancer, liver cancer, lymphoma.

Nanoparticles exhibit unique physical, chemical, and biological properties. They find wide-ranging applications in fields such as biomedical research (Schmalz et al., 2017). The characteristics of small size and large area to volume ratio of nanoparticles enable them to efficiently bind, absorb and deliver small molecules of drugs (Yetisgin and Cetinel, 2020). Their variable size, shape and surface characteristics also enable them to have high stability, high carrying capacity, properties of binding hydrophilic or hydrophobic substances, and compatibility of different drug delivery routes. Because of their own advantages, nanomaterials can play a certain advantage in tumor treatment. Nanomaterials can wrap drugs or combine drugs to be targeted and delivered near the tumor area, so that drugs can act on tumor cells more accurately. The targeted therapy of nanomaterials can be divided into passive and active targeting according to different targeting pathways (Alavi and Hamidi, 2019). The former refers to that after the combination of nanomaterials and therapeutic drugs enters the human body, taking into account the differences in the specific biochemical microenvironment of organs, tissues, cells and specific lesions, the drugs will stop, stay or accumulate in special sites, so as to increase the efficacy and concentration of drugs at the tumor site, so as to achieve targeted treatment. The latter uses artificial means to deliver nanomaterials and drugs near the tumor site for selective treatment (Figure 1).

There is a difference between targeted drugs and nanomaterial targeted therapy, targeted drugs are targeted to the tumor site through the specific binding of drug molecules to specific receptors on the surface of tumor cells, while nanomaterial is targeted to the tumor site through the unique physical and chemical properties of nanomaterials, such as magnetic properties, EPR effects, and binding tumor recognition ligands. Compared with direct intravenous drug input, encapsulation or combination of nanomaterials has the following advantages (Hou et al., 2020; Barani et al., 2021; Dutta et al., 2021; Kashyap et al., 2023): 1) It can improve drug targeting for tumor and reduce the damage to normal tissues and organs. 2) It can improve drug stability, reduce drug delivery by enzymatic hydrolysis, resulting in drug destruction. It can reduce the side effect of anticancer agents. 3) It can make the drug in the body controlled release. For example, the prodrug nanoassemblies (LPNAs) and the pH-reduction dual responsive drug delivery system designed by Ding et al. (2019) can precisely control drug release, resulting in better therapeutic effects (Ding et al., 2019; Ding et al., 2023). In addition, while delivering drugs, nanomaterials can also produce photothermal effects and enhance the killing effect on tumors. Based on the numerous advantages of nanomaterials, nanomaterials have been widely used in the drug-loaded targeted therapy of cancer. This paper will review the research progress in this direction, and provide certain reference value for the subsequent research.

2 Commonly used nanomaterials

Due to the numerous advantages, nanomaterials have been wildly used in clinical and laboratory researches (Figure 2). In this section, we summary the commonly used nanomaterials in cancer therapy, including organic nanomaterials and inorganic nanomaterials (Khalid et al., 2020). At present, some nano-drugs have been applied in clinical practice. For example, Abraxane and Paclitaxel liposome are commonly used in the treatment of breast cancer, ovarian cancer, and non-small cell lung cancer. Adriamycin liposomes is often used in the treatment of ovarian cancer, non-Hodgkin lymphoma, breast cancer, and uterine tumors.

2.1 Organic nanomaterials

Organic nanomaterials are substances that mostly naturally existing in organisms or synthesized by chemicals. Such nanomaterials are less cytotoxic and biodegradable, so they are currently a research hotspot and widely used (Khizar et al., 2023). Organic nanomaterials have the advantages of controllable size, large specific surface area, easy surface modification, high permeability and retention effect, and good biocompatibility (López-Dávila et al., 2012; Hussein Kamareddine et al., 2019). Organic nanomaterials can carry both hydrophilic and hydrophobic drugs. Modification of endogenous molecules of some receptors on the surface of organic nanomaterials can significantly improve the targeting of tumor tissue. At present, organic nanomaterials mainly include liposome, protein and polymeric nanomaterials (Palazzolo et al., 2018; Wang et al., 2021).

2.1.1 Liposome nanomaterials

Liposomes are nanocapsules with closed spherical vesicle structure surrounded by phospholipid bilayer and contain hydrophilic water nuclei, which can bind both hydrophilic and hydrophobic drugs (Yang et al., 2021). Compared with other nanocarriers, liposome show good biocompatibility and high drug loading capacity, showing lower toxicity, low immunogenicity, and can be cleared through normal metabolism.

At present, the clinical application of liposome preparations contain different chemotherapy drugs, such as Doxil1/Caelyx1/Myocet1, DaunoXome1, and DepoCyte1, respectively, were used to treat patients with ovarian cancer, AIDS-associated Kaposi's sarcoma, multiple myeloma, lymphoma, or leukemia combined with meningeal diffusion (Kaspers et al., 2013; Bhowmik et al., 2018; Le Rhun et al., 2020). In addition, there are a number of drugs are being studied. Anthracyclines (ANT) are aromatic polyketo antitumor drugs, representative of which are doxorubicin (DOX), daunorubicin (DNR), aclarubicin, epirubicin, pirarubicin, etc. Doxil is FDA approved for the treatment of ovarian cancer and Kaposi's sarcoma (Addeo et al., 2008). One of the most common dose-limiting toxicities of anthracyclines is cardiotoxicity, especially in the elderly and in patients with severe complications such as diabetes and coronary heart disease. However, cardiotoxic events with

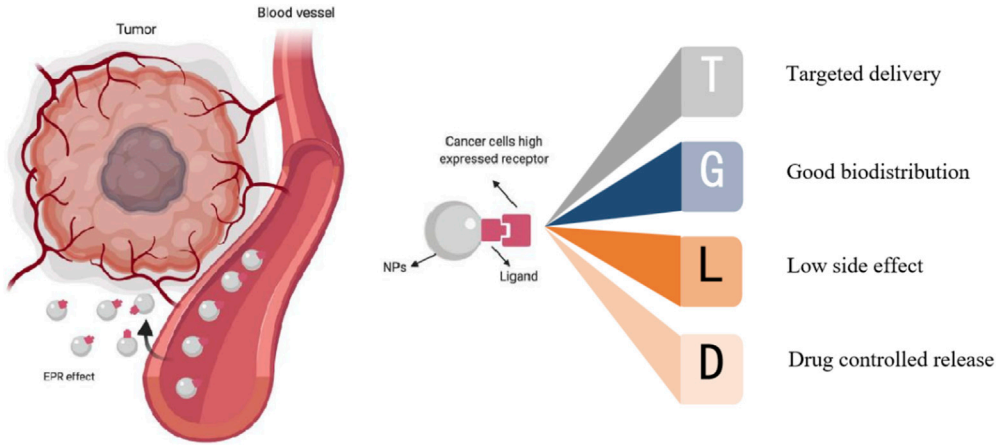

FIGURE 1
Targeting of nanoparticles: active targeting and passive targeting (Sanità et al., 2020).

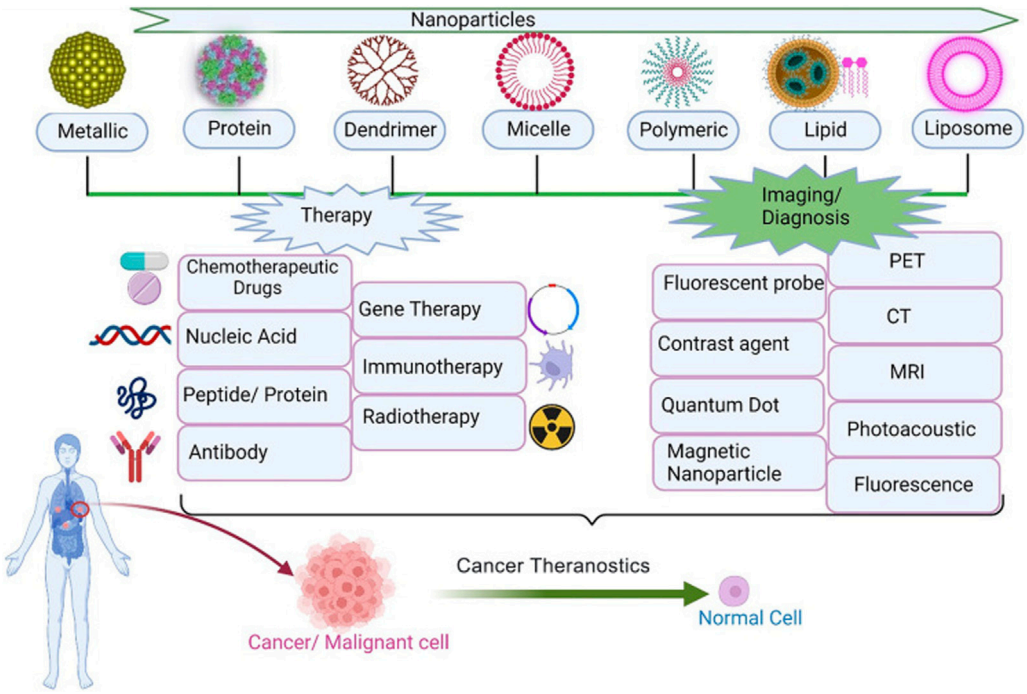

FIGURE 2
Application of nanoparticles in tumor therapy and diagnosis (Kashyap et al., 2023).

anthracyclines encapsulated in liposomes are significantly reduced during tumor therapy (Fassas et al., 2002). As is shown in Figure 3A, Yoshizaki et al. (2016) a pH-sensitive fusogenic polymer-modified liposomes. The liposomes were loaded with antigenic peptides derived from ovalbumin (OVA) OVA-I (SIINFEKL), and OVA-II, which can significantly enhance the activation efficiency of cytotoxic T lymphocyte (ctl), so as to achieve efficient cancer immunotherapy. Matbou Riahi et al. (2018) developed celecoxib (CLX) liposome nanomaterials to overcome the shortcomings of poor water solubility and low anti-tumor titer, and found that CLX liposome preparation had the slowest release curve and the strongest anti-tumor effect *in vivo*. Compared with free CLX, the accumulation of CLX liposomes in tumor sites increased by 3 times. It is proved that CLX liposome is a safe and effective antitumor agent and can release the drug slowly. Wang S. et al. (2020b) used the copper acetate gradient method to prepare As_2O_3 liposomes. By forming a complex of aqueous copper acetate and As_2O_3 in the liposomes, the encapsulation rate reached 83.1%, the

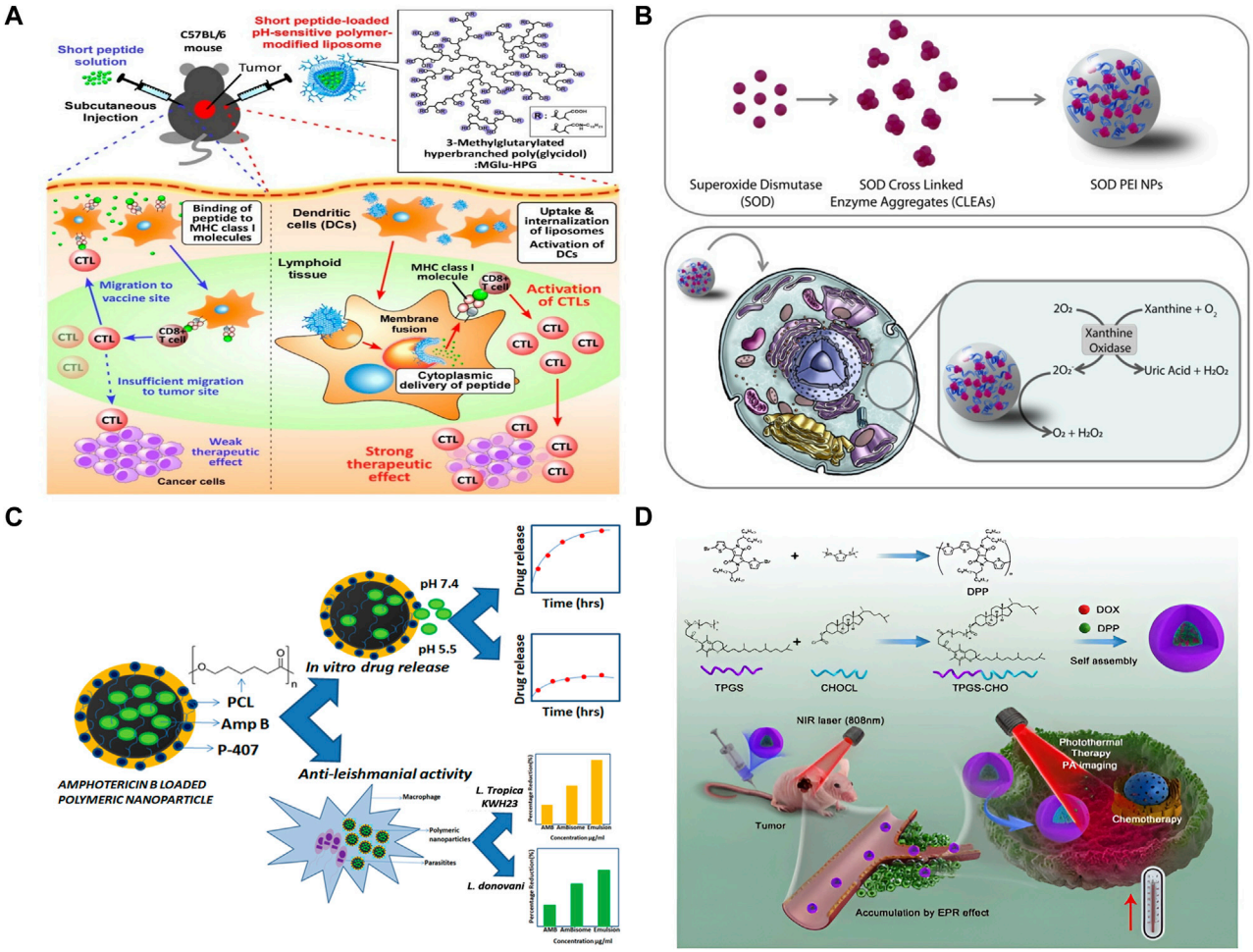

FIGURE 3
Organic nanomaterial. **(A)** Antigen delivery of pH-sensitive polymer-modified liposomes (Yoshizaki et al., 2016). **(B)** The synthesis, *in vitro* assay, and activity in cell of SOD NPs (Galliani et al., 2019). **(C)** From Amphotericin B (Amp B) loaded polymeric nanoparticles preparation to *in vitro* drug release (Saqib et al., 2020). **(D)** Polymer-Based nanocarriers for Co-Delivery and combination of diverse therapies against cancers (Yan et al., 2018).

tumor inhibition rate reached 61.2%, and the toxicity of arsenic trioxide (ATO) was greatly reduced. *In vivo* pharmacokinetic experiments showed that plasma clearance rate of As_2O_3 liposomes was significantly reduced, and the *in vivo* circulation time was doubled compared with intravenous injection of As_2O_3 solution, which improved drug distribution in tumor tissues. Further research showed that the strong skeleton formed by arsenic and metal ions increased the stability of the drug, and the liposome lasted in the body for 6 months longer than the original.

2.1.2 Protein nanomaterials

Protein nanomaterials is a kind of nano-drug loading system composed of drugs and animal, plant or recombinant proteins as carriers. Protein nanomaterials have the advantages of biodegradability, good biocompatibility, low immunogenicity, high drug-loading and stability, and can accumulate in tumor through EPR effect (Ding et al., 2020; Carrion et al., 2021). The types of protein nanomaterials commonly used in tumor therapy include albumin, whey protein, lipoprotein, zein, soy protein, recombinant ferritin and filamentin (Katouzian and Jafari, 2019).

Wamel's (van Wamel et al., 2016) study showed that paclitaxel albumin nanoparticle (Abraxane) uses human serum albumin as a carrier, and through the natural transport pathway of albumin in the body, it can rapidly distribute and aggregate in tumor tissues, improve the efficacy of chemotherapy and reduce toxicity. Jayaprakasha et al. (2016) prepared whey protein-coated curcumin nanoparticles by solvent removal method. Compared with free curcumin, the uptake of colon cancer cells and prostate cancer cells increased significantly. The cytotoxicity and bioavailability of nano curcumin were significantly improved. Wu et al. (2013) prepared paclitaxel-fibroin nanoparticles (PTX-SF-NPs) in aqueous solution at room temperature for the treatment of local gastric cancer. The anti-tumor effect of PTX-SF-NPs was evaluated on the *in vitro* model of gastric cancer in nude mice, and the results showed that PTX-SF-NPs significantly enhanced the effect of delaying tumor growth and reducing tumor weight, with high safety. Sonekar et al. (2016) prepared folic acid conjugated curcumin-melololin nanoparticles by desolvation method, which can be taken orally and targeted for delivery to colon cancer cells, significantly improving the bioavailability and targeting of drugs.

2.1.3 Polymeric nanomaterials

Polymeric nanoparticles are colloidal systems with a wide size range (10–1000 nm). Polymeric nanoparticles have high immunogenicity and stability, and can effectively encapsulate and display antigens. Polymeric nanoparticles can effectively protect drugs from *in vitro* and *in vivo* degradation, cross the blood-brain barrier, control drug release sites and improve drug targeting, and thus have a better therapeutic prospect in the targeted delivery of anti-tumor drugs (Elzoghby, 2017). In general, polymeric nanocarriers are more stable than liposomes. Common polymeric nanomedicine delivery carriers include polymeric micelles, dendritic macromolecules, polymeric nanogels, polymeric nanospheres, etc (Salari et al., 2022).

As is shown in Figure 3B, Galliani et al. (2019) developed a PLGA-based nanostructure, which can protect the structure of the enzymes from being destroyed and accurately deliver it to the cytoplasm. In the Figure 3C, Polyacaprolactone (PCL) nanoparticles loaded with Amp B were developed. The IC50 of the nanoformulations was significantly lower as compared to free Amp B, so it can greatly enhance the effect of Amp B. Wang et al. (2017) prepared gemcitabine (GEM) chitosan nanoparticles (FA-PEG-GEM-NPs) with surface modification of folic acid (FA) and polyethylene glycol (PEG). It was confirmed by cell experiments that FA-PEG-GEM-NPs had high selectivity and high toxicity to human non-small cell lung cancer A549 cells. Wu et al. (2018) designed a stimulus-responsive drug delivery system combining radiotherapy and chemotherapy. They modified L-cysteine (L-Cys) on the surface of polyamidoamine (PAMAM) polymer. On the one hand, the sulfhydryl group of L-Cys can act as a radiation protection agent by removing free radicals. On the other hand, disulfide bonds formed by sulfhydryl groups can be used to trigger the release of anti-cancer drugs. Low doses of gamma rays (5 Gy) trigger reactive oxygen species (ROS) production, which breaks disulfide bonds and releases anticancer drugs DOX. Gu et al. (Wang et al., 2018) designed a therapeutic nano hydrogel. When injected *in situ* into the tumor, the coated gemcitabine (GEM) and immune checkpoint inhibitor anti-PD-L1 antibody (aPDL1) were released in response, realizing the synergistic tumor suppression by chemotherapy and immunization. This gel can achieve ROS responsive degradation and programmed release of therapeutic drugs in ROS rich tumor microenvironments. The results showed that nano gel containing aPDL1-GEM significantly promoted immune-mediated tumor killing in tumor-bearing mice, thus it greatly prevented the recurrence of tumor after resection. Docetaxel (DTX) is a first-line chemotherapy drug for the treatment of metastatic breast cancer. Encapsulated in alendronate (AlN)-modified micelles, docetaxel can achieve sustained release and improve pharmacokinetics. DTX micelles can inhibit tumor growth and significantly prolong animal survival in a model of advanced disseminated breast cancer with bone metastases (Liu, 2019). Yan et al. Repoated a polymer-Based nanocarrier for Co-Delivery and combination of diverse therapies against cancers (Figure 3D).

2.2 Inorganic nanomaterials

Inorganic nanomaterials are nanocarriers synthesized by metallic and semi-metallic materials, which can be used for drug delivery. At present, inorganic nanomaterials used in tumor therapy mainly include metal nanomaterials, non-metallic nanomaterials, magnetic nanomaterials, etc, (Pei et al., 2023). Inorganic nanomaterials are easy to prepare and modify, which has become one of the important research directions of nanocarriers.

2.2.1 Metallic nanomaterials

Metallic nanomaterials, which are synthesized based on metallic elements, not only have the function of targeted drug delivery of conventional carriers, but also enhance the ability of chemotherapy drugs to interfere with cell metabolism, inhibit proliferative cell signal transduction and induce cell apoptosis (Jin et al., 2018).

In the Figure 4A, a hydrogen peroxide (H_2O_2)-triggered nanomaterial (LV-TAX/Au@Ag) was developed. When the nanomaterial reach the tumor tissues, it will release taxol and recovere the photothermal properties of AuNRs. With this combined chemo-photothermal therapy, tumor growth was significantly inhibited. Sun et al. (2015) prepared BioMOF ZnBTCA as a drug delivery vector to promote the uptake and release of anticancer drugs, which showed strong cytotoxicity to A2780cis (ovarian cancer cells) *in vitro*. ZnBTCA itself is not significantly cytotoxic to cancer cells, while drug@ZnBTCA will release the drug continuously and slowly to inhibit the cell growth of A2780cis. Compared with free drugs, drug@ZnBTCA reduces toxicity to normal cells. Tomuleasa et al. (2012) studied the therapeutic effects of different Au NPs loaded with adriamycin, cisplatin or capecitabine respectively on liver cancer, and the drug molecules were non-covalently combined with aspartic acid coated Au NPs. Compared with free drugs, Au NP-drug conjugations significantly improved the therapeutic efficacy of tumor cells, and were equally effective on drug-resistant cells. Rotello et al. (Zhu et al., 2008) demonstrated that Au NPs with surface charge and hydrophobicity are very conducive to cell uptake. Silver nanomaterials (Ag NPs) exhibit dose-dependent toxicity to tumor cells, killing tumor cells by inducing oxidative stress and DNA damage. TNBC tumor cells are sensitive to oxidative stress and DNA damage. Ag NPs have high selectivity for TNBC tumor cells, and have little damage to normal breast tissue cells, liver, kidney, and monocyte system cells (Simard et al., 2016). Curcumin and its derivatives are effective on TNBC tumor cells cultured *in vitro*, and it has been found that curcumin has greater damage to normal cells *in vivo* experiments. Li et al. (2017) found that in TNBC mouse model, the use of copper nanocomplex coating curcumin can improve its anticancer activity without significant adverse reactions (Li et al., 2017).

2.2.2 Nonmetallic nanomaterials

At present, the most widely used nonmetallic nanomaterials mainly include carbon nanomaterials and silica nanomaterials. Mesoporous silica nanoparticles (MSN) have a larger specific surface area due to their unique mesoporous structure, and thus have better drug loading capacity.

In the Figure 4B; Diaz-Diestra et al. (2018) developed a nanocomposite (FA-rGO/ZnS:Mn). This nanocomposite can increase the drug loading rate and enhance the anti-tumor effect without increasing the toxicity to normal cells. Xiong et al. (2015) designed a novel MSN modified with two ligand (folic acid and dexamethasone), as a targeted delivery system for tumor nuclei.

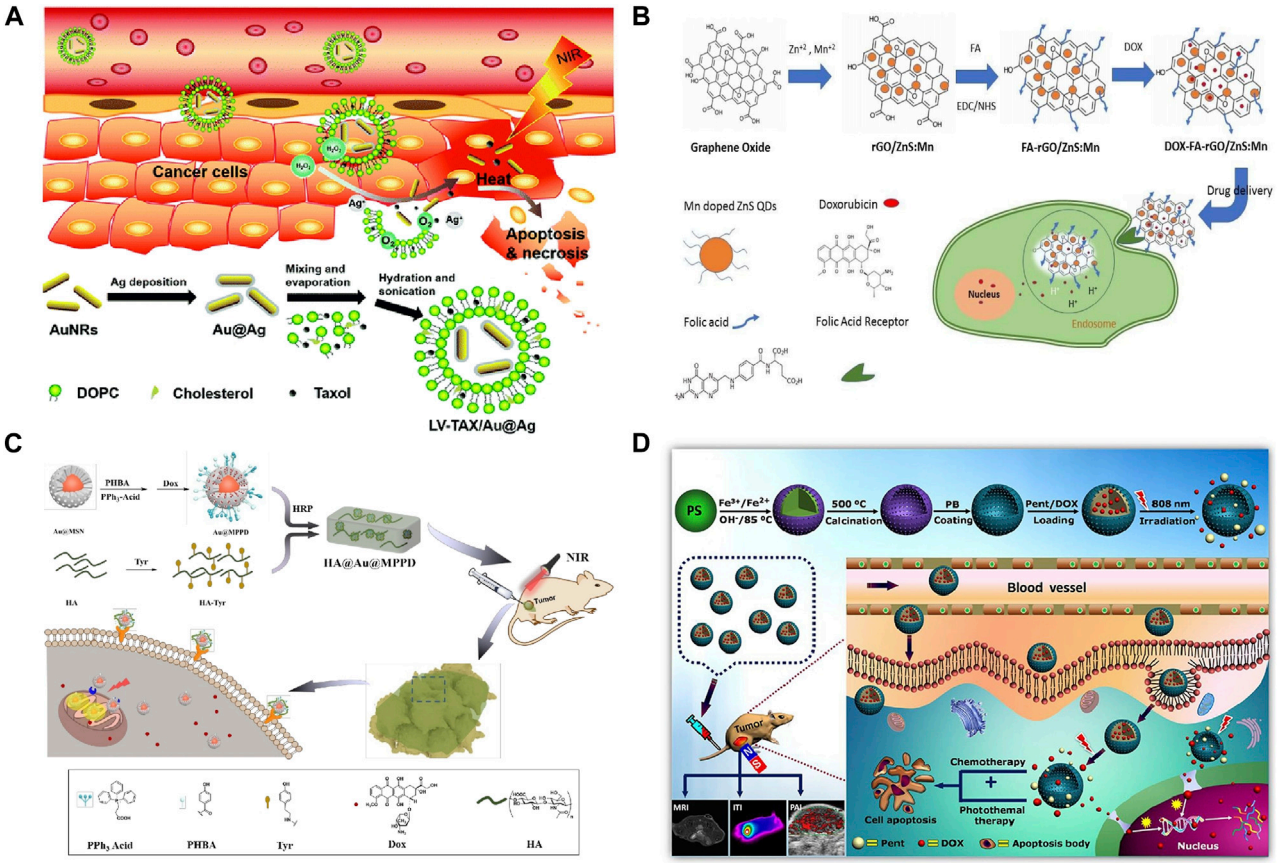

FIGURE 4
(A) Combination therapy of LV-TAX/Au@Ag (Wang K. et al., 2020a). **(B)** FA-rGO/ZnS:Mn as a drug delivery system to release DOX into the cancer cell nucleus (Diaz-Diestra et al., 2018). **(C)** FA-rGO/ZnS:Mn as a drug delivery system to release DOX into the cancer cell nucleus (Zhou et al., 2020). **(D)** Magnetic nanoparticles enhance drug targeting through magnetic fields (Estelrich et al., 2015; Gul et al., 2019).

Folic acid modification can increase the targeting ability of MSN to tumor cells. Dexamethasone is a glucocorticoid, which can bind to the nuclear receptor of tumor cells, namely glucocorticoid receptor, and the formed dexamethasone-glucocorticoid receptor complex can be actively transported from cytoplasm to nucleus. By combining these two ligand to MSN, the novel delivery vector will target DOX into the tumor nucleus and increase its accumulation in the nucleus, thereby improving the inhibition of HeLa (human cervical cancer cells) and reducing the toxic and side effects on normal cells through receptor-mediated cell selectivity. Kumar et al. (2017) successfully prepared DOX-FA-MSNPs nanomaterials loaded with doxorubicin based on MSNs, and examined the uptake at the level of breast cancer cells by confocal microscopy and flow cytometry, and the results indicated that the uptake of nanomaterials in cell lines was high. Cytotoxic results showed that DOX-FA-MSNPs had higher cytotoxic effects on breast cancer cells. Khodadadei et al. (2017) loaded methotrexate (MTX) onto nitrogen-containing graphene quantum dots (GQDs) and found that its entry into tumor cells was slower than that of free MTX, but its effect time was longer and it had strong cytotoxicity. Liu et al. (2022) prepared nano-scale functional hydroxyapatite particles by reversibly combining hydroxyapatite with adriamycin. The nanoparticle is applied locally to the lesion area and can enter the lysosome of tumor cells. In acidic environment, the combination of hydroxyapatite and adriamycin is destroyed, and the released adriamycin accumulates in mitochondria. Further tests on osteosarcoma mice showed that local delivery of adriamycin via hydroxyapatite granules had a stronger tumor eradication effect than traditional application of adriamycin. Mesoporous silica is also a commonly used nanomaterial. A hyaluronic acid (HA) hydrogel covalently embedded with doxorubicin loaded and triphenylphosphine (TPP) modified core-shell gold mesoporous silica nanoparticles was developed by Zhou et al. (2020) This nanomaterial can accurately target tumor cells via CD44 and generate chemophotothermal synergistic cancer therapy (Figure 4C).

2.2.3 Magnetic nanomaterials

Magnetic nanoparticles (MNPs) have magnetic properties and can be targeted to the target area by an external magnetic field. MNPs are generally magnetic composite materials composed of iron, nickel, cobalt and other metals and their oxides, which have been extensively studied in tumor targeted drug delivery. At present, magnetic nanocarriers used for tumor therapy mainly include core-shell structure nanoparticles (made from silica or polymeric micelles wrapped magnetic nuclei and drugs) (Oh and Park, 2011), magnetic

liposomes (Song et al., 2020), and magnetic nanoparticles (transport modes are determined by particle size, morphology, surface charge, surface-to-coupled drugs or targeted molecules) (de Smet et al., 2011). Magnetic ferric oxide nanoparticles (MNP-Fe_3O_4) are magnetic nanomaterials approved by FDA for clinical application, which have attracted wide attention in the field of tumor targeted therapy (Zhao et al., 2018). In addition, multifunctional magnetic nanoagents (MMNs) is of great value for cancer precision therapy (Ding et al., 2021).

Figure 4D shows the process of a magnetic nanomaterial accurately delivering drugs to tumor tissues through magnetic fields, and killing tumors in coordination with photothermal effects. Wu et al. (2020) developed) a novel chitosan superparamagnetic ferric oxide nanocrystals (PECs), loaded with indocyanine green (ICG) fluorescent dye and irinotecan (IRT). By applying magnetic field, real-time fluorescence monitoring of the efficiency of magnetic targeted drug delivery to the tumour was realized. Centelles et al. (2018) designed imaged thermosensitive liposomes (iTSLs) for targeted Hycamtin delivery. iTSL accumulation at the tumor site can be detected by near infrared fluorescence imaging (NIRF), and its release at the tumor site can be detected by topotecan enhanced fluorescence. High intensity focused ultrasound (HIFU) can promote drug release from liposomes *in vivo*, induce subablative hyperthermia, change the permeability of tumor vessels and enhance the absorption of nanoparticles. Shao et al. (2016) designed a kind of magnetic Fe_3O_4/mesoporous silicon "nano bullet" particles. The magnetic Fe_3O_4 nanoparticles of "nano bullet" can provide magnetic targeting ability, and mesoporous silicon can adsorb chemotherapy drugs Dox. Therefore, the designed "nanobullets" can be targeted and enriched to the liver cancer area under the effect of magnetic targeting to realize the chemotherapy effect on tumors. Lu et al. (2018) constructed a PH-sensitive dual-targeting magnetic nanoparticle, and prepared graphene oxide (MGO) by deposition of Fe_3O_3 magnetic nanoparticles on graphene oxide (GO) by chemical coprecipitation. MGO- PEG-CET was obtained by modifying MGO with polyethylene glycol (PEG) and cetuximab (CET). EGFR is highly expressed on tumor cell surface, so MGO-PEG-CET can be used for dual targeted delivery of DOX.

3 Summary and outlook

Drug loading and targeted delivery of nanomaterials is one of the hot spots in biomedical research. Although many studies have demonstrated their advantages, most nanomaterials are still in the experimental stage and need to be improved in many aspects: 1) The biological toxicity of materials should be reduced as much as possible; 2) The pharmacokinetic characteristics, metabolism, distribution and cumulative effects *in vivo* need to be clarified. 3) How to improve the drug loading rate and the controllability of drug release of nanomaterials more effectively; 4) To improve the targeting of nanomaterials and reduce the toxicity to normal cells as much as possible. The real clinical use of nanomaterials requires more interdisciplinary and cross-field collaborative research. With the deepening of various researches, the application of nanomaterials will continue to make breakthrough progress.

Author contributions

PZ, JL, XZ, and WJ: conceptualization, project administration, funding acquisition and editing. PZ, GY, and GX: writing—Review and editing. All authors contributed to the article and approved the submitted version.

Funding

The present study was supported in part by the Guangdong Basic and Applied Basic Research Foundation (2021A1515010970); Shenzhen Innovation of Science and Technology Commission (Nos. JCYJ20210324132407019, LGKCYLWS2022002, LGKCYLWS2021000027, and LGKCYLWS2020099); Shenzhen Key Medical Discipline Construction Fund (No. SZXK039).

Conflict of interest

The authors declare that the research was conducted in the absence of any commercial or financial relationships that could be construed as a potential conflict of interest.

Publisher's note

References

Addeo, R., Faiola, V., Guarrasi, R., Montella, L., Vincenzi, B., Capasso, E., et al. (2008). Liposomal pegylated doxorubicin plus vinorelbine combination as first-line chemotherapy for metastatic breast cancer in elderly women ≥65 years of age. *Cancer Chemother. Pharmacol.* 62 (2), 285–292. doi:10.1007/s00280-007-0605-6

Alavi, M., and Hamidi, M. (2019). Passive and active targeting in cancer therapy by liposomes and lipid nanoparticles. *Drug Metab. Pers. Ther.* 34 (1). doi:10.1515/dmpt-2018-0032

Barani, M., Bilal, M., Sabir, F., Rahdar, A., and Kyzas, G. Z. (2021). Nanotechnology in ovarian cancer: Diagnosis and treatment. *Life Sci.* 266, 118914. doi:10.1016/j.lfs.2020.118914

Bhowmik, S., Bhowmick, S., Maiti, K., Chakra, A., Shahi, P., Jain, D., et al. (2018). Two multicenter Phase I randomized trials to compare the bioequivalence and safety of a generic doxorubicin hydrochloride liposome injection with Doxil(®) or Caelyx(®) in advanced ovarian cancer. *Cancer Chemother. Pharmacol.* 82 (3), 521–532. doi:10.1007/s00280-018-3643-3

Carrion, C. C., Nasrollahzadeh, M., Sajjadi, M., Jaleh, B., Soufi, G. J., and Iravani, S. (2021). Lignin, lipid, protein, hyaluronic acid, starch, cellulose, gum, pectin, alginate and chitosan-based nanomaterials for cancer nanotherapy: Challenges and opportunities. *Int. J. Biol. Macromol.* 178, 193–228. doi:10.1016/j.ijbiomac.2021.02.123

Centelles, M. N., Wright, M., So, P. W., Amrahli, M., Xu, X. Y., Stebbing, J., et al. (2018). Image-guided thermosensitive liposomes for focused ultrasound drug delivery:

Using NIRF-labelled lipids and topotecan to visualise the effects of hyperthermia in tumours. *J. Control Release* 280, 87–98. doi:10.1016/j.jconrel.2018.04.047

de Smet, M., Heijman, E., Langereis, S., Hijnen, N. M., and Grüll, H. (2011). Magnetic resonance imaging of high intensity focused ultrasound mediated drug delivery from temperature-sensitive liposomes: An *in vivo* proof-of-concept study. *J. Control Release* 150 (1), 102–110. doi:10.1016/j.jconrel.2010.10.036

Diaz-Diestra, D., Thapa, B., Badillo-Diaz, D., Beltran-Huarac, J., Morell, G., and Weiner, B. (2018). Graphene oxide/ZnS:Mn nanocomposite functionalized with folic acid as a nontoxic and effective theranostic platform for breast cancer treatment. *Nanomater. (Basel).* 8 (7), 484. doi:10.3390/nano8070484

Ding, Y., Hu, X., Piao, Y., Huang, R., Xie, L., Yan, X., et al. (2023). Lipid prodrug nanoassemblies via dynamic covalent boronates. *ACS Nano* 17 (7), 6601–6614. doi:10.1021/acsnano.2c12233

Ding, Y., Liu, J., Li, X., Xu, L., Li, C., Ma, L., et al. (2019). Rational design of drug delivery systems for potential programmable drug release and improved therapeutic effect. *Mater. Chem. Front.* 3 (6), 1159–1167. doi:10.1039/C9QM00178F

Ding, Y., Xu, Y., Yang, W., Niu, P., Li, X., Chen, Y., et al. (2020). Investigating the EPR effect of nanomedicines in human renal tumors via *ex vivo* perfusion strategy. *Nano Today* 35, 100970. doi:10.1016/j.nantod.2020.100970

Ding, Y., Zeng, L., Xiao, X., Chen, T., and Pan, Y. (2021). Multifunctional magnetic nanoagents for bioimaging and therapy. *ACS Appl. Bio Mater.* 4 (2), 1066–1076. doi:10.1021/acsabm.0c01099

Dutta, B., Barick, K. C., and Hassan, P. A. (2021). Recent advances in active targeting of nanomaterials for anticancer drug delivery. *Adv. Colloid Interface Sci.* 296, 102509. doi:10.1016/j.cis.2021.102509

Elzoghby, A. O. (2017). Editorial: Polymeric nanocarriers as robust platforms for cancer therapy. *Curr. Pharm. Des.* 23 (35), 5211–5212. doi:10.2174/1381612823999171106125801

Estelrich, J., Escribano, E., Queralt, J., and Busquets, M. A. (2015). Iron oxide nanoparticles for magnetically-guided and magnetically-responsive drug delivery. *Int. J. Mol. Sci.* 16 (4), 8070–8101. doi:10.3390/ijms16048070

Fassas, A., Buffels, R., Anagnostopoulos, A., Gacos, E., Vadikolia, C., Haloudis, P., et al. (2002). Safety and early efficacy assessment of liposomal daunorubicin (DaunoXome) in adults with refractory or relapsed acute myeloblastic leukaemia: A phase I-ii study. *Br. J. Haematol.* 116 (2), 308–315. doi:10.1046/j.0007-1048.2001.03292.x

Galliani, M., Tremolanti, C., and Signore, G. (2019). Nanocarriers for protein delivery to the cytosol: Assessing the endosomal escape of poly(lactide-co-glycolide)-poly(ethylene imine) nanoparticles. *Nanomater. (Basel)* 9 (4), 652. doi:10.3390/nano9040652

Gul, S., Khan, S. B., Rehman, I. U., Khan, M. A., and Khan, M. I. (2019). A comprehensive review of magnetic nanomaterials modern day theranostics. *Front. Mater.* 6. doi:10.3389/fmats.2019.00179

Hou, J., Sun, X., Huang, Y., Yang, S., Liu, J., Feng, C., et al. (2020). The design and application of nanomaterials as drug carriers in cancer treatment. *Curr. Med. Chem.* 27 (36), 6112–6135. doi:10.2174/0929867326666190816231409

Hussein Kamareddine, M., Ghosn, Y., Tawk, A., Elia, C., Alam, W., Makdessi, J., et al. (2019). Organic nanoparticles as drug delivery systems and their potential role in the treatment of chronic myeloid leukemia. *Technol. Cancer Res. Treat.* 18, 153303381987990. doi:10.1177/1533033819879902

Jayaprakasha, G. K., Chidambara Murthy, K. N., and Patil, B. S. (2016). Enhanced colon cancer chemoprevention of curcumin by nanoencapsulation with whey protein. *Eur. J. Pharmacol.* 789, 291–300. doi:10.1016/j.ejphar.2016.07.017

Jin, G., He, R., Liu, Q., Dong, Y., Lin, M., Li, W., et al. (2018). Theranostics of triple-negative breast cancer based on conjugated polymer nanoparticles. *ACS Appl. Mat. Interfaces* 10 (13), 10634–10646. doi:10.1021/acsami.7b14603

Kashyap, B. K., Singh, V. V., Solanki, M. K., Kumar, A., Ruokolainen, J., and Kesari, K. K. (2023). Smart nanomaterials in cancer theranostics: Challenges and opportunities. *ACS Omega* 8 (16), 14290–14320. doi:10.1021/acsomega.2c07840

Kaspers, G. J., Zimmermann, M., Reinhardt, D., Gibson, B. E., Tamminga, R. Y., Aleinikova, O., et al. (2013). Improved outcome in pediatric relapsed acute myeloid leukemia: Results of a randomized trial on liposomal daunorubicin by the international BFM study group. *J. Clin. Oncol.* 31 (5), 599–607. doi:10.1200/jco.2012.43.7384

Katouzian, I., and Jafari, S. M. (2019). Protein nanotubes as state-of-the-art nanocarriers: Synthesis methods, simulation and applications. *J. Control Release* 303, 302–318. doi:10.1016/j.jconrel.2019.04.026

Khalid, K., Tan, X., Mohd Zaid, H. F., Tao, Y., Lye Chew, C., Chu, D. T., et al. (2020). Advanced in developmental organic and inorganic nanomaterial: A review. *Bioengineered* 11 (1), 328–355. doi:10.1080/21655979.2020.1736240

Khizar, S., Alrushaid, N., Alam Khan, F., Zine, N., Jaffrezic-Renault, N., Errachid, A., et al. (2023). Nanocarriers based novel and effective drug delivery system. *Int. J. Pharm.* 632, 122570. doi:10.1016/j.ijpharm.2022.122570

Khodadadei, F., Safarian, S., and Ghanbari, N. (2017). Methotrexate-loaded nitrogen-doped graphene quantum dots nanocarriers as an efficient anticancer drug delivery system. *Mater Sci. Eng. C Mater Biol. Appl.* 79, 280–285. doi:10.1016/j.msec.2017.05.049

Kumar, P., Tambe, P., Paknikar, K. M., and Gajbhiye, V. (2017). Folate/N-acetyl glucosamine conjugated mesoporous silica nanoparticles for targeting breast cancer cells: A comparative study. *Colloids Surf. B Biointerfaces* 156, 203–212. doi:10.1016/j.colsurfb.2017.05.032

Le Rhun, E., Wallet, J., Mailliez, A., Le Deley, M. C., Rodrigues, I., Boulanger, T., et al. (2020). Intrathecal liposomal cytarabine plus systemic therapy versus systemic chemotherapy alone for newly diagnosed leptomeningeal metastasis from breast cancer. *Neuro Oncol.* 22 (4), 524–538. doi:10.1093/neuonc/noz201

Li, Y., Jiang, C., Zhang, D., Wang, Y., Ren, X., Ai, K., et al. (2017). Targeted polydopamine nanoparticles enable photoacoustic imaging guided chemo-photothermal synergistic therapy of tumor. *Acta Biomater.* 47, 124–134. doi:10.1016/j.actbio.2016.10.010

Liu, T., Romanova, S., Wang, S., Hyun, M. A., Zhang, C., Cohen, S. M., et al. (2019). Alendronate-modified polymeric micelles for the treatment of breast cancer bone metastasis. *Bone Metastasis* 16 (7), 2872–2883. doi:10.1021/acs.molpharmaceut.8b01343

Liu, Y., Nadeem, A., Sebastian, S., Olsson, M. A., Wai, S. N., Styring, E., et al. (2022). Bone mineral: A trojan horse for bone cancers. Efficient mitochondria targeted delivery and tumor eradication with nano hydroxyapatite containing doxorubicin. *Mater Today Bio* 14, 100227. doi:10.1016/j.mtbio.2022.100227

López-Dávila, V., Seifalian, A. M., and Loizidou, M. (2012). Organic nanocarriers for cancer drug delivery. *Curr. Opin. Pharmacol.* 12 (4), 414–419. doi:10.1016/j.coph.2012.02.011

Lu, Y. J., Lin, P. Y., Huang, P. H., Kuo, C. Y., Shalumon, K. T., Chen, M. Y., et al. (2018). Magnetic graphene oxide for dual targeted delivery of doxorubicin and photothermal therapy. *Nanomater. (Basel).* 8 (4), 193. doi:10.3390/nano8040193

Matbou Riahi, M., Sahebkar, A., Sadri, K., Nikoofal-Sahlabadi, S., and Jaafari, M. R. (2018). Stable and sustained release liposomal formulations of celecoxib: *In vitro* and *in vivo* anti-tumor evaluation. *Int. J. Pharm.* 540 (1-2), 89–97. doi:10.1016/j.ijpharm.2018.01.039

Meric-Bernstam, F., Johnson, A. M., Dumbrava, E. E. I., Raghav, K., Balaji, K., Bhatt, M., et al. (2019). Advances in HER2-targeted therapy: Novel agents and opportunities beyond breast and gastric cancer. *Clin. Cancer Res.* 25 (7), 2033–2041. doi:10.1158/1078-0432.ccr-18-2275

Oh, J. K., and Park, J. M. (2011). Iron oxide-based superparamagnetic polymeric nanomaterials: Design, preparation, and biomedical application. *Prog. Polym. Sci.* 36 (1), 168–189. doi:10.1016/j.progpolymsci.2010.08.005

Palazzolo, S., Bayda, S., Hadla, M., Caligiuri, I., Corona, G., Toffoli, G., et al. (2018). The clinical translation of organic nanomaterials for cancer therapy: A focus on polymeric nanoparticles, micelles, liposomes and exosomes. *Curr. Med. Chem.* 25 (34), 4224–4268. doi:10.2174/0929867324666170830113755

Pei, Z., Lei, H., and Cheng, L. (2023). Bioactive inorganic nanomaterials for cancer theranostics. *Chem. Soc. Rev.* 52 (6), 2031–2081. doi:10.1039/d2cs00352j

Robert, J. (2013). Biology of cancer metastasis. *Bull. Cancer* 100 (4), 333–342. doi:10.1684/bdc.2013.1724

Rouviere, D., Bousquet, E., Pons, E., Milia, J. D., Guibert, N., and Mazieres, J. (2015). New targets and new drugs in thoracic oncology. *Rev. Mal. Respir.* 32 (8), 867–876. doi:10.1016/j.rmr.2015.02.091

Saito, M., Suzuki, H., Kono, K., Takenoshita, S., and Kohno, T. (2018). Treatment of lung adenocarcinoma by molecular-targeted therapy and immunotherapy. *Surg. Today* 48 (1), 1–8. doi:10.1007/s00595-017-1497-7

Salari, N., Faraji, F., Torghabeh, F. M., Faraji, F., Mansouri, K., Abam, F., et al. (2022). Polymer-based drug delivery systems for anticancer drugs: A systematic review. *Cancer Treat. Res. Commun.* 32, 100605. doi:10.1016/j.ctarc.2022.100605

Sanità, G., Carrese, B., and Lamberti, A. (2020). Nanoparticle surface functionalization: How to improve biocompatibility and cellular internalization. *Front. Mol. Biosci.* 7, 587012. doi:10.3389/fmolb.2020.587012

Saqib, M., Ali Bhatti, A. S., Ahmad, N. M., Ahmed, N., Shahnaz, G., Lebaz, N., et al. (2020). Amphotericin B loaded polymeric nanoparticles for treatment of leishmania infections. *Nanomater. (Basel)* 10 (6), 1152. doi:10.3390/nano10061152

Schmalz, G., Hickel, R., van Landuyt, K. L., and Reichl, F. X. (2017). Nanoparticles in dentistry. *Dent. Mater* 33 (11), 1298–1314. doi:10.1016/j.dental.2017.08.193

Shao, D., Li, J., Zheng, X., Pan, Y., Wang, Z., Zhang, M., et al. (2016). Janus "nano-bullets" for magnetic targeting liver cancer chemotherapy. *Biomaterials* 100, 118–133. doi:10.1016/j.biomaterials.2016.05.030

Siegel, R. L., Miller, K. D., Fuchs, H. E., and Jemal, A. (2022). Cancer statistics, 2022. *CA Cancer J. Clin.* 72 (1), 7–33. doi:10.3322/caac.21708

Simard, J. C., Durocher, I., and Girard, D. (2016). Silver nanoparticles induce irremediable endoplasmic reticulum stress leading to unfolded protein response dependent apoptosis in breast cancer cells. *Apoptosis* 21 (11), 1279–1290. doi:10.1007/s10495-016-1285-7

Sonekar, S., Mishra, M. K., Patel, A. K., Nair, S. K., Singh, C. S., and Singh, A. K. (2016). Formulation and evaluation of folic acid conjugated gliadin nanoparticles of curcumin for targeting colon cancer cells. *J. Appl. Pharm. Sci.* 6 (10), 068–074. doi:10.7324/japs.2016.601009

Song, Y., Li, D., Lu, Y., Jiang, K., Yang, Y., Xu, Y., et al. (2020). Ferrimagnetic mPEG-*b*-PHEP copolymer micelles loaded with iron oxide nanocubes and emodin for enhanced magnetic hyperthermia–chemotherapy. *hyperthermia-chemotherapy* 7 (4), 723–736. doi:10.1093/nsr/nwz201

Sun, R. W., Zhang, M., Li, D., Zhang, Z. F., Cai, H., Li, M., et al. (2015). Dinuclear gold(I) pyrrolidinedithiocarbamato complex: Cytotoxic and antimigratory activities on cancer cells and the use of metal-organic framework. *Chemistry* 21 (51), 18534–18538. doi:10.1002/chem.201503656

Tomuleasa, C., Soritau, O., Orza, A., Dudea, M., Petrushev, B., Mosteanu, O., et al. (2012). Gold nanoparticles conjugated with cisplatin/doxorubicin/capecitabine lower the chemoresistance of hepatocellular carcinoma-derived cancer cells. *J. Gastrointestin Liver Dis.* 21 (2), 187–196.

van Wamel, A., Sontum, P. C., Healey, A., Kvåle, S., Bush, N., Bamber, J., et al. (2016). Acoustic Cluster Therapy (ACT) enhances the therapeutic efficacy of paclitaxel and Abraxane® for treatment of human prostate adenocarcinoma in mice. *J. Control Release* 236, 15–21. doi:10.1016/j.jconrel.2016.06.018

Wang, C., Wang, J., Zhang, X., Yu, S., Wen, D., Hu, Q., et al. (2018). *In situ* formed reactive oxygen species-responsive scaffold with gemcitabine and checkpoint inhibitor for combination therapy. *Sci. Transl. Med.* 10 (429), eaan3682. doi:10.1126/scitranslmed.aan3682

Wang, F., Wang, Y., Ma, Q., Cao, Y., and Yu, B. (2017). Development and characterization of folic acid-conjugated chitosan nanoparticles for targeted and controlled delivery of gemcitabinein lung cancer therapeutics. *Artif. Cells Nanomed Biotechnol.* 45 (8), 1530–1538. doi:10.1080/21691401.2016.1260578

Wang, K., Cai, Z., Fan, R., Yang, Q., Zhu, T., Jiang, Z., et al. (2020a). A tumor-microenvironment-responsive nanomaterial for cancer chemo-photothermal therapy. *RSC Adv.* 10 (37), 22091–22101. doi:10.1039/d0ra04171h

Wang, S., Liu, C., Wang, C., Ma, J., Xu, H., Guo, J., et al. (2020b). Arsenic trioxide encapsulated liposomes prepared via copper acetate gradient loading method and its antitumor efficiency. *Asian J. Pharm. Sci.* 15 (3), 365–373. doi:10.1016/j.ajps.2018.12.002

Wang, Z., Zhi, K., Ding, Z., Sun, Y., Li, S., Li, M., et al. (2021). Emergence in protein derived nanomedicine as anticancer therapeutics: More than a tour de force. *Semin. Cancer Biol.* 69, 77–90. doi:10.1016/j.semcancer.2019.11.012

Wu, D., Zhu, L., Li, Y., Wang, H., Xu, S., Zhang, X., et al. (2020). Superparamagnetic chitosan nanocomplexes for colorectal tumor-targeted delivery of irinotecan. *Int. J. Pharm.* 584, 119394. doi:10.1016/j.ijpharm.2020.119394

Wu, P., Liu, Q., Li, R., Wang, J., Zhen, X., Yue, G., et al. (2013). Facile preparation of paclitaxel loaded silk fibroin nanoparticles for enhanced antitumor efficacy by locoregional drug delivery. *ACS Appl. Mater Interfaces* 5 (23), 12638–12645. doi:10.1021/am403992b

Wu, S. Y., Chou, H. Y., Yuh, C. H., Mekuria, S. L., Kao, Y. C., and Tsai, H. C. (2018). Radiation-sensitive dendrimer-based drug delivery system. *Adv. Sci. (Weinh)* 5 (2), 1700339. doi:10.1002/advs.201700339

Xiong, L., Du, X., Kleitz, F., and Qiao, S. Z. (2015). Cancer-cell-specific nuclear-targeted drug delivery by dual-ligand-modified mesoporous silica nanoparticles. *Small* 11 (44), 5919–5926. doi:10.1002/smll.201501056

Yan, G., Li, A., Zhang, A., Sun, Y., and Liu, J. (2018). Polymer-based nanocarriers for Co-delivery and combination of diverse therapies against cancers. *Nanomater. (Basel)* 8 (2), 85. doi:10.3390/nano8020085

Yang, B., Song, B. P., Shankar, S., Guller, A., and Deng, W. (2021). Recent advances in liposome formulations for breast cancer therapeutics. *Cell Mol. Life Sci.* 78 (13), 5225–5243. doi:10.1007/s00018-021-03850-6

Yetisgin, A. A., Cetinel, S., Zuvin, M., Kosar, A., and Kutlu, O. (2020). Therapeutic nanoparticles and their targeted delivery applications. *Molecules* 25 (9), 2193. doi:10.3390/molecules25092193

Yoshizaki, Y., Yuba, E., Komatsu, T., Udaka, K., Harada, A., and Kono, K. (2016). Improvement of peptide-based tumor immunotherapy using pH-sensitive fusogenic polymer-modified liposomes. *Molecules* 21 (10), 1284. doi:10.3390/molecules21101284

Zhang, Q. Y., Wang, F. X., Jia, K. K., and Kong, L. D. (2018). Natural product interventions for chemotherapy and radiotherapy-induced side effects. *Front. Pharmacol.* 9, 1253. doi:10.3389/fphar.2018.01253

Zhao, Y., Zhao, X., Cheng, Y., Guo, X., and Yuan, W. (2018). Iron oxide nanoparticles-based vaccine delivery for cancer treatment. *Mol. Pharm.* 15 (5), 1791–1799. doi:10.1021/acs.molpharmaceut.7b01103

Zheng, R., Zhang, S., Zeng, H., Wang, S., Sun, K., Chen, R., et al. (2022). Cancer incidence and mortality in China, 2016. *J. Natl. Cancer Cent.* 2 (1), 1–9. doi:10.1016/j.jncc.2022.02.002

Zhou, J., Wang, M., Han, Y., Lai, J., and Chen, J. (2020). Multistage-targeted gold/mesoporous silica nanocomposite hydrogel as *in situ* injectable drug release system for chemophotothermal synergistic cancer therapy. *ACS Appl. Bio Mat.* 3 (1), 421–431. doi:10.1021/acsabm.9b00895

Zhu, Z. J., Ghosh, P. S., Miranda, O. R., Vachet, R. W., and Rotello, V. M. (2008). Multiplexed screening of cellular uptake of gold nanoparticles using laser desorption/ionization mass spectrometry. *J. Am. Chem. Soc.* 130 (43), 14139–14143. doi:10.1021/ja805392f

frontiers | Frontiers in Bioengineering and Biotechnology

TYPE Review
PUBLISHED 28 July 2023
DOI 10.3389/fbioe.2023.1249875

OPEN ACCESS

EDITED BY
Chang Li,
Tongji University, China

REVIEWED BY
Yating Xiao,
UCAS, China
Xun Li,
Chinese Academy of Sciences (CAS), China

*CORRESPONDENCE
Jianshuang Guo,
jshguo@mail.nankai.edu.cn
Jianheng Li,
lijianheng@hbu.edu.cn

†These authors have contributed equally to this work

RECEIVED 29 June 2023
ACCEPTED 14 July 2023
PUBLISHED 28 July 2023

CITATION
Yang Y, Lin M, Sun M, Zhang G-Q, Guo J and Li J (2023), Nanotechnology boosts the efficiency of tumor diagnosis and therapy.
Front. Bioeng. Biotechnol. 11:1249875.
doi: 10.3389/fbioe.2023.1249875

Nanotechnology boosts the efficiency of tumor diagnosis and therapy

Ying Yang†, Mali Lin†, Mengfan Sun, Guo-Qiang Zhang, Jianshuang Guo* and Jianheng Li*

Pharmacology and Toxicology Research Laboratory, College of Pharmaceutical Science, Hebei University, Baoding, Hebei, China

The incidence and mortality of cancer are gradually increasing. The highly invasive and metastasis of tumor cells increase the difficulty of diagnosis and treatment, so people pay more and more attention to the diagnosis and treatment of cancer. Conventional treatment methods, including surgery, radiotherapy and chemotherapy, are difficult to eliminate tumor cells completely. And the emergence of nanotechnology has boosted the efficiency of tumor diagnosis and therapy. Herein, the research progress of nanotechnology used for tumor diagnosis and treatment is reviewed, and the emerging detection technology and the application of nanodrugs in clinic are summarized and prospected. The first part refers to the application of different nanomaterials for imaging *in vivo* and detection *in vitro*, which includes magnetic resonance imaging, fluorescence imaging, photoacoustic imaging and biomarker detection. The distinctive physical and chemical advantages of nanomaterials can improve the detection sensitivity and accuracy to achieve tumor detection in early stage. The second part is about the nanodrug used in clinic for tumor treatment. Nanomaterials have been widely used as drug carriers, including the albumin paclitaxel, liposome drugs, mRNA-LNP, protein nanocages, micelles, membrane nanocomplexes, microspheres et al., which could improve the drug accumulate in tumor tissue through enhanced permeability and retention effect to kill tumor cells with high efficiency. But there are still some challenges to revolutionize traditional tumor diagnosis and anti-drug resistance based on nanotechnology.

KEYWORDS

nanotechnology, nanomaterials, tumor imaging, biomarker detection, tumor therapy

1 Introduction

Cancer is still considered as a major threat to human health (Lu, 2023). According to World Health Organization's estimates, approximately 10 million individuals pass away globally each year due to cancer. Low income countries and middle-income countries account for a large proportion, and the incidence rate is rising rapidly (Tavallaii et al., 2023).

According to the investigation, malignant tumors can be detected by physical examination, which can prevent their further deterioration in a timely manner. Tumor cells are highly invasive and metastatic, making detection difficult. Most tumor cells are only discovered at a late stage. So far, several imaging techniques have been used for tumor diagnosis, such as magnetic resonance imaging (MRI), computed tomography (CT), and ultrasound imaging (USI). However, these techniques have certain limitations, for example, the low spatial resolution of CT (Sharma et al., 2023). MRI provides high-resolution

anatomical images, but its sensitivity is low and tissue penetration is poor (Montiel Schneider and Lassalle, 2017).

Commonly used treatment methods include chemotherapy, surgery, and radiation therapy (Liu et al., 2023). Surgical resection is recognized as the preferred choice for treating solid tumors. Given the limitations of tumor resection, additional methods will be used to assist in targeting tumor residues (Khan et al., 2022). Chemotherapy and radiation therapy are relatively important treatment methods, but there are also many side effects, such as toxicity, drug resistance, and a high probability of late recurrence (Shao et al., 2022; Richardson et al., 2023).

Along with the deep understanding of cancer, more and more studies have begun to focus on the application of nanotechnology for tumor theranostic. The application of nanotechnology in diagnostic and therapeutic applications holds bright prospects. Nanomedicine can enhance the bioavailability of drugs, reduce side effects and extend the duration of drug effectiveness *in vivo* (Teja et al., 2022; Hu et al., 2023). New nanomedicine is constantly being applied in the clinic. Nanotechnology has also made new breakthroughs in cancer diagnosis. Utilizing nanoimaging technology, the sensitivity can be significantly improved, offering the possibility of early detection and timely treatment of cancer. Based on the physical properties of nanomaterials, their applications are becoming more and more extensive. In the diagnosis and treatment of cancer, nanotechnology is seen as a more convenient, highly targeted delivery system with fewer side effects (Gulia et al., 2023). At present, there are still many potential problems with nanotechnology in cancer diagnosis and treatment. This paper reviews the clinical applications of various nanomedicines and their applications in the field of tumor diagnosis and treatment.

2 Application of nanotechnology in tumor detection

With the emergence and development of nanotechnology, the small size advantage of nanocarriers can be used to harnessed to enable drugs to engage in nano-level interactions with cells, thereby enhancing the precision of tumor diagnosis (Chen et al., 2023). At present, nanotechnology has made great progress *in vivo* imaging [magnetic resonance imaging (MRI), fluorescence imaging (FI), photoacoustic imaging (PAI), ultrasound imaging (USI)] and *in vitro* detection (exosome).

2.1 Nanomaterials imaging *in vivo*

In vivo imaging is a powerful strategy in life science research and medical diagnosis. People could better understand the occurrence and development of diseases. The technology is now widely used in the field of oncology. The combination of imaging technology with nanomaterials has led to new breakthroughs in magnetic resonance imaging, fluorescence imaging and photoacoustic imaging.

2.1.1 Magnetic resonance imaging

MRI is one of the most commonly used imaging modalities for tumors, but its image resolution is low. The use of contrast agents such as magnetic nanoparticles (MNPs) can effectively solve this problem. MNPs are nanoscale particles centered on a magnetic material and encapsulated in a biopolymer core-shell structure. MNPs has the advantages of both magnetic materials and nanoparticles. They have the advantages of large surface area, strong magnetic responsiveness, high adsorption capacity, good biocompatibility, and easy manipulation by external magnetic fields (Eivazzadeh-Keihan et al., 2021). In the field of tumor-imaging, biomolecule-coated small superparamagnetic iron oxide nanoparticles (SPIOs) and ultramicroscopic paramagnetic iron oxides (USPIOs) have been widely used as magnetic resonance imaging contrast agents for cancer imaging detection. Subsequently, more MNPs for tumor diagnosis have been explored through ongoing in-depth studies. In a study conducted by Rezayan et al. (2016), the impact of nanoparticles used as contrast agents in MRI was explored. SPIOs were synthesized by co-precipitation method according to the synthetic route (Figure 1). The nanoparticles that have undergone modifications exhibit superparamagnetic properties, and they are well-dispersed and highly stable in water. Furthermore, studies have demonstrated that iron oxide nanoparticles modified with amino acids are the most efficient contrast agents for MRI. In a study performed by Eivazzadeh-Keihan et al. (2021), MNPs were subjected to modifications using various materials such as carbon-based nanomaterials, metal oxide nanoparticles, synthetic and natural polymers, antibodies, biomolecules, and amphiphilic polymers. The research highlight that the adsorption mechanism of magnetic nanoparticles is influenced by their size, surface energy and charge. Furthermore, the hydrophilicity of magnetic nanoparticles is a crucial factor in influencing the selectivity of protein binding and separation processes.

2.1.2 Fluorescence imaging

FI is an important modality for tumor detection. It is an indispensable instrument in both physiological and pathological research and drug development. In recent years, nanomaterials have many applications in FI for tumor detection, such as inorganic quantum dots (QDs).

QDs refer to be aggregates composed of a certain number of atoms in a certain way, which can be used to display the distribution and concentration of biomarkers in tissues. QDs have exceptional optical characteristics such as high brightness, strong stability and the ability to perform multiplexing, so they are expected to be a promising optical detector (Cheng et al., 2021). The surface of QDs can be modified to enable object localization imaging. Li et al. (2023d) used a simple strategy to combine Mn: ZnS QDs, and TEMPO-CNFs to detect different types of biological molecules. The biosensor is portable and accurate, make it a valuable tool in fluorescence detection, not only for the targeted substances but also potentially for other compounds in samples. It is expected to provide new ideas for environmental monitoring and biomedical diagnosis.

Carbon quantum dots (CQD) are fluorescent carbon nanoparticles with promising applications in cell imaging and bioimaging due to their photoluminescent properties. Through the use of photobleaching treatment, Huang et al. (2019) synthesized highly stable fluorescent carbon quantum dots

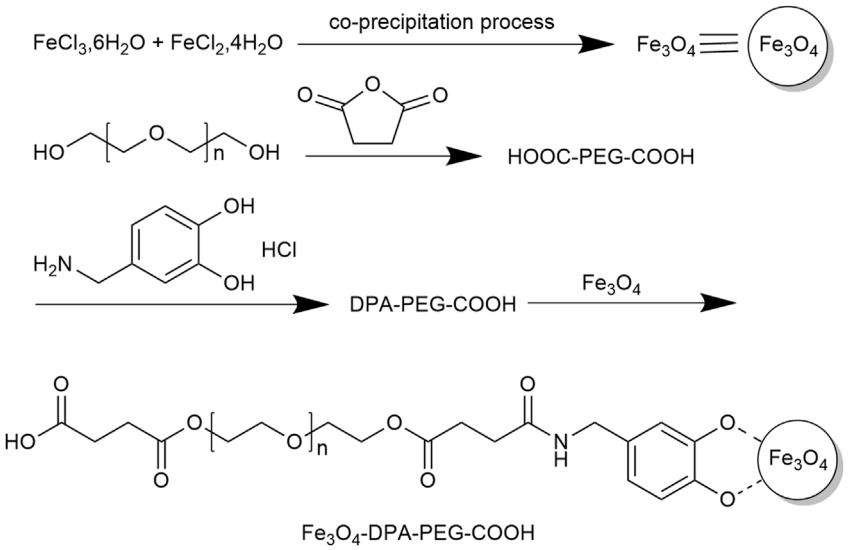

FIGURE 1
Synthesis of Fe_3O_4-DPA-PEG-COOH.

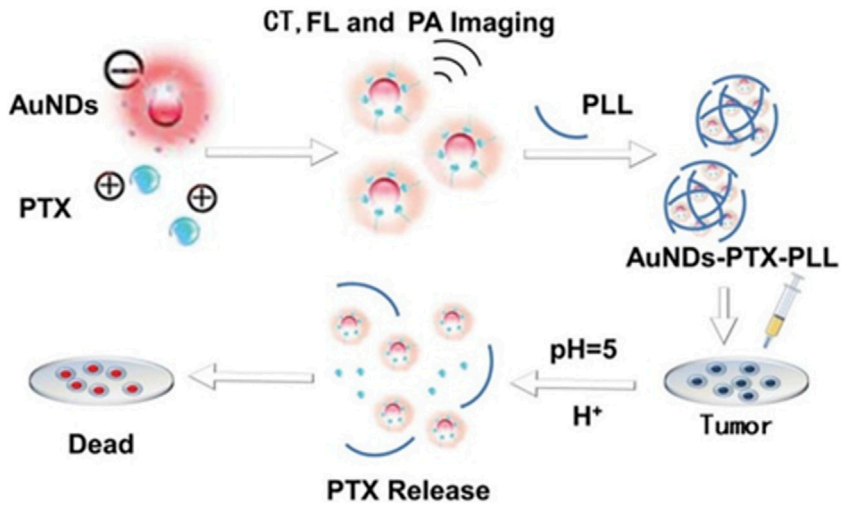

FIGURE 2
The procedure involved in producing AuNDs-PTX-PLL and its utilization for responsive drug release in chemotherapy applications.

(FCQDs) and obtain fluorescence images at different time intervals. The FCQDs exhibited fluorescence 5 min after administration and accumulated at the tumor sites after 3 h. The authors reported that the total accumulation in tumors was observed at 12 h and this extended the imaging period. The researchers also found that the FCQDs efficiently accumulated in tumors, kidneys, and liver based on anatomical images of mouse organs. However, there was no detection of fluorescent signal in organs such as the heart, lung, and spleen. Experiments involving *in vivo* cell imaging and bioimaging demonstrated that the FCQDs exhibited excellent bioimaging properties, low cytotoxicity, and antioxidant activity.

2.1.3 Photoacoustic imaging

PAI is an advanced technology that integrates ultrasound imaging with optical imaging systems, offering both precise spatial resolution and enhanced contrast. But the resolution of photoacoustic imaging is influenced by many factors. Photoacoustic imaging and gold nanoparticles can be used in combination to achieve more accurate biomedical imaging. Gold (Au) is one of the most chemically stable elements, and Au nanomaterials have good biocompatibility. Gold nanoparticles (AuNPs) are easily adsorbed on other biomaterials (Li H. et al., 2022), and the surface is always covered with protectant molecules. These molecules are used to interact with specific reagents in order

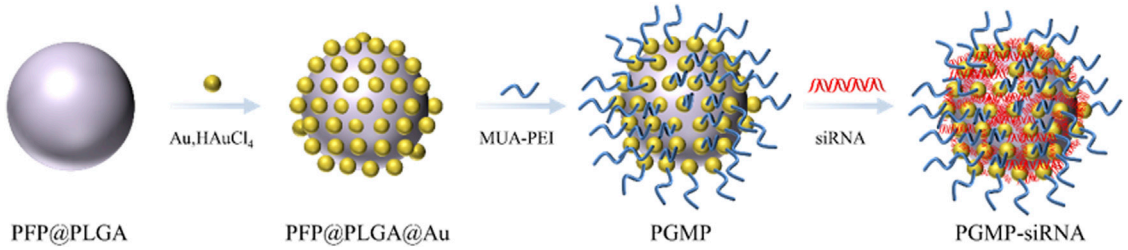

FIGURE 3
Synthesis of PGMP-siRNA NPs.

to generate certain functional groups with special functions. With this property, AuNPs can be chemically modified and applied to imaging analysis, tumor detection and other fields. In particular, surface passivators, such as protein and peptide capped gold nanoparticles, are widely used for imaging (Shelar et al., 2023). Wang et al. (2022) constructed a core-shell integrated diagnostic and therapeutic nano-system of gold nanodots-paclitaxel-polylysine (AuNDs PTX-PLL) (Figure 2). AuNDs and PTX are encapsulated in PLL, with a size of around 30 nm to facilitate the enrichment of nanoparticles in tumors. Besides, AuNDs can be used for PAI. Given the direct relationship between the concentration of AuNDs and the imaging effect, it becomes feasible to employ them for quantitative analysis. For optimal results, an AuNDs concentration of 1–1.5 mg/mL is recommended, as the signal strength remains relatively consistent within this range. The utilization of AuNDs enables non-invasive and real-time monitoring of drug delivery and release procedures, showcasing their potential for valuable clinical applications.

PAI has become a research hotspot and researchers need to develop ideal nanoparticle transport systems to work with this imaging technology. Indocyanine green (ICG) is a water-soluble tricarbocyanine dye, which is one of the most commonly used PAI agents. Thangavel et al. (2022) added dehydrated ethanol to human serum albumin aqueous solution, and synthesized ICG-PTX nanoparticles by using a desolvation process. ICG-PTX nanoparticles are being used to guide drug delivery targeting CD44-positive non-small cell lung cancer (NSCLC). The size of the nanoparticle is about 315.24 nm and the PDI is less than 0.3. HA (hyaluronic acid) -functionalized-ICG-PTX-loaded nanoparticles had strong PAI average strength signal with nanoparticles excited by light with a wavelength of 806 nm. The maximum PAI intensity was obtained with a detection signal depth of about 10 mm.

2.1.4 Ultrasonic imaging

USI involves the transmission and reception of ultrasound waves, which encounter varying levels of impedance depending on the tissue they pass through, resulting in different degrees of transmission and reflection at the boundaries between different tissues. Examining the reflected signal can provide insights into the internal structure of bodily tissues.

Lv et al. (2022) created a type of gold-based nanocarriers called PGMP-siRNA NPs, which were specifically designed to carry small interfering RNA (siRNA) targeting STAT6, with a particle size of about 200 nm (Figure 3). *In vitro* experiments, PGMP-siRNA NPs had strong absorption of light in the wavelength range of 600–900 nm. It can efficiently transform near-infrared light into thermal energy and regulated the temperature by controlling the laser power. In the *in vitro* contrast-enhanced ultrasound (CEUS) mode, the PGMP-siRNA NPs exhibited remarkable improvement in echo intensity. It displayed uniform fine point ultrasonic echo, and the echo was enhanced with the increase of nanocore concentration. Based on their superior ultrasound imaging performance, *in vivo* USI of nanoparticles has been characterized. Tumor sites in PGMP-siRNA NPs-treated mice were significantly enhanced in CEUS mode compared to the control group. These findings provide further validation of the potential of nanoparticles in advancing contrast imaging techniques. Wu et al. (2023) (Figures 4A, B) synthesized a PDLIM5 siRNA delivery system (MSN-siRNA@PVA (polyvinyl alcohol) NPs) based on mesoporous silicon dioxide (MSN) nanobubbles for the treatment of gefitinib resistant NSCLC. The nanoparticles have an approximate size of around 200 nm. In the CEUS test, the MSNsiRNA@PVA NPs echo enhancement is evident, showing a uniform fine-dot high echo. MSN-siRNA@PVA NPs was compared with SonoVue, a commonly used clinical ultrasound contrast agent, to produce similar contrast enhancement at the same concentration (Figure 4C). Therefore, nanoparticles have the potential to be applied in clinical NSCLC diagnosis.

2.2 Biomarker detection with nanomaterials *in vitro*

In tumor detection, the conventional approach is to confirm the diagnosis with a biopsy, which is invasive and costly for the patient. Exosomes are ideal analytical targets for liquid biopsies because of the capacity of carrying genetic molecules (Zhang et al., 2021). High quality, low-cost nanosensors are a promising method for exosome protein detection. Compared with other methods, exosomes exhibit excellent performance in biological analysis, including liquid biopsy (Zhang L. et al., 2022; Li et al., 2023b). Nanosensors are typically made of metal or semiconductor nanoparticles whose surfaces are modified with specific biomolecule recognition molecules (e.g., antibodies or nucleic acids) that allow them to bind selectively to the target biomolecule. Kuznetsov et al. (2022) explored a cost-efficient approach to create fluorescent nanosensors utilizing semiconductor nanocrystals. The sensor has excellent photostability and can be used for *in vitro* diagnosis of c-Met positive cells. It exhibits high binding efficacy to the target

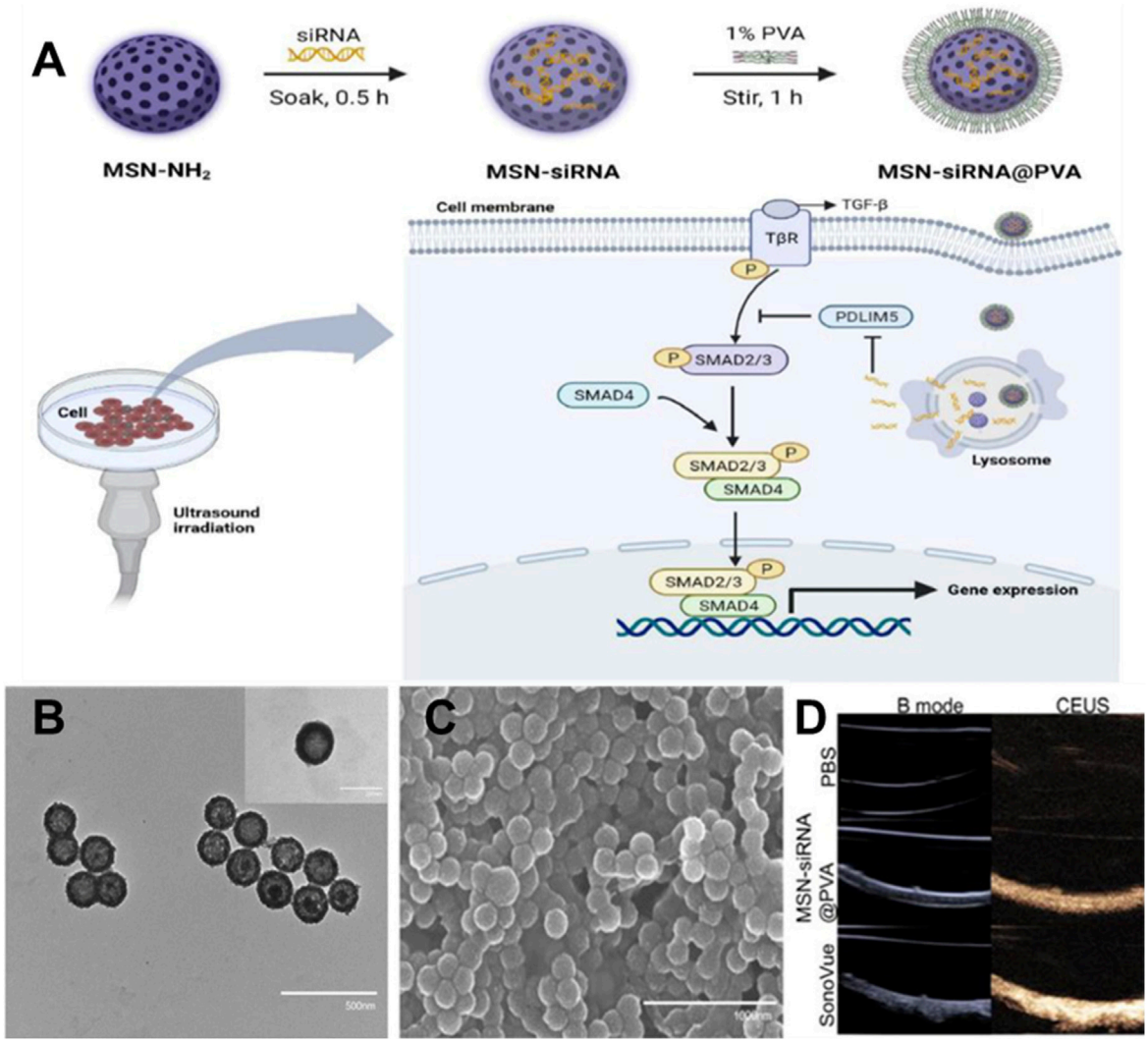

FIGURE 4
(A) Preparation process and antagonistic strategy of siRNA-MSN@PVA NPs. Characterization of MSN-siRNA@PVA nanoparticles. **(B)** TEM **(C)** and SEM images of MSN-siRNA@PVA nanoparticles. **(D)** *In vitro* CEUS imaging of MSN-siRNA@PVA nanoparticles and SonoVue.

antigen present on the cell surface and can be utilized for molecular profiling of tumor tissue. The resulting product is expected to be useful for biomarker visualization. Ganesh et al. (2022) designed a self-functionalized nanosensor capable of pathologically identifying metastatic cancer at an early stage and predicting the likelihood of metastatic cancer onset. By attaining a sensitivity rate of 98%, this approach successfully meets the requirements for early detection and prognosis of cancer metastasis through the identification of metastasis-initiating cells (MIC). It demonstrates a remarkable specificity of 99.62% in distinguishing MIC within a diverse population of tumor-initiating cells. Additionally, the predictive accuracy of the MIC assay as a biomarker for metastasis in heterogeneous tumor spheres is 84.6%. In general, this technique is highly relevant for the early identification of metastatic tumors. A near-infrared fluorescent biosensor called α-Fuc-DCM was created by Zhang J. et al. (2022) to enable the quick and ratiometric monitoring of α-L-fucosidase (AFU) activity in cells and mouse models of hepatocellular carcinoma (HCC). The biosensor was found to emit light as a result of the effective catalysis of α L-fucose residues by AFU. The α-Fuc-DCM nanoparticles are a stable biosensor that can be used for the early detection of endogenous AFU activity in a mouse model of HCC. Moreover, the α-Fuc-DCM probe is capable of detecting AFU in serum samples from patients with HCC. This approach offers an effective means of detecting AFU activity, which can be beneficial for the timely diagnosis of HCC.

3 Application of nanotechnology in tumor treatment

With the development of nanotechnology, nanomaterials have contributed to the further development of therapeutic tools such as hormone therapy, radiotherapy, transplantation, targeted therapy and immunotherapy. The role of nanomaterials in tumor therapeutic tools can be briefly summarized into two aspects: the

first is the direct fabrication of drug molecules into nanoscale particles to address the poor dispersion and high toxicity of existing drugs, such as nanocrystalline drugs; second, nanomaterials are used as drug delivery systems (including albumin paclitaxel, liposome drugs, mRNA-LNP, protein nanocages, micelles, membrane nanocomplexes) for drug delivery.

3.1 Drug nanocrystal

In the past few years, an increasing number of scientists have centered their attention on utilizing targeted and controlled-release nanotechnology in the therapy of cancer. with nanocrystalline drugs in the spotlight. Nanocrystals do not require carrier materials. The system is comprised of submicron particles made entirely from drugs, which are arranged in a colloidal dispersion, and there are no limitations on the encapsulation rate. Nanocrystalline drugs often exist as crystalline dispersed particles, and when in liquid form, they are known as nanocrystalline suspensions, which can be defined as nanoparticles made of pure drugs. This is a general formulation method that can improve the delivery efficiency of hydrophobic drugs. This method holds great promise in enhancing the pharmaceutical attributes of active pharmaceutical ingredients that have poor-solubility in water (Ma et al., 2023).

PTX nanocrystals are based on this property to enhance the poor water solubility of paclitaxel. Wei et al. (2015) characterized the saturation solubility, *in vitro* release, stability, and pharmacokinetic properties of PTX nanocrystals. Pharmacokinetic and tissue distribution experiments have shown that PTX nanocrystals can reduce the side effects of cancer therapies and are a promising formulation. PTX nanocrystals have different effects when combined with other drugs. Patel et al. (2014) developed stable PTX nanocrystals with high solubility and dissolution. Clarithromycin was used as a double multi-drug resistance gene cytochrome P450 3A4 inhibitor to enhance PTX penetration and anti-cancer efficacy, and its therapeutic effect on xenografted solid tumor mice was studied. The findings revealed that the nanocrystalline formulation considerably improved the solubility and permeability of PTX, resulting in enhanced therapeutic outcomes. At the same time, co-administration with CLM is a better way to improve the oral bioavailability of taxanes.

Multidrug resistance predisposes to chemotherapy failure, and the fabrication of nanoparticles of celastrol (CST) is an effective solution to overcome the challenges posed by multidrug resistance. The small size and surface modification of nanoparticles of CST can improve the bioavailability and targeting of the drug while reducing drug side effects. Xiao et al. (2022) developed dispersed nanodrugs by directly assembling CST into nanoparticles. The study also investigated the impact of these CST nanoparticles (CNPs) on P-glycoprotein (P-gp) inhibition. Results showed that CNPs were effective in inhibiting P-gp expression and preventing drug efflux by inducing HSF-1 expression and promoting nuclear translocation of HSF-1. The study also found that CNPs promoted apoptosis of newly established doxorubicin (DOX) resistant cell (MCF-7/ADR) by activating the ROS/ERK/JNK signaling pathway, compared to free CST. Moreover, CNPs showed significant inhibitory effects on the proliferation of MCF-7/ADR spheroids, confirming their potential to reverse drug resistance. These findings demonstrated that CNPs have the capability to serve as a translational nanomedicine for addressing drug resistance in cancer treatment. It has also been investigated to synergistically combine ryanodine with doxorubicin Nanocrystals carrier-free for better therapeutic effects through synergistic effects. Through a straightforward and eco-friendly precipitation approach, Xiao et al. (2018) created biocompatible nanoparticles (CST/DOX NPs) that do not require a carrier. The nanoparticles consisted of CST and DOX, two small-molecule drugs that are used clinically, and were developed to enable a synergistic combination chemotherapy strategy that can overcome resistance to DOX. The findings revealed that CST/DOX NPs had a substantial impact on the water solubility of CST and led to an enhanced accumulation of the drug in MCF-7/ADR cells by activating HSF-1 expression and suppressing P-gp expression through the NF-κB pathway. Additionally, the study discovered that CST/DOX NPs triggered apoptosis and autophagy in MCF-7/ADR cells via the ROS/JNK signaling pathway. Furthermore, CST/DOX NPs exhibited significant accumulation and infiltration capabilities in MCF-7/ADR multicellular spheroids (MCs) and had a notable inhibitory effect on MCF-7/ADR MCs. These findings suggest that CST/DOX NPs have great potential as a novel and effective strategy for combating DOX resistance in cancer treatment.

3.2 Nanodrug delivery system

Nanoplatforms can be designed as a vehicle to co-deliver multiple drugs, facilitating combination therapy to overcome drug resistance and improve treatment effectiveness (Li et al., 2023c). Nanocarriers can reduce the toxicity level of a drug and improve its therapeutic index. It enables the drug to maintain homeostatic levels for a longer period of time, thus improving efficacy (Chatterjee and Kumar, 2022). Several nanomedicines are gradually entering clinical applications, including nucleic acid-based nanoparticles, polymeric NPs, and classical liposomes (Chatterjee and Kumar, 2022; Zhang et al., 2023). The subsequent parts will discuss the significance of albumin paclitaxel, liposomes, mRNA-LNP, protein nanocages, micelles, Membrane-Nanoparticle Composites, and microspheres in the process of delivering drugs.

3.2.1 Albumin paclitaxel

PTX (Figure 5A) is a commonly used chemotherapy drug. In 2005, the FDA approved albumin binding paclitaxel for the treatment of metastatic breast cancer (MBC) (Karthikeyan et al., 2023). It was later approved in 2012 for the treatment of locally advanced or metastatic NSCLC, and in 2013 for metastatic pancreatic cancer (Kundranda and Niu, 2015). Shi et al. (2023) compared the efficacy of solvent-based paclitaxel, liposomal paclitaxel, nanoparticle albumin-bound paclitaxel (Nab-P), and DOX (Figure 5B) in human epidermal growth factor receptor 2 (HER2) positive and HER2 negative breast cancers. It showed that the group containing Nab-P was the most effective in treating breast cancer. Nano-albumin-bound paclitaxel (Abraxane) and solvent-based paclitaxel (i.e., Cre-paclitaxel) have different advantages in clinical applications (Spada et al., 2021). Albumin-bound paclitaxel showed a higher response rate and better tolerance in patients with advanced MBC and NSCLC compared to solvent-based paclitaxel

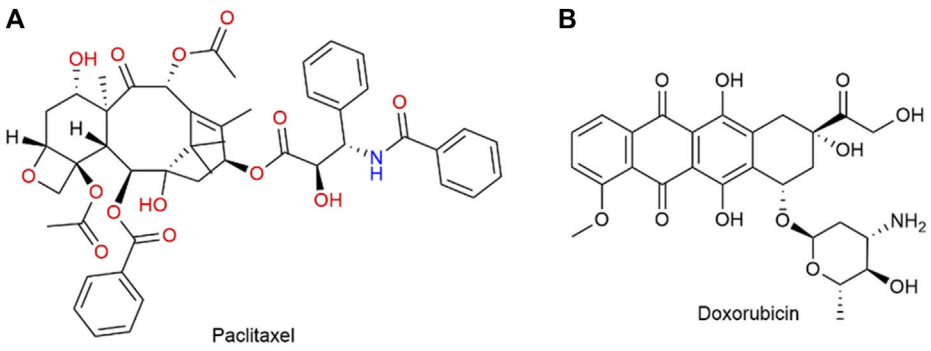

FIGURE 5
(A) Structure of paclitaxel. **(B)** Structure of doxorubicin.

(Yardley, 2013). Yoneshima et al. (2021) compared the therapeutic effects of Nab-P and DOX n patients diagnosed with either squamous or non-squamous NSCLC. Finally, the objective remission rate of albumin-bound paclitaxel was notably higher compared to that of DOX. These findings strongly indicate that albumin-bound paclitaxel demonstrates remarkable efficacy, particularly in patients with advanced NSCLC. The utilization of albumin-bound paclitaxel in the management of advanced NSCLC was also progressing and advancing clinically. And Spigel et al. (2021) evaluated maintenance Nab-P for the treatment of advanced squamous non-epithelial cell lung cancer. A Phase III trial revealed that the combination of Nab-P and carboplatin provided significant benefits for a subgroup of patients with advanced squamous NSCLC. In addition to advanced NSCLC, Nab-P may also have potential benefit for patients with recurrent small cell lung cancer. The progress made in nanotechnology has resulted in the utilization of Nab-P in conjunction with other drugs, with the goal of augmenting its efficacy. A retrospective analysis conducted by Koyama et al. (2018) examined the clinicopathological characteristics of patients who had stage IIIb or IV non-small cell lung cancer (NSCLC) and received a combination treatment consisting of Nab-P and carboplatin (CBDCA). Based on the results of clinical studies, the combination of Nab-P and CBDCA may be considered as a viable treatment alternative for patients with NSCLC and malignant pleural effusion. Multi-drug combination therapies are also emerging. Paglizumab as a targeting antibody modified on the surface of the nanoparticle, which enveloped the carboplatin and albumin paclitaxel by Mazieres et al. (2020). The use of this technique led to a noteworthy enhancement in the overall survival rate, progression-free survival rate, and objective response rate among patients who was untreated metastatic squamous cell carcinoma. The application of paclitaxel combined with Nab-P for clinical cancer treatment is a very promising method, but there are some side effects, such as numbness in the hands and feet, which is one of the more noticeable side effects. The better application of Nab-P to clinical treatment still needs to be improved.

3.2.2 Liposomal drugs

Liposomes are phospholipid vesicles composed of single or more concentric lipid bilayer with hydrophobic and hydrophilic cores, are also the most widely used nanocapsules. The therapeutic function of liposomal drugs is strongly related to their lipid composition. In addition, liposomes have been shown to enhance drug dissolution rates and modulate drug delivery (Andresen and Larsen, 2020; Khafoor et al., 2023). Polyethylene glycol doxorubicin liposomes (Doxil) are the first FDA-approved liposomal formulation to form adriamycin sulfate nanocrystals within liposomes during active drug loading (Chakravarty and Dalal, 2018). Researchers are working on the development of novel liposomes, such as long-acting liposomal drugs, cationic liposomes drugs, immune agents, and environmentally sensitive liposomes drugs, in order to enhance drug effectiveness and safety. Modification of empty liposomes with new materials can further improve the targeting ability and safety of liposomes and prolong the half-life of liposomes (He and Tang, 2018). By modifying their surface with hydrophilic polymers, liposomes as drug delivery systems have the advantage of lower leakage rates and longer cycle times. de Oliveira Silva et al. (2019) synthesized long-cycling PH-sensitive folic acid-coated DOX-supported liposomes (SpHL-DOX-Fol). The efficacy of the liposome against tumors was evaluated by conducting both *in vitro* and *in vivo* experiments using a 4T1 breast cancer model (Figure 6). The novel multifunctional nanoplatform demonstrated significant tumor targeting and antitumor effectiveness both *in vitro* and *in vivo*.

Cationic liposomes have a positive surface charge and, unlike their electrically neutral and anionic counterparts. Its low immunogenicity and toxicity, easy quality control and simplicity of preparation make it a common delivery system (Halevas et al., 2019). Various therapeutic payloads can be encapsulated with the help of phospholipid bilayer vesicles of liposome nanoparticles. Doping antibodies (immune liposomes/ILP) on the bilayer surface can amplify the active targeting ability of liposomes. By increasing the affinity for the target cell, the absorption of the drug by the target cell can be selectively enhanced, the off-target effects on normal cells can be mitigated, and the drug efflux can be reduced (Goswami et al., 2022).

The pH-sensitive liposomes are composed of sensitive lipids that remain stable at physiological pH but are unstable under acidic conditions. They possess membrane fusion properties and have attracted attention for achieving rapid drug release in tumor tissue. This function stimulates reactive drug release and decreases drug toxicity. Multi-drug resistance is a key factor in the failure of NSCLC

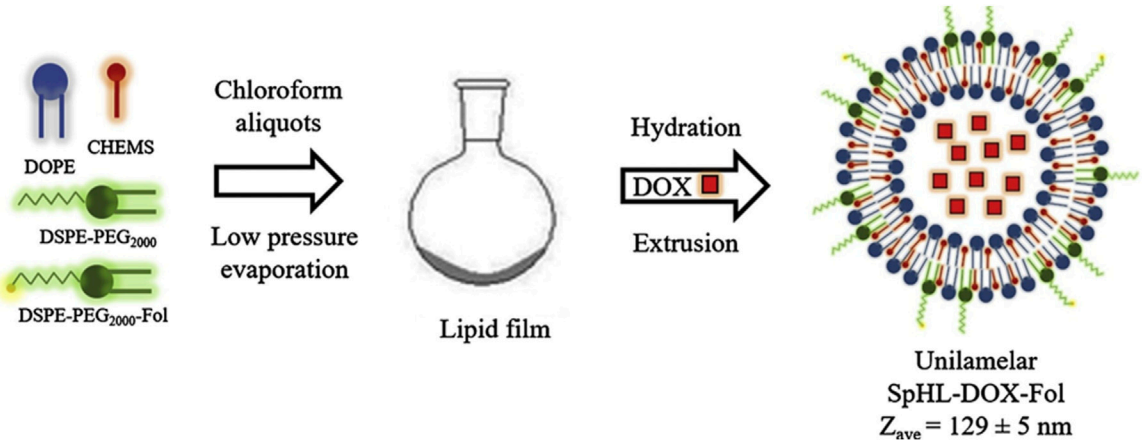

FIGURE 6
Synthesis of SpHL-DOX-Fol.

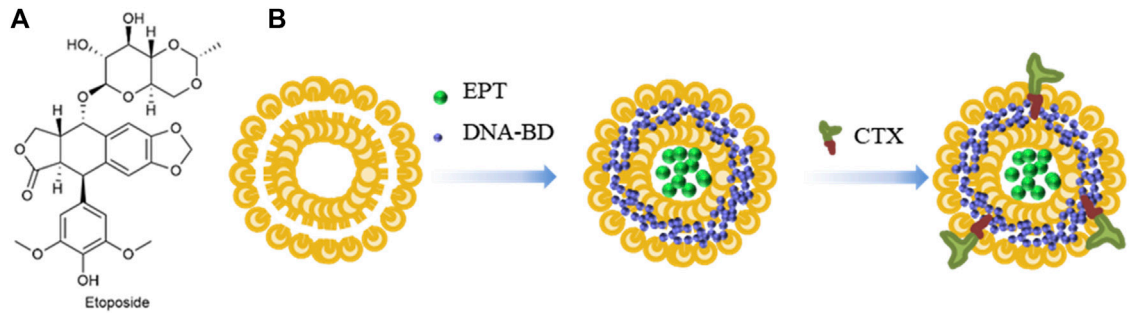

FIGURE 7
(A) Structure of Etoposide. **(B)** Synthesis of liposomes loaded with Etoposide and DNA-BD and coated with Cetuximab.

treatment. Wang et al. (2021) prepared porous hybrid paclitaxel-supported liposomes (PPL) containing ambroxol (Ax). It can re-sensitize resistant tumor cells and increase the retention of the drug in the lungs. The combined use of PPL and Ax can achieve outstanding tumor cell killing effect in multiway and multi-aspect, and has a broad range of applications. Liposomal drugs do have clear targeting advantages, but there are also drawbacks, such as the need for sophisticated instruments, high production costs, short half-lives, and the need for newer and better technology.

As shown in Figure 7A, Etoposide (ETP) is a widely used chemotherapy agent and eukaryotic topoisomerase II inhibitor. It breaks down the DNA structure, leading to cytotoxicity (Le et al., 2023). Cetuximab (CTX) is a monoclonal antibody that binds to the epidermal growth factor receptor (EGFR), thereby inhibiting the development of cancer (Baysal et al., 2020). Jha et al. (2020) used liposomes to encapsulate DNA biopoints (DNA-BD) and ETP with CTX as a target agent to modify the surface of nanoparticles. Carboxylated Vitamin-E TPGS (Vit-E TPGS) liposomes loaded with ETP were prepared using an improved solvent injection method, and CTX was coupled to the surface of Vit-E TPGS liposomes by carbodiimide reaction (Figure 7B), with a binding rate of 75%. The size range of liposomes was 140–190 nm, PDI < 0.3, and pH 5.5 was the optimal pH for ETP release. CTX-targeted liposomes have shown strong cytotoxic effects in A549 cells. EGFR-mediated endocytosis enables liposomes to target lung cancer cells and deliver site-specific drugs.

Inhalation administration is a common method for the treatment of lung disease, which reduces the distribution of chemotherapy drugs in the body and alleviates systemic toxicity. In addition, inhalation delivery can improve drug pharmacokinetics and increase drug retention in lungs (Lee et al., 2018). In order to overcome the insufficient pulmonary drug deposition caused by conventional drug delivery methods for treating NSCLC, Sarvepalli et al. (2022) prepared indomethacin liposomes (IND-Lip) by thin film hydration method. The fine particle fraction of nanoparticles was 82.5% ± 0.8%. The median mass values of aerodynamic diameter and geometric standard deviation are 4.3 ± 0.1 μm and 2.3 ± 0.1 μm, in that order. It was shown that the nanoparticles have good atomization behavior and can efficiently enter the tumor and deposit. The cytotoxicity of IND-Lip on three NSCLC cell lines (H460, H1299, and A549) was detected by MTT assay, and the

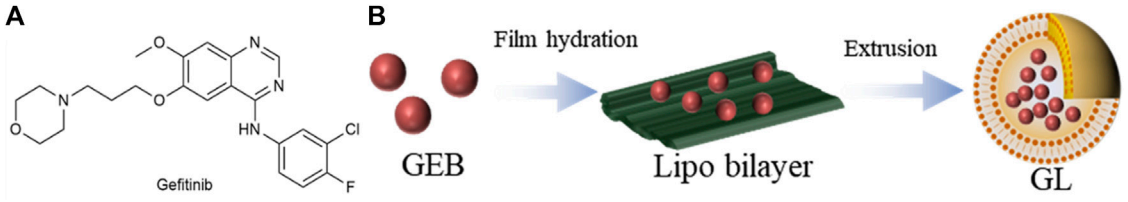

FIGURE 8
(A) Structure of gefitinib. **(B)** Synthesis of GL.

results showed that the IC_{50} value of IND-Lip was 1.5–4 times lower than that of ordinary IND. The efficacy of IND-Lip was better than that of ordinary IND. *In vitro* 3D globular cell administration experiments, the IND-Lip at 200 μM could reduce the original tumor volume by approximately 20%.

Gefitinib (GEB) (Figure 8A) is a selective EGFR-tyrosine kinase inhibitor (EGFR-TKI) (Lai et al., 2019). In light of the severe side effects of GEB and the limited effectiveness of using single drugs, Hu et al. (2020) opted to utilize a thin film dispersion method that incorporated anhydrous ethanol as a lipid solvent to produce liposomes containing GEB, denoted as GL (Figure 8B). GL has a particle size of about 190 nm, the PDI is 0.248, and the IC_{50} value is 29.63 μg/mL. When the ratio of phospholipid to cholesterol was 3, the highest encapsulation rate of 60.26% was obtained. The drug release time of GL is about 12 h, and the cumulative release rate reaches 80%, which indicates that the GL nanocomposite structure has a certain stability and can effectively prolong the drug action time. In *in vivo* anti-cancer model experiments, the GL group consistently maintained a tumor size of approximately 100 mm^3, which was significantly smaller than that of the PBS group. The mean tumor weight was 0.066 g in the GL group and 1.167 g in the PBS group. Nanoparticle liposomal carriers have promising applications in the treatment of lung cancer.

Bevacizumab (Beb) is an antibody targeting vascular endothelial growth factor and it is the first-line drug for metastatic colorectal cancer. As the first drug approved to target tumor angiogenesis, Beb is also being used to treat other cancers, including NSCLC and renal cell carcinoma (Muhsin et al., 2004). Zhang J. et al. (2022) prepared cationic liposomes containing anticancer drugs Geb and Beb by thin-film hydration method. The diameter of the nanoparticle is approximately 160 nm. Dialysis was utilized to evaluate the release properties of Geb and Beb. According to the *in vitro* release kinetics curves obtained in a PBS buffer at pH 5.0 and pH 7.4, it can be observed that the nanoparticles exhibit a pH-responsive behavior for the release of Geb and Beb. In addition, the drug release rate of MnO_2-PDA@Lipo@Geb@Beb nanomaterial is faster in high glutathione (GSH) conditions than in non-redox conditions, indicating that the nanoparticles have GSH response properties. MnO_2-PDA@Lipo@Geb@Beb also significantly inhibits tumor blood vessel formation. The results obtained during experimentation in a mouse tumor model validated that it displayed a more pronounced impact in inhibiting the growth of NSCLC cells compared to the unbound pharmaceutical agent.

3.2.3 mRNA-LNP

Messenger RNA (mRNA) is an emerging and intriguing form of tumor vaccine that provides antigen delivery and intrinsic immune activation-mediated co-stimulation in a spatiotemporally synchronized manner. mRNA vaccines are designed to instruct cells to express almost all essential proteins in host cells and tissues. These proteins may have a preventive effect, which play the therapeutic role in treating multiple diseases (Granados-Riveron and Aquino-Jarquin, 2021). Lipid nanoparticles (LNP) are simple, biocompatible, inexpensive, and versatile nanocarriers, which can be used to design multifunctional nanosystems (Granja et al., 2023). Initially, researchers used LNP as a vector to encapsulate full-length mRNA encoding novel coronavirus stinger proteins. Immune cells are able to recognize and ingest viral mRNA. Protein antigens can be efficiently expressed by directed mRNA. Tahtinen et al. (2022) discovered that the RNA and lipid formulation of RNA vaccines played a crucial role in the induction of interleukin 1 (IL-1) cytokine production in human immune cells. The IL-1 pathway is known to be vital for initiating innate signaling in response to RNA vaccines. Interestingly, specific lipids used in vaccine formulations containing N1-methylpseudouracil modified RNA unexpectedly increased this effect, thereby enhancing the activation of toll-like receptor signaling. These findings highlight the significance of the lipid component of LNP in stimulating immune responses to mRNA vaccines.

To achieve effective cancer vaccines, it is essential to generate a durable and high-quality $CD8^+$ T cell response. Although systematic vaccination is widely recognized as the most effective strategy, it is crucial to meticulously adjust the composition of the LNP carrier to ensure the successful delivery of mRNA to antigen-presenting cells (Bevers et al., 2022). The delivery of mRNA-encapsulated LNPs to the lungs is not without its challenges. One of the difficulties is that the nebulization process of LNPs can subject them to shear stresses caused by air dispersion, air jets, ultrasound and vibrational nets. This shear stress can lead to the clustering or leakage of LNPs, which can disrupt cross-cellular transport and endosomal escape. To overcome this problem, Miao et al. (2023) optimized the LNP formulation, nebulization method, and buffer system to keep the stability of LNPs during nebulization and preserve mRNA efficiency.

As a potential substitute for traditional drugs, mRNA-based therapies show great promise in cancer treatment. By encoding inactivated genes, mRNA therapy can restore the function of tumor suppressor genes that have been deleted or inactivated, thus inhibiting the growth of tumors that result from such mutations (Zong et al., 2023). Additionally, mRNA is translated in the

cytoplasm, allowing temporal control of immunotherapy. The benefits of mRNA immunotherapies have made them an attractive option for clinical applications, including cancer treatment modalities such as chimeric antigen receptor T cell (CAR-T) therapy and tumor infiltrating T cell therapy. The use of LNPs as a delivery platform is particularly promising, as they are able to efficiently deliver mRNA to T cells while minimizing toxicity during *in vivo* transfection (Patel et al., 2022). LNPs can be engineered to respond to external stimuli, such as the presence of tumors or the acidic environment of the endosome, thereby releasing mRNA in a targeted manner. Furthermore, LNPs can undergo modifications with targeting ligands and other substances to augment their affinity for overexpressed target proteins, like HER2 on cancer cells, and facilitate enhanced absorption by the intended tissue (Wang et al., 2023). The effectiveness of mRNA delivery through LNPs is heavily influenced by the lipid composition of the LNP, with the ionizable lipids being the primary determinant of delivery efficiency (Zeng et al., 2023). Snow et al. (2022) developed a new minor histocompatibility antigen (mHA) LNP vaccine using UNC-GRK 4-V as a target. They hypothesized that the vaccine might induce an antigen-specific immune response. The result showed that the UNC-GRK 4-V mRNA LNP vaccine based on ionizable amino lipids (SM-102) could trigger a robust antigen-specific T cell response. This could be an effective treatment to reduce the recurrence rate of tumors after allografts. Zeng et al. (2023) developed a LNP to deliver mRNA to bone marrow dendritic cells and evaluated its ability to activate T cells. The researchers confirmed that the LNP proved to be efficient and well-tolerated in delivering mRNA, demonstrating its exceptional suitability as a carrier for mRNA vaccines. Four different LNP formulations were identified, which effectively induced T cell expansion and cytokine production, and these formulations will be subjected to additional *in vivo* investigations as part of the efforts to create cancer vaccines.

3.2.4 Protein nanocages

Protein nanocages have attracted significant attention in different areas of nanomedicine owing to their inherent characteristics, such as biocompatibility, biodegradability, high structural stability, and easily modifiable surfaces and internal cavities (Wang and Douglas, 2021). Protein-based nanocages have great potential as diagnostic systems in cancer treatment. Protein-based nanocages, with their physiological properties and bioengineering versatility, make them a promising candidate for clinical applications. The integration of imaging and therapeutic functions within ferritin nanocages is currently considered the most promising and attractive frontier in cancer diagnostic and therapeutic approaches (Truffi et al., 2016). Nanocages based on ferritin contain anthracyclines, including adriamycin, which is widely used in cancer treatment to inhibit cell proliferation by blocking isomerase 2 (Palombarini et al., 2020). Protein cage nanoparticles such as ferritin, coated insulin, and virus-like particles (VLPs) have significant applications in vaccine development and imaging. These protein-based nanoparticles offer unique advantages compared to chemically synthesized nanomaterials as drug or vaccine carriers. They have many applications in vaccine development, for example, where they can be efficiently targeted and retained in the lymph nodes. Protein nanoparticles can enhance the immune response in various ways, such as facilitating efficient uptake by antigen-presenting cells and forming multiple connections with B cell receptors, thereby improving immunogenicity. Li et al. (2021) developed a new peptide antigen using VLPs from the phage P22 vaccine delivery system. The peptide antigens were expressed by fusion expression on the protein fraction of P22 VLPs. The produced vaccine particles stimulated a significant production of specific antibodies, with titers reaching 5.0×10^5. These findings suggest that P22 VLPs are vehicles for delivering peptide antigens in vaccines and present a versatile and straightforward technology platform for developing personalized therapeutic oncology vaccines.

3.2.5 Micelles

Micelles are mostly spherical structures formed by association of amphoteric molecules at specific temperatures and appropriate concentrations, with particle sizes ranging from 5–100 nm. The micelle's center is created by hydrophobic segments of amphoteric molecules, while the micelle's outer layer is made up of hydrophilic fragments (Milovanovic et al., 2017). Many drugs made from micelles have been applied in clinical (Sun et al., 2018), and micelles are mostly used to deliver insoluble chemotherapy drugs in cancer treatment (Ghosh and Biswas, 2021).

Curcumin (Cur) (Figure 9A) is extracted from the rhizome of Curcuma longa, which contains two *O*-methylphenols and one *β*-Polyphenol compounds of diketones. Curcumin can regulate various pathways (NF-*k*B and PI3K/AKT signaling pathways, etc.) to induce tumor cell apoptosis and improve its sensitivity to radiotherapy and chemotherapy (Wang L. et al., 2019). Baicalin (Bai), which is shown in Figure 9B, is a flavonoid that originates from the root of Scutellaria baicalensis Georgi. Its capacity to target multiple signal pathways enables it to inhibit various forms of cancer (Singh et al., 2021). Wang et al. (2019a) synthesized quercetin-dithiodipropionic acid-oligomeric hyaluronic acid-mannose-ferulic acid (QHMF), prepared self-assembled targeting nano micelles (nano Taraxacum) (Figure 10A), which can simultaneously target to the tumor tissue. In addition, Taraxacum nanoparticles targeting CD44 receptors would recruit more nanoparticles at tumor sites. In addition, Man could specifically bind to CD206, making the nanoparticle more susceptible to tumor-associated macrophage (TAM) engulfment. The disulfide bond connected the hydrophobic part and the hydrophilic part, which can be destroyed by the excessive concentration of GSH in the tumor microenvironment (TME), thus releasing Cur/Bai (Figure 10B). The particle size of nanometer Taraxacum was 121.0 ± 15 nm, and the Zeta potential was −20.33 ± 4.02 mV. It was easy to enter tumor tissue and could be released for a long time (Figures 10C, D). Nanotaxacum has good cell penetration and tumor cytotoxicity with fewer side effects.

Itraconazole (ITA) (Figure 11A) is a widely used antifungal drug with strong anti-angiogenic activity, which can affect multiple angiogenic pathways (Aftab et al., 2011). Zhang et al. (2018) co-encapsulated PTX and ITA in PEG-PLA (poly lactic acid) micelles (PIM) (Figure 11B). There were strong intermolecular interactions between ITA and PTX, so the micelle stability was high and the critical micelle concentration was low. It was concluded from *in vitro* cell

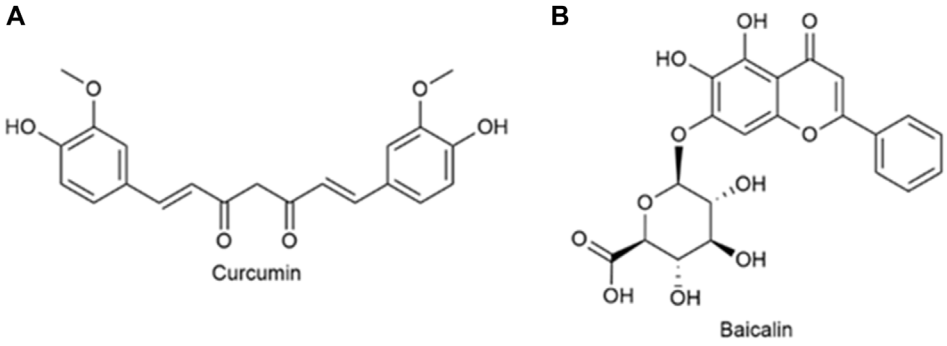

FIGURE 9
(A) Structure of curcumin. **(B)** Structure of Baicalin.

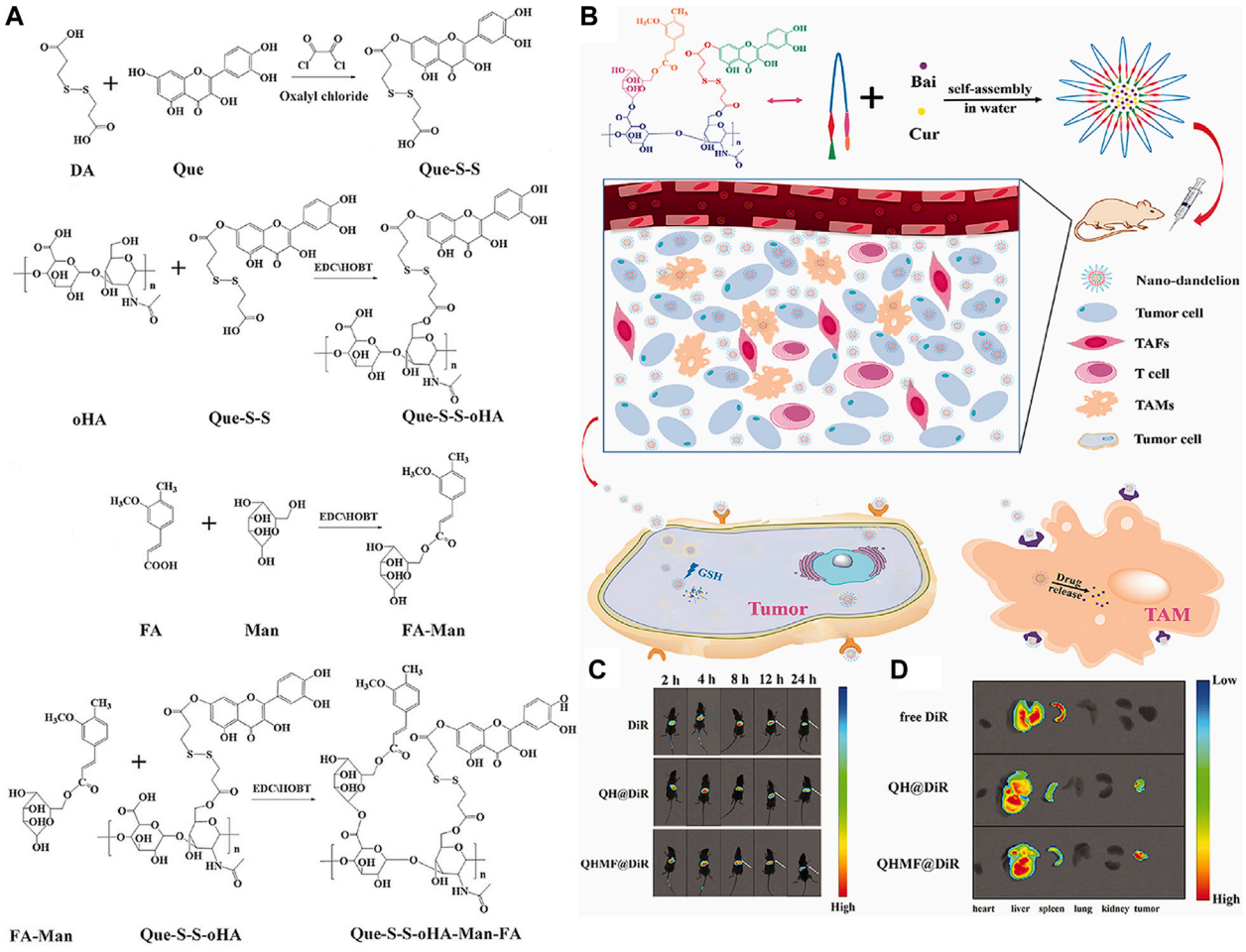

FIGURE 10
(A) Synthesis of QHMF. **(B)** Synthesis process of nano-dandelion and schematic diagram of nano-dandelion targeting A549 cells and TAMs. **(C)** The *in vivo* fluorescence imaging of A549 tumor-bearing mice was conducted at various time intervals (2, 4, 8, 12, and 24 h) subsequent to the intravenous injection of free DiR, QH@DiR, and QHMF@DiR. (Dir: Near-infrared fluorescent dye) **(D)** Distribution of free DiR, QH@DiR, and QHMF@DiR in the heart, liver, spleen, lung, kidney, and tumor.

experiments that PIM enters cells mainly through endocytosis and could bypass the elevated efflux caused by P-glycoprotein over-expression. *In vitro* experiments showed that PIM was effective in significantly inhibiting PTX-resistant NSCLC. Meanwhile, ITA acted as a P-glycoprotein inhibitor, blocking P-glycoprotein-mediated efflux and increasing the cellular

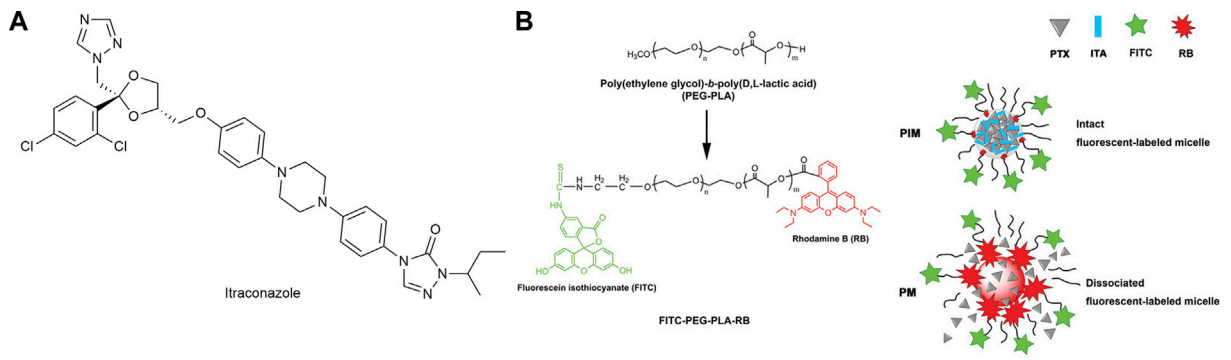

FIGURE 11
(A) Structure of Itraconazole. **(B)** Construction of fluorescent-labeled PEG-PLA and PEG-PLA micelles.

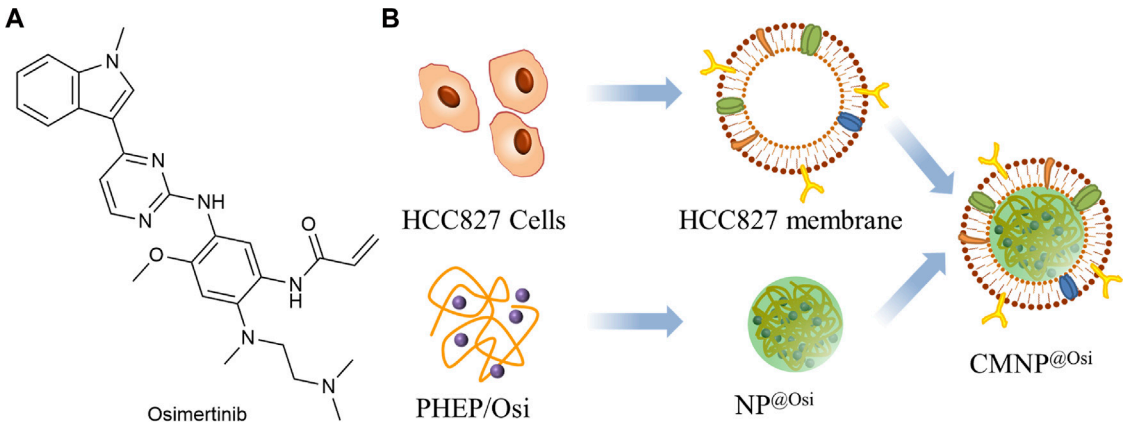

FIGURE 12
(A) Structure of Osimertinib. **(B)** Synthesis of CMNP$^{@Osi}$.

uptake of PTX. In xenografts obtained from patients with Kras mutation, orthotopic models, and subcutaneous models of paclitaxel resistance, PIM was found to significantly suppress tumor growth.

3.2.6 Membrane-nanoparticle composites

Biological nanocarriers sourced from bacteria, viruses, and mammalian cells have become a popular area of research due to their biodegradable nature and specific functions in the body. They possess the ability to evade immune system attacks, prolong circulation time, and enhance selective targeting, making them an attractive option for various applications (Yoo et al., 2011). Biofilms also have the function of biological self-recognition and signal transduction. Based on these characteristics, membrane camouflage nanocarriers with good biocompatibility, targeting, and long clearance time were developed (Fang et al., 2014; Liu et al., 2022). Moreover, this method is easy to prepare with lower cost (Xu et al., 2023).

As shown in Figure 12A, Osimertinib (Osi) is the third-generation EGFR-TKI used to treat patients with first or second generation acquired resistance to EGFR-TKI (Hognasbacka et al., 2023). Xu et al. (2023) prepared the inner core NP$^{@Osi}$ nanoparticles by nanoprecipitation using polymeric polyphosphoester (PHEP) (Figure 12B). The cell membranes were extracted from HCC827 cells and fused with NP$^{@Osi}$ to obtain CMNP$^{@Osi}$. The average particle size was 100 nm, the IC50 value was 14.23 nM, while the release of Osi was not affected by the cell membrane. *In vivo* administration of HCC827 xenografted BALB/c nude mice confirmed that the nanoparticles had good anti-tumor activity and biocompatibility. Compared to other cell types, CMNP$^{@Osi}$ exhibited better affinity and stronger targeting of its homologous cells. Therefore, homologous targeting can be considered as a specific targeting function of biofilms. At the same time, Osi, as a targeted drug, has been selectively used for EFGR sensitivity mutations and T790M resistance mutations. CMNP$^{@Osi}$ implemented the dual targeting strategy and facilitated the application of the membrane coating technique.

Over the past few years, the research for immune checkpoint blocking (ICB) drugs has progressed significantly with the development of inhibitors targeting programmed cell death protein 1 (PD-1) and its associated ligand, PD-L1. Although the use of antibody inhibitors targeting PD-1 or PD-L1 has

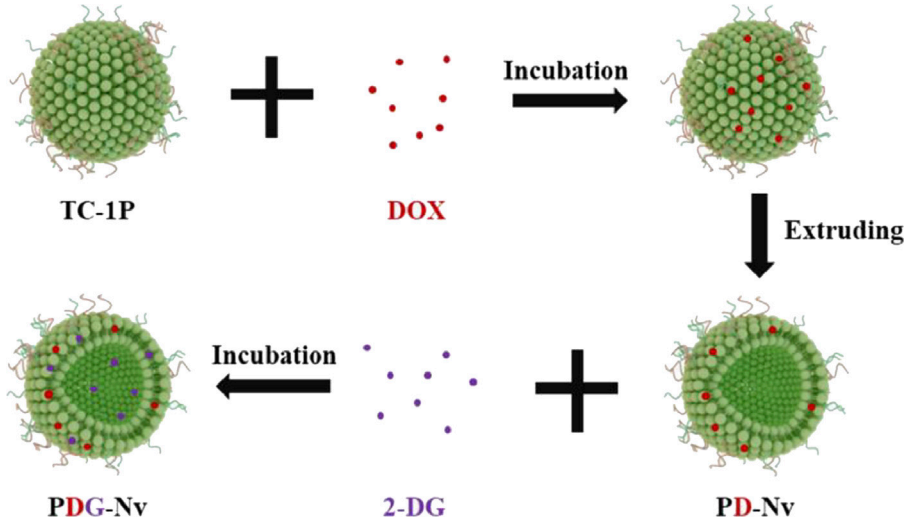

FIGURE 13
The assembly process of DOX and 2-DG loaded P-NV.

shown effectiveness in the treatment of lung cancer, they are unfortunately only effective in 10%–30% of patients (Li B. et al., 2023). Li et al. (2023a) designed TC1 cells (mouse NSCLC cell line), prepared PD-1 nanovesicles (P-NVs) by extrusion method, and loaded DOX and 2-deoxy-D-glucose (2-DG) into P-NVs to obtain PDG-NV for targeted treatment of NSCLC (Figure 13). The enhancement of tumor targeting capability was achieved by incorporating PD-1 onto NVs. Moreover, the combination of efficient loading of 2-DG and DOX exhibited a synergistic therapeutic effect on NSCLC in both *in vitro* and *in vivo* experiments, leading to significant cytotoxicity on tumor cells. PDG-NVs were also found to effectively reduce PD-L1 expression in the TME and improve the antitumor immune response mediated by $CD4^+$ and $CD8^+$ T cells. Thus, PDG-NV had great therapeutic potential, but this needs to be confirmed by further clinical trials.

Cisplatin (CDDP) is a platinum complex and is considered one of the most efficacious chemotherapy drugs for cancer treatment (Wang and Lippard, 2005). Despite its considerable anticancer activity, cisplatin's clinical application is restricted because of its acquired resistance and severe side effects (Yimit et al., 2019). Liang et al. (2021) used tannic acid (TA) to chelate Fe-rich metal-organic framework nanoparticles (MOF) to create MOF/TA. To create MOF/TA-CDDP-APT (MTCA), they further equipped the MOF/TA with CDDP and utilized antagonistic DNA aptamers (Apt) that specifically target PD-L1. The MTCA was further enveloped in the cancer cell membrane to create M@MTCA. The complex delivered the contents precisely to the tumor under the acidic conditions of TME, then released therapeutic substances and iron ions (Fe^{2+}) reactively with degradation. In addition to chemotherapy, CDDP can also be used to treat NSCLC through chemodynamic therapy. The level of H_2O_2 in the cell was raised by cascade reaction, and H_2O_2 was continuously converted to high cytotoxic •OH by Fenton reaction. Moreover, the nanocomplex was capable of converting "cold" tumors into "hot" tumors by promoting immunogenic cell death in tumor cells, which can enhance the therapeutic effectiveness when combined with ICBs (Apt).

Outer membrane vesicles (OMVs) are phospholipid bilayer structures with a spherical shape, ranging in size from 20 to 250 nm. These vesicles are generated from the outer membrane and periplasm of Gram-negative bacteria. They are naturally released from the bacterial cell envelope during their growth process (Schwechheimer and Kuehn, 2015). OMVs are engaged in a diverse array of physiological activities, such as intracellular and extracellular communication, quorum sensing, and stress responses. Kuerban et al. (2020) obtained OMV from attenuated *Klebsiella pneumoniae* and loaded DOX onto them (DOX-OMV) (Figure 14). The results of confocal microscopy and *in vivo* distribution studies indicated that the DOX-OMV delivery system effectively delivered DOX to NSCLC A549 cells. DOX-OMV also demonstrated a powerful cytotoxic effect, resulting in the triggering of cancerous cell death. When tested on BALB/c nude mice with A549 tumors, DOX-OMV was observed to significantly inhibit tumor growth, while being well-tolerated and exhibiting desirable pharmacokinetic properties. Moreover, OMVs are immunogenic and can recruit macrophages in TME causing corresponding immune responses, so they have great potential in tumor chemical immunotherapy.

3.2.7 Microspheres

Recently, the importance of long-acting implants has been increasingly recognized due to their unique advantages such as fewer medication administrations, high patient compliance, and low toxicity and side effects (Qiu et al., 2022). Biodegradable polymer microspheres possess the aforementioned advantages. These microspheres not only exhibit excellent biocompatibility but can also be prepared as sustained or controlled release formulations according to needs. Furthermore, their particle size distribution is narrow, eliminating the need for screening of improperly sized microspheres in later stages. As a result, this

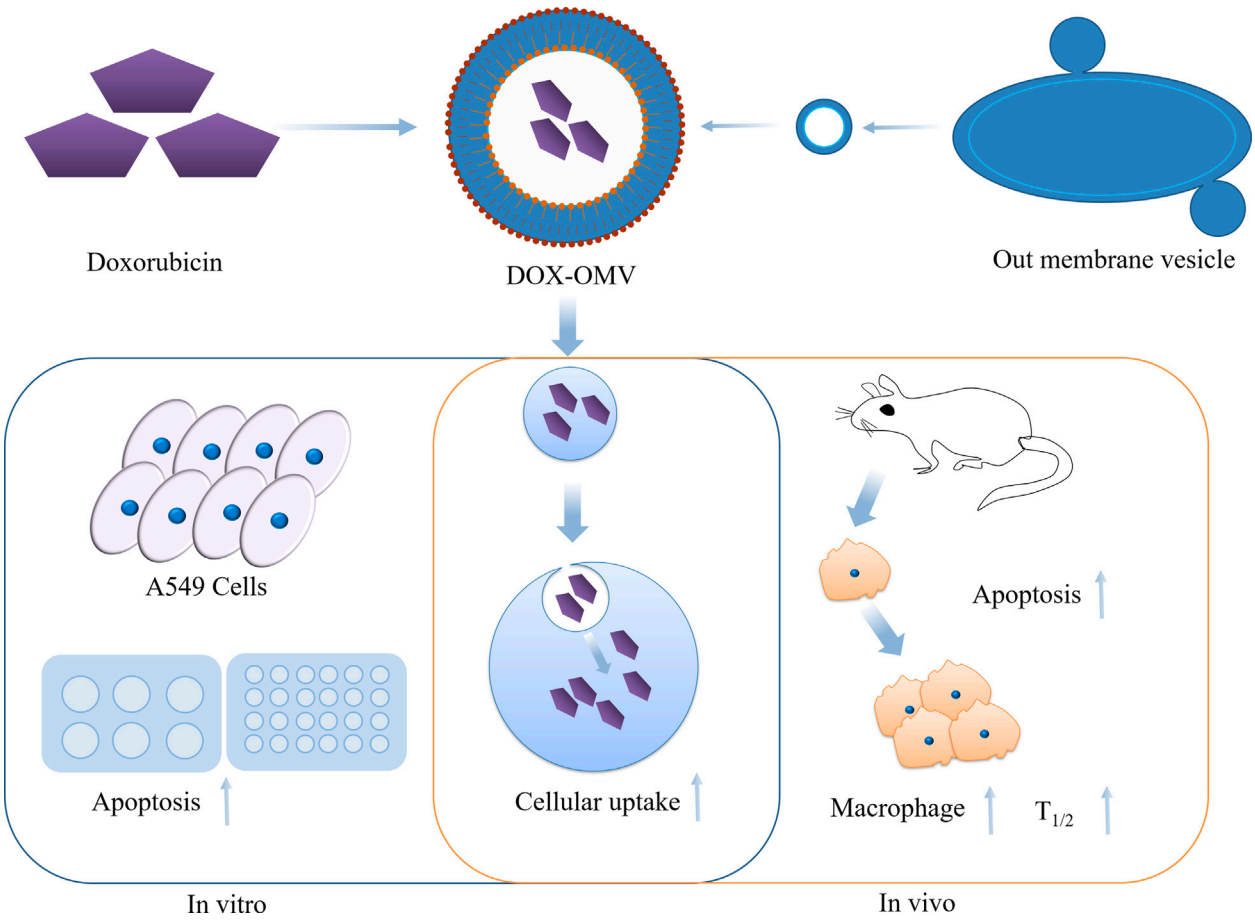

FIGURE 14
Overview of the anti-NSCLC effects of DOX-OMV. *In vitro*, DOX in OMV is delivered into A549 cells, resulting in strong cytotoxicity and apoptosis. *In vivo*, OMV also induces the recruitment of macrophages in tumor microwells.

characteristic reduces raw material waste and lowers preparation costs. Additionally, microspheres demonstrate good batch-to-batch reproducibility and repeatable release behavior, showcasing significant clinical value (Jin et al., 2020). Microsphere formulations belong to the high-end and complex field of pharmaceutical development, with a higher threshold. There is relatively little homogeneous competition in the pharmaceutical market for such formulations. For most drugs, there is a significant market capacity and room for growth, making their commercial prospects vast.

Poly lactic-co-glycolic acid (PLGA) formulations consist of different types, such as microspheres, *in situ* gel systems, and solid implants, and are commonly utilized for controlled and sustained drug release (Li X. et al., 2022). So far, there are more than twenty PLGA microsphere-based commercial products accessible in the market, including Decapeptyl Depot (Anwar et al., 2023), Lupron Depot, and Eligard (Kapoor et al., 2015). Sorafenib is a receptor tyrosine kinase inhibitor that can be taken orally, and it targets multiple receptors. The drug is capable of suppressing the proliferation of tumor cells, hindering angiogenesis, and promoting apoptosis of tumor cells. Sorafenib is primarily utilized to treat advanced renal cell carcinoma. Li et al. (2020) used a double-emulsion solvent diffusion method to encapsulate sorafenib (SOR) and catalase (CAT) into PLGA microspheres, forming SOR-CAT-PLGA microspheres (SOR-CAT-PLGA MSs). The size of these microspheres is approximately 73.5 ± 8.3 μm, with encapsulation efficiencies of 68.7% ± 1.9% for SOR and 76.5% ± 2.3% for CAT. The combined application of SOR and CAT demonstrates a significant synergistic effect in promoting cancer cell apoptosis while causing minimal damage to surrounding normal cells. During *in vivo* experiments, SOR-CAT-PLGA microspheres were found to fill tumor blood vessels effectively, impede neovascularization, and result in the shrinkage of tumor volume or prompt necrosis in rabbits. Moreover, these microspheres also downregulate the expression of PD-L1, suppress $CD8^+$ T cell apoptosis, and elevate IFN-γ levels. Therefore, the combined use of SOR and CAT may be an effective treatment method for liver cancer.

Porous microspheres (pMS) possess a large specific surface area and excellent adsorption performance, with interconnected inner and outer channels. pMS have broad application prospects in gastric retention drug delivery, pulmonary targeting drug delivery, high-speed chromatography, tissue regeneration scaffold development, and serving as carriers for biopharmaceuticals (Ghosh Dastidar

et al., 2018). Due to the low density and light weight of pMS, Yang et al. (2019) designed a dry powder inhalation drug delivery system based on pMS for treating EGFR TKI-resistant NSCLC. They loaded AFT lipid nanoparticles (AFT-SLN) and PTX into PLGA-pMS, creating AFT-SLN-PTX-pMS. This microsphere complex exhibited two distinct drug release phases, with PTX releasing faster than AFT. The aerodynamic properties of AFT-SLN-PTX-pMS were found to be favorable, with an MMAD value of about 3.25 μm, indicating successful deposition in the alveolar region of the lungs. According to pharmacokinetic parameters, both drugs maintained high concentrations within 96 h and were predominantly concentrated in the lungs. Additionally, the combination of the two drugs showed synergistic effects, with PTX significantly enhancing the cancer cell growth inhibitory effect of AFT. Moreover, AFT's sustained release inhibited cancer cell migration. These results suggest that AFT-SLN-PTX-pMS can evade phagocytic cells and achieve prolonged retention in the lungs. This drug delivery system demonstrates passive lung targeting characteristics, enhancing tumor killing efficacy while reducing systemic side effects.

Tumor treatment is a long-term process, and direct injection of drugs into the tumor presents a promising approach. Some drugs have been attempted to be administered directly into tumor tissues. However, these drugs have poor retention at the administration site and may leak out of the tumor within a few hours. This significantly affects drug efficacy and may increase systemic toxicity of the medication (Nakajima et al., 2000; Wang et al., 2003; Muñoz et al., 2021). Drug depot technology may be a potential approach to address these issues. Drugs diffuse and gradually release within a polymer matrix, (such as PLA or PLGA). However, the stability of sensitive drugs may be impacted by the properties of the polymer matrix, including its hydrophobic nature, internal pH, and reactive functional groups (Lessmann et al., 2023). Thermosensitive hydrogel is a drug delivery system whose physical state changes with temperature. By enhancing the adhesiveness of drugs to the affected area and prolonging local residence time, thermosensitive hydrogels can effectively improve drug bioavailability (Fan et al., 2022). Gel solutions undergo a phase transition with changes in environmental temperature and quickly solidify to block blood vessels, thereby cutting off the blood supply to tumors. Additionally, it can effectively address issues of embolism caused by non-uniform sizes of lipids and microspheres. Compared to common tumor treatment approaches, thermosensitive hydrogels can serve as drug depots for controlled release of drugs and targeted delivery into tumor tissues. The irregular shape of the affected area in tumor treatment poses challenges for drug administration, making thermosensitive hydrogels an ideal drug carrier (Ma and Yan, 2021).

Yu et al. (2019) utilized a modified double emulsion-solvent evaporation technique to fabricate microspheres of losartan potassium (LP MSs), with gelatin serving as the inner phase. These microspheres were then combined with cisplatin-loaded nanoparticles (CDDP NPs) made of poly (*α*-*L*-glutamate) grafted polyethylene glycol mono methyl ether (PLG-gmPEG). The microspheres and CDDP NPs were then dissolved in a temperature-responsive hydrogel, which could prevent drug leakage from the needle hole and greatly improve the drug retention time in the tumor. In *in vivo* experiments, LP MSs/CDDP NPs gel was found to effectively suppress tumor growth, decrease tumor volume, and caused no damage to the surrounding muscle tissue. This microsphere-gel composite has practical significance for the treatment of solid tumors. Tan et al. (2021) developed an injectable platform (Cur-MP/IR820 gel) for the treatment of osteosarcoma and the regeneration of bone tissue, which consisted of a composite methylcellulose hydrogel containing Cur microspheres and IR820. In *in vitro* experiments, after laser irradiation and heating, Cur was released rapidly, and the cytotoxicity against tumor cells was significantly higher than in other groups. Then, the mice in the group that received laser irradiation and were given Cur-MP/IR820 experienced high temperatures (approximately 51°C) at the tumor site, leading to tumor elimination. Subsequently, the platform continued to release Cur, killing the remaining cancer cells and promoting the differentiation of mesenchymal stem cells into osteoblasts and calcium deposition. The Cur-MP/IR820 hydrogel platform offers a promising avenue for the treatment of bone tumors and the regeneration of bone tissue, thereby providing a source of inspiration for future research in this area.

4 Conclusion

The development of nanotechnology has provided an excellent platform for tumor diagnosis, tumor cell imaging, early prevention and targeted therapy. The introduction of nanomaterials has provided novel functional technologies for the early diagnosis and treatment of major diseases such as cancer. In this paper, we have summarized the progress of nanotechnology in the early diagnosis of tumors, including the development status of nanomaterials for *in vivo* imaging and *in vitro* imaging techniques. The challenges and future directions of nanoprobe technology in image-guided oncology diagnostics are discussed, as well as the prospects for the development of biosensors for high sensitivity detection of tumor biomarkers. They have their advantages, such as magnetic nanoparticles that can be used as medical contrast agents for increased sensitivity, nanocrystalline QDs with high stability, and gold nanoparticles with low toxicity. These nanoparticles enable ultra-fast, highly sensitive and highly selective detection and diagnosis. At the same time, however, these tumor detection techniques suffer from several drawbacks, such as the large amount of residual nanoprobes in the body, and the possibility of cell death, oxidative stress and inflammation, among other side effects, due to too long residence time.

Conventional cancer therapies, targeted therapies and immunotherapies all come with their own set of limitations, including resistance, systemic toxicity and rapid elimination rates. New modalities of cancer treatment may be combined with nanotechnology to alter the status of treatment with excessive systemic chemotherapy. There is a growing clinical focus on the application of nanotechnology with targeted and slow-release properties to conventional oncology treatments, with nanomedicine being the leading candidate.

Nanomedicines for the treatment of tumors are generally natural nanomedicines, polymeric nanodrug carriers, and nanoliposomes. The emergence of emerging Nab-P, mRNA-LNP, protein nanocages, micelles, membrane-nanoparticle composites and

microspheres has solved many problems in clinical cancer prevention and treatment. Nevertheless, there exist certain obstacles in the practical implementation of these nanomedicines in clinical settings. The instability of the phospholipid component of liposomal drugs has hampered the translation of liposomal research into clinical practice for more than 50 years. The emergence of mRNA-LNP has represented a significant advancement in cancer prevention, yet there is still ample scope for enhancing LNP effectiveness. This can be accomplished through the refinement of lipid composition and customizing LNPs to cater to specific objectives. Cell membrane-coated biomimetic nanoparticles have shown great potential for cancer targeted therapies due to their superior molecular identification specificity and cancer cell targeting. However, there is still a lack of key indicators that can assess the quality of these bio-inspired nanoparticles and the resulting therapeutic effects. Additionally, only a few of these nanoparticles have received clinical approval due to their toxicity, immunogenicity and reticuloendothelial system isolation. Microsphere formulations are a type of sustained-release drug delivery system that can stably release drugs over a prolonged period. They are mainly used for diseases that require frequent dosing, such as cancer and psychiatric disorders. This drug delivery system can significantly improve the bioavailability of drugs and patient compliance. However, the development and production of microsphere formulations are challenging, and there are high barriers to entry in the industry. Therefore, it is necessary to accelerate the development of corresponding technologies. There is no denying that nanotechnology will play an important role in the future of medicine, but there are many aspects of nanotechnology that are not yet perfect. For nanotechnology to benefit humanity, further exploration by relevant researchers is needed.

Author contributions

YY and ML: Collection, writing original draft. MS: Investigation. G-QZ: Supervision, review and editing. JG and JL: Writing, review and editing. All authors contributed to the article and approved the submitted version.

Funding

This work was supported by the National Natural Science Foundation of China (52203171), the Postdoctoral Science Foundation of China (2021M701791) and Natural Science Foundation of Hebei Province (H2021201060).

Conflict of interest

The authors declare that the research was conducted in the absence of any commercial or financial relationships that could be construed as a potential conflict of interest.

Publisher's note

All claims expressed in this article are solely those of the authors and do not necessarily represent those of their affiliated organizations, or those of the publisher, the editors and the reviewers. Any product that may be evaluated in this article, or claim that may be made by its manufacturer, is not guaranteed or endorsed by the publisher.

References

Aftab, B. T., Dobromilskaya, I., Liu, J. O., and Rudin, C. M. (2011). Itraconazole inhibits angiogenesis and tumor growth in non-small cell lung cancer. *Cancer Res.* 71 (21), 6764–6772. doi:10.1158/0008-5472.CAN-11-0691

Andresen, T. L., and Larsen, J. B. (2020). Compositional inhomogeneity of drug delivery liposomes quantified at the single liposome level. *Acta Biomater.* 118, 207–214. doi:10.1016/j.actbio.2020.10.003

Anwar, A., Sun, P., Rong, X., Arkin, A., Elham, A., Yalkun, Z., et al. (2023). Process analytical technology as in-process control tool in semi-continuous manufacturing of PLGA/PEG-PLGA microspheres. *Heliyon* 9 (5), e15753. doi:10.1016/j.heliyon.2023.e15753

Baysal, H., De Pauw, I., Zaryouh, H., De Waele, J., Peeters, M., Pauwels, P., et al. (2020). Cetuximab-induced natural killer cell cytotoxicity in head and neck squamous cell carcinoma cell lines: Investigation of the role of cetuximab sensitivity and HPV status. *Br. J. Cancer* 123 (5), 752–761. doi:10.1038/s41416-020-0934-3

Bevers, S., Kooijmans, S. A. A., Van de Velde, E., Evers, M. J. W., Seghers, S., Gitz-Francois, J. J. J. M., et al. (2022). mRNA-LNP vaccines tuned for systemic immunization induce strong antitumor immunity by engaging splenic immune cells. *Mol. Ther.* 30 (9), 3078–3094. doi:10.1016/j.ymthe.2022.07.007

Chakravarty, K., and Dalal, D. C. (2018). Mathematical modelling of liposomal drug release to tumour. *Math. Biosci.* 306, 82–96. doi:10.1016/j.mbs.2018.10.012

Chatterjee, P., and Kumar, S. (2022). Current developments in nanotechnology for cancer treatment. *Mater. Today Proc.* 48, 1754–1758. doi:10.1016/j.matpr.2021.10.048

Chen, F., Wang, M., Du, Z., Pu, X., and Zhu, B. (2023). 131I labeled pH-responsive gold nanoparticles for bimodal tumor diagnosis. *Mater. Lett.* 330, 133202. doi:10.1016/j.matlet.2022.133202

Cheng, Y., Ling, S. D., Geng, Y., Wang, Y., and Xu, J. (2021). Microfluidic synthesis of quantum dots and their applications in bio-sensing and bio-imaging. *Nanoscale Adv.* 3 (8), 2180–2195. doi:10.1039/d0na00933d

de Oliveira Silva, J., Fernandes, R. S., Ramos Oda, C. M., Ferreira, T. H., Machado Botelho, A. F., Martins Melo, M., et al. (2019). Folate-coated, long-circulating and pH-sensitive liposomes enhance doxorubicin antitumor effect in a breast cancer animal model. *Biomed. Pharmacother.* 118, 109323. doi:10.1016/j.biopha.2019.109323

Eivazzadeh-Keihan, R., Bahreinizad, H., Amiri, Z., Aliabadi, H. A. M., Salimi-Bani, M., Nakisa, A., et al. (2021). Functionalized magnetic nanoparticles for the separation and purification of proteins and peptides. *TrAC Trends Anal. Chem.* 141, 116291. doi:10.1016/j.trac.2021.116291

Fan, R., Liu, Y., Zhang, T., Wang, Z., Zhang, H., Li, J., et al. (2022). Based on clinical application research progress of thermosensitive gel in different drug delivery sites. *Acta Pharm. Sin.* 57 (05), 1235–1244. doi:10.16438/j.0513-4870.2021-1209

Fang, R. H., Hu, C. M., Luk, B. T., Gao, W., Copp, J. A., Tai, Y., et al. (2014). Cancer cell membrane-coated nanoparticles for anticancer vaccination and drug delivery. *Nano Lett.* 14 (4), 2181–2188. doi:10.1021/nl500618u

Ganesh, S., Venkatakrishnan, K., and Tan, B. (2022). Early detection and prediction of cancer metastasis – unravelling metastasis initiating cell as a dynamic marker using self-functionalized nanosensors. *Sensors Actuators B Chem.* 361, 131655. doi:10.1016/j.snb.2022.131655

Ghosh, B., and Biswas, S. (2021). Polymeric micelles in cancer therapy: State of the art. *J. Control Release* 332, 127–147. doi:10.1016/j.jconrel.2021.02.016

Ghosh Dastidar, D., Saha, S., and Chowdhury, M. (2018). Porous microspheres: Synthesis, characterisation and applications in pharmaceutical & medical fields. *Int. J. Pharm.* 548 (1), 34–48. doi:10.1016/j.ijpharm.2018.06.015

Goswami, S., Chiang, C.-L., Zapolnik, K., Nunes, J., Ventura, A., Mo, X., et al. (2022). ROR1 targeted immunoliposomal delivery of OSU-2S shows selective cytotoxicity in t(1;19)(q23;p13) translocated B-cell acute lymphoblastic leukemia. *Leukemia Res.* 118, 106872. doi:10.1016/j.leukres.2022.106872

Granados-Riveron, J. T., and Aquino-Jarquin, G. (2021). Engineering of the current nucleoside-modified mRNA-LNP vaccines against SARS-CoV-2. *Biomed. Pharmacother.* 142, 111953. doi:10.1016/j.biopha.2021.111953

Granja, A., Lima-Sousa, R., Alves, C. G., de Melo-Diogo, D., Nunes, C., Sousa, C. T., et al. (2023). Multifunctional targeted solid lipid nanoparticles for combined photothermal therapy and chemotherapy of breast cancer. *Biomater. Adv.* 151, 213443. doi:10.1016/j.bioadv.2023.213443

Gulia, M., Nishal, S., Maddiboyina, B., Dutt, R., Kumar Desu, P., Wadhwa, R., et al. (2023). Physiological pathway, diagnosis and nanotechnology based treatment strategies for ovarian cancer: A review. *Med. Omics* 8, 100020. doi:10.1016/j.meomic.2023.100020

Halevas, E., Mavroidi, B., Swanson, C. H., Smith, G. C., Moschona, A., Hadjispyrou, S., et al. (2019). Magnetic cationic liposomal nanocarriers for the efficient drug delivery of a curcumin-based vanadium complex with anticancer potential. *J. Inorg. Biochem.* 199, 110778. doi:10.1016/j.jinorgbio.2019.110778

He, K., and Tang, M. (2018). Safety of novel liposomal drugs for cancer treatment: Advances and prospects. *Chemico-Biological Interact.* 295, 13–19. doi:10.1016/j.cbi.2017.09.006

Hognasbacka, A., Poot, A. J., Kooijman, E., Schuit, R. C., Schreurs, M., Verlaan, M., et al. (2023). Synthesis and preclinical evaluation of two osimertinib isotopologues labeled with carbon-11 as PET tracers targeting the tyrosine kinase domain of the epidermal growth factor receptor. *Nucl. Med. Biol.* 120-121, 108349. doi:10.1016/j.nucmedbio.2023.108349

Hu, Y., Zhang, J., Hu, H., Xu, S., Xu, L., and Chen, E. (2020). Gefitinib encapsulation based on nano-liposomes for enhancing the curative effect of lung cancer. *Cell Cycle* 19 (24), 3581–3594. doi:10.1080/15384101.2020.1852756

Hu, Z., Zhang, R., Xu, S., Wang, J., Li, X., Hu, J., et al. (2023). Construction of nano-drug delivery and antitumor system of stimuli-responsive polypeptides. *Colloids Surfaces B Biointerfaces* 226, 113310. doi:10.1016/j.colsurfb.2023.113310

Huang, C., Dong, H., Su, Y., Wu, Y., Narron, R., and Yong, Q. (2019). Synthesis of carbon quantum dot nanoparticles derived from byproducts in bio-refinery process for cell imaging and *in vivo* bioimaging. *Nanomater. (Basel)* 9 (3), 387. doi:10.3390/nano9030387

Jha, A., Viswanadh, M. K., Burande, A. S., Mehata, A. K., Poddar, S., Yadav, K., et al. (2020). DNA biodots based targeted theranostic nanomedicine for the imaging and treatment of non-small cell lung cancer. *Int. J. Biol. Macromol.* 150, 413–425. doi:10.1016/j.ijbiomac.2020.02.075

Jin, H., Chong, H., Zhu, Y., Zhang, M., Li, X., Bazybek, N., et al. (2020). Preparation and evaluation of amphipathic lipopeptide-loaded PLGA microspheres as sustained-release system for AIDS prevention. *Eng. Life Sci.* 20 (11), 476–484. doi:10.1002/elsc.202000026

Kapoor, D. N., Bhatia, A., Kaur, R., Sharma, R., Kaur, G., and Dhawan, S. (2015). Plga: A unique polymer for drug delivery. *Ther. Deliv.* 6 (1), 41–58. doi:10.4155/tde.14.91

Karthikeyan, L., Sobhana, S., Yasothamani, V., Gowsalya, K., and Vivek, R. (2023). Multifunctional theranostic nanomedicines for cancer treatment: Recent progress and challenges. *Biomed. Eng. Adv.* 5, 100082. doi:10.1016/j.bea.2023.100082

Khafoor, A. A., Karim, A. S., and Sajadi, S. M. (2023). Recent progress in synthesis of nano based liposomal drug delivery systems: A glance to their medicinal applications. *Results Surfaces Interfaces* 11, 100124. doi:10.1016/j.rsurfi.2023.100124

Khan, M. I., Batool, F., Ali, R., Zahra, Q. u. A., Wang, W., Li, S., et al. (2022). Tailoring radiotherapies and nanotechnology for targeted treatment of solid tumors. *Coord. Chem. Rev.* 472, 214757. doi:10.1016/j.ccr.2022.214757

Koyama, N., Watanabe, Y., Iwai, Y., Miwa, C., Nagai, Y., Aoshiba, K., et al. (2018). Effectiveness of nanoparticle albumin-bound paclitaxel plus carboplatin in non-small lung cancer patients with malignant pleural effusion. *Neoplasma* 65 (1), 132–139. doi:10.4149/neo_2018_170206N78

Kuerban, K., Gao, X., Zhang, H., Liu, J., Dong, M., Wu, L., et al. (2020). Doxorubicin-loaded bacterial outer-membrane vesicles exert enhanced anti-tumor efficacy in non-small-cell lung cancer. *Acta Pharm. Sin. B* 10 (8), 1534–1548. doi:10.1016/j.apsb.2020.02.002

Kundranda, M. N., and Niu, J. (2015). Albumin-bound paclitaxel in solid tumors: Clinical development and future directions. *Drug Des. Dev. Ther.* 9, 3767–3777. doi:10.2147/DDDT.S88023

Kuznetsov, D., Dezhurov, S., Krylsky, D., and Neschisliaev, V. (2022). Fluorescent nanosensors for molecular visualization of the c-Met tumor marker. *Nano-Structures Nano-Objects* 31, 100890. doi:10.1016/j.nanoso.2022.100890

Lai, K. C., Chueh, F. S., Hsiao, Y. T., Cheng, Z. Y., Lien, J. C., Liu, K. C., et al. (2019). Gefitinib and curcumin-loaded nanoparticles enhance cell apoptosis in human oral cancer SAS cells *in vitro* and inhibit SAS cell xenografted tumor *in vivo*. *Toxicol. Appl. Pharmacol.* 382, 114734. doi:10.1016/j.taap.2019.114734

Le, T. T., Wu, M., Lee, J. H., Bhatt, N., Inman, J. T., Berger, J. M., et al. (2023). Etoposide promotes DNA loop trapping and barrier formation by topoisomerase II. *Nat. Chem. Biol.* 19 (5), 641–650. doi:10.1038/s41589-022-01235-9

Lee, W. H., Loo, C. Y., Ghadiri, M., Leong, C. R., Young, P. M., and Traini, D. (2018). The potential to treat lung cancer via inhalation of repurposed drugs. *Adv. Drug Deliv. Rev.* 133, 107–130. doi:10.1016/j.addr.2018.08.012

Lessmann, T., Jones, S. A., Voigt, T., Weisbrod, S., Kracker, O., Winter, S., et al. (2023). Degradable hydrogel for sustained localized delivery of anti-tumor drugs. *J. Pharm. Sci.* S0022-3549, 00227-7. doi:10.1016/j.xphs.2023.05.018

Li, B., Yang, T., Liu, J., Yu, X., Li, X., Qin, F., et al. (2023a). Genetically engineered PD-1 displaying nanovesicles for synergistic checkpoint blockades and chemo-metabolic therapy against non-small cell lung cancer. *Acta Biomater.* 161, 184–200. doi:10.1016/j.actbio.2023.03.002

Li, H., Lin, L., Yan, R., Chen, Z., Wen, X., Zeng, X., et al. (2022a). Multi-functional Fe3O4@HMPDA@G5-Au core-releasable satellite nano drug carriers for multimodal treatment of tumor cells. *Eur. Polym. J.* 181, 111647. doi:10.1016/j.eurpolymj.2022.111647

Li, J., Lou, K., Dang, Y., Tian, H., Luo, Q., Huang, C., et al. (2023b). Precise tumor resection under the navigation of Tumor-Microenvironment pH-activated NIR-II fluorescence imaging via calcium Carbonate/Polydopamine Co-packed Nd-doped downshifting nanoprobes. *Mater. Des.* 227, 111703. doi:10.1016/j.matdes.2023.111703

Li, J., Zhu, L., and Kwok, H. F. (2023c). Nanotechnology-based approaches overcome lung cancer drug resistance through diagnosis and treatment. *Drug Resist. Updat.* 66, 100904. doi:10.1016/j.drup.2022.100904

Li, W., Jing, Z., Wang, S., Li, Q., Xing, Y., Shi, H., et al. (2021). P22 virus-like particles as an effective antigen delivery nanoplatform for cancer immunotherapy. *Biomaterials* 271, 120726. doi:10.1016/j.biomaterials.2021.120726

Li, X., Qin, J., and Hu, Y. (2023d). Switch-on hydrogel biosensor based on self-assembly Mn-doped ZnS QDs and cellulose nanofibrils for glutathione detection. *Microchem. J.* 191, 108763. doi:10.1016/j.microc.2023.108763

Li, X., Yu, H., Huang, Y., Chen, Y., Wang, J., Xu, L., et al. (2020). Preparation of microspheres encapsulating sorafenib and catalase and their application in rabbit VX2 liver tumor. *Biomed. Pharmacother.* 129, 110512. doi:10.1016/j.biopha.2020.110512

Li, X., Zhang, Z., Harris, A., and Yang, L. (2022b). Bridging the gap between fundamental research and product development of long acting injectable PLGA microspheres. *Expert Opin. Drug Deliv.* 19 (10), 1247–1264. doi:10.1080/17425247.2022.2105317

Liang, L., Wen, L., Weng, Y., Song, J., Li, H., Zhang, Y., et al. (2021). Homologous-targeted and tumor microenvironment-activated hydroxyl radical nanogenerator for enhanced chemoimmunotherapy of non-small cell lung cancer. *Chem. Eng. J.* 425, 131451. doi:10.1016/j.cej.2021.131451

Liu, H., Miao, Z., and Zha, Z. (2022). Cell membrane-coated nanoparticles for immunotherapy. *Chin. Chem. Lett.* 33 (4), 1673–1680. doi:10.1016/j.cclet.2021.10.057

Liu, J., Zhang, J., Gao, Y., Jiang, Y., Guan, Z., Xie, Y., et al. (2023). Barrier permeation and improved nanomedicine delivery in tumor microenvironments. *Cancer Lett.* 562, 216166. doi:10.1016/j.canlet.2023.216166

Lu, Q. (2023). Bioresponsive and multifunctional cyclodextrin-based non-viral nanocomplexes in cancer therapy: Building foundations for gene and drug delivery, immunotherapy and bioimaging. *Environ. Res.* 234, 116507. doi:10.1016/j.envres.2023.116507

Lv, W., Xu, C., Wu, H., Zhu, Y., Akakuru, O. U., Du, H., et al. (2022). Ultrasound-visualized nanocarriers with siRNA for targeted inhibition of M2-like TAM polarization to enhance photothermal therapy in NSCLC. *Nano Res.* 16 (1), 882–893. doi:10.1007/s12274-022-4767-7

Ma, N., and Yan, Z. (2021). Research progress of thermosensitive hydrogel in tumor therapeutic. *Nanoscale Res. Lett.* 16 (1), 42. doi:10.1186/s11671-021-03502-5

Ma, Y., Cong, Z., Gao, P., and Wang, Y. (2023). Nanosuspensions technology as a master key for nature products drug delivery and *in vivo* fate. *Eur. J. Pharm. Sci.* 185, 106425. doi:10.1016/j.ejps.2023.106425

Mazieres, J., Kowalski, D., Luft, A., Vicente, D., Tafreshi, A., Gümüş, M., et al. (2020). Health-related quality of life with carboplatin-paclitaxel or nab-paclitaxel with or without pembrolizumab in patients with metastatic squamous non-small-cell lung cancer. *J. Clin. Oncol.* 38 (3), 271–280. doi:10.1200/jco.19.01348

Miao, H., Huang, K., Li, Y., Li, R., Zhou, X., Shi, J., et al. (2023). Optimization of formulation and atomization of lipid nanoparticles for the inhalation of mRNA. *Int. J. Pharm.* 640, 123050. doi:10.1016/j.ijpharm.2023.123050

Milovanovic, M., Arsenijevic, A., Milovanovic, J., Kanjevac, T., and Arsenijevic, N. (2017). "Nanoparticles in antiviral therapy," in *Antimicrobial nanoarchitectonics.* (Elsevier), 383–410. doi:10.1016/B978-0-323-52733-0.00014-8

Montiel Schneider, M. G., and Lassalle, V. L. (2017). Magnetic iron oxide nanoparticles as novel and efficient tools for atherosclerosis diagnosis. *Biomed. Pharmacother.* 93, 1098–1115. doi:10.1016/j.biopha.2017.07.012

Muhsin, M., Graham, J., and Kirkpatrick, P. (2004). Bevacizumab. *Nat. Rev. Drug Discov.* 3 (12), 995–996. doi:10.1038/nrd1601

Muñoz, N. M., Williams, M., Dixon, K., Dupuis, C., McWatters, A., Avritscher, R., et al. (2021). Influence of injection technique, drug formulation and tumor

microenvironment on intratumoral immunotherapy delivery and efficacy. *J. Immunother. Cancer* 9 (2), e001800. doi:10.1136/jitc-2020-001800

Nakajima, S., Koshino, Y., Nomura, T., Yamashita, F., Agrawal, S., Takakura, Y., et al. (2000). Intratumoral pharmacokinetics of oligonucleotides in a tissue-isolated tumor perfusion system. *Antisense Nucleic Acid. Drug Dev.* 10 (2), 105–110. doi:10.1089/oli.1.2000.10.105

Palombarini, F., Di Fabio, E., Boffi, A., Macone, A., and Bonamore, A. (2020). Ferritin nanocages for protein delivery to tumor cells. *Molecules* 25 (4), 825. doi:10.3390/molecules25040825

Patel, K., Patil, A., Mehta, M., Gota, V., and Vavia, P. (2014). Oral delivery of paclitaxel nanocrystal (PNC) with a dual Pgp-CYP3A4 inhibitor: Preparation, characterization and antitumor activity. *Int. J. Pharm.* 472 (1), 214–223. doi:10.1016/j.ijpharm.2014.06.031

Patel, S. K., Billingsley, M. M., Frazee, C., Han, X., Swingle, K. L., Qin, J., et al. (2022). Hydroxycholesterol substitution in ionizable lipid nanoparticles for mRNA delivery to T cells. *J. Control. Release* 347, 521–532. doi:10.1016/j.jconrel.2022.05.020

Qiu, X., Li, S., Li, X., Xiao, Y., Li, S., Fen, Q., et al. (2022). Experimental study of beta-TCP scaffold loaded with VAN/PLGA microspheres in the treatment of infectious bone defects. *Colloids Surf. B Biointerfaces* 213, 112424. doi:10.1016/j.colsurfb.2022.112424

Rezayan, A. H., Mousavi, M., Kheirjou, S., Amoabediny, G., Ardestani, M. S., and Mohammadnejad, J. (2016). Monodisperse magnetite (Fe3O4) nanoparticles modified with water soluble polymers for the diagnosis of breast cancer by MRI method. *J. Magnetism Magnetic Mater.* 420, 210–217. doi:10.1016/j.jmmm.2016.07.003

Richardson, N. H., Althouse, S. K., Ashkar, R., Cary, C., Masterson, T., Foster, R. S., et al. (2023). Late relapse of germ cell tumors after prior chemotherapy or surgery-only. *Clin. Genitourin. Cancer* S1558-7673, 00087-3. doi:10.1016/j.clgc.2023.03.018

Sarvepalli, S., Parvathaneni, V., Chauhan, G., Shukla, S. K., and Gupta, V. (2022). Inhaled indomethacin-loaded liposomes as potential therapeutics against non-small cell lung cancer (NSCLC). *Pharm. Res.* 39 (11), 2801–2815. doi:10.1007/s11095-022-03392-x

Schwechheimer, C., and Kuehn, M. J. (2015). Outer-membrane vesicles from gram-negative bacteria: Biogenesis and functions. *Nat. Rev. Microbiol.* 13 (10), 605–619. doi:10.1038/nrmicro3525

Shao, Y., Xiang, L., Zhang, W., and Chen, Y. (2022). Responsive shape-shifting nanoarchitectonics and its application in tumor diagnosis and therapy. *J. Control. Release* 352, 600–618. doi:10.1016/j.jconrel.2022.10.046

Sharma, A., Sharma, N., Singh, S., and Dua, K. (2023). Review on theranostic and neuroprotective applications of nanotechnology in multiple sclerosis. *J. Drug Deliv. Sci. Technol.* 81, 104220. doi:10.1016/j.jddst.2023.104220

Shelar, S. B., Barick, K. C., Dutta, B., Basu, M., and Hassan, P. A. (2023). Selective targeting of gold nanoparticles for radiosensitization of somatostatin 2 receptor-expressing cancer cells. *J. Drug Deliv. Sci. Technol.* 82, 104381. doi:10.1016/j.jddst.2023.104381

Shi, W., Wan, X., Wang, Y., He, J., Huang, X., Xu, Y., et al. (2023). Nanoparticle albumin-bound paclitaxel-based neoadjuvant regimen: A promising treatment option for HER2-low-positive breast cancer. *Nanomedicine* 49, 102666. doi:10.1016/j.nano.2023.102666

Singh, S., Meena, A., and Luqman, S. (2021). Baicalin mediated regulation of key signaling pathways in cancer. *Pharmacol. Res.* 164, 105387. doi:10.1016/j.phrs.2020.105387

Snow, A., Lin, L., Hunsucker, S. A., Wang, Y., Liu, R., and Armistead, P. M. (2022). Development of a mRNA lipid nanoparticle (mRNA-LNP) cancer vaccine to prevent leukemia relapse after stem cell transplant. *Blood* 140, 7382–7383. doi:10.1182/blood-2022-160218

Spada, A., Emami, J., Tuszynski, J. A., and Lavasanifar, A. (2021). The uniqueness of albumin as a carrier in nanodrug delivery. *Mol. Pharm.* 18 (5), 1862–1894. doi:10.1021/acs.molpharmaceut.1c00046

Spigel, D. R., Jotte, R. M., Aix, S. P., Gressot, L., Morgensztern, D., McCleod, M., et al. (2021). Nanoparticle albumin-bound paclitaxel plus carboplatin induction followed by nanoparticle albumin-bound paclitaxel maintenance in squamous non–small-cell lung cancer (ABOUND.sqm): A phase III randomized clinical trial. *Clin. Lung Cancer* 22 (1), 6–15.e4. doi:10.1016/j.cllc.2020.09.007

Sun, X., Wang, G., Zhang, H., Hu, S., Liu, X., Tang, J., et al. (2018). The blood clearance kinetics and pathway of polymeric micelles in cancer drug delivery. *ACS Nano* 12 (6), 6179–6192. doi:10.1021/acsnano.8b02830

Tahtinen, S., Tong, A. J., Himmels, P., Oh, J., Paler-Martinez, A., Kim, L., et al. (2022). IL-1 and IL-1ra are key regulators of the inflammatory response to RNA vaccines. *Nat. Immunol.* 23 (4), 532–542. doi:10.1038/s41590-022-01160-y

Tan, B., Wu, Y., Wu, Y., Shi, K., Han, R., Li, Y., et al. (2021). Curcumin-Microsphere/IR820 hybrid bifunctional hydrogels for *in situ* osteosarcoma chemo-co-thermal therapy and bone reconstruction. *ACS Appl. Mater Interfaces* 13 (27), 31542–31553. doi:10.1021/acsami.1c08775

Tavallaii, A., Meybodi, K. T., Nejat, F., and Habibi, Z. (2023). Current status of research on targeted therapy against central nervous system tumors in low- and lower-middle-income countries. *World Neurosurg.* 174, 74–80. doi:10.1016/j.wneu.2023.03.030

Teja, P. K., Mithiya, J., Kate, A. S., Bairwa, K., and Chauthe, S. K. (2022). Herbal nanomedicines: Recent advancements, challenges, opportunities and regulatory overview. *Phytomedicine* 96, 153890. doi:10.1016/j.phymed.2021.153890

Thangavel, K., Lakshmikuttyamma, A., Thangavel, C., and Shoyele, S. A. (2022). CD44-targeted, indocyanine green-paclitaxel-loaded human serum albumin nanoparticles for potential image-guided drug delivery. *Colloids Surf. B Biointerfaces* 209 (1), 112162. doi:10.1016/j.colsurfb.2021.112162

Truffi, M., Fiandra, L., Sorrentino, L., Monieri, M., Corsi, F., and Mazzucchelli, S. (2016). Ferritin nanocages: A biological platform for drug delivery, imaging and theranostics in cancer. *Pharmacol. Res.* 107, 57–65. doi:10.1016/j.phrs.2016.03.002

Wang, B., Zhang, W., Zhou, X., Liu, M., Hou, X., Cheng, Z., et al. (2019a). Development of dual-targeted nano-dandelion based on an oligomeric hyaluronic acid polymer targeting tumor-associated macrophages for combination therapy of non-small cell lung cancer. *Drug Deliv.* 26 (1), 1265–1279. doi:10.1080/10717544.2019.1693707

Wang, D., and Lippard, S. J. (2005). Cellular processing of platinum anticancer drugs. *Nat. Rev. Drug Discov.* 4 (4), 307–320. doi:10.1038/nrd1691

Wang, L., Wang, C., Tao, Z., Zhao, L., Zhu, Z., Wu, W., et al. (2019b). Curcumin derivative WZ35 inhibits tumor cell growth via ROS-YAP-JNK signaling pathway in breast cancer. *J. Exp. Clin. Cancer Res.* 38 (1), 460. doi:10.1186/s13046-019-1424-4

Wang, R., Sun, Y., He, W., Chen, Y., Lu, E., and Sha, X. (2021). Pulmonary surfactants affinity Pluronic-hybridized liposomes enhance the treatment of drug-resistant lung cancer. *Int. J. Pharm.* 607, 120973. doi:10.1016/j.ijpharm.2021.120973

Wang, Y., and Douglas, T. (2021). Protein nanocage architectures for the delivery of therapeutic proteins. *Curr. Opin. Colloid & Interface Sci.* 51, 101395. doi:10.1016/j.cocis.2020.101395

Wang, Y., Hu, J. K., Krol, A., Li, Y. P., Li, C. Y., and Yuan, F. (2003). Systemic dissemination of viral vectors during intratumoral injection. *Mol. Cancer Ther.* 2 (11), 1233–1242.

Wang, Z., Ma, W., Fu, X., Qi, Y., Zhao, Y., and Zhang, S. (2023). Development and applications of mRNA treatment based on lipid nanoparticles. *Biotechnol. Adv.* 65, 108130. doi:10.1016/j.biotechadv.2023.108130

Wang, Z., Zhao, Y., Yang, Z., Li, X., Xing, H., Qu, W., et al. (2022). Construction of intelligent responsive drug delivery system and multi-mode imaging based on gold nanodots. *Macromol. Rapid Commun.* 43 (10), e2200034. doi:10.1002/marc.202200034

Wei, L., Ji, Y., Gong, W., Kang, Z., Meng, M., Zheng, A., et al. (2015). Preparation, physical characterization and pharmacokinetic study of paclitaxel nanocrystals. *Drug Dev. Ind. Pharm.* 41 (8), 1343–1352. doi:10.3109/03639045.2014.950272

Wu, H., Lv, W. H., Zhu, Y. Y., Jia, Y. Y., and Nie, F. (2023). Ultrasound-mediated mesoporous silica nanoparticles loaded with PDLIM5 siRNA inhibit gefitinib resistance in NSCLC cells by attenuating EMT. *Eur. J. Pharm. Sci.* 182, 106372. doi:10.1016/j.ejps.2023.106372

Xiao, Y., Li, X., Mao, J., Zheng, H., Ji, R., Wang, Z., et al. (2022). Reverse anti-breast cancer drug resistance effects by a novel two-step assembled nano-celastrol medicine. *Nanoscale* 14 (21), 7856–7863. doi:10.1039/d2nr02064e

Xiao, Y., Liu, J., Guo, M., Zhou, H., Jin, J., Liu, J., et al. (2018). Synergistic combination chemotherapy using carrier-free celastrol and doxorubicin nanocrystals for overcoming drug resistance. *Nanoscale* 10 (26), 12639–12649. doi:10.1039/c8nr02700e

Xu, B., Zeng, F., Deng, J., Yao, L., Liu, S., Hou, H., et al. (2023). A homologous and molecular dual-targeted biomimetic nanocarrier for EGFR-related non-small cell lung cancer therapy. *Bioact. Mater* 27, 337–347. doi:10.1016/j.bioactmat.2023.04.005

Yang, Y., Huang, Z., Li, J., Mo, Z., Huang, Y., Ma, C., et al. (2019). PLGA porous microspheres dry powders for codelivery of afatinib-loaded solid lipid nanoparticles and paclitaxel: Novel therapy for EGFR tyrosine kinase inhibitors resistant nonsmall cell lung cancer. *Adv. Healthc. Mater* 8 (23), e1900965. doi:10.1002/adhm.201900965

Yardley, D. A. (2013). nab-Paclitaxel mechanisms of action and delivery. *J. Control. Release* 170 (3), 365–372. doi:10.1016/j.jconrel.2013.05.041

Yimit, A., Adebali, O., Sancar, A., and Jiang, Y. (2019). Differential damage and repair of DNA-adducts induced by anti-cancer drug cisplatin across mouse organs. *Nat. Commun.* 10 (1), 309. doi:10.1038/s41467-019-08290-2

Yoneshima, Y., Morita, S., Ando, M., Nakamura, A., Iwasawa, S., Yoshioka, H., et al. (2021). Phase 3 trial comparing nanoparticle albumin-bound paclitaxel with docetaxel for previously treated advanced NSCLC. *J. Thorac. Oncol.* 16 (9), 1523–1532. doi:10.1016/j.jtho.2021.03.027

Yoo, J. W., Irvine, D. J., Discher, D. E., and Mitragotri, S. (2011). Bio-inspired, bioengineered and biomimetic drug delivery carriers. *Nat. Rev. Drug Discov.* 10 (7), 521–535. doi:10.1038/nrd3499

Yu, M., Zhang, C., Tang, Z., Tang, X., and Xu, H. (2019). Intratumoral injection of gels containing losartan microspheres and (PLG-g-mPEG)-cisplatin nanoparticles improves drug penetration, retention and anti-tumor activity. *Cancer Lett.* 442, 396–408. doi:10.1016/j.canlet.2018.11.011

Zeng, Y., Escalona-Rayo, O., Knol, R., Kros, A., and Slutter, B. (2023). Lipid nanoparticle-based mRNA candidates elicit potent T cell responses. *Biomaterials Sci.* 11 (3), 964–974. doi:10.1039/d2bm01581a

Zhang, J., Xu, L., Hu, H., and Chen, E. (2022a). The combination of MnO(2)@Lipo-coated gefitinib and bevacizumab inhibits the development of non-small cell lung cancer. *Drug Deliv.* 29 (1), 466–477. doi:10.1080/10717544.2022.2032872

Zhang, L., Liu, Z., Kong, C., Liu, C., Yang, K., Chen, H., et al. (2018). Improving drug delivery of micellar paclitaxel against non-small cell lung cancer by coloading Itraconazole as a micelle stabilizer and a tumor vascular manipulator. *Small* 14 (51), e1802112. doi:10.1002/smll.201802112

Zhang, L., Loh, X. J., and Ruan, J. (2022b). Photoelectrochemical nanosensors: An emerging technique for tumor liquid biopsy. *J. Photochem. Photobiol. A Chem.* 429, 113942. doi:10.1016/j.jphotochem.2022.113942

Zhang, L., Wang, H., Zhao, G., Li, N., Wang, X., Li, Y., et al. (2021). Anti-Tim4 grafting strongly hydrophilic metal-organic frameworks immunoaffinity flake for high-efficiency capture and separation of exosomes. *Anal. Chem.* 93 (16), 6534–6543. doi:10.1021/acs.analchem.1c00528

Zhang, P., Xiao, Y., Sun, X., Lin, X., Koo, S., Yaremenko, A. V., et al. (2023). Cancer nanomedicine toward clinical translation: Obstacles, opportunities, and future prospects. *Med* 4 (3), 147–167. doi:10.1016/j.medj.2022.12.001

Zong, Y., Lin, Y., Wei, T., and Cheng, Q. (2023). Lipid nanoparticle (LNP) enables mRNA delivery for cancer therapy. *Adv. Mater. Deerf. Beach, Fla)* 2023, e2303261. doi:10.1002/adma.202303261

Frontiers in
Bioengineering and Biotechnology

Accelerates the development of therapies, devices, and technologies to improve our lives

A multidisciplinary journal that accelerates the development of biological therapies, devices, processes and technologies to improve our lives by bridging the gap between discoveries and their application.

Discover the latest Research Topics

See more →

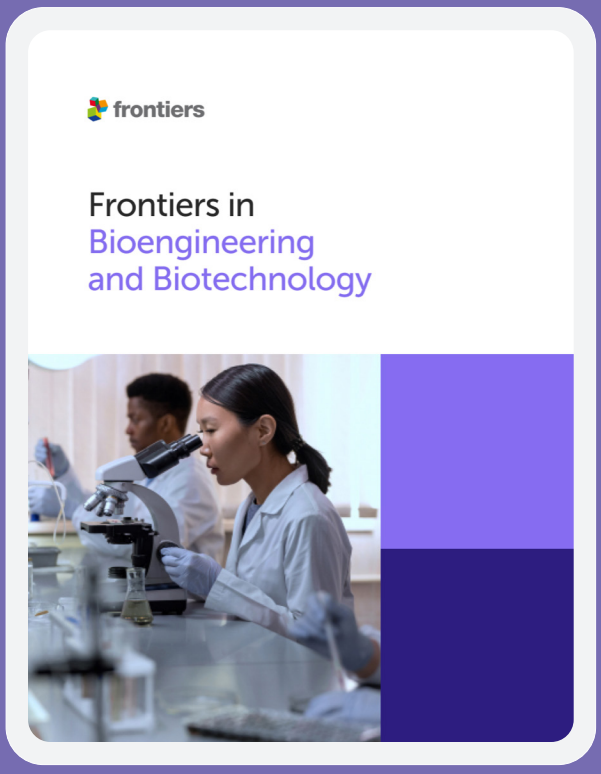

Frontiers

Avenue du Tribunal-Fédéral 34
1005 Lausanne, Switzerland
frontiersin.org

Contact us

+41 (0)21 510 17 00
frontiersin.org/about/contact